

# Development of Dual View Displays

*submitted by*

Jonathan F Mather

To the University of Exeter as a thesis for the degree of Doctor of  
Philosophy in the Faculty of Science, October 2007.

This thesis is available for library use on the understanding that it is copyright material and that no quotation from the thesis may be published without proper acknowledgement.

I certify that all material in this thesis which is not my own work has been identified and that no material has previously been submitted and approved for the award of a degree by this or any other University.

Signed.....

Confidential information from SLE to the University of Exeter, November 2007.

To my parents.



*Sharp announce that they will make dual view displays, July 2005 Tokyo Japan.*

## **Abstract**

This thesis is about 'Dual View' displays. These are displays that can show different images to different people. For example, the driver of a car could view a GPS map, whilst the passenger who looks at the display from a different angle, could watch a movie.

This thesis describes some of the research that took the project from an idea to a refined product. Sharp's first dual view display is prototyped, and problems such as crosstalk between the two views are seen. These problems are analysed and rectified to bring the device up to a high standard. In July 2005 Sharp used this technology to launch the world's first dual view product.

Since then a new design of dual view display has been investigated. This design is theoretically optimised and experimentally tested. The new design is shown to provide dual view with greater head freedom, greater efficiency, and lower crosstalk than the original parallax barrier design.

# Table of contents

<b>Development of Dual View Displays.....</b>	<b>1</b>
<b>Abstract.....</b>	<b>4</b>
<b>Table of contents .....</b>	<b>5</b>
<b>List of figures .....</b>	<b>10</b>
<b>List of tables.....</b>	<b>20</b>
<b>List of publications.....</b>	<b>23</b>
<b>Description of the publications .....</b>	<b>25</b>
<b>Acknowledgements.....</b>	<b>29</b>
<b>A special thanks to .....</b>	<b>29</b>
<b>INTRODUCTION .....</b>	<b>30</b>
<b>CHAPTER 1: PRIOR ART.....</b>	<b>34</b>
<b>Introduction .....</b>	<b>35</b>
<b>1. An introduction to dual view displays.....</b>	<b>35</b>
1.1 What is a dual view display .....	35
1.2 Why are dual view displays needed.....	36
<b>2. Dual view prior art.....</b>	<b>38</b>
2.1 Dual view paintings .....	39
2.2 Dual view toys - still images.....	40
2.3 Dual view displays .....	41
2.3.1 Concept .....	41
2.3.2 Multi-view.....	44
2.3.3 Parallax barrier dual view .....	46
2.4 Dual view prior art summary .....	46
<b>3. Extending 3D prior art towards dual view .....</b>	<b>46</b>
3.1 What are auto-stereoscopic 3D displays .....	47
3.2 Parallax optical technology .....	49
3.2.1 Basic design principles for 3D .....	49
3.2.2 Extension of parallax barrier design principles to dual view .....	53
3.2.3 Techniques to increase image splitting .....	56
3.2.4 Techniques for switching.....	67
3.2.5 Time multiplexing to increase resolution.....	74
3.2.6 Techniques to make a black central window .....	78

3.2.7 Crosstalk reduction .....	87
3.3 Alternative methods of image splitting .....	89
<b>4. A spin off application for dual view .....</b>	<b>92</b>
<b>5. Summary .....</b>	<b>94</b>
<b>CHAPTER 2: CREATING DUAL VIEW WITHOUT THIN GLASS .....</b>	<b>96</b>
<b>Introduction .....</b>	<b>97</b>
<b>1. The basic operation of the design .....</b>	<b>97</b>
<b>2. Design optimisation (theoretical) .....</b>	<b>100</b>
2.1 Lenticular thickness .....	101
2.1.1 Other magnification ratios.....	101
2.2 Radii of the lenses .....	101
2.2.1 Radius of the 2 <sup>nd</sup> lenticular.....	101
2.2.2 Radius of the 1 <sup>st</sup> lenticular. ....	102
2.3 Barrier –1st Lenticular separation.....	103
2.4 Pitch for each element.....	103
2.4.1 1 <sup>st</sup> lenticular pitch.....	104
2.4.2 Barrier pitch .....	104
2.4.3 2 <sup>nd</sup> lenticular pitch.....	104
2.4.5 Summary for all element pitches .....	105
2.5 Alignment of elements .....	105
2.6 ‘Barrier pitch correction’ .....	107
2.7 Summary table .....	107
<b>3. Optimisation of design by ray tracing.....</b>	<b>108</b>
3.1 Success criteria for the design procedure.....	109
3.1.1 Success criteria for computer optimisation.....	109
3.1.2 Success criteria for use in manual inspection .....	112
3.2 Method for optimisation.....	112
3.3 Summary of the design procedure .....	115
<b>4. Modelling results and analysis .....</b>	<b>115</b>
4.1 Design procedure implementation .....	115
4.2 Design procedure version 2.....	116
4.3 Design procedure version 2 implementation .....	116
4.3 Why is the performance of the system not perfect?.....	117
4.4 Design procedure version 3.....	119

4.5 Design procedure version 3 implementation .....	120
4.7 Summary of the modelled optimum design .....	123
<b>5. Experimental testing of the device.....</b>	<b>123</b>
5.1 Designing the device .....	123
5.2 Constructing the device.....	126
5.2.1 Creating the correct spacing between the components .....	126
5.2.2 Alignment of the components .....	127
5.3 Characterisation of the device.....	127
5.4 Conclusions on the double lens system.....	138
<b>6.0 Summary.....</b>	<b>139</b>
<b>CHAPTER 3: INVESTIGATION OF CROSSTALK IN A DUAL VIEW LCD. ....</b>	<b>141</b>
<b>Introduction .....</b>	<b>142</b>
<b>1. The new dual view display, and the crosstalk problem.....</b>	<b>142</b>
1.1 Description of the new design.....	143
1.2 The crosstalk problem .....	145
<b>2. Causes of crosstalk .....</b>	<b>146</b>
2.1 Hypothesis on the causes of crosstalk.....	146
2.2 Evidence for electrical crosstalk .....	147
2.2.1 Test images .....	148
2.2.2 Observations of single view panel. ....	151
2.2.3 A redesign of the panel electronics .....	153
2.3 Evidence for optical crosstalk and its sources.....	155
2.3.1 Test images that show optical crosstalk.....	155
2.3.2 Measurement of crosstalk .....	156
2.3.3 Microscope pictures of optical crosstalk.....	159
2.3.4 Further discussion supporting diffraction as a cause of crosstalk.....	165
2.3.5 Further investigation of light leakage through the parallax barrier.....	181
2.3.6 A new panel design .....	185
2.3.7 Further evidence of diffractive crosstalk.....	186
2.3.8 Could crosstalk be caused by edge reflection? .....	192
2.3.9 Could reflections from the underside of the barrier cause crosstalk? .....	196
2.3.10 Could crosstalk be caused by scatter at the polariser? .....	201
2.3.11 Experimentation on a giant dual view model.....	202
2.3.12 Summary of evidence for crosstalk causes. ....	213

<b>3. Human factors study</b> .....	<b>216</b>
3.1 Review of factors influencing crosstalk visibility.....	217
3.2 Experiments specific to dual view crosstalk visibility.....	219
3.3 Human factors techniques to reduce crosstalk visibility.....	223
<b>4. Reducing crosstalk</b> .....	<b>225</b>
4.1 Reducing electrical crosstalk.....	226
4.1.1 Crosstalk correction for electrical crosstalk.....	226
4.1.2 Redesign of TFT layout to reduce parasitic capacitance. ....	232
4.2 Reducing optical crosstalk .....	234
4.2.1 Crosstalk correction .....	234
4.2.2 Reducing diffraction.....	235
4.2.2 Reducing crosstalk from the polariser.....	248
4.3 Summary of solutions .....	249
4.4 Experimental demonstration of a low crosstalk dual view display.....	251
<b>5.0 Summary</b> .....	<b>252</b>
<b>CHAPTER 4: A MICROLENS DUAL VIEW SYSTEM</b> .....	<b>255</b>
<b>Introduction</b> .....	<b>256</b>
<b>1. Development of the idea</b> .....	<b>257</b>
1.1 How a 3D lenticular system works .....	257
1.2 Why the 3D lenticular system does not work for dual view .....	258
1.3 New lenticular design for dual view .....	259
1.4. What is the best lens- barrier design? .....	260
1.4.1 Cylindrical lenses and barrier.....	261
1.4.2 Prisms + barrier .....	265
1.4.3 A custom lens shape for dual view .....	267
1.4.4 Further possible improvements to the lens system .....	271
1.5 Summary of theoretical parallax optic designs .....	273
<b>2. Experimental testing of the device</b> .....	<b>274</b>
2.1 Why test the device? .....	275
2.2 How to make the lenses.....	277
2.2.1 Prototyping by photo-resist micro-lenses .....	277
2.3 Summary .....	289
<b>3. Optimisation tool for lens + barrier design</b> .....	<b>289</b>
3.1 Requirements of the theoretical model .....	290

3.2 The assumptions used in the model .....	290
3.4 Finding the best design .....	295
3.4.1 Success criteria for the dual view design .....	295
3.4.2 The optimisation algorithm .....	295
3.5 Summary .....	298
<b>4. Making a Manufacturable clear lens system .....</b>	<b>298</b>
4.1 Idea proposals .....	299
4.2 Experimental testing .....	299
4.2.1 Under development of resist .....	300
4.2.2. Dry etching red resist lenses into glass .....	301
4.2.3 Create rounded blocks in negative resist by use of a diffusive mask.....	301
4.2.4 Greyscale lithography on clear negative resist.....	302
4.2.5 Print negative resist blocks and then melt them.....	303
4.2.6 Using resist pillars to shape clear resist .....	304
4.2.7.....	305
Lenses by transfer technique.....	305
4.2.8 Capillary lenses .....	306
4.2.9 Embossing .....	307
4.2.10 Patterned de-wetting.....	308
4.3 Embossing clear micro-lenses.....	309
4.4 Making clear micro-lenses by capillary action .....	311
4.5 Summary .....	315
<b>5. Spin off designs for 3D and VAR.....</b>	<b>315</b>
5.1 Novel 3D systems .....	315
5.2 Improved view-angle restriction systems .....	317
<b>6. Summary.....</b>	<b>317</b>
<b>SUMMARY.....</b>	<b>319</b>
<b>APPENDICES .....</b>	<b>321</b>
Appendix 1 .....	321
Appendix 2.....	322
Appendix 3 .....	325
Appendix 4 .....	327
Appendix 5 .....	328
<b>References .....</b>	<b>335</b>

## List of figures

- Figure 1: A cross section of Sharp's first dual view prototype. The parallax barrier blocks light from pixels showing the other user's view.
- Figure 2: A novel configuration of micro-lenses that creates the dual view effect by directing light through the display pixels in different directions.
- Figure 3: A cross section of Sharp's first product quality dual view display. Much work was done to reduce crosstalk between the left and right views.
- Figure 4: A dual view display using a novel microlens and a parallax barrier configuration.
- Figure 5: A dual view display being used in a car application.
- Figure 6: Computer game applications for dual view.
- Figure 7: A cash machine using tri-view can advertise to passers by.
- Figure 8: The technology of the first known dual view painting.
- Figure 9: A patent application made in 1923, on which many dual view images are based today.
- Figure 10: An example of a modern day advertising campaign using lenticular poster technology
- Figure 11: An extract from a patent in 1994, which attempts to claim the concept dual view in a car.
- Figure 12: An extract from a patent from Nippon Denso, showing the use of lenticular lenses with a display.
- Figure 13: An extract from a patent filed by Ricoh. The diagrams show the operation of a device that creates 4 different views in different directions. The system is based on a parallax barrier design.
- Figure 14: The concept of stereoscopic displays.
- Figure 15: A cross sectional diagram of a parallax barrier, with all its important dimensions labelled.

- Figure 16: Calculating the correct distance between the pixels and parallax barrier for a 3D display.
- Figure 17: Calculation of a parallax barrier pitch.
- Figure 18: 'Barrier pitch correction' for a dual view display.
- Figure 19: The head freedom of a dual view display is linked to the slit widths in the parallax barrier.
- Figure 20: The two most promising ideas for creating dual view with a parallax barrier.
- Figure 21: Improved pixel design for dual view displays.
- Figure 22: A design to improve the quality of a 3D display using head tracking, created by company SeeReal.
- Figure 23: Parallax barrier designs for dual view with different groupings of pixels used to form the interlacing pattern for the left and right views.
- Figure 24: Parallax barrier systems on LCDs with different types of interlacing for the left and right images. The appearance of the display depends on the pitch of the slits in the parallax barrier.
- Figure 25: A photo of an early dual view prototype display. A mirror is used to show that a different image is being shown in another direction.
- Figure 26: An autostereoscopic display that is switchable between 2D and 3D.
- Figure 27: The Sharp system for 2D to 3D switchable displays.
- Figure 28: A switchable diffuser could be used to convert a dual view display into a conventional display.
- Figure 29: A new parallax barrier switching system.
- Figure 30: A diagram showing how 3D can be created using time multiplexed parallax barrier.
- Figure 31: A diagram showing how 3D can be created using time multiplexed backlighting.
- Figure 32: This diagram shows how Mitsubishi achieve directional illumination from their backlight.

- Figure 33: For a conventional parallax barrier dual view design, a region of angles exists on axis, where both images can be viewed.
- Figure 34: A double barrier design for a 3D display by Sanyo Electric Co.
- Figure 35: The use of colour filters in a parallax barrier.
- Figure 36: The transmission spectrum of colour filters used in an LCD television.
- Figure 37: A typical automotive backlight for an LCD.
- Figure 38: Light extracted from the waveguide.
- Figure 39: A backlight that emits light only to the left and right and not on-axis.
- Figure 40: Calculation of crosstalk.
- Figure 41: Transmission versus grey level curves for a TN LCD panel when viewed from above and below.
- Figure 42: Photographs of a TN LC mode operating as a dual view panel.
- Figure 43: An explanation of how a mirror works with a dual view display.
- Figure 44: Possible applications of a dual view display with a mirror.
- Figure 45: Diagram of a 'double lens' directional illumination system.
- Figure 46: The cumulative effect of all the lenses in a double lens dual view system.
- Figure 47: Design parameters that must be optimised in a double lens dual view system.
- Figure 48: Operation of the lenses in a double lens dual view system.
- Figure 49: Different ways of aligning the lenses and barrier.
- Figure 50: Head freedom requirements of a dual view display.
- Figure 51: Ray tracing of the double lens dual view system.
- Figure 52: Assessing crosstalk by ray tracing.
- Figure 53: The success criteria for the 1st lenticular and barrier.
- Figure 54: Crosstalk and brightness versus angle for the 2 lens directional illumination system.
- Figure 55: This diagram shows only rays passing through the system that cause crosstalk between 0 and 52 °.

- Figure 56: Brightness and crosstalk versus angle for the 2 lens directional illuminations system.
- Figure 57: This diagram shows only rays passing through the system that cause crosstalk between 0 and 52 ° for the 1mm system.
- Figure 58: Construction details of prototype.
- Figure 59: Using a laser to align the lenticular lenses.
- Figure 60: A photograph of the double lens dual view system in operation.
- Figure 61: Brightness versus angle from the thick glass prototype system.
- Figure 62: A comparison of data from the experimental system and simulated data whereby the parameters have been fitted match the experimental data.
- Figure 63: A cross sectional photograph of the lenticular lenses used to prototype the double lens dual view system.
- Figure 64: Experimental data from the double lens dual view system compared with simulation which takes into account the rounded areas at the lens joins.
- Figure 65: Experimental data from the double lens dual view system compared with simulation which takes into account the rounded areas at the lens joins and Fresnel reflections from the lenses.
- Figure 66: The operation of a 'thin glass' parallax barrier display.
- Figure 67: Comparison of simulated and experimentally measured dual view performance.
- Figure 68: Photos shows the effect of crosstalk on the dual view display.
- Figure 69: The proposed causes of crosstalk are electrical interference between pixels, and optical diffraction.
- Figure 70: Test images showing electrical crosstalk.
- Figure 71: Electrical crosstalk only 'travels' in one direction.
- Figure 72: Which pixels influence others via electrical crosstalk.
- Figure 73: Could optical effects cause the inverted crosstalk.
- Figure 74: A test image used to show up inverted crosstalk on a conventional single view panel.

- Figure 75: Parasitic capacitance (shown in red) amongst the pixels is the thought to be the cause of electrical crosstalk.
- Figure 76: A test image to show optical crosstalk. a). A green map in the left view produces faint green crosstalk to the right view.
- Figure 77: A sketch of crosstalk measurement for a dual view system.
- Figure 78: Experiment to show where optical crosstalk comes from. Using this set-up with the microscope, it is possible to see the crosstalk on a microscopic level.
- Figure 79: Set up of an experiment to see the source of crosstalk.
- Figure 80: Microscope images of crosstalk from a dual view panel.
- Figure 81: The equation for Fresnel diffraction.
- Figure 82: The geometry of the dual view system.
- Figure 83: Simulated Fresnel diffraction fringes in the plane of the barrier in the dual view system.
- Figure 84: A sketch of the variations in E field and intensity across the pixel aperture and slit respectively.
- Figure 85: The predicted intensity profile across the parallax barrier slit based on Fresnel diffraction from an incoherent backlight.
- Figure 86: The predicted intensity profile across the parallax barrier slit based on Fresnel diffraction from a coherent backlight.
- Figure 87: The E field contribution to a position on the slit from each point emitter on the backlight.
- Figure 88: Fringe contrast predicted by diffraction theory for different levels of spatial coherence at the backlight.
- Figure 89: A simplified diagram of a microscope with focal length  $f$  and lens diameter  $D$ .
- Figure 90: Photographs of fringes at the slit of a parallax barrier dual view system when viewed from the left side and the right side.
- Figure 91: The intensity pattern across the parallax barrier slit in a dual view systems for a backlight with a  $2\ \mu\text{m}$  spatial coherence length.

- Figure 92: A photograph of diffraction fringes created by a green laser and a dual view system compared with a theoretical simulation based on Fresnel diffraction theory.
- Figure 93: Transmission of the parallax barrier material with wavelength.
- Figure 94: A graph of transmission of white light from the dual view panel through the parallax barrier material.
- Figure 95: The optical path that causes crosstalk via parallax barrier material transmission.
- Figure 96: Light from a laser beam heading through the right view of a dual view LCD appears to spread into the left view by diffraction.
- Figure 97: Measurement of slit width versus crosstalk indicating that diffraction is the dominant effect in crosstalk production.
- Figure 98: The intensity of diffracted light with angle, for collimated light incident on a 38  $\mu\text{m}$  slit.
- Figure 99: Crosstalk versus wavelength in a dual view panel.
- Figure 100: A diagram showing a potential route via reflection from the edge of the parallax barrier.
- Figure 101: Fresnel reflections from air to the parallax barrier material.
- Figure 102: A sketch showing a possible route for crosstalk to occur.
- Figure 103: A microscope image of the LCD pixels when illuminated from above. Reflective metallic structures seem to be present.
- Figure 104: An experiment to measure the reflectivity of the pixels.
- Figure 105: The graph shows the amount of crosstalk given by a standard dual view panel.
- Figure 106: A cross sectional sketch of a macroscopic model of the dual view system.
- Figure 107: Identifying sources of crosstalk.
- Figure 108: A cross sectional sketch of the macroscopic dual view model showing all the light paths that can be seen to cause crosstalk.
- Figure 109: Light from different input angles causes different types of crosstalk. By measuring the amount of crosstalk caused from light illumination at

different angles, we can quantify the contribution of crosstalk from each source.

Figure 110: An experimental set-up for measuring the effect of light illuminating the panel from different angles

Figure 111: How light from different illumination angles affect the brightness and crosstalk in a dual view display.

Figure 112: A graph showing the contribution to crosstalk that each illumination angle causes.

Figure 113: The key factors in crosstalk visibility are the intensity of the crosstalk and the intensity of the background.

Figure 114: Contrast sensitivity of the human eye for different background intensities.

Figure 115: Test image showing varying levels of crosstalk intensity.

Figure 116: Typical images that may be shown on a dual view display.

Figure 117: The principle of crosstalk correction.

Figure 118: By illuminating the correct pixels, and by using a colour filter, electrical crosstalk can be decoupled from optical crosstalk.

Figure 119: Measurement of electrical crosstalk between left and right pixels in a dual view panel.

Figure 120: The intensity output of the blue pixels, versus the data level that is given to them.

Figure 121: Pixel designs that have/ have much reduced electrical crosstalk.

Figure 122: Electrical crosstalk on a panel with side-by-side ITO lines.

Figure 123: Crosstalk versus angle.

Figure 124: Soft edged parallax barriers.

Figure 125: A diagram of the equipment used to measure the amount of diffraction from hard and soft edged parallax barriers.

Figure 126: A graph showing that soft edge barriers diffract on axis light out to 30 ° on axis, by about 10 times less than a hard edge barrier.

Figure 127: A comparison of the crosstalk and brightness of the hard and soft edge barrier systems.

- Figure 128: A graph showing which angles of light from the backlight cause crosstalk.
- Figure 129: A graph of the illumination intensity versus angle for the standard and directional backlights.
- Figure 130: Crosstalk versus angle is tested for two dual view displays. The displays are identical except for the angle of separation between the images. The results show that increasing the angle of separation between the left and right images decreases the crosstalk.
- Figure 131: By rotating the LCD sub pixels by 90 °, the parallax barrier slit widths can be made 3 times larger.
- Figure 132: A comparison of crosstalk between standard and rotated pixel designs.
- Figure 133: The conventional design of an auto-stereoscopic 3D display.
- Figure 134: The concave regions between lenticular lenses are typically ~2% of the lens pitch.
- Figure 135: Standard auto stereoscopic 3D lens design applied to dual view. The focal lengths of the lenses should be at the pixels. This focal length is very small and difficult to achieve.
- Figure 136: A new design for dual view with lenses.
- Figure 137: A cross sectional view of a novel lens-barrier dual view system.
- Figure 138: Defocusing the lenses for better dual view performance.
- Figure 139: The angular brightness profiles of the new lens system versus the conventional parallax barrier system.
- Figure 140: Prisms can be used not to image light from the pixels, but simply bend light from the pixels into the correct direction to create a dual view display.
- Figure 141: The angular brightness profiles of the new lens system, prism system, and conventional parallax barrier system for dual view displays.
- Figure 142: Are lenses the best possible shape for a dual view system?
- Figure 143: An aspherical lens shape designed to create dual view.
- Figure 144: A custom lens shape design that creates dual view without any secondary windows.

- Figure 145: Theoretical predictions of the performance of a custom lens shape versus a spherical lens shape and parallax barrier.
- Figure 146: An explanation of how the maximum aperture of a dual view lens system is limited by the maximum refractive bending that can be achieved.
- Figure 147: Sketches of ideas that could provide more brightness than a single lens system.
- Figure 148: An effect that could reduce the contrast ratio of a lens dual view system.
- Figure 149: LCD pixels modulate light by changing polarisation.
- Figure 150: Method used to prototype the first dual view lens system.
- Figure 151: The transmission spectrum of the resist lens material.
- Figure 152: UV exposure before melting the resist makes the lenses 70% transmitting.
- Figure 153: The lens system creates dual view with low crosstalk, and good head freedom.
- Figure 154: The dual view display made from a new lens system has about the same brightness as the parallax barrier system.
- Figure 155: The dual view display made from a new lens system has lower crosstalk and more head freedom than the parallax barrier system.
- Figure 156: Contrast ratio of a dual view display with parallax barrier versus that of a lens system.
- Figure 157: Iso-azimuth plots of the contrast ratio of the parallax barrier and lens dual view systems.
- Figure 158: Grey level inversion in a dual view display with lenses.
- Figure 159: A paper representation of a cylindrical lens in the dual view system.
- Figure 160: A simulation of a dual view system based on geometric optical ray tracing.
- Figure 161: How the modelling software operates to predict the performance of a lens system
- Figure 162: Comparison of theory and experimental performance of the red lens system.
- Figure 163: Graphs to show the links between different design parameters in a dual view lens system.

- Figure 164: The extreme rays in the viewing windows come from the edges of the pixel. It is only necessary to ray trace these rays to determine the head freedom.
- Figure 165: Cross sections of resist blocks that are created with various exposure and development conditions.
- Figure 166: A method for making clear lenses with reactive ion etching.
- Figure 167: Apparatus used to expose resist with diffuse light.
- Figure 168: Resist blocks created by exposure with diffuse light.
- Figure 169: Apparatus used to create lithographic structures by using greyscale lithography.
- Figure 170: A picture of lenses made by depositing resist through a screen printing mask taken with an electron microscope by Micro-Stencil ltd.
- Figure 171: A method proposed to make lenses with clear negative resist.
- Figure 172: A photograph of clear negative resist after it has fused with red positive resist.
- Figure 173: A method proposed to create clear lenses by using a 'transfer technique'.
- Figure 174: Photographs of lenses created by using a transfer technique.
- Figure 175: A method proposed to create clear lenses by using capillary action.
- Figure 176: Photographs of lenses created using a capillary action.
- Figure 177: A cross sectional photograph of embossed lenses with black mask.
- Figure 178: A photograph of a water droplet on a glass surface.
- Figure 179: A cross section of the embossed lens demo structure.
- Figure 180: Comparison of theory and experimental performance of the clear lens system.
- Figure 181: Capillary lenses can be brighter than embossed lenses because of a bigger change in refractive index that can be achieved.
- Figure 182: Three options for assembling lenses (formed by capillary action) into a dual view display.

Figure 183: Modelling of crosstalk created by Fresnel reflection in ‘low index capillary lenses’.

Figure 184: Experimental measurement of a dual view made with a capillary lens system.

Figure 185: Lens barrier 3D versus standard 3D system.

Figure 186: The new lens and barrier system gives a 3 times brightness increase compared to a parallax barrier, when it is applied to ‘View angle restriction’.

## **List of tables**

Table 1: The barrier-pixel separation required to create dual view when mediums of various refractive index are used between the pixels and barrier.

Table 2: A comparison of the key dual view parameters for a colour filter barrier and a conventional parallax barrier.

Table 3: A comparison of brightness and contrast ratio between a standard TN LC mode and an LC mode that can create dual view due to its natural viewing angle characteristics.

Table 4: A table showing the head freedom produced by an LC mode that creates dual view due to its natural viewing angle characteristics.

Table 5: The section number in which each parameter of the double lens dual view system is discussed.

Table 6: How different 2nd lenticular lens pitches image the 1st lenticular.

Table 7: Formulae for the optimum parameters in the double lens dual view system based on thin lens approximations.

Table 8: How well the barrier and 1st lenticular perform in the double lens dual view system for different slit apertures.

Table 9: The performance of different slit and lens systems designed using different methods.

Table 10: The performance of different double lens dual view systems designed using different methods.

- Table 11: A comparison of possible designs for the double lens dual view system that could be created using off the shelf lenses.
- Table 12: The target values for the remaining variables of the prototype double lens dual view system.
- Table 13: The target specifications for the double lens prototype and the actual specifications.
- Table 14: A comparison of the double lens system of chapter 2 and the parallax barrier system of chapter 3.
- Table 15: Methods to detect electrical crosstalk in a single view panel.
- Table 16: Theoretical reflectivity between glue and two types of parallax barrier material
- Table 17: A table showing the type of crosstalk that illumination from different angles causes in the microscopic dual view system.
- Table 18: A summary of the different causes of crosstalk in a parallax barrier dual view system and the magnitude of each effect.
- Table 19: Crosstalk levels and their visibility to the human eye.
- Table 20: Methods to mask the visibility of crosstalk.
- Table 21: An example of test images that can be used to measure electrical crosstalk in the dual view system.
- Table 22: A comparison of the performance of soft and hard edged parallax barriers.
- Table 23: The effect of different illumination profiles on crosstalk.
- Table 24: A summary of methods to reduce electrical crosstalk.
- Table 25: A summary of methods to reduce optical crosstalk.
- Table 26: A summary the causes of crosstalk in a parallax barrier system and their magnitudes.
- Table 27: A first iteration of the micro-lens dual view design.
- Table 28: The performances of spherical and custom designed lens shapes in a dual view system.
- Table 29: A comparison of dual view systems based on different micro-optic lens shapes.

- Table 30: A comparison of a parallax barrier dual view system and the first micro-lens dual view system based on red lens material.
- Table 31: The complexity of modelling that might be required to predict different dual view parameters.
- Table 32: The variables that must be optimised in the parallax barrier and micro-lens dual view systems.
- Table 33: An estimate of the amount of time required to test all possible combinations of variables in the micro-lens system.

## List of publications

<i>GB Patent Pub.no.</i>	<i>GB Filing date</i>	<i>Title</i>	<i>Authors</i>
2404106	16/07/2003	Method to Allow Visual Estimate of Crosstalk on a 3D Display.	JM,GB, RW, DJM, GJ
2399653	21/03/2003	Parallax barrier and multiple view display.	DK, DJM, GB, JM
2405043	13/08/2003	Multiple view directional display	JM, DJM, GB, RW
2415850	28/06/2004	A multiple-View directional display	DK, JM, RW, DJM, HS
2405516	30/08/2003	Display showing Two Images from one uniform Panel	HS, JM, DUK
2405517	30/08/2003	Two Panel Stack	HS, JM, DUK
2405544	30/08/2003	A light control element and a display incorporating the same.	AE, PB, GB, LH, JM, MT, EW, RW, PS, MS
2405542	30/08/2003	Techniques to put a Barrier close to an LCD	JM, DK, RW, GB, AN
2405489	30/08/2003	Display that produces an image larger than the display size	JM, KS, GB
2405543	30/08/2003	A Multiple-View Directional Display.	DJM, JM, AJ, GB, GJ
2405546	30/08/2003	A multiple view directional display.	DJM, JM, GB, GJ
2405519	30/08/2003	A Multiple-View Directional Display.	JM, DJM, RW, GB, NB
2405545	30/08/2003	Parallax Optics using colour filters	JM, DJM, DUK, GJR, GB

2406731	20/01/2004	A multiple view display and a multi-direction display	JM, EJW, NB, GB, DUK, TWP
2410116	17/01/2004	Illumination system and display device.	PB, GB, AE, AJ, MDT, EJW, RW, JM, NJS
2418315	21/09/2004	Novel barrier and colour filter designs for multi-view displays	JM, AE, GRJ
2422737	26/01/2005	A multi-view display and display controller	JM, DJM, GRJ, DUK
2426351	19/05/2005	Dual view backlight barrier	JM, EL, DJM
2428303	08/07/2005	Front lights for VAR	EL, JM
2428129	08/07/2005	A multiple view directional display	JM, HS, GB, DK
2428344	08/07/2005	Multiple view directional display	DK, JM
Not yet published.	13/06/2006	Switching parallax optics using thermal rewritable technology	EL, JM

See Appendix 5 for the key to the initials.

## Description of the publications

GB Pub.no.	Description	My contribution
2404106	Methods to allow the crosstalk level of a multi-view display to be assessed by eye rather than by optical measurement. This document describes test images whereby the viewer can assess the crosstalk level by comparing intensity levels shown on the screen.	Co-invention of the test images.
2399653	This document describes the display designs which use novel groupings of pixels and parallax barrier slit widths presented in Chapter 1 section 3.2.3.	Co-invention of the NP2 design. Invention of the NP6 design that the first prototype dual view display was based on.
2405043	This document describes a parallax barrier in which the pitch is variable to compensate for the refraction of light that occurs whilst viewing at high angle.	Realisation that this compensation would be needed in some instances, and co-invention of the solutions.
2415850	A multi-view display that works in landscape or portrait mode without a change in viewing distance.	Co-invention of the design.
2405516	This document describes different types of liquid crystal mode that inherently provide dual view without any additional optics. The concept of this idea is described in Chapter 1 section 3.3.	Co-discovery of the TN mode as a 'dual view liquid crystal mode', and co-development of the idea.

2405517	Methods of creating dual view with directional liquid crystal modes. This patent covers ideas that use two panels one in front of the other to create the dual view effect.	Co-invention and analysis of many of the ideas.
2405544	A method for producing a privacy display which can switch between wide and narrow angles of view. This is based on a 'micro-louver' design that acts like a louver blind to block off axis light. The device is switchable using polarisation optics.	Co-invention of a minor embodiment of the design.
2405542	This document is about different ways of manufacturing a dual view display by putting the parallax optics close to the pixels. This patent also includes the idea of combining microlenses with the parallax barrier that is described in chapter 4.	Co-invention of the manufacturing techniques to put the parallax optics close to the pixels, and invention of the microlens system.
2405489	The use of a dual view display and a mirror to increase the apparent size of a display. The patent also contains ideas for mirrors that reflect an image off-axis so that the mirror is easier to position next to the display.	The design of off-axis mirrors for use with the dual view display.
2405543	This patent describes the lens system that is investigated in Chapter 2. Other single lens systems that work to re-image a parallax barrier to the pixels are also described.	The design of the double lens dual view system.
2405546	Designs for dual view displays in which the driver view has more head freedom than the passenger view.	Co-invention of the asymmetric designs.

2405519	Using a colour filter barrier with dual view to get better head freedom and brightness. Using colour filter barriers with secondary colours, using a colour filter barrier where the pixels are rearranged so the barrier may be closer to the display.	Design of colour filter barriers designed for use with dual view.
2405545	Using optics to increase the image separation between left and right images. This could allow a simple to make stereoscopic system to be converted into a dual view system.	Invention of the lens embodiments of the idea, co-invention of the other micro-optic systems.
2406731	Use of micro-prisms to redirect the backlight only into the dual view windows (increasing brightness, and creating a black central window). Also, use of double barriers, colour filter barriers etc, to block light going into the central window.	Co-invention of the backlights all configurations of the design.
2410116	This document is about directional backlights. The main idea is a backlight that can switch between on-axis and uniform illumination. The on-axis only illumination prevents off-axis viewers seeing private information on a display whilst the on axis viewer is unaffected. The document also includes an idea for a backlight that can switch between single view and dual view illumination modes.	Invention of the switchable backlight for dual view.
2418315	Different types of arrangements for colour filters in an LCD that work well with the dual view parallax optics.	Co-invention of the colour filter configurations.
2422737	Methods to reduce crosstalk in a dual view display including software compensation, apodized barrier slits, and rotating the pixels to reduce diffractive effects.	Co-invention of the software compensation algorithm.

2426351	A backlight waveguide that emits light only from stripes on its surface. The backlight functions as a waveguide and a parallax optic to create the dual view effect.	Invention of the main design.
2428303	A front light for an LCD that emits light only in the left and right directions thus preventing people at the left and right from seeing the LCD image whilst the on-axis user can still see the image.	Design of the front light which has these characteristics.
2428129	A collection of ideas including the use of directional micro-reflectors for brighter reflective dual view, a polariser that only diffuses one polarisation (half of the ambient light) whilst not diffusing the other polarisation (emitted by the dual view display), a dual view system for giant LED based displays, dual view with micro-optics internal to the liquid crystal cell, and a novel barrier design to compensate for brightness non-uniformity that may arise when using asymmetric pixels.	Invention of the novel barrier that compensates for brightness non-uniformity, and co-invention of the other ideas.
2428344	More techniques to reduce the crosstalk of DV displays. 1) add a microlens array some distance from the parallax barrier to split the central image mixing region. 2) Add patterned retarder behind or at the edges of barrier slits to compensate for crosstalk (similar to software compensation for crosstalk but done with optical elements).	Invention of the micro-lens idea, co-invention of the retarder idea.
Not yet published.	Methods using thermal rewritable material to create switchable parallax elements that could be used in directional displays such as multi-view displays and VAR displays.	Invention of parallax optics using thermally switchable material.

## **Acknowledgements**

The dual view project started at Sharp Laboratories of Europe Ltd (SLE) late in 2002. SLE is a research arm of Sharp, whose role is to primarily to create, prototype, and develop new technology. At SLE typically 2 to 3 people have been working on the dual view project, of which I am one.

Following successful design and prototyping at SLE, the dual view display has been exploited commercially by Sharp Corporation Japan. This has been a huge project, involving numerous people from sales, marketing, production, and product development.

The bulk of the work in this PhD is restricted to that which is my work or mostly my work. There are some exceptions where I briefly describe interesting results produced by colleagues. The table in appendix 5 shows in detail who made contributions to each section of the thesis, and what they did.

### **A special thanks to**

Professor Roy Sambles for giving me the opportunity to work on this PhD, and his encouragement to think a little deeper than I otherwise would have.

David Montgomery for teaching me about diffraction.

Diana Kean, Allan Evans, and Paul Gass for supervision, encouragement and advice.

Grant Bourhill for kick starting my career, showing me good working practices, and of course good Japanese izakayas.

Heather Stevenson, Etienne Lesage, Michel Sagadoyburu, and Lesley Parry-Jones who have at some point worked on the dual view project.

Jin Yu for providing all the SEM pictures.

Phelim Daniels and Safo Asia for arranging the contracts, and dealing with the mountain of paperwork that patents create. Marks and Clark patent attorneys who convert the information in all of SLE's patents into sound legal documents.

All the people at Sharp Corporation Japan who work at the business and product development end of the project, and to everyone else that has helped me at Sharp.

# INTRODUCTION

This thesis is about the development of a dual view display.

A dual view display shows different images to different viewers. For example, a driver in a car looking at the display from one angle could view information from a global positioning system, whilst the passenger who views the display from another angle could watch a movie.

A dual view display would enable a passenger to continue watching a movie whilst the car is in motion, with no visual distractions to the driver. A dual view display also takes up less space on a crowded dashboard than two displays, and one dual view display can be produced more cheaply than two displays.

In chapter 1 of this thesis prior art on dual view displays is revised. The concept of dual view can be dated back to a painting made in 1692 and is commonly seen in posters and toys. However there were no commercially available dual view displays that could show moving images, furthermore potential designs for dual view displays presented a serious engineering challenge since they required optics to be placed remarkably close to the display's pixels.

A novel design for dual view was created that did not need the optics- display separation to be small. This method was used to create Sharp's first prototype display, which had a good angular viewing range. The display had poor image quality but it proved that the concept of a dual view display was very popular (Figure 1).

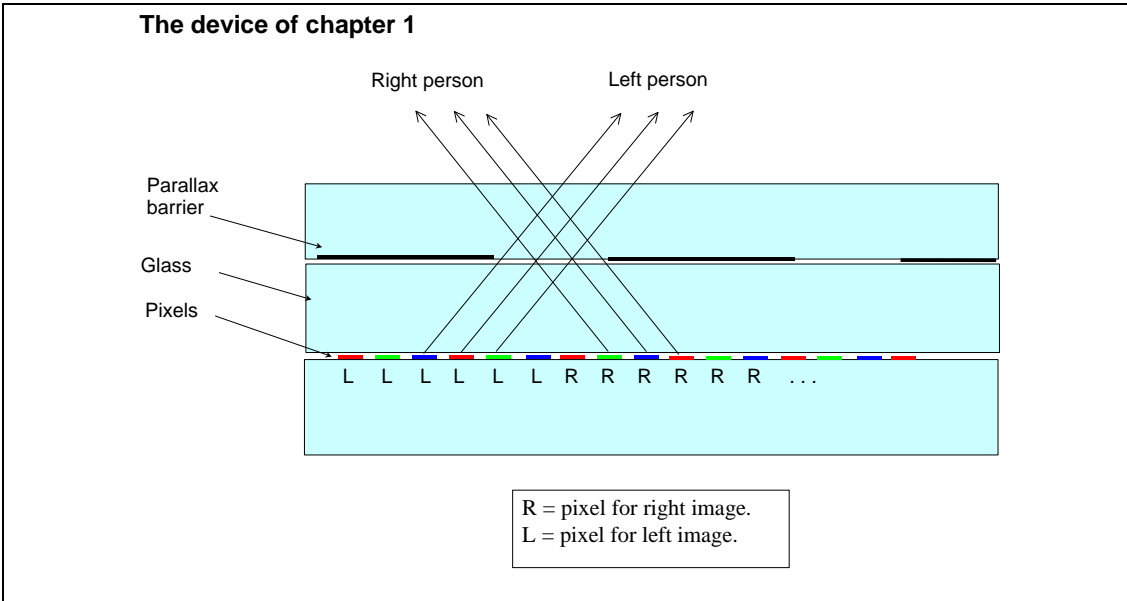


Figure 1: A cross section of Sharp's first dual view prototype. The parallax barrier blocks light from pixels showing the other user's view.

This display showed that a design for dual view was needed that was easy to make, bright, had good head freedom, and good image quality.

In chapter 2 a new design was created that would potentially meet all of these requirements. It was based on an arrangement of micro-optical elements as shown below.

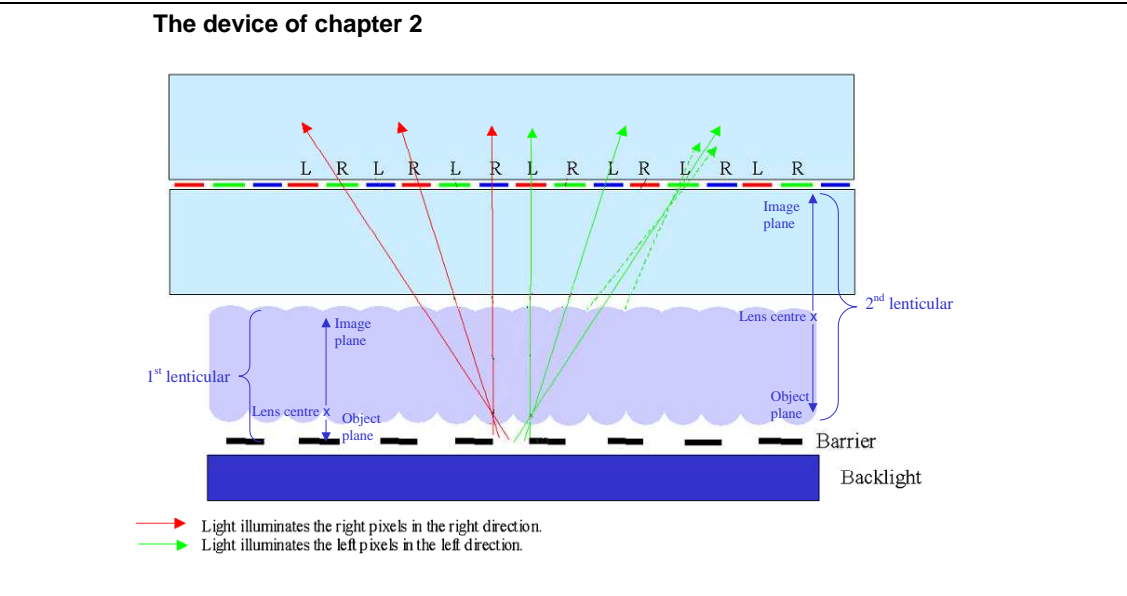
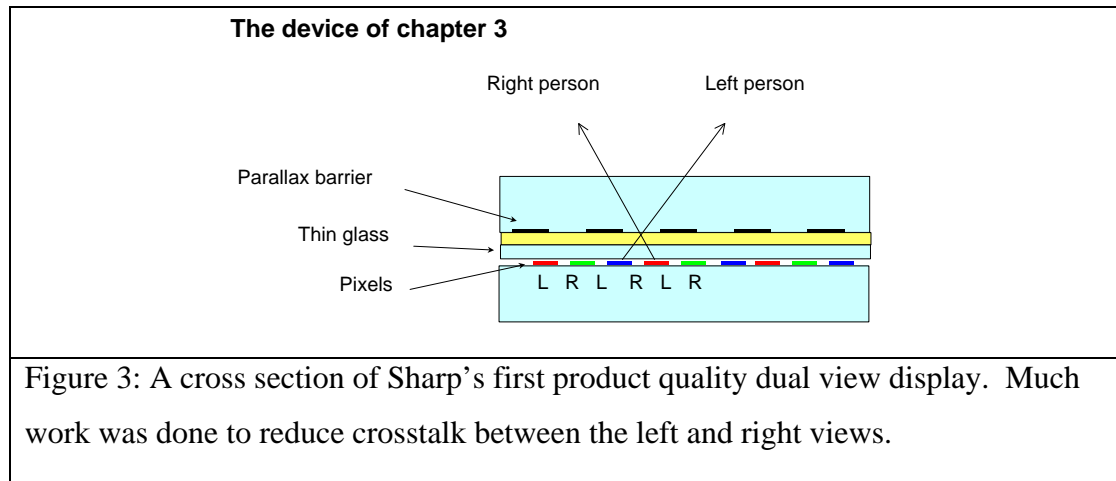


Figure 2: A novel configuration of micro-lenses that creates the dual view effect by directing light through the display pixels in different directions.

The design was optimised theoretically and tested experimentally. The results demonstrated that this technique could be used to make a dual view display, however it

was superseded by a design investigated in Chapter 3. The Chapter 2 design was superseded because subtle effect in the design caused an unacceptable amount of crosstalk between the two views. This created a possible distraction hazard for the driver and made the display appear of low quality.

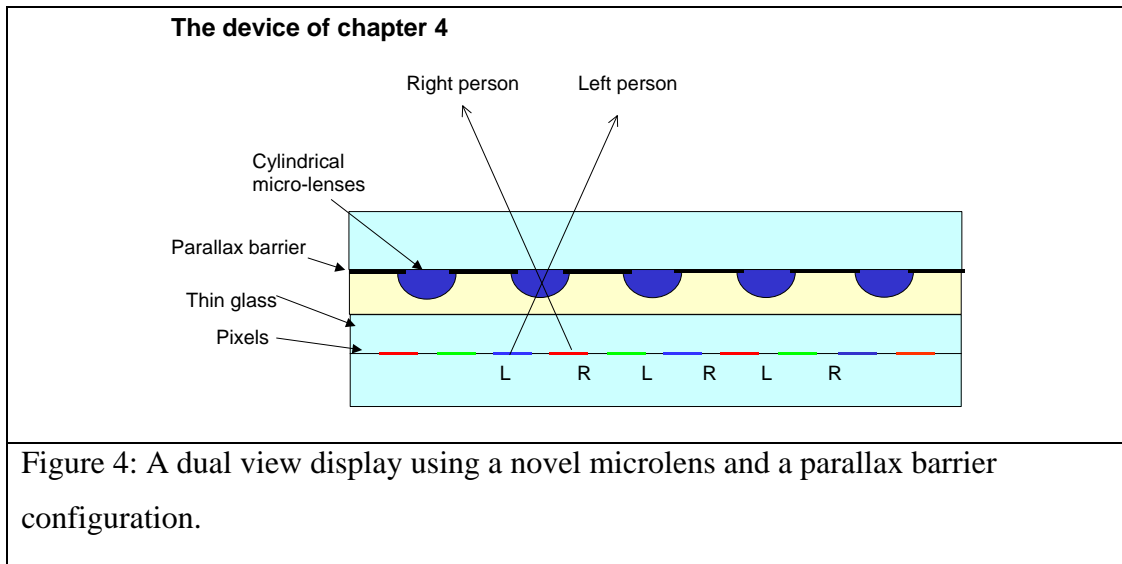
The device of Chapter 3 was the first known dual view display in which optics were positioned less than 100 $\mu$ m from the display. This was produced with remarkable engineering at Sharp Corporation Japan. A cross section of the design is shown below.



This device had good head freedom, good image quality and less crosstalk than the Chapter 2 design. However the crosstalk level was still too high. The causes of this crosstalk were analysed and quantified. The main causes were shown to be scatter at the polariser, diffraction in the optics, and electrical interference between the pixels. Many solutions to this problem were considered and successfully demonstrated.

In July 2005 Sharp released the world's first dual view product. This product incorporated crosstalk remedies that reduced the crosstalk to a level that would not be seen unless the user is actively seeking to perceive it.

The design of Chapter 3 is fundamentally of low brightness. Chapter 4 presents the development of an idea to increase its brightness by using a novel micro-lens design as below.



This idea is optimised and prototyped. The design is shown to give (in comparison with Sharp’s first product) a brightness improvement of 1.7 times, or an increase in angular viewing freedom of 40%. In addition the system seems to suffer less from diffraction so that crosstalk is further reduced.

This design is the subject of a key patent that looks set to provide Sharp with a strong competitive advantage in the field of dual view displays.

In summary, dual view displays have been developed from concept to a high quality Sharp product. The table below shows how the performance of the device progressed throughout the thesis.

<i>Device</i>	<i>Device 1</i> <i>(Chapter 1)</i>	<i>Device 2</i> <i>(Chapter 2)</i>	<i>Device 3</i> <i>(Chapter 3)</i>	<i>Device 4</i> <i>(Chapter 4)</i>
Brightness	Poor	Satisfactory	Poor	Good
Head freedom	Satisfactory	Satisfactory	Satisfactory	Good
Image quality	Poor	Good	Good	Good
Crosstalk	Not measured	Poor	Satisfactory	Good

# CHAPTER 1: PRIOR ART

# Introduction

A dual view display shows different images to different viewers, as shown in figure 1.

This chapter is an examination of literature on dual view displays that provides the background to this thesis.

The first section describes what a dual view display is and what its applications are.

The second section reviews dual view literature from the first known dual view painting created in 1692 up to the start of this thesis (late 2003).

Although dual view prints are well known, publications on dual view displays are surprisingly limited. There are just a few papers suggesting the idea with very brief descriptions of how the dual view effect could be created. These designs are poorly thought through and very difficult to make. It is thought that none of these designs had ever been made.

No literature was found discussing the drawbacks of dual view displays, or proposed refinements necessary for a high quality device.

The closest such literature relates to stereoscopic 3D displays. This is the subject of section 3. It discusses 3D literature from basic design to more complex ideas that improve its functionality. Many problems that exist in 3D displays also affect dual view, so the philosophies used to improve 3D displays are extended towards dual view.

Consequently this chapter is a combination of literature review and original work.

In particular, a design is created enabling the first prototype dual view display to be made. Problems with the device are seen, and in the absence of solutions from the literature, the research presented in chapters 2, 3, and 4, is carried out.

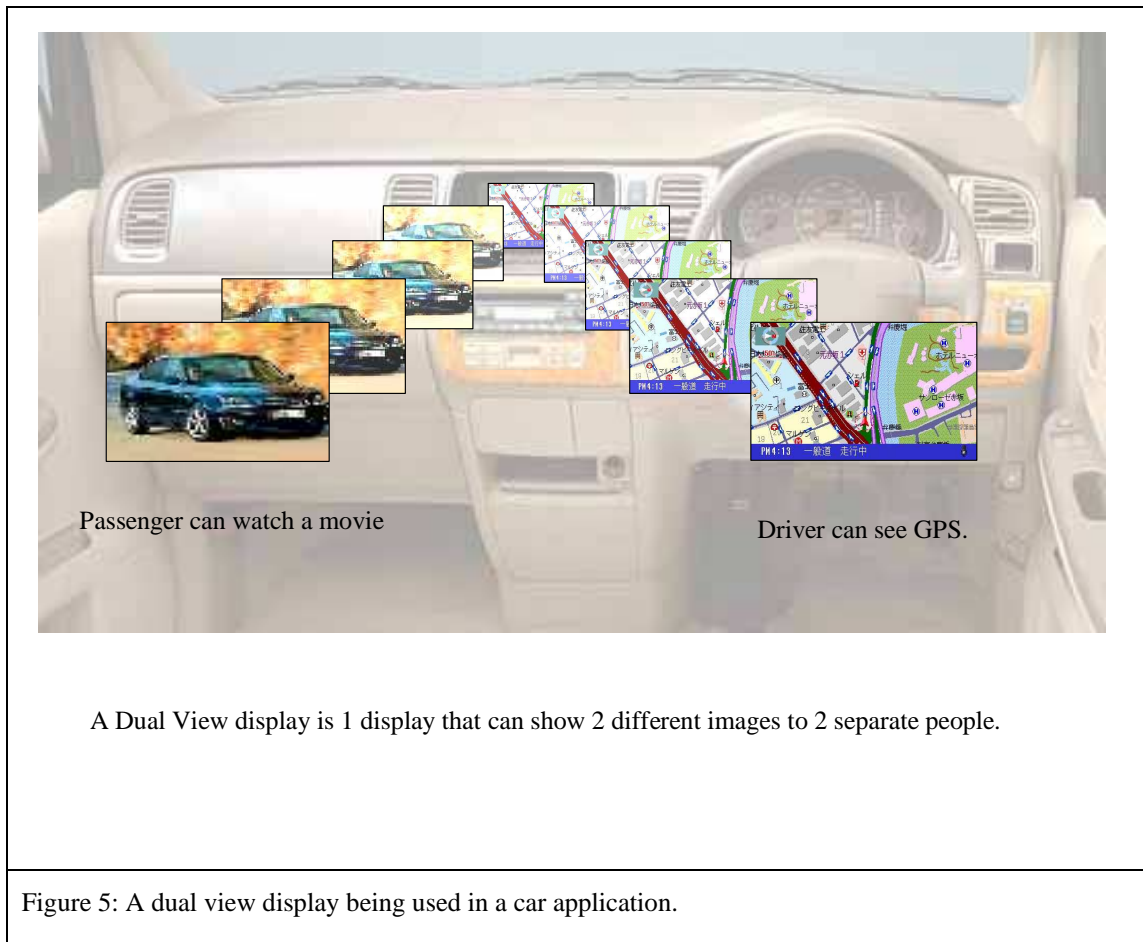
Finally section 4 of this chapter presents a novel spin off application. Dual view may have more uses than first expected.

## **1. An introduction to dual view displays**

### **1.1 What is a dual view display**

A dual view display is a display that can show different images in different directions.

An illustration of this is shown in the following figure.



## **1.2 Why are dual view displays needed**

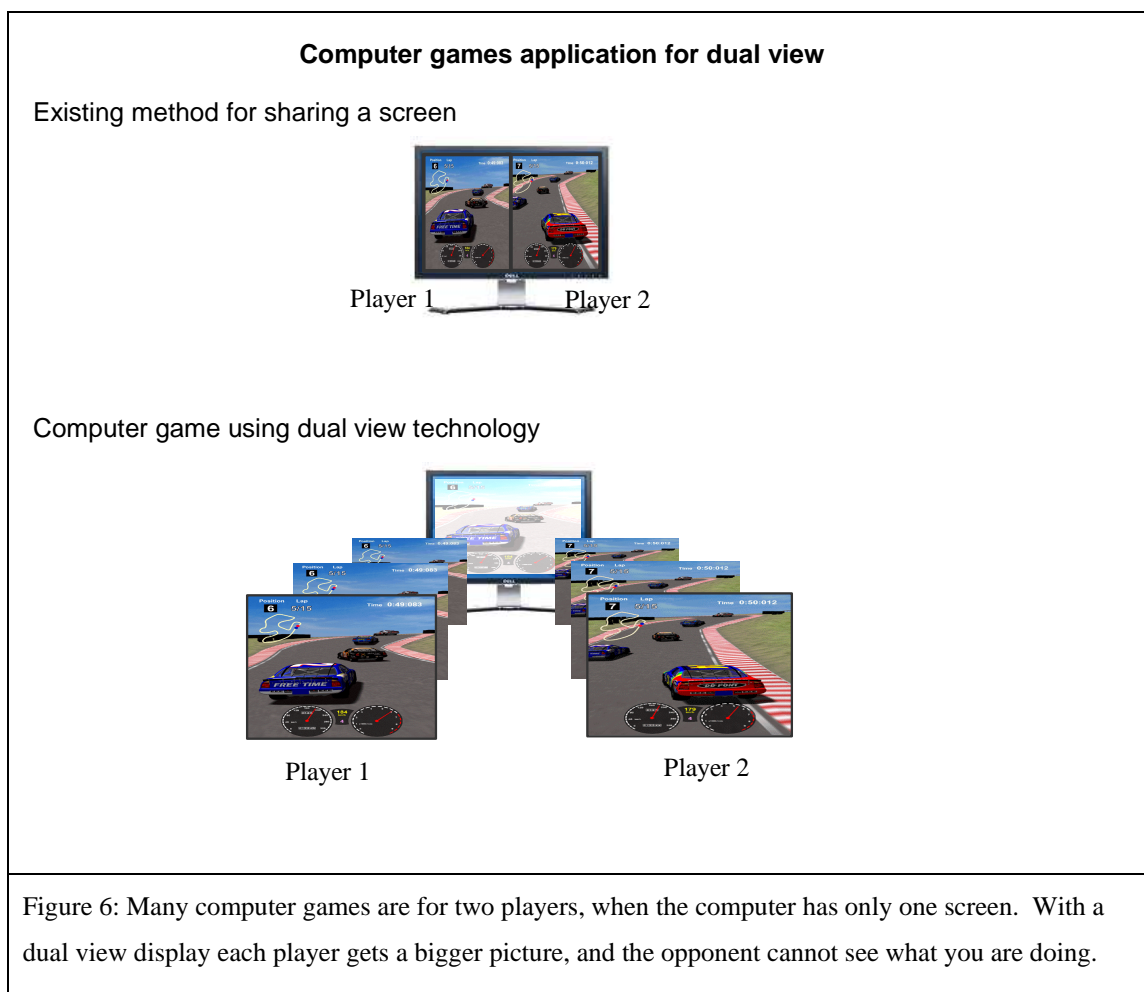
Motion picture displays such as liquid crystal displays (LCDs) and cathode ray tubes (CRTs) are widely used in today's technology. These displays assume the users require the same information from the display, no matter what angle they view it from. However, there are many applications where it would be desirable to see different information from the same display depending on the position of the user.

For example in an automobile the driver may wish to view satellite navigation data, while the passenger may wish to watch a movie. If two displays were used in this case (one showing the satellite data to the driver, one showing a movie) it would be possible for the driver to view the movie which could be dangerously distracting. In fact this situation is forbidden by law in many states in the US and other countries. It is conventional that a driver/ passenger television is disabled whilst a car is in motion.

A dual view display would enable a passenger to continue watching a movie whilst the car is in motion, with no visual distractions to the driver. There are many other advantages in using a dual view display here. A dual view display takes up less space

on a crowded dash board than two displays. One dual view display can also provide a cost advantage over the use of two displays.

In a computer game, two players may wish to view the game from their own perspective. This is currently done by using half of a conventional display to display the view for one player and the other half of the display for the other player. This means that each player can only use half of a display. Alternatively two screens may be used, one for each user, but this reduces portability. Use of a dual view display solves all these problems.



On an aeroplane passengers would ideally like the ability to choose their own movie channel or computer game. This can be achieved by giving every passenger their own display, however, a dual view (or triple view/quad view etc.) display would be able to provide multiple passengers with their own views, with fewer displays. This would give significant cost, space and weight savings.

A dual view display has the ability to prevent users from seeing each other's views. This might be desirable to increase the security and privacy of devices such as cash point machines. This is shown in Figure 7.



Figure 7: A cash machine using tri-view can advertise to passers by, whilst keeping the bank details of the user confidential.

## 2. Dual view prior art

This section reviews the major advances in dual view technology up to the start of my PhD in 2003.

The first dual view picture is described – a painting from 1692. The next major advance was the creation of dual view pictures using lenticular lenses. This idea was patented in 1922 and the design is still used today to create dual view pictures and toys that are often found in cereal packets or on children’s rulers.

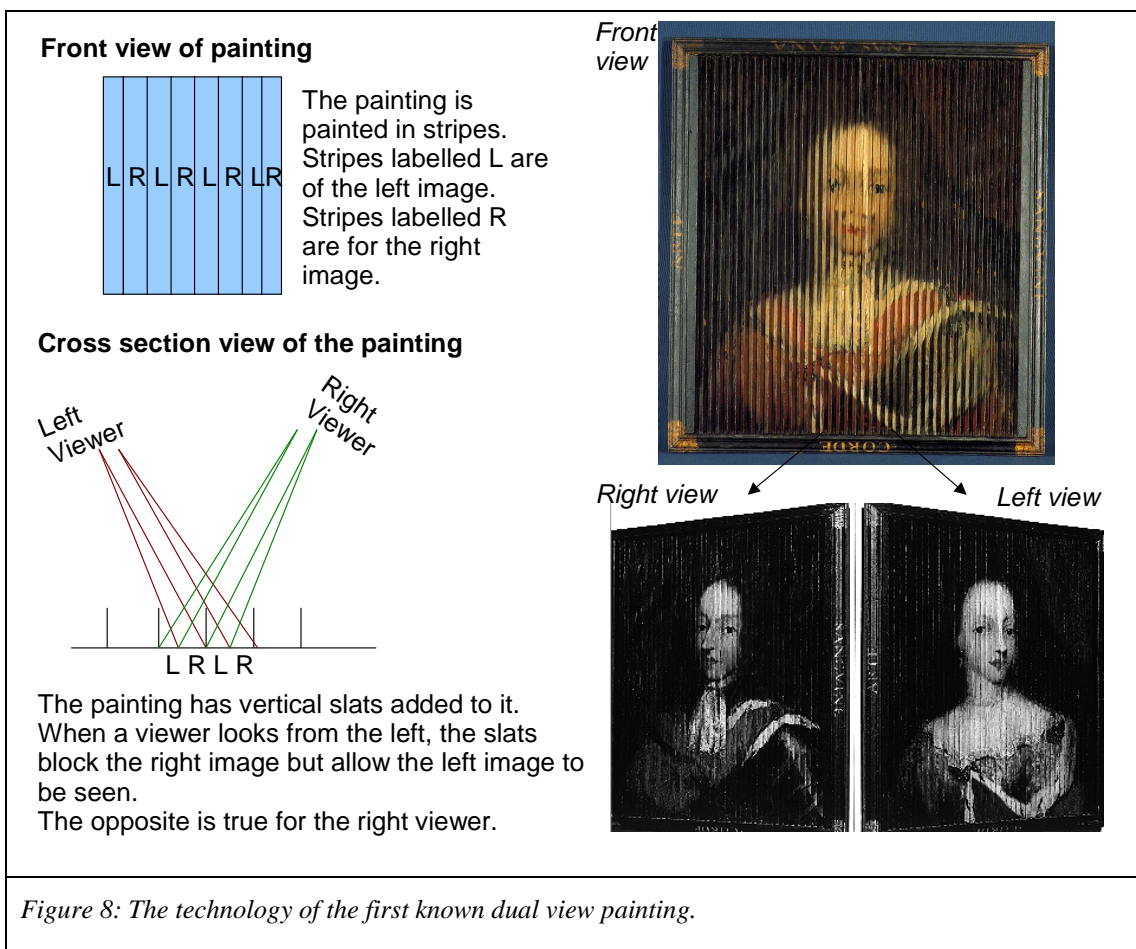
The first mention of a dual view display (capable of creating moving dual view images) was, as far as we know, published in 1994. The idea is presented in a patent, however the design of the display is poorly thought through. Section 2.3.1 roughly calculates the dimensions of the design, and shows that it is impractical to make.

Finally in 2000 Sumitomo publish a workable dual view design based on a parallax barrier.

This PhD started when the basic parallax barrier dual view design was known, but had seemingly never been made. Consequently, there had been no study of secondary issues (such as interference between left and right images) that arise when creating a dual view LCD.

## 2.1 Dual view paintings

Dual view has been known about since at least 1692. In 1692 a French painter called Bois-Clair created the dual view effect, by using a technique described in the figure below.



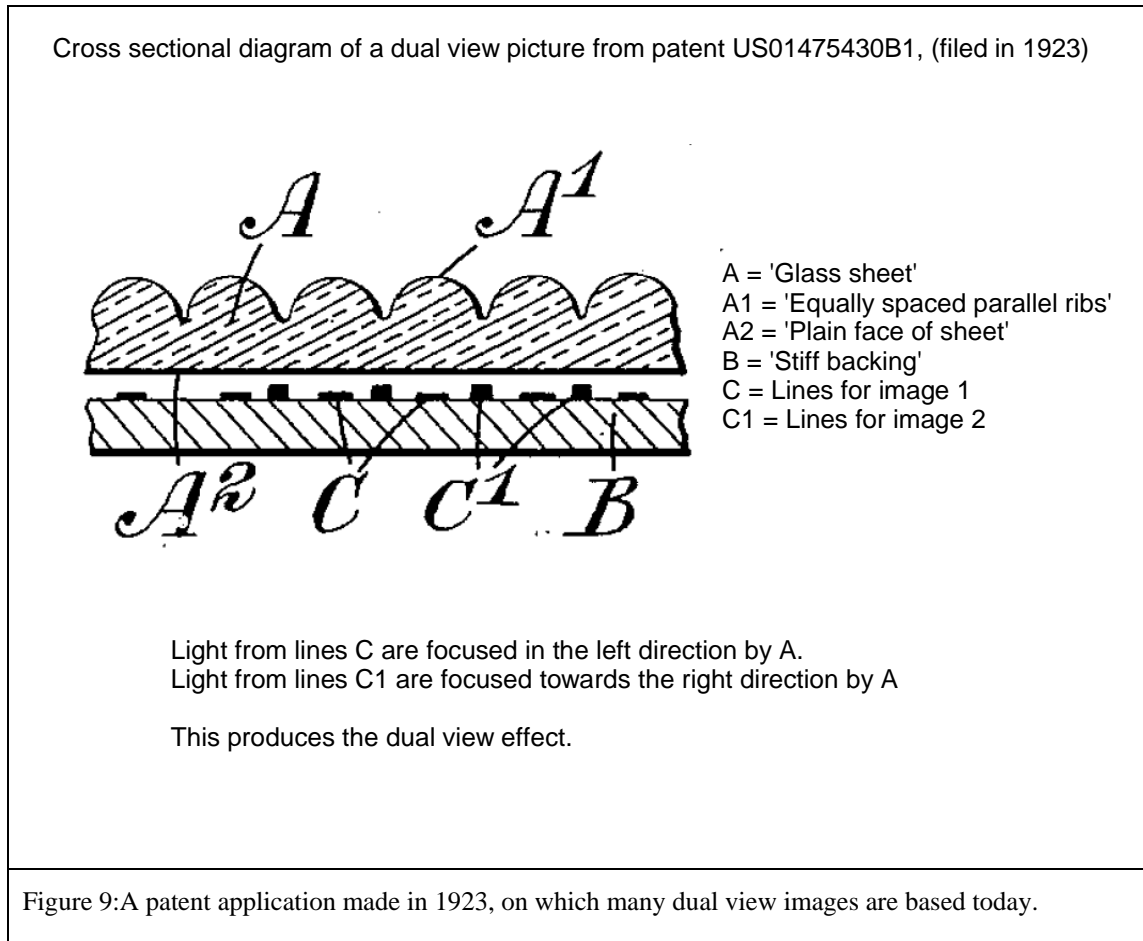
Examples of this work can be seen at Rosenberg Castle in Copenhagen and Brussels museum of arts [1].

One assumes that this technique works well for large painting when viewed from a distance, but that to create high resolution images to be viewed close up would be too difficult with a paint brush.

It was 200 years later when high resolution dual view images became prevalent. These images are described in the next section.

## 2.2 Dual view toys - still images

In 1923 a patent was filed explaining how a high resolution dual view image may be created by using a lenticular lens array [2]. The stated applications of this device, included advertising boards and toys. The method of operation is described in the following figure.



This technique for dual view is still used today in toys and adverts.



Right view

On axis view

Left view

Figure 10: An example of a modern day advertising campaign using lenticular poster technology. The poster advertises the movie 'The Incredible Hulk', [3].

## **2.3 Dual view displays**

### **2.3.1 Concept**

All prior art mentioned earlier relates to still images. To create moving dual view images the dual view technology needs to be applied to display technology.

Surprisingly, the first example of this (that I know) is in a patent application published in 1994, by Japanese electronics company Nippon Denso [4].

Perhaps the reason why moving image dual view had taken so long to be considered is due to development of display technology. Only in the last ten years have LCDs become prolific. Before this cathode ray tubes (CRTs) were standard technology, and CRTs do not lend themselves to parallax barrier technology. The front glass of a CRT is very thick, such that it is not easy to put the parallax barrier close enough to the pixels, and the pixels are generated by a scanning electron beam, which is difficult to align with any parallax optics. In an LCD the situation is much different. The pixels are placed in very well fixed positions, and they are close to the front of the display. This makes the use of parallax optical technology possible.

The patent aims to cover the concept of using a dual view video display in a car, so that the driver could see satellite navigation information whilst the passenger can watch television.

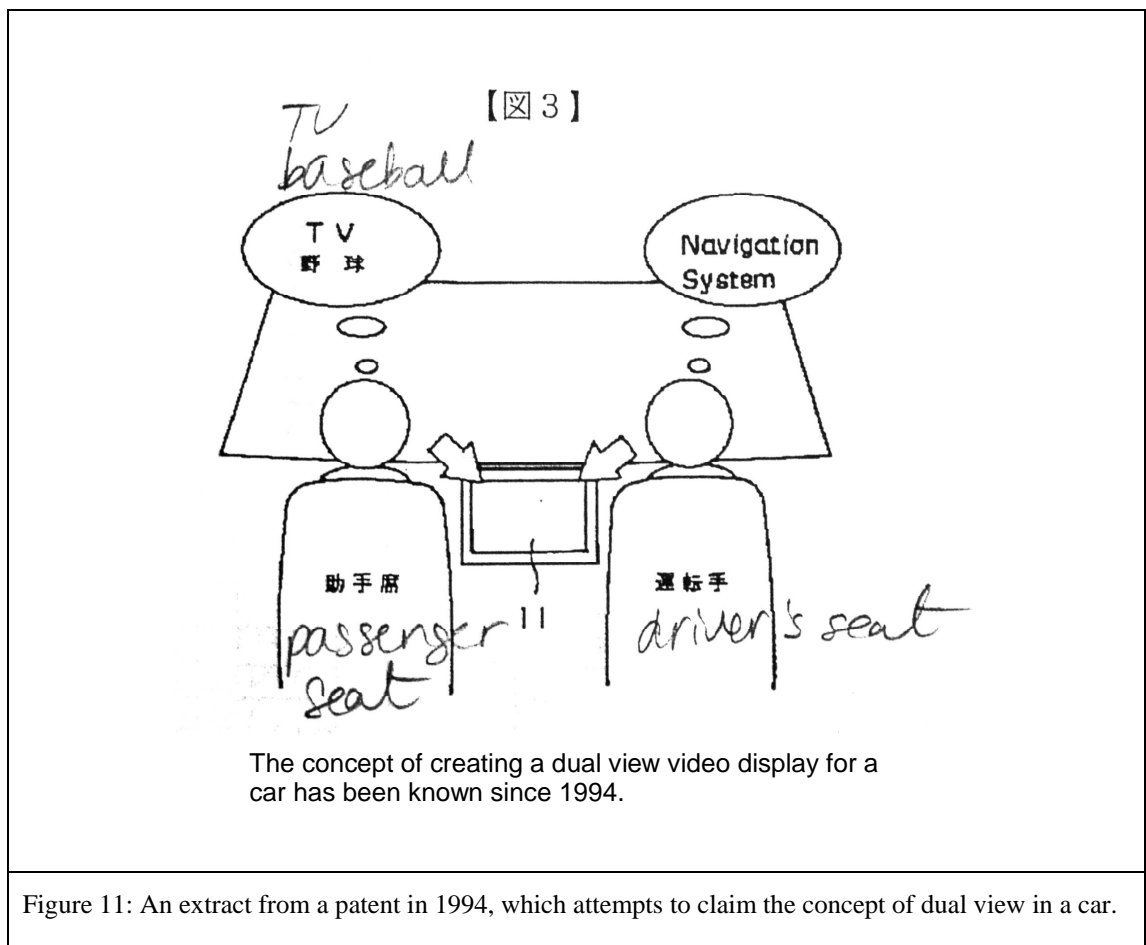


Figure 11: An extract from a patent in 1994, which attempts to claim the concept of dual view in a car.

The method given is identical to that used for dual view toys in 1923 patent, but applied to a video display.

Although the concept of a dual view display for cars is presented here, very little thought has been given to the technical design. In fact the design stated in this patent is virtually unusable.

The main reasons for its failings are presented below.

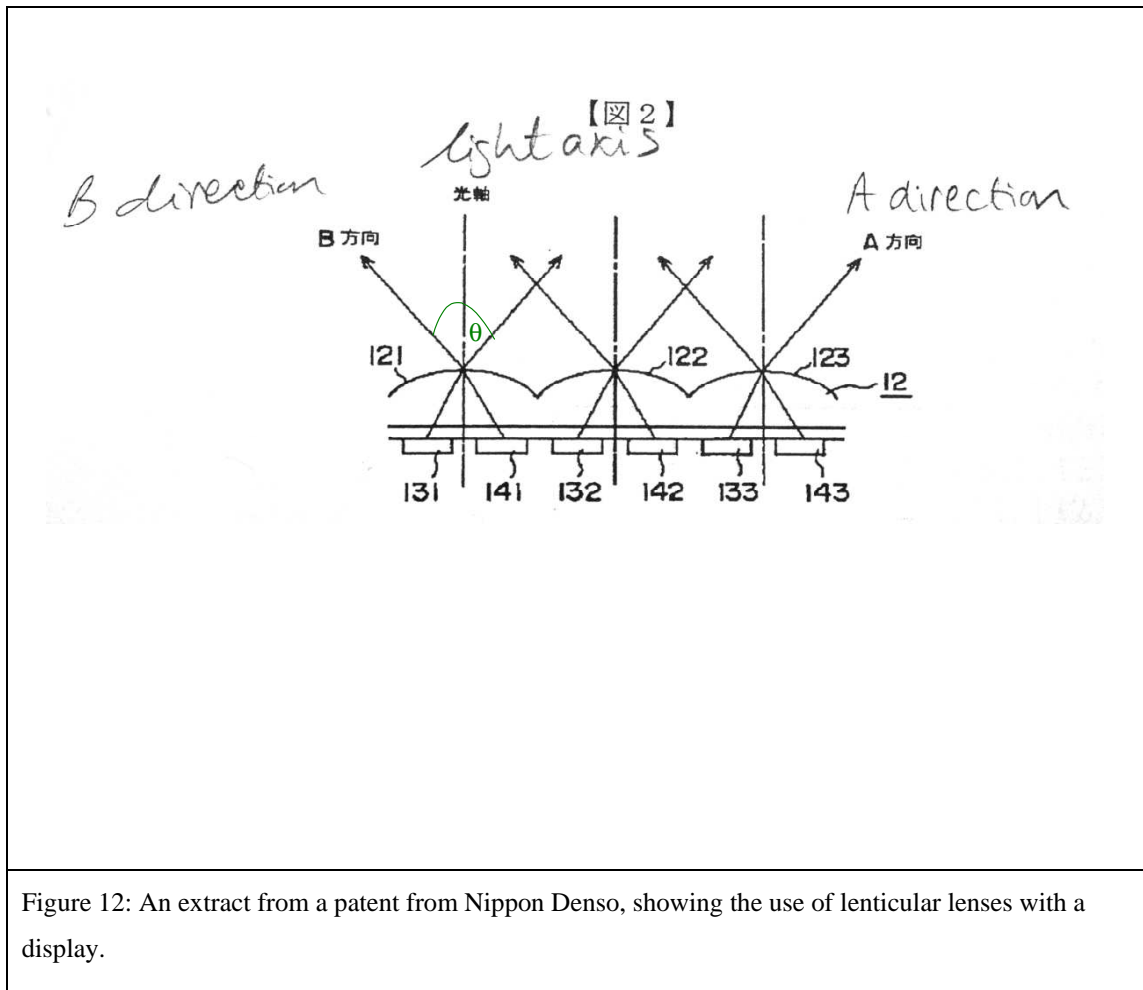


Figure 12: An extract from a patent from Nippon Denso, showing the use of lenticular lenses with a display.

A typical high-resolution automotive display has a 7-inch diagonal screen size, and 800 by 480 white pixels. Each white pixel consists of 3 sub pixels – one for the red, green and blue pixel data to enable colour images. In this case each sub pixel must be 65 $\mu$ m wide.

In a typical car the distance between the noses of the passenger and driver would be about 70 cm and the distance between the driver and the display is also about 70 cm. This means that the left and right images from the dual view display should be separated by about 60° (labelled  $\theta$  in Figure 12).

Looking at the diagram of Figure 12, if the pixels, 131, 141 etc., are 65 $\mu$ m wide, the substrate refractive index is 1.5, and theta needs to be 60°, then the lens centre needs to be approximately 80  $\mu$ m from the pixels, (based on the equation given in section 3.2.2).

Now consider standard automotive video display technology, i.e. a liquid crystal display (LCD). A detailed description of an LCD can be found in [5], the key point to be made here is that the device requires the liquid crystal to be sandwiched between two glass substrates.

There are many reasons why the substrates that hold the liquid crystal need to be glass, but the main one is due to the construction of thin film transistors (TFTs). Thin film transistors are needed to provide high quality electronic addressing of the liquid crystal. Research into the production of TFTs on plastic is a large field, but this technology has many problems, and is not standard technology [6].

The TFTs are produced on one of the glass substrates. On the other glass substrate colour filters (CF) are produced. These colour filters must align with the TFTs and so this other substrate must also be made from glass to avoid misalignment due to thermal expansion problems (the problem of thermal misalignment between glass and plastic is explained in more detail in chapter 4).

In summary, in an LCD both the TFT substrate and the CF substrate must be made from glass, and the Nippon Denso design requires that one of these substrates is less than 80  $\mu\text{m}$  thick.

A glass substrate that is less than 80  $\mu\text{m}$  thick is (from experience in handling such substrates) too weak to be used in a product; shock and vibrations can cause the glass to break. No method of supporting the thin substrate is given in the patent, and indeed it would be difficult to do so. For example, adhering an additional supporting substrate would not be possible, since in the Nippon Denso design a glass - air interface is needed to create lenses of sufficient focal power to create dual view (see chapter 4).

The Nippon Denso design for dual view is impractical.

Matsushita, Siemens, and Phillips have all published similar documents based on the same 1923 patent, with the same problems of mechanical instability when used in high-resolution displays [7, 8, 9].

### **2.3.2 Multi-view**

Several companies have considered making multi-view displays where the display gives out at least 4 views to different angles. The example in the figure below was published by Ricoh in early 1998 [10].

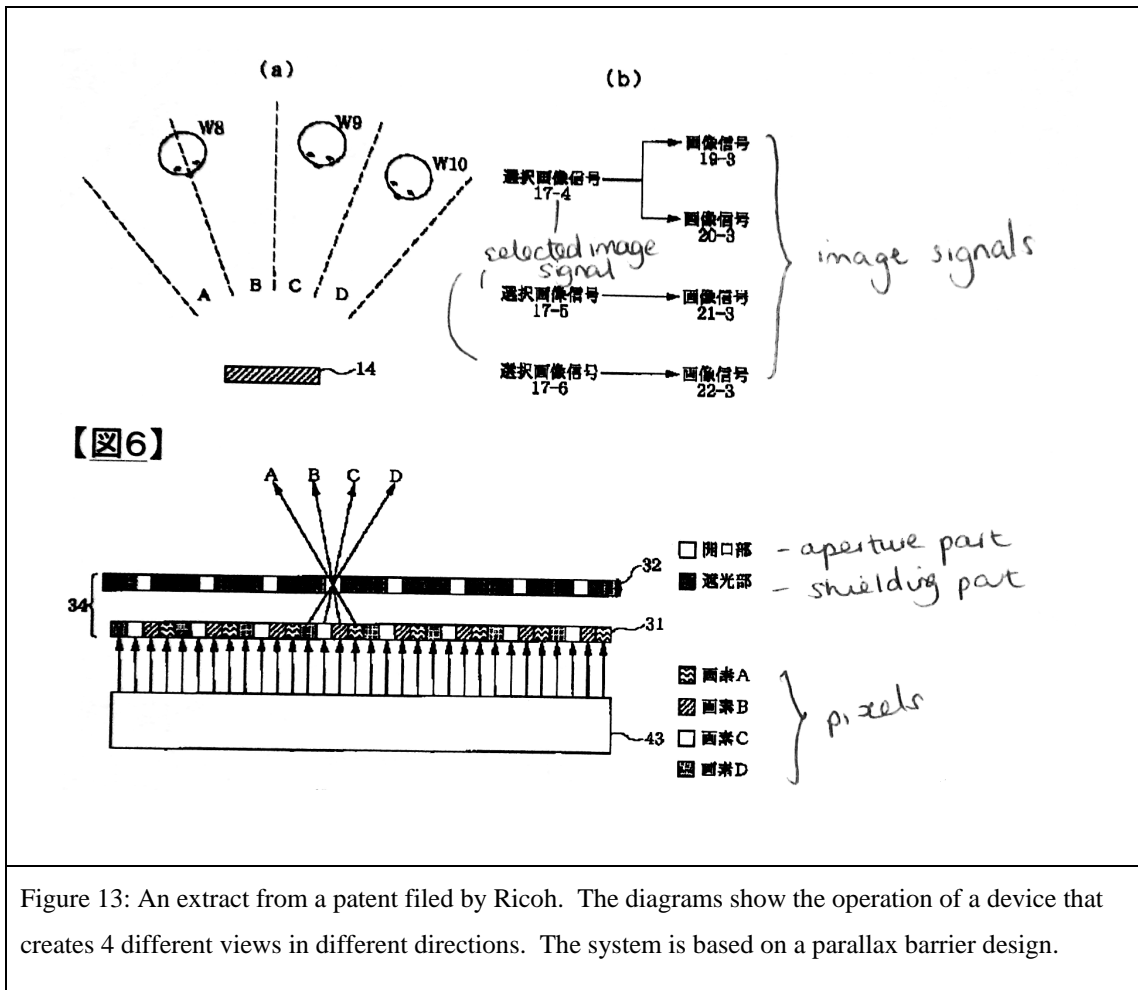


Figure 13: An extract from a patent filed by Ricoh. The diagrams show the operation of a device that creates 4 different views in different directions. The system is based on a parallax barrier design.

The design works in a similar way to the lenticular design of the 1923 patent, however it uses a parallax barrier instead of lenses. A parallax barrier is to a lenticular lens array as a pinhole camera is to a camera with a lens. The parallax barrier functions in a similar way as a lens to enable only light from the correct pixels to go to the correct viewing position. This can be seen in the figure above. They are simpler to make.

The design creates views that are each separated by about 20°. This implies that the barrier should be about 280 μm from the pixels in an automotive display.

Because the separation between parallax barrier and pixels can be 280 μm, the device is easier to make.

Because the device uses a parallax barrier, supporting substrates can be adhered to the thin glass, giving it structural support. This means that the design is mechanically strong and workable.

However, to move from a design which has four views to a design that has two views (as required in the automotive application) glass of 80 μm thickness would need to be used. The publications shy away from proposing this idea, probably because this is a tough manufacturing challenge.

### **2.3.3 Parallax barrier dual view**

Only as recently as the year 2000, was a workable dual view design published. This patent was filed by Sumitomo [11], and is a design based on a parallax barrier and thin glass.

Very little detail is given about solutions to inevitable problems that would be encountered in making such a device, such as how to create such thin glass and, as far as we know, Sumitomo has exhibited no prototype. This suggests that Sumitomo's work in this field remains untested.

### **2.4 Dual view prior art summary**

To summarise, when I started work on my PhD, the concept of dual view displays, and their use in cars was known (from Nippon Denso).

The idea of creating dual view displays with lenticular lenses was known, but the idea had been considered in such poor detail that all designs mentioned are of no practical use.

Workable parallax barrier designs were known that would create dual view (from Sumitomo). However, it is thought that none of these designs were ever built. Consequently, there was no analysis of secondary issues that arise from creating the basic dual view design. For example, there are no publications related to crosstalk between the left and right views, manufacturing techniques for thin glass, or brightness and head freedom enhancements.

## **3. Extending 3D prior art towards dual view**

There was surprisingly little research that had been done in the field of dual view displays. There is much more literature available concerning 3D displays. These displays give the illusion of depth by sending different perspectives of an image to the different eyes.

This idea is very similar to dual view, the primary difference being that in 3D two images are separated by about  $6^\circ$  to target the left and right eyes, in dual view the images need to be separated by about  $60^\circ$  to target the views towards different viewers.

Therefore, many issues such as how to increase the distance between the parallax barrier and pixels, have been considered for 3D. These ideas can be built on to help the construction of dual view systems. This is the subject of section 3.

Section 3.1 describes the basics of 3D parallax barrier technology.

Section 3.2.1 describes the fundamentals of 3D parallax barrier design, and then section 3.2.2 proposes how the design could be better optimised for dual view.

Section 3.2.3 states the difficulties in putting a parallax barrier close to the pixels to create dual view, and looks at 3D literature for solutions. No good solution is found, but one 3D design can be extended to produce an easy-to-make prototype dual view display. The quality of this display is flawed, but it is enough to prove that the dual view concept is highly desirable.

Section 3.2.4: Dual view would benefit from the ability to be switched in to a conventional single view mode, just as 3D displays benefit from a 2D mode. Methods of creating switchable parallax barriers are looked at for 3D displays and no suitable ideas are found. A new technique for dual view is proposed and discussed.

Section 3.2.5 shows how time multiplexing has been considered for use in 3D displays to increase the perceived resolution of the display. There is potential to apply this to dual view, but at the present time LCD switching speeds are too slow.

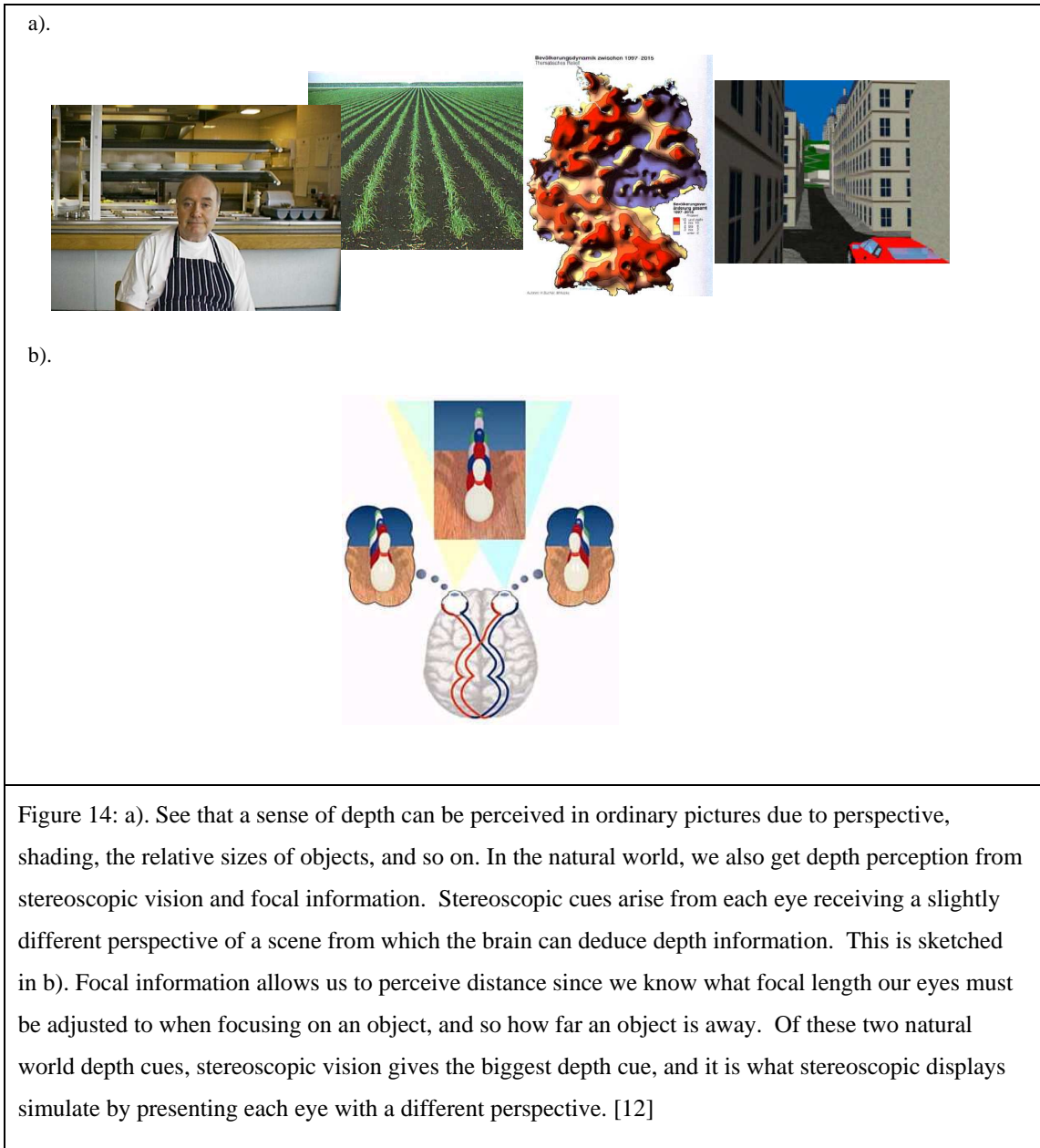
Section 3.2.6: In a car a dual view system can show the driver and passenger different images. The rear passenger unfortunately sees an unpleasant mix of the two. In a dual view system the on-axis view would ideally be black. Designs exist for 3D displays which happen to create a black view in between the eyes. These designs are assessed, and a new system is proposed and tested. This idea is perhaps more suitable for dual view, it relies on simple modification of the backlight optics.

Section 3.2.7: Reviews the studies that have been done on crosstalk between the left and right views of a 3D display. No such studies exist for dual view. This is the subject of chapter 3.

Finally, section 3.3 looks to the 3D literature to inspire alternative methods for creating dual view. Some research has been done on the use of LC modes alone to create 3D. An LC mode is found that produces dual view without any additional optics, but it is outperformed by parallax barrier technology.

### **3.1 What are auto-stereoscopic 3D displays**

When we look at a scene we perceive distance in many ways. This is described in the figure below.



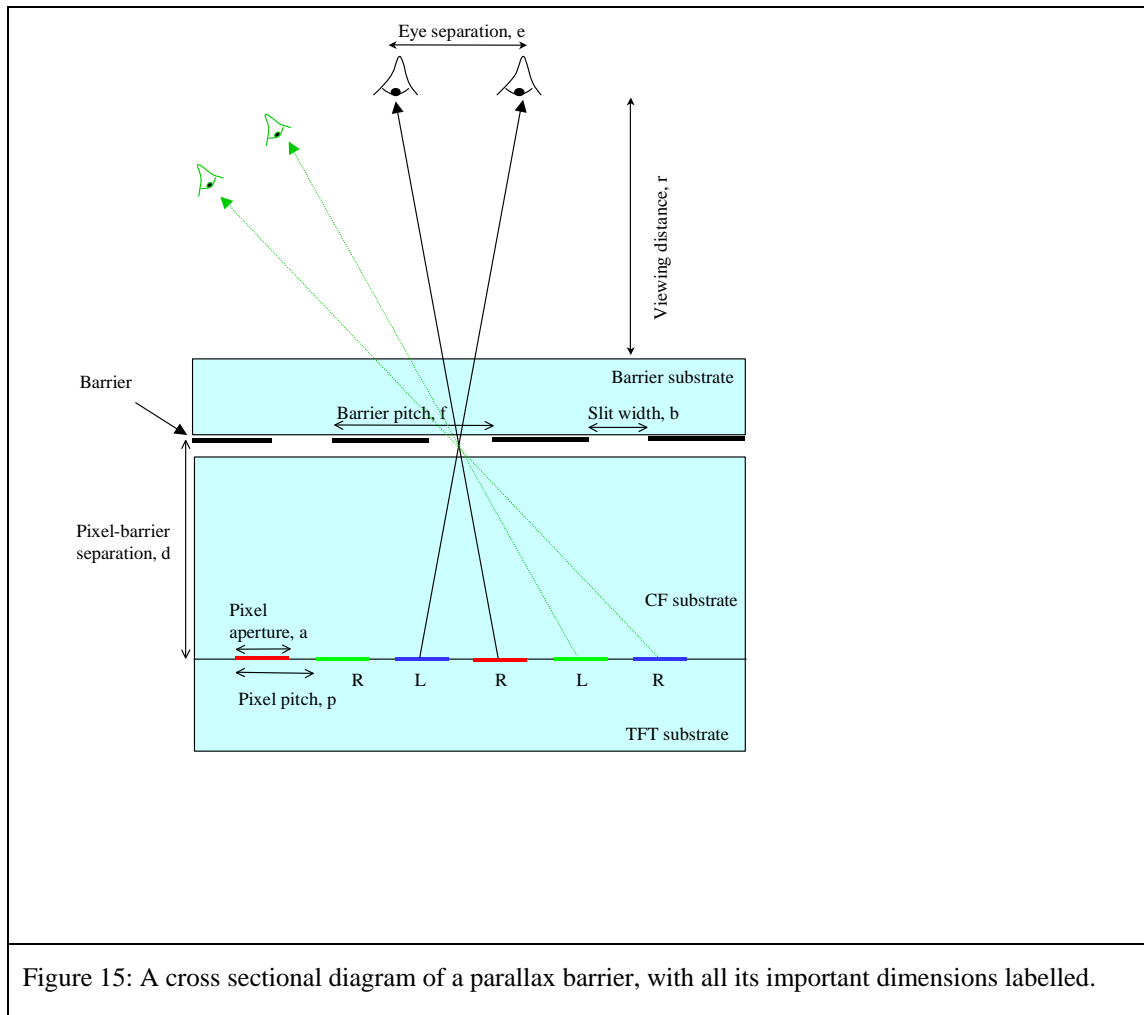
A stereoscopic display gives the illusion of depth by giving each eye a different perspective of a scene, as would happen in reality. This may be done by displaying one perspective with one polarisation, and the other perspective in a different polarisation. A viewer can then see stereoscopic depth by wearing glasses where each ‘lens’ only allows the appropriate polarisation to pass.

An auto-stereoscopic display is a display that gives stereoscopic depth without the user needing to wear glasses. It does this by projecting a different image into each eye. These displays can be achieved by using parallax optical technology.

## 3.2 Parallax optical technology

### 3.2.1 Basic design principles for 3D

The design and operation of a parallax barrier for 3D is well described in a paper from the University of Tokushima Japan [13]. Below follows a summary of the parallax barrier operation and design.



The figure shows a cross sectional diagram of an auto-stereoscopic parallax barrier design.

The images for the left and right eye are interlaced on alternate columns of pixels, as for previous designs.

The slits in the parallax barrier allow the viewer to see only left image pixels from the position of their left eye, right image pixels from the right eye, just as for a dual view parallax barrier.

The viewer may look on axis at the display to see a stereoscopic view, but note that they may also see a stereoscopic view off axis as shown in the figure above in green. The on

axis view is termed the primary viewing window, and the off axis view is called the secondary viewing window.

Note that the parallax barrier may also be placed behind the LCD pixels. In this case, light from a slit passes the left image pixel in the left direction, and vice versa. This is called a rear parallax barrier and it creates the same effect as a front parallax barrier.

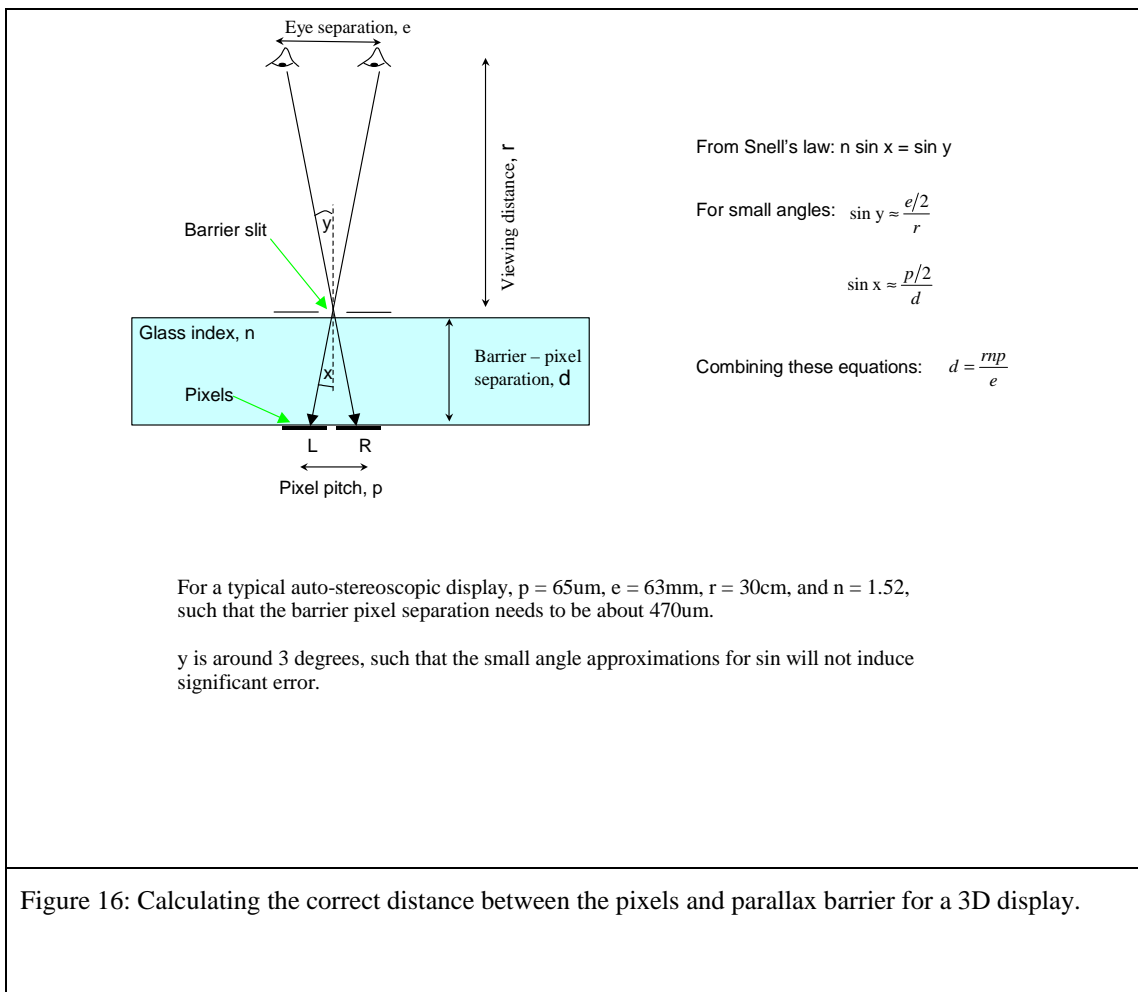
When choosing the geometry of the parallax barrier the important parameters that need to be optimised are; the pixel – barrier separation  $d$ , the parallax barrier pitch  $f$ , the pixel aperture  $a$ , and the parallax barrier slit width  $b$ .

#### *Optimum design values for an auto-stereoscopic display*

Optimum design parameters for a stereoscopic system have been well discussed in the literature [13], and they are summarised here.

#### *Parallax barrier – pixel separation*

The closer the parallax barrier is to the pixels, the wider the angle between the left and right images. For a stereoscopic display the left and right images must hit the left and right eyes, which means they must be separated by only a few degrees. The pixel-barrier separation for this case is derived in the figure below.



In the derivation of this formula small angle approximations are used.  $\sin x$  is approximated to  $x$ . Physically this means that in Snell's law refraction is still considered although with reduced accuracy. For example if the internal angle is  $10^\circ$  and the index is 1.5 then the external angle is assumed to be 1.5 times 10 which is  $15^\circ$ . In reality from Snell's law the external angle should be the inverse sin of (1.5 times the sin of  $10^\circ$ ), which is  $15.1^\circ$ .

### *Parallax barrier pitch*

In Figure 15 the pitch of the parallax barrier is two times the pitch of the pixels. For the optimum design it should be slightly less than this. This perturbation of the barrier pitch is called 'barrier pitch correction'. The reason that it improves the display is given below.

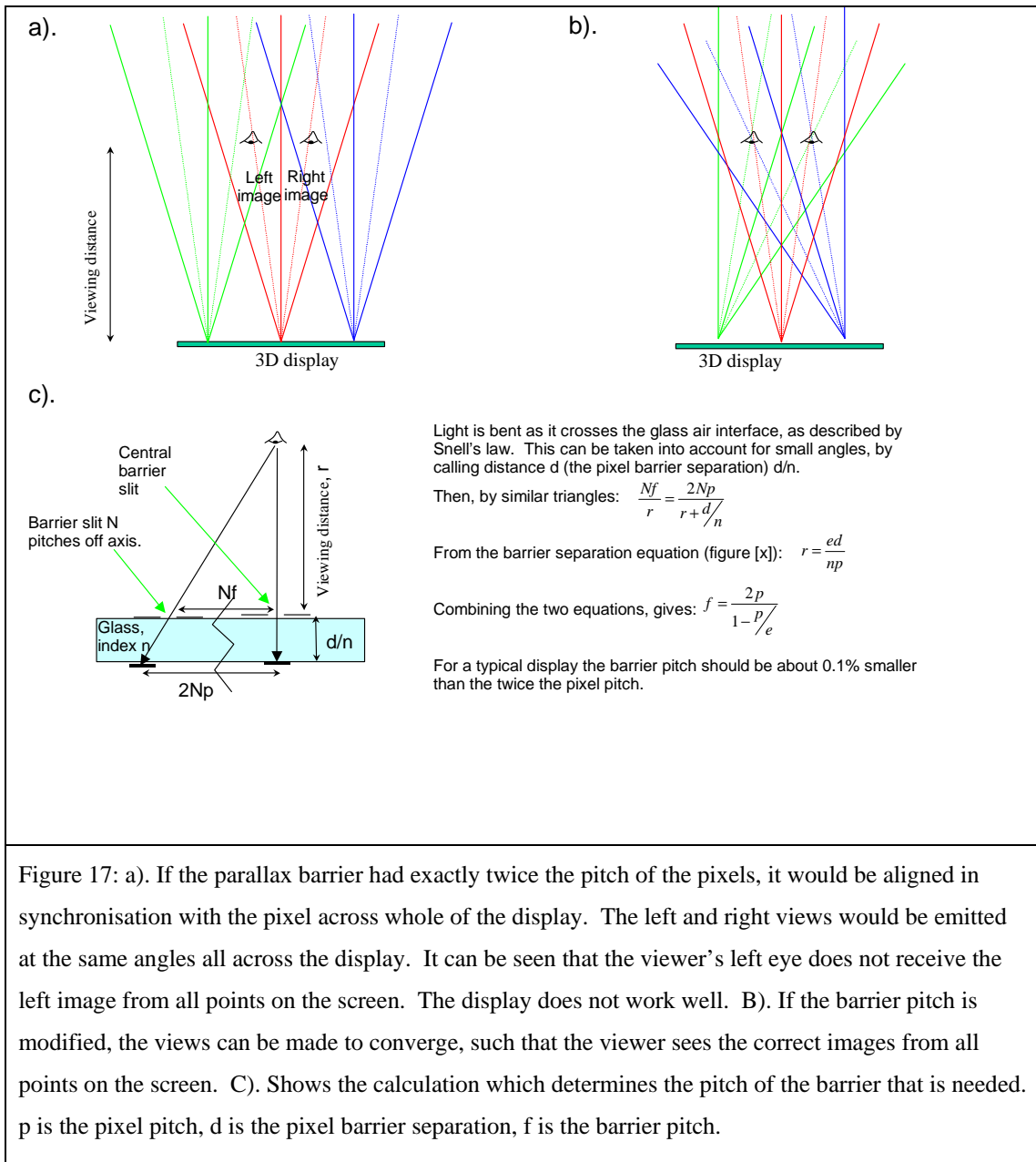


Figure 17: a). If the parallax barrier had exactly twice the pitch of the pixels, it would be aligned in synchronisation with the pixel across whole of the display. The left and right views would be emitted at the same angles all across the display. It can be seen that the viewer's left eye does not receive the left image from all points on the screen. The display does not work well. B). If the barrier pitch is modified, the views can be made to converge, such that the viewer sees the correct images from all points on the screen. C). Shows the calculation which determines the pitch of the barrier that is needed.  $p$  is the pixel pitch,  $d$  is the pixel barrier separation,  $f$  is the barrier pitch.

### *Optimum pixel aperture and barrier slit width*

The influences of the barrier and slit width have been well investigated by David Montgomery [14]. In this paper he shows that the performance of a 3D display can be simulated by Fresnel diffraction theory. From these simulations, the following can be deduced.

- If the slit width is small, light passing the slits is diffracted heavily causing crosstalk. The brightness of the display is also reduced.
- If the slit width is large, light passing the slit does not diffract so much, but the wider slits create crosstalk due to geometric ray paths. Therefore the design suffers more crosstalk. The brightness of the display is increased.

Therefore the best slit width is given by a trade off between crosstalk and brightness [15].

### 3.2.2 Extension of parallax barrier design principles to dual view

When designing a parallax barrier for dual view the same design parameters need to be optimised as for 3D. This section looks at how the optimum design differs for dual view rather than 3D.

#### *Parallax barrier – pixel separation*

The calculation for dual view barrier separation is substantially the same as for the 3D calculation, except that small angle approximations used in Figure 16 need to be removed. This is because in the case of a dual view display, the left and right images exit the screen at about  $\pm 30^\circ$ ; small angle approximations in this case would lead to a noticeable error.

This makes the barrier separation formula:  $d = \frac{p}{2 \tan\left(\sin^{-1}\left(\frac{\sin \theta}{n}\right)\right)}$ .

## Parallax barrier pitch

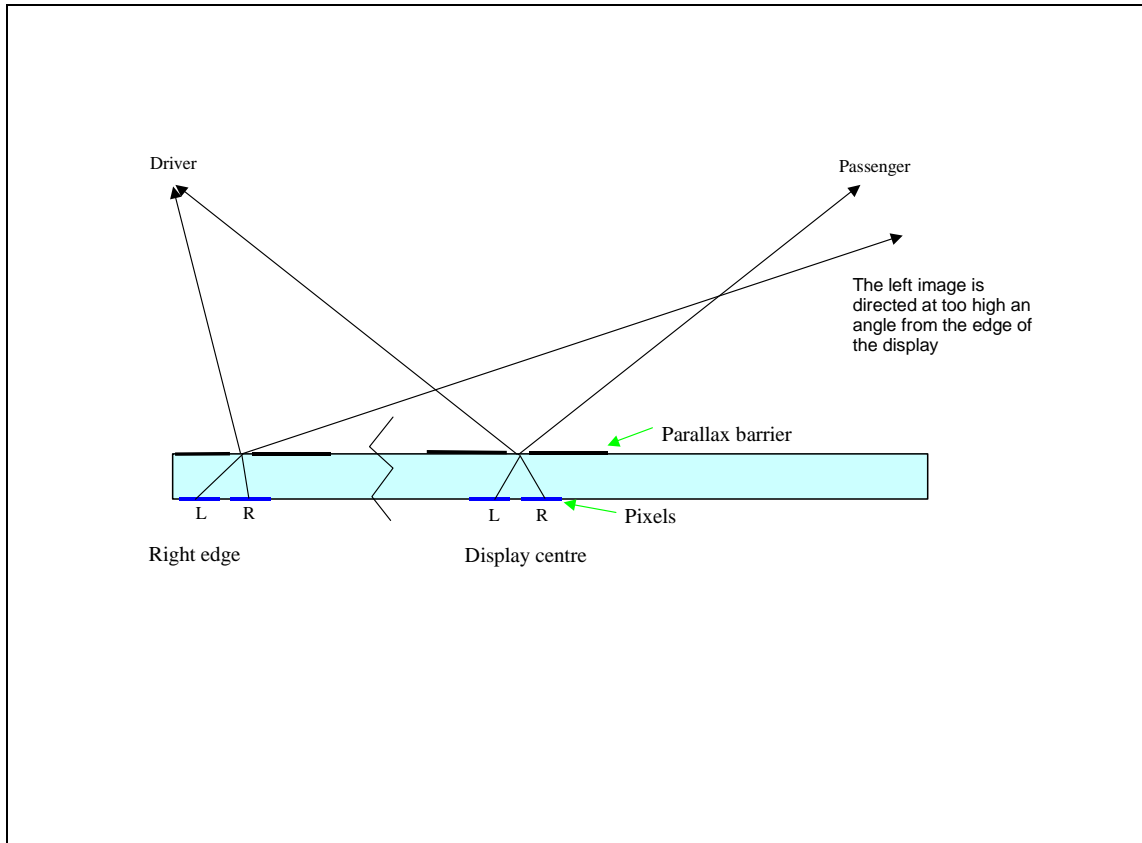


Figure 18: 'Barrier pitch correction' for a dual view display. At the centre of the display the left and right pixels are seen by the driver and passenger as desired. At the right edge of the display, the position of the slit should be adjusted to compensate for the viewers looking at this part of the display from a different angle. This is much harder for a dual view display than for a 3D display. If Snell's law (governing the refraction as the light exits the panel) was linear then adjusting the position of the slit at the edge of the display can provide good compensation for the driver and the passenger. By linear it is meant that external angle is  $n$  times the internal angle (which is approximately the case for the 3D systems where light only exits at small angles). In the case of dual view, light exits the panel at high angles such that Snell's law becomes non-linear. That is to say that the external angle is given by  $\sin^{-1}(n \sin \text{internal angle})$ . The slit can be positioned exactly for the driver, but light going to the passenger which exits the display at higher angle, is refracted considerably more, as shown. 'Barrier pitch correction', can not work well for dual view.

The figure above describes how a dual view barrier pitch cannot be modified to create the benefits of 'barrier pitch correction' used in 3D displays.

A solution to this is to use the standard barrier pitch correction formulae given in section 3.2.2 for dual view, and in addition adjust the positions of the left and right pixels across the panel. By doing this, the directions of the left and right images can be tuned individually across the panel. This is the subject of reference [16]. A slight advantage can be achieved by doing this.

### Optimum pixel aperture and barrier slit width

In choosing the optimum apertures I propose that diffraction effects can be ignored. This is because, based on Fraunhofer diffraction through a typical barrier slit aperture of  $38\ \mu\text{m}$  with light of  $550\ \text{nm}$  wavelength the first diffraction minima is calculated to be at about  $1^\circ$ . This is significant in a 3D system where the images are only separated by  $6^\circ$ , but in DV the images are separated by about  $60^\circ$ .

This assumption is tested later in Chapter 3 and shown to be sensible. The proposal for the best apertures is based on geometric optics as follows.

There are optimum values for  $a$  and  $b$  (Figure 15) in a dual view systems. The effect of 'a' is described in the figure below.

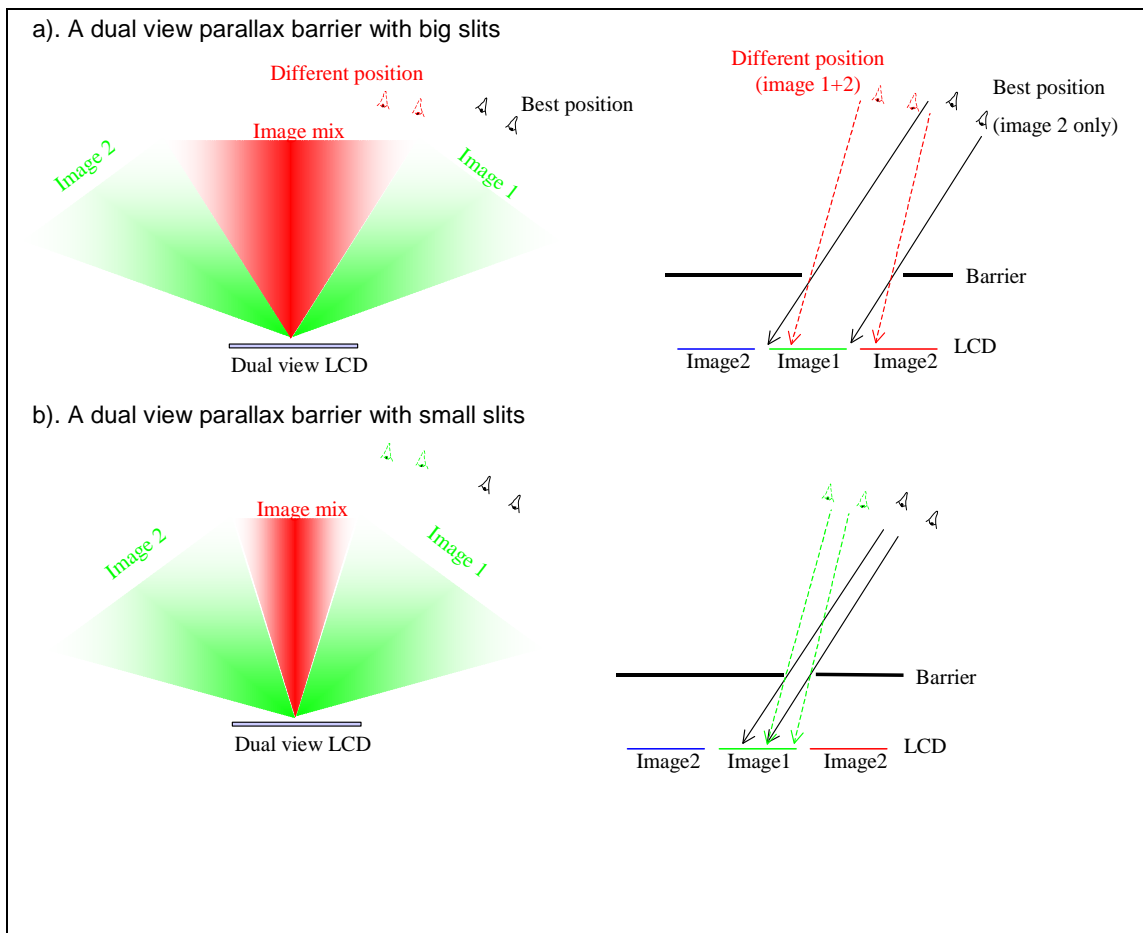


Figure 19: The head freedom of a dual view display is linked to the slit widths in the parallax barrier. A). shows the geometric optics of a large slit system. The correct image can be seen in one position (labelled best position), but as soon as the viewer moves away from this position, they can see a percentage of light from image 2 which spoils the view. B). shows the situation where the parallax barrier slits are small. Image 1 can be seen over a wider range of angles.

In addition, the smaller the parallax barrier slits, the less light passes the barrier and the dimmer the display becomes.

A similar diagram can be drawn to show that the smaller the pixel apertures (variable b), the greater the head freedom, and the smaller the pixel apertures the less light passes the LCD panel, making the display dimmer.

There is a trade off between head freedom and brightness and there are many variables that can be adjusted to achieve a given head freedom requirement.

The question is: for a given head freedom what is the brightest design?

Head freedom is a function of a, b, d, and n. Head freedom can be calculated by elementary trigonometry. By solving the problem numerically it seems that for the brightest design  $a = b$ .

### *Summary*

In this section (3.2.2) the techniques used to develop parallax barriers for 3D displays have been extended to dual view displays. It is proposed that a good dual view design could be made by following the formulae summarised below.

1). The pixel-barrier separation d, should be given by:  $d = \frac{p}{2 \tan\left(\sin^{-1}\left(\frac{\sin \theta}{n}\right)\right)}$ .

2). The pitch of the barrier f, should be given by:  $f = \frac{2p}{1 - p/e}$ . A slight improvement

could be gained by adjusting the pitch of the pixels across the display also.

3). The apertures of the pixels and barrier should be equal. Experimental evidence given in chapter 3, section 1.1 suggests that taking diffraction into account would not improve the choice of pixel aperture and slit width.

Since the effects of diffraction would not modify the choice of design, it is not necessary to take diffraction into account when choosing the dual view design parameters above. Therefore I propose that the formulae above (based on geometric optics) provide the best possible dual view design.

### **3.2.3 Techniques to increase image splitting**

As mentioned previously, one of the biggest challenges to make a dual view display is in placing the parallax barrier close enough to the pixels.

The question is – are there any alternative designs that do not require such a small pixel – barrier separation?

In this section some methods for producing the thin glass are described and the difficulties discussed. Since this approach is difficult, the 3D literature is also examined in search of alternative designs that would enable dual view to be created without thin glass.

The pixel - barrier separation does not cause a big problem for 3D displays, but 3D designs that have been published could help this problem in a dual view system. These are, 1). Rotated pixel designs, 2). Grouped pixel designs.

These designs are not perfect either – they do not enable displays of marketable quality to be made, but they do allow a prototype display to be made which demonstrates the concept of dual view.

A more radical redesign of the dual view system is investigated in Chapter 2, which discusses a dual view design that might allow high quality dual view displays to be created without needing thin glass.

### **Methods of making parallax barrier dual view with an 80 $\mu\text{m}$ pixel barrier separation**

Two methods for putting a parallax barrier 80  $\mu\text{m}$  from the LCD pixels are shown in the figure below.

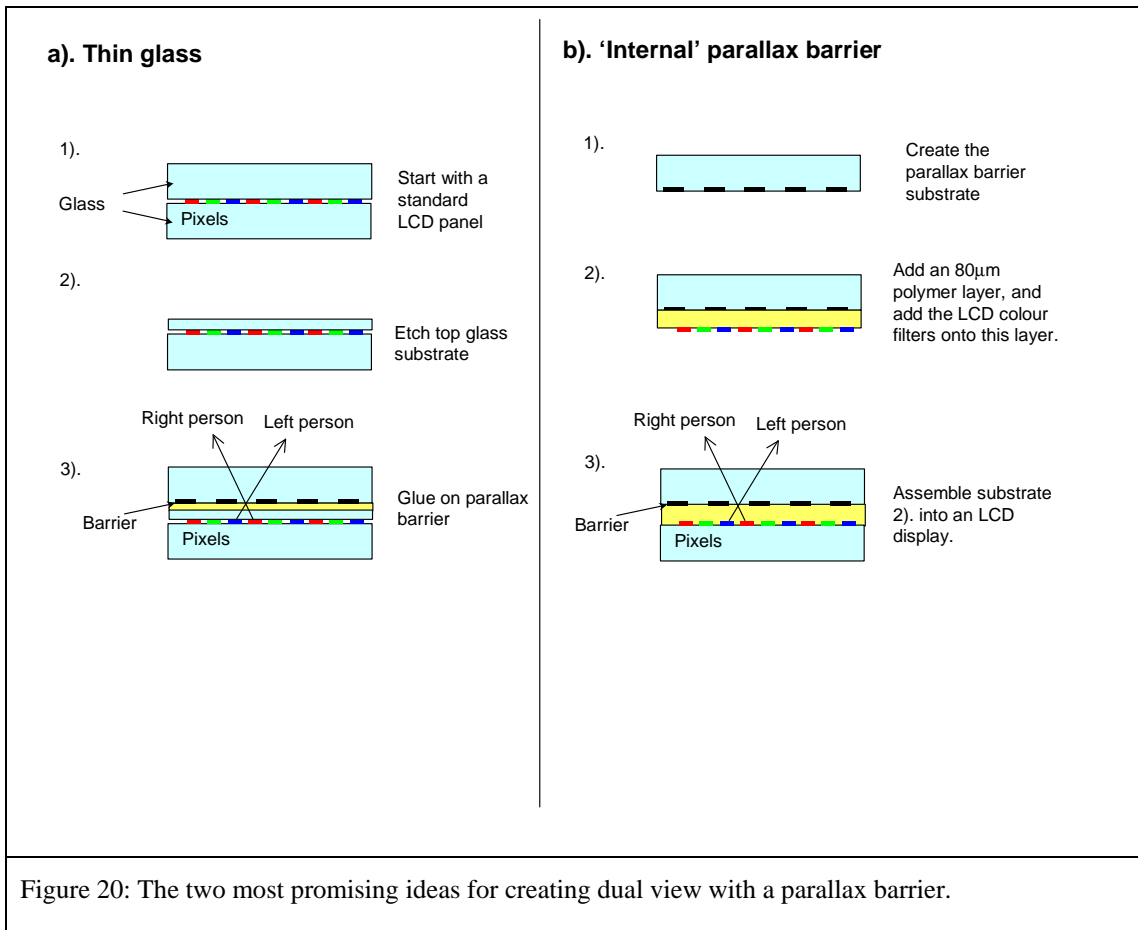


Figure 20: The two most promising ideas for creating dual view with a parallax barrier.

In the above figure, part a). describes how the top glass substrate of an LCD could be etched to about 50 µm, so that a parallax barrier can be adhered on top (with a 30 µm glue layer). This technique is possible, but in between etching the glass and attaching the parallax barrier the display is exceptionally fragile. The difficulty in this method is to avoid breakages. Any breakage results in an almost complete LCD panel being lost incurring considerable cost.

Part b of the figure, describes an alternative method. The parallax barrier is created on a substrate, and spaced off the LC pixels by a spacer layer (for example a clear polymer). The major difficulty in using this technique is in keeping the LC cell gap uniform. The LC material is typically 5 µm thick, with a tolerance of about +- 0.5 µm. Therefore the clear polymer material (which forms one side of the LC cell) must be coated in an 80 µm film, and this film must vary in thickness be less than +- 0.5 µm. The polymer film must have a thickness variation of less than 1%, which is very difficult to achieve.

These techniques and others are described in more detail in reference [17]. The difficulty that the 80 µm barrier separation produces a strong need for new dual view designs.

## Rotated pixel designs

The following diagram shows how rotating the sub pixels allow the pixel – barrier separation to be increased by 3 times. This idea has been presented for use in 3D displays [18].

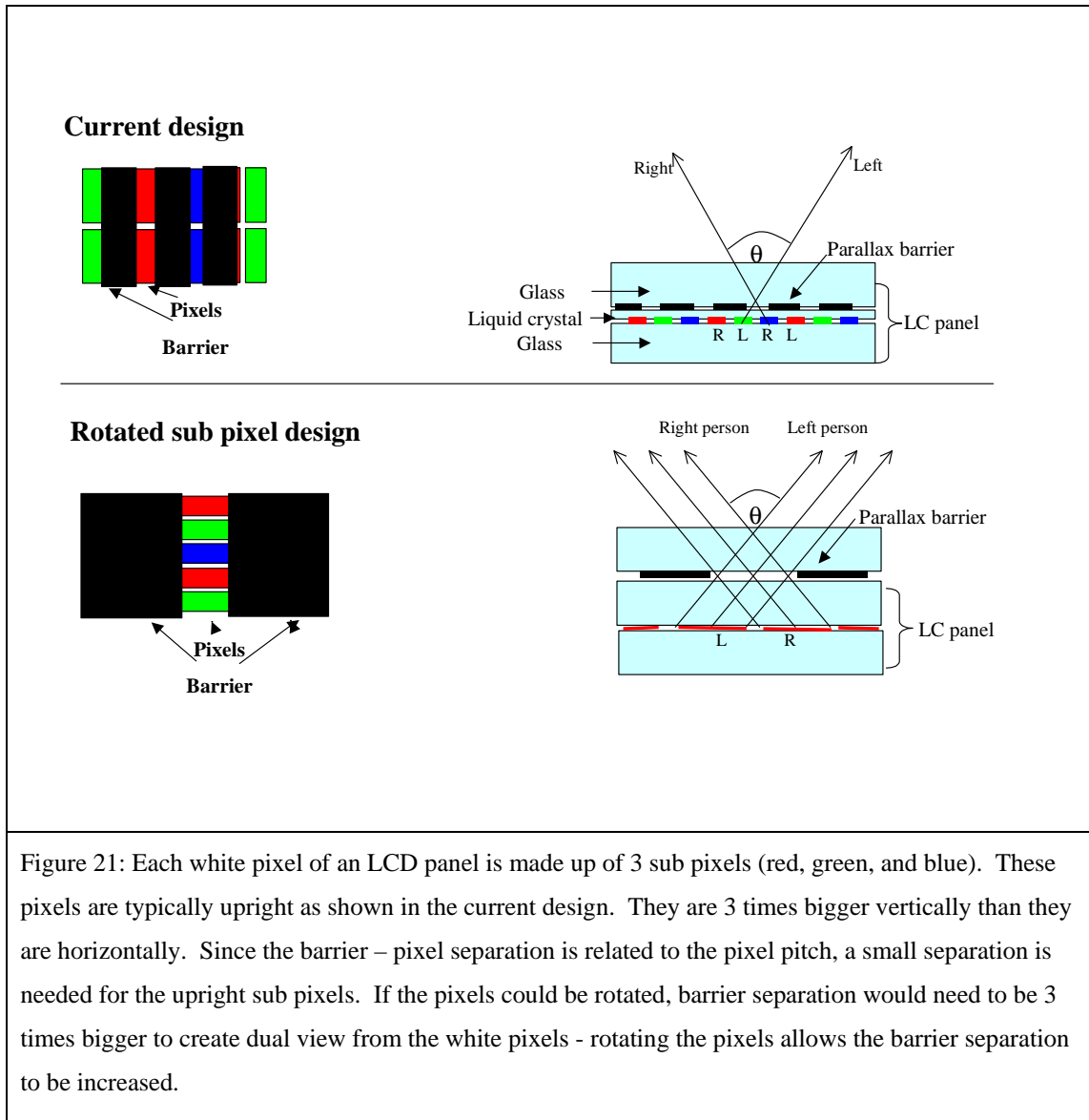


Figure 21: Each white pixel of an LCD panel is made up of 3 sub pixels (red, green, and blue). These pixels are typically upright as shown in the current design. They are 3 times bigger vertically than they are horizontally. Since the barrier – pixel separation is related to the pixel pitch, a small separation is needed for the upright sub pixels. If the pixels could be rotated, barrier separation would need to be 3 times bigger to create dual view from the white pixels - rotating the pixels allows the barrier separation to be increased.

This seems to be a promising idea. However it has drawbacks. The idea requires the TFT layout to be completely redesigned. The redesign would require massive and extremely costly development work to create the new design, rather than using the tried and tested existing pixel designs.

Therefore this is not an ideal solution.

### *Grouped Pixel designs*

A small company working on auto-stereoscopic displays called See Real Technologies published a paper containing an idea to increase the angle of separation between views without decreasing the pixel – barrier separation [19].

The idea is described as a method for creating 'tracked 3D'. It is described in the figure below.

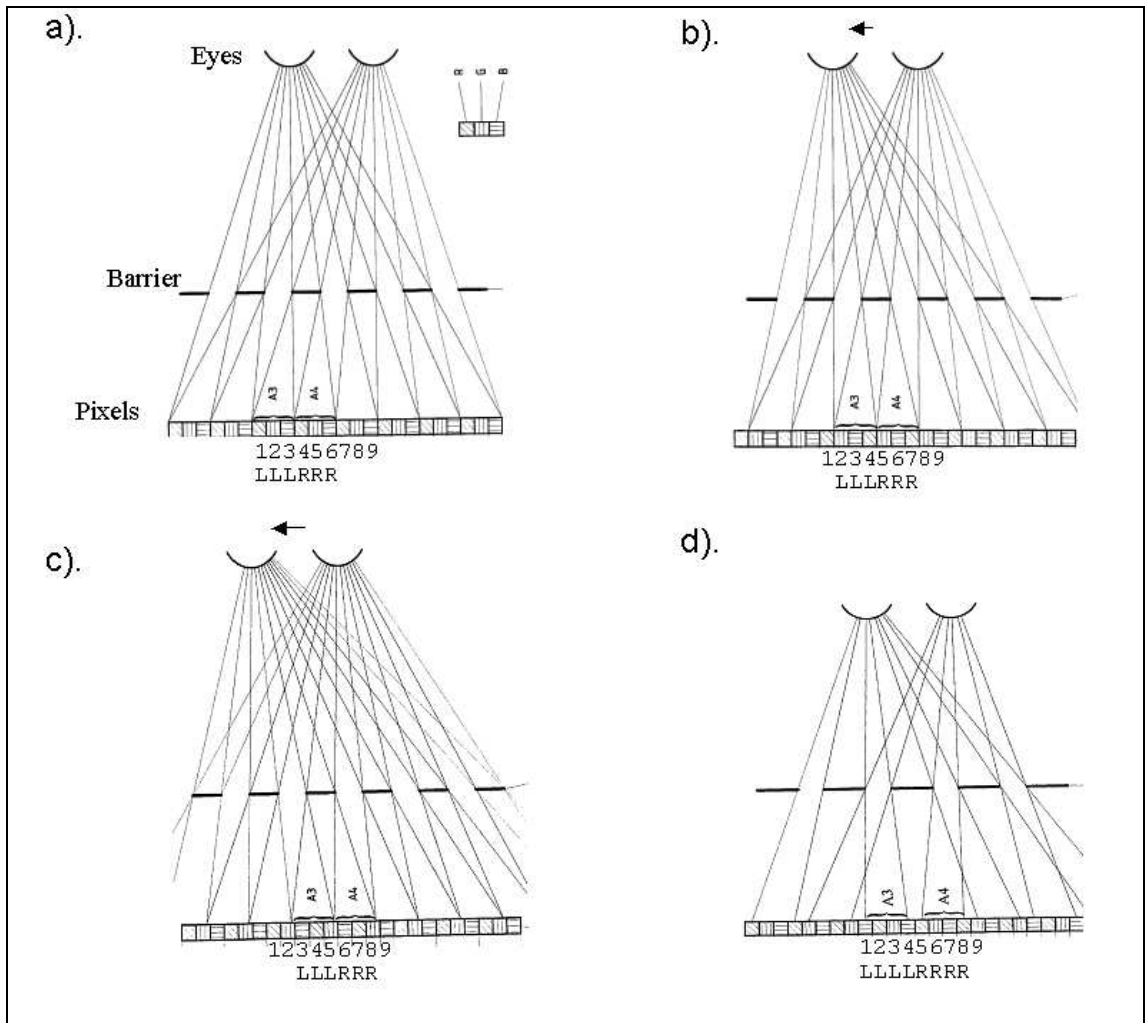


Figure 22: A design to improve the quality of a 3D display using head tracking, created by company See Real. a) Shows a parallax barrier design for 3D. The left eye sees pixels 123, and the right eye sees pixels 456. B) When the viewer moves to this position, the left eye sees pixels 234, and the right eye 456. This would be a problem since the left eye is seeing pixels 2 and 3 (L image pixels), and pixel 4 (a R image pixel), i.e. a mix of both images. However, the See Real system uses head tracking. This means that the system has some means of knowing where the user's head is, so the system knows the viewer's head has moved and it knows which pixels the viewer can see. Therefore the system can set pixels 234 to be L image pixels, and 567 to be R image pixels. In this case the viewer maintains a good 3D image from this position. C) shows a problem with this design. The viewer can move into a position where the left eye sees half of pixel 2, pixels 3, 4, and half of pixel 5. The right eye sees half of pixel 5, pixels 6, 7 and half of pixel 8. So the left and right eye can see some of pixel 5. Pixel 5 must be half L image and half R image, which is not possible. This means that from some positions crosstalk is seen. D) shows a solution to this problem. Four pixels are used for each image, the parallax barrier pitch is increased accordingly but the slits remain at 3 pixel wide. There is no viewing position where the user can see parts of more than 4 pixels, so that the pixels can always be adjusted to send the correct images to the correct eyes.

Notice how in the above design, the eyes in part d are closer to the display than in the other parts. This is because the angle of image separation has been changed by the way See Real have changed the grouping of the left and right pixels.

In parts a, b, c, the pixels are grouped in threes - LLL RRR LLL RRR ... . In part d the pixels are grouped in fours – LLLL RRRR LLLL RRRR ... .

The principle can be applied to dual view systems. There are two issues to consider.

Firstly, the more the pixels are grouped together the greater the separation between images.

Secondly, a clever way of adjusting the slit width of the parallax barrier is needed so that no problems occur. For example, had See Real in part d, used a parallax barrier with slits 2 pixels wide, then the viewer would see a red and a green pixel, or a green and a blue pixel – the colour of the image would depend on the angle it is seen from, which is no good. By using a slit 3 pixels wide the viewer always sees one red, green, and blue pixel, so that the colour balance is maintained.

Potential dual view systems made by grouped pixels are shown below, considering only the first issue.

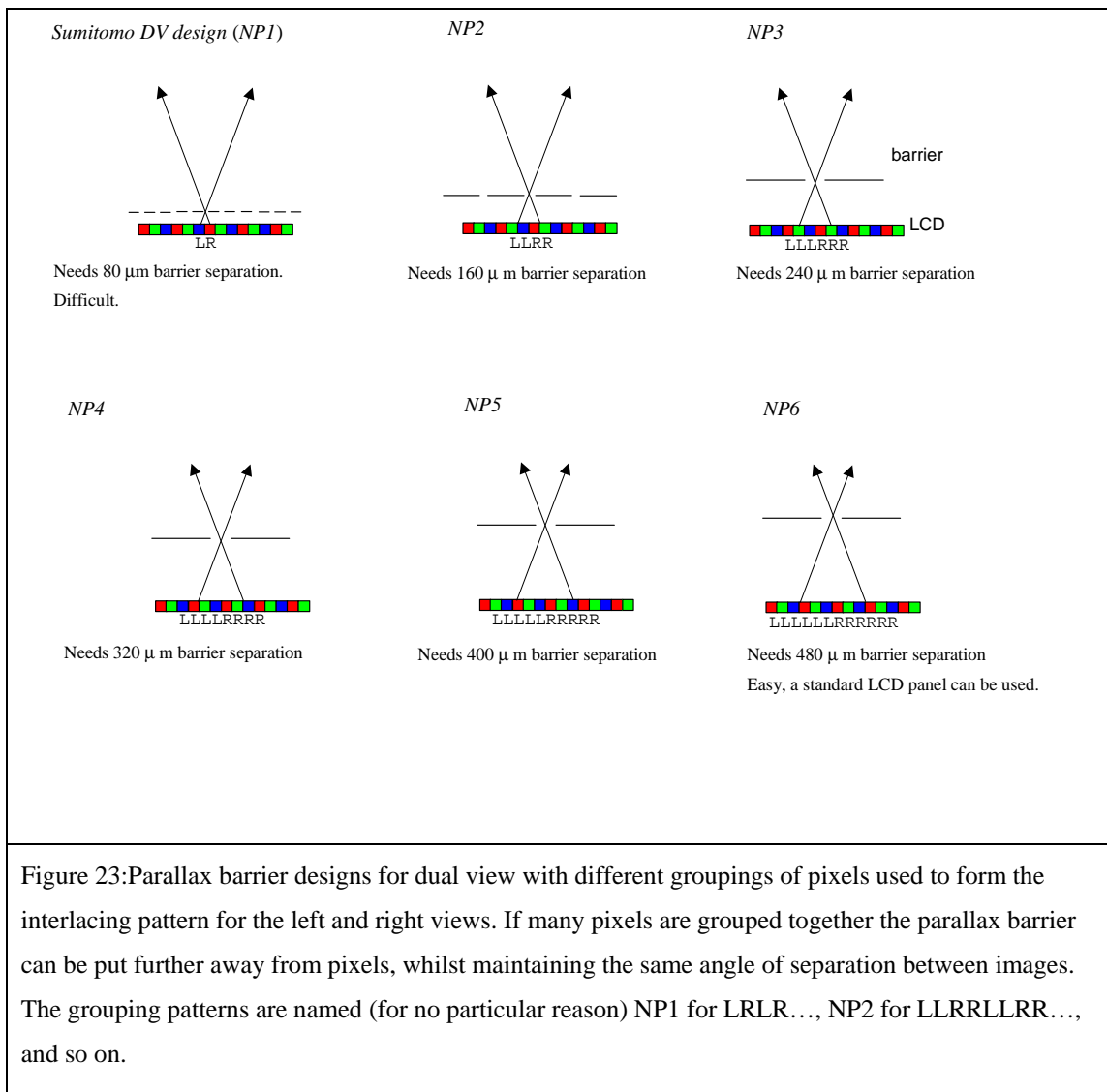
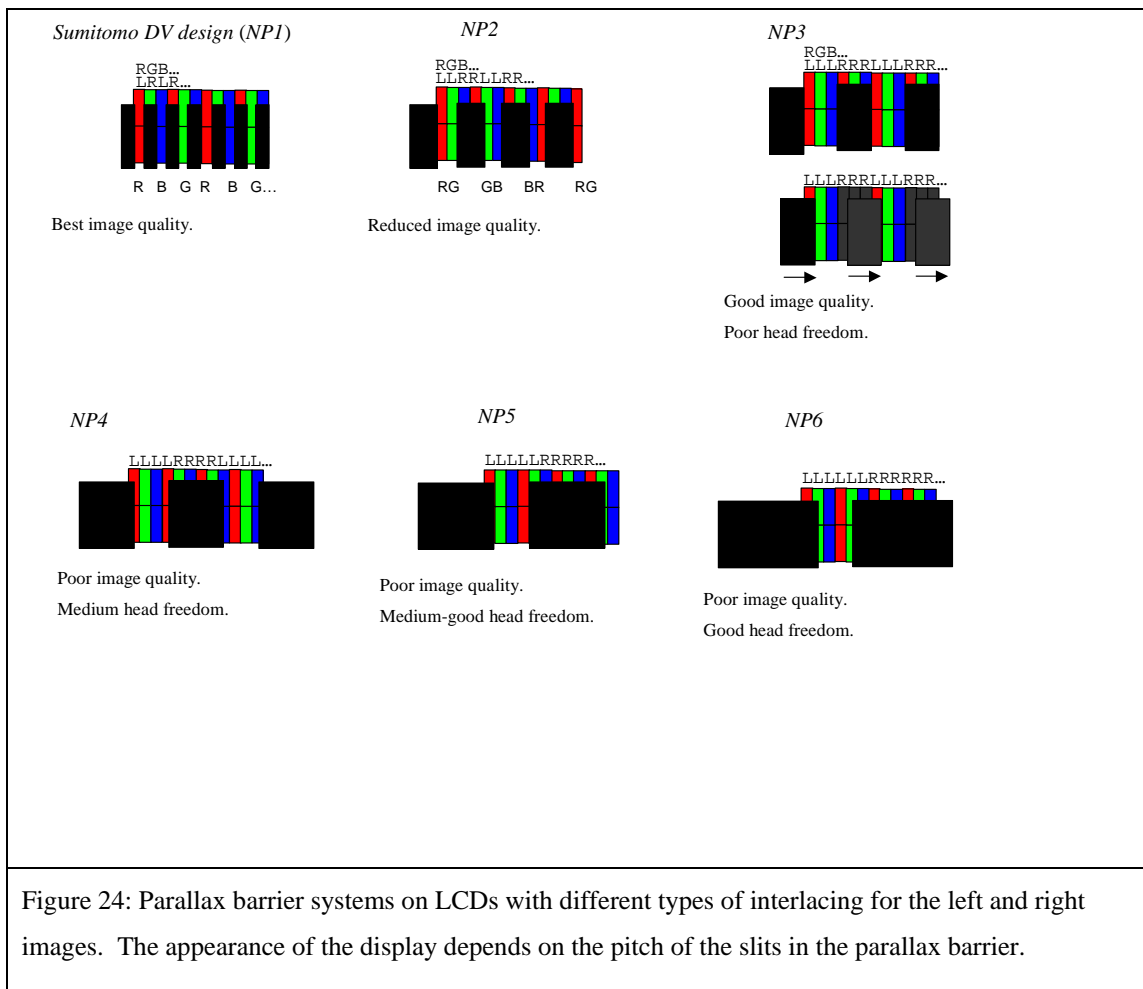


Figure 23: Parallax barrier designs for dual view with different groupings of pixels used to form the interlacing pattern for the left and right views. If many pixels are grouped together the parallax barrier can be put further away from pixels, whilst maintaining the same angle of separation between images. The grouping patterns are named (for no particular reason) NP1 for LRLR..., NP2 for LLRRLLR..., and so on.

The next figure tries to describe the second issue with these designs.



From the designs shown in figure 20, the ‘NP6’ design was chosen for prototyping. The line of thought for this decision went as follows.

Many factors are likely to need consideration when judging each design for image quality and head freedom.

The first factor that will affect image quality is barrier pitch. The smaller the barrier pitch the less visible it will be, and the less it will degrade the image. According to [20], the best human eyes cannot see gratings of more than 35 cycles per degree. For a display with 65µm wide sub pixels, with the viewer 700 mm away, it would be predicted that the NP1 and NP2 barriers are invisible, and that the other barriers are visible and so increasingly degrade the image.

Another factor is the separations between the colour pixels. In the NP1 design the RGB pixels of each view are spread over 6 sub pixels. In the NP2 design notice how the colour filter pattern beats with the barrier slits. For example, when looking at only the left image, there are 9 sub pixels separating the red pixels, then the next two red pixel come close together. The colour filter pattern repeats over a period of 9 sub pixels (20 cycles per degree), which theoretically degrades the image quality. In NP3 designs and

higher this problem does not exist. The problem is rectifiable to some extent by rearranging the colour filter layout. This is the subject of reference [21].

A third factor influencing image quality relates to NP4, 5 and 6. Take the NP6 design as an example. The viewer only sees three sub pixels out of every twelve sub pixels. Therefore the viewer only sees a quarter of the total resolution from the display, which must reduce the image quality.

Regarding head freedom, in the NP1 design there is freedom to choose any slit width and pixel aperture to get the brightest design with the head freedom desired. This is true to some extent for the NP2 design because the slit size can be adjusted to adjust head freedom. It is difficult to change the pixel sizes without changing the sub pixel spacing – which is difficult. In the NP3 design the slit widths must be 3 sub pixels wide so that the viewer sees an even proportion of red green and blue pixels. This reduces head freedom. As soon as the viewer moves away from the best viewing position they see crosstalk from the other image. The NP4, 5 and 6 designs must all have slit widths that are 3 sub pixel widths for the same reason as the NP3 design. However, as the NP4, 5 and 6 designs have an increasing ratio of pixel pitch to slit width they have increasing head freedom.

Taking all the above into account it can be seen that an alternative design exists to the Sumitomo 'NP1' design. The NP6 design allows dual view to be created without thin glass. It should give the same good head freedom characteristics that the NP1 design does the only side effect being that the pitch of the parallax barrier would be about 1mm, making the barrier visible to the eye and degrading the resolution of the image.

This NP6 design was prototyped by myself to provide a proof of concept demonstration of a dual view display. It is shown in the photo below.



Figure 25: A photo of an early dual view prototype display. A mirror is used to show that a different image is being shown in another direction.

This display inspired significant interest from many car companies, and demand for the further developmental efforts described in this thesis.

### *Refractive index*

If we consider the equation relating to the image separation for the images in a parallax barrier dual view system (section 3.2.2), we see that it is a function of the pixel pitch and the refractive index. In the literature there are various ways of changing pixel size, but no mention of changing the refractive index.

For completeness, the table below shows the barrier separation required to create an image separation of 30 °, for a 65  $\mu\text{m}$  pixel pitch, for different refractive indices between the barrier and pixels.

Refractive index	Barrier separation for 30 ° image separation (um)
1	46
1.5	79
2	130

Table 1: The barrier-pixel separation required to create dual view when media of various refractive index are used between the pixels and barrier.

By using a high refractive index such as 2, the required barrier separation can be increased by about 50  $\mu\text{m}$ . Materials with such high refractive indices bring other problems without significantly reducing the problem creating LCDs with substrates of less than 130  $\mu\text{m}$  is still difficult.

### *Summary*

In this section we have seen various ways of creating dual view with a parallax barrier and without using a very small pixel – barrier separation.

Using pixels rotated by 90 ° enables the separation to be increased by 3 times but this is not significant enough to solve the problem. The required pixel barrier separation is still small. In addition it is an expensive option.

Grouping pixels enables a dual view display to be created with such a large pixel-barrier separation that it is trivial to make. However, these designs reduce the image quality of the display such that they are not a realistic solution.

Modifying the refractive index of the system doesn't have a significant enough effect on the problem to make the materials issues worth tackling.

In summary, there is a big requirement to create a radically new design of dual view system that is simpler to make. Such a design is considered in Chapter 2.

### **3.2.4 Techniques for switching**

In a dual view display, the left viewer sees only half the pixels (that is to say the left image pixels). Therefore the resolution of the display is halved.

An ideal dual view display would be switchable between dual view and single view modes as necessary.

This is a well known problem in the field of 3D for similar reasons. Two techniques used to switch 3D displays between 3D and 2D modes are described below, and there

applicability to dual view is discussed. They both have big problems when applying them to dual view.

Some technology developed by other companies is considered for its applicability to dual view single view switching, and one new idea is shown to have potential.

### *Liquid crystal parallax barriers*

A small 3D display company DTI use a liquid crystal (LC) parallax barrier to create the 3D. In this way the barrier can be switched on and off like a conventional LCD.

The construction is shown in the figure below.

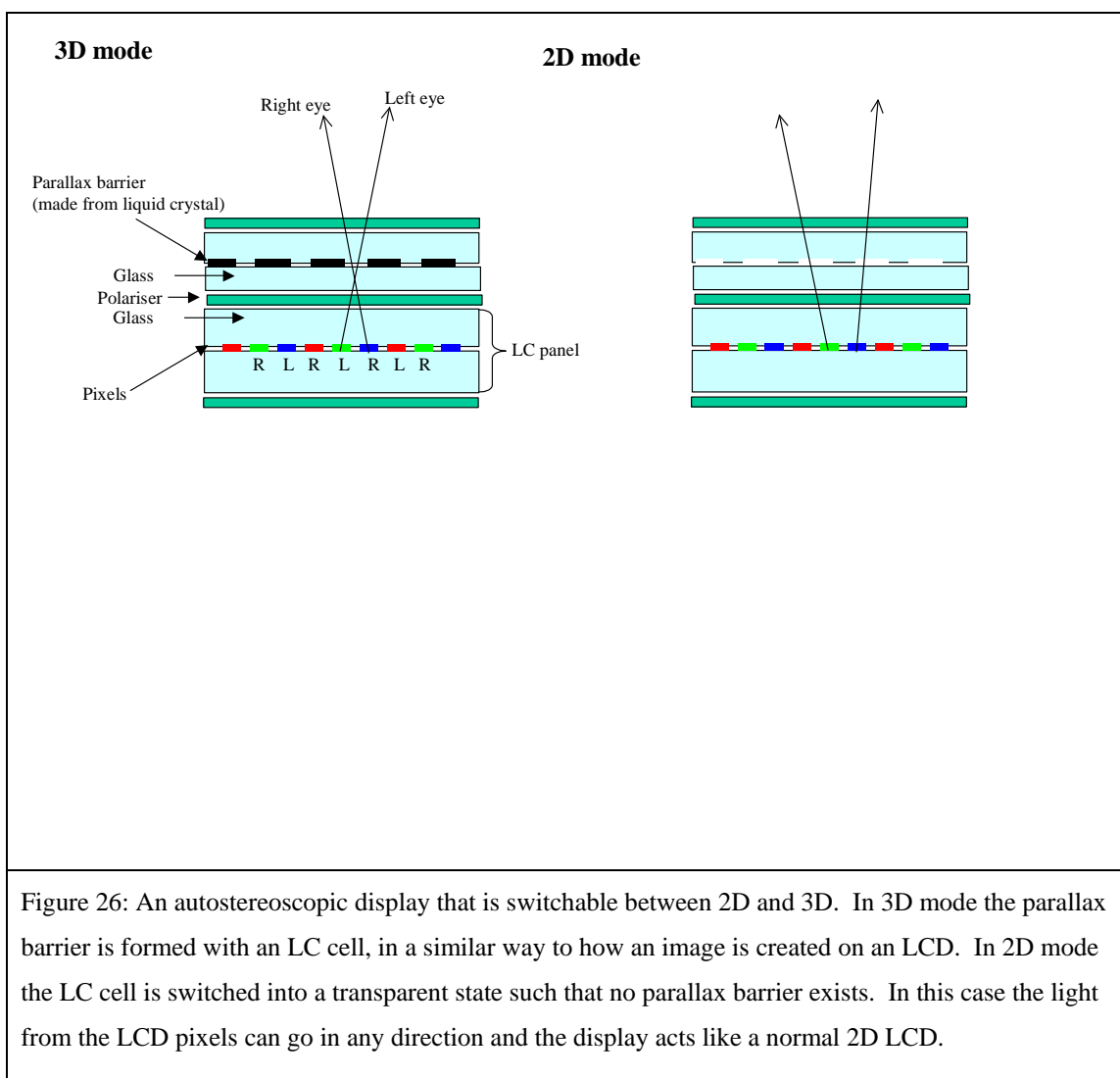


Figure 26: An autostereoscopic display that is switchable between 2D and 3D. In 3D mode the parallax barrier is formed with an LC cell, in a similar way to how an image is created on an LCD. In 2D mode the LC cell is switched into a transparent state such that no parallax barrier exists. In this case the light from the LCD pixels can go in any direction and the display acts like a normal 2D LCD.

It is necessary to have a polariser in between the LCD and the LC barrier for the LCD to function. Therefore between the pixels and the barrier there is a thick stack of; LCD glass substrate (typically 0.4 mm), polariser (typically 0.2 mm), LC barrier substrate (typically 0.4 mm). The total distance between the pixels and barrier is therefore about 1 mm. This is large even for a 3D display such that an 'NP3' design would be needed if

small high resolution pixels are to be used. The NP3 design degrades the head freedom of the device as mentioned in section 3.2.3.

### *Patterned retarders by Sharp*

Around 2002, Sharp produced a 3D display based on a novel design of switchable barrier that could be placed closer to the pixels. It is based on a reactive mesogen (RM) which is similar to an LC except that it can be cured into a solid. This enables the RM to be formed into a parallax barrier on just one substrate rather than needing two substrates to contain it like an LC. The method of operation is described below.

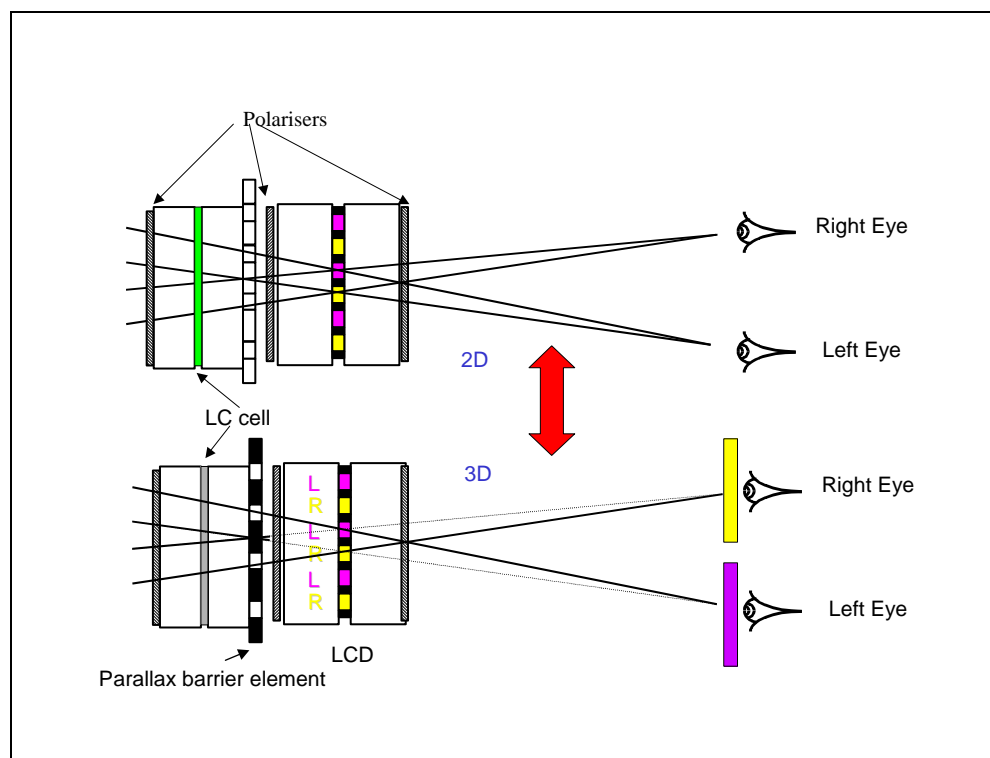


Figure 27: The Sharp system for 2D to 3D switchable displays. The parallax barrier is made from an LC which can be aligned and cured into a solid. It needs only one supporting substrate, and so can be placed very close to the pixels, which is advantageous for high resolution 3D. The cured LC acts as a retarder. In 3D mode the retarder either rotates the polarisation of the light so that the final polariser blocks it, or passes it depending whether the light passes a part of the retarder representing a ‘slit’ or a ‘barrier’. The alignment (and optical axis) of the cured LC in the ‘slit’ and ‘barrier’ regions is different to enable this to happen. In 2D mode the LC cell changes the polarisation of light such that the light passes all regions of the parallax barrier equally so that the 3D effect is lost. See reference [22] for further details.

The only components needed between the pixels and the barrier are a glass substrate (typically 0.4 mm) and a polariser (typically 0.2 mm). These components are almost

half as thick as the DTI design, which allows a high-resolution switchable 3D system to be created with an NP1 design. This gives better head freedom and image quality.

### **A dual view switchable parallax barrier system.**

#### *Polarisation based systems*

The switchable systems above for 3D are both based on changing the polarisation of light. They therefore need a polariser between the LCD and the barrier to initialise the polarisation of light correctly for the switching barrier.

The thinnest polarisers (using conventional technology) are at least 0.13 mm which alone is thicker than the 80  $\mu\text{m}$  pixel-barrier separation required for dual view.

This suggests that any polarisation based switching mechanism is no good.

#### *Electro-wetting dyes*

Phillips have created prototype displays using electro wetting dyes [23]. These displays rely on moving black dye around in a pixel to either block light or let light pass. Such dyes could be used to create a parallax barrier. The problem here is that the dyes need to be encapsulated between two substrates. The additional substrates would put the parallax barrier too far away from the pixels. If the thin glass front substrate of the LCD were to be used as one of the substrates for switching the dye then layers such as ITO would need to be added. This would require extra processing steps on a weak layer which is likely to increase the number of breakages.

#### *Switchable diffusers*

Seiko have developed a switchable diffuser [24], it can be switched between transparent and scattering states. This could be placed over a parallax barrier – when the diffuser is clear the barrier would generate dual view, when the diffuser is scattering it would mix the two images to create a single view mode.

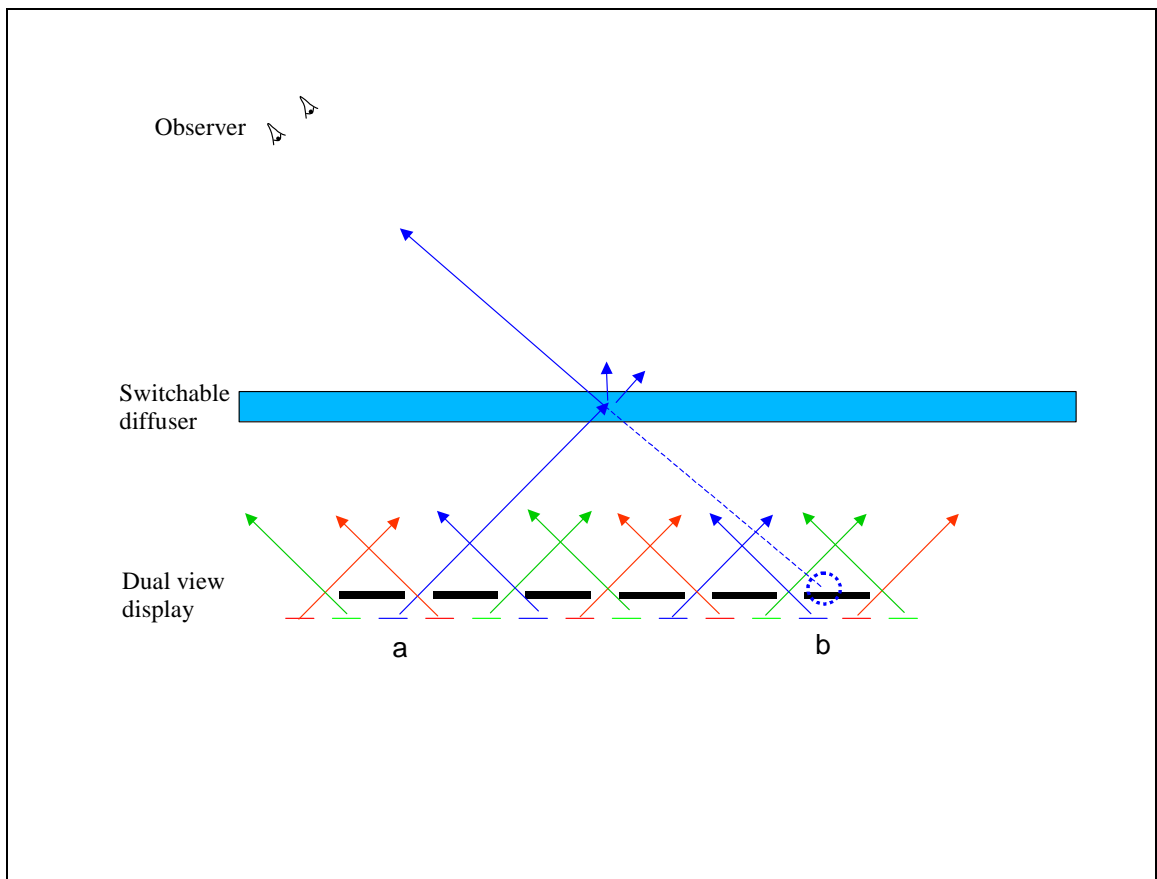


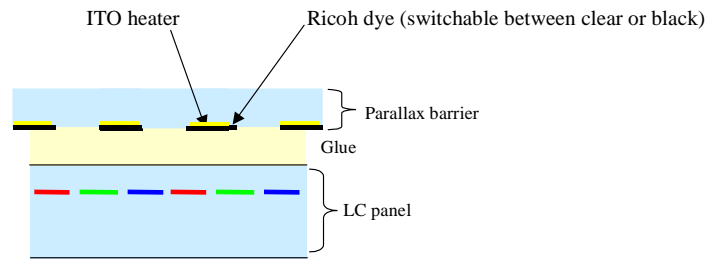
Figure 28: A switchable diffuser could be used to convert a dual view display into a conventional display, however it is thought that the diffuser would need to be placed very close to the pixels to avoid blurring of the image. The diagram shows how this blurring would come about. Light from a pixel at point 'a' would, without any diffusion, travel away from the observer. With the diffuser, the ray would be scattered towards and be seen by the observer. The problem is that this ray will appear to have come from position b on the panel, and as can be seen 'b' is some distance from 'a', such that the image will be blurred. A diffuser could be used to remove the dual view effect, but it would have to be placed in the plane of the barrier to avoid blurring. In addition to problems putting a switching layer so close to the barrier, the switchable diffuser would need to be polarisation preserving so that the polarisation state of the light passing each pixel is preserved up to the polariser that is positioned after the barrier.

The figure above shows why it is thought that the diffuser would need to be placed closer to the parallax barrier than is possible.

#### *Thermally switchable dyes*

A new technology developed by Ricoh may provide a workable solution to the switching problem. It is based around a bi-stable thermal dye that can change from opaque to transparent and back again by heating [25]. Its operation as a parallax barrier is described below.

### Novel parallax barrier switching system for dual view



#### Switching procedure

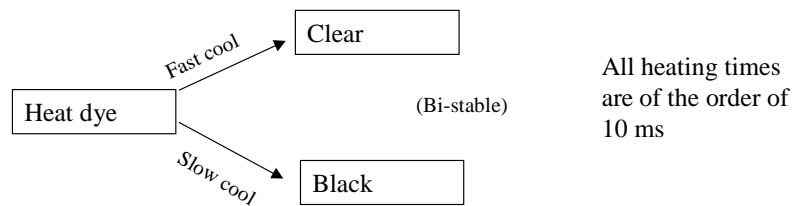


Figure 29: The new parallax barrier switching system above would allow the parallax barrier to be placed close enough to the pixels to create dual view. The switching system is based on a new type of dye made by Ricoh. The dye can be switched between opaque and transparent states by heating (creating dual view, and single view respectively). To switch the dye is heated then for an opaque state the dye is cooled slowly (by slow reduction of the heating current through the indium tin oxide (ITO) heating lines. For a transparent state the heating is removed rapidly, the rapid cooling causes the dye to become clear.

This idea provokes many questions regarding its practicability. These include the lifetime and absorption of the new material.

Perhaps the biggest concerns are how much energy does it require to switch, how much power does it require to switch, and will the heating damage the LCD? These questions are discussed below.

#### Switching energy:

If the material has a specific heat capacity of  $1000 \text{ J kg}^{-1} \text{ K}^{-1}$ , a density of  $1000 \text{ kg m}^{-3}$  (typical for polymers [26]), a layer of  $30 \text{ }\mu\text{m}$  is needed for sufficient absorption over an area of a 15 by 8 cm automotive LCD, and a temperature rise from  $25^\circ\text{C}$  to  $90^\circ\text{C}$  is needed to switch the material, then 23 Joules of energy would be needed to switch the

dye. This is a conservative estimate since it assumes that all this energy goes into the dye, rather than being dissipated into the surroundings.

This energy is not significant compared to the 4 MJ stored in the car battery [27].

#### Switching power:

Supposing the dual view display needed to be switched from dual view to single view only 3 times in every hour of use, then at 23 J per switch this would only add an average of 20 mW to the power consumption of the device, which is insignificant compared with the 5 W consumed by the backlight [28].

However, a property of the material is that the change in temperature must occur in a period of about 10 ms, which makes the power requirement during switching about 2300 W. A car battery is capable of delivering 4800 W on starting the engine [27], but handling this power makes the design quite impractical.

A thick ITO layer has a resistance of about 1  $\Omega$  per square [29]. In the heating element there is an ITO line under every strip of barrier. Each barrier strip has a width of about 90  $\mu\text{m}$  and a length of 8 cm, and there are about 1000 strips. This would make the total resistance of the heating elements 0.7  $\Omega$ .

Given that power = current x voltage, and voltage = current x resistance, the voltage V, needed across the heating element (with resistance R) to dissipate power P, is  $V = \sqrt{PR}$ . For the above device 40 V needs to be applied to the heating element to dissipate 2300 W.

This voltage could be generated by a step up transformer, the problem is that the heating element is only 0.7 ohms, comparable to copper wires that might be used to transfer power from the circuitry to the heating element, and in the step up transformer.

Therefore there would be as much power dissipated in the circuitry as in the dye, which is likely to cause damage (without an impractically cumbersome design).

We can increase the resistance of the heater but then the voltage requirement rises. It doesn't seem sensible to use high voltages for safety reasons.

Therefore this design is not practical.

Ricoh use this dye as the ink in a re-printable paper. This paper is printed one line at a time, so that only a small area of dye is switched at a time. Consequently, the power requirement is low.

We can use the same approach by heating only 1 strip of the barrier at a time. There are about 1000 barrier strips on an automotive LCD. This would reduce the power requirement by 1000 times, to 2.3 W. The resistance of the heating element (in this case 1 strip of the barrier) would be 700  $\Omega$  (1000 times that of the whole heating element). So, the voltage required for each strip would remain at 40 V. However, since the resistance of the heating element is much higher than the rest of the circuitry, and the peak power requirement is only 2.3 W, this is a much more manageable design. The time taken to switch the display increased 1000 times from 10 ms to about 10 seconds, which would produce an interesting switching effect but overall with this time the design is potentially feasible.

#### Heat damage to the LCD:

The operating temperature of a typical automotive LCD is from  $-30^{\circ}\text{C}$  to  $+85^{\circ}\text{C}$ , and the storage temperature is from  $-40^{\circ}\text{C}$  to  $+85^{\circ}\text{C}$ . Therefore the dye must not clear much before  $85^{\circ}\text{C}$  or else the operating temperature of the display will be reduced. Supposing the dye is developed to be 'written' at  $90^{\circ}\text{C}$ . This exceeds the storage temperature of the LCD. The idea should be tested to find out if this causes damage, but it is possible that the display will be OK. Firstly the  $90^{\circ}\text{C}$  temperature only needs to exist for milli-seconds, and secondly, only the 30  $\mu\text{m}$  dye layer is heated to this temperature. It is possible that the heat will dissipate as it spreads throughout the display such that the sensitive components never reach a damaging temperature.

#### *Summary*

This section stated the advantages that switchable dual view optics could provide, i.e. when the dual view mode is not needed, the dual view optics could be switched off and all the viewers can benefit from higher resolution and more brightness.

No such design is known in the literature for dual view, and designs that work for 3D do not work for dual view because the switching optics cannot be placed close enough to the pixels. A new idea was proposed that may be compatible with a dual view system. No in-depth experimental work has been carried out on this design but back of the envelope calculations suggest it is feasible, and the idea has been patented [30].

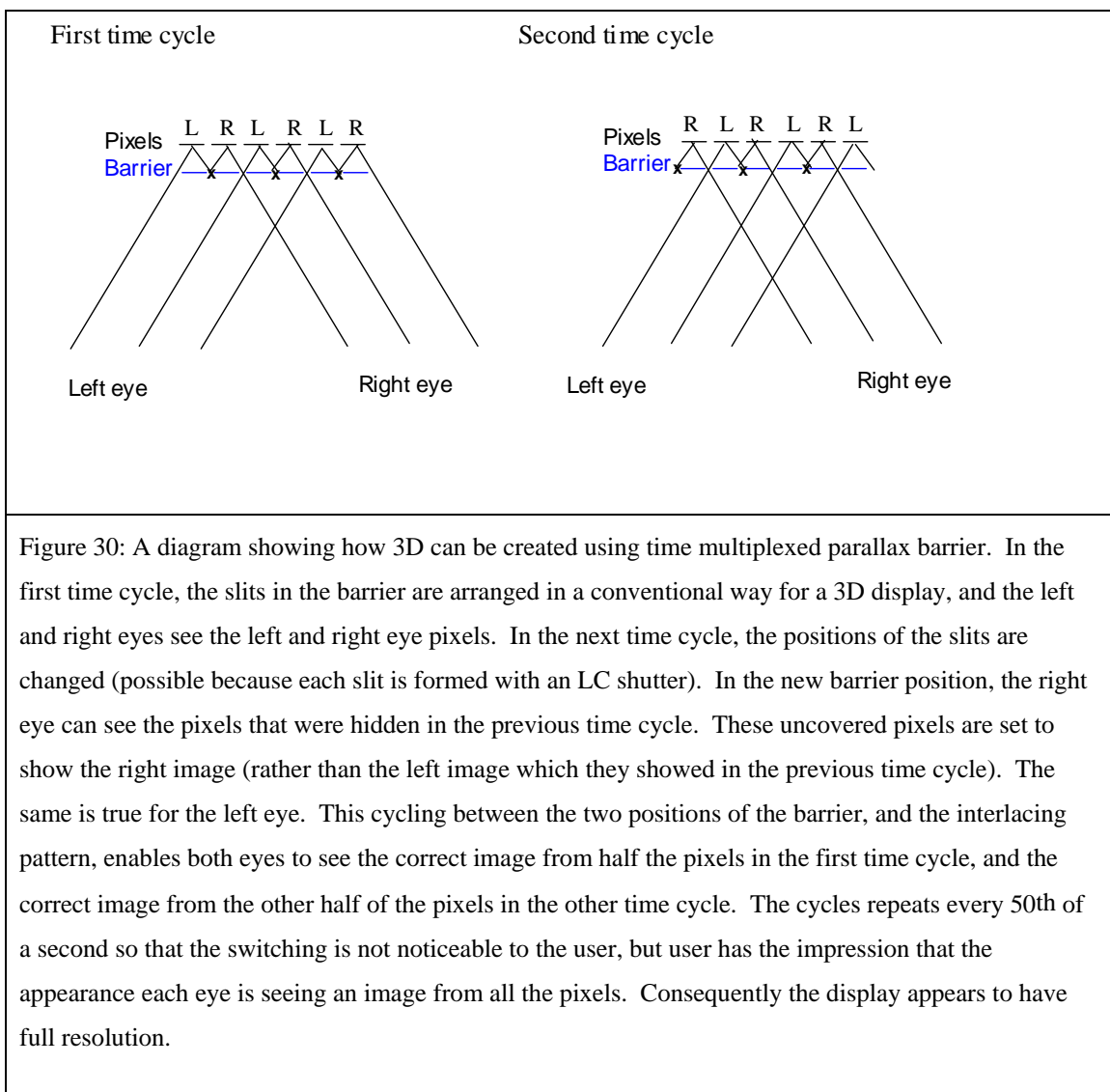
### **3.2.5 Time multiplexing to increase resolution**

A problem with dual view displays is that in the left or right image viewing positions a viewer only sees half the pixels (the pixels showing their image). Therefore resolution is halved.

The same problem exists for 3D, such that a drop in resolution is noticeable when switching from 2D to 3D.

### *A time multiplexed parallax barrier*

In 1998, a Kenneth Erbey, not affiliated with any company, disclosed his work on a solution to this problem [31]. His design uses time multiplexing to allow each eye to see the full resolution of the panel.



This system seems entirely feasible, though difficult to implement because of the need for a display and parallax barrier that can switch fast enough to avoid the display flickering. Such panels exist but are expensive.

### *A time multiplexed backlight*

Mitsubishi developed an idea to overcome the resolution problem in 2002 [32]. It is based on time multiplexing. Its operation is described below.

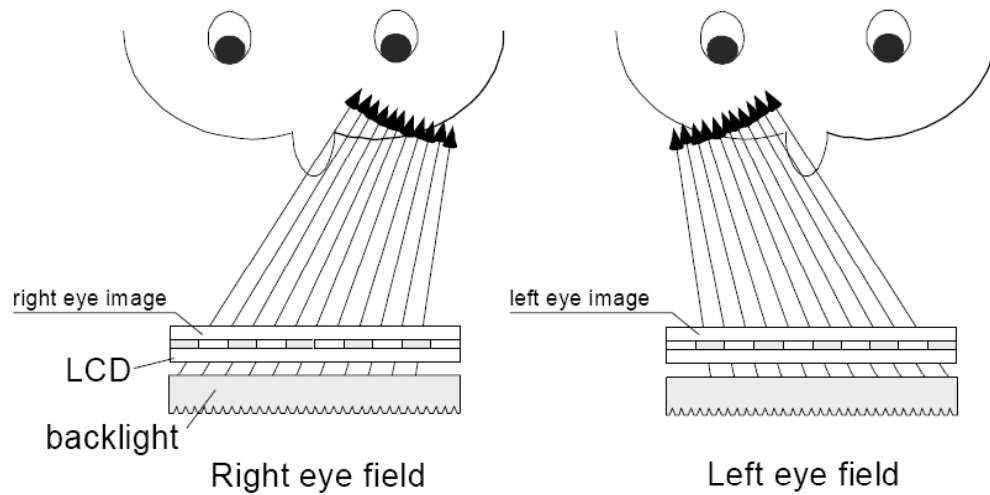


**Figure 1. Field sequential method**

Figure 31: A diagram showing how 3D can be created using time multiplexed backlighting. In time frame 1 (or the right eye field), the backlight only sends light in the direction of the right eye. During this time the LCD shows the right eye image. In the next time frame, the backlight only illuminates the left eye, and the LCD shows the left eye image. This cycle repeats every 50<sup>th</sup> of a second so that it is not noticeable to the user. Notice that in this method, the left and right eye images can use all the pixels in the LCD, so that the 3D image has the full resolution of the display.

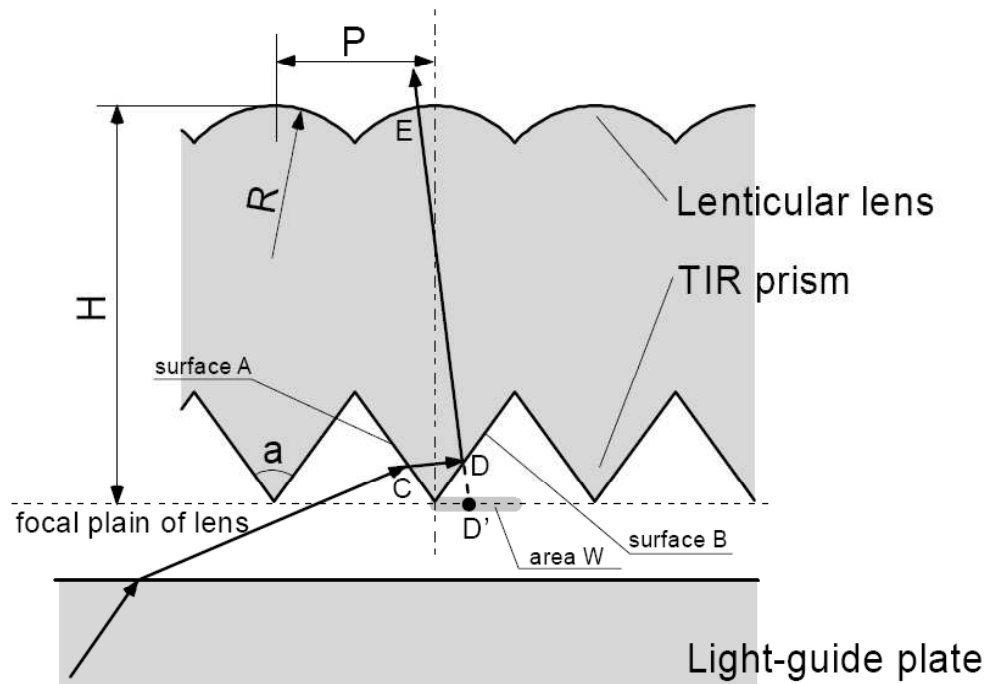


**Figure 3. Structure of the prism sheet**

Figure 32: This diagram shows how Mitsubishi achieve directional illumination from their backlight. Light from a source such as an LED is guided down the light guide plate by total internal reflection (TIR). It travels from left to right in the diagram because the light source is at the left edge of the light guide plate. The light is extracted uniformly behind the display by some distortions in the light guide plate. The extracted light enters the prisms and is reflected by TIR towards the lenticular lenses. The lenses focus the light towards the right eye direction. To illuminate the left eye direction, the LED at the left edge of the plate is switched off, and an LED at the right edge of the plate is switched on. The system now works in reverse to illuminate the left eye.

The paper shows that the Mitsubishi system is also feasible, if a high switching speed panel is used. By creating the time multiplexing system in the backlight Mitsubishi have probably created a cost advantage over the Erbey system. The Mitsubishi system components needed are similar to those used in inexpensive plastic backlights, and the switching is done by flashing light emitting diodes (LEDs), whereas the Erbey system requires an additional switching LC cell to form the parallax barrier, which is complicated to make.

## *Summary*

In summary, these time multiplexing techniques could generate full resolution dual view, however both the techniques described suffer switching speed problems. The LCD needs to operate at twice video rate to prevent the image appearing to flicker. This is a very difficult challenge for LCDs because the time taken for the LC to change is typically only just fast enough for one times video rate. This is especially true in cars where the display may have to operate at temperatures much less than 0°C. At these temperatures the LC becomes more viscous and switches more slowly.

For this reason, the use of time multiplexing to create high-resolution dual view was not pursued further in the study reported in this thesis.

### **3.2.6 Techniques to make a black central window**

If a dual view display is created with a parallax barrier such as that shown in section 3.2.2, then left and right views will be visible from the left and right. For a small range of angles in between the left and right views, both images are visible. This image-mixing region is a little unsightly, it would be better if it were blacked out.

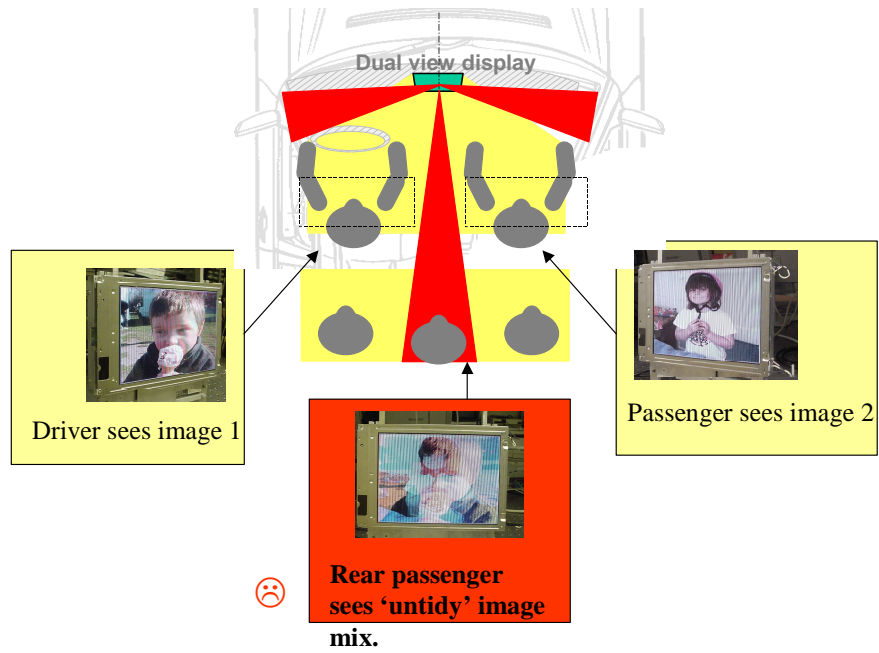
This section shows photographs of the problem (based on the 'NP6' barrier design), and then presents two solutions from the 3D literature. These are; double parallax barriers, and parallax barriers using colour filters, both designed by Sanyo. These ideas are assessed. They have potential but are not taken further for dual view due to their various drawbacks.

A new method of creating a black on axis view was developed and prototyped based on the modification of an LCD backlight. This is simpler than the two Sanyo designs.

#### *The image mixing problem*

The central image-mixing problem is illustrated in the diagrams below.

## The image mixing problem



## The ideal solution

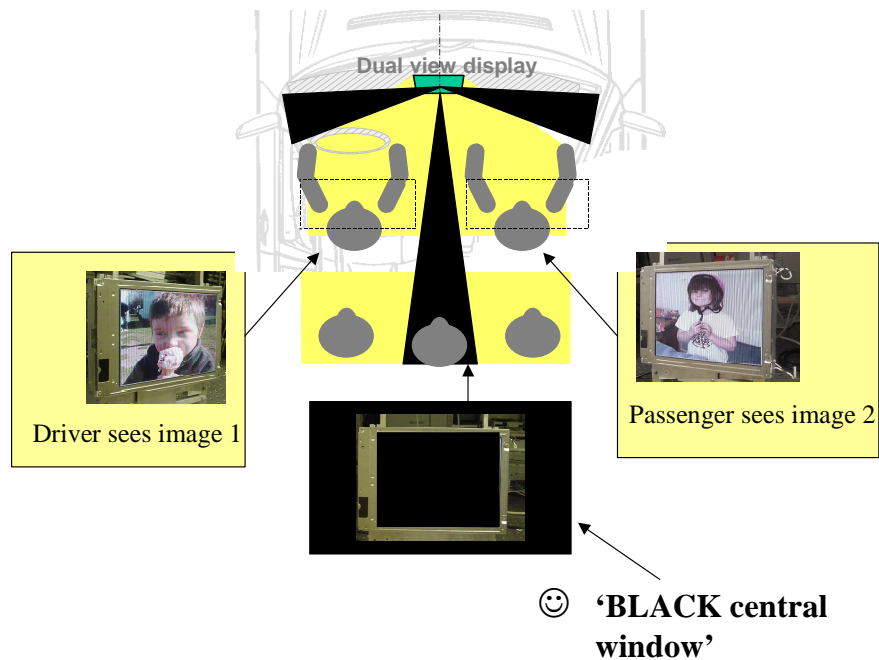
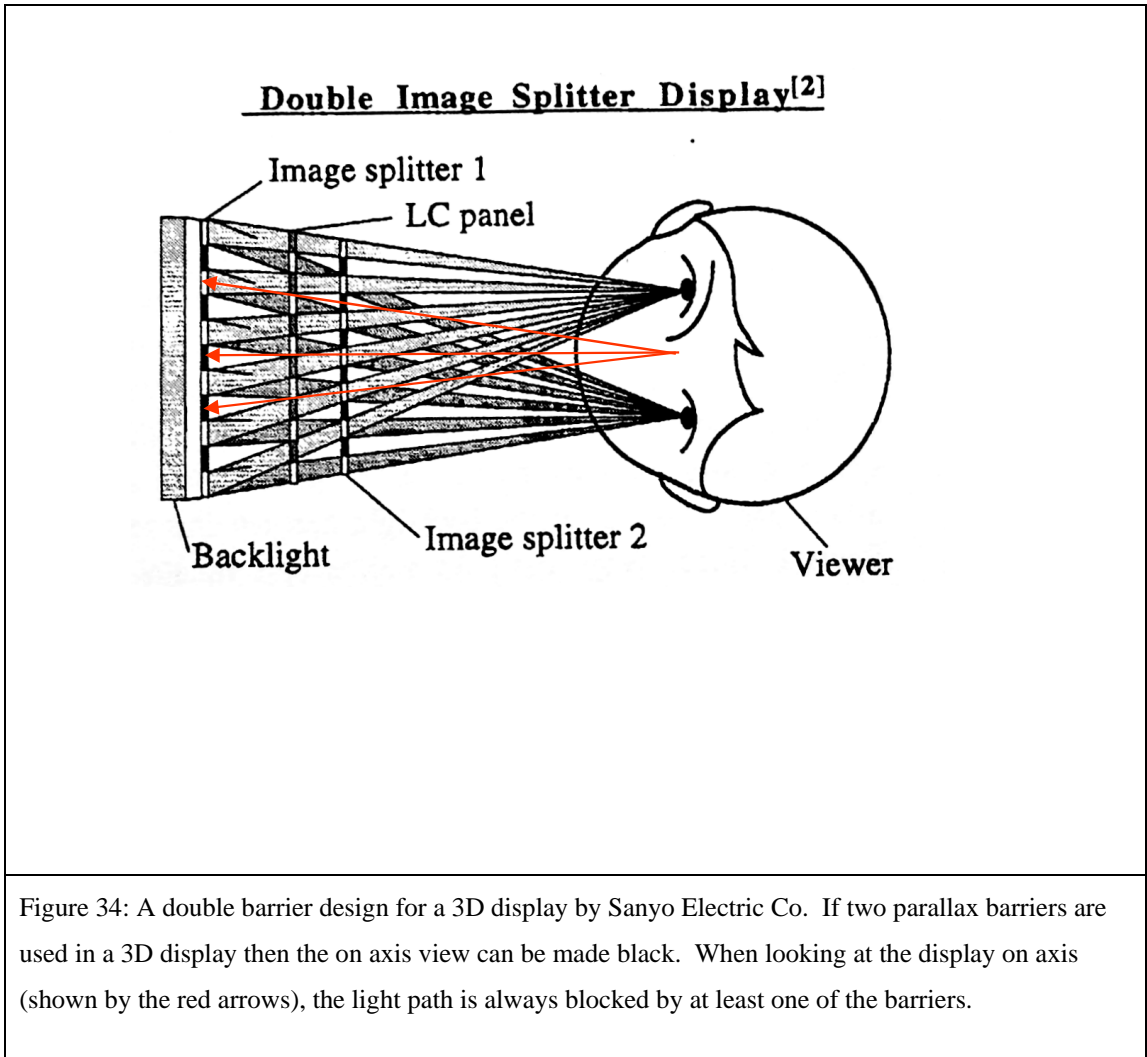


Figure 33: For a conventional parallax barrier dual view design, a region of angles exists on axis, where both images can be viewed. As shown in the diagram, this looks unsightly. Ideally this problem would be solved by making the on axis view black.

### *Double barriers by Sanyo*

Sanyo had developed a method of creating a black region between the left and right views in a 3D display by using two parallax barriers. Its operation is as shown in Figure 34 [33].



The paper reports that good head freedom can be produced, with reasonable brightness. The disadvantage in this design is that for dual view, both barriers must be put close to the pixels, which is difficult, and adds to cost. Modelling carried out by a colleague suggested that the brightness and head freedom increase, would not be as great as that generated by the use of micro lenses developed in Chapter 4. Therefore this idea is not well suited to dual view.

### Colour filter barriers by Sanyo

Sanyo (a Japanese electronics company), have proposed a more effective parallax barrier design than the conventional black and clear barriers [34]. Sanyo propose that a parallax barrier making use of colour filters could be used with an LCD. An explanation of its workings is shown below.

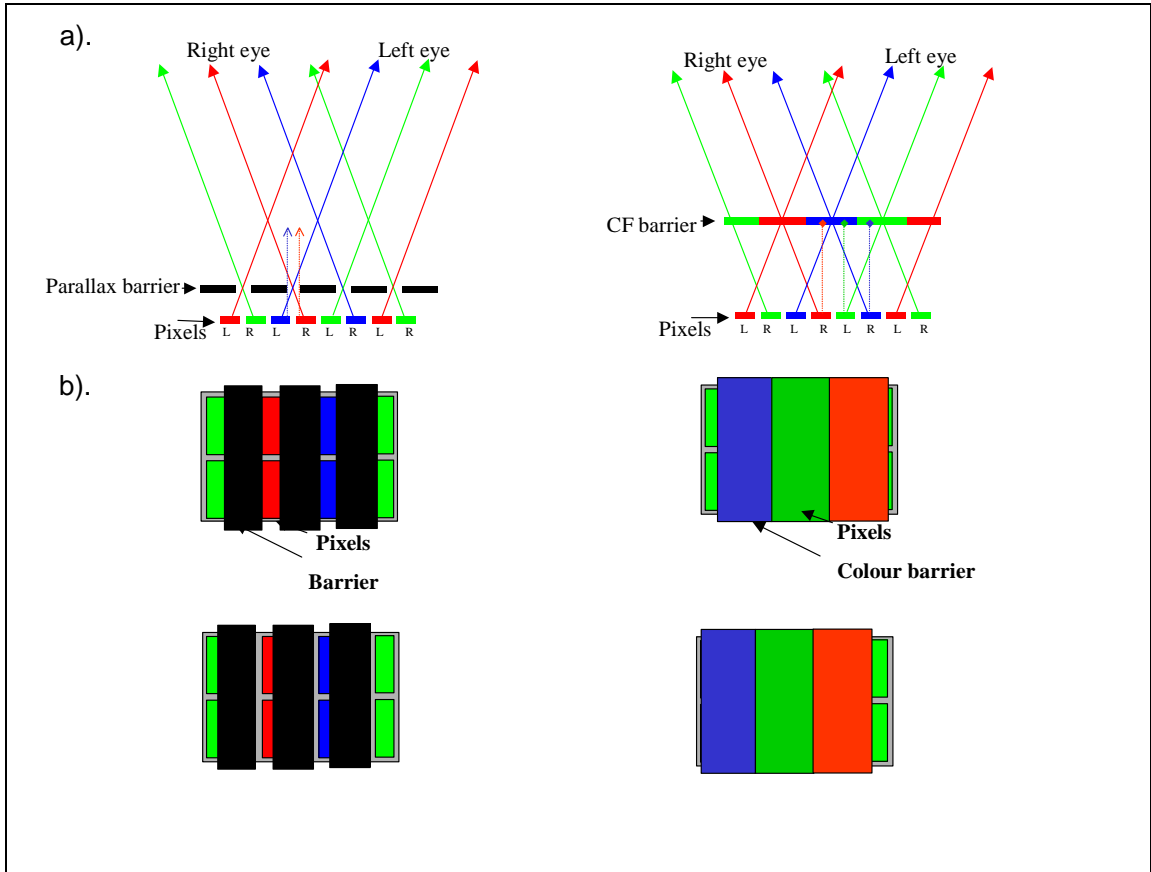


Figure 35: Diagrams a) show cross sections of the standard black and clear parallax barrier (left) and the Sanyo colour filter barrier (right). The Sanyo barrier can be placed 3 times further away than the standard barrier, it creates a black on axis view, and it has more head freedom and brightness. The dotted lines on diagrams a) show how light can pass on axis through the standard barrier, but on axis light is blocked by the colour filter barrier. Diagram b) shows how the increase in head freedom and brightness come about. The diagrams are of top views of the barriers, the diagrams at the top are shown as viewed from the left eye position. At the left eye position, the viewer can see all the apertures of all the left eye pixels, and so sees the full brightness from the pixels. However, as soon as the left eye moves slightly off the left eye position (as shown bottom left), the viewer only sees part of the pixel apertures, and so sees reduced brightness. This is not true for the colour filter barrier, because the barrier 'slits' are much wider than the pixel apertures. The viewer sees full brightness from a wider range of angle.

The Sanyo design has several advantages over a conventional parallax barrier;

- The on axis light (which would normally illuminate the image mixing region) is blocked, to create a black view on axis.

- The parallax barrier can be placed 3 times further away from the pixels than a black and white parallax barrier, whilst maintaining the same image separation.
- There is an improvement in brightness and head freedom.

These advantages are quantified in the figure below, based on simulated data using a model developed in Chapter 4.

The simulations are based on the use of a real LCD panel design (that with low electrical crosstalk shown in Chapter 3). The standard parallax barrier is designed to give a dual view display with head freedom suitable for a car (10 to 56 °), whilst the colour filter barrier is designed as described in the Sanyo patent (so that the barrier consists of equal proportions of red green and blue colour filters).

The simulations provide predictions of the head freedom and brightness that each design should produce if made. The predictions are shown below.

Dual view design	Barrier- pixel separation (um)	Head freedom (degrees)	Average brightness from 20 to 50 ° (arb)
Standard parallax barrier	80	10 to 56	1
Colour filter barrier	240	5 to 70	1.28

Table 2: A comparison of the key dual view parameters for a colour filter barrier and a conventional parallax barrier.

The colour filter barriers are better than the standard design in all the key parameters. However, the simulations above assume that perfect colour filters are used. That is to say, the red colour filters pass all the red light, and block all the blue and green light. The transmission spectrum of commercially available colour filters is shown below.

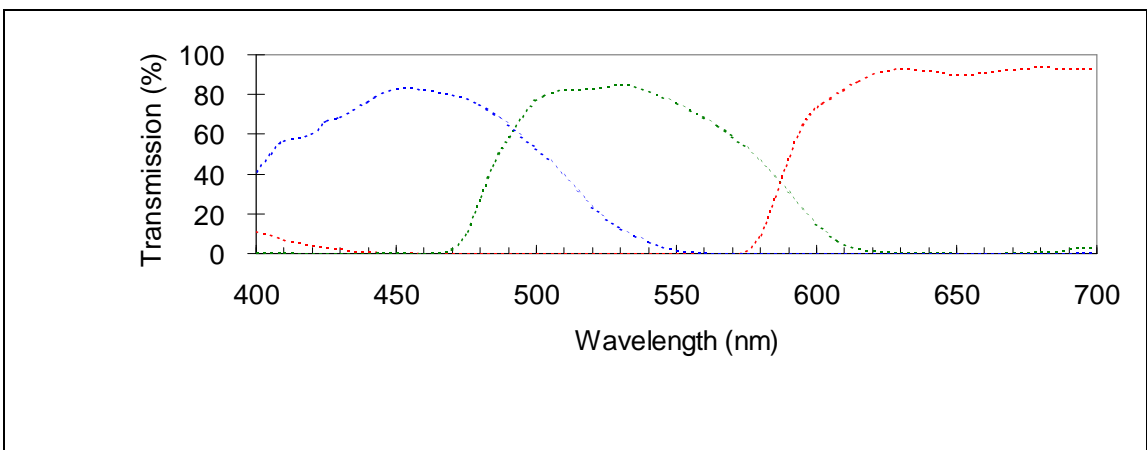


Figure 36: The transmission spectrum of colour filters used in an LCD television.

It can be seen that the colour filters only transmit about 80% of the colour they are supposed to. If these colour filters were used in the parallax barrier the brightness of the system would be reduced by 20%. With this loss factored into the simulations, the standard parallax barrier and colour filter barrier would have about the same brightness.

Also, note that the colour filter spectrums overlap. This means that (for example) light from a red pixel (at 600nm) could pass the green colour filter in the barrier and cause crosstalk. The colour filters must be made more narrow band to avoid crosstalk. Such filters exist (made by Kodak), but they have severely reduced transmission in the wavelength regions that they are supposed to transmit. About 50% of red light will pass the red filter. A device using these filters would be even dimmer than a standard parallax barrier.

However, if perfect colour filters could be produced this design would create a very high performance dual view display. No substantial work was done on colour filter barriers during this thesis for two reasons. Firstly, the research required to create good colour filters is outside my field of expertise. Secondly, it seemed easier to achieve a performance improvement by using micro-lenses, as described in chapter 4.

### *Directional backlights*

One method of making a black on-axis view, is to modify the backlight so that it does not emit any light on axis.

The figures below describe how a typical automotive LCD backlight works, and how it can be modified so that it does not emit on axis. The data in these figures is obtained by disassembly and measurement of a commercially available backlight. A paper describing the construction of a backlight is given in reference [35].

## Standard automotive backlight design - operation of the waveguide

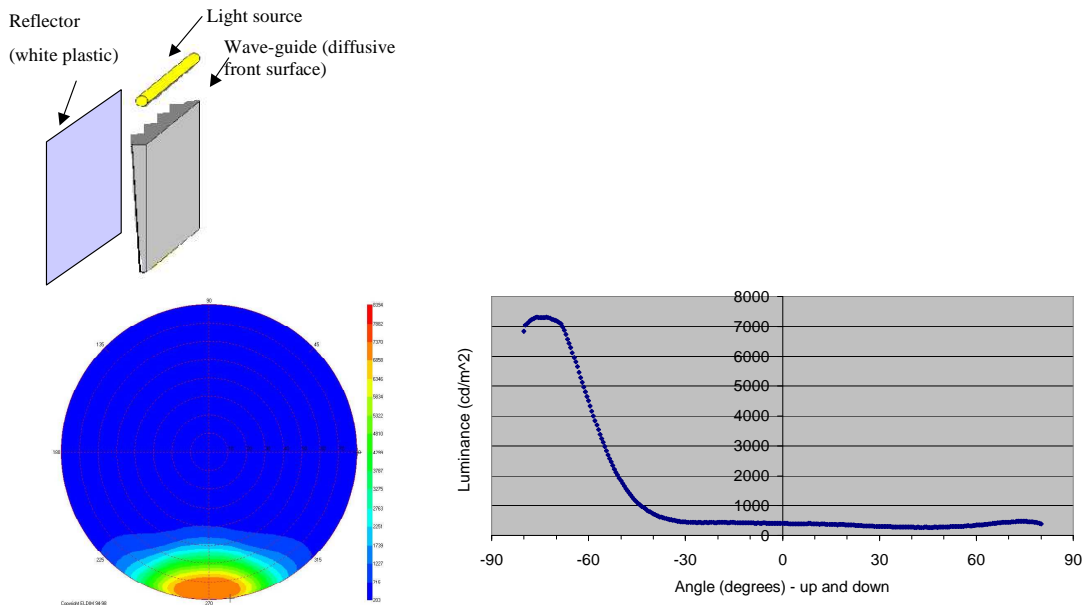


Figure 37: A typical automotive backlight for an LCD consists of a light source such as a cold cathode fluorescent tube (CCFL), and a waveguide. Light from the CCFL travels along the waveguide by total internal reflection (TIR), until it is extracted by scattering by the diffusive front surface of the waveguide. This provides a uniform illumination over the entire area of the waveguide. The light is emitted at high angles, but external micro-prism sheets shown in the next figures correct this. Any light extracted backwards is reflected to the correct direction by the reflector.

## Standard automotive backlight design - operation of the whole system

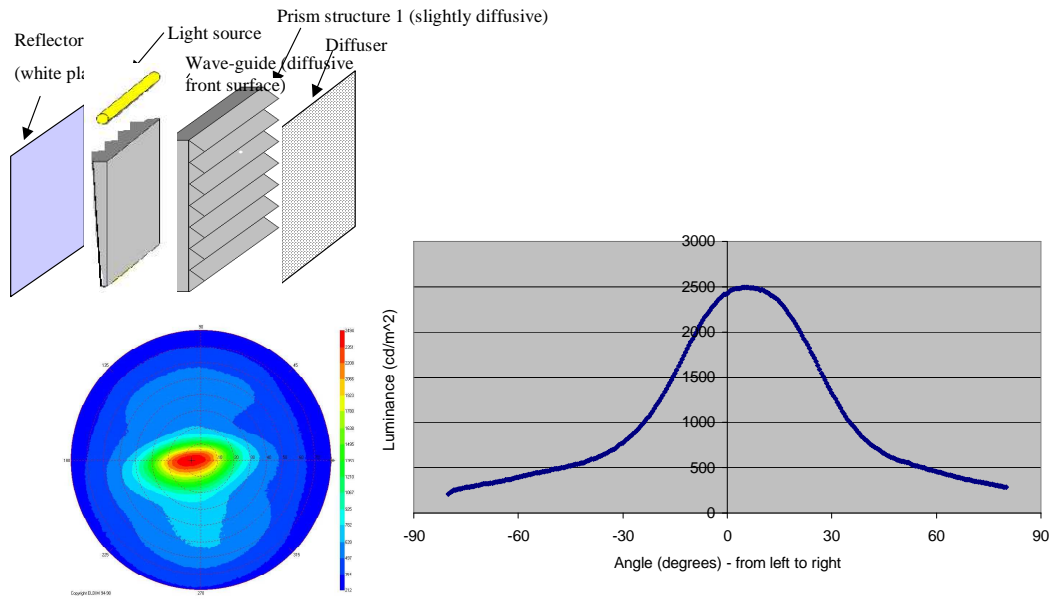
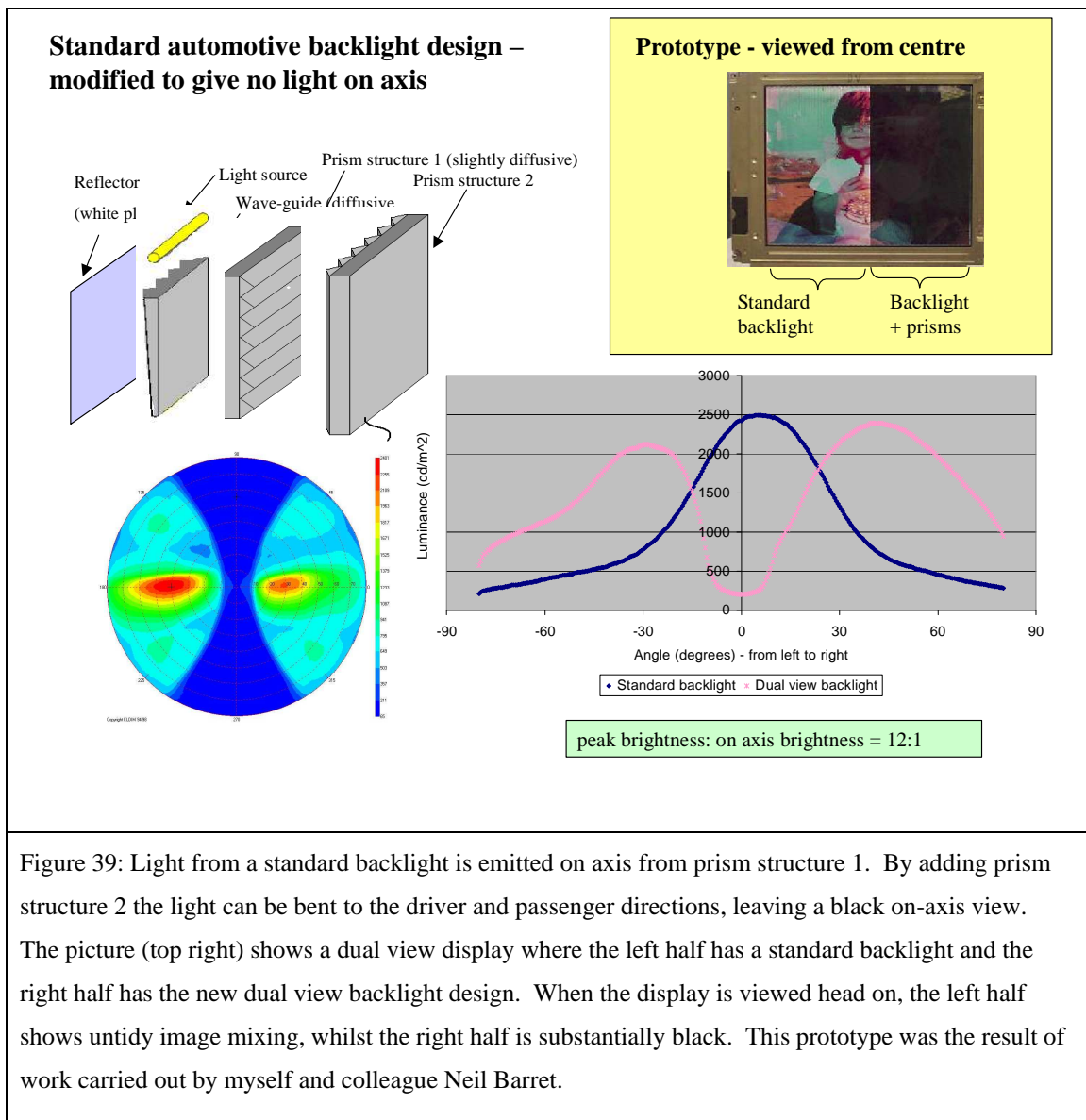


Figure 38: Light extracted from the waveguide, is extracted at high angles. The 'prism structure 1' bends this light on axis, so that it is suitable for illuminating an LCD display. The diffuser on the front of the backlight is to prevent the prism sheet structure being visible.



### Summary

Colour filter barriers have potential to create dual view with no on-axis image mixing. They might also give a brightness increase and require an advantageous larger barrier – pixel separation. The disadvantage with this design is the development of colour filter material that is needed to allow high transmission and low crosstalk. It seems as though current technology is a long way from meeting this criteria.

Double barriers are said to give an advantage in brightness and head freedom for 3D and so are likely to improve dual view displays. They also produce a black on-axis view. The key disadvantage is the cost in producing two parallax barriers <100 µm apart.

The new backlight design is wonderfully simple to create. It uses only off the shelf components to suppress the on-axis illumination, and as a bonus, the light that would

have illuminated the on-axis view is redirected to the driver and passenger to provide a boost in brightness for the driver and passenger. Its disadvantage is that the on-axis light suppression is not perfect. Overall, it is still advantageous and could be used. It is the subject of a patent application [36].

### **3.2.7 Crosstalk reduction**

Crosstalk is the interference that exists between the left and right views in a 3D or dual view display. In a display with high crosstalk the viewer of the left image would be able to see the right image faintly in the background.

It is shown in chapter 3 that crosstalk in dual view displays is a big problem. There is no known previous literature on dual view crosstalk.

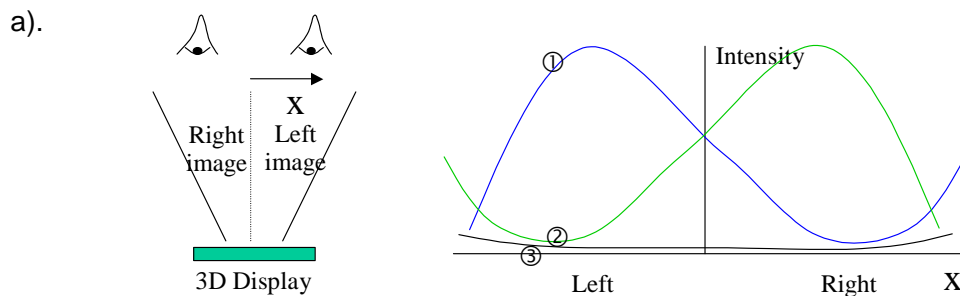
There has been some work done on the crosstalk in parallax barrier based 3D systems. This section describes two papers published in this area. The first paper described below is about measurement of crosstalk and the use of apodized parallax barrier slits to reduce crosstalk by diffraction. The paper proposes that the main cause of crosstalk in a 3D display is diffraction from the parallax barrier. The paper suggests that theoretically, apodized slits in the barrier would reduce crosstalk by about 30 times.

The second paper is one of many about removing crosstalk by image processing. The paper also includes some assessment of the level of crosstalk that is tolerable in a 3D display. It concludes that crosstalk should be kept below 1 to 2%.

#### *Soft edge barriers by Sharp*

This paper [14] defines a measurement technique that can be used to quantify crosstalk from the parallax barrier system. The technique involves measuring the percentage of light that deviates from one view to the other, as described in the figure below.

### Measurement of crosstalk



b).

Label on graph	Display output	What the measurement shows
①	Left image = white, Right image = black	This gives the maximum intensity possible to the left eye.
②	Left image = black, Right image = white	Theoretically no light should go to the left eye, but actually some light will be measured due to; a). Light leakage (crosstalk) from the right to left eye. b). Light from the imperfect black of the pixels for the left eye.
③	Left image = black, Right image = black	Measurement only of the light from the imperfect black of pixels for the left eye.

c).

$$\text{Crosstalk} = \frac{\text{②} - \text{③}}{\text{①} - \text{③}} \times 100$$

Figure 40: Crosstalk is the percentage of light from one view leaking to the other view. The measurements and calculations above show how crosstalk is defined when measuring crosstalk in the left image.

Diagrams a) sketch the intensity measurements that need to be made for different outputs from the 3D display. Table b) describe their purpose. Equation c) is used to derive the crosstalk. It is the ratio of the light leakage from the right image into the left image, but note that the imperfect black level of the LCD is subtracted out from the result so that it does not change the crosstalk ratio.

The crosstalk in a typical parallax-barrier based 3D system at the best eye position is 3%.

The paper hypothesises that the cause of this crosstalk is diffraction. In this paper the diffraction from the parallax barrier was modelled and found to tie in with experimental crosstalk measurements.

The paper goes on to predict that the amount of crosstalk caused by the parallax barrier will be highly dependent on the sharpness of the edges of the slits. For example, if the transmission of the barrier goes from opaque to transparent sharply as it moves from barrier to slit then this produces a wide diffraction pattern and consequently more

crosstalk. If the transition is smoother then the diffraction will not spread so widely and less crosstalk will be produced.

This prediction is consistent with experimental results for a slightly soft edged barrier (whose pitch is 182  $\mu\text{m}$ , slit width is 48  $\mu\text{m}$ , and transition between opaque and transmissive occurs over a region of about 3  $\mu\text{m}$ ). The slightly soft edged barrier has a crosstalk of 2.3% which is slightly lower than the crosstalk from a harder edged barrier which was about 2.7%.

The main suggestion (theoretical) is that an edge whose transmission decreases over as much as 10  $\mu\text{m}$  could have crosstalk as low as 0.1 %. This would be a very useful result. All of this work is quoted from reference [14].

### *Crosstalk removal by image processing*

This paper [37] studies crosstalk in 3D displays. It presents results of subjective tests carried out to determine the image quality of 3D images. It concluded that for high quality 3D, crosstalk should be 'no greater than around 1 to 2%'.

Video processing is stated as a method of countering crosstalk – that is to say using image processing to compensate for the effects of crosstalk (as described in more detail in Chapter 3).

### **3.3 Alternative methods of image splitting**

There are a few other techniques that can be made to create auto stereoscopic displays. These include holographic image splitting, and optical combination of the images from two LCD panels [38,39], but these require cumbersome optics.

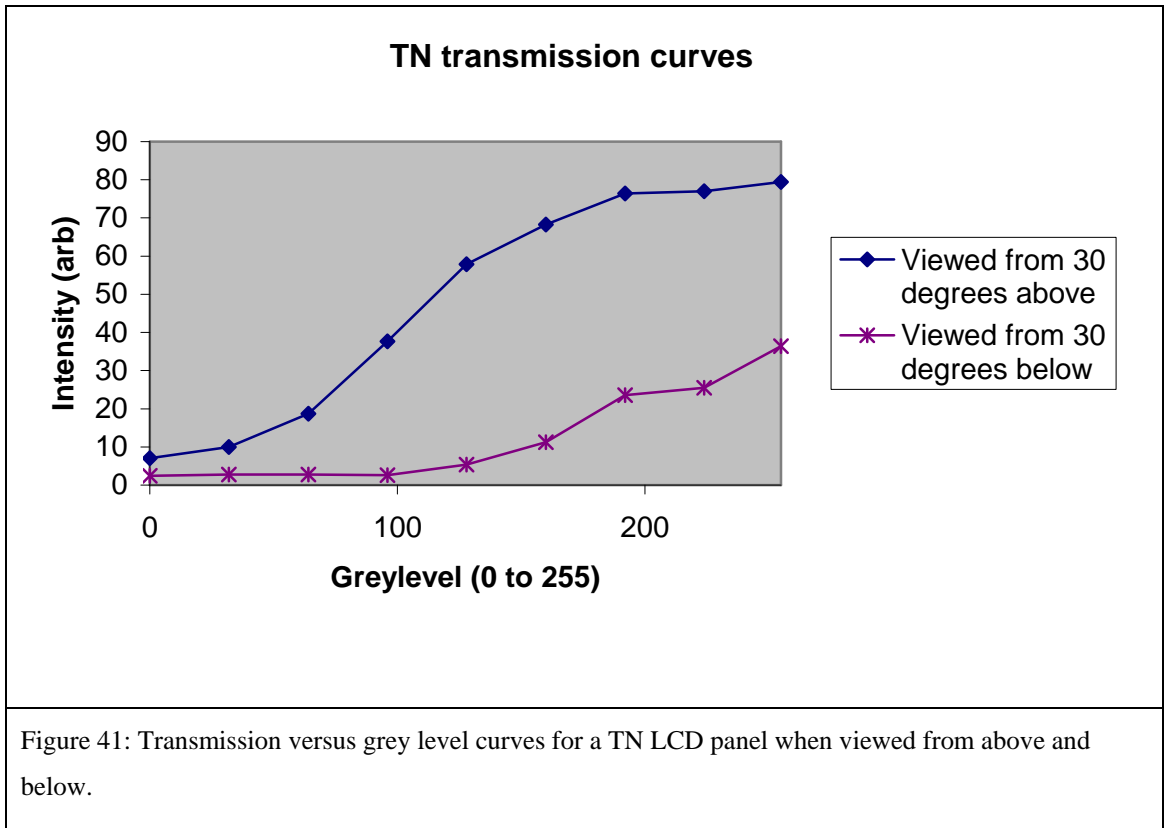
One method stands out as radically different and potentially advantageous. It was presented by Toyama University, Japan, in 1998 [40].

It is based on the use of LC viewing angle properties. An LCD is created where some pixels have view angle characteristics such that an image can only be seen from them from the right direction, and some pixels are similarly made for the left view.

The key advantage of this system is that no additional optics need be added to the LCD, thus keeping it thin, and potentially simple to make.

We managed to create a similar device with a new LC mode that worked for dual view [41]. This work is described below, which also illustrates how the device works.

An LC mode with the suitable characteristics was discovered by accident whilst working on a rotated pixel parallax barrier design for a twisted nematic (TN) LCD. It was found that when the intensity versus grey level curves are measured on a TN LCD at  $\pm 30^\circ$  in the vertical direction, the following graphs are obtained.



To create a dual view display, firstly we rotated the panel  $90^\circ$  so that the ‘up and down’ grey level curves become ‘right and left’ grey level curves. See how we can put an image to the left by using 0 to 128, and that if these pixels are viewed from the right then the image appear substantially black, the image cannot be seen.

Similarly we may make an image that is visible to the right by using data levels 128 to 255, and when we view these pixels from the left, the pixels all appear substantially white such that the image can not be seen.

Therefore, we can interlace left image data (which uses the 0 to 128 data range), and the right image data (using the 128 to 255 data range) to create a dual view image. When the viewer looks from the left, he sees an image from the left pixels, and the right image pixels all look black. When the viewer looks from the right, they see an image from the right pixels and the left image pixels all look white.

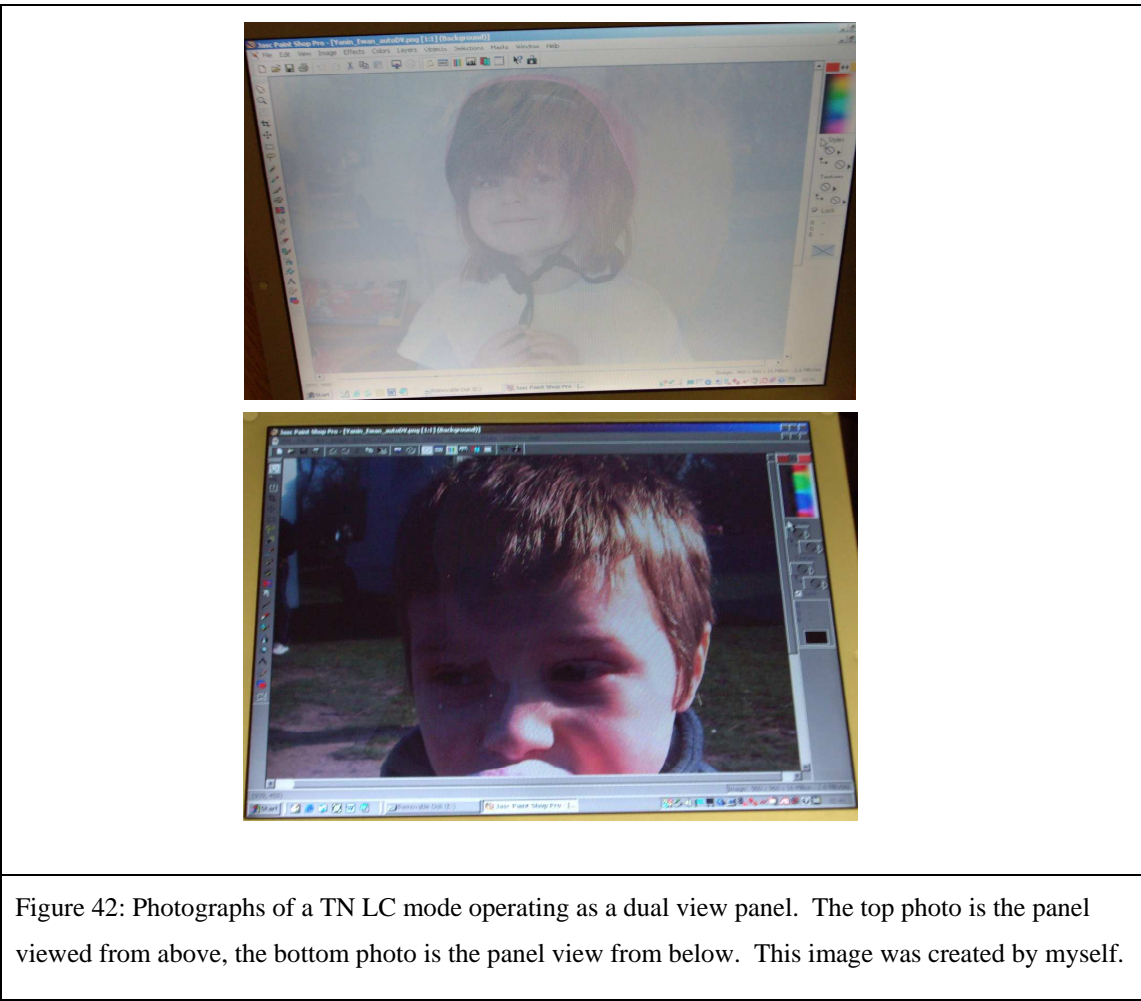


Figure 42: Photographs of a TN LC mode operating as a dual view panel. The top photo is the panel viewed from above, the bottom photo is the panel view from below. This image was created by myself.

This device is not perfect, there are problems with contrast ratio and brightness. For example, when the viewer looks at the left image the right pixels show white. This washes out the contrast of the display. When the viewer looks at the right image, the display becomes very dim, since the transmission of the LC mode at this angle is very low.

The contrast and brightness of the device is shown in the following table.

		<b>Brightness (cd/m<sup>2</sup>)</b>	<b>Contrast ratio</b>
Rotated TN used to create dual view, viewed at 30 °.	Left	51	17
	Right	104	15
Normal single view TN	Left	200	43
	Right	216	38

Table 3: A comparison of brightness and contrast ratio between a standard TN LC mode and an LC mode that can create dual view due to its natural viewing angle characteristics.

The contrast and brightness of the dual view LC mode are significantly degraded compared with that of a conventional TN.

The dual view head freedom of the LC mode is good when viewing the right image, but poor for the left image.

		Approx. head freedom, subjectively assessed.
Rotated TN used to create dual view	Left view	20 °
	Right view	40 °

Table 4: A table showing the head freedom produced by an LC mode that creates dual view due to its natural viewing angle characteristics.

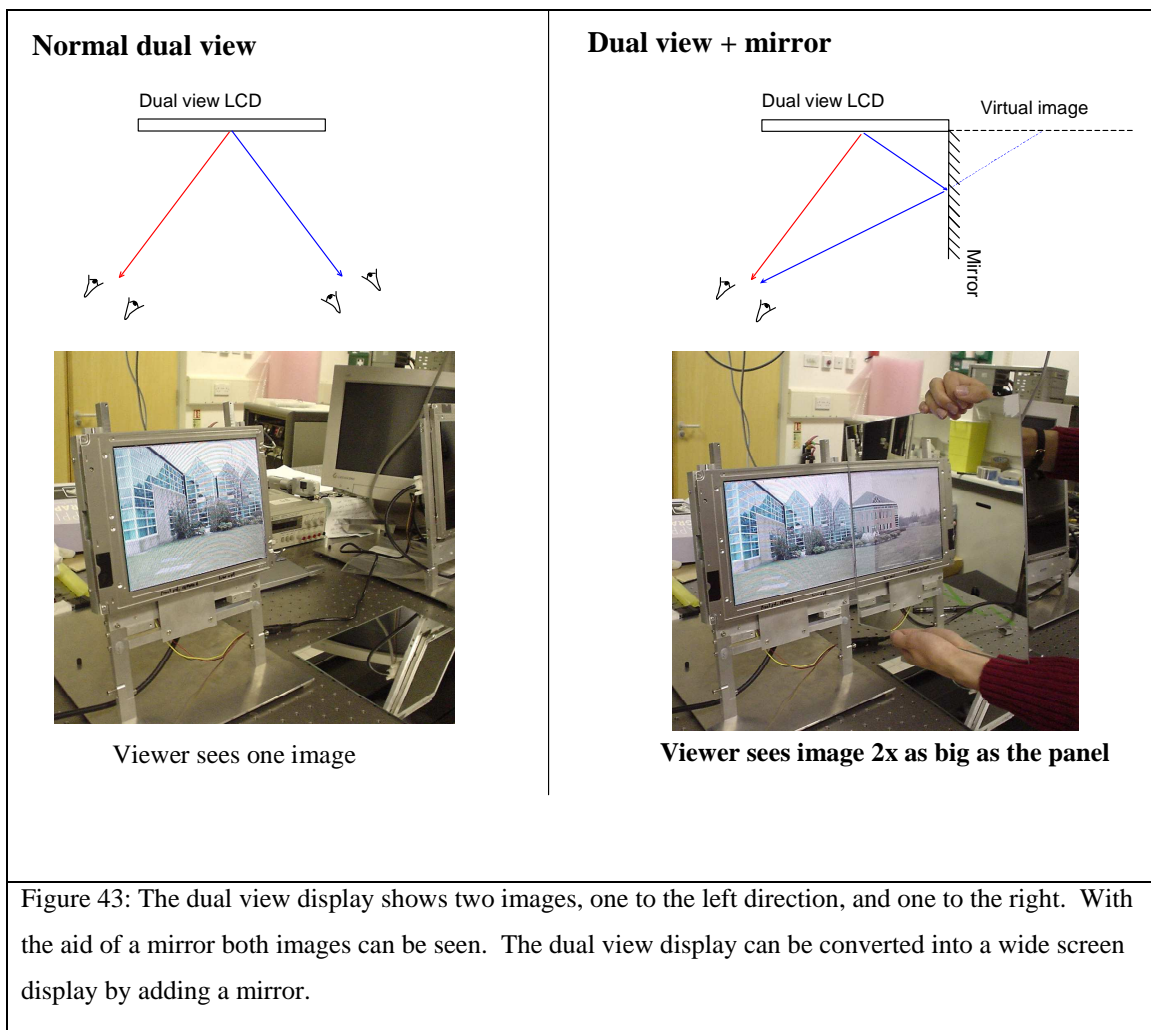
The device is therefore not usable as a display. A colleague spent some considerable effort to optimise the LC mode however they failed to make a significant improvement. It is difficult to get the viewing angle properties of an LC mode to change rapidly as a viewer moves from the left to right image, but then maintain high brightness and contrast ratio for a wide range of head movement within the left or right view.

A good LC mode may exist, but for the reasons above it seems unlikely, such that no more mention of this method is made in the thesis.

## **4. A spin off application for dual view**

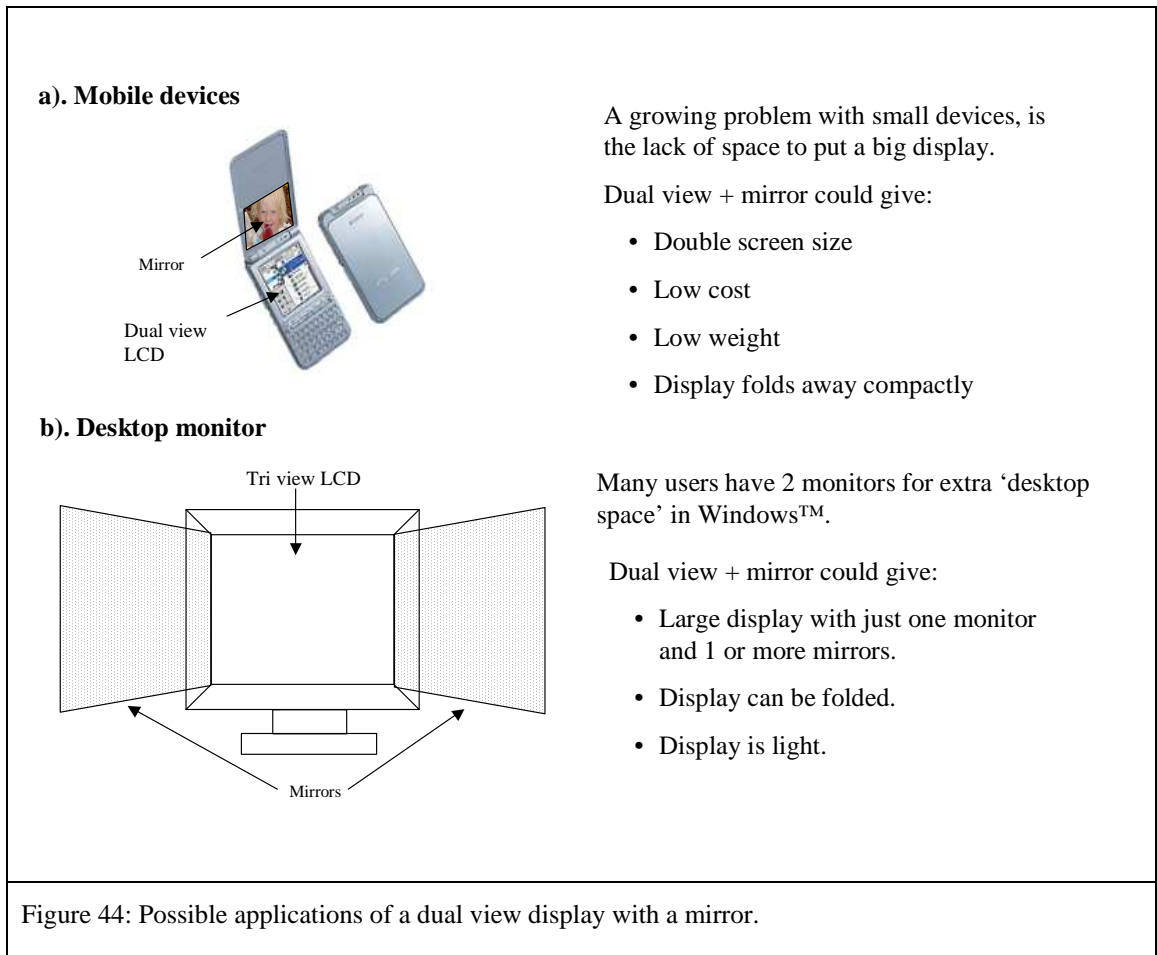
Notice that if a mirror is held up to a dual view display, it enables one person to see both images – the first directly from the panel, and the second, reflected back from the

mirror. The reflection from the mirror shows a different image from the screen than that seen by viewing it directly. This peculiar effect is illustrated in the following figure.



Effectively, by adding a mirror, the active area of the screen is doubled. This could have applications in mobile technology where the need for big displays on small devices is high. A patent application has been made on this subject, [42].

The following figure suggests a couple of applications of this technology.



## 5. Summary

In this chapter literature on dual view and 3D displays was reviewed. Literature on dual view displays is limited, but many ideas from 3D display research could be extended to help dual view displays.

In particularly, a design was found that enabled a prototype dual view display to be easily fabricated and tested. From this the key problems that plague dual view were seen to be;

- The small barrier – pixel separation that makes manufacture difficult.
- Crosstalk between the left and right views.
- The brightness and head freedom of each image.

No satisfactory solutions to these problems were found in the literature, and so these problems are the subject of investigation in the rest of the thesis.

Chapter 2 investigates a new design, which enables dual view to be created on LCDs with thick glass substrates. In Chapter 3, the causes of crosstalk in a parallax barrier

dual view system are investigated. In Chapter 4, a method for brightness and head freedom enhancement is designed and tested.

# **CHAPTER 2: CREATING DUAL VIEW WITHOUT THIN GLASS**

# Introduction

Chapter 1 described the current literature about dual view displays, and some new ideas that might be used to create dual view. It concludes that none of these ideas provide a satisfactory solution.

This chapter is about the development of a new lens system that should create a good dual view effect. By this it is meant that the dual view can be constructed by adding optical elements far away from the displays pixels making manufacture easier. The interlacing pattern that is used is NP1, which will give high image quality. The system does not use time multiplexing, so it is compatible with conventional LCDs, rather than needing expensive high switching speed displays.

This idea is currently patent pending in application GB03020362.7.

In this chapter the design is optimised theoretically and then tested experimentally. The results demonstrate that it should be possible to create a high quality dual view display by using this technique, but it is superseded by the design investigated in Chapter 3.

Section 1 describes the basic concept of the system.

Sections 2 to 4 are about optimising all of the design parameters to try to minimise crosstalk, and maximise brightness and head freedom. The system is initially optimised by assuming that the lenses in the system act as simple thin lenses. This allows variations of the design to be understood conceptually which allows us to deduce which particular configuration of lenses is optimum. The design is then fine-tuned using optical ray tracing.

Section 5 describes the experimental testing of the system. This verifies that the device functions broadly in line with the predictions made by theory, with the exception that the simulated results underestimate crosstalk. Crosstalk in the system is its main downfall.

## 1. The basic operation of the design

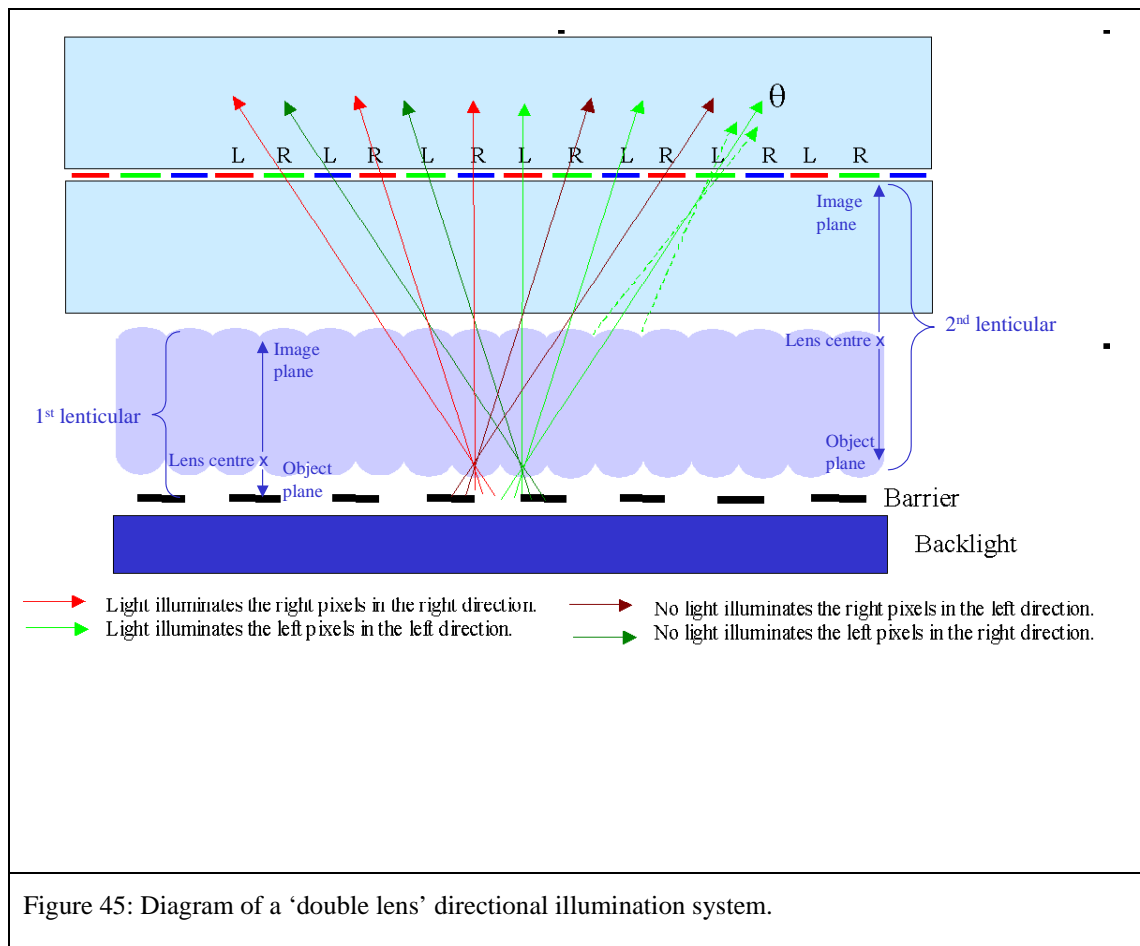
The aim of this invention is create a dual view display by illuminating each pixel directionally.

The pixels on the display contain information for the left and right images interwoven with each other so that the first, third, and fifth ... columns show the left image and

other columns show the right image. This is the same as for a parallax barrier dual view system.

The optics of the system then aim to illuminate the left pixels with light travelling only in the left direction and illuminate the right pixels with light travelling only in the right direction thereby creating a multi view display.

The following figure shows the operation of the system.



The basic operation of the design is as follows. The barrier and 1<sup>st</sup> lenticular create regions of directional illumination. That is to say the lenses of the 1<sup>st</sup> lenticular alternate between emitting light travelling in the left direction and right direction.

The 2<sup>nd</sup> lenticular images the 1<sup>st</sup> lenticular to the pixels with 1 to 1 magnification, creating directional illumination.

Note that in the preceding figure each pixel is illuminated with a small angular cone of light (labelled  $\theta$ ) from one lens of the 2<sup>nd</sup> lenticular. This angular range is insufficient to create good head freedom. Figure 46, shows how the whole system combines to create

more head freedom. Head freedom of the design is only limited by aberrations that may occur at high angles.

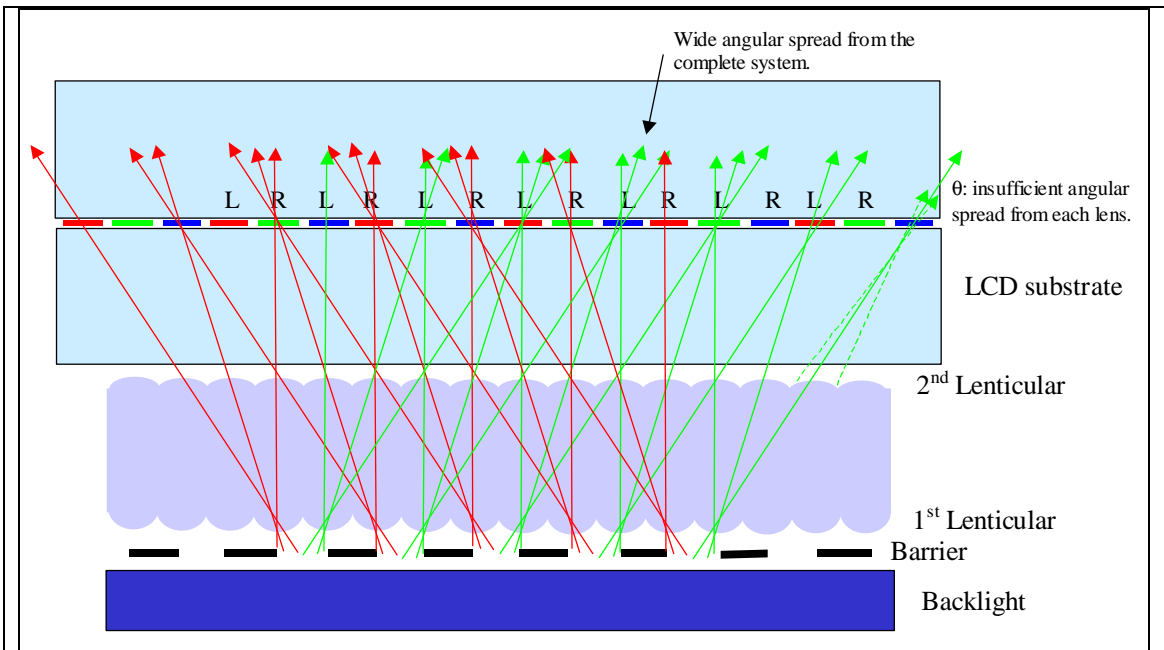


Figure 46: Each individual lens of the 2nd lenticular illuminates the pixels with a small angular range  $\theta$ . The cumulative effect of all the lenses produces a much wider angular spread, giving excellent head freedom.

This design has many potential advantages over a parallax barrier method.

The slit widths in a parallax barrier design must be very narrow to produce enough head freedom; a typical aperture ratio for a dual view parallax barrier might be 30%. The aperture ratios of the barrier used in the double lens design could be up to 50% (as described in section 2). This means that less light is absorbed and the system is more efficient.

We will see that assuming the lenses act as simple thin lenses the design will not create a region of image mixing on-axis. Instead the on-axis view will be black.

All of the optics can be added on to a standard LCD panel. In contrast to the parallax barrier design which requires the barrier to be 80  $\mu\text{m}$  from the pixels which requires difficult modification of the base LCD panel. It should be possible to make the optics in the double lens system function when positioned at any distance from the panel.

These potential advantages provide the motivation for optimising, constructing and testing the system to find out if they can really be achieved.

## 2. Design optimisation (theoretical)

Section 1 described a particular design of the lens system. Many variations of this design are possible which all work on the same basic principle.

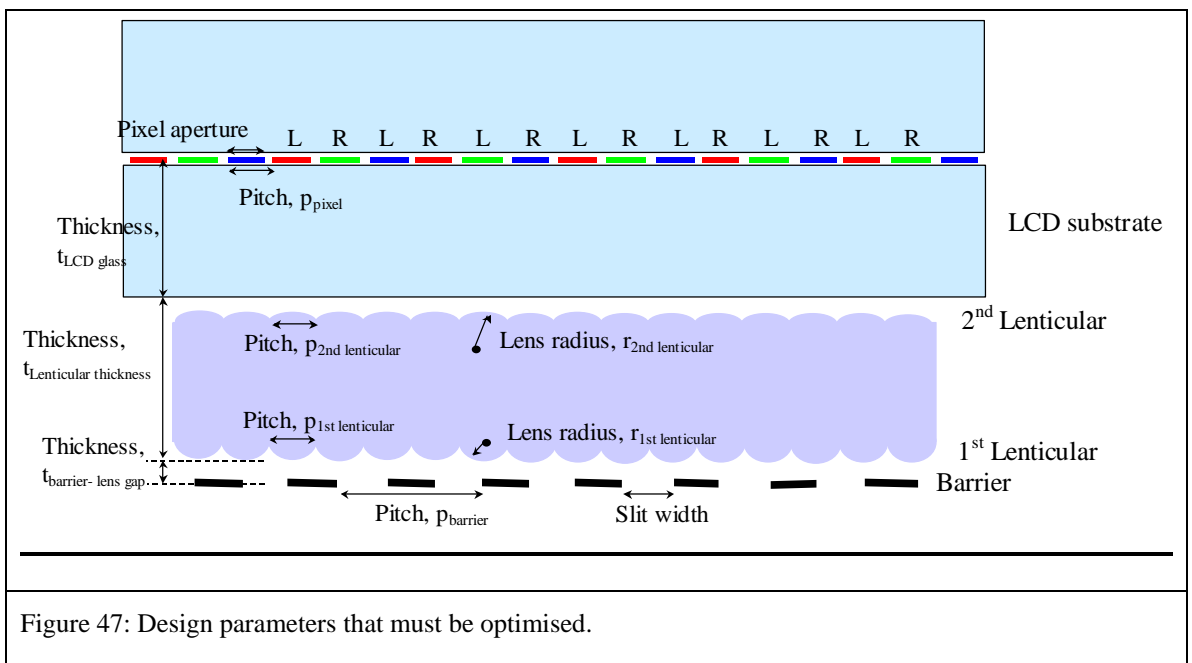
Here ‘variations’ is used to describe the discrete variables in the system that may be changed. For example section 1 shows the design where the 2<sup>nd</sup> lenticular pitch is equal to the first lenticular pitch. In fact the design works when the 2<sup>nd</sup> lenticular pitch is equal to  $n$  times the 1<sup>st</sup> lenticular pitch, where  $n=1,2,3, \dots$

The design in section 1 is thought to be optimum. This section runs through the thought processes that were used to reach that conclusion.

The result is a table of formulae that determine the optimum parameters of the lens system, given the design parameters of LCD panel.

In fact these formulae only provide a first approximation of the lens design parameters because they are based on thin lens formulae. These approximations provide a starting point for sections 3 to 5, which go on to optimise the system further by use of ray tracing.

Figure 47 below shows the design parameters that must be optimised. They are listed in table 1.



Section number	Parameter
2.1	Lenticular thickness
2.2	Radius of lenses
2.2.1	- 2 <sup>nd</sup> lenticular
2.2.2	- 1 <sup>st</sup> lenticular
2.3	Barrier – lens separation
2.4	Pitches
2.4.1	- 1 <sup>st</sup> lenticular
2.4.2	- Barrier
2.4.3	- 2 <sup>nd</sup> lenticular
2.5	Alignment of elements

Table 5: The section number in which each parameter of the double lens dual view system is discussed.

## **2.1 Lenticular thickness**

The thickness of the lenticular is governed by the need for the 2<sup>nd</sup> lenticular to image the 1<sup>st</sup> lenticular to the pixels. A 1:1 magnification is optimum because this makes the system as thin as possible for a given lens power. For a 1:1 magnification: LCD glass thickness = Lenticular thickness.

### **2.1.1 Other magnification ratios**

Other designs exist where the 1<sup>st</sup> lenticular is magnified by 3x, 5x, 7x, and so on. However, upon sketching such designs, it is seen that these designs are thicker, and offer no obvious advantage.

Designs exist where magnification is any arbitrary value, e.g. 0.8x. These designs are thicker, and there are disadvantages. The lens pitches must be modified so that they are not the same size as the pixels. In this case translational symmetry is lost (described further in section 2.4). Without translational symmetry the lens pitch would move in and out of phase with the pixel pitch causing brightness variations.

## **2.2 Radii of the lenses**

### **2.2.1 Radius of the 2<sup>nd</sup> lenticular**

The 2<sup>nd</sup> lenticular lenses must focus the 1<sup>st</sup> lenticular lenses to the pixels.

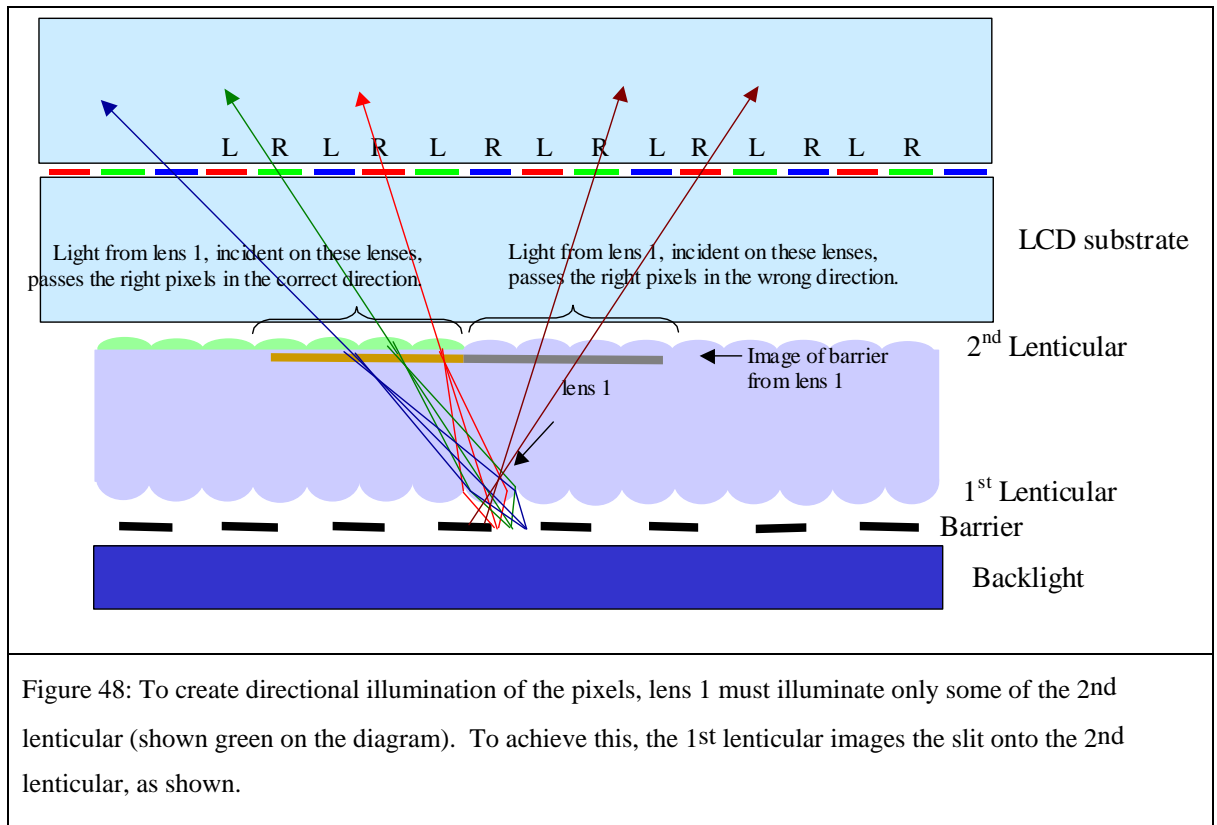
From formulae for thin lenses, and for 1:1 imaging:

$$\text{Focal length of 2nd lenticular} = \frac{\text{LCD glass thickness}}{2}$$

$$\text{Radius of 2nd lenticular} = \frac{\text{LCD glass thickness} \times (n_{\text{air}} - n_{\text{lent}})}{2 \times n_{\text{glass}}}$$

### 2.2.2 Radius of the 1<sup>st</sup> lenticular.

The function of the 1<sup>st</sup> lenticular lenses is to illuminate only the correct lenses on the 2<sup>nd</sup> lenticular, as shown in Figure 48.



To do this the 1<sup>st</sup> lenticular must image the barrier to the 2<sup>nd</sup> lenticular. Therefore from the thin lens formulae:

$$\text{Focal length of 1st lenticular} = \frac{t_{\text{barrier-lens gap}} \times t_{\text{Lenticular thickness}}}{t_{\text{barrier-lens gap}} + t_{\text{Lenticular thickness}}}$$

$$\text{Radius of 1st lenticular} = \frac{t_{\text{barrier-lens gap}} \times t_{\text{Lenticular thickness}} \times (n_{\text{lenticular}} - n_{\text{air}})}{(t_{\text{barrier-lens gap}} + t_{\text{Lenticular thickness}}) \times n_{\text{lent}}}$$

## **2.3 Barrier –1st Lenticular separation**

The distance between the barrier and 1<sup>st</sup> lenticular is a trade off between two effects.

1. If the barrier is too far from the lenses, there will be secondary windows.
2. If the barrier is too close to the lenses, the lenses must have a very high focal power. This will induce aberrations – light is likely to be sent in the wrong directions, causing crosstalk.

The 1<sup>st</sup> lenticular lenses are very powerful, so thin lens formulae are unlikely to give satisfactory estimates of the secondary window positions.

Knowing that we need an image separation angle of approximately +/- 30° implies that the barrier should be approximately one pixel pitch away from the 1<sup>st</sup> lenticular based on thin lens formulae, however final optimisation is best done by ray tracing.

## **2.4 Pitch for each element**

Translational symmetry requirement

The pitches of all elements are fixed to some extent by a requirement for translational symmetry. In Figure 48 the light from one slit in the barrier is considered as it propagates through the system. It is assumed that the light from other slits in the barrier will perform identically because the system has ‘translational symmetry’. That is to say a position on the system is the same as another position in the system that is one barrier pitch away in the horizontal direction. If this was not the case then the performance of the display would vary across its length which would not be desirable. Therefore the display system must have ‘translational symmetry’.

Translational symmetry requires that under every left and right pixel there are  $n$  or  $1/n$  lenses and slits, where  $n=1,2,3\dots$

For example, the translational symmetry on in figure 1, is created by having, under each left and right pixel pair:

- Exactly two 1<sup>st</sup> lenticular lenses.
- Exactly two 2<sup>nd</sup> lenticular lenses.
- Exactly 1 slit pitch.

So, each element will have the same alignment for each left right pixel pair, giving the system translational symmetry.

### **2.4.1 1<sup>st</sup> lenticular pitch**

In addition to translational symmetry, the 1<sup>st</sup> lenticular pitch is fixed as below. The 1<sup>st</sup> lenticular must be imaged to the pixels by the 2<sup>nd</sup> lenticular with a 1:1 magnification ratio. For each 1<sup>st</sup> lenticular lens to be aligned with the pixels, the pitch of the 1<sup>st</sup> lenticular must be the same as the pixels.

A 1<sup>st</sup> lenticular pitch that is equal to the pixel pitch is the only value that satisfies the requirements for translational symmetry and design functionality.

### **2.4.2 Barrier pitch**

The barrier pitch should be a multiple of the 1<sup>st</sup> lenticular pitch so that the two elements remain aligned across the display. Different multiples could be used to provide different effects, for example dual view is created by using a barrier pitch of 2 times the 1<sup>st</sup> lenticular lens pitch. A triple view device could be created by using a barrier pitch of 3 times the 1<sup>st</sup> lenticular lens pitch, and so on.

### **2.4.3 2<sup>nd</sup> lenticular pitch.**

#### *Introduction*

This pitch depends on three criteria;

1. Translational symmetry requires that there must be 0.5, 1, 2, 3, ... lenses per left right pixel pair.
2. Design functionality requires that there are 1, 2, 3, ... lenses per left right pixel pair.
3. A requirement for low aberrations means that low f-number lenses are the best.

These factors imply that there should be two 2<sup>nd</sup> lenticular lenses for each left right pixel pair. Each factor is explained in more detail below.

#### *Translational symmetry*

This requirement is explained in section 2.4.

#### *Design functionality*

The table below shows how the design would function for the pitches that meet the requirement for translational symmetry.

<i>Lens pitch</i>	<i>A 1<sup>st</sup> lenticular lens is imaged to</i>
2 x Left right pixel pair	every 4 <sup>th</sup> pixel: e.g. every other Left pixel
1 x Left right pixel pair	every 2 <sup>nd</sup> pixel: e.g. every Left pixel
0.5 x Left right pixel pair	every pixel: i.e. every left and right pixel. This is no good, each lens should be imaged only to the left pixels.

Table 6: How different 2<sup>nd</sup> lenticular lens pitches image the 1<sup>st</sup> lenticular.

In summary, the pitch of the 2<sup>nd</sup> lenticular lens can be n times the barrier pitch where n = 1, 2, 3, ... .

### *Low aberrations*

When considering perfect thin lenses there are no advantages/ disadvantages of larger 2<sup>nd</sup> lenticular lens pitches (for example, 1 x, or 2 x, ... , a left right pixel pair, should give the same results).

When aberrations are considered, lenses with a higher f-number would be thinner and more like a thin lens and so would be expected to have fewer aberrations. Therefore the pitch of the 2<sup>nd</sup> lenticular should be as small as possible.

### *Summary for 2<sup>nd</sup> lenticular pitch*

When all above considerations are taken into account, the optimum 2<sup>nd</sup> lenticular pitch = 1x the pitch of a left right pixel pair.

### **2.4.5 Summary for all element pitches**

For a given pixel pitch, p;

- Barrier pitch = 2 x p
- 1<sup>st</sup> lenticular pitch = p
- 2<sup>nd</sup> lenticular pitch = p

## **2.5 Alignment of elements**

The 1<sup>st</sup> and 2<sup>nd</sup> lenticular, barrier, and pixels can all be aligned in different ways which give subtly different results. This section shows all the ways that the elements can be aligned and explains which is best.

The dual view display output should be symmetrical which implies that the alignment of the elements should also be symmetrical. Figure 49 shows all the symmetrical ways of aligning the barrier and lenses.

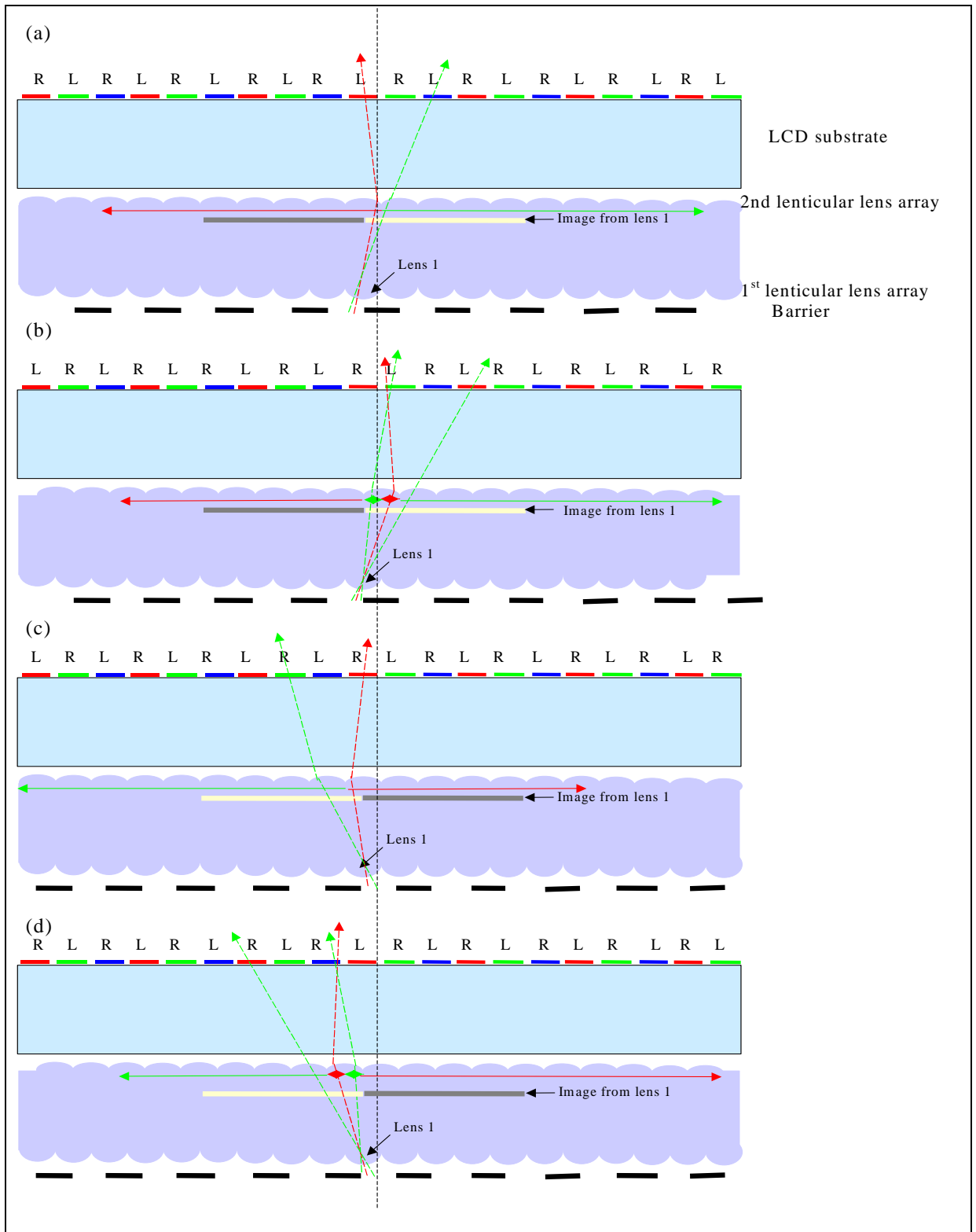


Figure 49: (a) to (d) show different ways of aligning the lenses and barrier. Solid red and green lines show which parts of the 2<sup>nd</sup> lenticular contribute/ do not contribute to crosstalk respectively. The dotted lines show example ray paths through each of the parts.

Figure 49b and Figure 49d, have a double sized central image mixing region compared with Figure 49a and Figure 49c. This makes it preferable to align the centres of the 2<sup>nd</sup> lenticular lenses directly above the centres of the 1<sup>st</sup> lenticular.

## **2.6 'Barrier pitch correction'.**

In section 2 it has been assumed that the dual view output must be uniform across the screen, therefore pitches are exact integer multiples. In fact, it is usual to add 'barrier pitch correction' to a dual view display (as described in chapter 1). This feature could be added to this design but it has not been considered here.

## **2.7 Summary table**

In section 2 all the design parameters have been calculated based on approximate analytical calculations. These provide starting points for computer optimisations performed in section 3.

The parameters and the optimum values are in the following table.

Design Parameters	Optimum value	Comment
LCD glass thickness	0.5mm	Given by panel designers.
$p_{\text{pixel}}$	0.110mm	Given by panel designers.
Pixel aperture	$\sim 0.9 \times p_{\text{pixel}}$	Given by panel designers.
$t_{\text{Lenticular thickness}}$	$\sim t_{\text{LCD glass}}$	
Radius of 1 <sup>st</sup> lenticular lenses	$\sim \frac{t_{\text{barrier-lens gap}} \times t_{\text{Lenticular thickness}} \times (n_{\text{lenticular}} - n_{\text{air}})}{(t_{\text{barrier-lens gap}} + t_{\text{Lenticular thickness}}) \times n_{\text{lent}}}$	Images barrier to 2 <sup>nd</sup> lenticular
Radius of 2 <sup>nd</sup> lenticular lenses	$\sim \frac{\text{LCD glass thickness} \times (n_{\text{air}} - n_{\text{lent}})}{2 \times n_{\text{glass}}}$	Images 1 <sup>st</sup> lenticular to pixels
$t_{\text{barrier-lens gap}}$	$\sim p_{\text{pixel}}$ (very approximate)	Optimisation is best done by ray tracing.
$p_{\text{barrier}}$	$2 \times p_{\text{pixel}}$	
$p_{\text{1st lenticular}}$	$1 \times p_{\text{pixel}}$	
$p_{\text{2nd lenticular}}$	$1 \times p_{\text{pixel}}$	
Alignment between 1 <sup>st</sup> and 2 <sup>nd</sup> lenticular	Lenses aligned in phase.	
Slit width	$0.5 \times p_{\text{barrier}}$	

Table 7: Formulae for the optimum parameters in the double lens dual view system based on thin lens approximations.

### 3. Optimisation of design by ray tracing

Section 2 gives a rough approximation for all the design parameters in the system.

These are based on thin lens approximations.

This section is about creating a design procedure to optimise the system based on results from ray tracing. An optimisation technique based on ray tracing should be more

effective than the results obtained by the thin lens approximations of section 2 because ray tracing takes into account the effects of lens aberrations which section 2 ignores.

The design procedure consists of; ray tracing the system, assessing the performance of the system, repeating these steps whilst iterating the design parameters towards the best system.

Section 3.1 is about choosing how to assess the performance of the system – to iterate the design parameters towards the best solution some criteria is needed to rate how good each design is.

Section 3.2 is about simplifying the task of optimisation. The system is split up into parts that may be independently optimised.

Section 3.3 summarises the resulting ‘design procedure’.

### **3.1 Success criteria for the design procedure**

To iterate the design parameters towards their best values, the computer must be able to rate each system it tries. Some success criteria is needed.

Two success criteria are used. The first is simple enough for a computer to use, the second is based on human inspection which is used as a final check that the results are sensible.

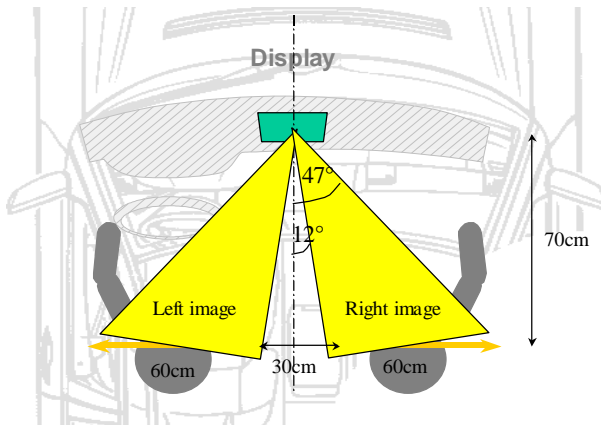
#### **3.1.1 Success criteria for computer optimisation**

The key requirement for a dual view display is low crosstalk over a wide viewing range. This requirement is stated in more detail in Figure 50 which shows the angular regions over which crosstalk must be low.

It was estimated that crosstalk of less than 2% would be acceptable for a dual view display.

### Head freedom for automotive dual view

(a) Minimum head freedom requirements



(b) Preferable head freedom requirements

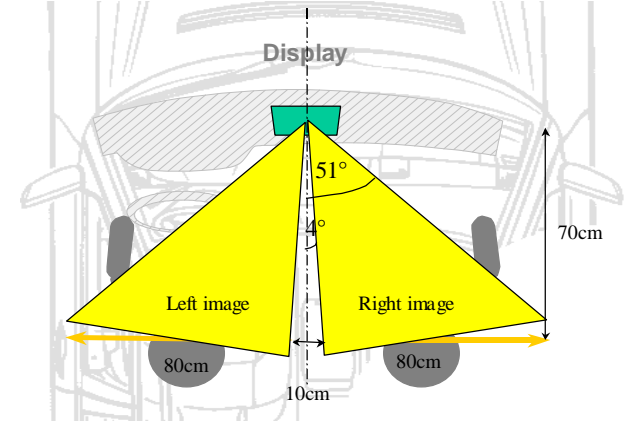


Figure 50: Within the yellow cones the image quality should be comparable with an ordinary LCD. Brightness must be uniform, and more importantly image mixing must be low. The dimensions of the cones (a) were provided by a car manufacturer. These specifications must be met for the display to be useable. The dimensions of the cones (b) exceed the minimum requirements, which is desirable for car manufacturers. These cones were determined by myself to be more desirable to the user. Cones (b) are used as the success criteria in this section in order to try for a high quality dual view display.

In the success criteria for the computer, the better the design, the lower the average crosstalk is in the angular range of 4 to 51 °.

The ray tracing is performed by the commercial software ‘Zemax’ (version of 11<sup>th</sup> June 2004). Figure 51 helps to show what it does. Light is assumed to be rays that obey geometric optics. Numerous rays with random directions are created at the slit in the barrier. The path of these rays through the lens system is calculated, so their direction is known after they exit the system.

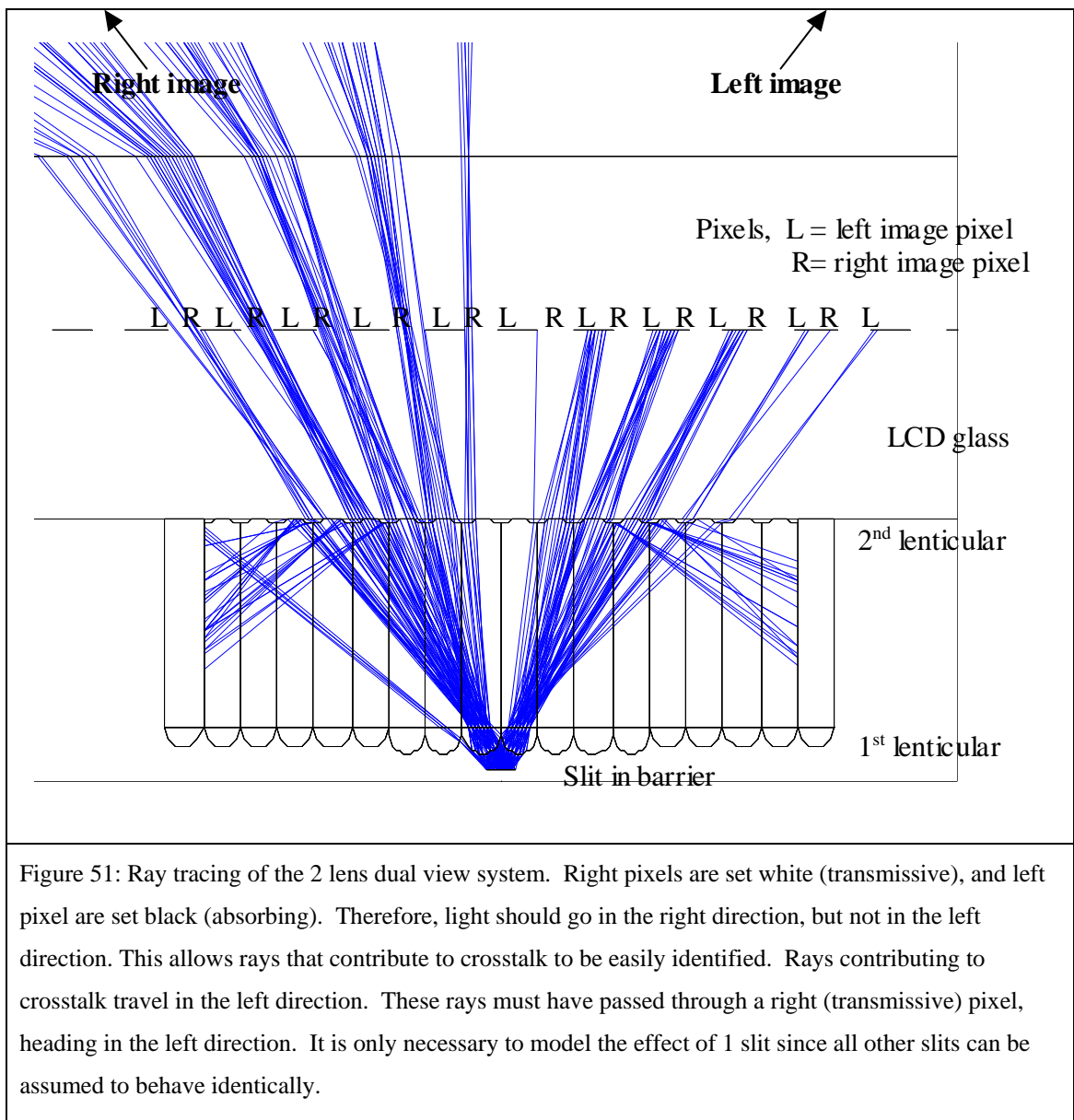
Fresnel reflections in the system are assumed to be negligible. This helps to speed up the calculations. The light source is assumed to consist of three wavelengths one red, one green, and one blue. The refractive indices of the materials and the dispersion are taken into account. The lenses are made from acrylic and the glass is a glass made by Schott called BK7. The dispersions of these materials are sourced from a database provided by the Zemax software, and this is assumed to be accurate.

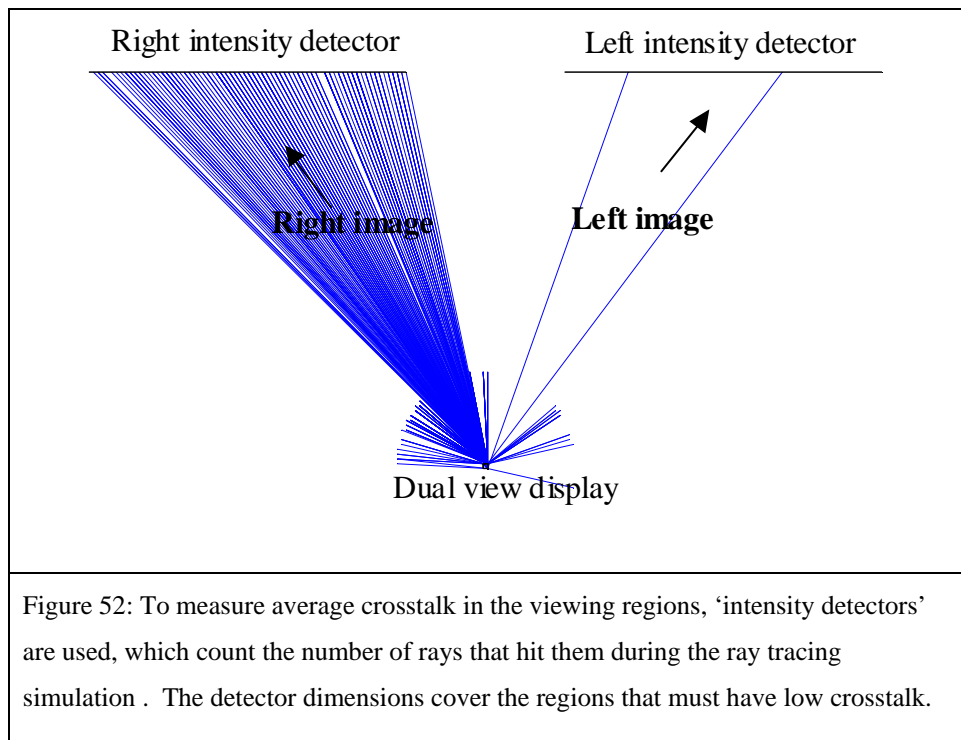
Figure 52 shows how the success criteria (average crosstalk from 4 to 51 °) is calculated by the software.

- The direction of light rays exiting the system is known from the ray tracing calculations. The computer counts the number of rays (A) that exit at 4 to 51 ° on the left side. No rays should exit at this angle since the dual view system is

set to be black in this direction. Any rays that do exit in this direction are due to crosstalk.

- The computer counts the number of rays (B) that exit at 4 to 51 ° to the right. There should be many of these rays since the dual view display is set to look white in this direction.
- Thus by dividing the number of rays (A) by the number of rays (B), average crosstalk from 4 to 51 ° is deduced.





### 3.1.2 Success criteria for use in manual inspection

The success criterion above (average crosstalk) is computationally simple for the optimisation routine but it has problems. The crosstalk uniformity is not considered and the brightness uniformity is not considered.

To check that crosstalk and brightness uniformity are satisfactory, measurements of crosstalk and brightness versus angle are needed. This measurement is performed by counting the number of rays exiting the display at many angles, for example, from 1 – 2°, from 2 to 3 ° and so on. Figure 54 shows an example of this type of graph

### 3.2 Method for optimisation.

There are 5 design parameters to optimise.

- 3 thicknesses/ separation distances
- 2 focal lengths

Two methods were considered to optimise these variables. All use an optimisation routine of ray tracing software Zemax, based on an “actively damped least squares method”. This iterates the design parameters towards local minima in the success criteria.

*Method 1: Iterate all 5 variables until the best system is found.*

This is potentially the best optimisation technique, however it would take too long for a computer to optimise so many variables.

*Method 2: Optimise in 2 steps.*

Step 1: Optimise 1<sup>st</sup> lenticular and barrier (2 variables: barrier – lens separation, and 1<sup>st</sup> lenticular radius).

Step 2: Optimise the rest of the system (3 variables: 2<sup>nd</sup> lenticular radius, lenticular thickness, and LCD glass thickness).

Breaking the system into two independent systems is faster (there are less combinations of variables to try). Therefore the optimisation algorithm works more effectively.

*Success criteria for step 1*

The function of the 1<sup>st</sup> lenticular and barrier is to illuminate only the correct lenses of the 2nd lenticular (as described in section 1). This is what the success criterion is based on for step 1. The success criteria is shown in more detail in Figure 53.

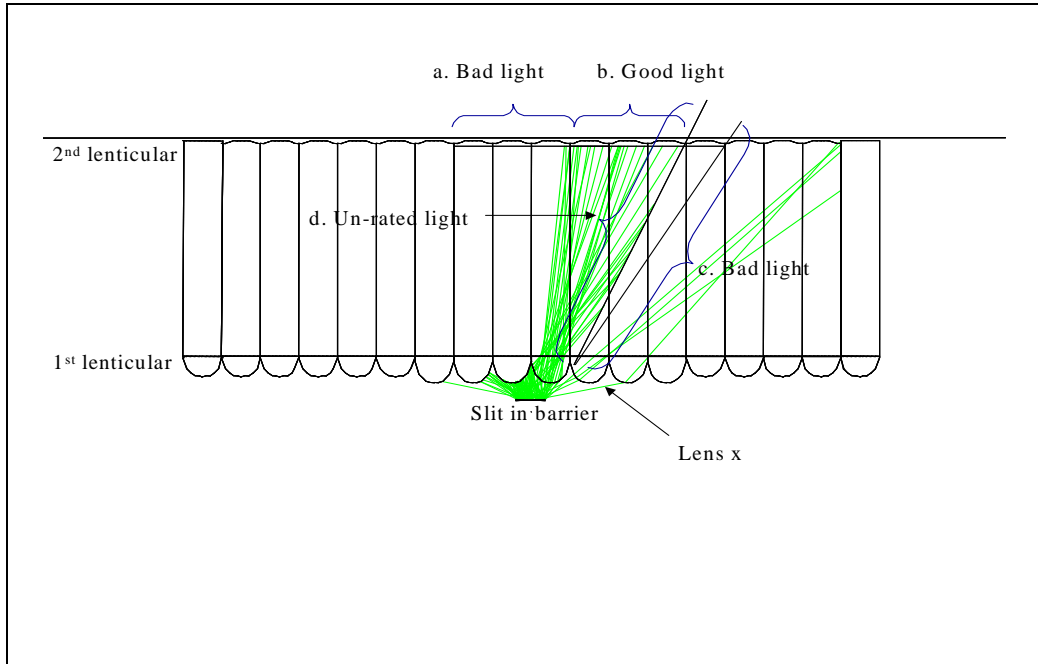


Figure 53: The success criteria for the 1<sup>st</sup> lenticular and barrier. (b) The 1<sup>st</sup> lenticular should illuminate only the correct lenses of the 2<sup>nd</sup> lenticular- labelled good light. (a) Light that illuminates the wrong lenses of the 2<sup>nd</sup> lenticular is ‘bad light’. (c) Light from the slit can also hit a different lens on the 1<sup>st</sup> lenticular (labelled ‘lens x’ on the diagram). Light could pass through lens x and then hit the 2<sup>nd</sup> lenticular in the correct place, however in this case the light would be travelling at the wrong angle and would cause crosstalk. Therefore this is intercepted by detector c and this is counted as ‘bad light’. (d) Light intercepted as ‘un-rated light’ will leave the display at >50°. This light does not contribute to the viewing zone so is disregarded in the success criteria.

$$\text{Success criteria for the 1st lenticular and barrier} = \frac{\text{Total bad light}}{\text{good light}}$$

Light which does not influence the viewing regions of the display (un-rated light) is disregarded in the calculation. A system that meets the success criteria should have a black central window and low crosstalk from secondary windows of the 1<sup>st</sup> lenticular – barrier system. It is assumed that the optimisation routine will not change the design so drastically that the amount of good light is radically changed, and therefore the brightness of the device should not be compromised.

### **3.3 Summary of the design procedure**

The result of sections 2 and 3 is a design procedure that can be followed to find the optimum parameters for the lens system.

The design procedure is summarised below;

Step 1: Calculate the design parameters approximately by the analytical equations of section 2.

Step 2: Optimise the 1<sup>st</sup> lenticular to illuminate the correct lenses on the 2<sup>nd</sup> lenticular by ray tracing and iteration.

Step 3: Optimise for low average crosstalk from 4 to 51 ° by ray tracing and iteration.

Step 4: Check crosstalk, and brightness uniformity are satisfactory by human inspection.

## **4. Modelling results and analysis**

In section 3 a design procedure was developed which should effectively optimise all the design parameters in the system.

In this section the design procedure is implemented and the results are seen to be poor.

The reasons for the poor performance are assessed and the design procedure is modified to counter the problems. This process is repeated until a good design procedure is achieved.

The final design, according to simulations, provides dual view with low crosstalk, good head freedom, and high brightness.

### **4.1 Design procedure implementation**

The design procedure of section 3.4 was run with the following inputs from the panel designers:

- Pixel pitch = 110  $\mu\text{m}$
- Pixel aperture = 99  $\mu\text{m}$
- LCD glass thickness = 0.5 mm

The main result was that after optimisation the 1<sup>st</sup> lenticular success criteria (used in step 2 of the design procedure) yielded a result of 21%. That is to say 21% of the light

from the 1<sup>st</sup> lenticular hit the 2<sup>nd</sup> lenticular in the wrong place, so that it would go on to cause crosstalk.

This level of ‘bad light’ was much more than expected, and is likely to cause an unacceptable amount of crosstalk. Due to the high focal power of the 1<sup>st</sup> lenticular lenses the lenses suffer significant aberrations and this disperses the light into unintended directions.

## **4.2 Design procedure version 2**

As a solution to this, the slit width in the barrier was reduced to reduce the spread of light from the 1<sup>st</sup> lenticular lenses. The performance of the 1<sup>st</sup> lenticular and barrier system are given below for different slit widths.

<i>Slit width (% of barrier pitch)</i>	<i>1<sup>st</sup> lenticular success criteria</i>
50%	21%
37.5%	4.1%
25%	3.2%

Table 8: How well the barrier and 1<sup>st</sup> lenticular perform in the double lens dual view system for different slit apertures.

Although 50% slits are satisfactory for ideal thin lenses, 50% slits width is too large for thick spherical lenses. Small slit widths decrease the ‘bad light’ that will cause crosstalk, but they also reduce the brightness of the system by absorbing more of the light from the backlight.

A slit width of 37.5% of the barrier pitch appears to be a good trade off between achieving low crosstalk and high brightness. Therefore, in version 2 of the design procedure, an empirical slit width of 37.5% of the barrier pitch will be used.

## **4.3 Design procedure version 2 implementation**

Version 2 of the design procedure was run with the following inputs:

- Pixel pitch = 110  $\mu\text{m}$
- Pixel aperture = 99  $\mu\text{m}$
- LCD glass thickness = 0.5 mm

The resulting average crosstalk from 4 to 51  $^{\circ}$  was 0.7%. Figure 54 shows the brightness and crosstalk uniformity of the display.

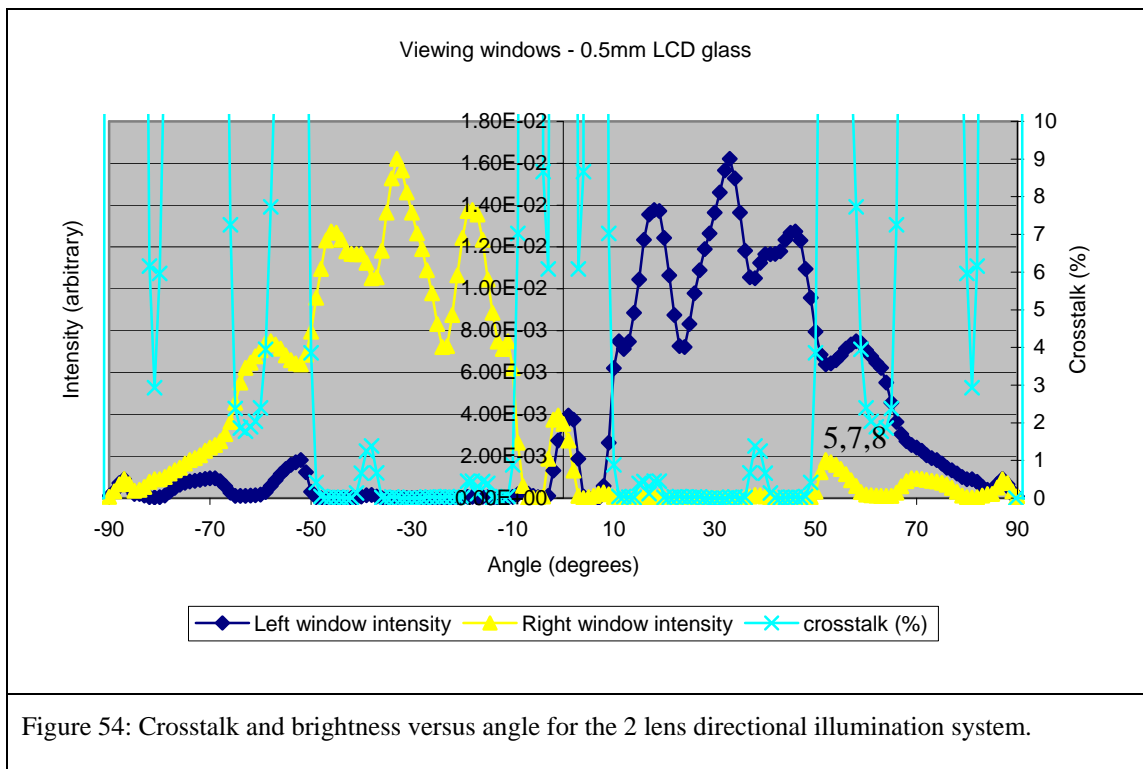


Figure 54: Crosstalk and brightness versus angle for the 2 lens directional illumination system.

The key points are firstly that crosstalk from 10 to 50 ° is satisfactory, (less than, but close to the estimated limit of 2%). Secondly the brightness uniformity is very poor, (~ +/-30% variation) between 10 to 50 °. Thirdly image-mixing exists on axis but the low on axis brightness may make this problem less noticeable.

### **4.3 Why is the performance of the system not perfect?**

Figure 54 shows that crosstalk exists. It is necessary to understand the origin of the crosstalk so that the crosstalk rays might be eliminated. This is the purpose of this section.

The ray paths which cause crosstalk can be shown by the ray traced diagram Figure 55. No light should exit the display to the left since the left image is set to be black. In the crosstalk ray diagram only rays from 0 to 52 ° to the left are shown, so all the rays on this diagram are contributing to crosstalk.

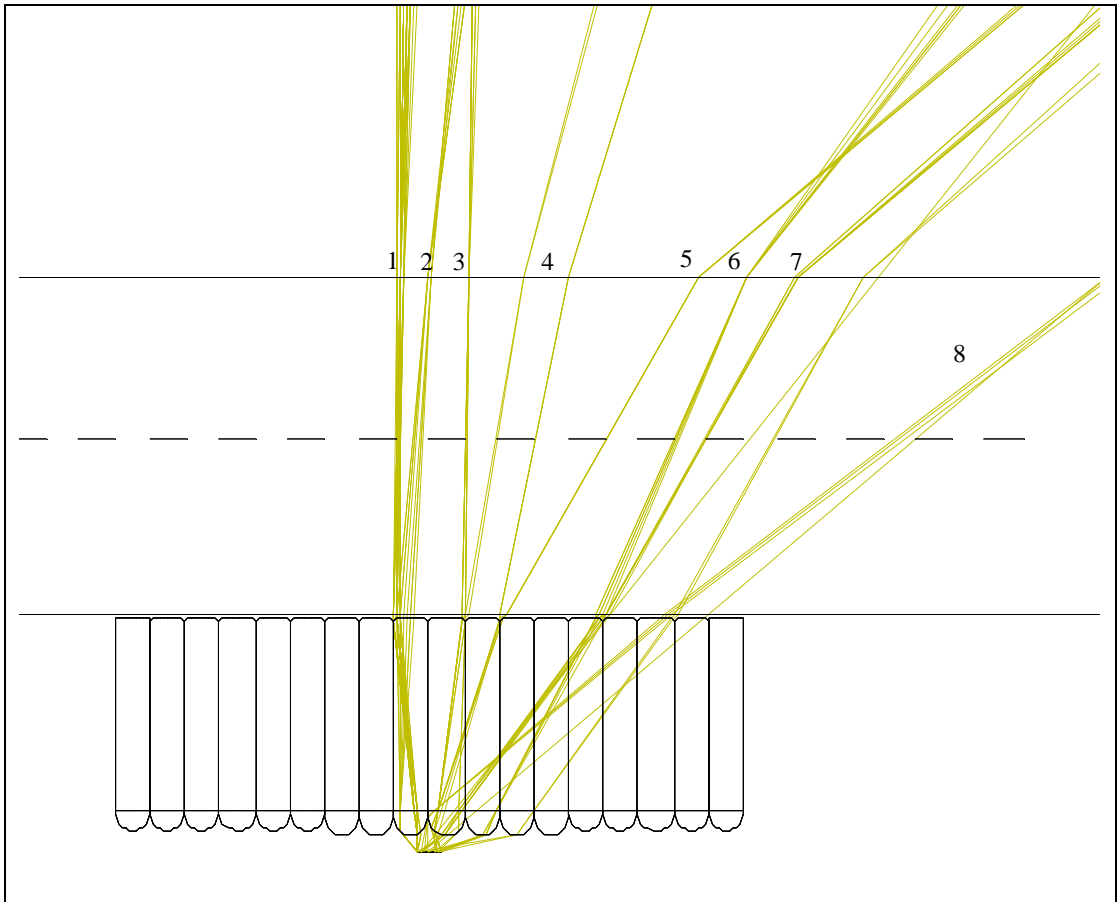


Figure 55: This diagram shows only rays passing through the system that cause crosstalk between 0 and 52 °. These problematic rays are labelled 1 to 8. The reason and effect of their problematic trajectory is given in the table below.

Ray label	Reason for problematic trajectory	Effect of problematic ray
1, 3	1 <sup>st</sup> lenticular aberration	On axis crosstalk.
2	1 <sup>st</sup> lenticular aberration	Crosstalk at ~ 8 °.
4	2 <sup>nd</sup> lenticular aberration	0.5% Crosstalk at ~ 15 °.
6	2 <sup>nd</sup> ary window of barrier and 1 <sup>st</sup> lenticular.	1.2% Crosstalk at ~ 40 °.
5, 7	2 <sup>nd</sup> lenticular aberration	~20% Crosstalk at ~ 50 °.
8	Due to 1 <sup>st</sup> and 2 <sup>nd</sup> lenticular aberration	

The effects of the problematic rays are also labelled on the graph (Figure 54). The main points from this analysis are that firstly problematic rays due to 1<sup>st</sup> lenticular aberrations

mostly cause on-axis crosstalk and secondly that problematic rays due to the 2<sup>nd</sup> lenticular aberrations cause a small amount of crosstalk in the viewing region. 2<sup>nd</sup> lenticular aberrations make the display unusable at angles  $> 50^\circ$ .

In addition the brightness of the display changes by up to 50% with angle. This would be noticeable to the user as an increase and decrease in display brightness as they move from one angle to another. This is not desirable. The origin of these brightness changes are thought to be Moiré fringe that are created by the 2<sup>nd</sup> lenticular array and the display pixels. From observations of the device in chapter 3 it is known that the human eye is not particularly sensitive to slow variations in brightness, and so these variation may be acceptable. It may also be possible to minimise them by careful choice of lens- pixel separation for example. For now this problem is ignored and the main problem of crosstalk is studied. If the crosstalk problem can be solved then it will be worth studying the brightness variations.

#### **4.4 Design procedure version 3**

The design procedure needs to be modified again to reduce the amount of crosstalk in the system from levels that are on the borderline of acceptability.

One method of reducing the crosstalk may be to increase the thickness of the LCD glass. This is because, from section 4.3, it is known that crosstalk occurs due to aberrations in the 1<sup>st</sup> and 2<sup>nd</sup> lenticular lens arrays. Increasing the LCD glass thickness will lower the focal power needed from the 1<sup>st</sup> and 2<sup>nd</sup> lenticular lenses and therefore I propose that aberrations should be reduced.

The 1<sup>st</sup> lenticular lens should focus the slit to the 2<sup>nd</sup> lenticular array, by increasing the thickness of the LCD glass we increase the thickness of the 1<sup>st</sup> to 2<sup>nd</sup> lenticular separation, which decreases the focal power requirement of the 1<sup>st</sup> lenticular.

The 2<sup>nd</sup> lenticular should focus the 1<sup>st</sup> lenticular to the pixels, so again increasing the LCD glass thickness will decrease the focal power requirement of the 2<sup>nd</sup> lenticular.

The system works perfectly if it is based on ideal lenses such as those approximated by the thin lens equations. In the thin lens equations the rays are assumed to be near the optical axis of the lens and making small angles with it. As the focal power of a lens is increased the rays are bent further away from the optical axis and so the system will deviate further from an ideal lens. Therefore I propose that lenses of lower focal power will suffer fewer aberrations.

Thus in version 3 of the design procedure the thickness of the LCD glass is made to be as thick as is acceptable, this was chosen to be 1mm.

#### **4.5 Design procedure version 3 implementation**

The tables below show a comparison of versions 2 and 3 of the design procedure. The only difference between the two design procedures is the thickness of the LCD glass.

	<b>Design procedure version 2 (LCD Glass thickness = 0.5mm)</b>	<b>Design procedure version 3 (LCD Glass thickness = 1mm)</b>
Slit width (% of barrier pitch)	1 <sup>st</sup> lenticular success criteria	1 <sup>st</sup> lenticular success criteria
50%	21%	14.2%
45%	-	5.1%
37.5%	4.1%	0.35%
25%	3.2%	-

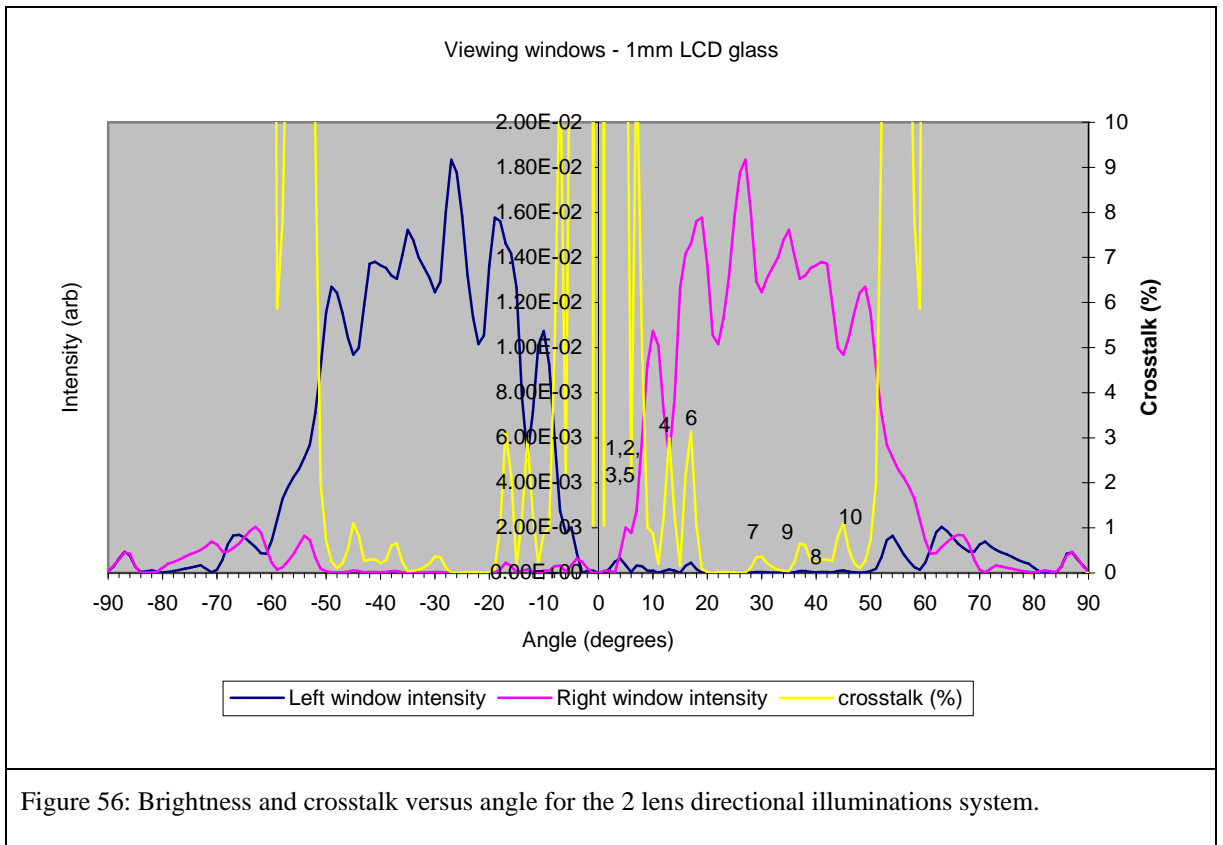
Table 9: The performance of different slit and lens systems designed using different methods.

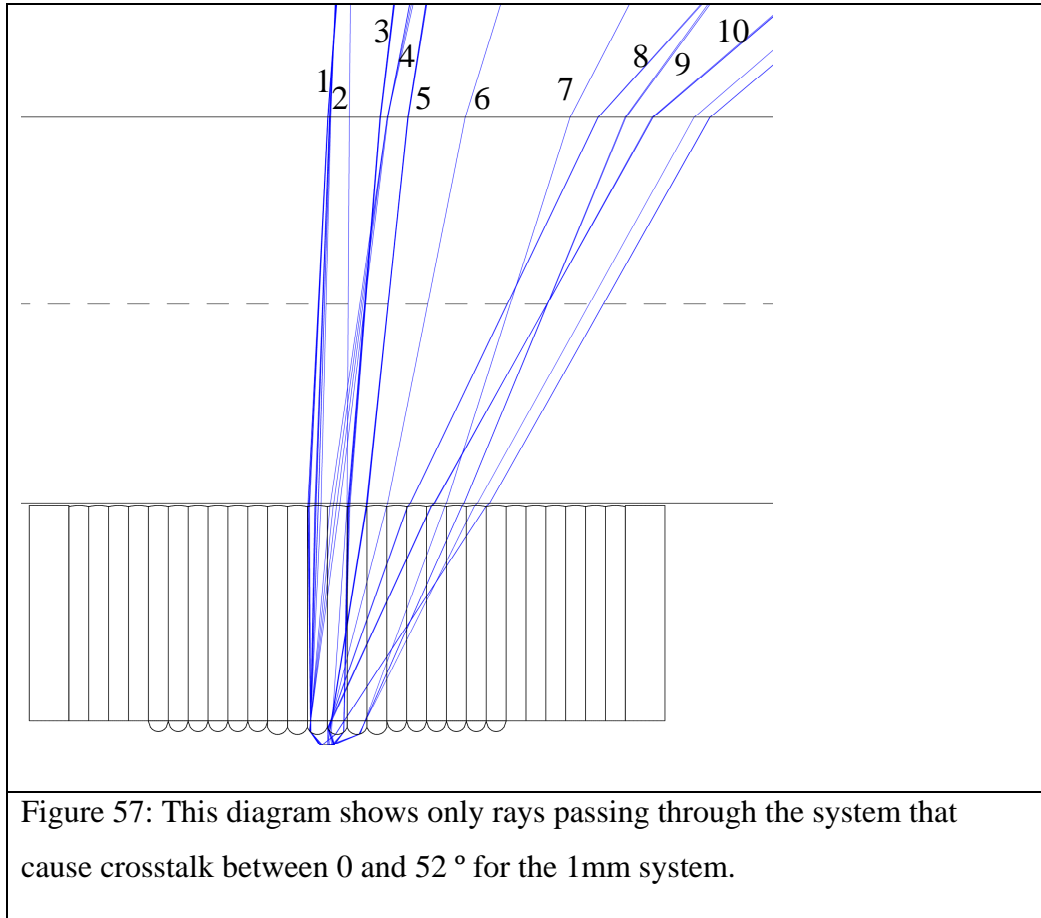
	<b>Design procedure version 2 (LCD Glass thickness = 0.5mm)</b>	<b>Design procedure version 3 (LCD Glass thickness = 1mm)</b>
Average crosstalk from 4 to 51° (slit width = 37.5% of barrier pitch)	0.7%	0.7%
Graph of angular light output	Figure 54	Figure 56

Table 10: The performance of different double lens dual view systems designed using different methods.

These tables are initially puzzling since the 1<sup>st</sup> lenticular and barrier system performs significantly better when thicker LCD glass is used. This would be expected to reduce the crosstalk, but the average crosstalk from the thick LCD glass system is the same as it was for the original 0.5mm LCD glass system. This is an unexpected result that is now investigated further.

More observations can be made by comparing graphs of brightness and crosstalk versus angle for the two systems, and also the problematic rays that cause crosstalk. These graphs are shown for the 0.5 mm thick glass in Figure 54, and the 1mm thick glass system in Figure 56. The problematic rays for the 1mm system are shown in Figure 57.





The graphs show that on axis the 1 mm LCD glass display is much darker than the 0.5 mm display. This is likely to be a result of the better 1<sup>st</sup> lenticular and barrier performance shown in the tables above. The 1<sup>st</sup> lenticular and barrier system successfully focus light to the correct lenses on the 2<sup>nd</sup> lenticular system, keeping it away from the central view, and making the central view darker.

Brightness drops off more rapidly at angles > 50 °. Black at angles > 50 ° is more desirable than a mix of images, which will look ‘untidy’. This is also a result of the improved 1<sup>st</sup> lenticular and barrier performance, which successfully keeps light away from the high angles where it is wasted.

However, despite the overall reduction in crosstalk from the 1<sup>st</sup> lenticular and barrier system there is a new path in the system that causes crosstalk at 12 °. It can be seen in Figure 57. Light from an aberration of the 1<sup>st</sup> lenticular can hit a different lens of the 2<sup>nd</sup> lenticular than in the 0.5mm system. This causes an unwanted spike of crosstalk at 12 °.

The spike in crosstalk at 18 ° is caused by aberration in the 2<sup>nd</sup> lenticular indicating that reduced focal power of the 2<sup>nd</sup> lenticular has not reduced aberrations significantly. This may be because the focal power of these lenses is not significantly changed.

The spikes in crosstalk at 30, 34 and 46 ° comes from the secondary window of the 1<sup>st</sup> lenticular and barrier system

In summary, the 1 mm system enables the focal power of the lenses to be reduced. This reduces aberrations in the 1<sup>st</sup> lenticular, which reduces much of the on-axis crosstalk caused by the 1<sup>st</sup> lenticular. However crosstalk caused by the secondary windows of the 1<sup>st</sup> lenticular is not reduced. In addition new paths of crosstalk exists in the system that are particularly problematic, and the crosstalk causing aberrations of the 2<sup>nd</sup> lenticular are also not significantly reduced. Therefore the system is not improved by this modification. Reducing crosstalk in the system further could be difficult.

#### **4.7 Summary of the modelled optimum design**

The double lens barrier system has been optimised by use of ray tracing. An average crosstalk of 0.7% is predicted from 4 to 51 °. The validity of such predictions is tested in section 5 by comparison with experimental data.

### **5. Experimental testing of the device**

All the work in previous sections of this chapter has been theoretical. The question remains – are the theoretical predictions a valid representation of a real system? In particular, do the theoretical simulations correctly predict the crosstalk and head freedom of the system.

In this section a thick glass system is designed and prototyped based on commercially available micro-lenses. The system substantially works as predicted but it suffers from more crosstalk than expected by theory. Some reasons as to why this might be are suggested.

It is concluded that a dual view system can be constructed using this technique but the crosstalk performance is inferior to the system discussed in Chapter 3.

#### **5.1 Designing the device**

Prototyping the device to the exact final design of section 5 is difficult. The difficulties are, firstly that it is time consuming to make a new set of micro lenses to a particular design, and secondly it can be expensive.

Options for constructing a prototype from ‘commercially available off the shelf’ (COTS) lenses were considered and are presented in the table below.

The aim is to find COTS lenses of the correct focal lengths, and custom make a pixel mask and parallax barrier to match the lens pitch. This approach also has problems. Ideally we need lenses of the same pitch but with different f-numbers. Numerous suppliers were searched and design 1 was the closest match of f-numbers and pitch. The pitch mismatch between the lenses (although small) is too severe. This design would only work over an area of 1 or 2 mm before the 2 sets of lenses became detrimentally out of phase with each other.

The solution to the pitch problem was to use the same COTS lenses for the 1<sup>st</sup> and 2<sup>nd</sup> lenticular, therefore the pitches of the lenses would match exactly.

Design 2 is one such possibility. The problem for this design is that the focal length of the 2<sup>nd</sup> lenticular is too strong, according to the design rules of section 2, the 2<sup>nd</sup> lenticular would need to be put very close to the pixels, which removes a significant point of the test. That is, that we demonstrate a dual view system that operates with optics far from the pixels.

Design 3 over comes this problem by applying index-matching glue over the 2<sup>nd</sup> lenticular to increase its f-number from 1.57 to 4. This is not a perfect solution because the high lens curvature means that more aberrations exist in the 2<sup>nd</sup> lenticular, and so the system suffers from more crosstalk. In addition, the f-number of the 1<sup>st</sup> lenticular could be lower. This would improve the design as shown in previous sections.

It was decided to proceed with the construction of design 3. It is not an optimum design but it should be suitable to check the validity of the model simulations.

<i>Design number</i>	<i>Summary of lenses used</i>	<i>Comments</i>
1	1270 $\mu\text{m}$ pitch lenticular, $f\# = 3$ 1263 $\mu\text{m}$ pitch lenticular, $f\#=1.7$	The mismatch between the lens pitches meant that this system would not work. The lenses would become out of alignment with each other over only a few lens pitches.
2	2500 $\mu\text{m}$ pitch lenticulars Both $f\# 1.57$	$F\#$ too low for 2 <sup>nd</sup> lenticular
3	<b>2500 <math>\mu\text{m}</math> pitch lenticulars</b> <b>1<sup>st</sup> lenticular <math>f\#=1.57</math>, refractive index=1.49.</b> <b>2<sup>nd</sup> lenticular, same lens surrounded by glue of index 1.37 to produce an <math>f\#</math> of about 4</b>	<b>These lenses could produce a prototype that is reasonable representative of the well optimised designs from section 4.</b>

Table 11: A comparison of possible designs for the double lens dual view system that could be created using off the shelf lenses.

The pixel pitch in this design is about 50 times larger than those in a conventional automotive display. This is a result of using the large pitch lenses. Scaling up the optics should not influence the results of the experiment, with the exception of diffraction. Since this prototype is 50 times larger than a conventional panel, diffraction will be reduced. The effect of diffraction on this design will have to be tested at a later date. This prototype should be sufficient to test the validity of the geometrical optical modelling, and should be easier to construct than a version which is 50 times smaller and has 50 times tighter tolerances.

The optimisation procedure was run with the lens pitch and lens radius fixed by the COTS lenses of design 3. These were measured at 2.5 mm and 1.616 mm respectively. The lens pitch was measured with a travelling microscope and the lens radius was measured by fitting a circle to a cross sectional photograph of the lenses (Figure 63). The size of the circle is deduced from the pitch of the lenses which is known to be 2.5 mm. The refractive index of the glue surrounding the 2<sup>nd</sup> lenticular was assumed to have an index of 1.37 at all wavelengths.

The 2<sup>nd</sup> lenticular to pixel separation (usually defined by the thickness of the LCD substrate) was set as 23 mm. This keeps the LCD substrate thickness in proportion to the pixel size.

The following parameters were returned for the rest of the variables.

<i>Parameter</i>	<i>Target value (mm)</i>
Pixel pitch	2.5
Barrier to 1 <sup>st</sup> lenticular lens separation	0.330
1 <sup>st</sup> lenticular to 2 <sup>nd</sup> lenticular separation	25.480

Table 12: The target values for the remaining variables of the prototype double lens dual view system.

## **5.2 Constructing the device**

The components in this design need to be assembled to tight positional tolerances. This is seen in the theoretical simulations, changing the positions of the lenses slightly makes a big impact on the angular light output. This section described how the components were spaced apart at the correct distance and aligned with each other.

### **5.2.1 Creating the correct spacing between the components**

Each component in the device is spaced apart by layers of glass or plastic as shown in the sketch below.

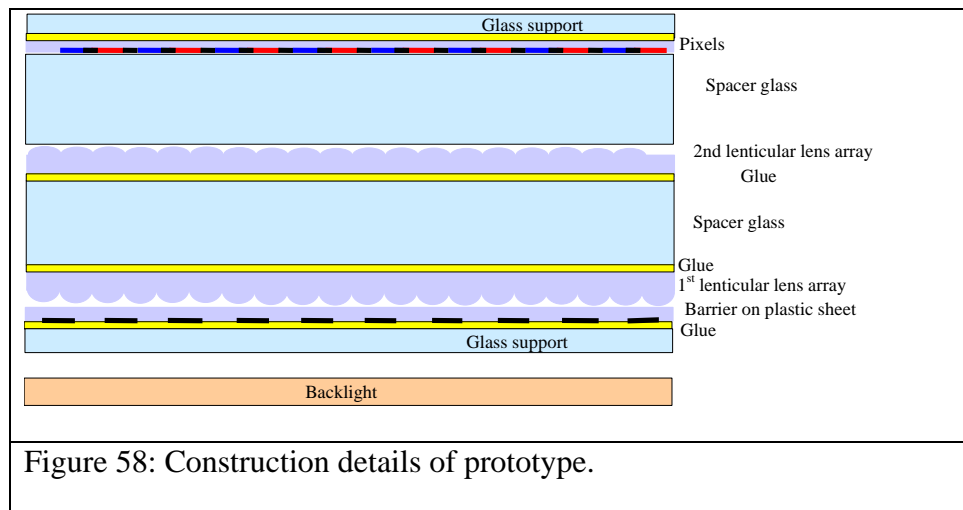


Figure 58: Construction details of prototype.

The glass spacer layers sometimes comprise two sheets of glass adhered to each other by transparent glue in order to obtain the correct thickness.

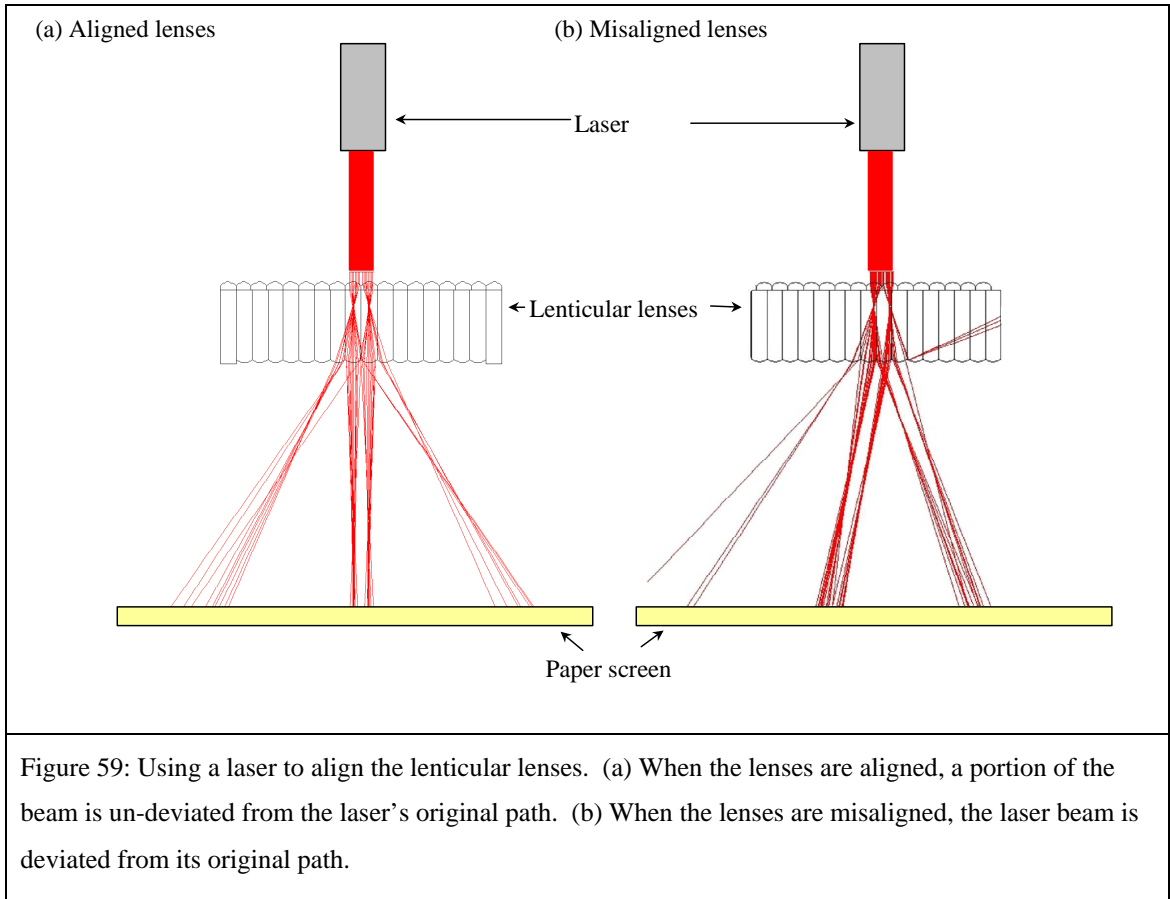
The glue used is a liquid polymer that can be cured by ultra-violet light. The refractive index of this glue is approximately 1.49 so that Fresnel reflections from the glass (of approximate refractive index 1.52) to glue should be minimal.

The lenses are made from acrylic, and the glass used is a glass from Schott called BK7. The pixels and the barrier were printed with a laser printer onto an acetate sheet.

The glue used to adhere the 2<sup>nd</sup> lenticular lenses to the glass is also a UV curable polymer but it has an index of 1.37. This index reduces the focal power of the 2<sup>nd</sup> lenticular, but does not remove the focal power completely.

### 5.2.2 Alignment of the components

The Lenticular lenses must be separated correctly and also aligned with the correct horizontal position and angle. The horizontal alignment was done as shown in Figure 59.



The angular alignment was done by rotating the two sets of lenses until the moiré fringes that they create became vertical. The pixels and slits were angularly aligned by inspection of the moiré fringes, and positionally aligned until the angular light output was symmetrical.

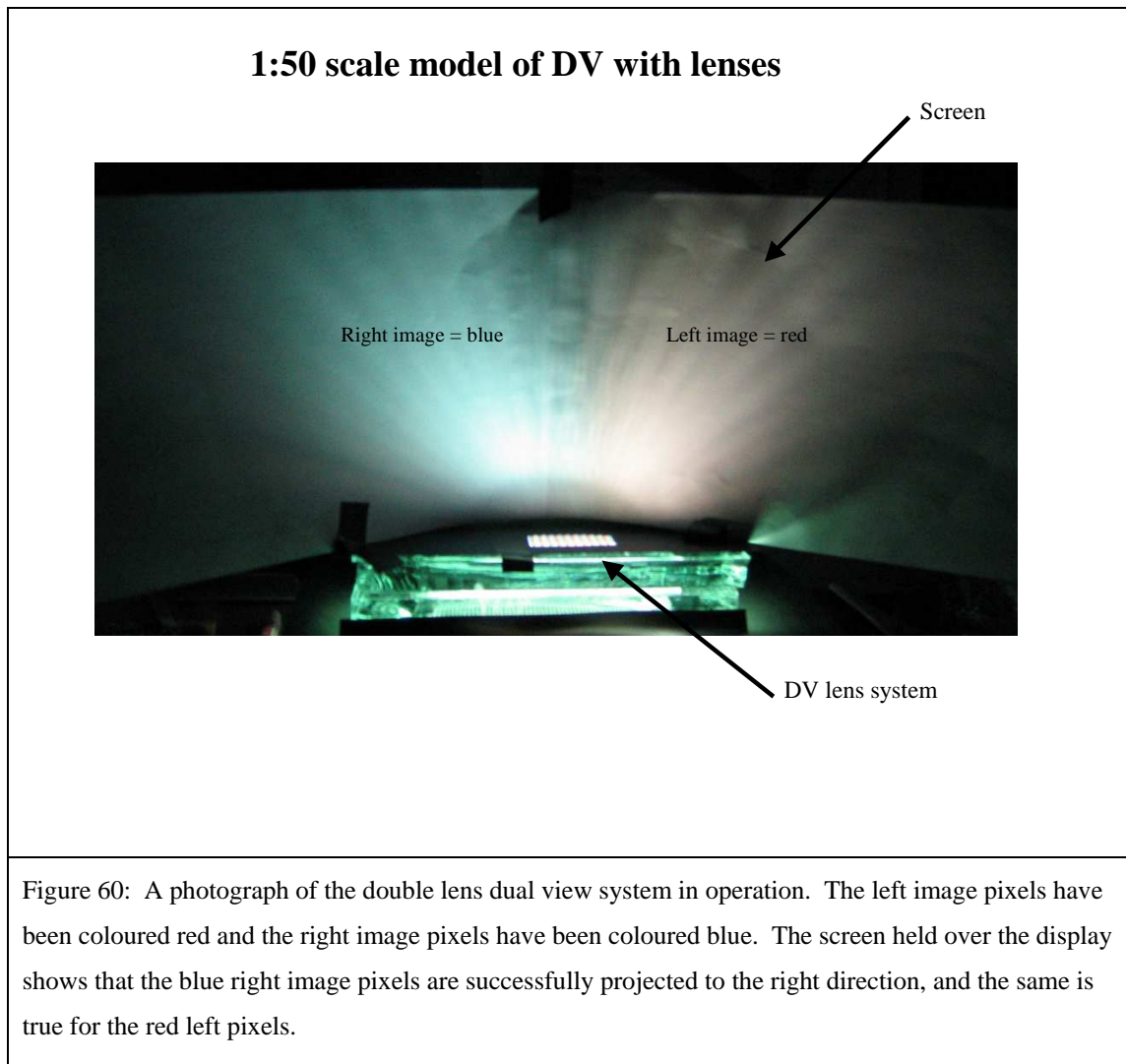
Following all of these steps the construction of the device was complete.

### 5.3 Characterisation of the device

The figure below shows a photo of the device in operation. In this section the performance of the device is compared with the theoretical predictions. It is seen that

the crosstalk performance is worse than predicted and some explanations for this are proposed.

For the photograph below the left image pixels have been coloured red, and the right image pixels have been coloured blue. By holding a screen close to the system, it can be seen that the red left image is projected to the left, and the blue image is sent to the right.



When looking at the display from the left the red pixels are more intense than the blue pixels, however the blue pixels can still be seen. That is to say a significant amount of crosstalk is present. This problem was quantified by measuring brightness versus angle when black left image pixels and white right image pixels were used. The data is presented in the figure below.

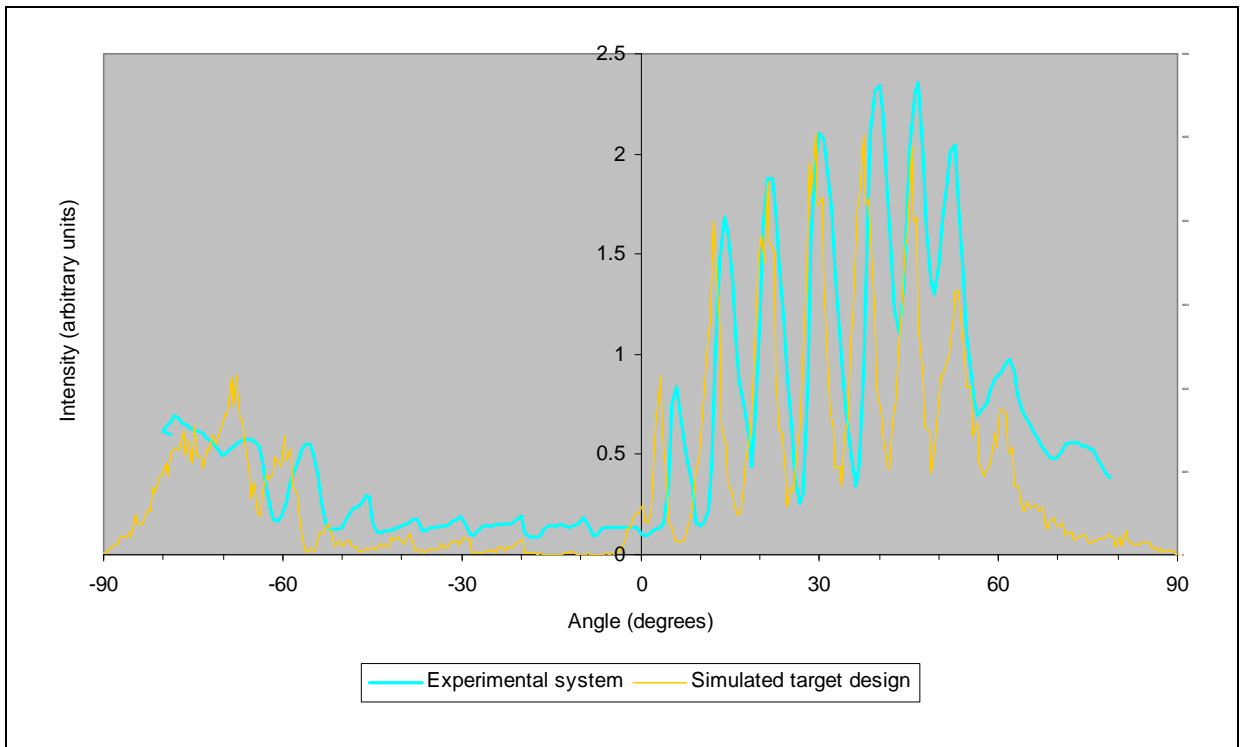


Figure 61: Brightness versus angle from the thick glass prototype system. The left image pixels have been coloured black, and the right image pixels are left transparent. Therefore there should be no light in the negative angular range, and maximum light intensity in the positive angular range. The orange plot shows the angular light output distribution predicted by the theoretical ray tracing.

We now discuss the question ‘Does the modelling technique used in this chapter make valid predictions of the experimental results?’

If we compare the plots of experimental and theoretical performance in the figure above we can see that the experimental system functions broadly in line with the function predicted by the theory. At positive angles the experimental system emits light to create a bright left view, and at negative angles the system does not emit much light, therefore the right view is substantially black as predicted. The peak intensity of the simulated data has been fitted to the experimental intensity.

The most significant mismatch between the theoretical predictions and the experiment are caused by the level of crosstalk in the system. That is to say the amount of light emitted in the negative angular range. It is seen that the theory predicts a lower level of crosstalk than produced by the experiment.

Looking at the peaks in the positive angular range suggests why this might be. Each peak is produced by a different lens in the 2<sup>nd</sup> lenticular. From geometric optics if the 2<sup>nd</sup> lenticular was moved close to the slit then the peaks would increase their angular

spread. If the horizontal displacement between the 2<sup>nd</sup> lenticular and the slits was changed the angular position of the peaks would be displaced. The experimental brightness peaks are different to those predicted. The experimental peaks have a different angular spread and displaced angular positions suggesting that the position of the 2<sup>nd</sup> lenticular is misaligned horizontally and spaced incorrectly from the slits.

It is likely that there are also errors in the positioning of the barrier slit, and the pixels since it is not possible to align these precisely experimentally. Therefore the positions of the components were measured so that the system could be remodelled as it was made. These measurements are summarised in the following table.

<i>Parameter</i>	<i>Target value (mm)</i>	<i>Measured value (mm)</i>	<i>Comment</i>
Lens pitch	2.5	2.500 +/- 0.005	The lens and pixel pitch were measured by use of a travelling microscope.
Pixel pitch	2.5	2.503 +/- 0.005	
Barrier to 1 <sup>st</sup> lenticular lens separation	0.33	0.64+/- 0.1	By using a microscope to focus on each components and measuring the resulting difference in microscope stage position.
1 <sup>st</sup> lenticular to 2 <sup>nd</sup> lenticular separation	25.480	25.6+/- 0.1	By micrometer measurement.
2 <sup>nd</sup> Lenticular to pixel separation	23.000	- 23.0 assumed	Could not be measured with sufficient accuracy with microscope or micrometer.
Barrier to lens alignment	Barrier slit is positioned at the midpoint between two lenses.	Barrier slit is positioned at the midpoint between two lenses +/- 0.01mm	Measured with a travelling microscope.
1 <sup>st</sup> to 2 <sup>nd</sup> lenticular alignment	No horizontal displacement	0.9 +/- 0.1	By measurement of the laser beam offset produced by the set up in Figure 59. The offset it derived from geometric optics from this.

Table 13: The target specifications for the double lens prototype and the actual specifications.

The system was remodelled with the measured positional data. There were still significant errors between the modelling and the experimental data. This might be

expected since the measured data is not of good accuracy. A measurement error of 0.1mm in the horizontal position of the pixels could cause a significant change in the angular output of the device as shown in Figure 62. Therefore an attempt was made to use the measurement data as starting point and then perturb this data until the experiment and theory match.

The procedure for this fitting was that firstly the pixels were removed from the experimental and modelled systems to remove the effect that their positioning errors would have. This simplifies the system by reducing the number of possible errors that could occur. Then once the system without pixels had been fitted the pixels would be added into the model so that the pixel positioning could be fitted separately.

The parameters iterated were the; pixel, 2<sup>nd</sup> lenticular, 1<sup>st</sup> lenticular and slit horizontal positions, and the pixel, 2<sup>nd</sup> lenticular, 1<sup>st</sup> lenticular, and slit separations. These were typically perturbed over a range of 0.5mm, which should be more than sufficient to cover any measurement errors that were made. Therefore the actual parameters of the experimental system should lie somewhere within this range.

This procedure used was a very long and manual process, meaning that the parameters could not be fitted to a high accuracy. The best fitting did not fit well. This could have been the result of bad fitting. Figure 62 shows the best-fitted data and shows how slight changes in a parameter radically affect the predicted angular output distribution.

As an aside, since a 100  $\mu\text{m}$  variation in just one parameter causes significant and unwanted variation in the devices performance this will make a final system difficult to construct. This system is a scale model that is 50 times bigger than a real device would be. Therefore the tolerances in the real device would be about 2  $\mu\text{m}$ , which is on the limits of standard LCD alignment capabilities.

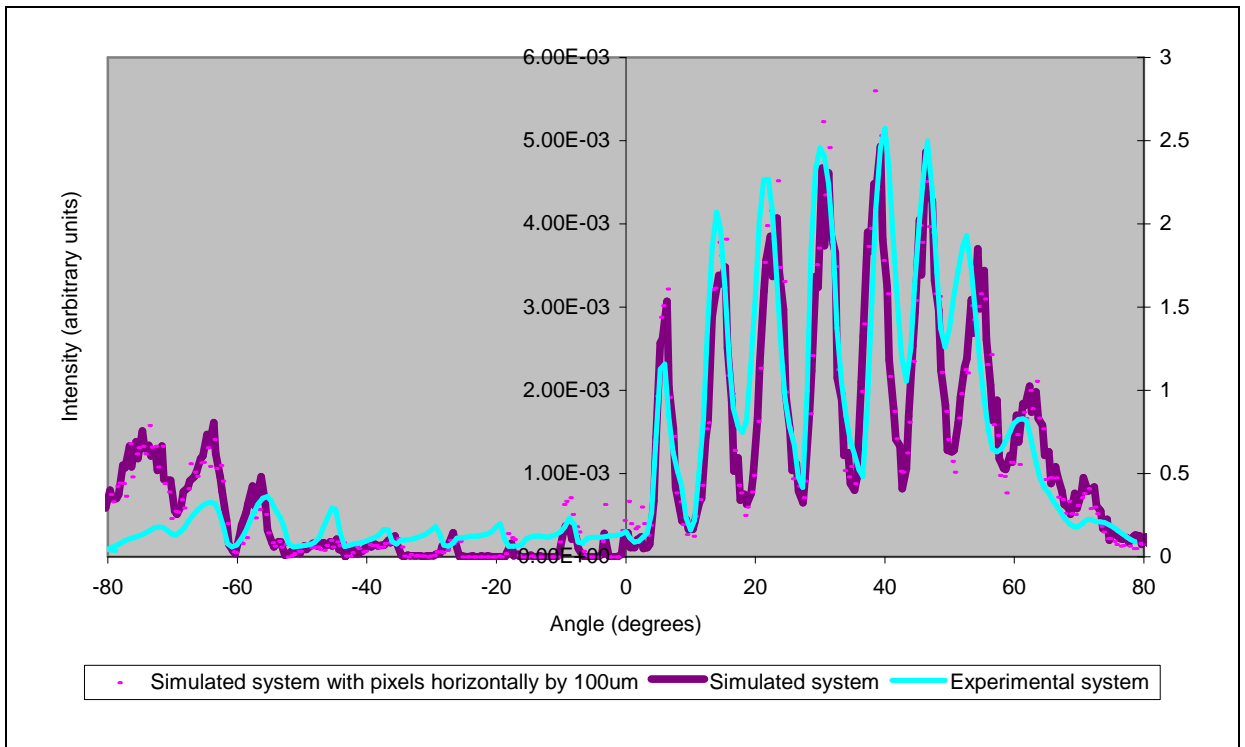


Figure 62: A comparison of data from the experimental system and simulated data whereby the parameters have been fitted to match the experimental data. The pink trace shows the effect on the system if one of the components is shifted by 100  $\mu\text{m}$ . The system is very sensitive to small changes in the alignment of the components.

However, looking at the shape of the peaks in intensity that cause crosstalk (particularly at  $-10^\circ$ ), the model appears to predict peaks that look the wrong shape. There is some unpredicted strong crosstalk (between the peaks) that could not be recreated by varying modelling parameters. Perhaps this suggests that the error in crosstalk prediction is more likely to be caused by factors other than the poor parameter fitting.

In the last section we identified which parts of the lens cause crosstalk at which angles by theory (an example of this is shown in Figure 55). We can compare where the crosstalk comes from experimentally with where we thought it would come from theoretically. This might show up where the errors are in the theory.

The theory predicted that crosstalk would come from the sides of the lenses on the 2<sup>nd</sup> lenticular where aberrations are most prominent, and that this crosstalk would occur at particular angles. The experiment showed that these aberrations did exist but in addition light seemed to be emitted from the sides between the lenses in nearly all directions rather than at one particular angle.

The figure below shows why this might be.

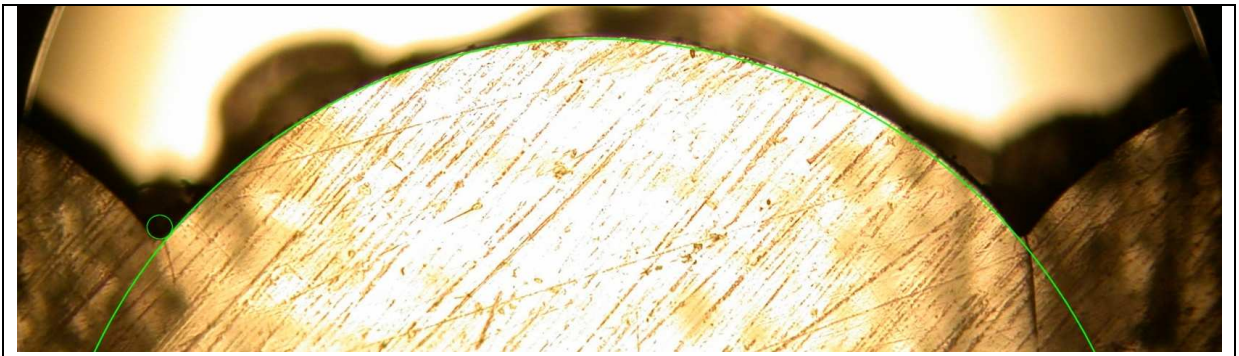
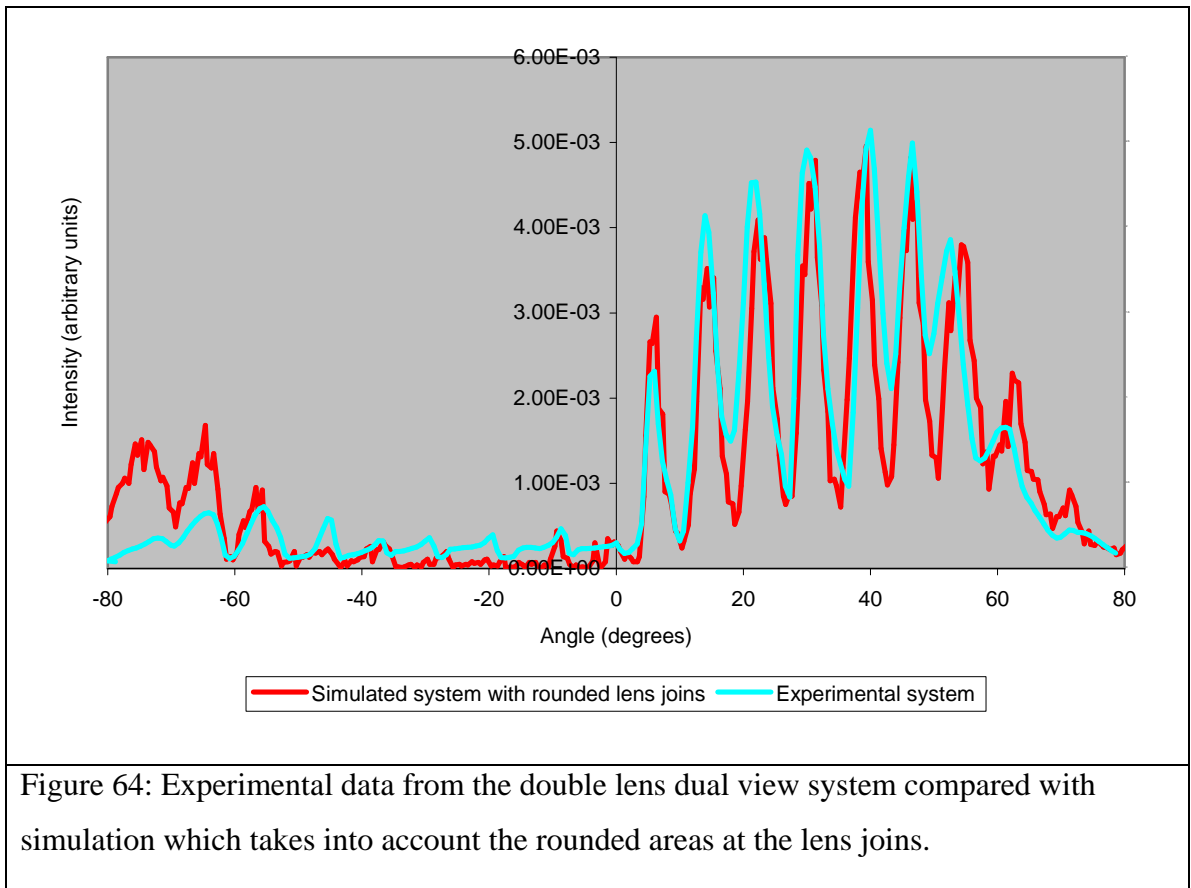


Figure 63: A cross sectional photograph of the lenticular lenses used to prototype the double lens dual view system.

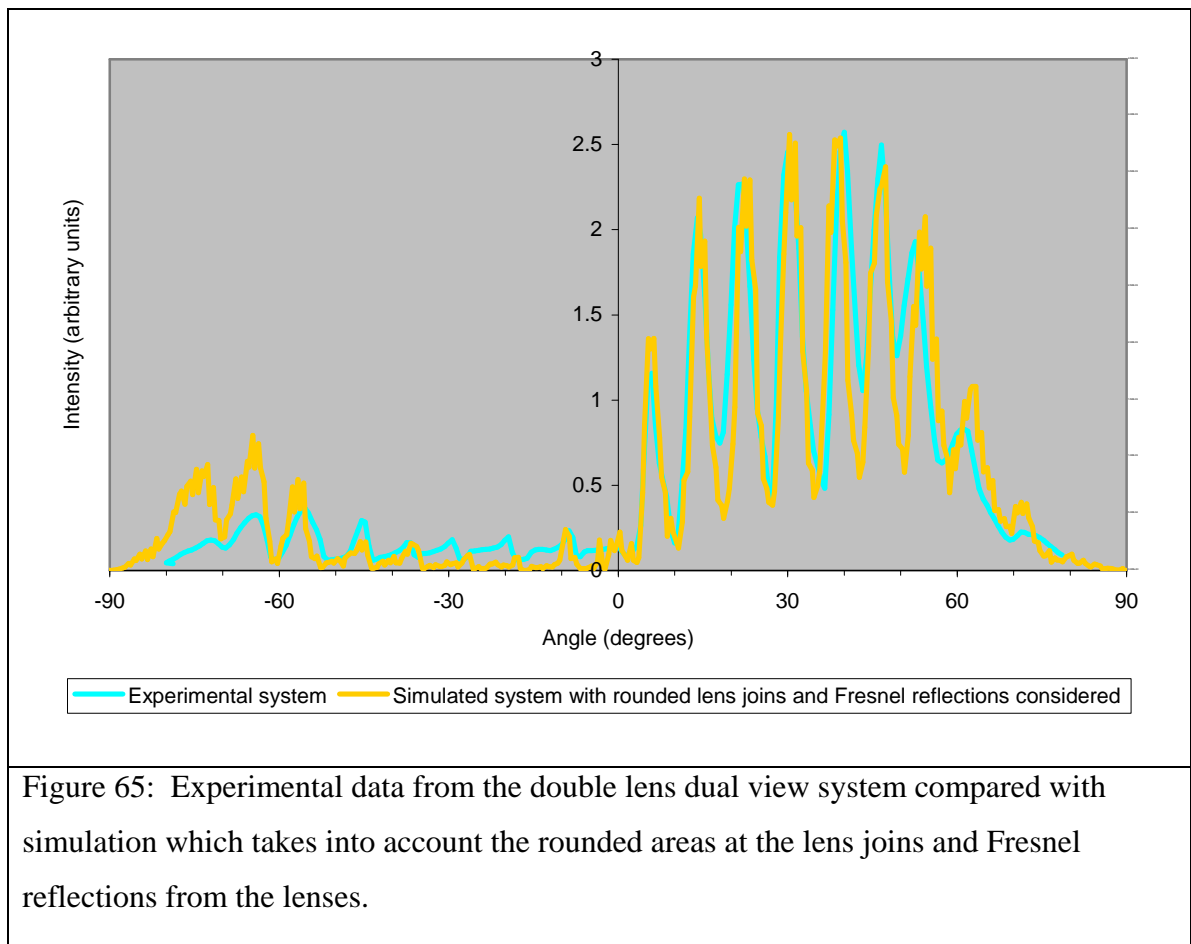
The cross section of the lenticular lenses shows that the joins between each lens is not perfectly sharp. There is a region between the lenses that forms a small concave lens that could be responsible for causing the light to be emitted in all directions at the sides of the lens. The original modelling assumes that the join between each lens is perfectly sharp so that no concave regions exist.

The modelling was adjusted so that the effect of the concave regions was accounted for. The figure below shows a comparison between the experimental data and the system simulated with concave regions between the lenses.



The concave regions seems to send crosstalk towards the same angles as seen in the experiment, but with the wrong magnitude. The model does not predict that the concave regions will scatter sufficiently to produce the level of crosstalk seen in the experiment. It is possible that these regions cause the extra crosstalk in the experiment and that the model is not predicting the magnitude correctly. However, there are other possible causes that also need consideration.

The modelling assumes that Fresnel reflections in the system are negligible. In fact light may be reflecting around the system to cause a general increase in crosstalk at all angles. Figure 65 shows the results of modelling which does and does not take Fresnel reflections from the lenses into account.



The figure shows that theoretically Fresnel reflections add a marginal level of crosstalk to the system at all angles, but the low level of crosstalk predicted suggests that this is not the cause of the high level of crosstalk seen in the experiment.

When the modelling results are considered (in particular at  $-10^\circ$ ) the experimental result looks like the peak predicted by theory but with an additional spreading error. That is to say crosstalk in the model is predicted to occur as a peak in the angular light distribution, but in the experiment the peaks are smeared or drop off in intensity gradually. This could be indicative of the type of effect that is causing the mismatch between theory and experiment. One factor which might cause this is dispersion in the lenses. The experiment was carried out with white light illumination, in the modelling the light was also assumed to be white (made up of red green and blue components) but it was assumed that there was no dispersion in the 1.37 index glue. Remodelling with the dispersion [43] of the glue accounted for made negligible different to the results. This makes conceptual sense since the refractive index of the glue varies by only 0.02 from 450 nm to 630 nm. The assumption that no dispersion occurs in the glue cannot be blamed for the mismatch.

Other factors that could produce a spread error might be angular misalignments and wedge errors (varying separation of the components across the system). This makes the task of accurately modelling the experimental system even more difficult since the inclusion of these errors would add more parameters that need to be identified.

Scattering could cause a raise in background crosstalk level as is seen in the experimental system, however this cause can be ruled out from experience gained in studying the device of chapter 3. Firstly the device of chapter 3 contains layers that scatter more than any of the layers in this chapter 2 device. That is to say the chapter 3 device contains scattering liquid crystal and view angle compensation films, whereas the chapter 2 device contains only smooth glass or plastic surface that should not scatter as much. The scatter in the device of chapter 3 was quantified as  $\sim 0.1\%$  which is not sufficient to account for the crosstalk in the chapter 2 device.

#### *Conclusions on the sources of crosstalk in the double lens system*

From the results above I suspect two main possibilities for the mismatch between theory and experiment. Firstly the system is very sensitive to misalignment of the elements. The experimental system can not be constructed with sufficient accuracy to replicate the design. The parameters in the model can not be fitted with sufficient accuracy to match the experiment. Perhaps these alignment and positioning errors do change the crosstalk level and the shape of the peaks that cause the crosstalk. Secondly there may be a specific factor that is influencing the system which we have not yet considered. For example the results may be influenced because the radius of the lens is not perfectly spherical or the dispersion of the glass is incorrectly modelled.

I believe the best way to find the causes of mismatch between theory and experiment would be to rebuild the system one component at a time, and at each step fitting the models alignment parameters and comparing the results with experiment. Firstly, this should allow the model and its parameters to be accurately fitted because at each step there will be less parameters to fit. Secondly, other discrepancies between the model and experiment should be more identifiable in a simpler system.

However, from the work done so far sufficient information has been gained. We have seen that in the thin lens system theoretically no crosstalk exists and the device works perfectly. With a more detailed model which incorporates the effect of lens aberrations an average crosstalk of  $0.7\%$  is predicted. In the experimental system crosstalk is higher than predicted by a factor of 4.

At this time an alternative dual view system had been successfully created (further investigated in Chapter 3). This was the product of an engineering project carried out by Sharp Japan, who successfully managed to create a dual view display by use of a parallax barrier and thin glass. This system had a crosstalk of 0.46% and it was seen that even this level of crosstalk was too high. This is far lower than earlier work suggested.

We can predict that if we were to make our best design of the double lens system the crosstalk would be at least 0.7% as predicted by modelling, and probably more given that inaccuracies and other effects occur in the manufacture of such a device. In addition a manufactured device could suffer crosstalk from diffraction since it would be 50 times smaller than the device tested in this section. Therefore this double lens system would be inferior to the thin glass system in terms of crosstalk.

A general statement might be made that since dual view systems require such low crosstalk levels, the optically simplest solutions are the best because there are less potential sources of crosstalk. This double lens system is too complicated.

## **5.4 Conclusions on the double lens system**

We are now in a position to make a comparison between the double lens system (of this chapter) and the performance of the system taken from chapter 3. The main points for comparison are shown in the table below.

<i>Parameter</i>	<i>Chapter 2 dual view system</i>	<i>Chapter 3 dual view system</i>
Image Quality	High	High
Brightness	Higher	Lower
Head freedom	~same	~same
Crosstalk	>1.5%	0.46%
Ease of manufacture	More difficult	Easier

Table 14: A comparison of the double lens system of chapter 2 and the parallax barrier system of chapter 3.

It seems that we could build a dual view display with high image quality based on the design in this chapter.

The brightness of the system was first predicted to be considerably brighter than the parallax barrier system because the barrier aperture could be 50% rather than 30% for

parallax barrier. After more detailed consideration it was seen that the barrier aperture needed to be reduced to about 37% to counter the effects of lens aberrations with the side effect of reduced brightness. However, according to the theory the system is still a little brighter than the parallax barrier system. This brightness advantage is enhanced because the lenses tend to bend light away from the on-axis view and secondary windows. The light is bent into the driver and passenger views where the light is useful. According to the predictions in the optimum theoretical design we get spikes of crosstalk that are about 1.5% in the viewing range in the double lens system. We know from testing that this will be higher in the finally constructed device. Therefore we write  $>1.5\%$  in table. This result is not favourable compared with the 0.46% crosstalk of the first device constructed in chapter 3.

After an engineering department at Sharp Corporation in Japan had spent some time working on the design of chapter 3, it became apparent that it was actually simpler to handle the very fragile thin glass panels than it would be to create the thick glass system by aligning two layers of micro-lenses. Therefore the design discussed in this chapter would be harder to make.

In conclusion it seems that the new design of dual view system that was optimised in this chapter could be produced to make a dual view display. The display would be of good image quality and reasonable head freedom and brightness, but inferior in terms of crosstalk and manufacturing ease. Brightness is the only parameter for which this system wins over the parallax barrier design, but requirements for low crosstalk and manufacturing easily dominate the brightness requirement.

## **6.0 Summary**

This chapter presented the details of an investigation into a new design of dual view display. This design is unique from other designs because it enables high resolution dual view to be created without the use of time multiplexing (which causes flickering) and without putting optical elements close to the LCD pixel (which creates a difficult engineering challenge).

The system was optimised and simulated using optical ray tracing, and it was predicted that the system would create the dual view effect with a head freedom from 4 to 51 ° and a maximum crosstalk in this range of about 1.5%.

The system was built and tested experimentally. The dual view effect was successfully created, and the head freedom was seen to be in line with predictions. A flaw was found in the system in that the crosstalk levels that it produced were too high. The prototype produced higher crosstalk than predicted, possibly because of misalignment of the elements during the device's construction. The elements in the system must be constructed to very tight tolerances. In addition it was seen that an alternative design of chapter 3 produced dual view with much lower crosstalk than could be expected from a perfectly made prototype, and that this low crosstalk level is essential in a dual view display.

In summary the new design was superseded by a design considered in the next chapter.

# **CHAPTER 3: INVESTIGATION OF CROSSTALK IN A DUAL VIEW LCD.**

# Introduction

In chapter 2 a dual view system was created using 2 micro-lens arrays. Chapter 3 describes a different dual view design, made with a new manufacturing technique developed by Sharp Corporation Japan. This design creates a very good dual view display (described in more detail in section 1.1) with only 0.5% crosstalk between left and right images.

However, the small amount of crosstalk that exists is noticeable and detracts from the quality of the display. This chapter is about deducing the causes of the crosstalk and attempts to reduce them. The low levels of crosstalk make this a challenging problem, but some improvements are made.

In section 1 the new design of dual view display and the crosstalk problem are described.

Section 2 presents experimental evidence that indicates where the crosstalk is from. The main causes of crosstalk are shown to be diffraction in the system, scatter at the LCD polariser and view angle compensation films, and parasitic capacitance within the thin film transistor electronics that drive the display pixels.

In section 3 the human visual system is tested to identify factors that influence the visibility of crosstalk. This information suggests that crosstalk of  $<0.03\%$  is required for zero visibility.

Section 4 is about the attempts made to reduce crosstalk. A modified dual view display is created with a substantially invisible crosstalk of  $0.05\%$ .

Section 5 summarises the key results from this chapter.

## **1. The new dual view display, and the crosstalk problem.**

Section 1.1 described the new dual view system. The system gives the chance to test the performance predictions that were made in chapter 1. They are seen to be satisfactory in predicting brightness and head freedom but not crosstalk.

In section 1.2 the problems that crosstalk causes are explained, showing the need to locate its causes and remove them.

## 1.1 Description of the new design

The design investigated in this chapter is shown in Figure 66. The display functions like a 3D display, but the parallax optics are  $<100\ \mu\text{m}$  from the pixels. This causes a wide angular separation of the left and right images as described in chapter 1.

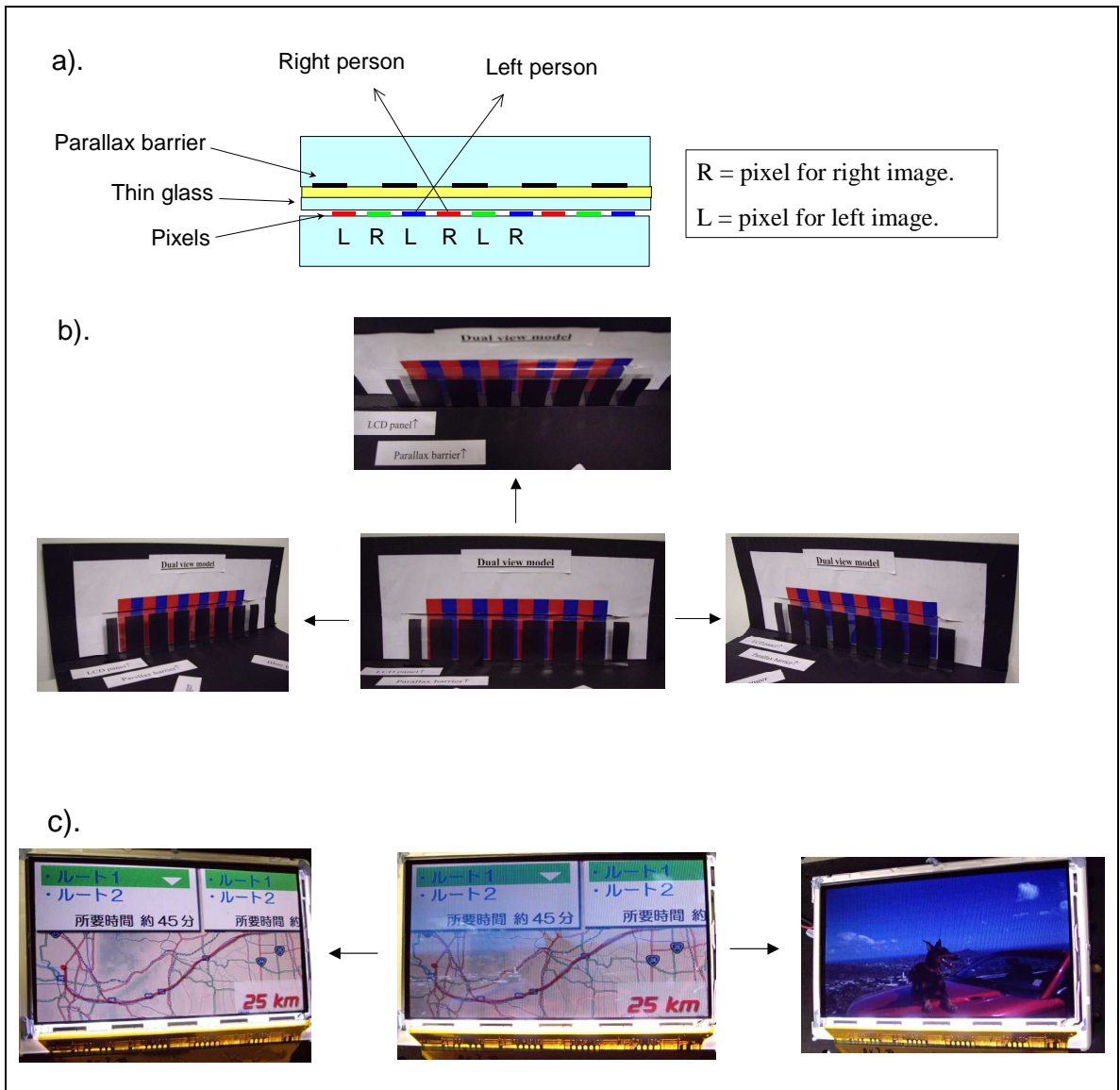


Figure 66 : a). shows a cross sectional diagram of the 'Thin glass' dual view system. The parallax barrier is placed very close to the pixels. B). Shows a cardboard model showing the effect of the parallax barrier. Some LCD pixels (shown in red) are used to display the passenger image, some LCD pixels (shown in blue) are used to display the driver image. When the model is viewed from the right, only the blue pixels can be seen through the parallax barrier, and only the red pixels can be seen from the left. C). Shows the final effect when the parallax barrier is applied to a display. From the left a map can be seen, from the right a TV picture can be seen, when viewed on axis a mix of both images can be seen. The system in this figure was designed by myself.

This design was initially thought to be too difficult to make, but in fact Sharp Corporation, Japan, achieved it with magnificent engineering skills.

This design creates a dual view display with:

- High (NP1) image quality.
- Simple optics (no lens systems)
- Low crosstalk (no lens aberrations)

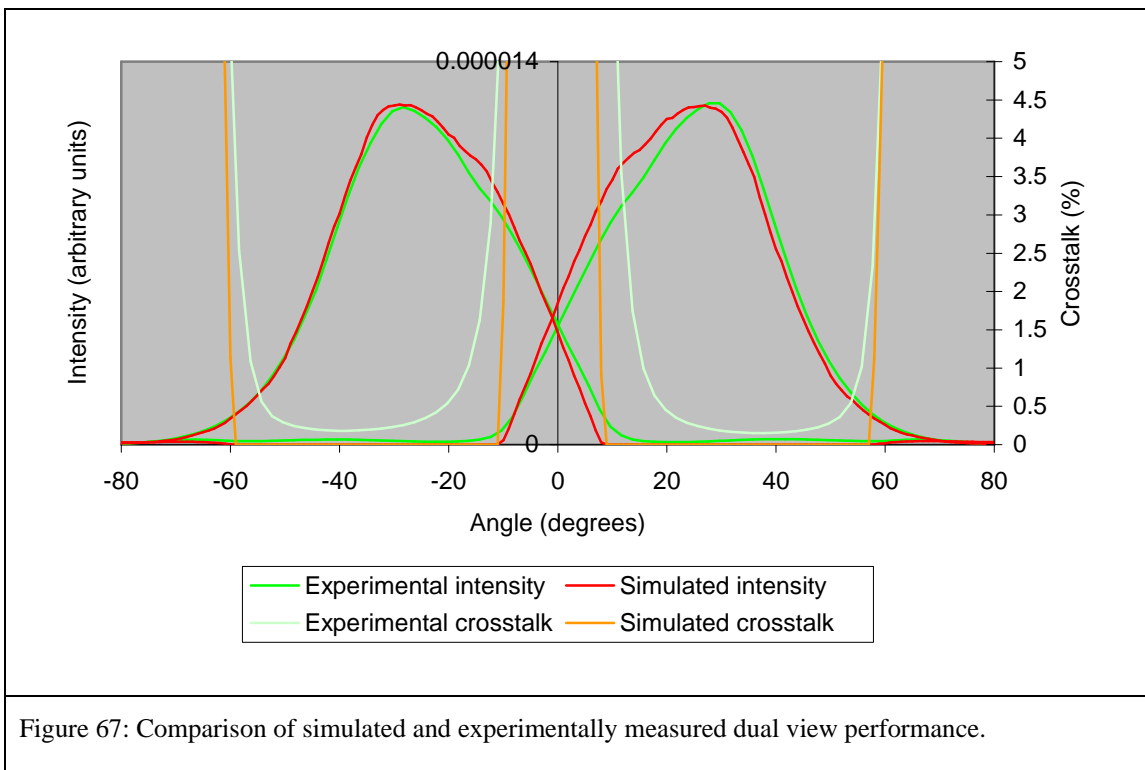
The problems with this design are that:

- It is inefficient. To allow good head freedom within each view the parallax barrier slits must be made very small. In this case the barrier absorbs approximately 75% of the light.

### *Experiment versus prediction based on geometric optics*

In chapter 1 all the design parameters in the dual view system were optimised theoretically. These calculations were based on the assumption that the system is successfully described by geometric optics. This assumption can now be tested with the new dual view panel.

Experimental results and theoretical results are shown below



Head freedom and brightness are well predicted by geometric optics, but crosstalk is not well predicted. The simulation predicts that no crosstalk exists in the proper viewing positions. In reality there is some percentage of crosstalk, and it is visible to the eye.

I believe that the geometric model is still the best tool to use in optimising a dual view display. This is because the head freedom and brightness are the most important consideration for dual view performance, so barrier has to be designed for head freedom and brightness, and therefore geometric optics can be used.

Crosstalk is a secondary issue that must be tackled without moving away from the optimum geometric design. This is because moving away from the best geometric design does not have a significant effect on crosstalk (see Figure 97), and it changes the brightness too much.

## 1.2 The crosstalk problem

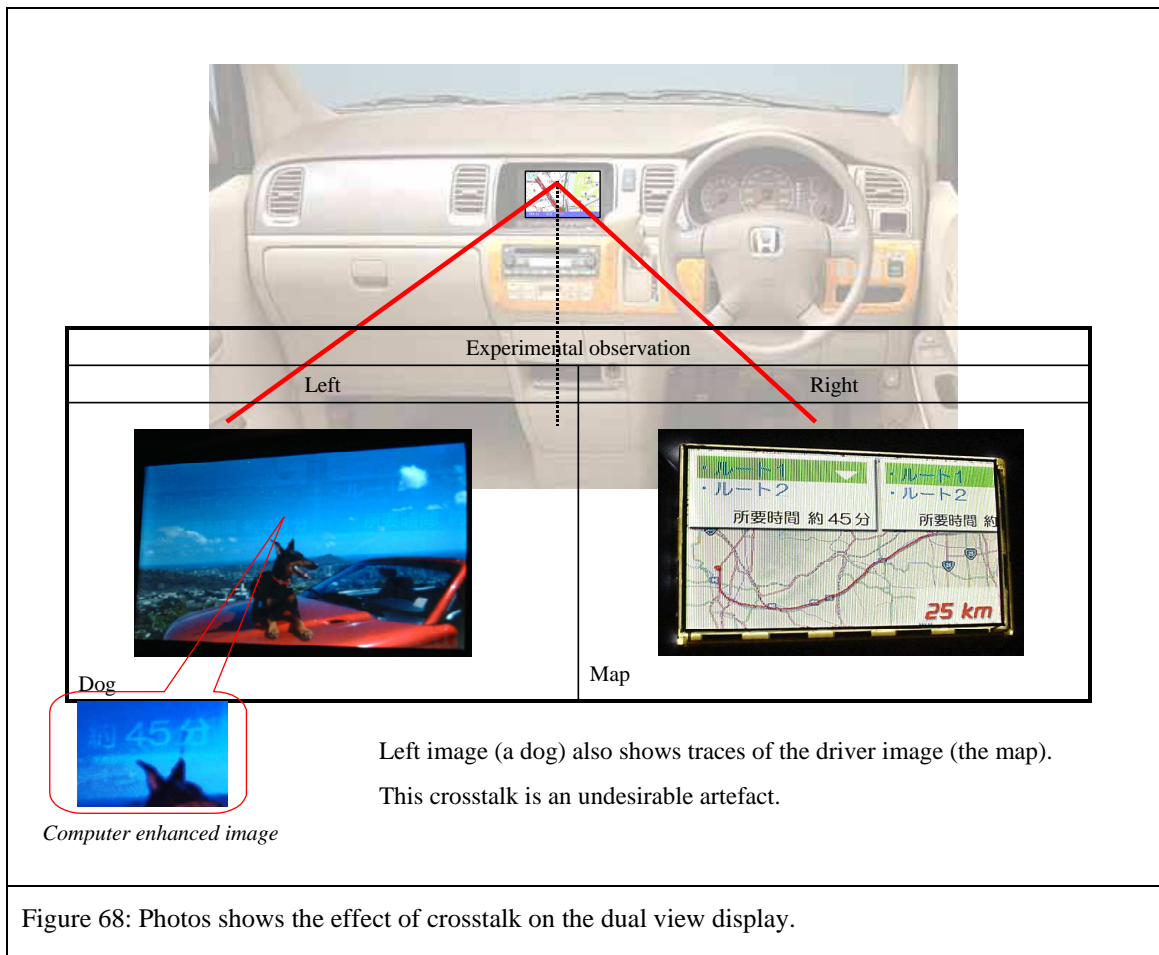


Figure 68: Photos shows the effect of crosstalk on the dual view display.

Figure 68 shows the effect of crosstalk in a dual view display. Crosstalk is undesirable because it is distracting to the viewer.

- The impact of crosstalk is hard to show by photography and printing due to the subtlety of the effect. To describe it in words - the effect of crosstalk is very slight, typically when both left and right views show an image, it is not noticed at first, but it can be seen. The problem is at its worse when one image is black and the other image is bright. The crosstalk can be seen quite clearly in this case.

The three main problems with crosstalk are;

1. The crosstalk may be distracting to the driver, and pose a safety risk.
2. In some countries the law states that the driver must not be able to see video images when the car is on motion. By looking at the crosstalk it could be argued that the driver can see the video image, so there is ambiguity in the legality of using a dual view display.
3. It makes the display appear poor quality.

Reducing or removing crosstalk will reduce or remove the above problems.

## **2. Causes of crosstalk**

This section is about deducing the causes of crosstalk. It contains results of experiments designed to indicate how the crosstalk occurs. Crosstalk in the dual view display is a very subtle effect, making it difficult to find experimental evidence that is conclusive.

Section 2.1 proposes our best hypothesis for the causes of crosstalk.

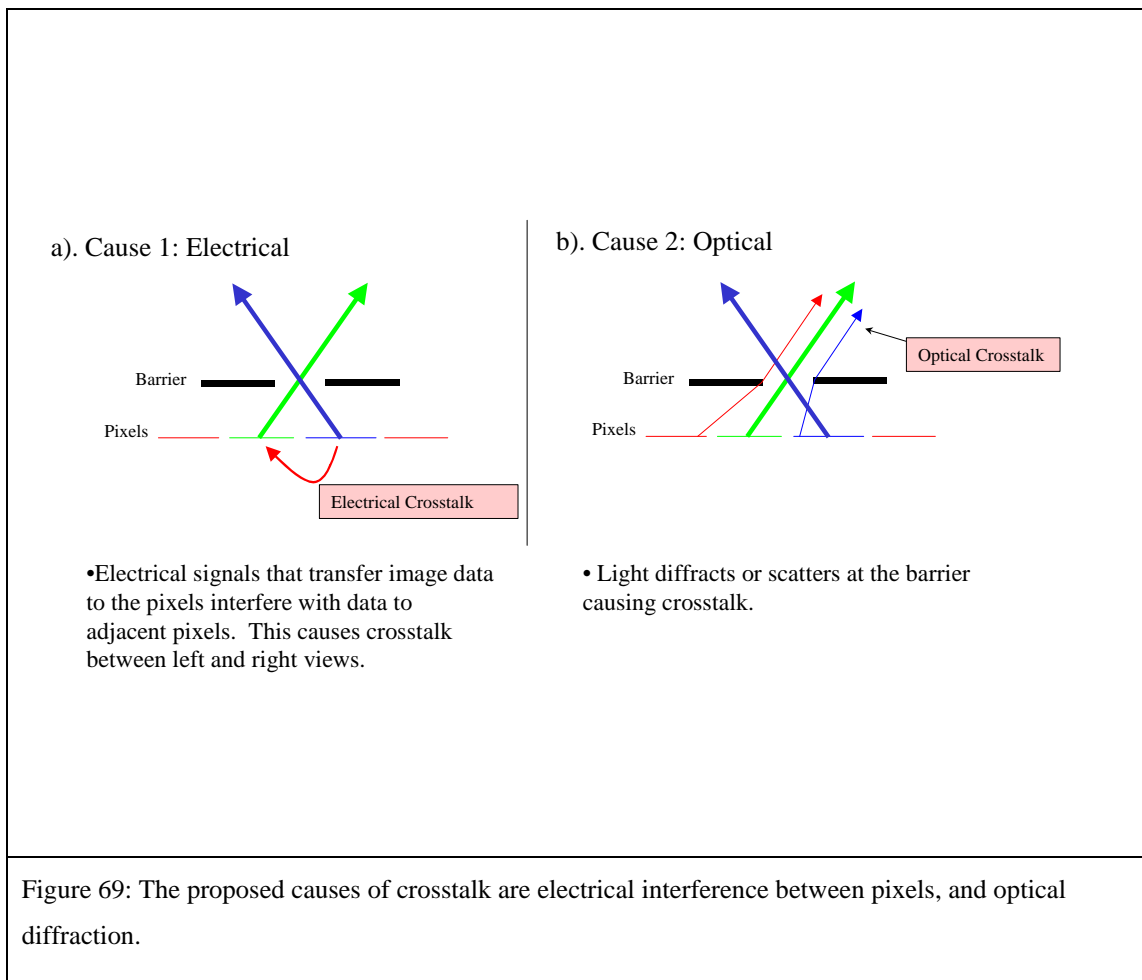
Sections 2.2 and 2.3 discuss the evidence that supports it.

### **2.1 Hypothesis on the causes of crosstalk**

It is thought that crosstalk is caused by;

Electrical crosstalk, as shown in Figure 69a,

1. Optical crosstalk as shown in Figure 69b



## 2.2 Evidence for electrical crosstalk

This section discusses the evidence that electrical crosstalk exists, as summarised below.

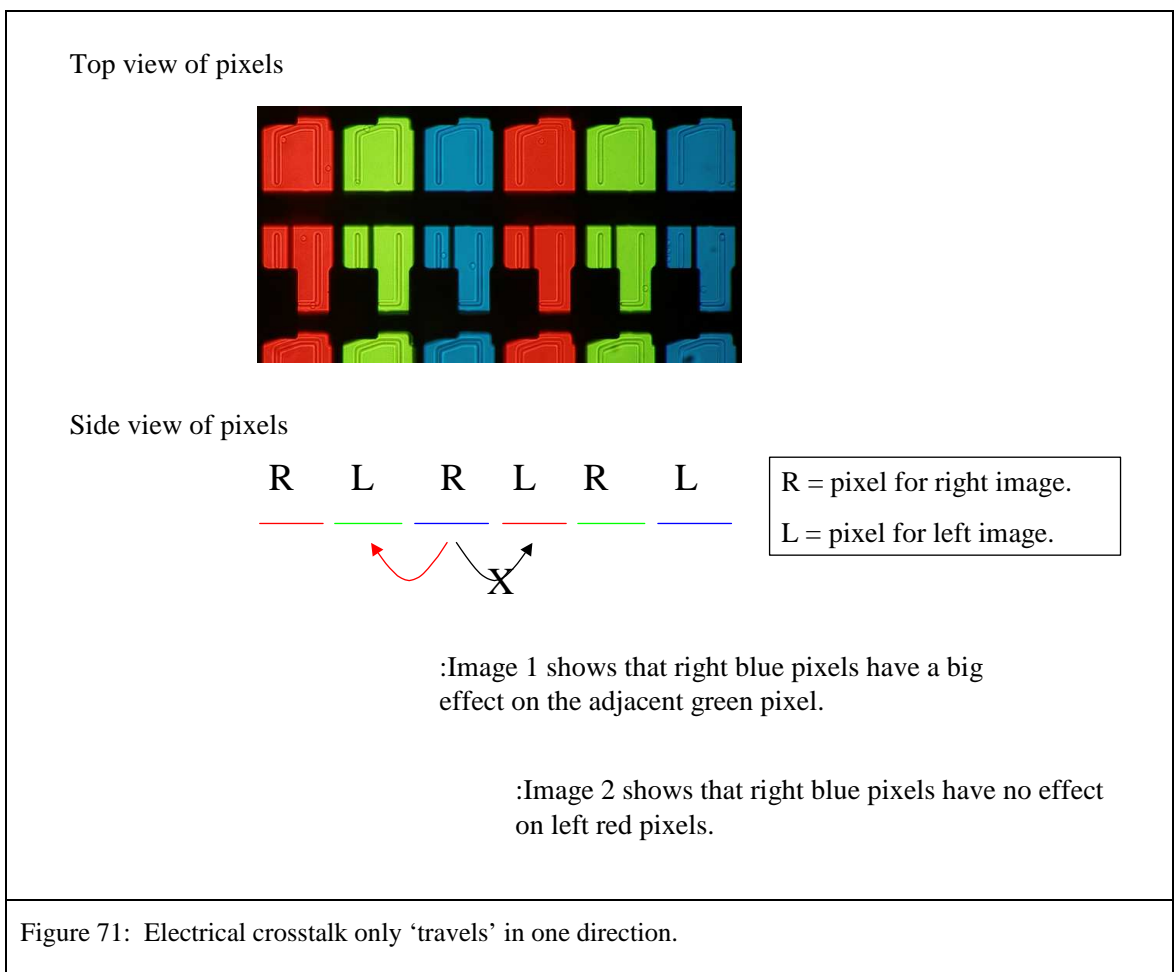
Certain test images show up particularly peculiar properties of crosstalk, which suggest the crosstalk is electrical in nature.

If crosstalk is electrical in nature, then such effects should be seen on a single view panel (independently of any dual view optics). These effects are not noticeable to the naked eye due to the subtleness of the intensity changes, and dazzling effects of surrounding pixels. However, a sensitive measurement technique is designed that allows the phenomenon to be seen, thus indicating this crosstalk is not caused by the dual view optics, but is simple **made visible** by the dual view optics.

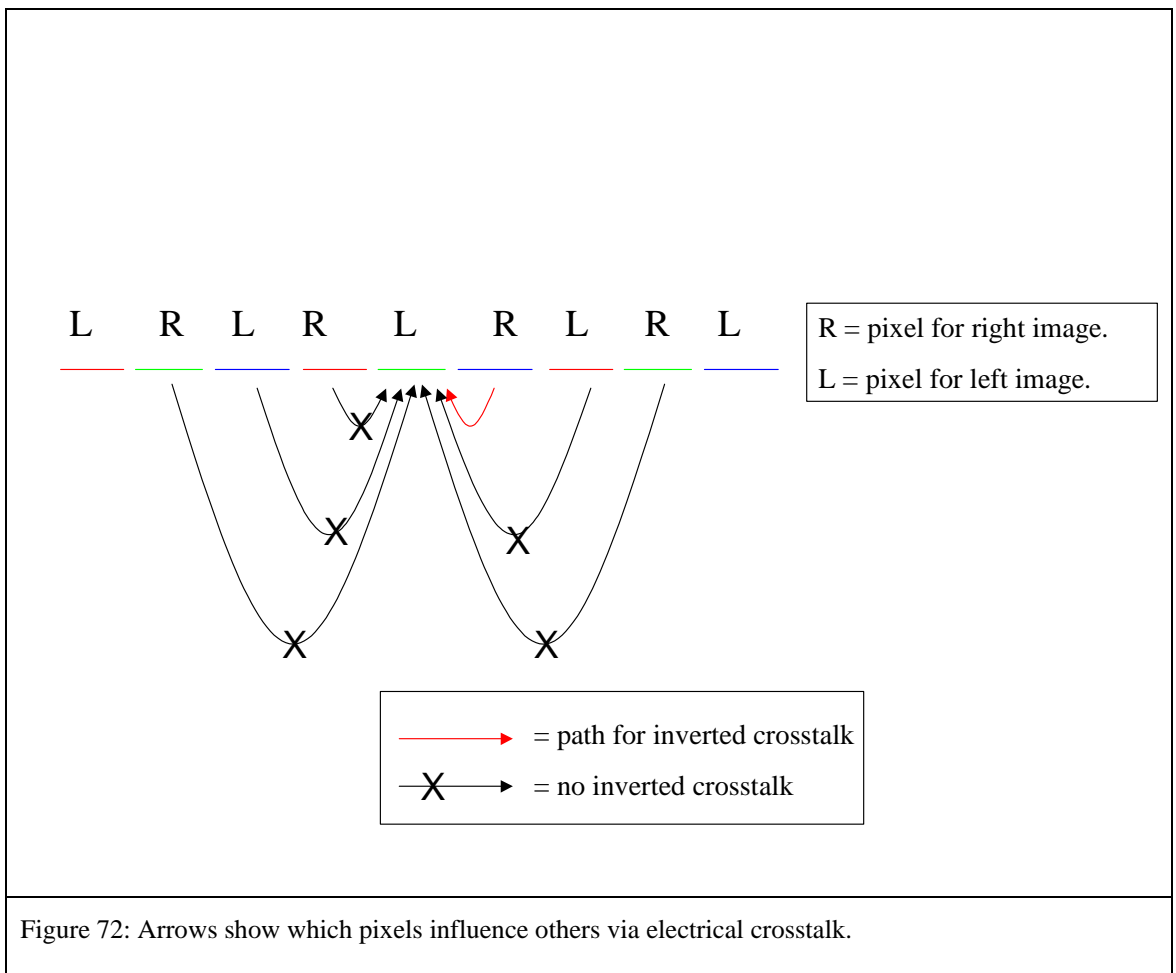
Final evidence that electrical crosstalk induces visible crosstalk effects in a dual view display comes when the single view panel is redesigned to remove the suspected causes of electrical crosstalk. The new redesigned panel exhibits much-reduced electrical crosstalk.



3. The magnitude of the inverted crosstalk depends on the left and right image data. For example, the inverted crosstalk is most visible when a medium green intensity is shown on the left image, and a high intensity is shown on the right image. This is unlike optical crosstalk. For optical crosstalk, crosstalk to the left view, would be caused by the right image, the left image would have no effect on the amount of light leakage from the right to the left.
4. Inverted crosstalk is massively asymmetrical. Blue causes significant crosstalk to green pixels (top of Figure 70), but blue does not cause any noticeable crosstalk to red (bottom of Figure 70). This point is elaborated in Figure 71.



Similar test images show that a pixel is only affected by inverted crosstalk by the pixel to its right, (Figure 72).



Whether or not an optical effect could cause this phenomenon, is discussed in Figure 73.

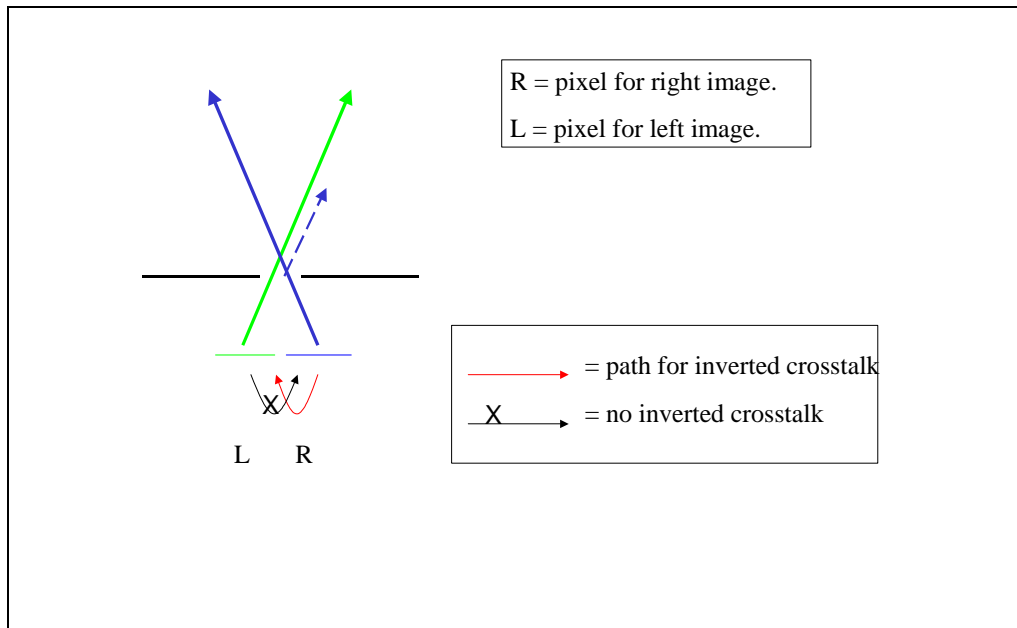


Figure 73: Could optical effects cause the inverted crosstalk. The red and black arrows show how the inverted crosstalk propagates in the panel. The blue and green arrows propose ray paths that might induce optical crosstalk. The blue ray travelling towards the right view would be deviated by some optical effect to cause crosstalk, however, the green ray travelling towards the left view would be un-deviated, causing no noticeable crosstalk. No asymmetry in the optical system could be thought of that could produce such a noticeable asymmetric optical effect. This suggests that the artefact is not optical in nature.

In summary;

- It is difficult to think of a significant optical effect that could cause optical crosstalk to become inverted.
- It is difficult to think of an optical effect that would cause the magnitude of crosstalk to depend on the intensity of the left and right pixels.
- It is difficult to think of a significant optical effect that could cause optical crosstalk to be so asymmetric.

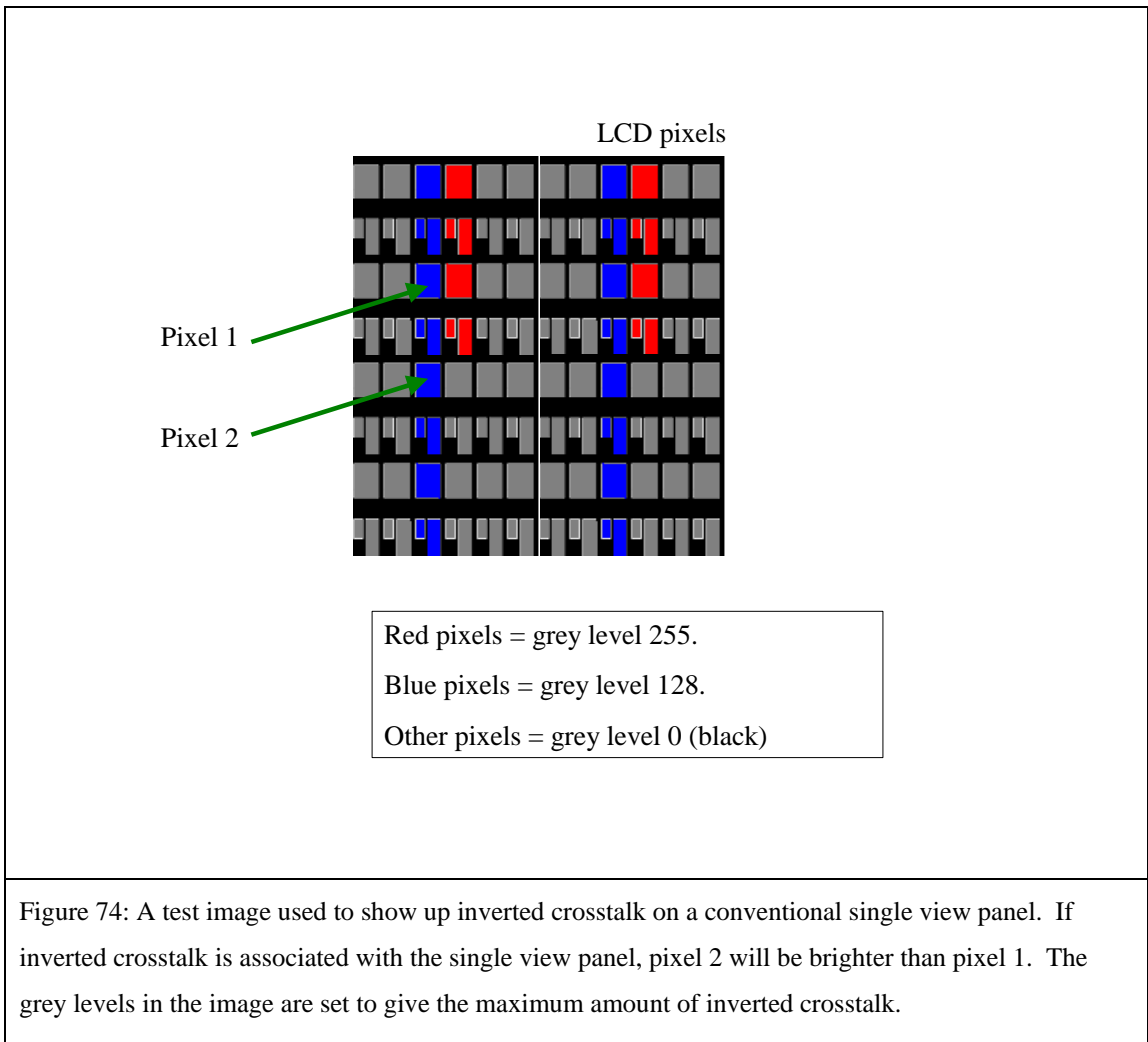
This suggests that the inverted crosstalk shown by the test images of Figure 70 are not optical in nature.

### 2.2.2 Observations of single view panel.

The above study of test images suggest that inverted crosstalk is not an effect related to a dual view parallax barrier, but that it is solely due to the conventional single view base panel on which the dual view optics is applied. If this is true then the effect should be visible on the single view panel before the parallax barrier is attached.

In this section, observation on a conventional single view panel are made, and inverted crosstalk is seen. This gives conclusive evidence that inverted crosstalk is not associated with the dual view optics.

Figure 74 shows the test image used to show up any inverted crosstalk inherent in the single view panel.



The table below shows the experimental techniques used to attempt measurement of inverted crosstalk on the single panel. The measurement is difficult because a very small change in the blue pixel must be detected, whilst the red pixel brightness varies hugely. This effect is measured in detail in section 4.1.2. The red pixel changes from 0.69 to 70  $\text{cd/m}^2$  whilst the blue pixel only changes from 9.5 to 11.4  $\text{cd/m}^2$ .

Experimental technique	Comment
1. Visual inspection with microscope	No change in brightness between pixel 1 and 2 could be seen due to the red pixels dazzling the viewer. Similarly a CCD array was not sensitive to detect a difference.
2. Use of high magnification (so that one pixel filled the field of view of the microscope) and measurement by PMT.	This technique is no good due to light from the red pixel scattering in the system and distorting the result.
3. Visual inspection with microscope, using only blue input light.	Pixel 2 could be seen to be brighter than pixel 1.

Table 15: Methods to detect electrical crosstalk in a single view panel.

Technique 3 was successful showing that inverted crosstalk exists in a single view panel.

### 2.2.3 A redesign of the panel electronics

A proposed cause of electrical crosstalk is shown in Figure 75.

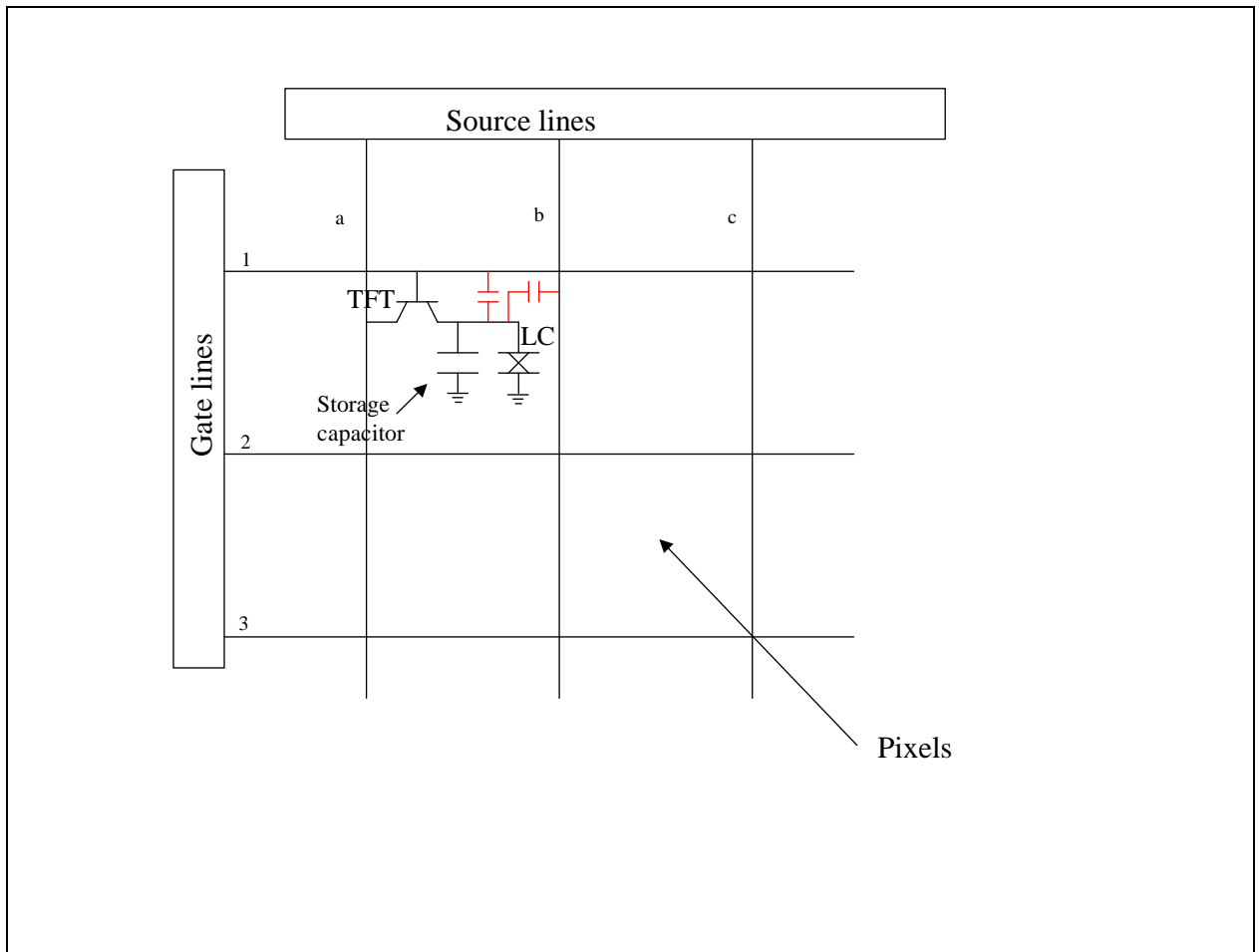


Figure 75: Parasitic capacitance (shown in red) amongst the pixels is thought to be the cause of electrical crosstalk.

Figure 75 shows the circuit diagram for a TFT LCD panel. The lines used to connect the TFTs are made of ITO. Lines of ITO that lie on top of other ITO lines cause ‘parasitic’ capacitance, which is thought to be the cause of electrical crosstalk [44].

This theory also suggests why the electrical crosstalk ‘travels’ only in one direction.

- Gate line 1 is switched on, which turns on all the TFTs in the row.
- The source lines are activated in sequence – a, b, c, ... to charge each pixels storage capacitor according to the image data.
- When line b is switched on, the data on pixel b1 is set, but data also leaks via the parasitic capacitance to lines a and c.
- Next, line c is switched on. Crosstalk from pixel b1 to c1 is over written in this step as fresh data is put on pixel c1. Again, data leaks onto lines b and d.

- Consequently, data on b1 has affected a1 but not c1, data from c1 has affected b1 but will not effect d1 because d1 will be rewritten in the next step.
- This continues such that electrical crosstalk from a pixel will only affect the pixel to its left.

Solutions to electrical crosstalk are considered in section 4.1. One of these solutions is to redesign the TFT layout so that ITO lines lie besides each other, rather than on top of each other. This should reduce such parasitic capacitance. The success of this technique provides the most conclusive evidence that parasitic capacitance is the cause of the inverted crosstalk.

## **2.3 Evidence for optical crosstalk and its sources**

This section discusses the evidence that optical crosstalk exists and evidence that indicates its origin.

Firstly test images are constructed which are known from section 2.2 to be free from electrical crosstalk. Some crosstalk is still present in these images. This is thought to be optical in nature.

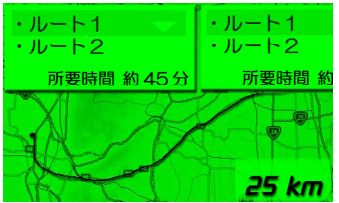
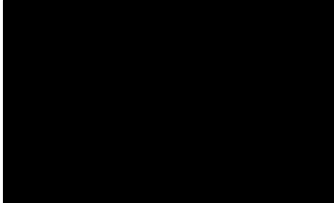
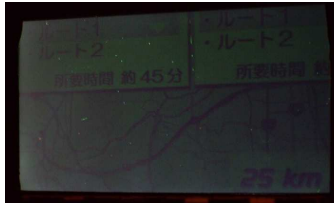
The remainder of this section is an investigation into the sources of this optical crosstalk, and the quantification of these sources. Solutions to these problems are investigated in the section 4.

This section attempts to find clear experimental evidence that conclusively shows all the sources of crosstalk. This has been an incredibly difficult challenge, and no such experiment was found; instead multiple experiments build up a picture of how the light leakage occurs in a dual view display. These experiments are almost entirely consistent with each other, suggesting that crosstalk is primarily from diffraction (60%) and scattering in the polariser (40%).

### **2.3.1 Test images that show optical crosstalk.**

Figure 76 shows how electrical crosstalk can be removed, to show up other sources of crosstalk.

a).

Test images		Result (Right view)
Left image	Right image	
 <p>Map (green channel only)</p>	 <p>Black</p>	 <p>Green map is faintly visible.</p>

b).

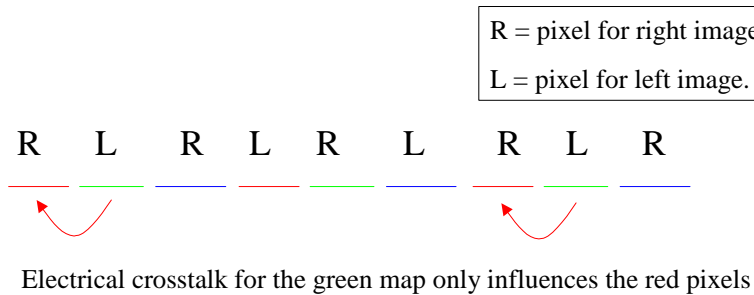


Figure 76: A test image to show optical crosstalk. a). A green map in the left view produces faint green crosstalk to the right view. The faint green crosstalk is thought to be optical in nature because; Electrical effects would produce red crosstalk (b). The faint green crosstalk does not show the inverted characteristic associated with electrical crosstalk.

After electrical crosstalk is removed by the carefully constructed test image of Figure 76, some crosstalk remains, which is thought to be optical in nature.

### 2.3.2 Measurement of crosstalk

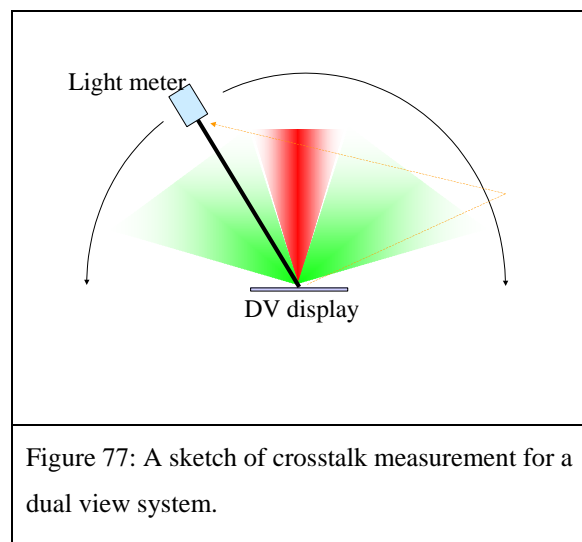
In order to quantify any improvements that are made in crosstalk, it is necessary to be able to measure the amount of crosstalk from a particular dual view system. This section describes the method used to quantify crosstalk.

It discusses the effect of stray reflections, ambient illumination, and factors that cause some crosstalk variation between dual view panels. These effects are investigated. Crosstalk measurements are thought to be accurate to +/- 10% of the value recorded.

From the literature, a method of crosstalk measurement from autostereoscopic 3D displays is known (and described in chapter 1). This technique involves moving a photodiode around the display and measuring the percentage of light that leaks from one image to the other.

This technique was replicated for a dual view display. It is sufficiently accurate to measure the typical crosstalk levels of 5-15% for a 3D display, however, the parallax barrier dual view display has a crosstalk of around 0.5%. Such low levels of crosstalk make the measurement harder.

The 3D measurement system is sensitive to stray reflections off the walls. This is shown in Figure 77, by the orange dotted line. That is to say, light is emitted in the left direction by the dual view display. Some of this light might leak into the right image within the display (genuine crosstalk), but in addition, light from the left view causes a general increase in the ambient illumination of the lab. Some of this light finds its way back to the photodiode by for example, reflecting off a wall. The latter light path increases the crosstalk reading given by the detector by an estimated quarter of a percent, producing a significant error.



For this reason dual view crosstalk measurements were made using a luminance meter from Minolta (model LS110), which focuses on a 1cm diameter spot on the display and accepts only light from this area.

The result of this measurement on the thin glass parallax barrier dual view panel, is shown in Figure 67.

The Minolta luminance meter should prevent light from the surroundings upsetting the result. However, it is possible that the general change in ambient illumination (when the left and right images are changed during the measurement) could change the intensity of light reflecting from the display into the Minolta meter. This would add error to the crosstalk reading.

The following experiment was done to quantify this effect.

Ambient light reflection from the display to the Minolta was measured at  $0.07 \text{ cd/m}^2$  per lux of room lighting. The increase in ambient illumination caused by setting the left image of the dual view display from black to white, was measured at 0.2 lux.

Therefore, the increase in signal from the Minolta due to room illumination from the dual view display would be about  $0.014 \text{ cd/m}^2$ . The influence that this has on the crosstalk reading at  $30^\circ$  is about 0.003%. This implies that changes in the ambient illumination caused by the dual view panel, do not significantly affect the crosstalk measurement.

With this effect eliminated, we believe that there is no significant offset error in the system.

In this section many dual view systems are constructed and their crosstalk is measured. It was noticed that there are further sources of error that can arise in these experiments. For example, if a dual view display is constructed with the parallax barrier slightly misaligned with the pixels (as is inevitable due to the tight tolerances required), different crosstalk readings are attained. Crosstalk in the left view might increase, whilst crosstalk in the right view might decrease. This may be due to the intensity with which each image is illuminated. If a barrier is horizontally displaced to the left, then the left image moves more off axis. Off axis the backlight illumination is less, and the transmission of the LC mode is reduced. Consequently the left image is illuminated with lower intensity. The right image moves more on axis, such that it is illuminated more strongly. Therefore the right image can dominate the left image such that the crosstalk in the left image is increased. Similarly the crosstalk in the right image is reduced.

Another error can result from misalignment of the Minolta detector. If the detector looks down at the panel with an azimuthal angle then the crosstalk reading is changed. Perhaps this is due to changes in the viewing angle properties of the LC at this angle, which, again, affect the intensities of each view.

To quantify the sum of the errors described above, and other sources of random error that may exist, we repeated the measurement of the same dual view display three times, each time disassembling and reassembling the panel. The crosstalk measurements were repeatable to about  $\pm 10\%$ .

In summary, it is believed that our system can measure crosstalk accurate to +/- 10%, with no significant offset error.

Note that it would have been less time-consuming, to measure crosstalk using an EZContrast machine made by ELDIM. This device produces crosstalk data for the whole hemi-sphere of angles that emerge from the display. However, the EZContrast reports that crosstalk is about 10 times higher than the Minolta, this is thought to be due to reflections between the EZContrast lens and dual view display which are brought very close to each other. The over reading of crosstalk may also be due to scattering inside the EZContrast system. The Minolta is trusted over the complex EZContrast system, because the Minolta style of measurement is simpler with less scope for errors to occur.

### **2.3.3 Microscope pictures of optical crosstalk.**

The test images of section 2.3.1 show what is thought to be optical crosstalk, however, little knowledge can be gained about its origin by visual inspection.

In this section, a microscope is used to create a magnified image of the crosstalk from the panel. A photograph is presented which shows some fascinating fringes thought to be from diffraction at the parallax barrier slit, and some light leakage through the parallax barrier. These are suspected to be the cause of the optical crosstalk.

#### *Experimental procedure*

Figure 78 shows a diagram of the set-up for the experiment.

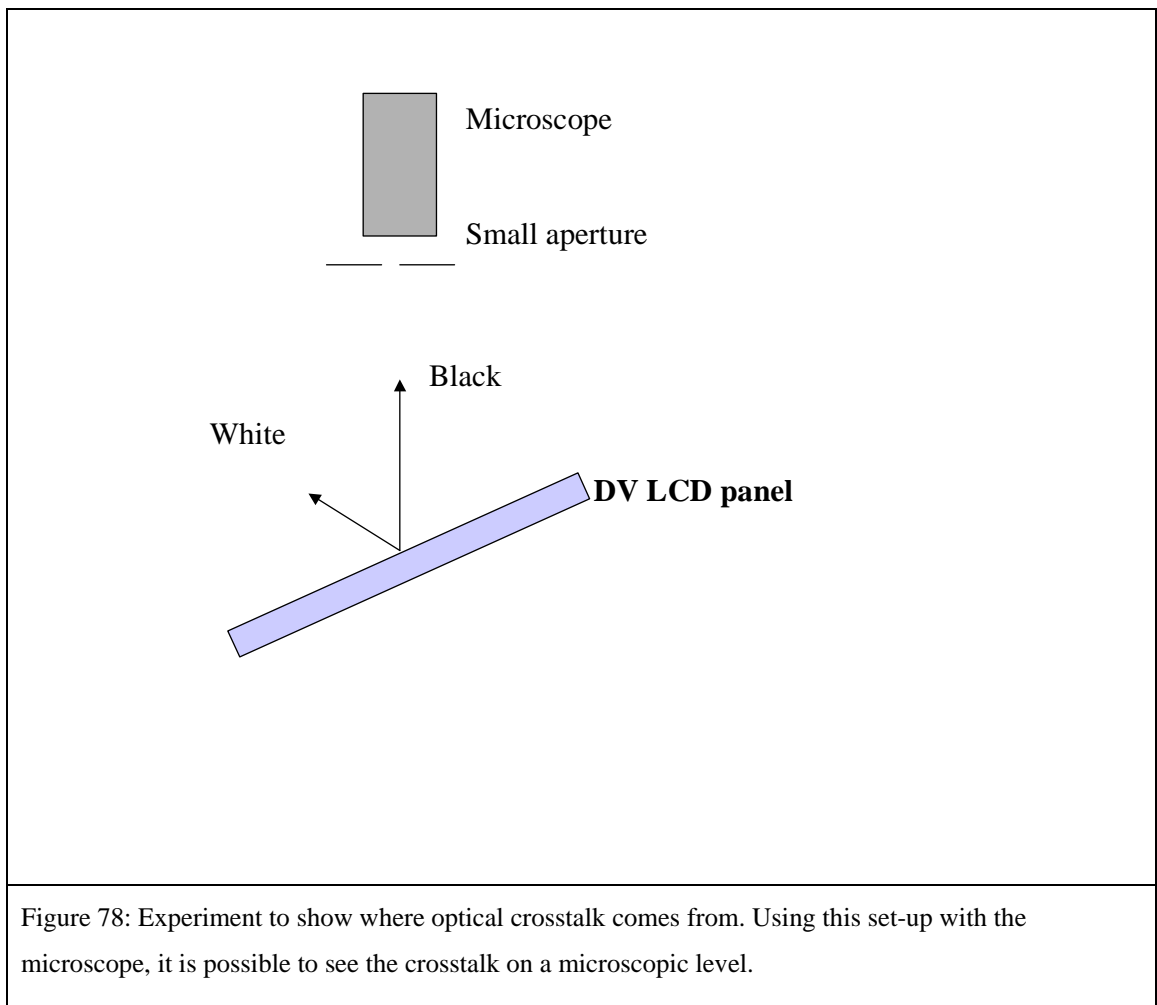


Figure 78: Experiment to show where optical crosstalk comes from. Using this set-up with the microscope, it is possible to see the crosstalk on a microscopic level.

The procedure for the experiment is as below;

1. A microscope is used to look at the dual view panel using sufficient magnification to see the features of the pixels and parallax barrier.
2. The dual view display is tilted so that the microscope views the display at 30 °. At this angle the microscope is looking straight at the left image.
3. The left image is set to be black.

The right image is set to be black.

In this case the microscope should see only LCD light leakage. I.e. when the LCD tries to display black, the black is not perfectly absorbing and some light leaks through the pixels. This is light that decreases the contrast ratio of the LCD.

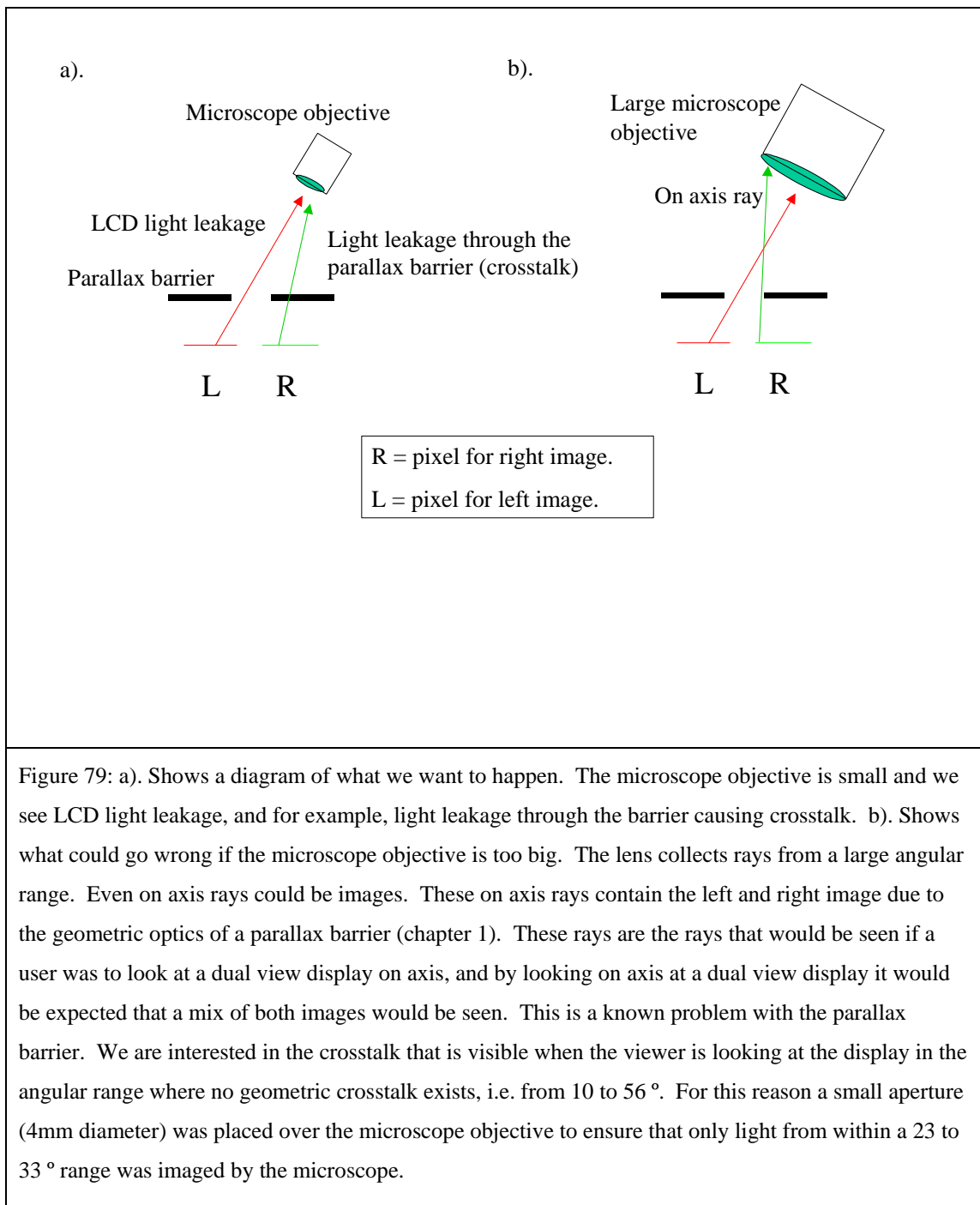
4. The left image is set to be black.

The right image is set to be white.

In this case the microscope should see;

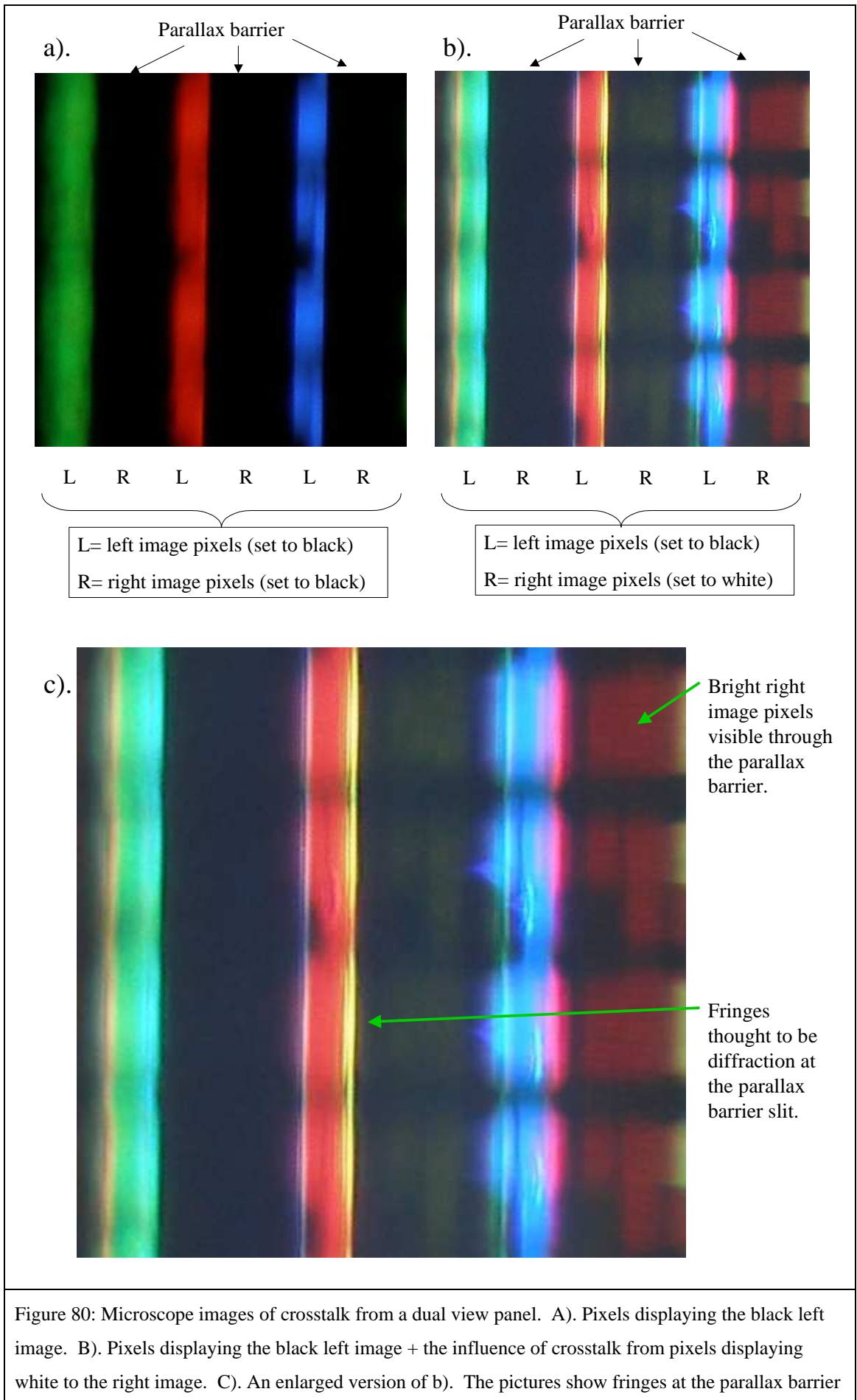
- a). LCD light leakage (as before).
- b). Light from the crosstalk. I.e. light from the right view that leaks into the left view. This is the extra light that causes the faint crosstalk image to be visible (as seen in Figure 76).

Note: A microscope objective typically has a short focal length, the microscope objective used must be positioned 2.3 cm away from the dual view panel. Also the microscope apertures can be very large. This could cause a problem as described below.



### Results

Figure 80 shows the images achieved from the above experiment. The photos were taken with a long exposure to attain bright images of the very low light level artefacts.



slit thought to be caused by diffraction, and a faint image of the right pixel, thought to be due to light leakage through the parallax barrier.

### *Observations and initial conclusions*

- The light from the left pixels is leakage from the black LCD pixels. This light causes a reduction in contrast ratio of the left image, but this light is not linked to the right image, so it is not a source of crosstalk.
- The right pixels can be seen slightly through the parallax barrier. This indicates that some light from the right image reaches the left viewer by simple transmission through the black dye in the parallax barrier.
- Transmission through the parallax barrier is wavelength dependent. Red can be seen to be transmitted through the barrier the most, followed by green, and then blue.
- The panel is at an angle to the microscope objective, therefore only the red left pixel is well focused. The green left, and blue left pixels are out of focus, and so the image is blurred.
- Fringes can be seen at the edges of the parallax barrier. This could be diffraction from the light from the right pixels.
- Fringes from the parallax barrier slit of the red left pixel are yellow (consistent with diffracted green from the adjacent right image pixel, plus red light from the left pixel LCD light leakage), and magenta (consistent with diffracted blue light from the other adjacent right image pixel, plus red light from the left pixel LCD light leakage). Other fringes also follow this pattern.
- There is too much noise present in the photograph to quantify each cause of crosstalk, and the linearity of the detector is not known.

### *Discussion*

In summary it seems that crosstalk is caused by light leakage through the parallax barrier, and diffraction from the parallax barrier slits.

The following sections discuss whether these conclusions are sensible, or whether other phenomenon could account for the effects seen.

### 2.3.4 Further discussion supporting diffraction as a cause of crosstalk

The fringes seen in the photograph of Figure 80 look similar to Fresnel diffraction fringes [45], but it is possible that they could be an artefact created by the microscope optics, such as lens flare. In this section a number of possible causes for the fringes are considered, and the conclusion is that the effect is a combination of diffraction and lens flare. The intensity of the effect suggests that this diffraction is a significant contributor to the total crosstalk.

The possible causes of these fringes that were considered when coming to this conclusion were;

- The fringes are caused by diffraction in the dual view system
- The fringes are caused by diffraction in the microscope system
- The fringes are caused by lens flare in the microscope system

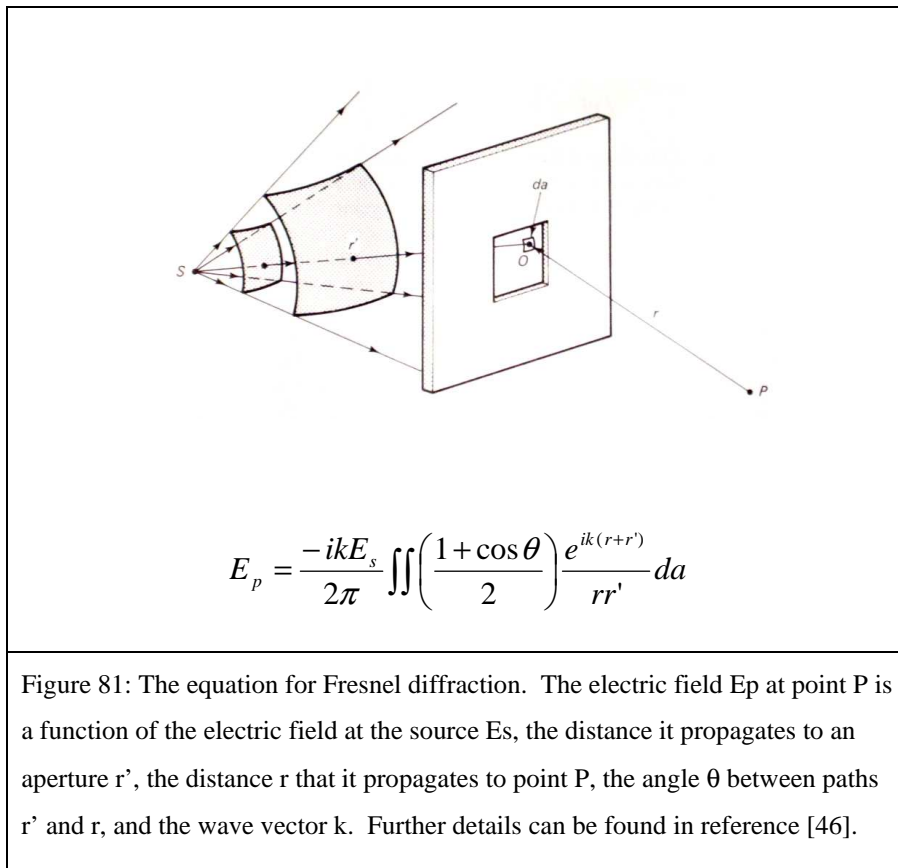
Each possibility is discussed in more details below.

#### *Diffraction in the dual view system*

We know the sizes of the apertures that diffract in the dual view system; that is to say, the sizes of the pixels apertures and the barrier slit apertures. Therefore we can predict the fringe spacing that we would see from Fresnel diffraction in this system. If the prediction matches the fringe spacing seen with the microscope then we can say that the fringes are likely to be Fresnel diffraction fringes.

Here we create a simulation of diffraction in the dual view system and find that the fringe spacing is almost identical to that seen experimentally with a microscope.

From [46] the formula for Fresnel diffraction is as below:



The equation is modified to fit the dual view system as follows. Firstly it is assumed that the equations can be simplified to a 2D system where  $s$  is not a point source, but a vertical line source emitting a cylindrical wave towards a vertical aperture. In this case integrating across the aperture horizontally is the same as integrating over the slit horizontally at any other vertical position on the slit. Therefore it is only necessary to integrate across the slit in one position.

Secondly, the equations can be further modified after considering the geometry of the dual view system.

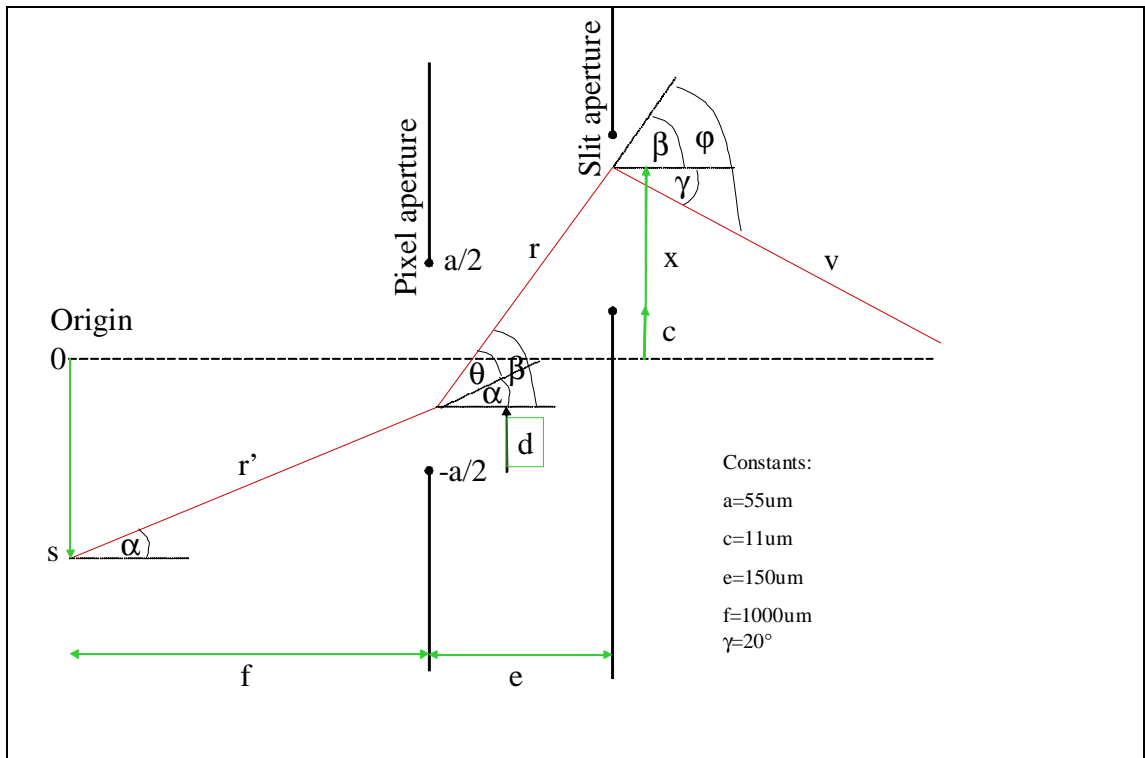


Figure 82: The geometry of the dual view system. A light source at position  $s$  propagates through the pixel aperture and slit aperture. The slit aperture is imaged at a detector a distance  $v$ .  $f$  is the distance from the source to the pixel aperture,  $e$  is the pixel-barrier separation. The pixel aperture width is  $a$ , and the slit is displaced from the origin a distance  $c$ .  $d$  and  $x$  are the positions that the light passes the pixel and slit respectively. The distances  $e$  and  $f$  have been multiplied by 1.5 to approximately take into account the 1.5 refractive index of the medium. The angles used all refer to angles internal to this medium.

Light from the backlight at position  $s$ , must be propagated through the pixel aperture, the barrier slit, and finally to the microscope objective. Therefore there are two obliquity factors in the equation, due to angles  $\theta$  and  $\phi$ . It is assumed that the intensity profile at the slit is imaged identically to the microscope CCD, and that distance  $v$  is long such  $v$  and  $\gamma$  are constant.

Therefore the electric field at position  $x$  is:

$$E_x = \frac{-ikE_s}{2\pi} \iint \left( \frac{1 + \cos \theta}{2} \right) \left( \frac{1 + \cos \phi}{2} \right) \frac{e^{ik(r+r'+v)}}{rr'v} dd$$

Since it is the fringe pattern that is of concern and not the absolute intensity, all constant factors in the equation are ignored so,

$$E_x = -i \iint \left( \frac{1 + \cos \theta}{2} \right) \left( \frac{1 + \cos \varphi}{2} \right) \frac{e^{ik(r+r')}}{rr'} dd \quad \text{and} \quad \text{Intensity} = E_x E_x^*$$

Where the equations for  $r$ ,  $r'$ ,  $\theta$  and  $\varphi$  are given by the geometry in the previous figure.

$$r' = \sqrt{f^2 + (s - (d - a/2))^2}$$

$$r = \sqrt{e^2 + (c + x - (d - a/2))^2}$$

$$\alpha = \tan^{-1} \left( \frac{(d - a/2) - s}{f} \right)$$

$$\beta = \tan^{-1} \left( \frac{c + x - (d - a/2)}{e} \right)$$

$$\theta = \alpha - \beta$$

$$\varphi = \gamma + \beta$$

These equations were evaluated numerically by a computer program written in C++.

The graph below shows the result when source position  $s=0$ . For  $s=0$ , the light source is a point source spaced quite far behind the pixel aperture such that the light is a slightly divergent wave when it reaches the pixel.

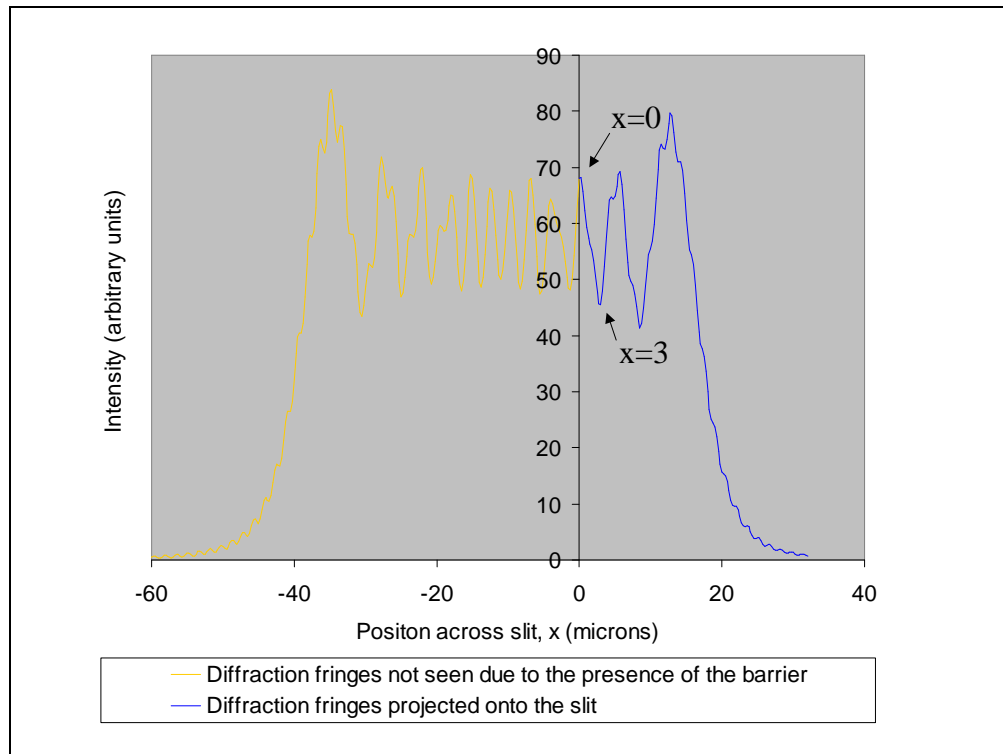
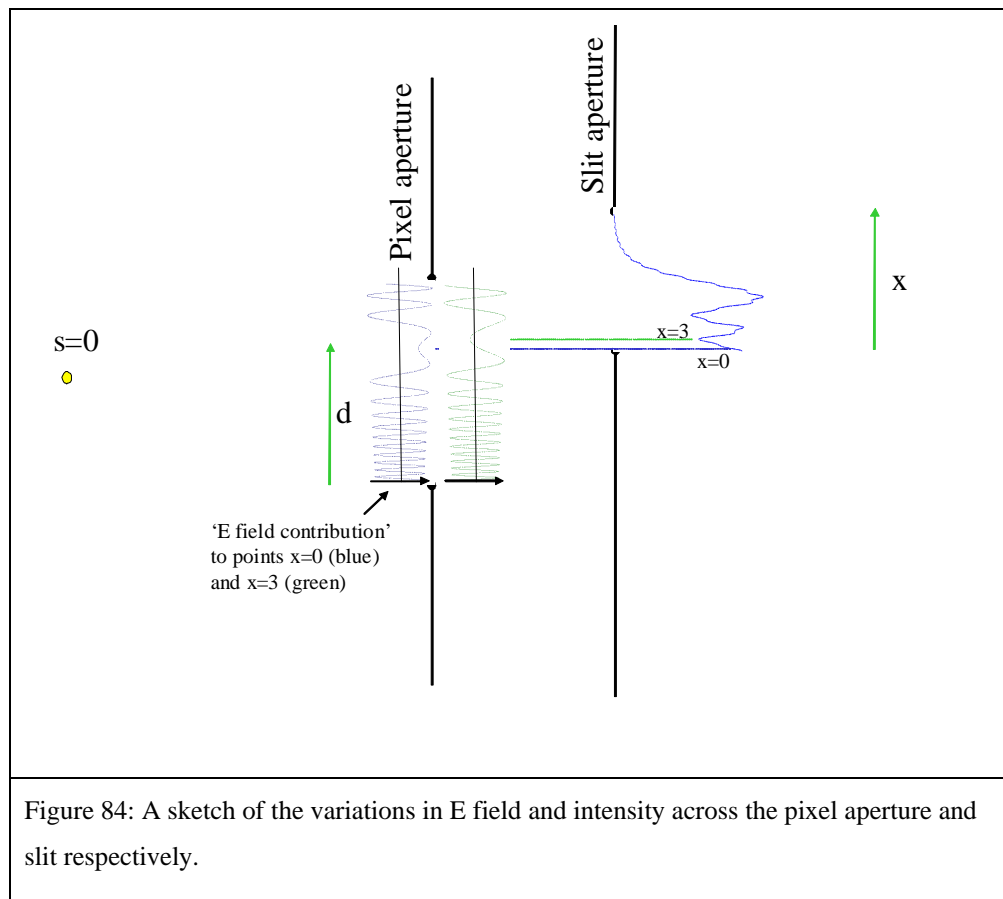


Figure 83: Simulated Fresnel diffraction fringes in the plane of the barrier in the dual view system. The barrier slit runs from  $x=0$  to  $32 \mu\text{m}$ .

The graph of intensity versus position on the slit  $x$  shows diffraction fringes at the slit. This is essentially a projection of the pixel aperture on the slit with some diffractive fringes.

It is possible to see how these fringes come about by considering points  $x=0$  (where the intensity is a maxima) and  $x=3$  (where the intensity is a minima).

The sketch below shows the E field contribution to these points from each position across the pixel aperture. The E field contribution is worked out as follows. For a point  $x$ , the phase and amplitude of the E field that comes from each point  $d$  is deduced. The sum of the E-fields from each point  $d$  gives the resultant E field at point  $x$ . The component of the E field at each point  $d$  that is in phase with the resultant E field at point  $x$  is called the 'E field contribution' since it is the contribution that each point  $d$  makes to the E field at  $x$ .

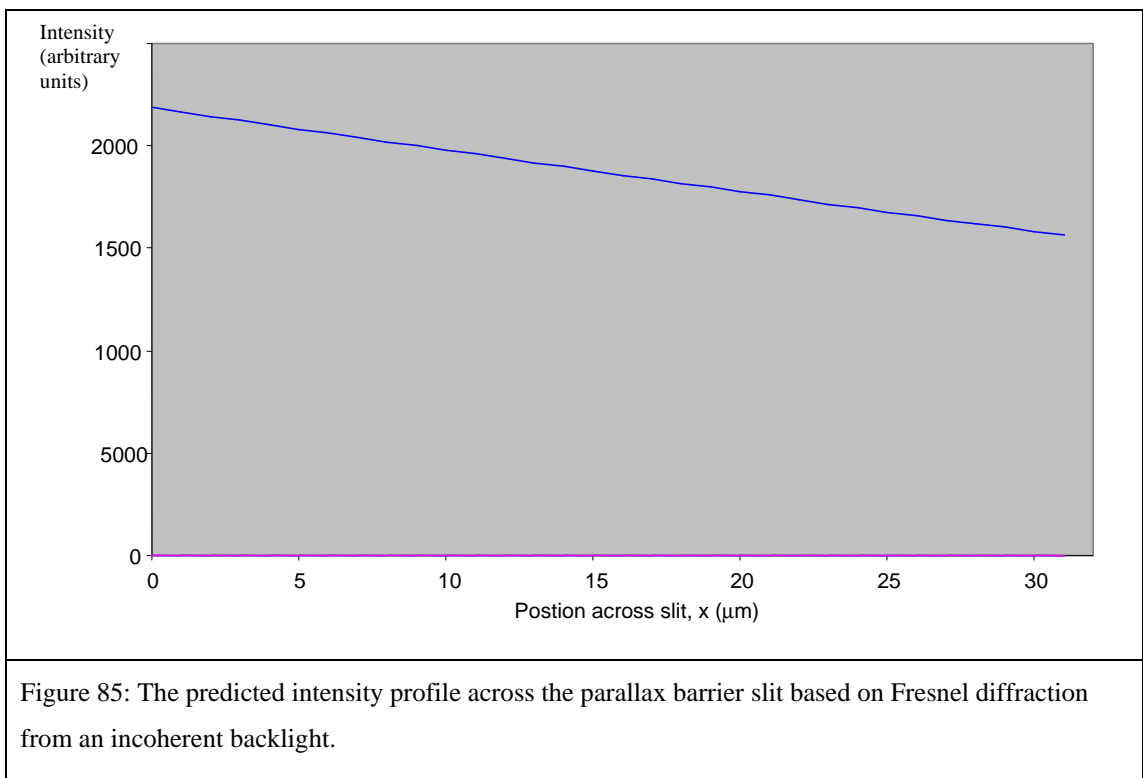


The intensity at a point  $x$  is modified by various factors. The amplitude of the E field varies across the pixel due to the obliquity factors and the distances  $r$  and  $r'$  that the light travels. However these are small effects. The main cause of the fringes at the slit is due to the variations in phase caused by  $r$  and  $r'$ . Also the pixel aperture blocks regions which either contribute positively or negatively to the E field at position  $x$ .

The case above where the dual view system is illuminated with a point source is not accurate. The microscope pictures were taken when the illumination source was the actual backlight used in the dual view display. This backlight is an extended source emitting light at all angles.

To calculate the intensity pattern of light at the slit when using an extended source, we should consider the effect of light illuminating the system from a range of different positions. Each point  $s$  on the backlight would emit light through the system at a different angle which would cause a different intensity profile at the slit. If we assume the backlight is spatially incoherent, then each point  $s$  will have a random phase such that they do not interfere with each other. In this case the total intensity at the slit will be the sum of the intensities created by each point  $s$ .

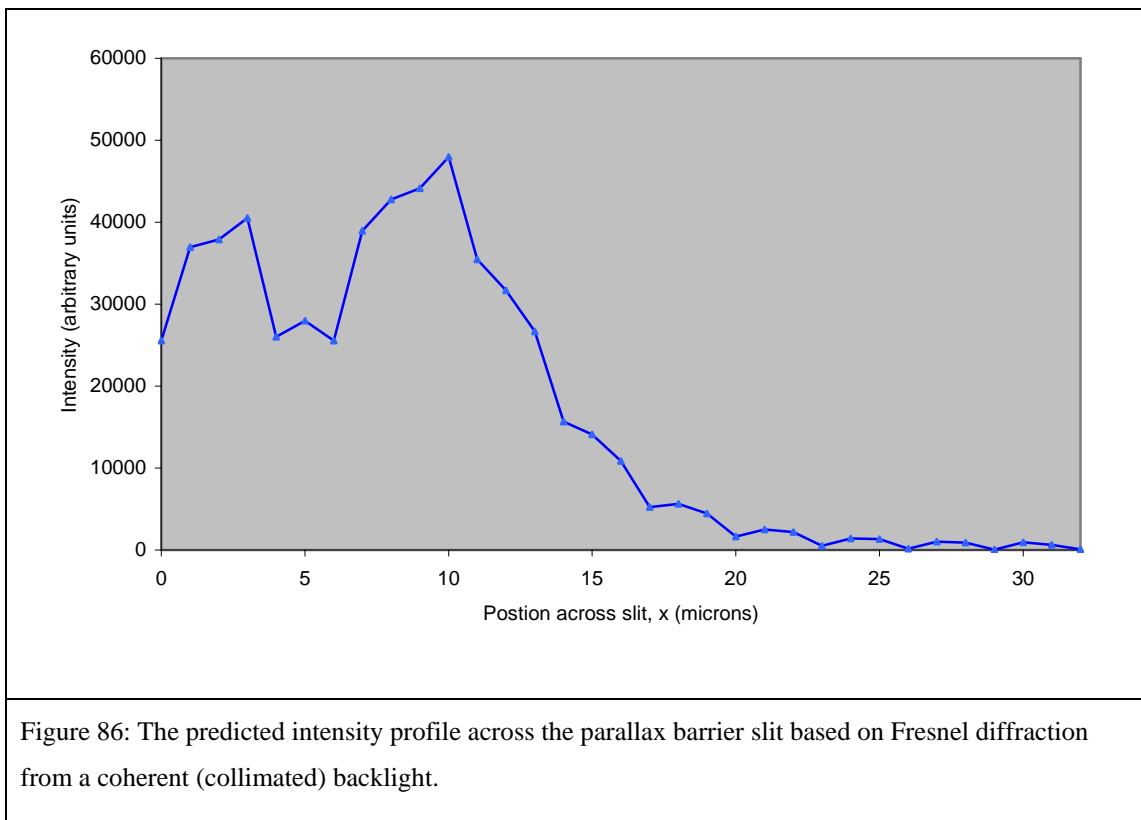
The graph below shows the simulated intensity pattern at the slit which is given by the E-field multiplied it complex conjugate. The intensities have been integrated over the range  $s=-1000$  to  $1000 \mu\text{m}$  ( $-45^\circ$  to  $45^\circ$ ).



Each angle of illumination produces a projection of the pixel aperture on the slit at a different position. When each of these projections is summed together the overall intensity at the slit does not have any fringes. The fringes are blurred to such an extent that they are not visible.

If we assume that each point source  $s$  is coherent with other points on the backlight then the different point sources can interfere with each other. In this case the intensity at the slit would be found by summing the E field contributions at the slit from each point source  $s$  on the backlight.

The graph below shows the result of such a calculation. Again the backlight source has been simulated over the range  $s=-1000$  to  $1000 \mu\text{m}$  ( $-45^\circ$  to  $45^\circ$ ).



When we assume that each point on the backlight is coherent with the others, the simulation predicts that fringes should be seen in the plane of the slit.

The fringes in this theoretical case have a pitch of  $8 \mu\text{m}$ . The fringes seen in the microscope picture of the crosstalk are spaced apart by  $9 \mu\text{m}$  (by measurement).

So, if we assume that the backlight is coherent then we predict that Fresnel diffraction will produce fringes that look very similar to those seen in the experiment. This supports the theory that the fringes result from Fresnel diffraction.

However, the modelling also shows that if we assume that the backlight is incoherent then we predict that diffraction cannot account for the experimentally observed fringes.

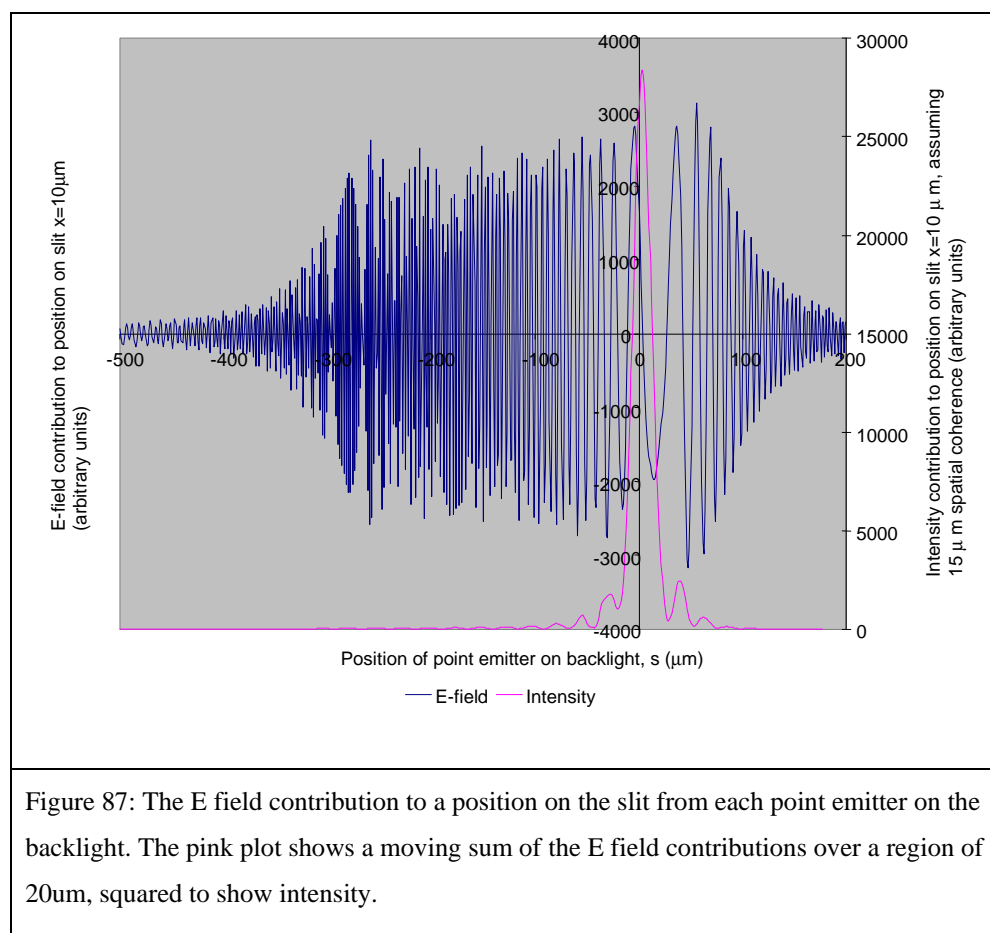
In reality the backlight is neither spatially incoherent nor coherent, it is somewhere in between. The modelling raises the question, ‘Is the small amount of coherence expected in a backlight capable of producing visible fringes at the slit?’ We attempt to answer this question next.

To create an ideal model of the actual backlight light source we would want to measure the exact phase profile across the extended source and propagate it through the dual view system using the Fresnel diffraction theory. This would tell us what intensity profile we would expect at the slit. This would be a difficult challenge.

A simpler method of modelling such partially coherent systems exists. By using this technique we can see the effect on the fringes of various levels of coherence in the backlight, and compare this with a predicted level of backlight coherence. The result states that the coherence in the backlight is not sufficient to produce fringes. The following text describes this approach in more detail.

In the approach that can be used to model partially coherent systems, the backlight is built up from many individual point sources (as before), but each point is only added coherently with nearby point sources. Each set of nearby point sources is added incoherently to other sets of point sources [47].

Below is a graph that helps to explain the effect of partial coherence in this particular dual view system.



The graph shows the contribution made to the E-field on the slit at position  $x=10\mu\text{m}$ , for different point emitters on the backlight at position  $s$ . The plot is a rapidly varying function. Its features can be understood as follows.

Firstly there is no significant contribution to the E field at the slit from point emitters where  $-380 \mu\text{m} < s < 180 \mu\text{m}$ . This can be understood geometrical optics. These point emitters have no geometric path from the backlight through the pixel aperture and to the slit. The path is blocked by the black mask that forms the pixel aperture.

For the range of point emitters that are inside the range  $-380$  to  $180 \mu\text{m}$ , the contribution to the E-field made to position  $x$  changes from positive to negative primarily due to change in phase as distance  $r'$  changes. The change from positive to negative is the slowest when the direct path from the slit to the backlight is perpendicular to the backlight since  $r'$  varies the slowest here.

If there is no coherence in the backlight each point emitter from  $s = -380$  to  $180 \mu\text{m}$  acts independently to produce an intensity pattern across the slit. This is as expected since a point emitter acting independently from its neighbours will emit in all directions, such that all of this range of emitters will add to the intensity of all points on the slit resulting in a blur of fringes and loss of fringe visibility.

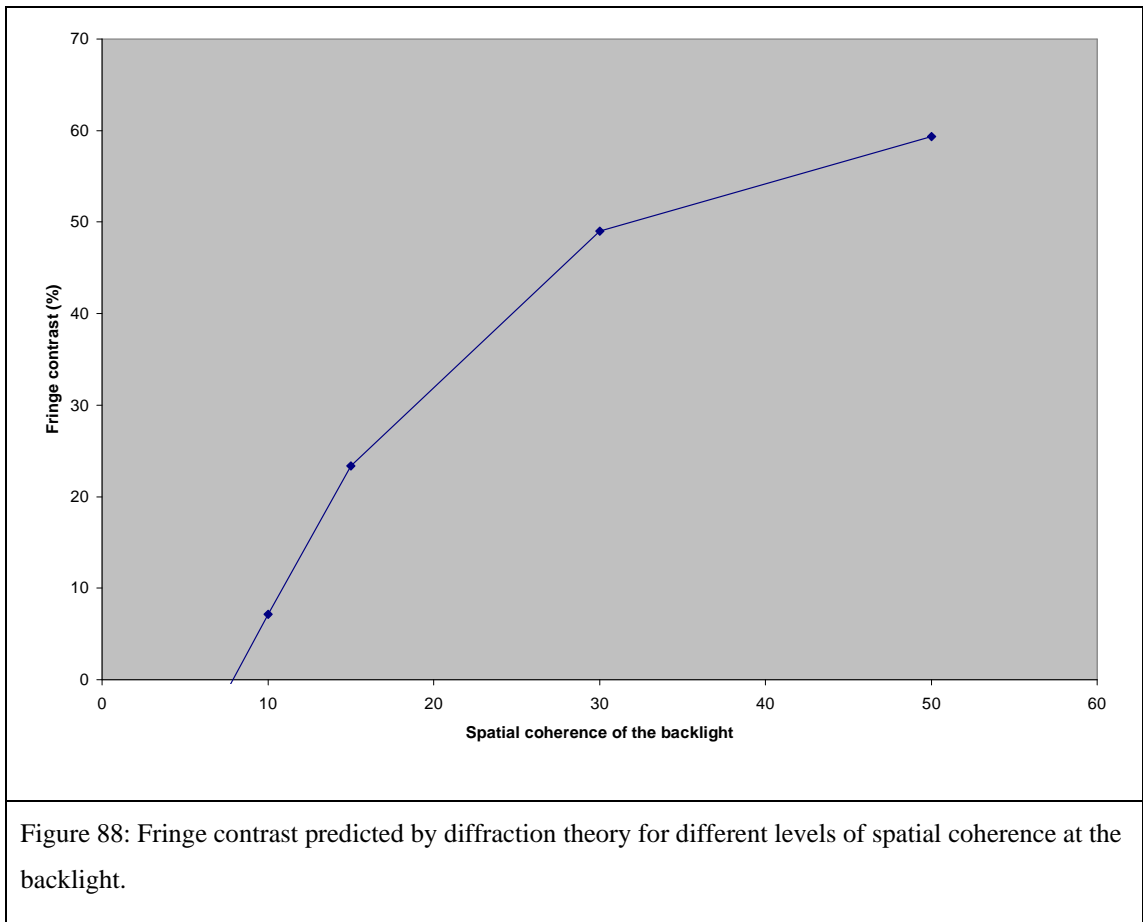
Suppose the backlight is coherent over a range of  $20 \mu\text{m}$ . If one considers the intensities created by each  $20 \mu\text{m}$  range of coherent point emits on the backlight one can see from Figure 87, that most of the point emitters will cancel each other due to their positive and negative variations such that they will make no contribution to the intensity at the slit.

This is as expected since point emitters partially in phase with their neighbours will emit partially collimated light. In this case the direct on-axis light path from the backlight to the slit will dominate the intensity pattern at the slit.

This is shown by the pink trace in Figure 87 which is a moving sum of a  $20 \mu\text{m}$  range over the point emitters. Most of the contributions to the slit intensity from the point emitters cancel. There is only a small region of point emitters which contribute to the intensity pattern at the slit at about  $s=10$ . This is the position on the backlight that is perpendicular to position  $x$  on the slit.

If the slit intensity profile is dominated by illumination from one angle like this, then the fringe patterns may not be smeared out so much and may become visible.

Figure 88 below shows the contrast of the slit pattern versus the spatial coherence length that the backlight is assumed to have in the Fresnel model.



The graph predicts that the fringes would still be visible (with about 10% contrast ratio) if the backlight was spatially coherent only over a 10  $\mu\text{m}$  range. In the photograph of the fringes it is difficult to be sure of the fringe contrast since the camera CCD is not linear with intensity, however the contrast of the fringes seem to be about 10%.

Next we need to determine what the spatial coherence of the backlight actually is. If the backlight is spatially coherent over 10  $\mu\text{m}$  or more then the theory predicts that the fringes should be easily seen. If not, then the theory predicts that the fringes at the slit should not be seen with illumination from a backlight.

From [46] the angular range over which a source emits  $\theta$ , with wavelength  $\lambda$ , in medium of index  $n$ , is related to its spatial coherence  $l$ , by the relationship:  $l = n\lambda/\theta$ .

10  $\mu\text{m}$  spatial coherence give an angular intensity distribution of about 5  $^\circ$ .

The backlight does not emit uniformly with angle. It consists of various optics including micro-prisms and so on, so that the backlight emits more light on-axis. The backlight has a light output distribution such that most of the light is emitted within a 25  $^\circ$  range once the light has entered a glass medium of index 1.52.

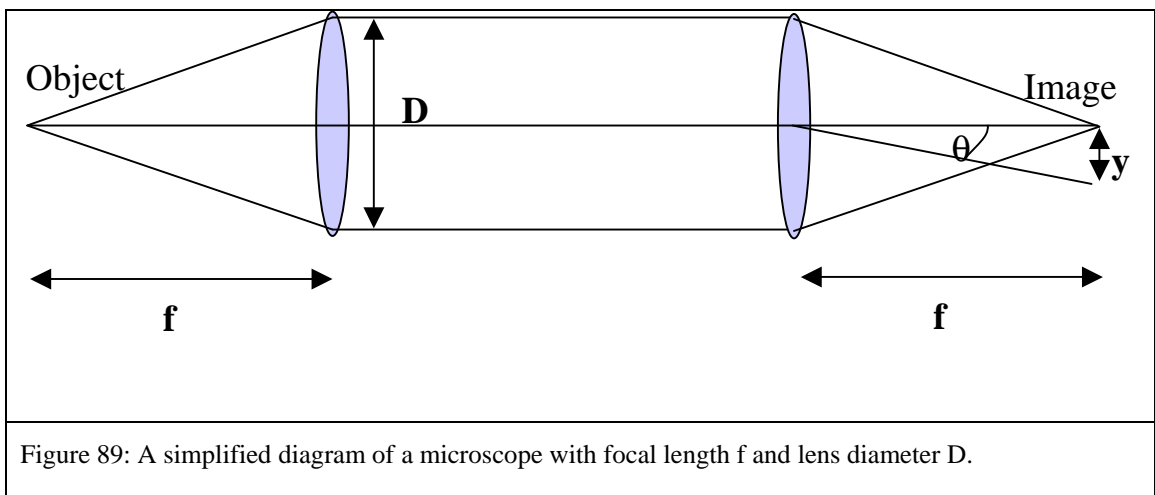
The theory predicts that the backlight needs a spatial coherence that is five times greater than it has for fringes to be formed at the slit. Therefore theory predicts that no fringes should be seen.

In addition to spatial coherence, the backlight also needs to have temporal coherence to produce clear diffraction fringes. The temporal coherence of the backlight can be seen to be more than adequate to produce diffraction fringes in this case.

The backlight has a surprising degree of temporal coherence. The backlight is white in colour, but this white is produced by a cold cathode fluorescent tube which emits light at particular frequencies in the red green and blue. The fringes seen in the microscope picture are from the green pixel. The green colour filters of the LCD panel remove the red and blue emission from the backlight, leaving the green emission peak only. A wavelength spectrum of the backlight shows that this peak is at 548nm with a FWHM (full width at half maximum intensity) of 7 nm.

From [46], this wavelength  $\lambda$ , and bandwidth  $\Delta\lambda$  are related to temporal coherence length  $t$ , by the formula,  $t = n\lambda^2 / \Delta\lambda$ . In the case of the above system  $t = 65 \mu\text{m}$ . The maximum path variation in the system (excluding the range  $s = -380$  to  $180 \mu\text{m}$  because these angles do not significantly contribute to the intensity at the slit) is about  $6 \mu\text{m}$ . Therefore we do not expect the temporal coherence of the backlight add much smear to the fringes.

*Diffraction in the microscope system*



From [46] the 1<sup>st</sup> diffraction maxima of a lens system at angle  $\theta$ , with an aperture diameter  $D$  is approximately given by  $\theta = 1.22 \lambda / D$ . If the lens is a focal distance  $f$  away

from the object then the distance between a spot and its first maximum  $y$  is approximately given by  $y=f\theta$ .

Given that the focal length of the microscope objective is 23 mm and the diameter of the aperture is 4mm, the fringe spacing that would arise from diffraction in the microscope system is about 4  $\mu\text{m}$ .

Since this is of similar pitch to the fringes seen in the photograph (which have a pitch of 9  $\mu\text{m}$ ) it is possible that diffraction in the microscope system could be responsible for the fringes. This is tested in more detail later on.

#### *Lens flare in the microscope system*

Lens flare as described by [48] is ‘the light scattered in lens systems through generally unwanted image formation mechanisms, such as internal reflection and scattering from material inhomogeneities in the lens’.



An example of this is shown in the picture opposite [48]. A bright sun causes rings and spots to appear in the photo. It could be possible that the relatively bright line of crosstalk causes fringes by lens flare artefacts. The system is tested as

explained below.

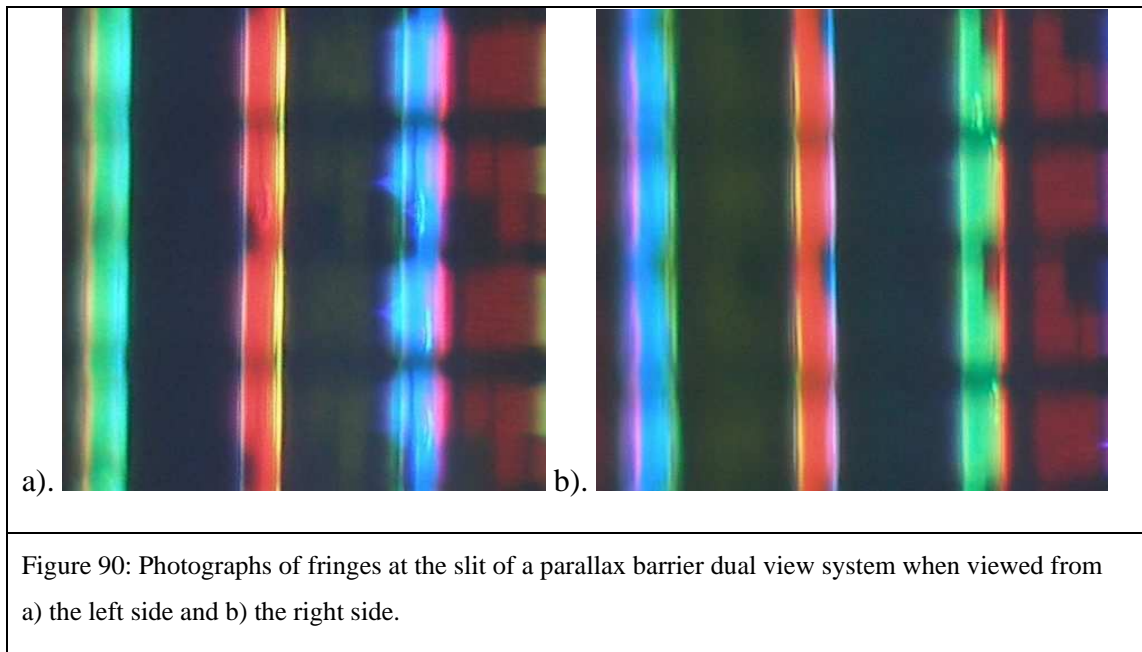
#### *Testing of camera flare and diffraction artefacts*

If microscope diffraction is causing the fringes to appear on the photograph, then we would expect the diffraction to be caused by the 4 mm aperture that was added onto the objective. We would expect the rest of the optics in the high quality microscope to have a diffraction limit that is based on its original objective size which was much larger than 4 mm. Therefore if we change the diameter of the aperture on the front of the microscope the pitch of the fringes in the photograph may change. If the pitch of the fringes does change then the fringe effect must be caused by the microscope objective, if not the fringes must be caused by some other effect.

The aperture placed on the objective was changed from 4 mm to 2 mm and no change in pitch was seen. This suggests that the fringes are not related to diffraction in the microscope system.

To test for lens flare the dual view panel was rotated under the microscope such that the objective viewed the right image rather than the left image. The left and right images

were then switched so that right pixels show black and the crosstalk comes from white left pixels. The figure below shows the results.



Observe the yellow fringes in the centre of the original photograph. The fringes drop off in intensity from right to left. In the photograph where the panel has been moved, the fringes still drop off in intensity from right to left. In the new picture the fringes appear to come from the black region of the barrier rather than the slit. This is hard to explain by any other mechanism than camera flare.

This suggests that the phenomenon is a flare artefact in the microscope rather than diffraction in the dual view system.

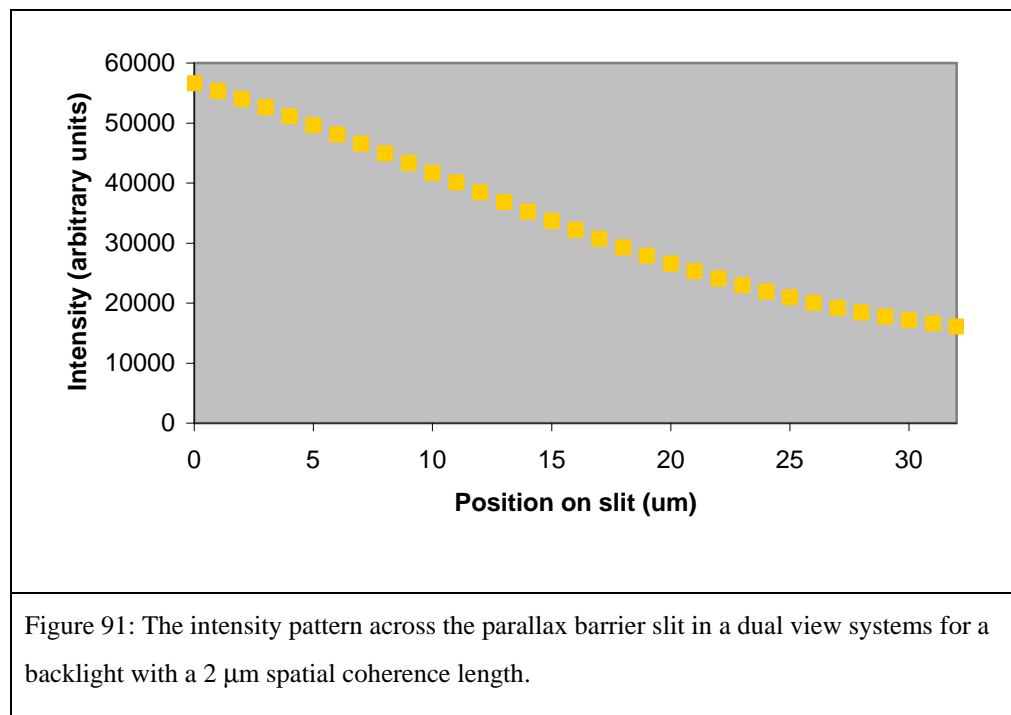
#### *Are the fringes a combination of diffraction and lens flare*

We wanted to know if the crosstalk at the edges of the slit was due to diffraction. We tried to explore this by studying the fringe pattern but now we believe that this is a result of camera flare.

However, the main fringe from which the lens flare is generated must be a real phenomenon. We now consider if there is any evidence to suggest that this main fringe is diffraction or not.

Now that we know the fringes are a microscope artefact, we can re-assess the Fresnel diffraction model fit with the experimental results. If the Fresnel diffraction model fits the data then this is evidence that the main fringe is caused by diffraction.

The backlight emits most of its light within a  $25^\circ$  range. This means that the spatial coherence of the backlight is about  $2\ \mu\text{m}$ . The graph below shows the intensity across the slit predicted by the Fresnel model and a  $2\ \mu\text{m}$  spatial coherence length.



The Fresnel model predicts that the main fringe should be very broad. Even with the effects of lens flare this is not seen in the photograph. The system being modelled is complicated and so there are many possible reasons for this.

The system is a partially coherent system, which is modelled by assuming that light from the backlight is spatially coherent over a length and that after this length the coherence stops suddenly. Others who have modelled such systems assume that coherence decreases gradually over distance [49].

It is possible that the main fringe in the photograph has an intensity profile that is similar to the modelling results, but that it is not visible because it is drowned out by the left view pixels.

The dual view system comprise two apertures which are modelled but it also comprises a liquid crystal layer, view angle compensation films, polarisers, and many photo resist structures that help to form the thin film transistors. These will alter the phase of the light in the system and could affect the diffraction pattern.

The shape and transmission profile at the edge of the slits are approximated to a perfectly thin and hard-edged aperture that may not be a valid assumption.

The microscope objective does not focus only on the slit. The objective has a certain depth of field that means that the image captured on the CCD is not just an image of the slit plane; the image contains effect from light outside the plane of the slit.

Our model does not convincingly fit the data seen experimentally in this case and therefore it does not provide convincing evidence that the main fringe results from diffraction.

The figure below presents a result from a simplified experimental set up.

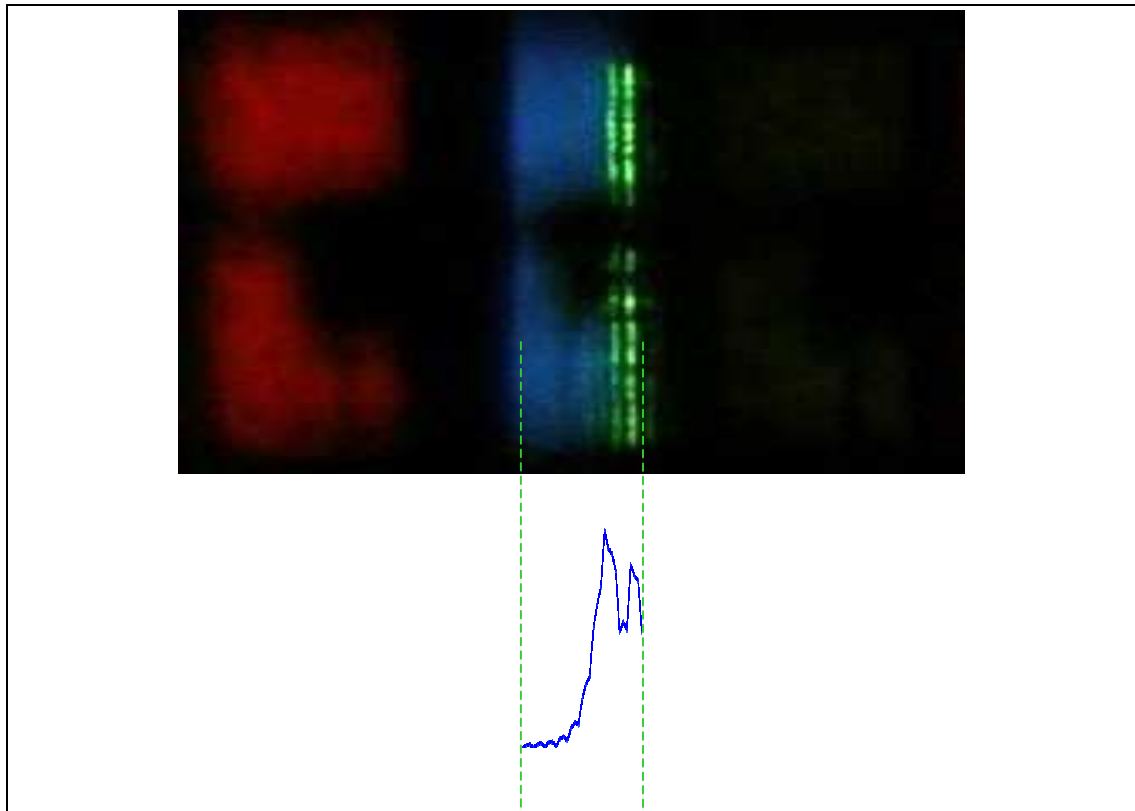


Figure 92: A photograph of diffraction fringes created by a green laser and a dual view system compared with a theoretical simulation based on Fresnel diffraction theory. The photograph shows a slit in the parallax barrier of the dual view system through which a blue pixel can be seen. The green fringes come from the green laser passing a green pixel covered by the barrier. The laser light is passed through the dual view system on axis with a small amount of white light illumination to enable the position of the slit to be seen. The theoretical simulation is taken from Figure 86.

In the simplified experimental set-up a coherent laser source is used and the system is only illuminated on axis. This simplifies the simulation because a partial coherence model is no longer needed, and since the laser light passes the system on axis I suspect that the effects of the liquid crystal and viewing films which are angularly dependant will have less effect.

The model provides a much better fit with the simplified system. The two fringes seen experimentally are seen in the simulation and these fringes do not resemble camera flare because they are of equal intensity rather than being of decreasing intensity as seen before.

The fringes seen experimentally fit with the diffraction hypothesis however the intensity of this effect is not given by the experiment (since no quantification of the laser power or the fringe intensity was made) or the simulation. Therefore it is not possible to state that diffraction is a significant effect or not.

Evidence that quantifies the effect of diffraction can be seen in section 2.3.11. It shows that diffraction is significant and the laser experiment above shows what diffraction looks like at the slit.

By knowledge of how the diffraction fringes would smear as the coherence of the light source decreases it seems plausible that these diffraction fringes would appear as one main fringe but that the simple model that we have developed does not predict this smear precisely.

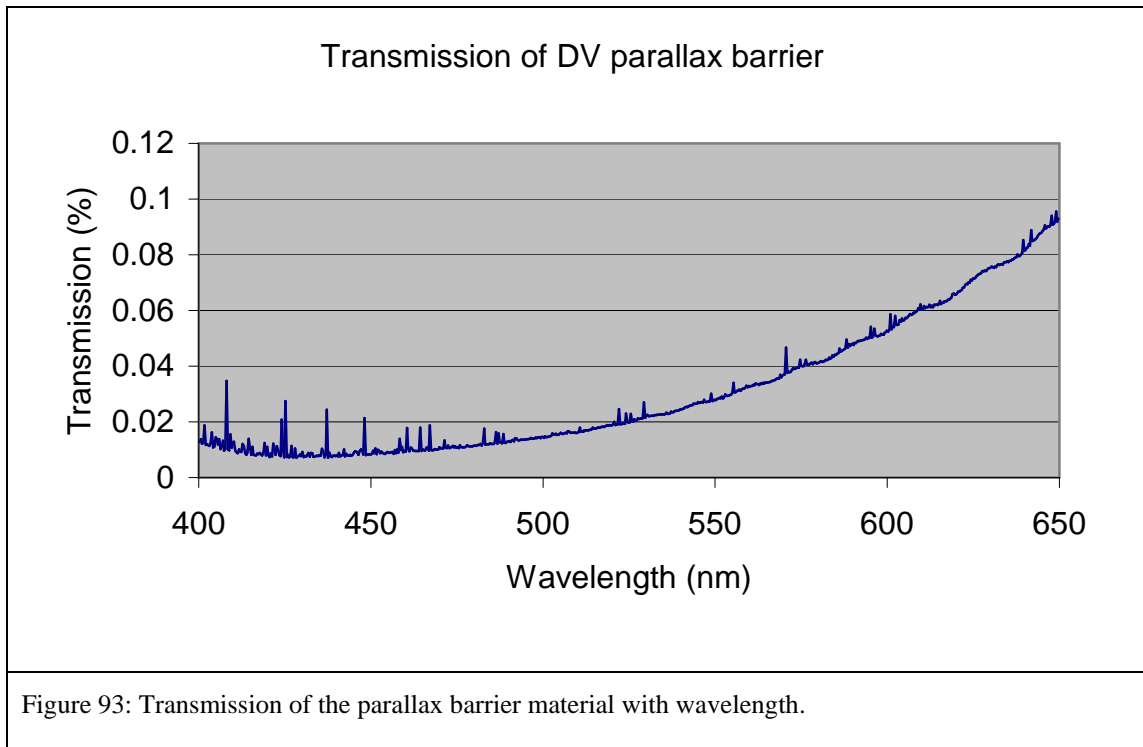
Based on this line of logic, we can suggest that light seen at the edge of the slits in Figure 80 is a result of diffraction.

This conclusion is not solid. The fit between predicted diffraction patterns and those seen experimentally are not perfect, but the results do suggest that diffraction is the cause. I suspect that the reason for the poor fits is due to inaccurate assumptions made in the model, however to rectify these errors would require substantial effort and is not considered further in the thesis.

### **2.3.5 Further investigation of light leakage through the parallax barrier**

The microscope pictures of crosstalk suggest that some crosstalk is caused by light leaking through the black barrier material. This section investigates the transmission properties of the barrier further. Firstly, the transmission versus wavelength properties are consistent with crosstalk seen in the microscope pictures. Secondly, the transmission of the barrier material is quantified in order to estimate the amount of crosstalk that is produced. Crosstalk by barrier transmission is thought to cause 6% of the crosstalk in the panel.

Figure 93 shows a measurement of the transmission versus wavelength of the parallax barrier, using a spectrometer.



*Experimental details.*

The equipment used was an Olympus BX60 microscope and a CCD spectrometer from Ocean Optics (model USB2000). The microscope rear illumination light source (a halogen light bulb) was focused to a 50µm spot in the plane of the sample. This light is collected by the microscope objective, and passed to the CCD spectrometer.

Firstly a reference spectrum was taken without the parallax barrier sample in place (just glass). The integration time of the CCD spectrometer was 3ms. The parallax barrier sample (processed onto glass) was put in place, and another spectrum was taken. Due to the high absorbance of the black barrier the CCD integration time was changed to 2500ms to enable enough light to be sampled. The transmission value given on the graph at any one wavelength is the ratio of the number of counts on the CCD for light through the parallax barrier to the number of counts on the CCD through glass, this value is then multiplied by the ratio of the different integration times used on the CCD.

*Conclusions*

The transmission spectrum shows that red is transmitted the most, then green, then blue. This is consistent with the parallax barrier leaking light in Figure 80, since the light suspected of being leaked through the parallax barrier in this photo also is most strong in the red, then green then blue.

### *Quantifying crosstalk caused by parallax barrier light leakage*

It is possible to predict the amount of crosstalk caused by leakage through the parallax barrier by using data about the transmission of the parallax barrier and geometric modelling.

Figure 93 shows how parallax barrier transmission depends on wavelength. The precise transmission of the parallax barrier will actually depend on a number of other factors, which need to be taken into account to get a more accurate prediction of the crosstalk actually caused.

For example,

- The wavelength spectrum of the panel: the transmission of the barrier depends on the wavelength, so the transmission will depend on which wavelengths the panel emits. The wavelength that the panel emits depends primarily on the backlight spectrum, and the colour filter spectrum.
- The angle at which light is passing the barrier. It would be expected that light passing the barrier at grazing incidence would pass through a longer cross section of the barrier, and so be absorbed more.

These factors can be taken into account by measuring the transmission of the barrier in a more realistic setting. Figure 94 shows the results of the barrier transmission, based on an experiment described as follows. An entirely uniform black square of parallax barrier material was made – with no slits. This square was placed over the LCD panel, and intensity versus angle was measured. This result was divided by a measurement of intensity versus angle without the black square. This yields the transmission of the parallax barrier material, with angle, at the wavelengths emitted by the LCD panel. This measurement was repeated for red green and blue light emitted from the LCD panel.

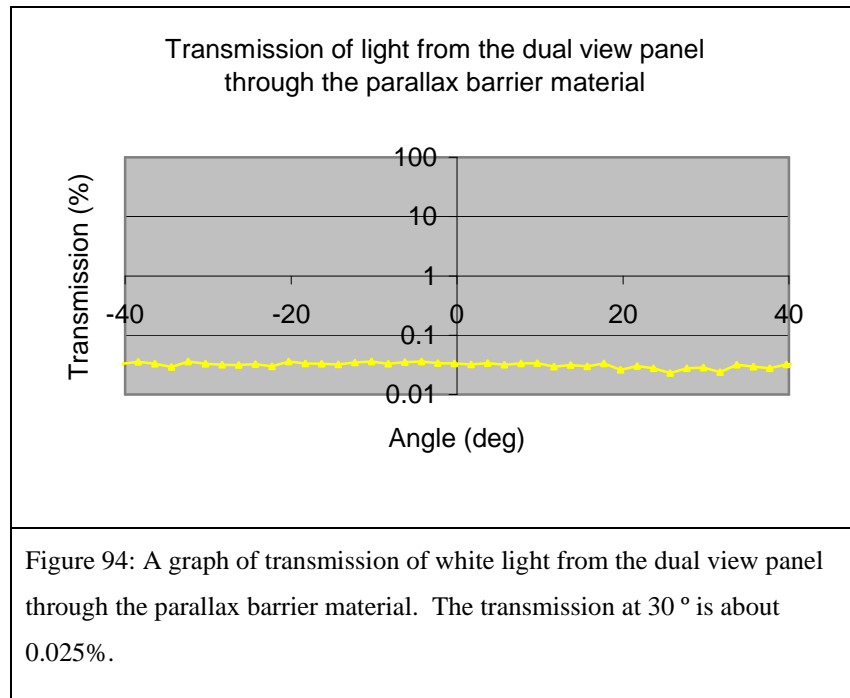
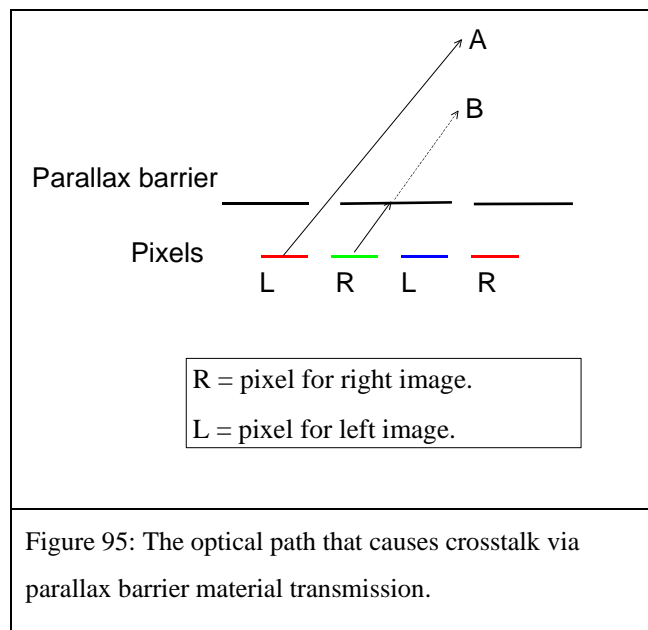


Figure 95 shows how the light leakage through the parallax barrier material causes crosstalk, at one viewing angle.



At 30 ° (left) the viewer sees light from the left image and light from the right image through the parallax barrier. To calculate the amount of crosstalk, the amount of light from each image must be determined, and the ratio taken.

The amount of light seen from the (correct) left image = Light from the left pixel passing through aperture C.

The amount of light seen from the (other) right image = Light from the right pixel passing through the barrier B.

The width of the left pixel is 44.5um, and the parallax barrier aperture is 38um, so 85% of the light passes the parallax barrier.

The width of the right pixel is also 44.5um, and due to the parallax barrier transmission, 0.025% of this light passes the parallax barrier.

Therefore we would expect the transmission of the barrier (for white light) to cause, 0.025/85% or 0.029% crosstalk. This is 6% of the total crosstalk in a dual view display.

### **2.3.6 A new panel design**

At this point in the diagnosis of the crosstalk origins, a new dual view panel design was made. This panel was built with the following additional features;

- The thickness of the parallax barrier material was doubled. The original transmission of the barrier material was 0.025% which caused 6% of the crosstalk. By doubling the material thickness the transmission becomes 0.000006%, making crosstalk by parallax barrier material transmission insignificant.
- The image separation angle of the display was increased by decreasing the thickness of the glue layer that adheres the parallax barrier. This reduces the amount of crosstalk in the display as described in section 4.2.2.3.
- The TFT design was modified to reduce the amount of electrical crosstalk in the display, as described in section 4.1.2.

These modifications were intended to reduce the crosstalk of the display, and they were successful. The new minimum crosstalk value for the display is 0.18%, compared with 0.46% for the first design. The bulk of the reduction is thought to be due to the increase in image separation angle.

This section continues to investigate the source of the 0.18% crosstalk. Note that repeating the microscope test of section 2.3.3 on the new panel design yields very similar pictures, but without crosstalk due to barrier transmission. Therefore the results from that test still hold for the new panel.

### **2.3.7 Further evidence of diffractive crosstalk**

It is thought that diffraction is a major source of crosstalk, but the evidence so far is not 100% convincing. This section looks for further evidence that diffraction causes crosstalk.

Laser light is seen to produce a diffraction pattern from the left view, all the way over to the right view, indicating that light does spread from one view to another via diffraction.

Measurement of barrier slit width versus crosstalk show that the smaller the barrier slits the more crosstalk is caused. This would be expected for diffractive crosstalk.

Measurement of the colour of crosstalk provides an anomalous result. If crosstalk were due to diffraction, then we would expect more crosstalk in the red than the blue. This is not the case. Which suggests that other causes of crosstalk are present. This is investigated in later sections.

#### *Diffraction patterns*

If diffraction is a significant cause of crosstalk then you would expect to see the maxima and minima of a diffraction pattern when a laser beam is shone through the LCD panel. In the figure below a green laser pointer is shone through the dual view LCD panel towards the right view. It can be seen that the light is spread out into the left window.

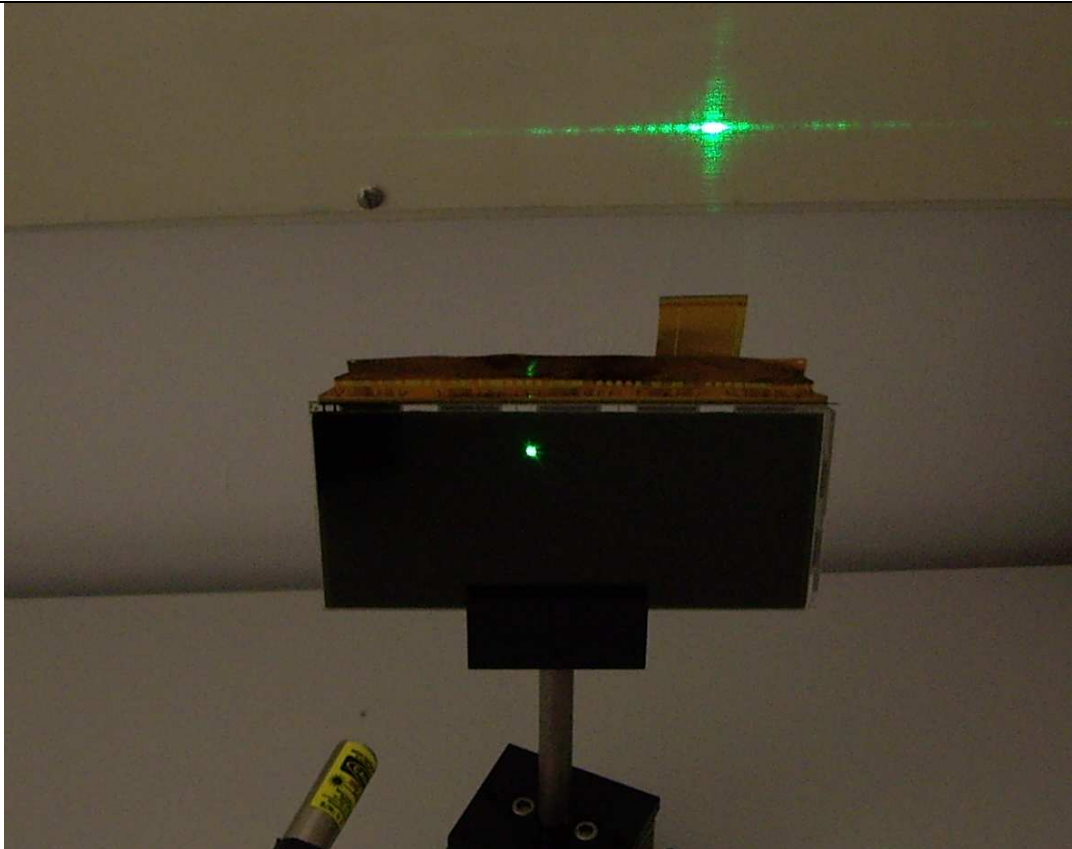


Figure 96: Light from a laser beam heading through the right view of a dual view LCD appears to spread into the left view by diffraction.

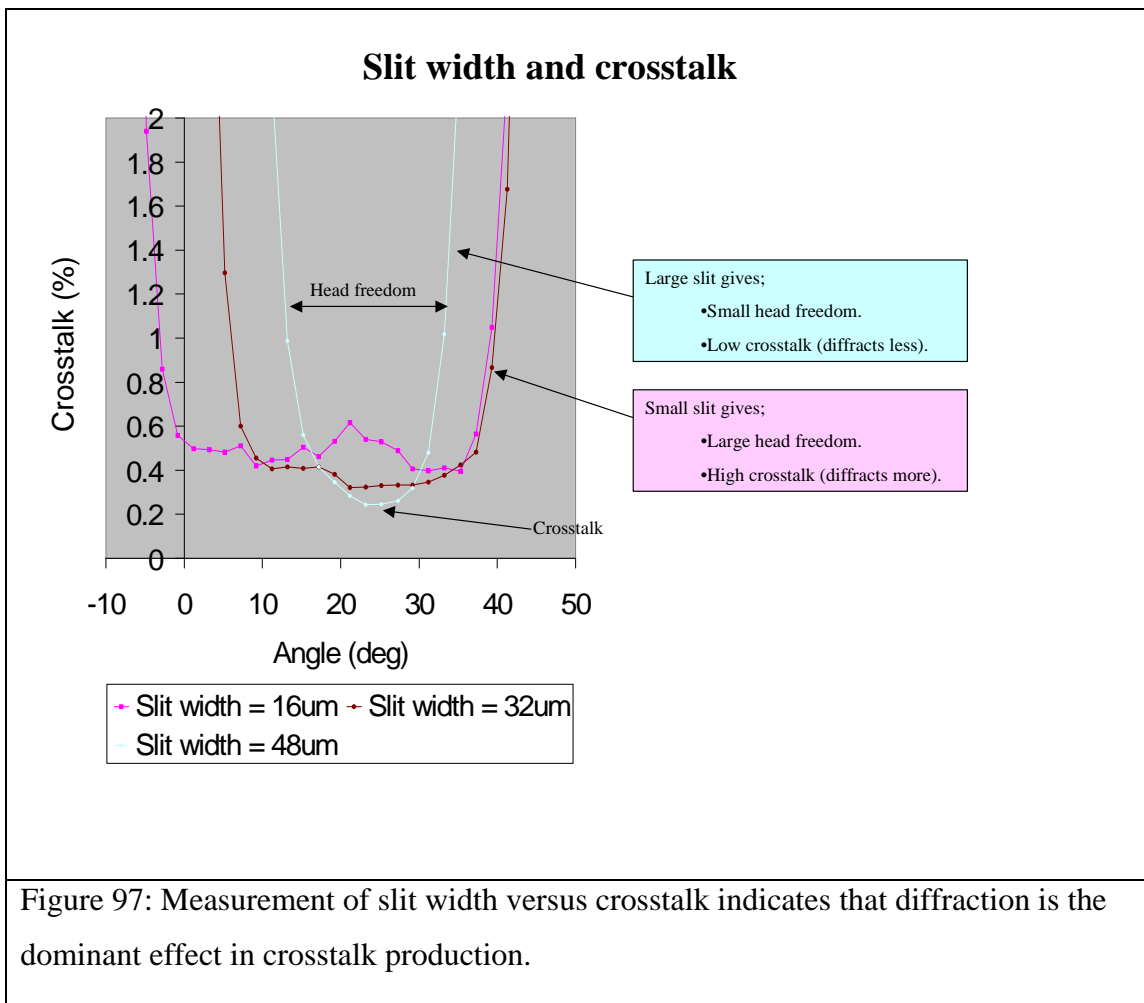
The light that is spread into the left window contains maxima and minima that are associated with spreading by diffraction. If crosstalk were mostly due to a scattering phenomenon, then we would expect that the light spread out smoothly into the left window without maxima and minima.

In conclusion, this test indicates that diffractive crosstalk is a feasible proposition.

#### *Slit width and crosstalk*

If diffraction is a significant cause of crosstalk, then one would expect crosstalk to be increased if smaller slits are used in the parallax barrier. Smaller slits should diffract the light more, and therefore cause more crosstalk.

The crosstalk from a range of parallax barrier slit apertures was measured, and the results are shown below.



### Conclusion

Parallax barriers with small slit widths give more head freedom (as would be expected from the geometric optics), however the crosstalk from these slits is higher. This is consistent with the smaller slits diffracting light more than the bigger slits.

### The colour of crosstalk

Measurement of optical crosstalk versus wavelength should provide more evidence that diffraction is the dominant cause of optical crosstalk. If diffraction is the main cause of crosstalk then long wavelength red light should diffract more and produce more crosstalk. Short wavelength blue light should diffract less giving less crosstalk.

If crosstalk was from another cause such as scattering, then blue light may cause more crosstalk.

In this section crosstalk versus wavelength is measured, and the results are not consistent with diffraction being the only cause of crosstalk. Other possible routes for crosstalk to occur are studied after this section.

### *Experimental set-up*

Crosstalk was measured by using the black and white test images as usual; however, red, green and blue filters would be placed over the detector for measurement of the crosstalk for these colours.

The measurements were all made at a viewing angle of 35 °, which was the angle of lowest crosstalk in the left view.

### *Predicted wavelength dependence of crosstalk from diffraction*

Diffraction in a dual view display is complicated. The main cause of diffraction will come from the pixel apertures and the barrier slits. The pixel apertures are close to the barrier slits such that the wave-front incident on the slits is curved. A Fresnel diffraction model would be needed to describe this.

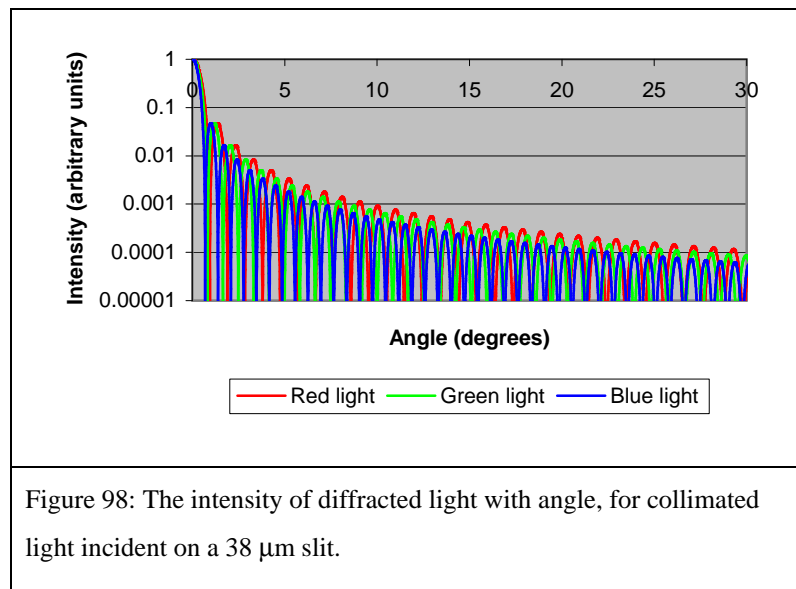
In this case however, I want to predict crudely which wavelengths will diffract more, and by about how much. Therefore I assume that a Fraunhofer diffraction model will provide results that are sufficiently accurate.

The Fraunhofer diffraction (collimated light through a single slit) is described by the following equation:

$$I \propto \text{sinc}^2\left(\frac{\pi b}{\lambda} \sin \theta\right)$$

where  $\lambda$  is the wavelength of the light,  $b$  is the width of the slit, and  $I$  is the intensity at angle  $\theta$  from the slit.

The angular spreading of light caused by diffraction through the 38  $\mu\text{m}$  barrier slit for red green and blue light (630 nm, 550 nm, and 460 nm respectively) is plotted in the following graph.



It can be seen that red diffracts more than green, which diffracts more than blue.

If the average intensity is taken over one of the diffraction peaks for each colour, then this implies that at about 30 °, the diffracted red irradiance is 1.35 times the green intensity, which is 1.43 times the blue intensity. Diffractive crosstalk should have a similar wavelength dependency to this.

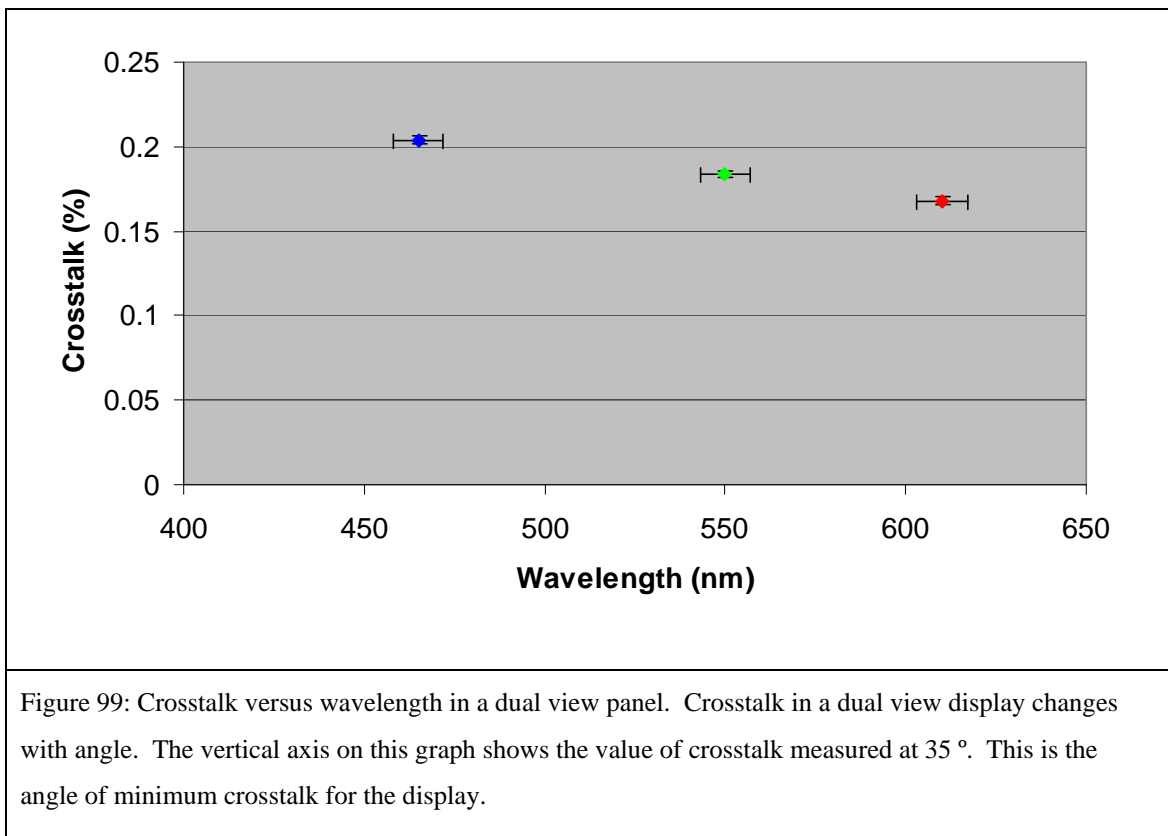
#### *Phenomenon that could cause more crosstalk for blue light*

Supposing the dual view system was scattering light on a sub wavelength scale. This would include for example, scattering in the polariser material, surface roughness in the many layers of glass, glue, and plastic films that make up the dual view display, and perhaps roughness at the edge of the parallax barrier. Sub wavelength scattering features would create Rayleigh scattering [46], which preferentially scatters blue light over red light. This could create more crosstalk in the blue than in the red.

Alternatively Fresnel reflections might exist in the system, for example due to a refractive index mismatch between the edge of the barrier slit and the surrounding. This could lead to Fresnel reflections from the edge of the barrier slit, which may cause crosstalk. These Fresnel reflections would be wavelength dependant if the refractive index of the materials concerned were wavelength dependant. There may be a larger difference in refractive index between the materials for blue light than red light, which would cause more Fresnel reflections and more crosstalk.

#### *Results*

The graph below shows the results of the measurements.



The notch filters have a bandwidth of  $\pm 10$  nm about their central transmission peak.

The accuracy of the crosstalk measurement in this experiment is much more accurate than usual. In most other measurements crosstalk is being compared between two different panels, which may have different pixel – barrier separations, and so give different crosstalk readings. In this case, the dual view panel is the same so it gives a consistent level of crosstalk for each measurement. It is only the detector that is modified. The accuracy of the measurement was (in the green)  $0.184 \pm 0.002\%$ .

### Conclusions

It can be seen that blue light causes more crosstalk than red light. As mentioned previously, if diffraction was the sole cause of crosstalk we would expect red light to spread more as it diffracts through the barrier slits, and cause more crosstalk. Since this is not the case, the experiment suggests that there must be other significant sources of crosstalk.

Examples of phenomenon that might cause more crosstalk for blue light are scattering and Fresnel reflections.

### *Summary of evidence for diffraction*

The evidence we have so far which suggests diffraction is a major source of crosstalk is;

- Microscope images showing crosstalk coming from the slit edges.
- Fringes in these photographs that resemble Fresnel diffraction, and have a pitch consistent with Fresnel diffraction.
- A laser can be seen to spread from the left view to the right view in a pattern characteristic of diffraction.
- Smaller barrier slits produce more crosstalk, as would be expected from diffraction.

There is also one piece of evidence that suggests that diffraction is not the only major cause of crosstalk;

- More crosstalk is created by blue light than for red light. This is inconsistent with diffraction being the only cause of crosstalk, and consistent with another effect (perhaps scattering) also contributing to crosstalk.

This section continues to consider other paths that may cause crosstalk.

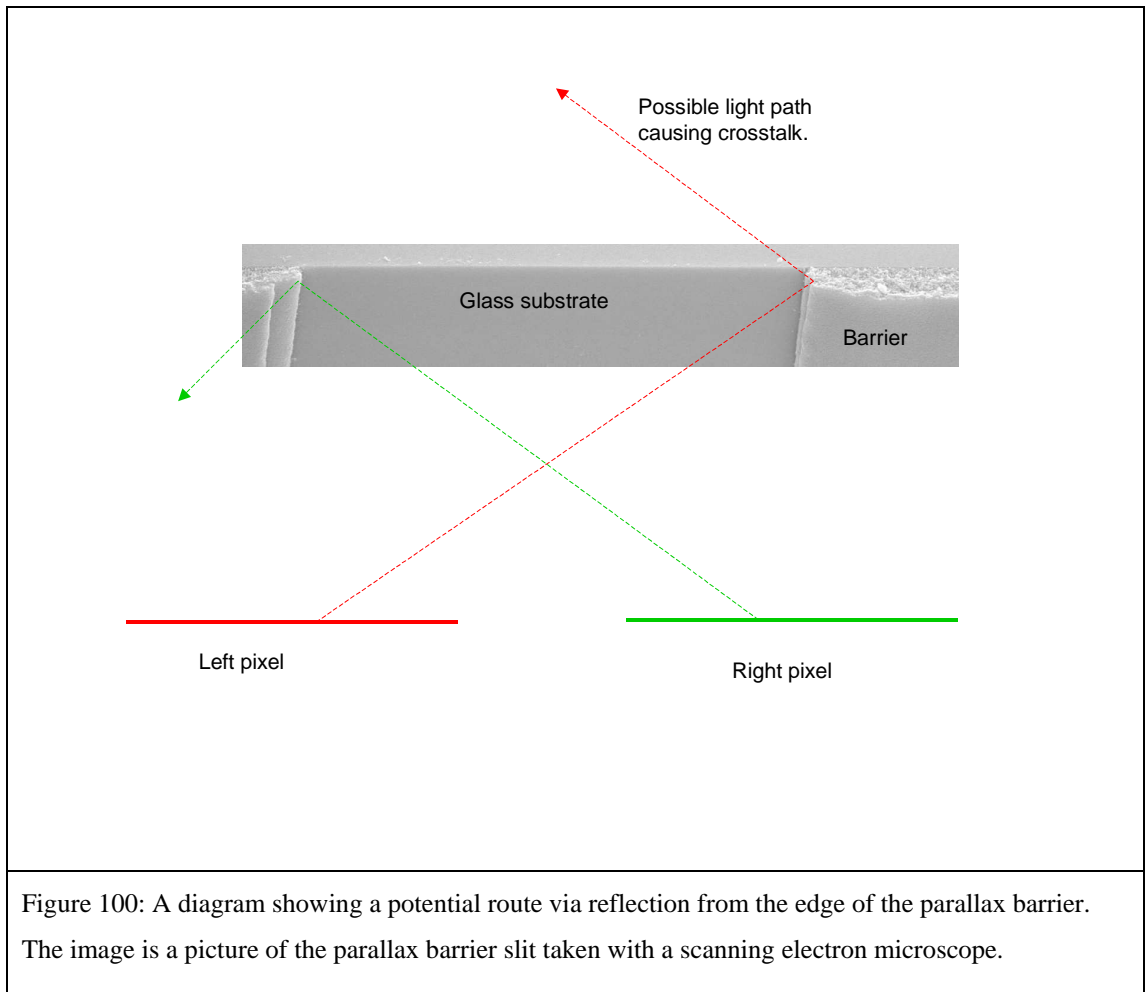
#### **2.3.8 Could crosstalk be caused by edge reflection?**

The most convincing evidence that a large component of crosstalk is diffraction comes from the microscope pictures showing that the crosstalk comes from the barrier slits. This section addresses the alternative explanation that this light is actually caused by reflections from the barrier edge.

This alternative explanation is described in more detail, and the amount of crosstalk that would be expected from this source is modelled based on the shape of the edge of the parallax barrier, and the amount of reflection from the black material. The result implies that this source of crosstalk is not significant.

#### *How edge reflections could occur*

The figure below shows how crosstalk from edge reflections could come about.



The figure shows a cross sectional picture of the parallax barrier material, (taken with a scanning electron microscope). The height of the parallax barrier material is about 3.4  $\mu\text{m}$ . It might be possible that light from the left pixel heading for the left view is reflected by the edge of the barrier, so that it causes crosstalk. The magnitude of this effect would depend on two parameters.

1. The shape (and height etc.) of the parallax barrier edge.
2. The amount of reflection from the black parallax barrier material.

The shape of the edge is known from the electron microscope picture.

As for the amount of reflection from the parallax barrier material, light hitting this black material should be absorbed, however, if the material has a different refractive index from its surrounding then there would be some Fresnel reflections from its surface. The refractive index of the glue is known to be 1.49 (from manufacturers specification), the refractive index of the black material is measured in the next section.

### *Refractive index measurement of the parallax barrier material*

The refractive index of the black layer was measured as follows.

We know [46] that reflectivity versus angle depends on the refractive index of a material as below:

For the TE polarisation:

$$\text{reflectivity} = \frac{\cos \theta - \sqrt{n^2 - \sin^2 \theta}}{\cos \theta + \sqrt{n^2 - \sin^2 \theta}}$$

For the TM polarisation:

$$\text{reflectivity} = \frac{n^2 \cos \theta - \sqrt{n^2 - \sin^2 \theta}}{n^2 \cos \theta + \sqrt{n^2 - \sin^2 \theta}}$$

where  $\theta$  is the angle of incidence of the light, and  $n$  is the complex refractive index of the black material.

Therefore we can find the refractive index by measuring the reflectivity of the material, and fitting  $n$  to the data.

The black material will have a complex refractive index because it is absorbing. This means there are two parameters to fit, the real and imaginary parts of the refractive index. We can simplify this situation by measuring the imaginary part of the index directly because it is related purely to the transmission coefficient of the material.

The expression for the imaginary part of the refractive index is:

$$\text{Im}(\text{refractive index}) = \frac{-\lambda}{4\pi r} \ln(a)$$

where  $\lambda$  is the wavelength of light,  $r$  is the thickness of the material, and  $a$  is the transmission of layer.

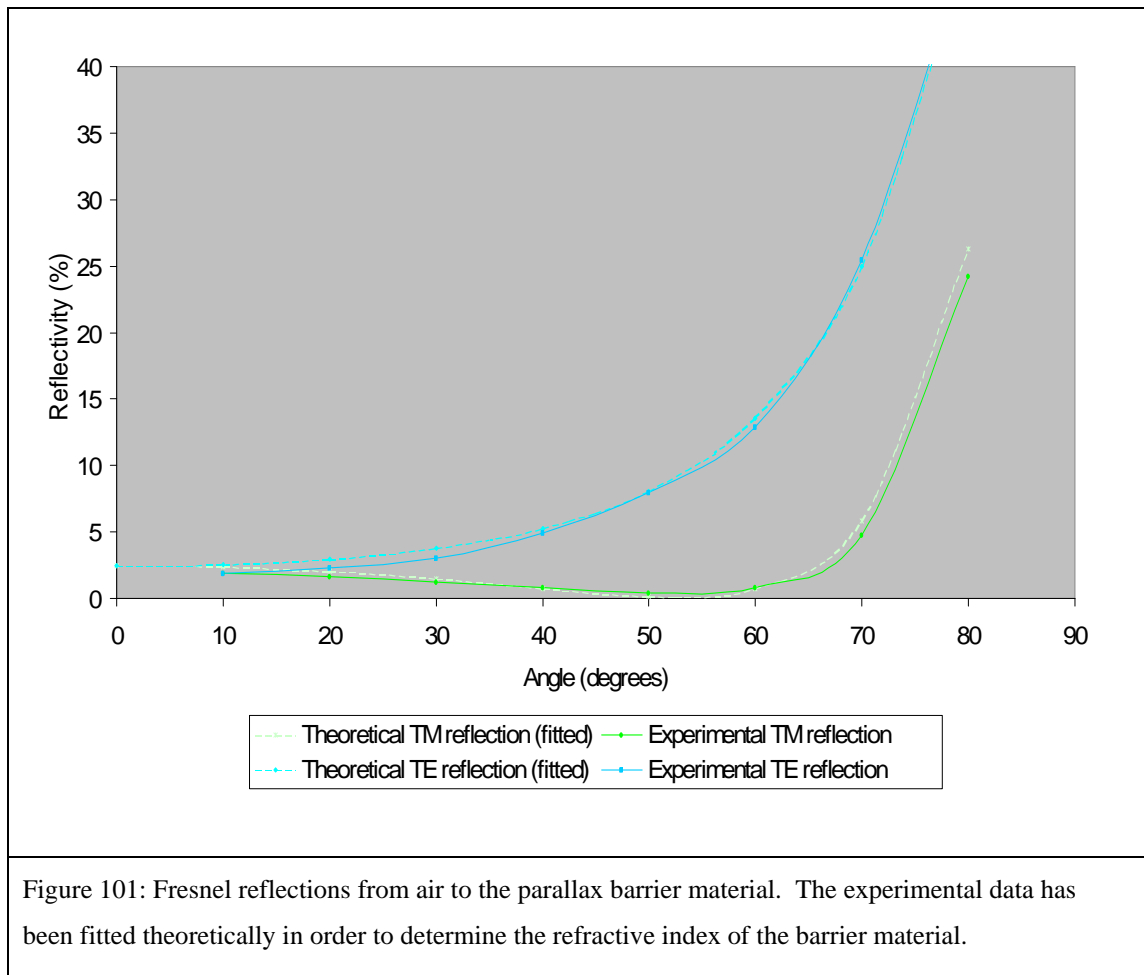
A uniform 1.7  $\mu\text{m}$  film (single layer) of the material was created on which these measurements could be made. The measurements were made using a HeNe laser (wavelength 632 nm) as a light source, and a photodiode as a detector.

The transmission of the film was measured at 0.08%, which implies an imaginary part of the refractive index of 0.211.

For the reflectivity measurement, the HeNe laser was directed at the black material and the photodiode was used to measure the intensity of the beam before and after the

reflection. The reflection was from an air to black film interface. One reflection measurement made in this way did not yield sufficient accuracy, primarily due to fluctuation in the laser intensity. So, the reflection was measured over a range of angles for TE and TM polarisations. The results are plotted in Figure 101.

The real part of the refractive index was found by fitting the equations to the data given that the imaginary part of the index is 0.211.



The graph shows the measured data along-side theoretical prediction based on fitted Fresnel equations.

The data implies that the refractive index of the material is  $1.29 + 0.211i$ . This is lower than the index of the surrounding glue of index  $1.49 + 0i$  (note that the imaginary part of the glue index is approximately zero because it is highly transmissive). Therefore Fresnel reflections would be expected from the edge of the barrier.

### *Modelling of the crosstalk caused by edge reflections*

The edge shape and refractive index of the parallax barrier were entered into a geometrical ray-tracing package which predicted that the amount of crosstalk produced by the edge reflections would be 0.0001%.

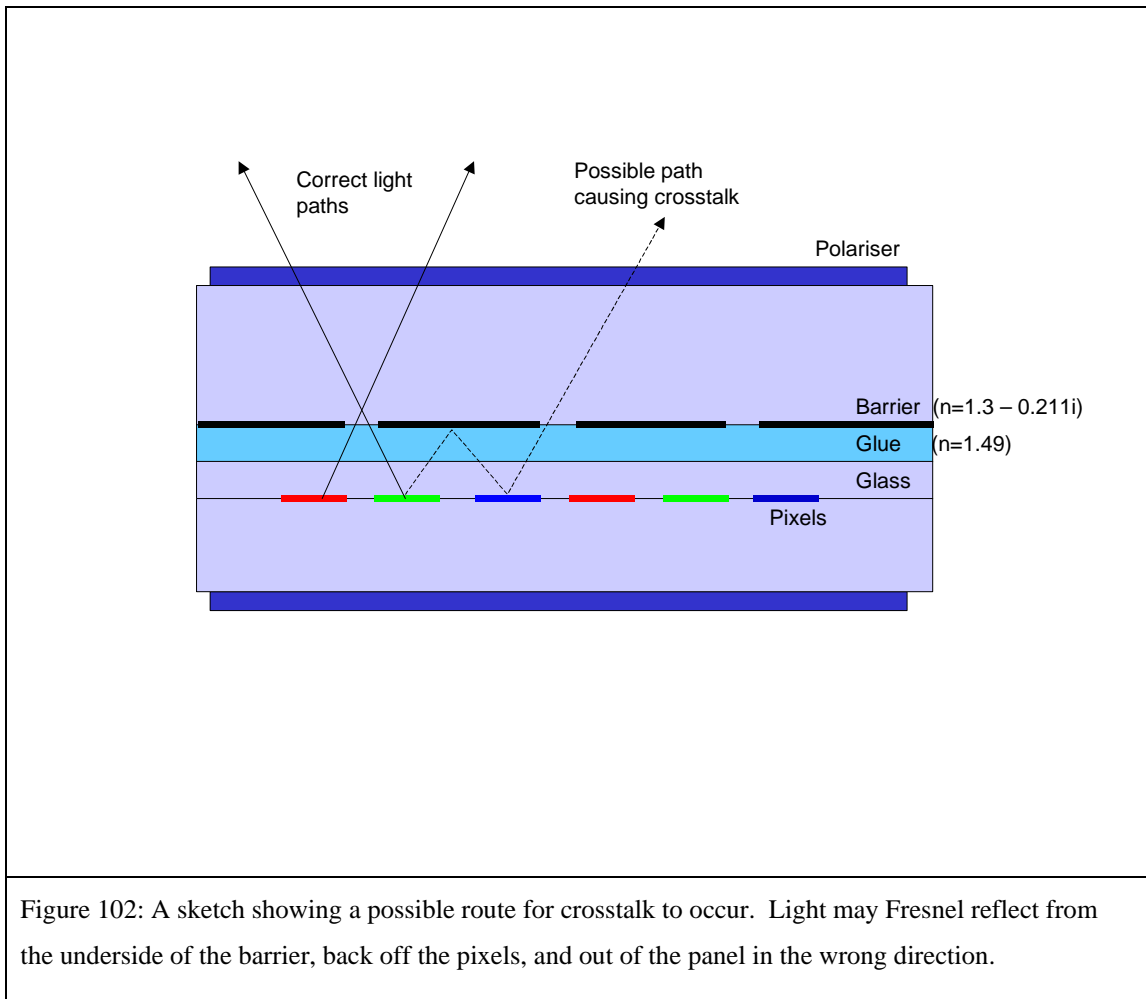
This value is insignificant when compared to the total amount of crosstalk that is seen from the dual view panel. The primary reason for the crosstalk being insignificant was due to the shape of the parallax barrier edge, which preferentially reflects light back into the panel, rather than in a direction that causes crosstalk.

This work predicts that edge reflections are not a significant cause of crosstalk.

### **2.3.9 Could reflections from the underside of the barrier cause crosstalk?**

In the last section it was found that there is a sizable refractive index difference between the parallax barrier and its surrounding material. The parallax barrier has an index of  $1.29 + 0.211i$ , whilst the glue has an index of about 1.49. This could lead to Fresnel reflections within the dual view system which could cause crosstalk. This section attempts to estimate the size of this effect. Calculations based in experimentally measured data provide an upper limit for this effect of 0.02% crosstalk. An experiment designed to remove all Fresnel reflections reduced crosstalk from 0.18% to 0.17%. Both tests imply that Fresnel reflections are not a significant source of crosstalk.

The figure below shows the path of light that could cause crosstalk if Fresnel reflections in the system are strong.



For this crosstalk path to be significant a strong reflection is needed from the underside of the barrier and the pixels.

According to the Fresnel reflection equations, the reflection from the  $1.29 + 0.211i$  index barrier when surrounded by  $1.49 + 0i$  index glue, at  $20^\circ$  is 1.59% for TE and 0.86% for TM. The polarisation of the light from the LC depends on the image data that is applied to the panel. In the worst case the barrier reflection would be 1.59%.

Crosstalk in the display is 0.18%. If the pixels reflected 5% of the 1.59% reflections from the barrier, then this would create a significant 0.08% crosstalk.

We need to know how much light is reflected by the pixels.

The next figure shows a microscope image of the LCD pixels illuminated from above. Bright areas in the photo correspond to areas on the pixel that reflect strongly.

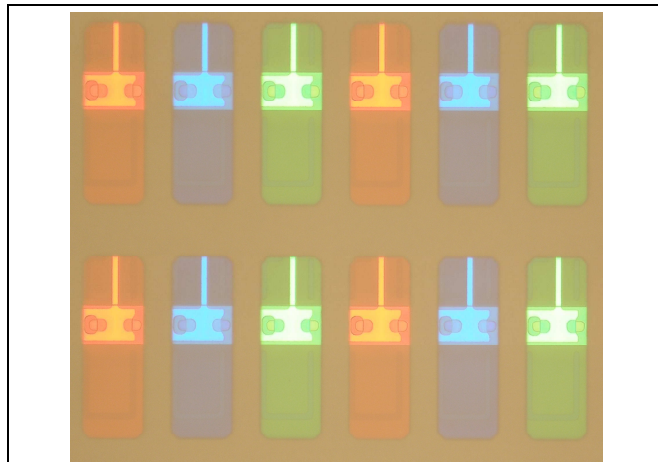
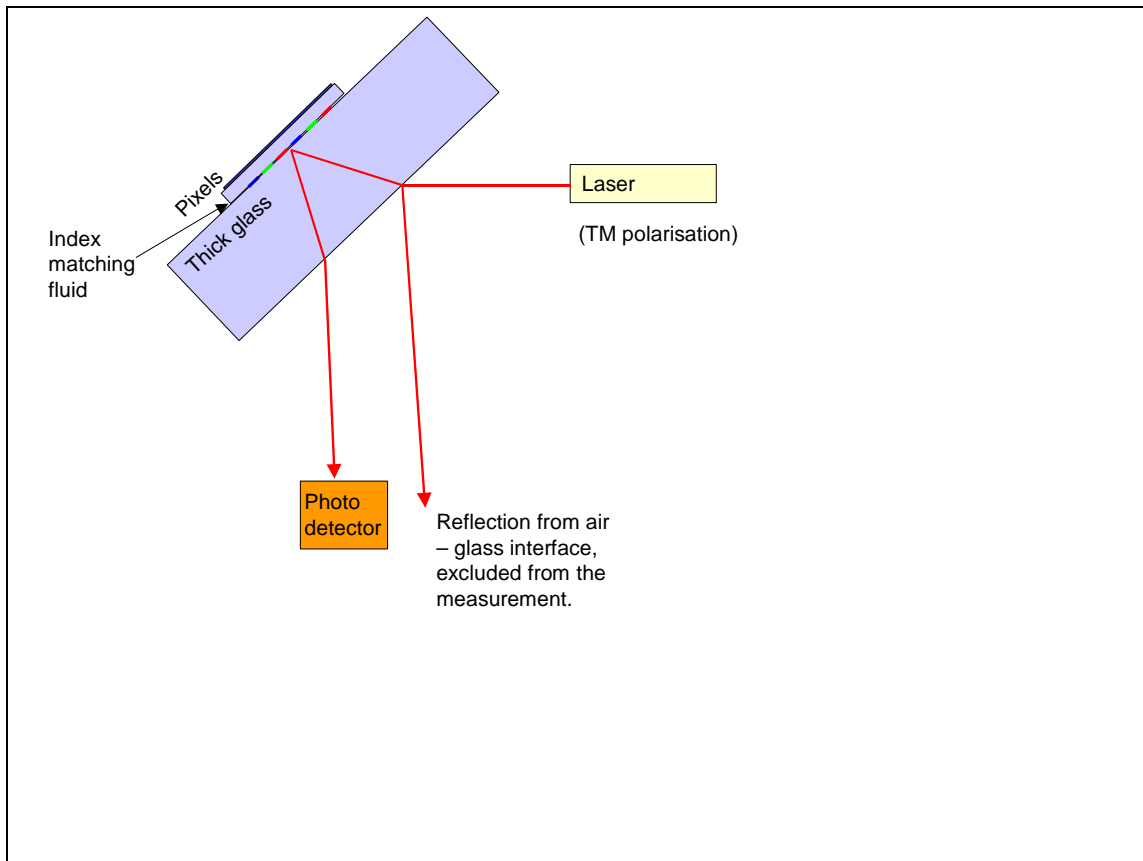


Figure 103: A microscope image of the LCD pixels when illuminated from above. Reflective metallic structures seem to be present.

There is reflection from all the area in the photo – even the black mask between the pixels. This may be due to Fresnel reflections from the black mask of the LCD pixels, or it may be due to Fresnel reflections from the glass – air interface at the front of the panel. More significantly, it appears that there are metallic areas in the pixels which could be reflecting very high percentages of the incoming light.

The microscope image suggests that reflections from the pixels could be significant, but does not quantify it. An experiment was carried out to quantify these reflections. It is described below.



*Figure 104: An experiment to measure the reflectivity of the pixels. It is difficult to measure the reflectivity of the pixels since the reflection from a panel is dominated by the reflection from the air – glass interface at its front surface. By adding a thick layer of glass to the front of the panel, the air-glass interface reflection becomes displaced from the pixel reflections. This enables the light from the pixels only to be measured.*

The result of this experiment is that for  $\theta = 20^\circ$ , 1.6% of the light is reflected from the pixels.

The main source of error in this experiment occurs as follows. Consider the light path that causes crosstalk by Fresnel reflection (Figure 102). In the figure, light from the green pixel reflects from the barrier onto a blue pixel. Green light passing the blue filter should be much reduced in intensity, such that reflections from the metallic areas of the pixel (under the colour filter) would not be as significant.

In the experiment we have red laser light (632 nm), hitting red green and blue pixels. Red light hitting the green and blue pixels will provide a representative reflectivity measurement, but red light reflecting off the red pixels will reflect more strongly than

would happen in the actual dual view system. Therefore the experiment will over estimate the reflectivity of the pixels.

The conclusion of the experiment is that the pixels reflect at most 1.6% of the light. The experiment does not tell us what percentage of light is actually reflected from the pixels.

So the crosstalk caused by such Fresnel reflections should be less than 1.59% (from the barrier) x 1.6% from the pixels. That is, crosstalk should be less than 0.02%. This is not significant compared with the 0.18% crosstalk that exists.

Note that Fresnel reflections within the panel would create crosstalk that is from a diffuse area. This does not show up in the microscope pictures of crosstalk, but these might not be sensitive to pick up a slight intensity increase over a large area, even though it might add up to a significant contribution to crosstalk.

*Experimental testing of the effect of Fresnel reflections*

These calculations can be tested by creating a parallax barrier from a new material which had an index of  $1.51 + 0.047i$ . This is much closer to the index of the glue, such that if edge reflections existed or reflections from the underside of the barrier existed, they would be much reduced, and crosstalk would be reduced. The material is a silver emulsion photo plate made by Konica Corporation.

Refractive index data for these materials is summarised below.

Refractive index of the original black film =  $1.29 + 0.211i$

Refractive index of the new black material =  $1.51 + 0.047i$

Refractive index of the glue =  $1.49 + 0i$

The reflectivity data for these materials for light incident at 20 ° is summarised in the following table. This data is derived from the Fresnel equations.

<i>Polarisation</i>	<i>Reflection from the glue and the original material.</i>	<i>Reflection from the glue and the new black material.</i>
TE	1.59%	0.03%
TM	0.86%	0.02%

Table 16: Theoretical reflectivity between glue and two types of parallax barrier material

The new black material should reduce Fresnel reflections by about 50 times.

Measurement of crosstalk from the two different barrier materials yielded minimum crosstalk values of 0.18% and 0.17% for the original and new materials respectively. This variation is within the experimental error of the measurements, indicating that Fresnel reflections do not cause a significant problem.

### *Discussion*

The new barrier material has a lower absorption coefficient, which means that it must be made thicker to prevent crosstalk by barrier transmission. In addition the shape of the edge (which acted to reduce crosstalk for the original material) may be different. These factors could create more edge reflections. So, crosstalk may be reduced due to the reduced Fresnel reflections, but increased due to the change in height and shape of the barrier edge.

Although it seems unlikely, it is possible that two effects cancel to some extent. With all such experiments involving complex systems, it is difficult to be sure about exactly what is happening.

In conclusion, experiment seems to show that Fresnel reflections do not cause crosstalk, but it is not 100% convincing.

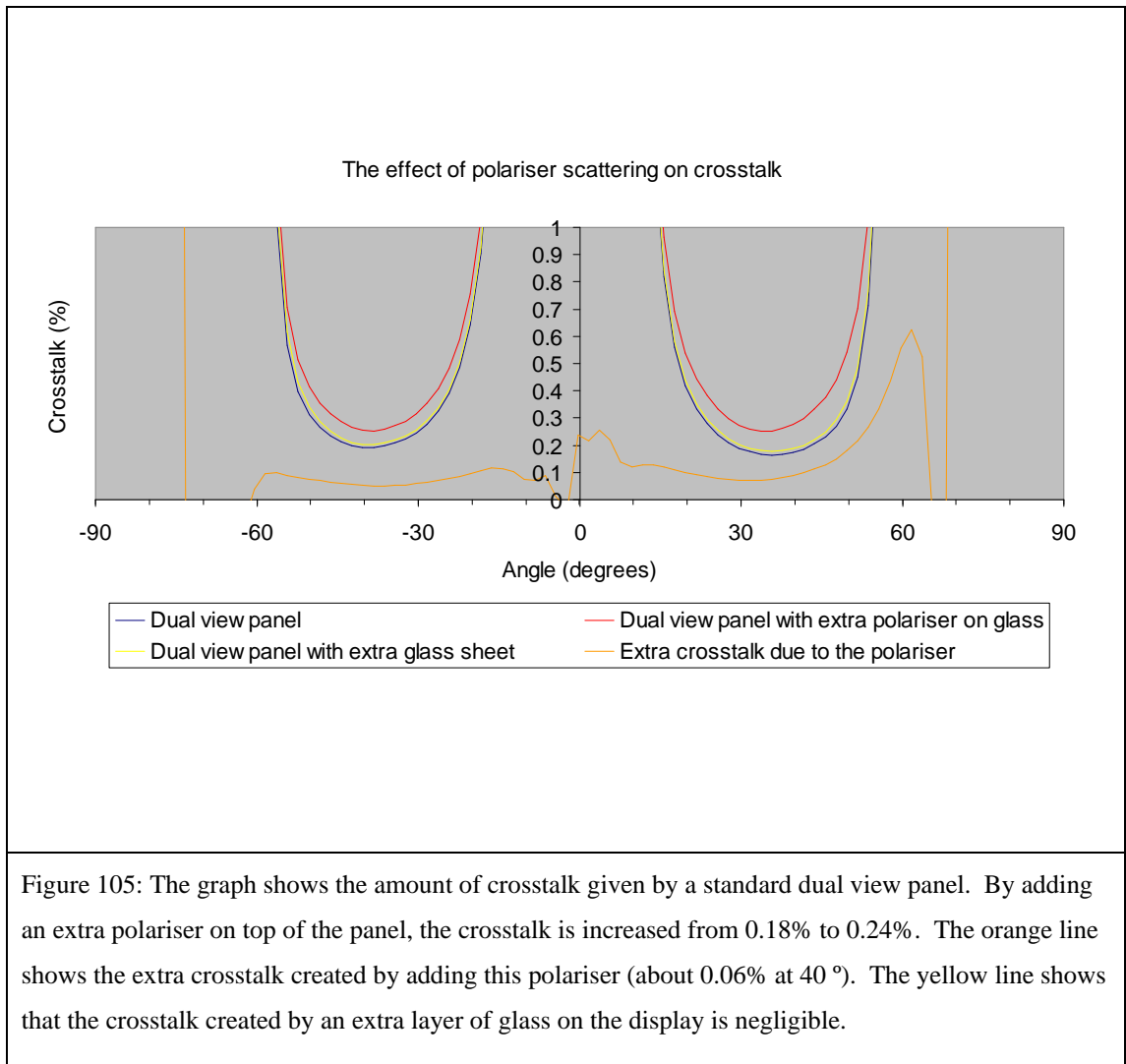
### **2.3.10 Could crosstalk be caused by scatter at the polariser?**

The microscope images of crosstalk show that crosstalk comes from the edges of the parallax barrier. However, if crosstalk was due to some scattering phenomenon, this would not show up strongly in the photograph. Instead, it would add a background haze to the image, which may not be detectable.

Light passes the pixels, the parallax barrier, and then the polariser, on its way to the passenger. If the polariser was scattering, then light heading for the passenger would be scattered towards the driver causing crosstalk. This section attempts to quantify the crosstalk caused by scatter in the polariser. It finds that scatter in the polariser could be causing a significant 0.06% crosstalk.

To quantify the amount of crosstalk caused by the polariser, a second polariser was laminated onto glass, and added to the top of the display. This should double the amount of crosstalk caused by the polariser, since there are now two polarisers in front of the dual view optics rather than one.

The graph below shows the results.



The experiment suggests that the front polariser in the dual view display will add 0.06% crosstalk to the system. This is significant, but it does not account for all the crosstalk that is present.

### 2.3.11 Experimentation on a giant dual view model

Many of the above tests are not conclusive because they rely on crude calculations, or experiments involving complex systems in which it is difficult to be sure that the result is accurate.

In an attempt to simplify the situation, a giant dual view display was built, with macroscopic dimensions. This section is about experiments done on this macroscopic system. These experiments lead to the most convincing evidence for the causes of crosstalk, and these results tally with the evidence so far.

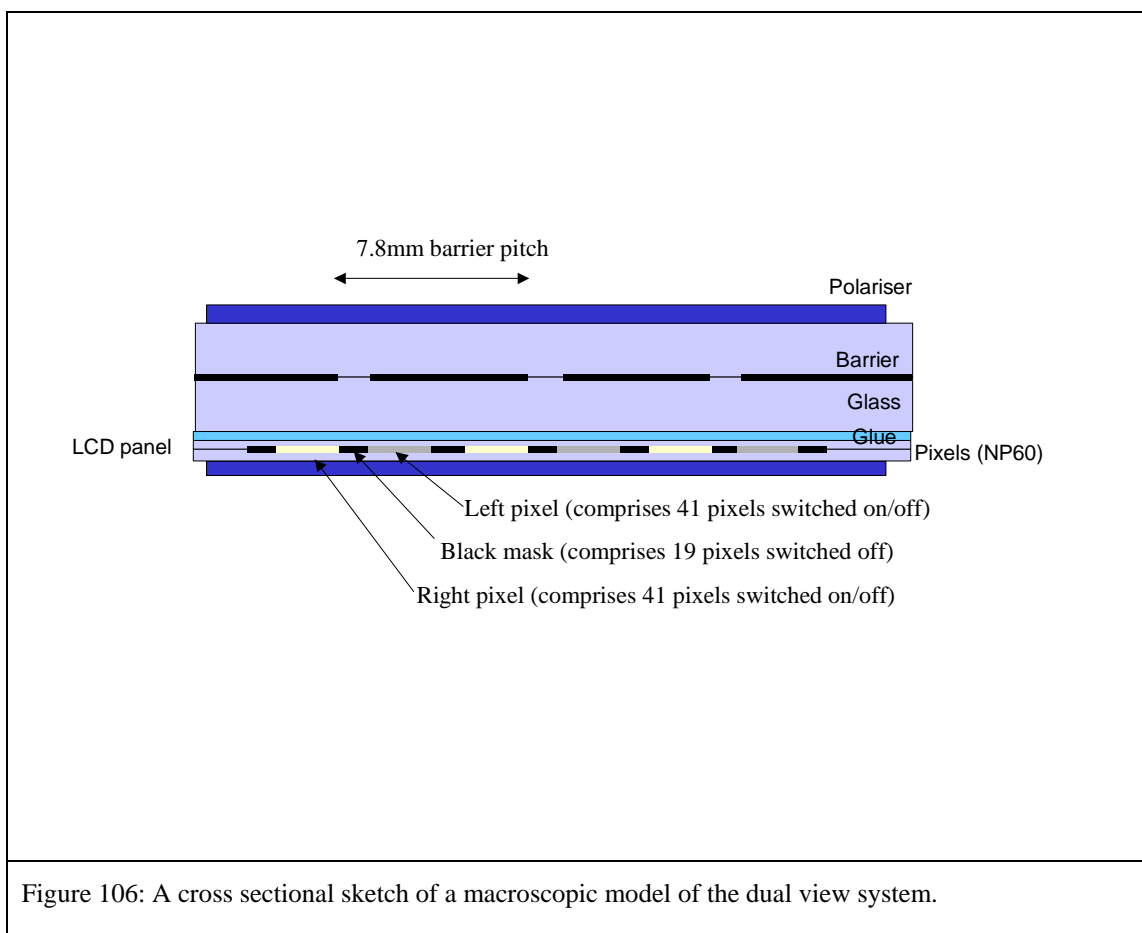
The advantages of a macroscopic system should be;

- Causes of crosstalk due to geometric optics, (such as Fresnel reflections, and barrier transmission) should be easy to see.
- The macroscopic size of the dual view system should make the wave properties of light that cause diffraction to become insignificant. Therefore, we can compare a system with diffractive effects to a system without diffractive effects. This means that we should be able to quantify diffraction in the standard system.

### Construction

The display was constructed using all the same materials as for the standard dual view display, such that the giant dual view display is substantially the same as the standard dual view apart from that it is 60 times bigger. This makes the pitch of the pixels 3.9mm rather than  $65\mu\text{m}$ , and the slit width of the barrier 2.28mm rather than  $38\mu\text{m}$ .

A diagram of the giant system is shown below.



The standard dual view barrier pitch is  $130\mu\text{m}$ , the pitch of the giant barrier is  $60 \times 130\mu\text{m} = 7.8\text{mm}$ . The barrier is made lithographically in the same way that the  $130\mu\text{m}$  standard barrier is made, using the same materials.

The pixels of the giant dual view display need to be 60 times bigger than the standard pixels. This was achieved by using a standard panel (which has the same ITO, colour filter, and TFT layers etc.), but grouping 60 pixels together with software. That is to say, where there should be a pixel aperture the pixels are switched on, where there should be a black mask between the pixels, the pixels are switched off.

The pixel – barrier separation needs to be 4.8 mm, which is achieved with a glass spacer layer.

The polariser (including viewing angle compensation films) on top of the display is the same polariser that is used in the standard dual view display. This polariser, if separated from the barrier to scale, would be positioned 24 mm from the barrier. The polariser was actually spaced 4.8 mm from the barrier to simplify the design.

In summary, the giant dual view model is simply 60 times bigger than the standard dual view display except for:

1. The polariser is closer to the barrier.
2. The thickness of the barrier is the same as the thickness of the barrier in the standard display, (about 4  $\mu\text{m}$ ).
3. The giant pixels comprise standard sized pixels (including red green and blue colours).

These factors are believed not to be important – they are discussed later.

### *Experiment 1: How much crosstalk does diffraction cause?*

In the standard dual view system the parallax barrier slits are 38  $\mu\text{m}$ . This is suspected of causing a significant amount of crosstalk by diffraction. The giant dual view model has slit widths of 2.2 mm, which is considerably larger than the wavelength of light, so that diffractive effects should be much less significant.

The minimum crosstalk in the standard dual view system is 0.18%, the minimum crosstalk in the giant dual view system was measured at 0.10%.

This suggests that diffraction adds about 0.08% crosstalk.

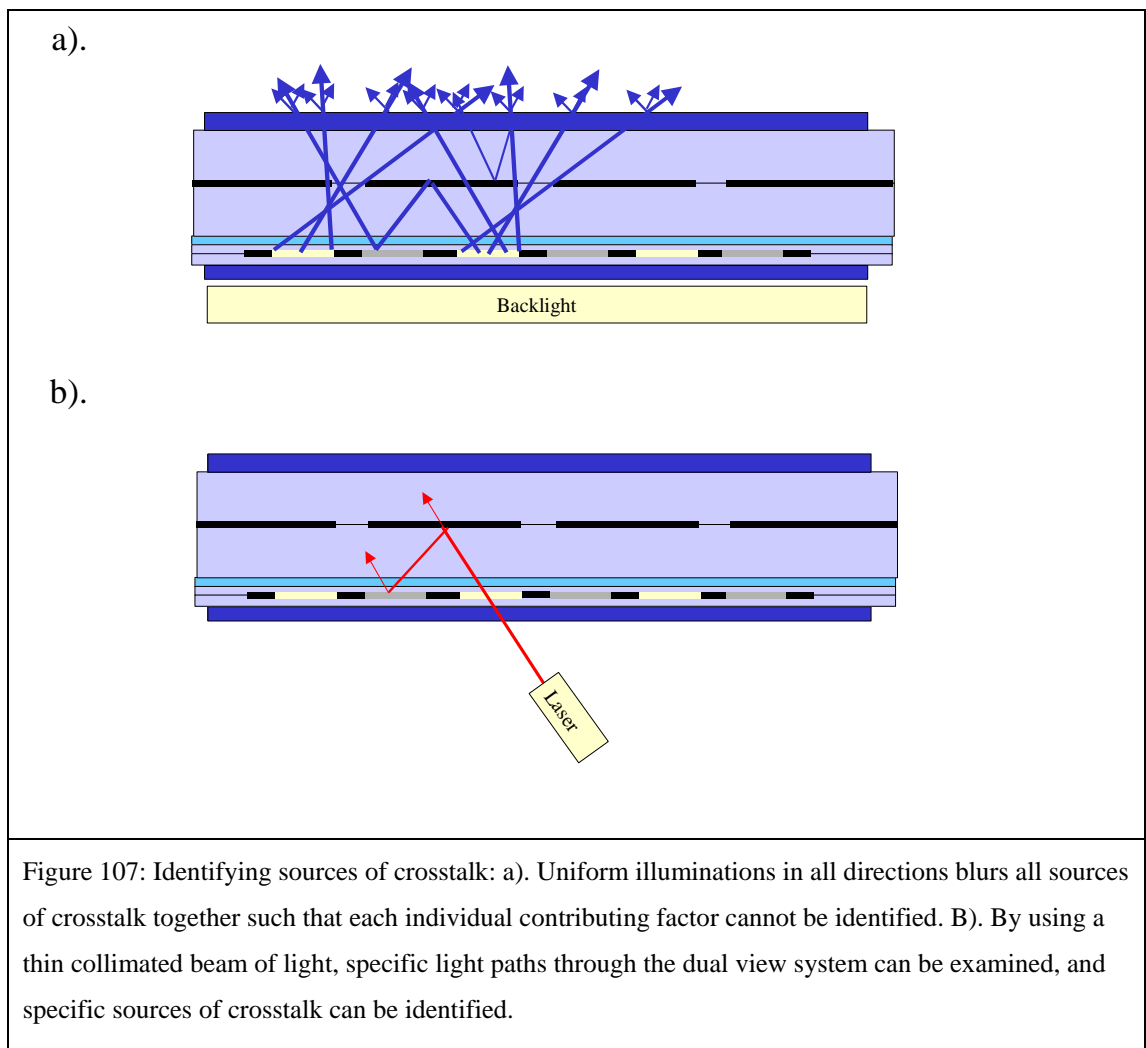
### *Experiment 2: Where is crosstalk from?*

A test was set up to enable the source of crosstalk to be seen for the macroscopic model. The procedure is similar to the method used to get microscope images of the standard dual view display (Figure 80).

Firstly, left and right images are set black, and an observer looks at the display from the left view. Then the right image is set to white. Any extra light that the observer can see from the display is crosstalk from the right image.

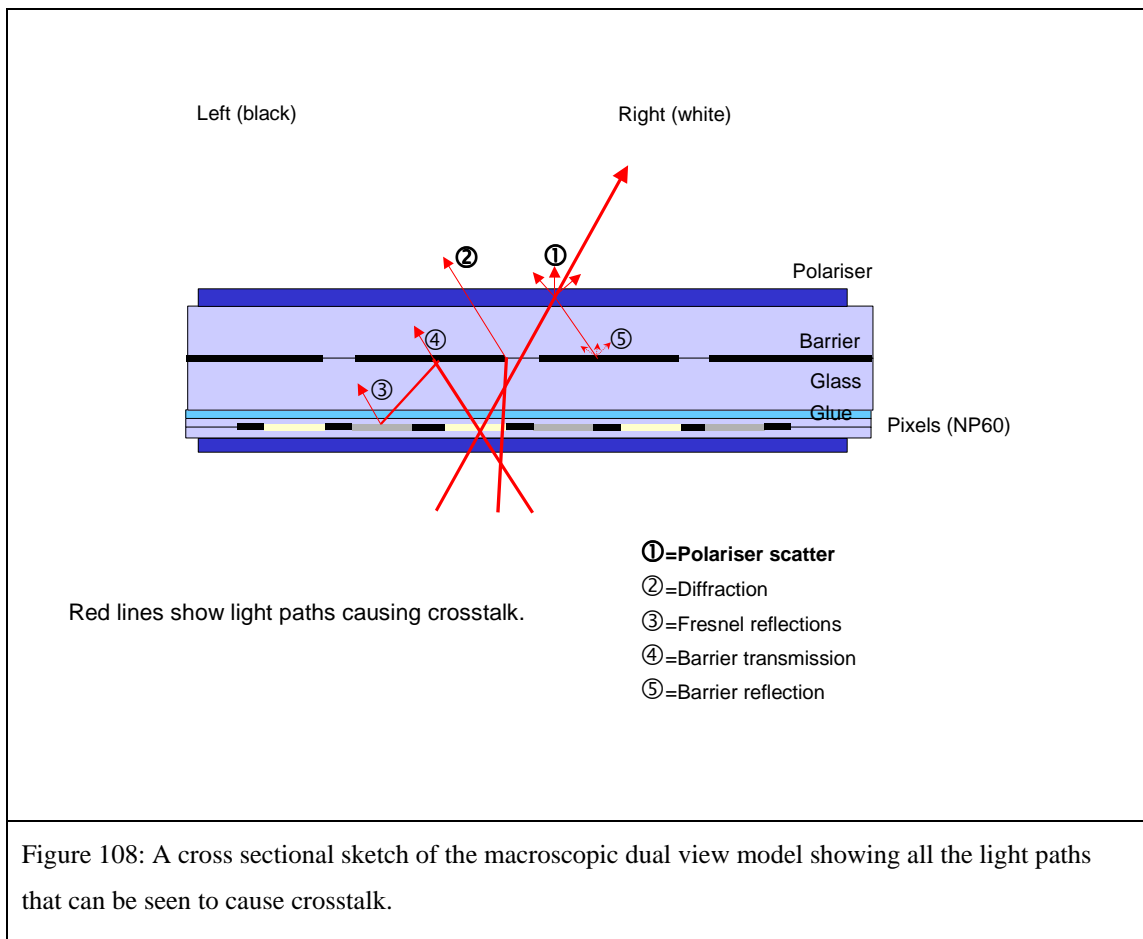
The result is that the observer can see a slight overall increase in intensity over the whole display, and it is not possible to identify any particular crosstalk causing features.

To simplify the system further a laser beam was used to inspect particular light paths through the system. The diagram below shows how this helps identify crosstalk-causing phenomenon.



In the case shown in the diagram the laser light can be seen to a). pass through the barrier to cause crosstalk (at very low levels of intensity), b). light reflects off the top of the right image pixel indicating that Fresnel reflections do exist.

The next figure shows all the other sources of crosstalk found by shining laser light into the panel at different angles.



Many new sources of crosstalk can be seen.

1. The polariser scatters light.
2. Even on the macroscopic dual view model light can be seen to diffract from the edge of the barrier slit, however, the intensity of this diffraction is small.
3. Light does reflect from the underside of the barrier, off the top of the right pixels, to cause crosstalk.
4. Light can be seen passing through the parallax barrier material.
5. Light appears to reflect from the glass-air interface at the top of the panel, and scatter from the top of the barrier material.

**Note that polariser scatter is the only major source of crosstalk in the macroscopic device.** Other sources can be seen but are much weaker in intensity. This is based on a visual assessment of the crosstalk, making it very difficult to quantify.

## Quantifying sources of crosstalk

Data on the sources of crosstalk would be considerably more useful if it could be quantified. This would enable us to identify which sources need to be tackled and which are insignificant. In this section the data is quantified.

Each input angle of laser light causes a different type of crosstalk. This is summarised in the figure below.

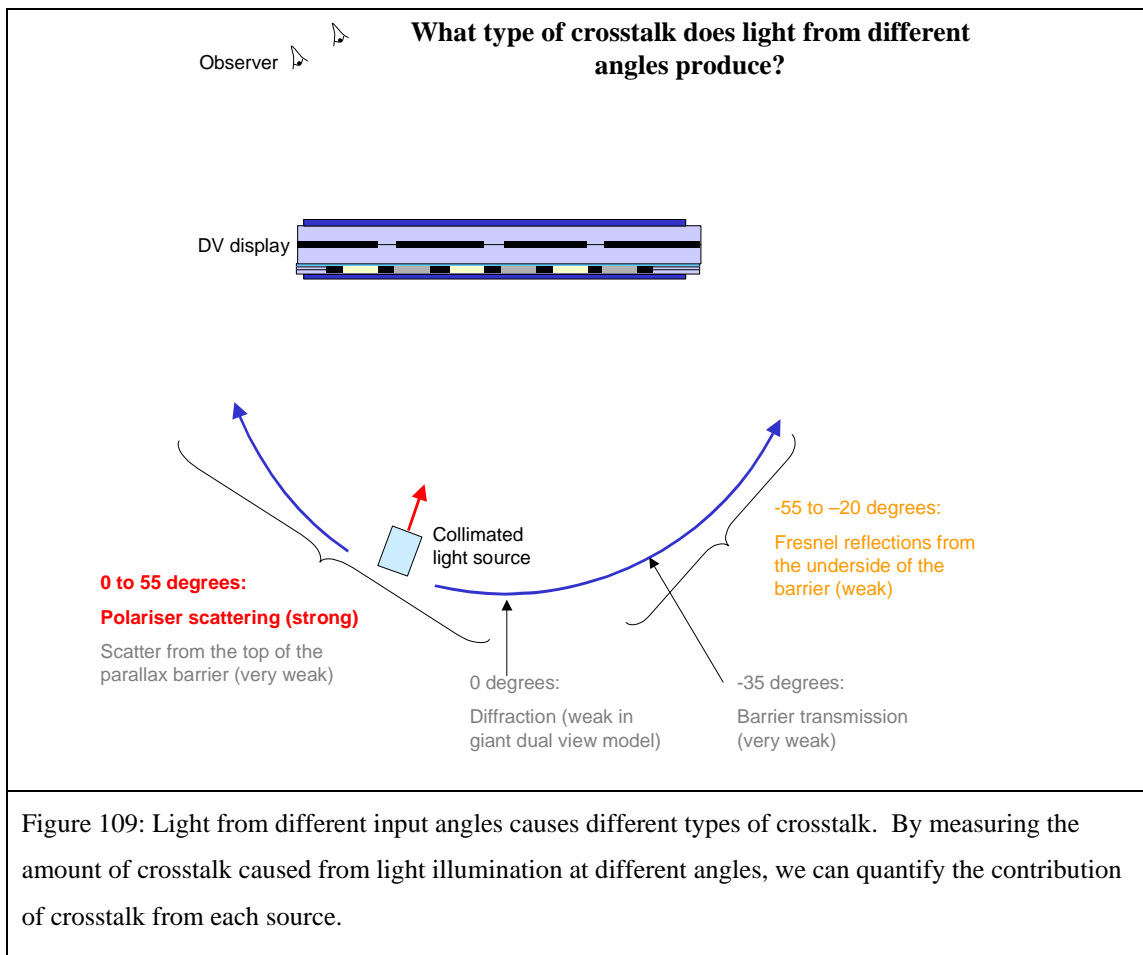


Figure 109: Light from different input angles causes different types of crosstalk. By measuring the amount of crosstalk caused from light illumination at different angles, we can quantify the contribution of crosstalk from each source.

This figure shows the results of visual observations made on the panel when illuminated with collimated light. The observer was looking at the display from  $35^\circ$  (at the centre of the left viewing position), and the collimated light source was shone into the panel at various angles. By observation it could be seen that (substantially) light entering the panel at a particular angle causes crosstalk from a particular source. Therefore, by measuring the amount of crosstalk caused by light at each particular input angle, we will know how much crosstalk is caused by each particular source.

This data was collected in the experiment below.

### Experimental set up

An experiment needs to be set up to measure the amount of crosstalk produced by light illuminating the panel at different angles. Figure 110 shows the set up that was used.

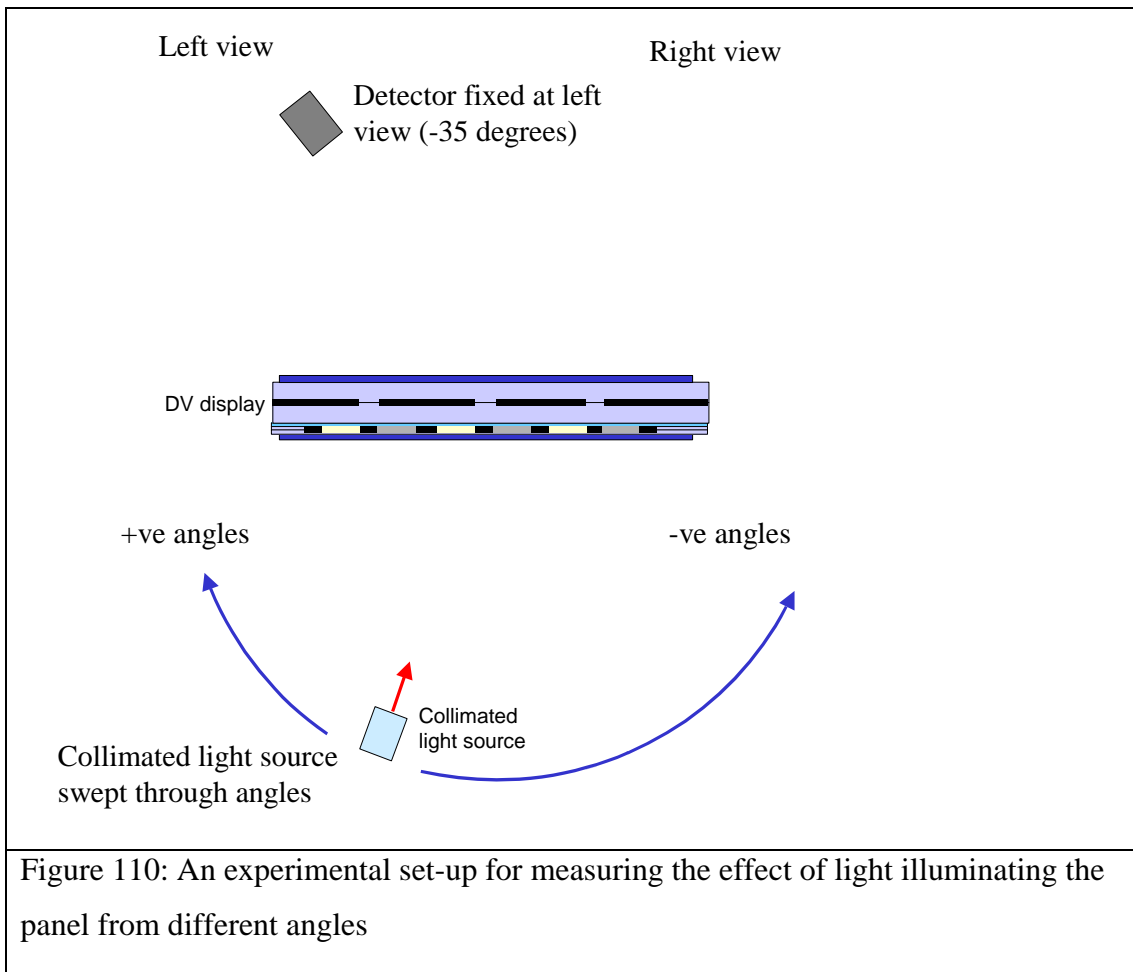


Figure 110: An experimental set-up for measuring the effect of light illuminating the panel from different angles

The light source was a halogen lamp. This was required to produce enough light intensity for the detector. It will have a wavelength spectrum similar to visible black body radiation, rather than an LCD cold cathode fluorescent tube backlight, which has a spectrum consisting of a few emission peaks in the red green and blue. Since both sources provide white light, and previous data shows that the effect of wavelength on crosstalk is small (Figure 99), I assume that there is no significant error induced by the change in wavelength spectrum used for this experiment.

The halogen light source has a diameter of 4 cm, and is placed 70 cm away from the panel. The aperture of the panel is 2 cm, and the detector is placed 28 cm away from the panel. This produces an angular resolution in the system of about 2°.

A set of cylindrical micro-lenses was placed behind the dual view panel to spread the collimated light source into a 'light slice' that is collimated only in one direction. The

light source is only diffuse perpendicular to the plane of the paper. The reason for this was as follows. Consider a purely collimated light source being used for this experiment. On axis light might diffract horizontally to cause crosstalk. Consider on axis light with an azimuthal input angle (such light would exist from a backlight), the barrier would diffract the light horizontally, but it would not change its azimuthal angle, therefore this light would not send crosstalk to the detector. Consider the same on axis light with an azimuthal angle scattering from a polariser. This light would be scattered in all directions, such that it would contribute to crosstalk at the detector. Therefore, the proportion of crosstalk generated by polariser scatter and diffraction will depend on the azimuthal angles of light used. Therefore it is important to use the same range of azimuthal angles of light as exists in the dual view backlight. By adding the micro-lenses to the collimated light source this is achieved to some extent. The collimated light source is spread into the azimuthal angles, however the angular distribution of this light is not identical to that in a dual view backlight. It is assumed that the light input angles are close enough to the actual dual view backlight that significant error is not induced.

### *Results*

Figure 111 and Figure 112 show graphs of the results. Figure 111 shows brightness data, and Figure 112 shows crosstalk data.

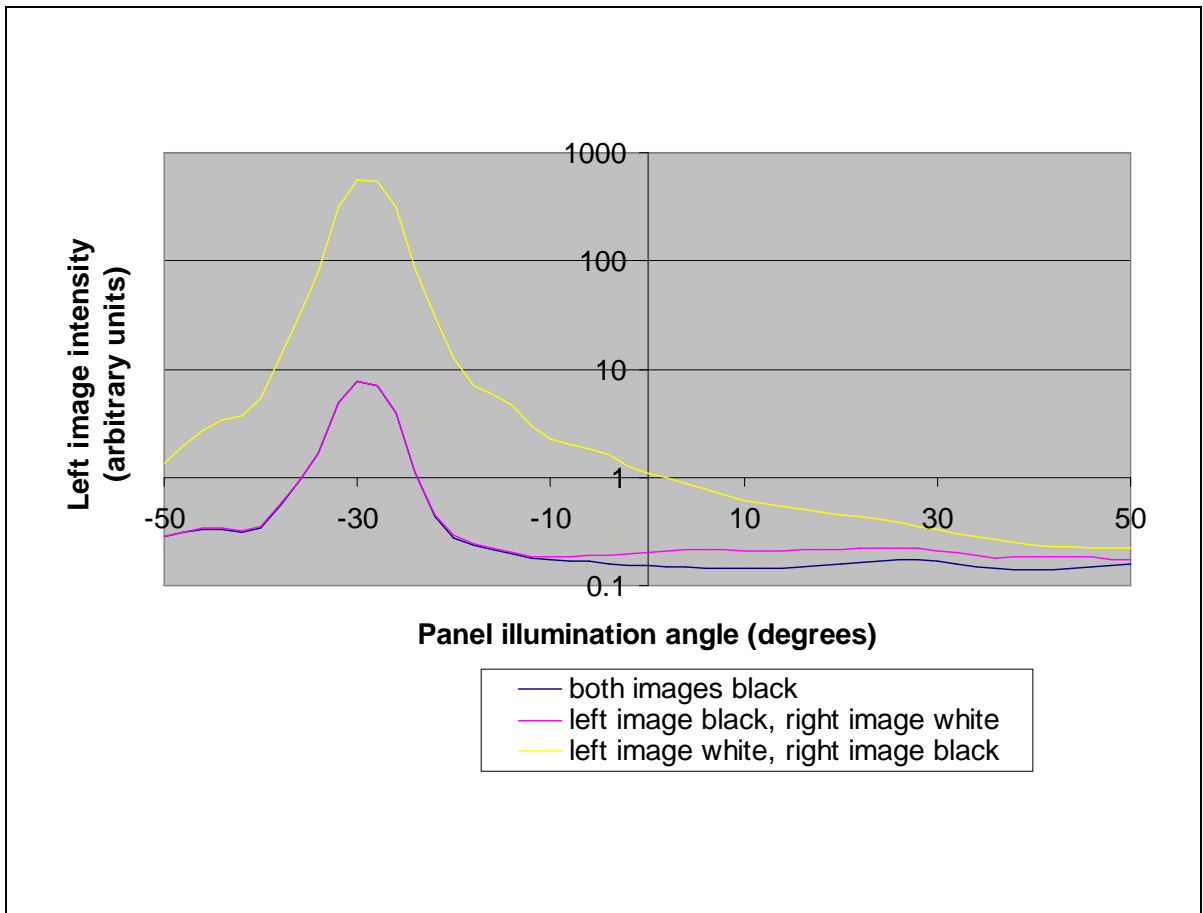


Figure 111: How light from different illumination angles affects the brightness and crosstalk in a dual view display. A detector at about  $-30^\circ$  measures the left image intensity, whilst the illumination angle of the panel is changed. The difference between the blue lines, and the pink line is a result of crosstalk in the display.

For Figure 111, the vertical axis shows the brightness at the left view, for a given angle of illumination light from the backlight. The horizontal axis shows how this changes for different illumination angles from the backlight.

In the yellow plot: the left image is showing white, so we expect high intensity in the left view, especially from light shining directly towards the left view (about  $-30^\circ$  on the horizontal axis).

In the blue plot: both images are set to show black, so we expect low intensity in the left view (only some light due to LCD light leakage).

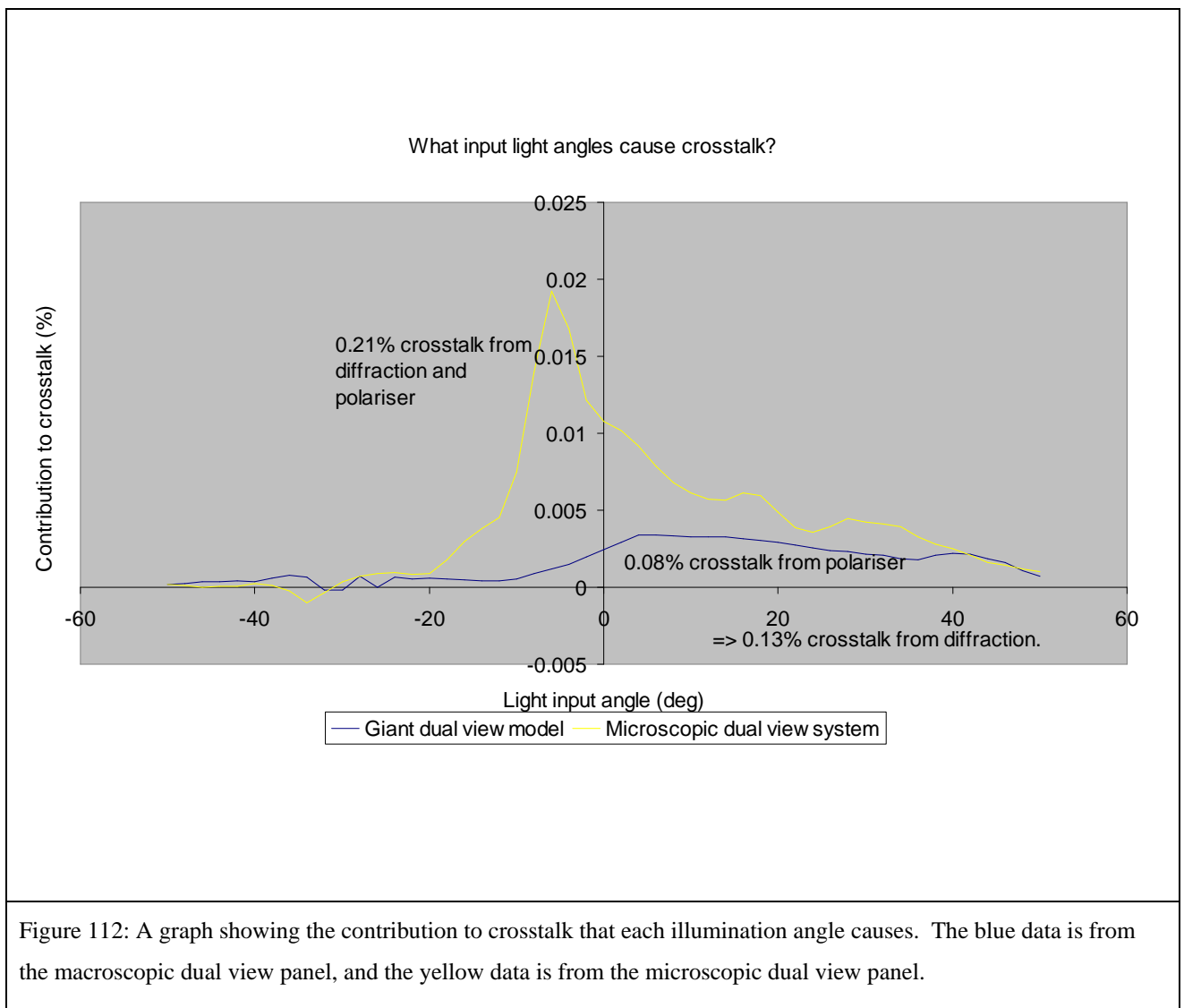
In the pink plot: the left image is set to show black, but the right image is set to white. If the panel had zero crosstalk, we would expect no extra intensity in the left view over the LCD light leakage shown in the blue plot.

The extra intensity in the pink plot (compared to the blue plot) is due to crosstalk.

Figure 112 shows crosstalk as a function of panel illumination angle. The vertical axis is calculated as follows.

$$\text{Contribution to crosstalk (at angle } \theta) = 100 \times \frac{\text{pink plot data (at angle } \theta) - \text{blue plot (at angle } \theta)}{\text{integrated area under all of the yellow plot}}$$

The numerator in the equation gives the absolute intensity of crosstalk caused by light illuminating the panel at angle  $\theta$ . This is divided by the total intensity of the white image (from all angles of illumination). The division normalises the data such that the area under the curves in the graphs below corresponds to crosstalk in (%).



For the giant dual view system, most crosstalk occurs when light illuminates the panel from  $-5$  to  $55^\circ$ . This light is known (by observation) to cause crosstalk by polarisation scatter. Integrating the crosstalk caused from these illuminations angles gives us the total crosstalk caused by polariser scattering. The result is that it causes 0.08% crosstalk.

Similarly, light from  $-55$  to  $-20^\circ$  is known to come from Fresnel reflections from the underside of the barrier. The data implies that this causes 0.01% crosstalk.

The yellow plot shows the same experiment repeated for a standard dual view display. We expect the same Fresnel, and polariser scatter to exist, and in addition we see extra crosstalk that must be due to diffraction.

Note that the total crosstalk measured by this technique is 0.21% for the microscopic system when the conventional measurement reads 0.18%.

As mentioned before, we expect errors in the results. Firstly, we expect an error from the differences in the wavelength spectrum of the actual backlight and that of the collimated light source. Secondly, we expect an error from the differences in the azimuthal angular spread of the actual backlight and the collimated light source. Thirdly, we expect an error since for example, light from the actual backlight is more intense on-axis than off-axis, so contribution to crosstalk from the collimated light source (which provides more uniform illumination) should be weighted more strongly for on-axis angles. Fourthly, angles from  $50^\circ$  to  $90^\circ$  are not measured in the collimated light experiment.

These errors are likely cause the difference between crosstalk measured by summing different illumination angles (0.21%) and that from the conventional measurement (0.18%). The purpose of this experiment is to identify the proportions of crosstalk from different sources, and an error of a few percent is acceptable for this case.

Light input angle  $-35^\circ$  tells us something else about the standard dual view panel. At this angle light passes the left image pixels and continues straight to the detector. If any electrical crosstalk exists between the right pixel and the left pixel, then changing the right pixel between black and white would change the intensity of the left pixel, and this would show up as crosstalk in Figure 112. The graph shows slight negative crosstalk at this angle, which suggests that some electrical crosstalk is present. However, in this particular case, where images are switched between full intensity blacks and whites, this negative electrical crosstalk is of insignificant proportion compared to the other diffractive and scattering sources. This is a good result as it means that in other tests done in this section for white and black test images, electrical crosstalk is insignificant and has not distorted the results.

### *Comparison with microscopic system*

I have assumed that the crosstalk in the standard system equals the crosstalk in the giant system plus diffraction.

This assumption is tested by observing crosstalk sources, in a similar way as was done with a laser in the giant model. However, to see the source sources of crosstalk on the standard microscopic scale dual view display, a microscope was used.

Table below shows the results of the visual observations.

<i>Light input angle (°)</i>	<i>Crosstalk caused by this light</i>
-30	Too dim to see
0	Mostly diffraction from the slit edges.
30	a). Diffraction from the slits edges. b). Scatter from the polariser.

Table 17: A table showing the type of crosstalk that illumination from different angles causes in the microscopic dual view system.

These results are consistent with the crosstalk seen in the giant dual view display, apart from;

- The weaker sources of crosstalk in the giant display cannot be seen (probably due to low light levels picked up by the microscope).
- Diffraction is much more significant.

As measured earlier in this section, the difference in crosstalk between the giant and standard dual view panels is 0.08%. It seems that this extra 0.08% crosstalk in the standard dual view display is due to diffraction.

#### **2.3.12 Summary of evidence for crosstalk causes.**

In section 2.3 many experiments have been done to identify sources of crosstalk and to quantify them. Here evidence from all the experiments is brought together to form a final conclusion.

The evidence from all the experiments is almost entirely consistent with each other, within experimental error. They point to a final conclusion that the 0.18% crosstalk has two primary causes: diffraction at the parallax barrier edge and scatter at the polariser.

These causes contribute in a ratio of about 60% to 40% respectively. There are many other sources of crosstalk, but these contribute to less than a few percent of the total crosstalk.

#### *Evidence for diffractive crosstalk*

Microscope images of dual view pixels show notable crosstalk coming from the edges of the parallax barrier slits. This crosstalk creates a fringe at the parallax barrier slit which is similar to that predicted by Fresnel diffraction, suggesting that it is diffractive in nature. A laser can be seen to spread from the left view to the right view in a pattern characteristic of diffraction. Smaller barrier slits produce more crosstalk, as would be expected from diffraction. This data does not quantify the diffractive crosstalk.

A giant dual view display should not suffer crosstalk due to diffraction because of its size. Since a standard dual view display has 0.13% more crosstalk than a giant dual view display this implies that diffraction is contributing 0.13% crosstalk.

#### *Evidence for crosstalk caused by polariser scattering*

Adding an extra polariser (and view film) to the top of the display increases crosstalk by 0.06%. This implies that a polariser adds 0.06% to the crosstalk in a dual view system.

In a giant dual view system, scattering from the polariser can be physically seen to be the dominant cause of crosstalk. Polariser scattering only contributes to crosstalk when light illuminating the panel is between about 0 to 55 °. Summing the contribution to crosstalk only for illumination between 0 and 55 ° implies that polariser scatter causes 0.08% crosstalk.

#### *Evidence for barrier edge reflections causing crosstalk*

Since there is a step in refractive index between the barrier and its surroundings, a Fresnel reflection might be expected from the barrier edge, which may cause crosstalk.

Modelling based on geometric optics, taking into account the refractive index step, and the shape of the barrier edge implies that such edge reflections will cause an insignificant 0.0001% crosstalk.

Constructing a dual view system in which the parallax barrier index is matched with its surroundings should remove edge reflection crosstalk. An index matched barrier, reduced crosstalk by an experimentally insignificant amount of 0.01%.

Within experimental error both modelling and experiment are consistent. Based on the modelling result it is likely that almost zero crosstalk originates from the barrier edge.

### *Evidence for reflections from the underside of barrier causing crosstalk*

It can be seen in the giant dual view model that light Fresnel reflects from the rear of the barrier, it reflects back off the pixels to cause crosstalk.

Calculation of the intensity of this effect, based on knowledge of the refractive index difference between the barrier and its surroundings, and based on experimental measurement of the reflection of light from the pixels, suggests that this effect should cause no more than 0.02% crosstalk.

Constructing a dual view system in which the parallax barrier index is matched with its surroundings should remove reflections from the underside of the barrier and remove the crosstalk. An index matched barrier reduced crosstalk by an insignificant amount of 0.01%

In a giant dual view system this crosstalk source can be physically seen. It only occurs when light illuminating the panel is between about  $-55$  to  $-20^\circ$ . Summing the contribution to crosstalk only for illumination between  $-55$  and  $20^\circ$  implies that this source causes 0.01% crosstalk.

With calculation and two experiments converging on a crosstalk contribution of 0.01%, I suggest that it is likely that this figure is genuine.

### *Crosstalk from barrier transmission*

From experimental measurement of the barrier transmission coefficient, thickness measurement, and geometrical modelling, crosstalk by barrier transmission should be 0.000006%.

This is consistent with visual observation of crosstalk from this source in the giant dual view model, which is negligible.

### *Crosstalk from upper side barrier reflections*

This source of crosstalk is seen in the giant dual view model. It is difficult to quantify, since the polariser scatter dominates the detector.

The quantification of this source of crosstalk relies on the fact that it is visually seen to be very weak. With good certainty, it can be said that this crosstalk source is not significant.

### *Summary table*

The table below summarises the sources of crosstalk and there intensities.

<i>Crosstalk source</i>	<i>Contribution to the total crosstalk in a standard dual view system</i>
Diffraction	~57%
Polariser scattering	~37%
Barrier edge reflection	<1%
Barrier underside reflection	<5%
Barrier transmission	~0%
Barrier upper side scatter	~0%

Table 18: A summary of the different causes of crosstalk in a parallax barrier dual view system and the magnitude of each effect.

Solutions to optical crosstalk are considered in section 4.2.

### **3. Human factors study**

#### *Introduction*

This section is about the use of a ‘human factors’ study with respect to crosstalk. The aim is to examine the human visual system to determine at what level crosstalk becomes invisible to a user and therefore by how much crosstalk must be reduced.

Section 3.1 reviews the current literature about factors that should influence the visibility of different intensities of light. The visibility of small changes in intensity (such as crosstalk) should be related to the change intensity and the intensity levels of the light.

This information is applied to a dual view display (with 0.18% crosstalk) to predict the reduction of crosstalk needed to make it acceptably invisible. The result implies that a 3.6 times reduction in the crosstalk level is needed, however no data could be found that matched the viewing conditions for a dual view display exactly, so this result is only a guide.

In section 3.2 specific crosstalk visibility experiments are performed on a dual view display. These show that crosstalk should be reduced by ~6 times for zero visibility. The section also comments on customer feedback about dual view displays which suggests zero visibility is highly desirable.

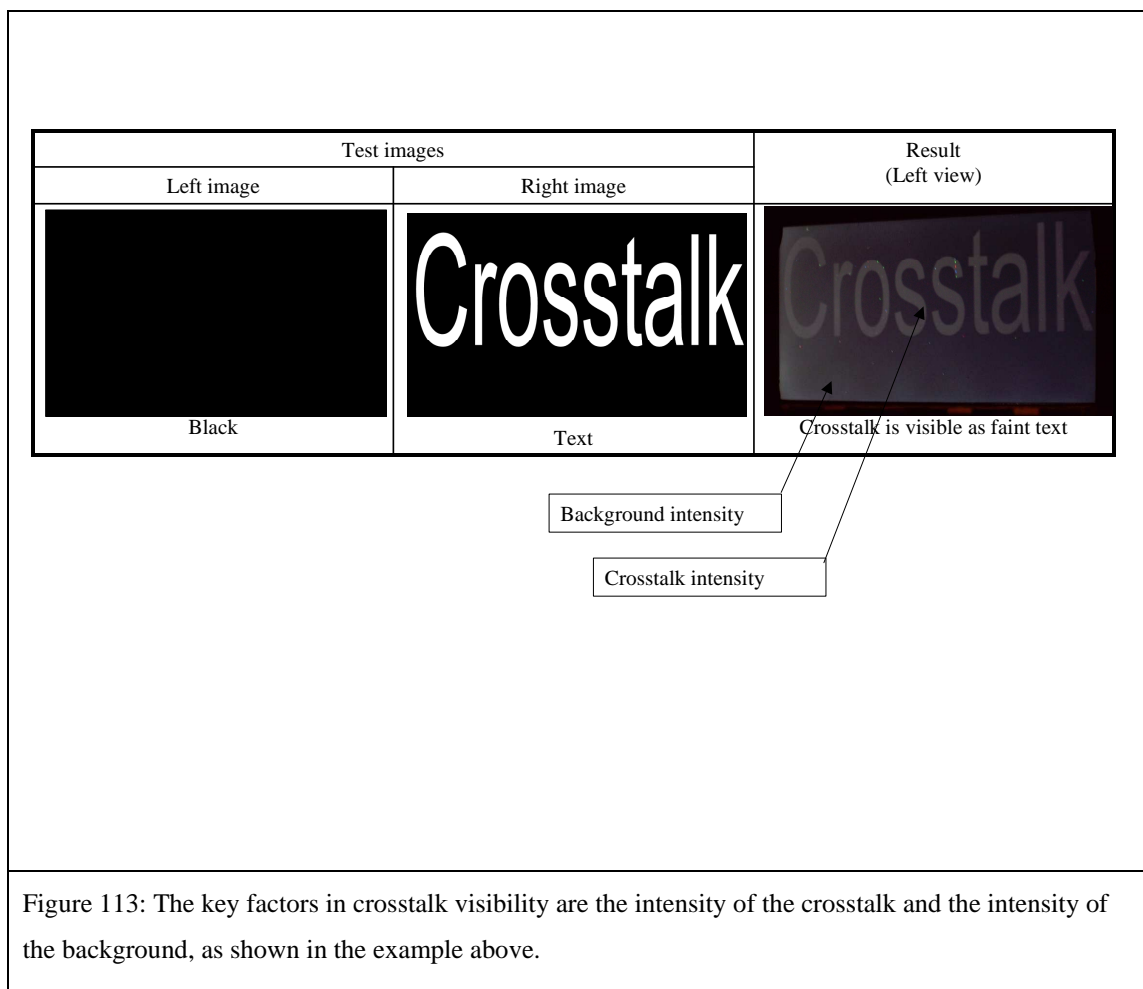
Section 3.3 attempts to make use of knowledge gained from the human factors studies to reduce crosstalk visibility. For example, theoretically, crosstalk should be ‘washed out’ and rendered invisible if the contrast ratio of a display is reduced, or the backlight intensity is dimmed. These methods are seen to be impractical.

### **3.1 Review of factors influencing crosstalk visibility**

From previous literature, crosstalk visibility would be expected to depend on; the intensity levels of the crosstalk and display, the spatial frequency of the crosstalk, the ambient lighting. This section describes each of them.

#### *Intensity levels and crosstalk visibility*

Figure 113 shows a diagram of the intensity levels involved in crosstalk visibility.



Weber’s law is a known formula for relating these intensity levels to visibility to the human eye [50].

It states, for a difference in intensity to be visible, W must be >0.02, where;

$$W = (\text{Intensity of crosstalk} - \text{Intensity of background}) / \text{Intensity of background}.$$

This means that the eye can always just perceive a 2% change in intensity. In fact what particular percentage change is perceivable depends a little on the absolute light levels that are being viewed. The 2% change rule is correct for typical display intensities of  $\sim 100 \text{ cd/m}^2$ .

Figure 114 shows the perceivable  $W$ , for different background intensities.

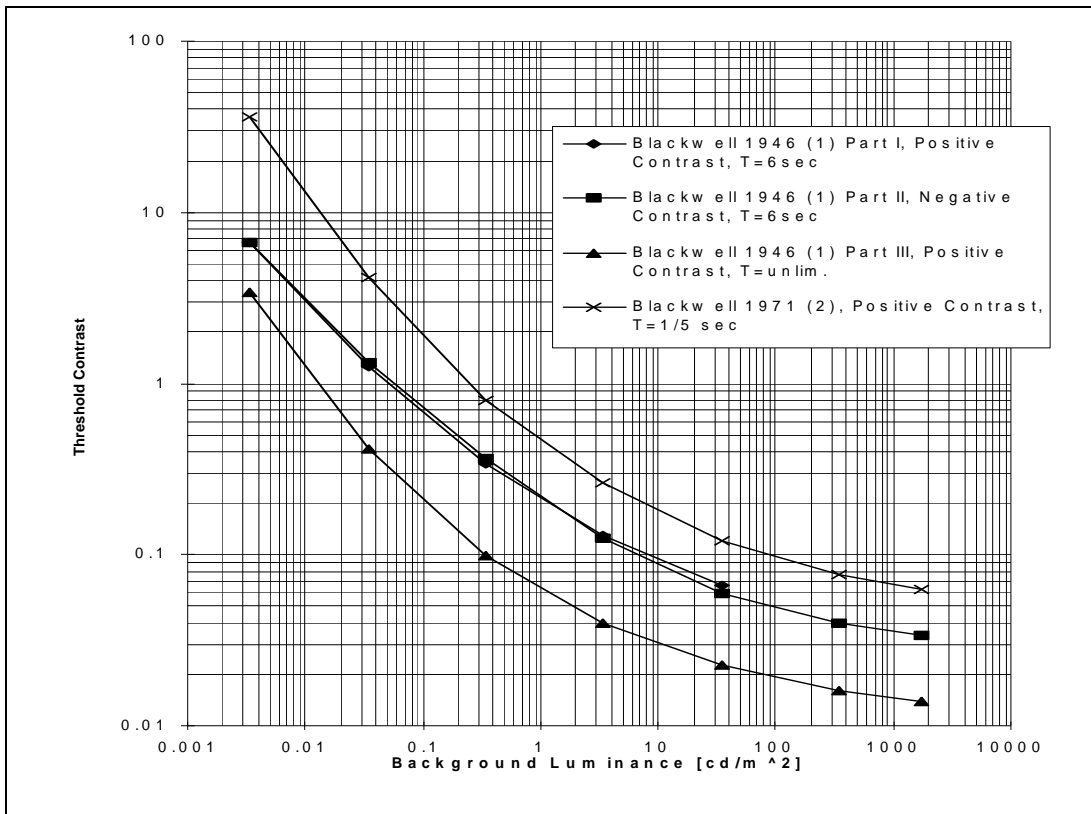


Figure 114: Contrast sensitivity of the human eye for different background intensities [51].

The data in figure 49 shows that the eye becomes less sensitive to changes in luminance when the luminance levels are lower. There is also some relationship between visibility of different luminance levels and the amount of time the user has to examine them. The more time the user has to examine an image of low contrast the more visible it becomes.

#### *Visibility predictions for dual view crosstalk*

In a dual view panel, the worst case for crosstalk visibility will be when the passenger view shows a full range of intensities, and the driver view shows black. The driver would see the maximum possible light leakage on the darkest possible background. The Weber's value is calculated below for this case.

The full passenger image intensity at  $35^\circ$  is  $375 \text{ cd/m}^2$ . 0.18% of this light leaks over to the driver view (see section 4.2.1), i.e. the intensity of crosstalk to the driver will be  $0.68 \text{ cd/m}^2$  higher than the background. The black of the driver image (background

intensity on Figure 113) is  $5.54 \text{ cd/m}^2$  at  $35^\circ$ . Therefore the driver sees a change in intensity due to the crosstalk of  $0.68 \text{ cd/m}^2$ , with a background intensity of  $5.54 \text{ cd/m}^2$ . This gives a Weber's value of 0.12.

For crosstalk to be invisible with a low background intensity of  $5.54 \text{ cd/m}^2$ , from Figure 114  $W$  must be less than 0.035. For this to be true, similar calculations show that crosstalk must be reduced to 0.05%. This is a reduction of 3.6 times.

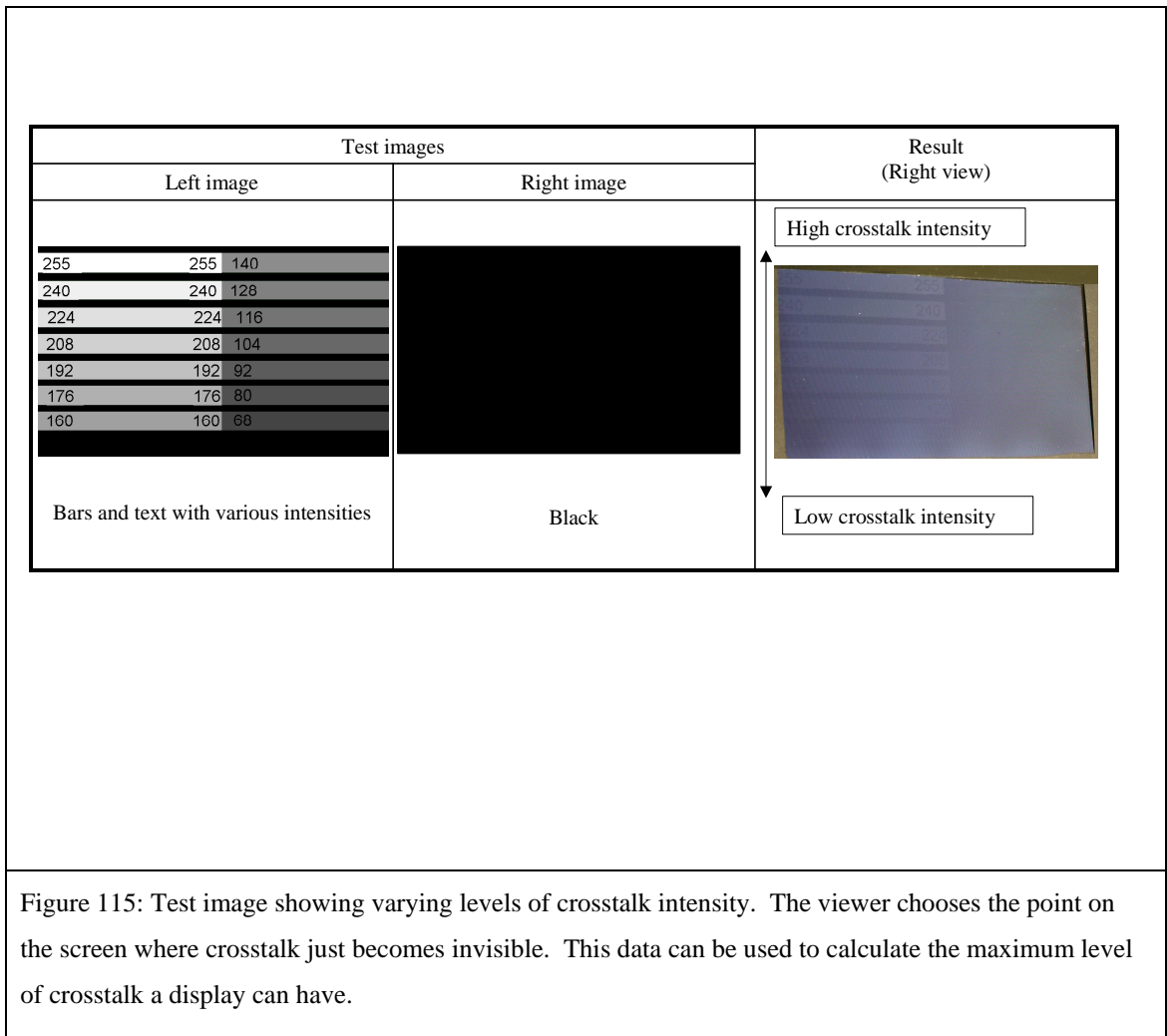
#### *Caveats*

From the literature [50], we would also expect crosstalk visibility to depend on the spatial frequency of the crosstalk, and the ambient lighting conditions. However, no data was found that tested the conditions as they would be for a dual view panel. The data can only be used as a guide. Testing specific to dual view panels is in section 3.2.

### **3.2 Experiments specific to dual view crosstalk visibility**

#### *Human factors experiment on crosstalk visibility*

Figure 115 shows the test image used to deduce what level of crosstalk is just perceivable.



On the right view black is displayed. A viewer looks at this black right image ready to identify any perceivable crosstalk coming from the left image.

The more intense the left image the more light leaks into the right image to cause crosstalk. This fact can be used to adjust the level of the crosstalk that the viewer sees, thus simulating the effect of panels with different crosstalk performance.

Specifically, an image of different intensities is shown on the left image (see Figure 115). This image has full brightness at the top fading to zero intensity at the bottom.

The viewer of the right image can see crosstalk at the top (from the full intensity left image), but cannot see crosstalk at the bottom (here the left image has zero intensity).

The viewer marks at what point from top to bottom, the crosstalk ceases to be visible. The crosstalk level at this point can be deduced from knowledge of the right image intensity. Consequently the crosstalk visibility threshold is found for a dual view display.

This test can be performed at 70 cm viewing distance (a typical viewing distance for a passenger), with various ambient lighting conditions, with typical font sizes used in GPS maps, on a display that has the same anti-reflection coatings as would be used on an automotive panel, and many other factors that match the actual usage of a dual view display. This makes the test more convincing than conclusions drawn from previously published literature.

## Results

As the crosstalk intensity is increased, its visibility goes through phases.

1. Firstly, the crosstalk is invisible.
2. At higher intensities, it is invisible when looked at, but can be seen when the point of gaze of your eye is just away from where the crosstalk exists.
3. At higher intensities, crosstalk becomes visible when looked at directly, but the detail cannot be seen sharply enough to read text.
4. At higher intensities, the crosstalk is bright enough so that text in the other image may be read.

The table below presents the crosstalk intensities for the four ‘phases of visibility’ described above.

‘Visibility phase’	Background intensity (from LCD light leakage), cd/m <sup>2</sup>	Grey level causing this level of crosstalk (0 to 255)	Crosstalk intensity (cd/m <sup>2</sup> )	Weber’s value	Crosstalk achieving this Weber’s value (%)
1	5.54	<104	<5.64	<0.019	<0.028
2	5.54	104 to 116	5.64 to 5.67	0.019 to 0.023	0.028 to 0.034
3	5.54	116 to 192	5.67 to 5.88	0.023 to 0.062	0.034 to 0.092
4	5.54	>192	>5.88	>0.062	>0.092

Table 19: Crosstalk levels and their visibility to the human eye.

This test was carried out in ambient lighting of 5 lux (similar to night time driving). The results do not change significantly up to 300 lux (room lighting), higher levels of ambient lighting were not tested, but it would be expected that the visibility of crosstalk would decrease. This is because the ambient lighting would increase the glare off the front of the panel, effectively increasing the brightness of the background intensity, and decreasing the Weber's value for a given crosstalk intensity.

The test was repeated with two different subjects. The results did not differ significantly between the two subjects.

The transition between the 'visibility phases' is not sharp; an error of about +/- 15% of the Weber's value is estimated. The table above is not a precise result, but it is intended to give a feeling for crosstalk intensity and visibility.

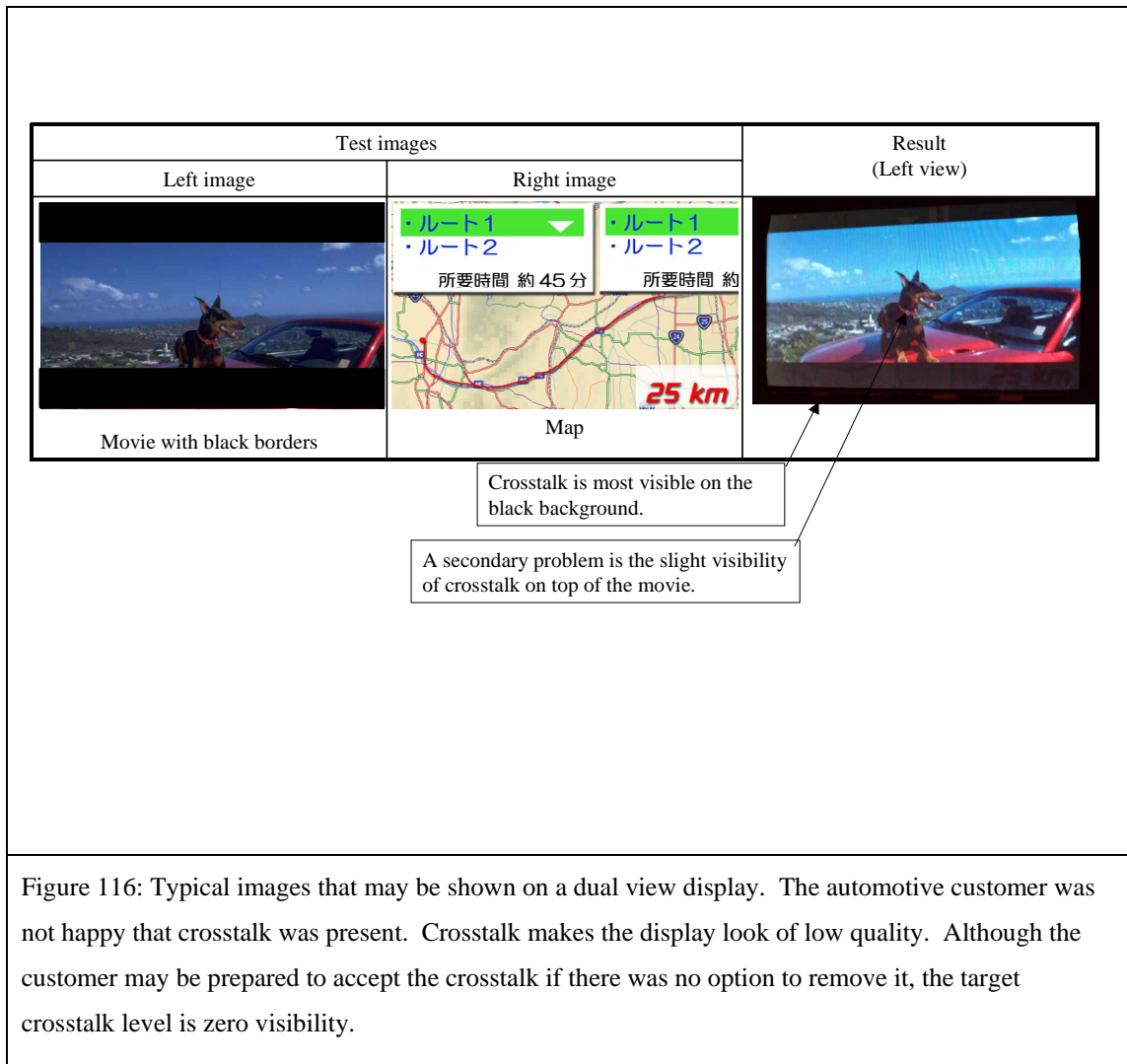
### *Conclusion*

It seems:

- According to tests on a dual view display, crosstalk must be reduced by about 1.9 to 5.3 times to make text on the opposing image illegible, and by 6.4 times to make crosstalk entirely invisible.
- The literature on visibility of different intensity levels is consistent with measurements made on a dual view panel. However, the literature's estimate of the reduction of crosstalk needed to make crosstalk invisible is generous.

### *Customer requests*

The dual view panel was sent to an automotive customer for feedback. The dual view panel was placed in a car and given typical usage. Figure 116 shows comments on a typical test image that was displayed.



### **3.3 Human factors techniques to reduce crosstalk visibility**

From the literature described in this section, the two methods below should make crosstalk less visible to the human eye.

1. Reduce the backlight intensity of the dual view LCD. This should work because the human eye is said to be less sensitive to changes in intensity at lower light levels. This technique could be used during nighttime driving, because the display needs to be dimmed anyway, so that it does not dazzle the driver.
2. Reduce the contrast ratio of the dual view LCD. If a small intensity is added to each pixel of the dual view display, the extra light should ‘drown out’ the crosstalk.

The results of trials using the above two methods are presented in the table below.

<i>Method</i>	<i>How much</i>	
	<i>Theoretical prediction</i>	<i>Experiment</i>
1.	At night displays are reduced to about 5cd/m <sup>2</sup> . This makes the background intensity 0.07cd/m <sup>2</sup> . At this low intensity level, the Weber's threshold for zero crosstalk visibility is 1.3. This means that a display should be able to have up to 1.9% crosstalk before crosstalk is noticeable.	0.18% crosstalk was tested under this illumination condition. The crosstalk was invisible.
2	If no less than 34 cd/m <sup>2</sup> is displayed on the left image, this should be sufficient to drown out the 0.18% crosstalk of the dual view display.	Only 19 cd/m <sup>2</sup> was needed to hide 0.18% crosstalk.

Table 20: Methods to mask the visibility of crosstalk.

The results show that method 1 would be able to eliminate crosstalk visibility at night, but it does not solve the daytime driving problem.

An experiment showed that method 2 was successful. I suspect that 19cd/m<sup>2</sup> is an underestimate of the intensity needed to mask 0.18% crosstalk because when a grey level is used to set the display to 19cd/m<sup>2</sup> electrical crosstalk will counter the optical crosstalk. Even so it was possible to see that the concept would work. The main point is that if 19cd/m<sup>2</sup> was used as the lowest grey level so that all crosstalk was masked then the contrast ratio of the display would effectively be 20:1, which is too low.

### *Conclusions*

Crosstalk needs to be reduced by ~6 times for it to become invisible. Grey levels can be added to drown out crosstalk, but the panel contrast ratio becomes poor. Reducing the backlight intensity at night can solve crosstalk visibility, but only at nighttime.

These results suggest that the only acceptable method of reducing the crosstalk visibility is to reduce the crosstalk intensity. Attempts to do this are presented in section 4.

## 4. Reducing crosstalk

Experiments described in section 2 suggest that crosstalk in the dual view panel originates from electrical interference between the pixels, and optical effects (mostly diffraction of light by the parallax barrier).

Section 3 showed that to solve the crosstalk problem completely (render it invisible to the human eye) a reduction in crosstalk of approximately 6 times is needed, a tough target considering that the current system gives only 0.18% light leakage from one image to the other (see section 4.2.1).

This section describes the attempts made to reduce electrical and optical crosstalk, and the results. A summary of this is given below.

### **Two methods of correcting electrical crosstalk were considered.**

1. 'Crosstalk correction', by image processing. This involves characterising how electrical crosstalk behaves, so that it may be predicted and compensated by modifying the images that are displayed. This technique was shown to be successful, however in order to implement this feature into a product, extra costly electronics would be needed.
2. A redesign of TFT layout in the LCD panel. This was carried out by colleagues in Sharp Corporation Japan, in an attempt to reduce the capacitance generated by multi level ITO lines suspected to cause the electrical crosstalk. This technique reduced the electrical crosstalk by about 8 times, rendering it significantly less visible.

### **The following methods were investigated to remove the optical crosstalk.**

1. 'Crosstalk correction', by image processing. This is similar to the technique used to remove electrical crosstalk, however optical crosstalk is more difficult to solve. The magnitude of optical crosstalk depends on the angle that the display is viewed from. Therefore crosstalk could be corrected for one angle, but not at all angles. This severely reduces its effectiveness.
2. Using apodised slit edges was considered, and shown to reduce the crosstalk by about 30%. This involves changing the transmission profile of the slit to change its diffraction properties. This technique has been used in 3D displays, and provides an option for optical crosstalk reduction.

3. Increasing the image separation by changing the geometry of the design is shown to reduce crosstalk, however, image separation is fixed by the passenger and driver positions, and so can not be changed.
4. Use of different pixel geometry is discussed. A dual view design can be created that uses wider slits which should diffract less.
5. Experiment suggests that by using backlighting which emits light in only specific angular ranges, crosstalk can be halved.
6. To help reduce the influence of polariser scattering on crosstalk, the polariser was spaced away from the display. This does not stop the polariser scattering, but it does prevent the polariser scattering a legible image, therefore, its effect on crosstalk becomes insignificant.

These methods are explained in more detail in the following sections.

Finally some of these solutions are combined into a modified dual view display. This display has an estimated crosstalk of 0.05%. This level of crosstalk is seen to be substantially invisible to the naked eye.

## **4.1 Reducing electrical crosstalk**

### **4.1.1 Crosstalk correction for electrical crosstalk**

Crosstalk correction involves the use of image processing to cancel out crosstalk. For example, predicted crosstalk from the left image is subtracted from the right image. When the images are displayed, the right viewer then sees: the right view (-predicted crosstalk from the left view) + crosstalk from the left view. Therefore the crosstalk from the left view is cancelled out.

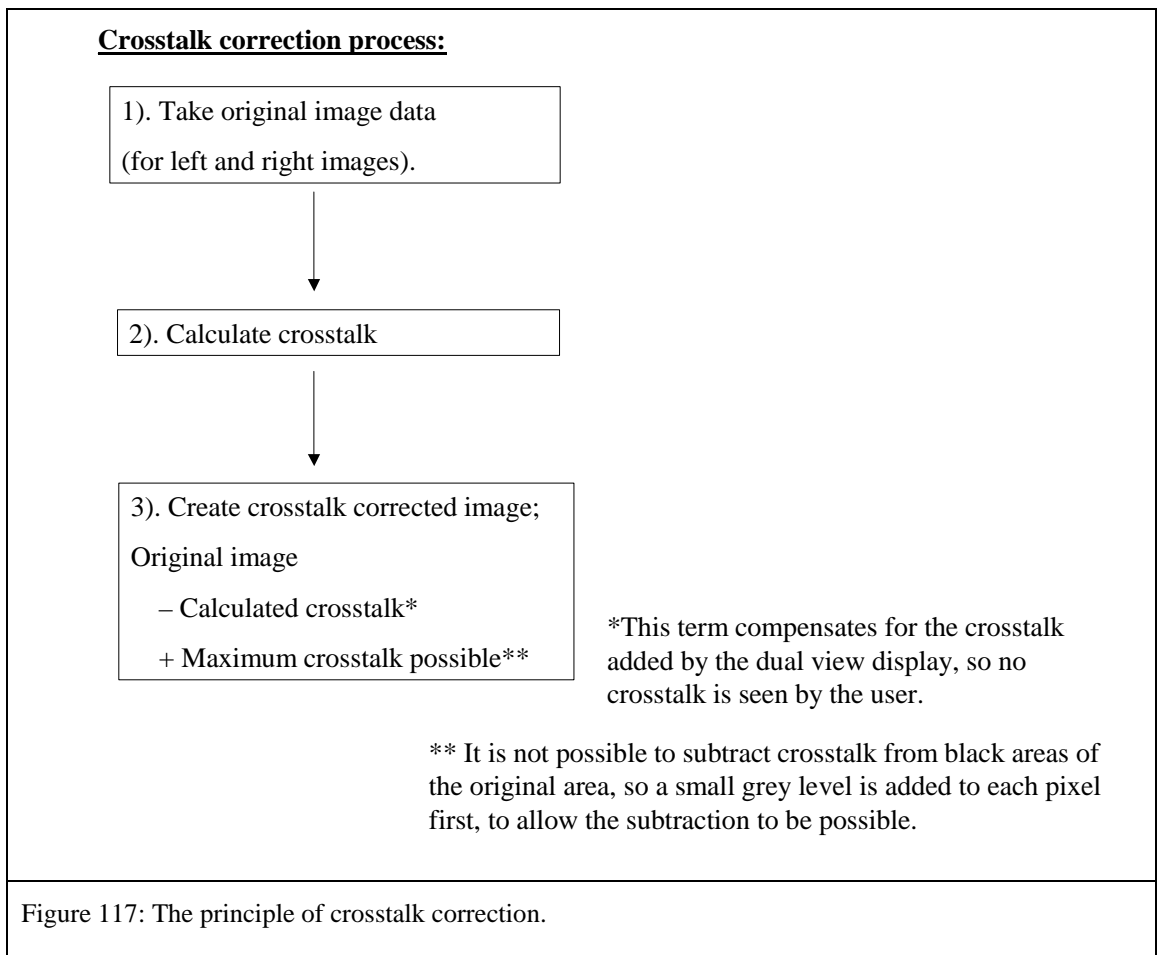
Section 4.1.1.1 describes the process in a little more detail.

Section 4.1.1.2 is about predicting the electrical crosstalk that will occur, which depends on the data that is sent to the pixels. A measurement system is set up to measure this empirically. In this measurement electrical crosstalk is decoupled from optical crosstalk, so that the electrical crosstalk alone was successfully measured.

Section 4.1.1.3 shows the final image processing result. The technique is seen to be successful.

#### *4.1.1.1 Image processing overview*

Figure 117 shows the principle behind crosstalk correction.



The details of steps 2 and 3 are considered in section 4.1.1.2

Results from the procedure are presented in section 4.1.1.3

#### *4.1.1.2 Implementation of electrical crosstalk correction*

##### *Characterising the crosstalk*

The test images of Figure 70 shows that the magnitude of electrical crosstalk depends on the data that is put onto both the left and right pixels. I.e. crosstalk from the left image to the right image depends on the left and right image data.

Therefore, the image-processing algorithm will need to know:

- What is the left pixel data?
- What is the right pixel data?
- What crosstalk does this combination of pixel data course?

The level of crosstalk that each combination of pixel data causes seems to be a complicated function resulting from the driving electronics. It is experimentally measured below.

*Electrical crosstalk measurement*

The measurement of electrical crosstalk is complicated by optical crosstalk, which could distort the results.

It is known from section 2.2.1 that electrical crosstalk only propagates in one direction across the panel, a distance of one pixel at a time. This is labelled in Figure 118.

Figure 118 shows that by using this fact, and knowledge of colour filters in the display, it is possible to design an experiment, which allows electrical crosstalk to be measured without optical crosstalk influencing the measurement.

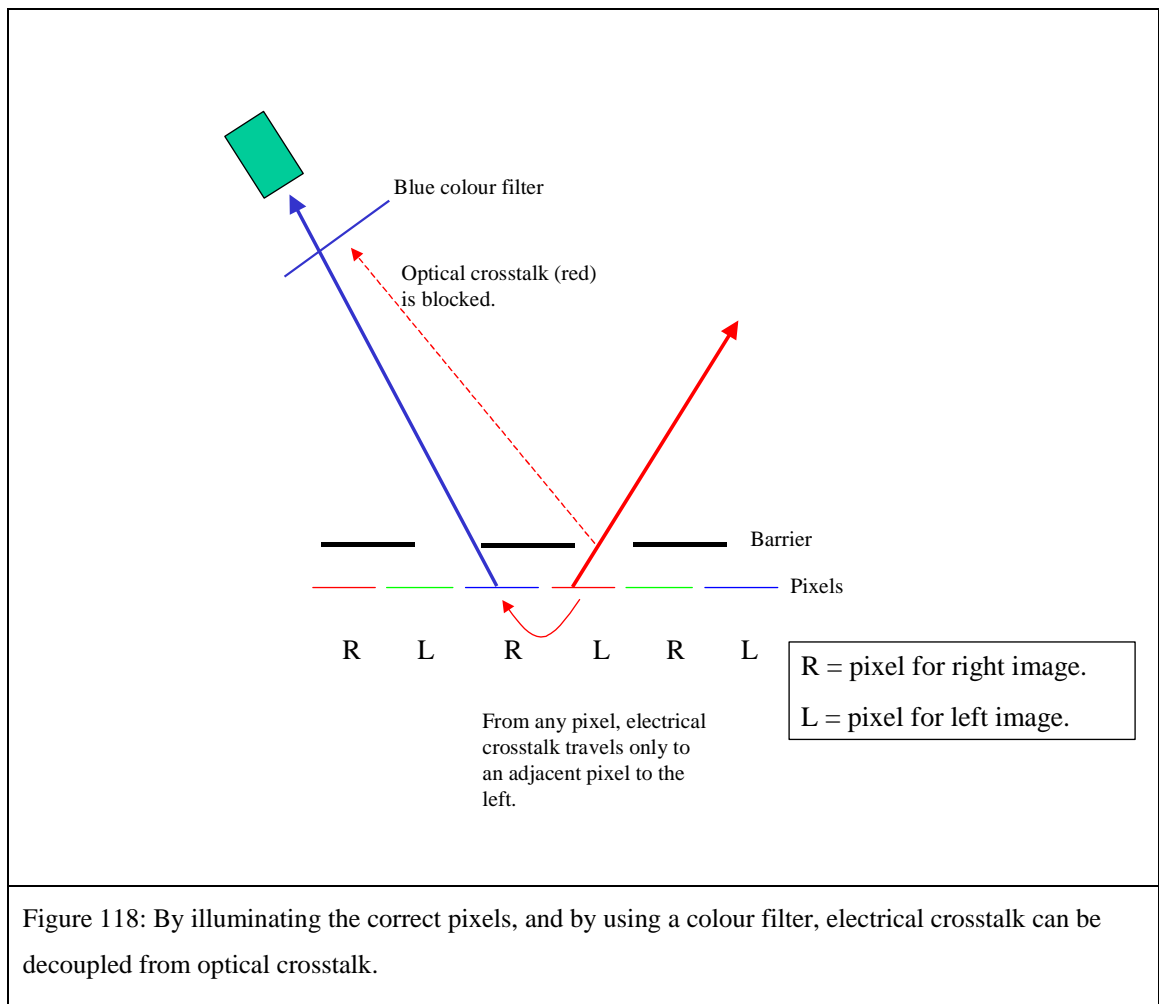


Figure 118: By illuminating the correct pixels, and by using a colour filter, electrical crosstalk can be decoupled from optical crosstalk.

In the case above a photodiode views the image from the blue right pixels.

The red left pixels generate;

- Electrical crosstalk to the blue right image.
- Optical crosstalk to the blue right image.

Electrical crosstalk induces a change in the blue pixel intensity, whilst optical crosstalk is red in colour. Therefore, by using a blue colour filter it is possible to filter out the optical crosstalk and measure only the electrical crosstalk.

For example, when the photodiode views the panel from the right with a blue colour filter, the following images can be used to measure electrical crosstalk.

<b>Right image</b>	<b>Left image</b>	<b>Photodiode measurement</b>
Blue (grey level 128)	Black	Reference level (no crosstalk)
Blue (grey level 128)	Red (grey level 255)	Reference level + electrical crosstalk only from the red pixel (optical crosstalk is red and is blocked by the colour filter).

Table 21: An example of test images that can be used to measure electrical crosstalk in the dual view system.

I can repeat the measurement for all combinations of left and right pixel data to determine how electrical crosstalk affects each case.

Each left and right pixel can take any one of 256 data levels, so to characterise electrical crosstalk for each case would require 256 x 256 measurements. Figure 119 shows a much-simplified data set.

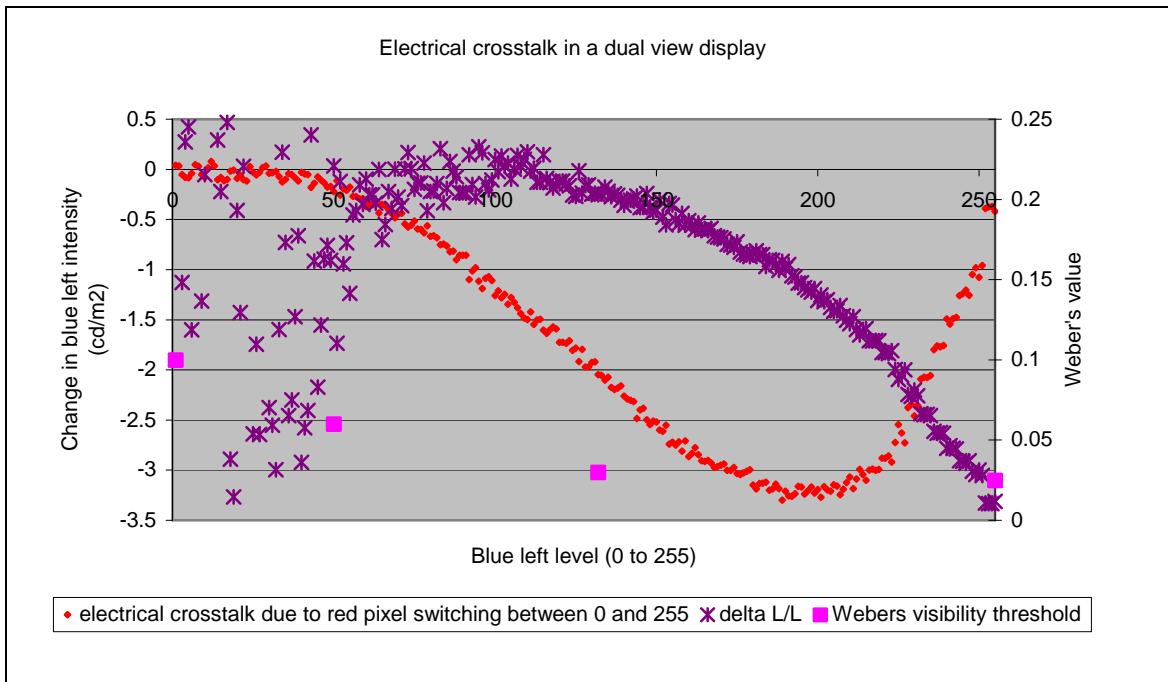


Figure 119: Measurement of electrical crosstalk between left and right pixels in a dual view panel. The vertical axis shows the change in intensity of a left pixel, due to a right (red) pixel switching between grey level 0 and 255. The horizontal axis shows how this electrical crosstalk changes with the intensity of the left pixel. The second set of data (purple \*s) is the Weber's value of the intensity change, i.e. the ratio of the change in brightness to the initial brightness.

The graph shows the behaviour of electrical crosstalk for different pixel data levels. For example, when the blue right image is at high or low intensities, the red left pixels have a small electrical effect. Maximum electrical crosstalk occurs when the blue right image is medium intensity.

#### *Experimental validity*

For the experiment to be valid no red light must leak through the blue colour filter, else optical crosstalk will interfere with the sensitive measurement of electrical crosstalk.

- The optical red crosstalk to the right image is measured to be 0.51% of the left image intensity. Full red intensity is  $23\text{cd/m}^2$ , corresponding to  $0.1\text{cd/m}^2$  crosstalk in the worst case of full intensity being used.
- The transmission of the red light from the panel through the blue colour filter was measured at 0.1%. The transmission of blue light from the panel through the blue colour filter was measured at 2.3%.
- Therefore the effect of the red optical crosstalk is approximately 1000 times less than the peak electrical crosstalk signal.

The noise in the graph is due to the very small changes in intensity that are being measured.

The vertical scale is scaled to  $\text{cd/m}^2$  without the blue colour filter present, (the intensity at the photo diode was actually a little less intense due to inefficiencies of the blue colour filter).

The measurements are consistent with visual observations made on the test images of section 2.2.1.

The above goes some way to suggesting a satisfactory measurement of the electrical crosstalk. Final confirmation will come with testing the resulting image processing algorithm.

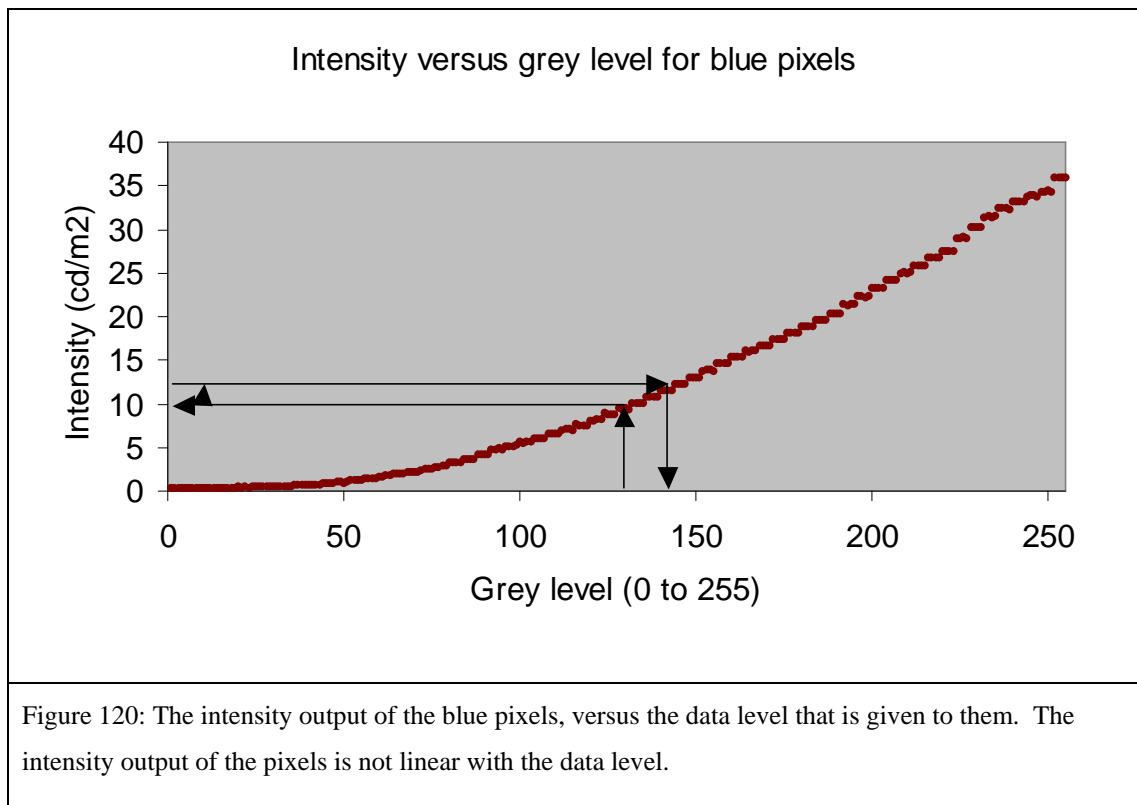
#### *Compensating for the crosstalk*

The following paragraphs show how the crosstalk may be compensated by use of an example. That is to say, from the experimental data we know that when a blue right pixel is set to grey level 128 and the adjacent red left pixel is changed from grey level 0 to 255, the blue right pixel intensity will be reduced by  $1.9 \text{ cd/m}^2$ .

To compensate for this  $1.9 \text{ cd/m}^2$  change in intensity we need to increase the blue right pixel intensity by the same amount.

To do this we need to know what change grey level (0 to 255) this corresponds to. The link between grey level and pixel intensity output is not linear.

The link is shown in Figure 120 below.



From the graph, for the example above, we can deduce the grey level increase needed to compensate the  $1.9 \text{ cd/m}^2$ .

1. Grey level 128 =  $9.5 \text{ cd/m}^2$
2.  $9.5 \text{ cd/m}^2 + \text{intensity needed to compensate electrical crosstalk} = 11.4 \text{ cd/m}^2$
3.  $11.4 \text{ cd/m}^2 = \text{grey level 141}$

We have shown that to compensate electrical crosstalk for this particular combination of pixel data, we need to increase the right pixel intensity by 13 grey levels. This should successfully cancel out the effect of electrical crosstalk.

#### 4.1.1.3 Result

Comparison of corrected/ non corrected images showed that electrical crosstalk became much less visible. However, the compensation algorithm requires extra electronics to be added to the display system to perform the processing. This adds cost to the system.

This line of investigation was dropped in favour of re-designing the TFT layout.

#### 4.1.2 Redesign of TFT layout to reduce parasitic capacitance.

Figure 121 shows how the TFT layout was re-designed to reduce electrical crosstalk.

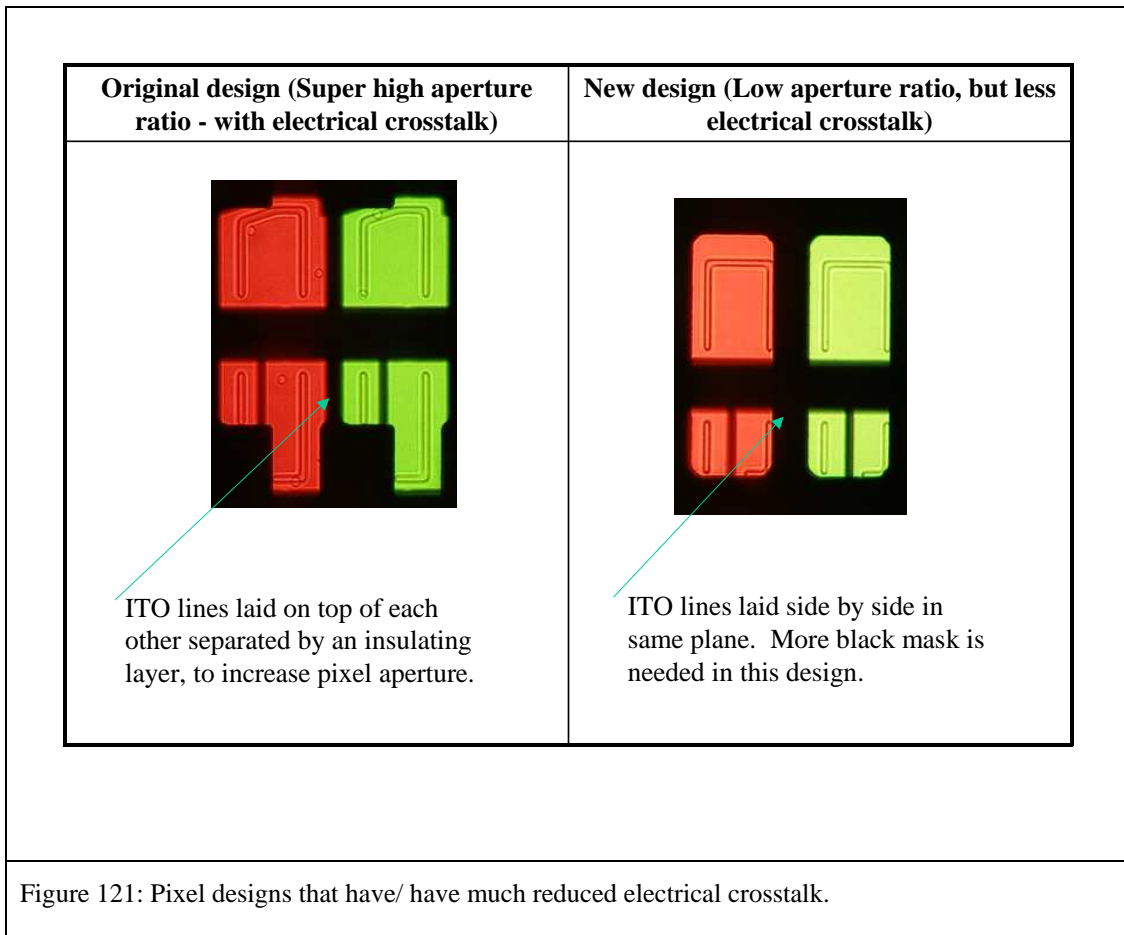
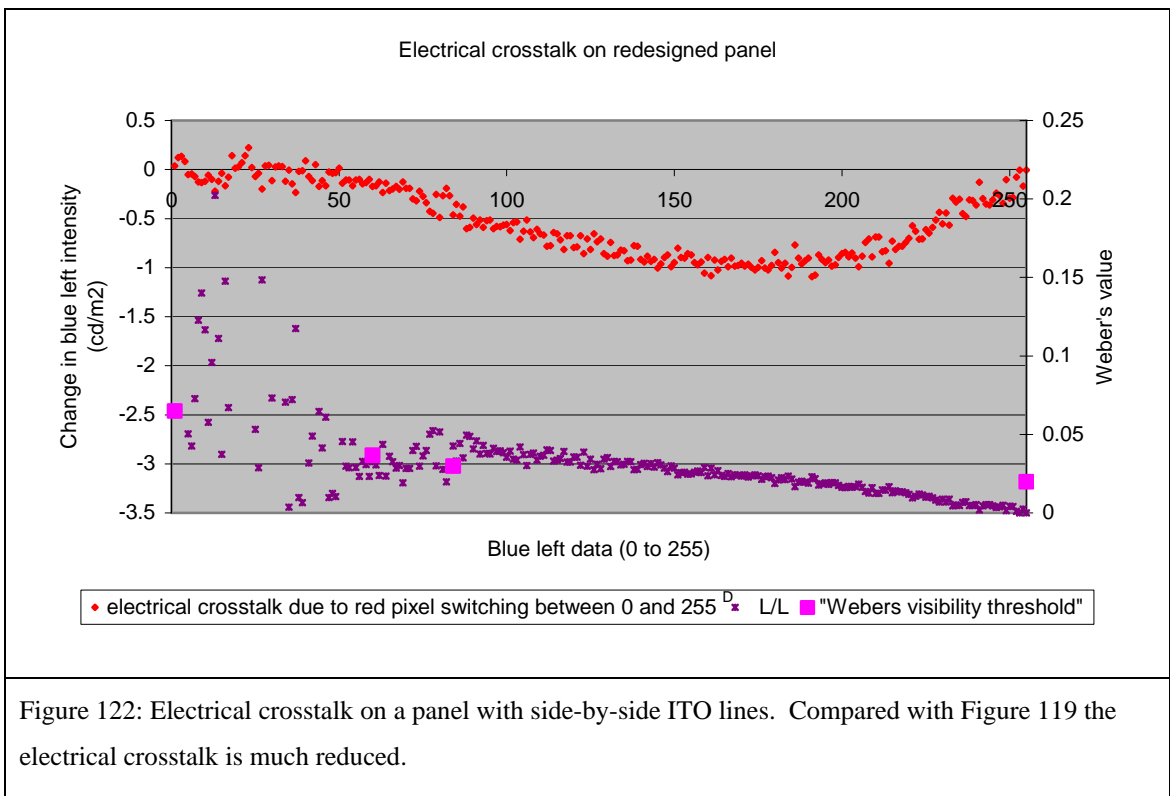


Figure 122 shows a graph of the electrical crosstalk for the new TFT layouts. It can be seen that electrical crosstalk is much reduced in the new design.



Visual observations show that electrical crosstalk is still slightly visible but very much improved.

### *Brightness of the new TFT design*

The aperture ratio of the new TFT design is reduced, but this is actually advantageous to dual view brightness. A smaller pixel aperture allows a larger slit aperture to be used.

The new TFT design is actually brighter than the old design when used in a dual view display [52].

## **4.2 Reducing optical crosstalk**

### **4.2.1 Crosstalk correction**

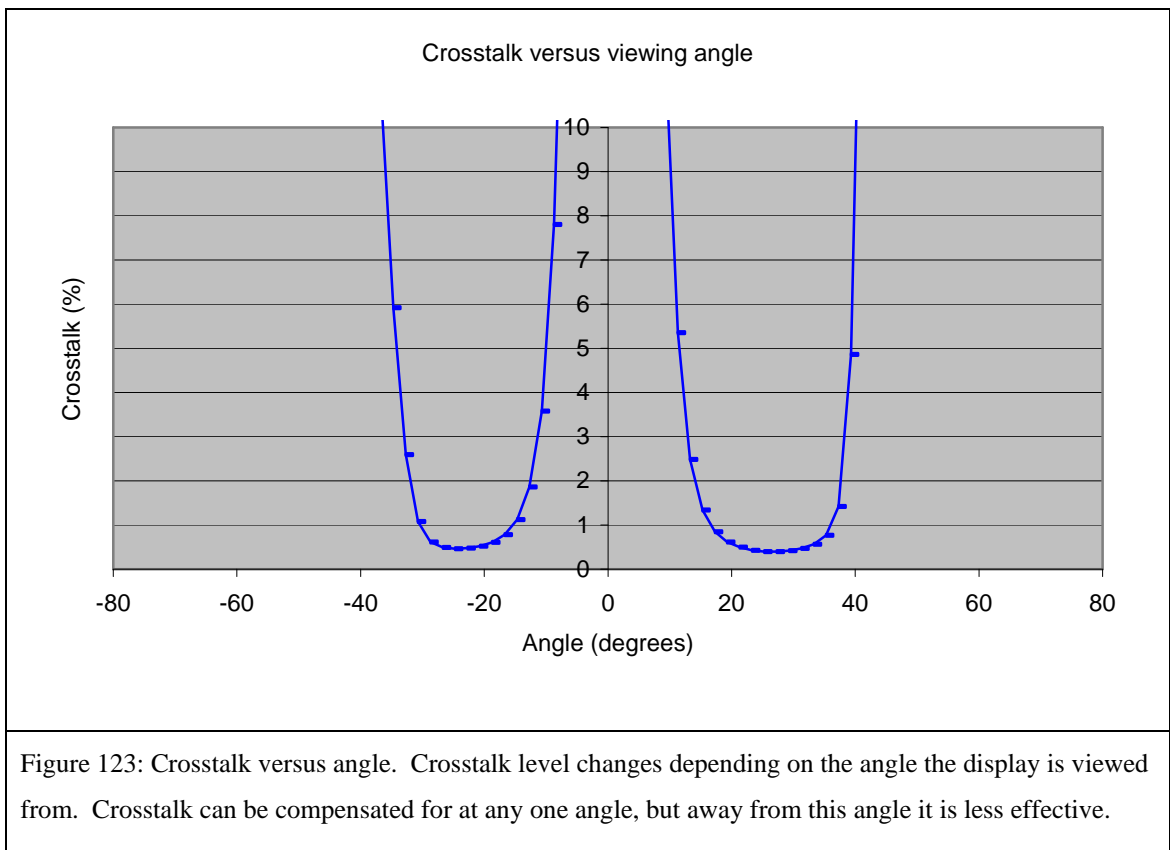
The principle of optical crosstalk correction is the same as for electrical crosstalk correction (section 4.1), however correcting optical crosstalk is simpler. Correction of a left pixel (for example) only depends on;

- a) The intensity of the adjacent right pixel (of the same colour).
- b) The level of optical crosstalk.
- c) Pixel intensity (cd/m<sup>2</sup>) versus pixel grey level (0 to 255), so the amount that the pixel grey level needs to be changed to compensate for crosstalk (cd/m<sup>2</sup>) can be calculated.

### *Results*

An algorithm was written to perform this optical crosstalk correction on the panel described in section 1.1 (with a crosstalk of 0.46%).

The result was that the correction works well at 30 °. When the user moves just off +/- 30 ° crosstalk becomes visible again. Figure 123 shows the reason for this. It is a graph of crosstalk versus angle.



Due to the sensitivity of the eye, even the slight change in crosstalk produced by moving a few ° away from 30 ° causes crosstalk to become visible again. Theoretically, since crosstalk increases away from 30 °, crosstalk correction should still reduce the visibility of crosstalk, even if it does not remove it entirely.

From a psychological point of view it seems that a reduction in crosstalk offers little advantage. Psychologically the crosstalk effect appears to be binary. It is either visible (and detracts from the display quality), or it is not visible (has no effect). This makes crosstalk correction for optical crosstalk of little use.

### *Conclusions*

Crosstalk correction is not an ideal solution;

- It only works for one viewing angle.
- To implement it in a product would require additional electronics to do the image processing. The performance of crosstalk correction does not justify this cost.

### **4.2.2 Reducing diffraction**

If diffraction is a major cause of crosstalk then reducing the diffraction from the barrier slits should reduce crosstalk. Some methods of doing this are discussed in this section.

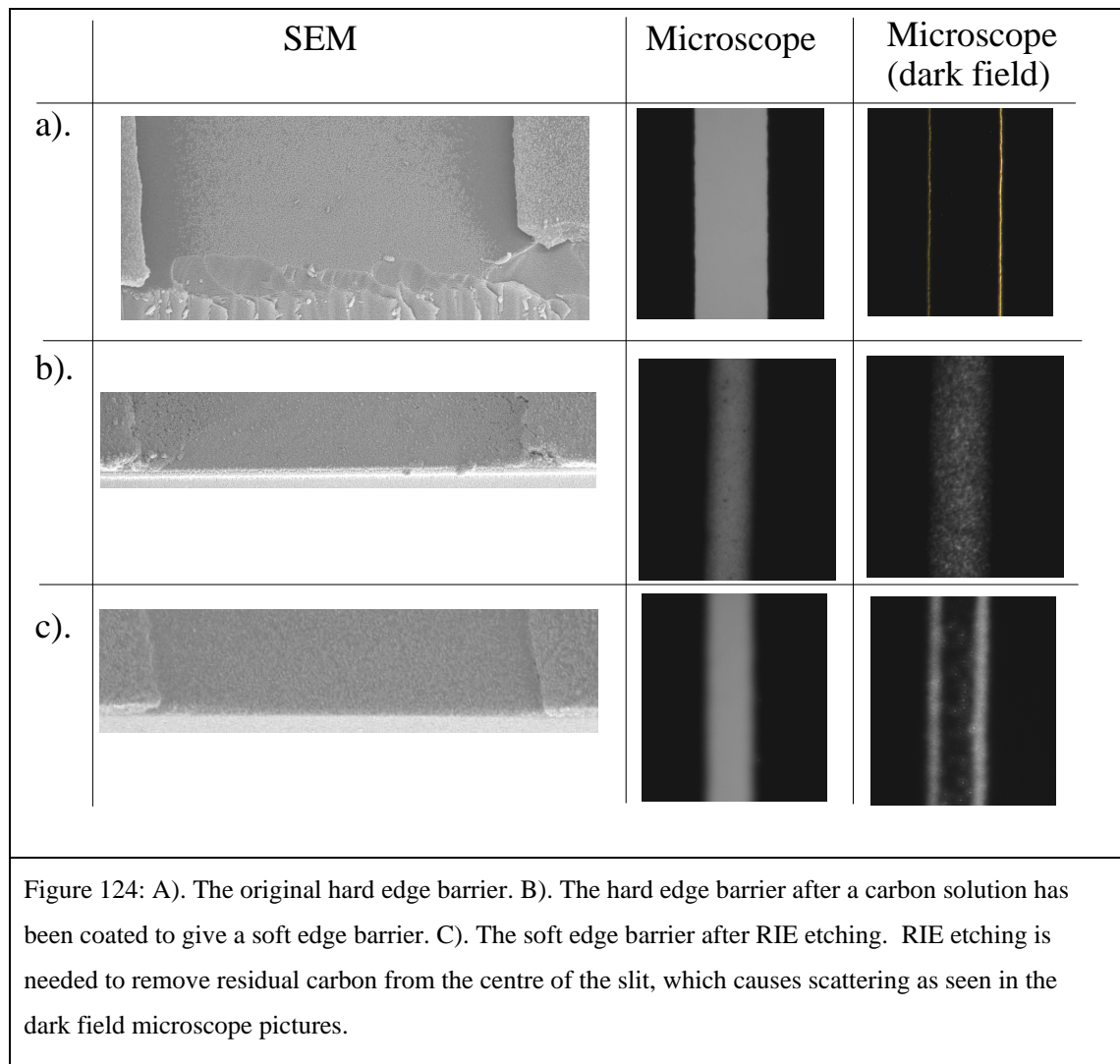
#### 4.2.2.1 Soft edge barrier

Apodising apertures in optical systems is a known method for reducing the effects of diffraction in optical systems [45].

In this section soft edges are made, and it is confirmed that they cause less diffraction at high angles. These barriers are constructed into a dual view display, and crosstalk is reduced by about 30%.

##### *Creating apodised slits*

In chapter 4 a simple technique is discovered to create lenses by surface tension effects. This technique was tested to see if it would work as a simple method of creating soft edge barriers. The technique is described below.

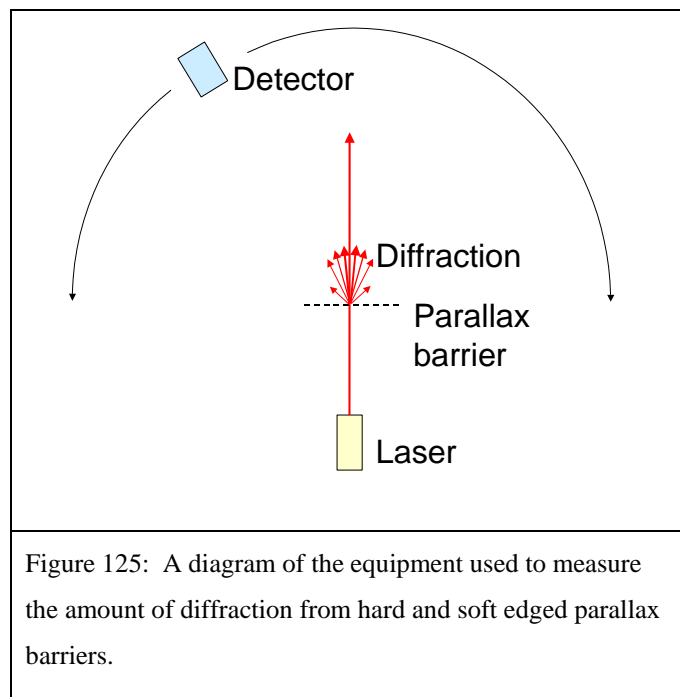


The technique was successful, as can be seen by looking at the microscope pictures of the original barrier edge a) and the processed barrier edge c).

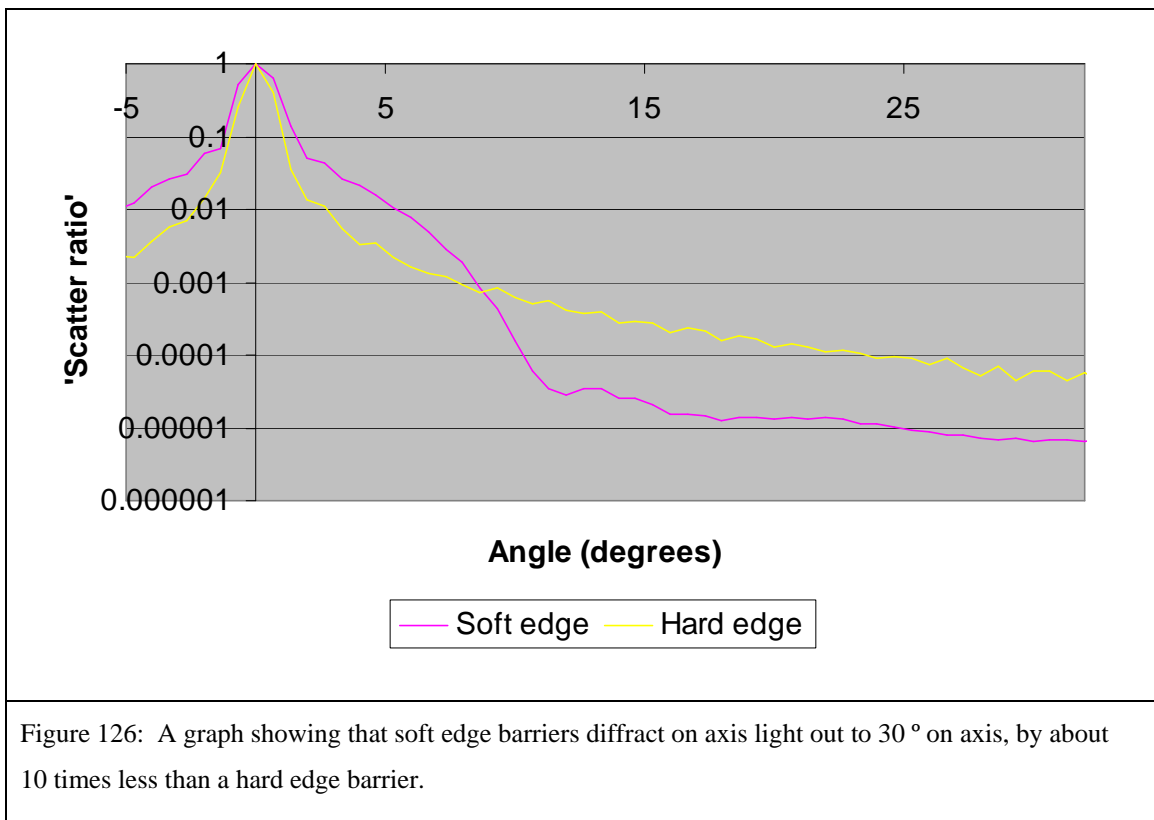
Unfortunately, residual carbon on the glass at stage b) would cause absorption and scatter, decreasing brightness and increasing crosstalk respectively. RIE (reactive ion etching) was needed to remove it. The use of RIE severely reduces simplicity of the manufacture technique, but the technique is still suitable for proving the principle of soft edges.

*Do the soft edges diffract less?*

An experiment was set-up as shown in the figure below, to measure the amount of diffraction from the hard and soft edged parallax barriers.



The results of this experiment are shown in the graph below.



#### *Experimental details*

The 'Scatter Ratio' refers to a calculation performed on the raw measurement data, which tries to normalise the results so that the slightly different transmissions of the barriers do not influence the results. The scatter ratio is the intensity of diffraction at each angle, expressed as a fraction of the on axis transmission.

Note that the actual diffraction patterns comprise multiple peaks with a spacing of about 0.2° due to interference from multiple slits of the barrier. These have been averaged out by use of large detector aperture, which gives an angular resolution of only 0.7°.

Therefore, the graph shows the diffraction envelope that results from the transmission profile of the slit.

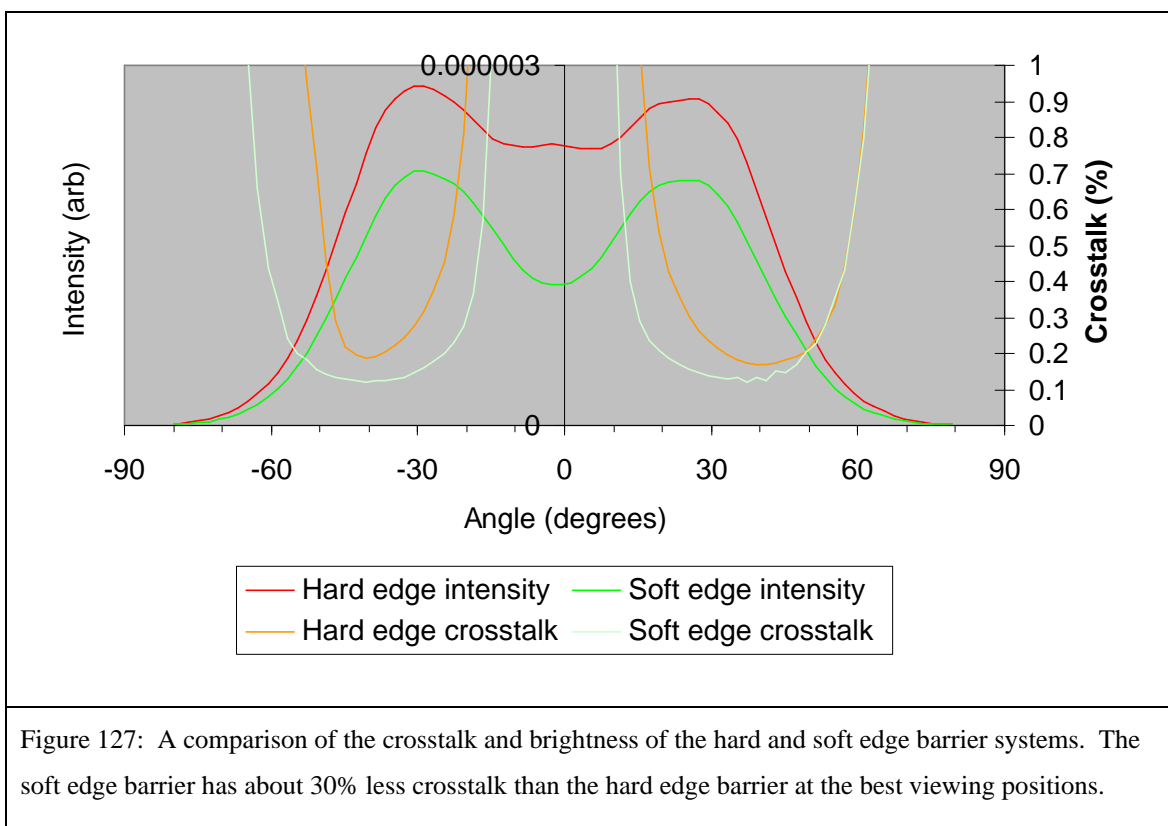
#### *Conclusions*

- There is more diffraction from the soft edge barrier at 5 ° than the hard edge barrier. At 30 ° there is about 10 times less diffraction from the soft edge barrier than the hard edge barrier.
- Look at Figure 112, it implies that most crosstalk is caused by light entering the panel on axis and diffracting 30 ° out towards the main 30 ° viewing position. Given light diffracted at 30° is 10 times less for the soft edge barrier, this implies that the crosstalk in a dual view panel should be reduced.

Diffraction from a dual view display is more complicated because the light propagates through two apertures: firstly the light passes the pixel aperture, and then the parallax barrier.

When we say that the barrier reduces diffraction by 10 times, this refers to the Fraunhofer diffraction case. When we say that this should lead to less diffraction in a dual view display we are assuming that the Fresnel diffraction in the display will behave in a similar way to Fraunhofer diffraction in the diffraction test involving the barrier alone. This assumption will be tested when the soft edge barrier is applied to a DV panel.

### Do the soft edges cause less crosstalk?



The results of the crosstalk test show that crosstalk is reduced by about 30%.

Brightness is also reduced. This is because the soft edge slits were made too narrow in error. The soft edge slit width should be made wider so that brightness is maintained and the test is a fair comparison.

I suggest that increasing the slit width of the soft edge barrier would cause two effects on crosstalk.

Firstly, the diffraction would be decreased since light spreads less due to diffraction when it passes wider slits. This would decrease crosstalk.

Secondly, the head freedom would be decreased as has been explained through geometric optic considerations. A decrease in head freedom would decrease the angle for which light needs to be scattered or diffracted for it to cause crosstalk. The centre of the viewing window is not as well angularly separated from the other view if the head freedom is reduced. This effect would increase crosstalk caused by the scatter and diffraction that exists.

We have seen from measurements of slit width versus crosstalk for hard edge barriers, that the first effect dominates over the second effect, so that smaller slits produce lower crosstalk.

In the case of soft edge barriers, the diffraction has been reduced, so it is difficult to predict whether the first effect will still dominate over the second.

The experiment was repeated with a soft edge slit that was wider. Unfortunately, this time the brightness of the soft edge barrier was slightly higher than the hard edge barrier, indicating that the soft edge slits were now too wide. The crosstalk reduction was 25% lower than the hard edge barrier. This is shown in the table below.

<i>Edge type</i>	<i>Brightness</i>	<i>Crosstalk</i>
Hard	Standard (38 $\mu$ m slit width)	Standard
Soft	Peak brightness reduced by 25% (slits too narrow)	Reduced by 30%
Soft	Peak brightness increased by 13% (slits too wide)	Reduced by 25%

Table 22: A comparison of the performance of soft and hard edged parallax barriers.

Since the crosstalk reduction for the wide and narrow soft edge slits is about the same in both cases, this implies that the first and second effects produce almost equal impact, and cancel each other out.

Therefore, had a soft slit width been produced of precisely the right width I suggest the crosstalk reduction would be about 25-30%, with brightness maintained the same as for the hard edge barrier.

There are two discrepancies here between basic diffraction theory and the experimental results. Firstly Figure 98 suggests that diffraction through a 38 $\mu$ m slit through an angle of 30 degrees should only give 0.01% crosstalk. From this it would seem that diffraction could not account for the 0.11% diffractive crosstalk that was measured experimentally. Secondly, figure Figure 126 implies that soft edge barriers should reduce crosstalk by 10 times whereas only a 2 times reduction in the diffractive crosstalk was seen.

I believe that the explanation of this discrepancy lies in the mismatch between set-ups examined in Figure 98 and Figure 126, and the set-up of the dual view display. Both these figures assume that light incident on the barrier is collimated and illuminates it on-axis. In the dual view system the barrier is positioned close to the pixel apertures and the backlight illuminates the panel from a range of angles. To model this diffraction regime would require Fresnel treatment of a two-aperture system with an un-collimated light source rather than the Fraunhofer diffraction model that applies to the collimated light systems.

A colleague (David Montgomery) developed a Fresnel diffraction model to represent the dual view system accurately. On modelling the diffractive crosstalk from the dual view panel the result stated that there should be 0.11% crosstalk from diffraction. This matches exactly with the experimental measurement. The main difference between this calculation and the calculation shown in Figure 98 is that light from many angles is incident on the panel. The calculation sums the contribution to crosstalk caused by light incident at all the angles present in the dual view system. Each angle adds an amount of crosstalk to the other view at 30 degrees, whilst substantially only illuminating a small region of the correct view. Therefore each angle of illumination light adds to the crosstalk at 30 degrees but it doesn't always add to the brightness of the correct view at -30 degrees. With this factor (and others) taken into account, the first discrepancy is explained.

The second discrepancy is about why the soft edge barriers reduce diffraction by 10 times with collimated light but by only 2 times on the dual view panel. Again I suggest that this is because testing the soft edge alone with collimated light is not representative of the case where it is fixed to a display. I believe that this experiment is sufficient to make an argument that the barrier reduces Fraunhofer diffraction and therefore the means by which the crosstalk is reduced in the display is likely to be diffraction reduction. However I believe that it is not sufficient to accurately quantify the reduction

that is likely to be achieved due to the complex situation that occurs when it becomes part of a dual view display. Further modelling of this situation could help theoretically quantify this effect.

#### *4.2.2.2 Directional backlighting*

##### *Introduction*

Notice that in Figure 112, most crosstalk is caused by light entering the panel on axis. This on-axis illumination only serves to illuminate the mix of images that occurs on axis, and so is of no use. This suggests that reducing the amount of on axis illumination is a good idea because it will reduce the diffraction that causes crosstalk, without reducing the brightness of the viewing windows.

In this section a prediction is made about the level of crosstalk reduction that should be seen. The idea is tested and shown to match with the predictions. That is to say, the backlight tested (with reduced on-axis illumination) reduced crosstalk by 30%. However, this backlight does not have the perfect directional output. If a perfect directional backlight could be made predictions suggest that crosstalk could be approximately halved.

##### *Crosstalk versus light input angle*

Note that in this section the tests were performed on the original thin glass dual view display (made before the design modifications of section 2.3.6). On this panel, the crosstalk contribution made by input light from different input angles was measured to be as below.

Figure 128, crosstalk as a function of panel illumination angle.

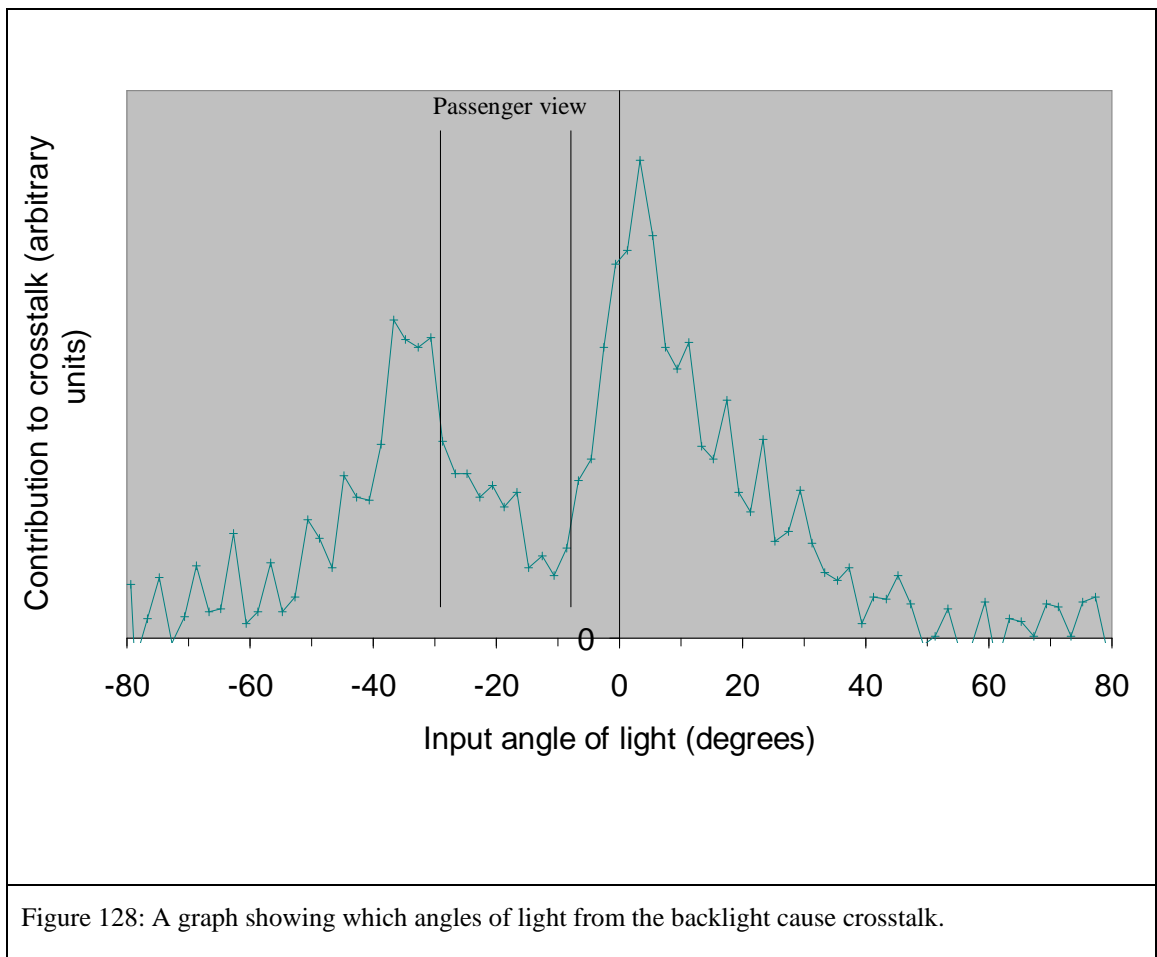


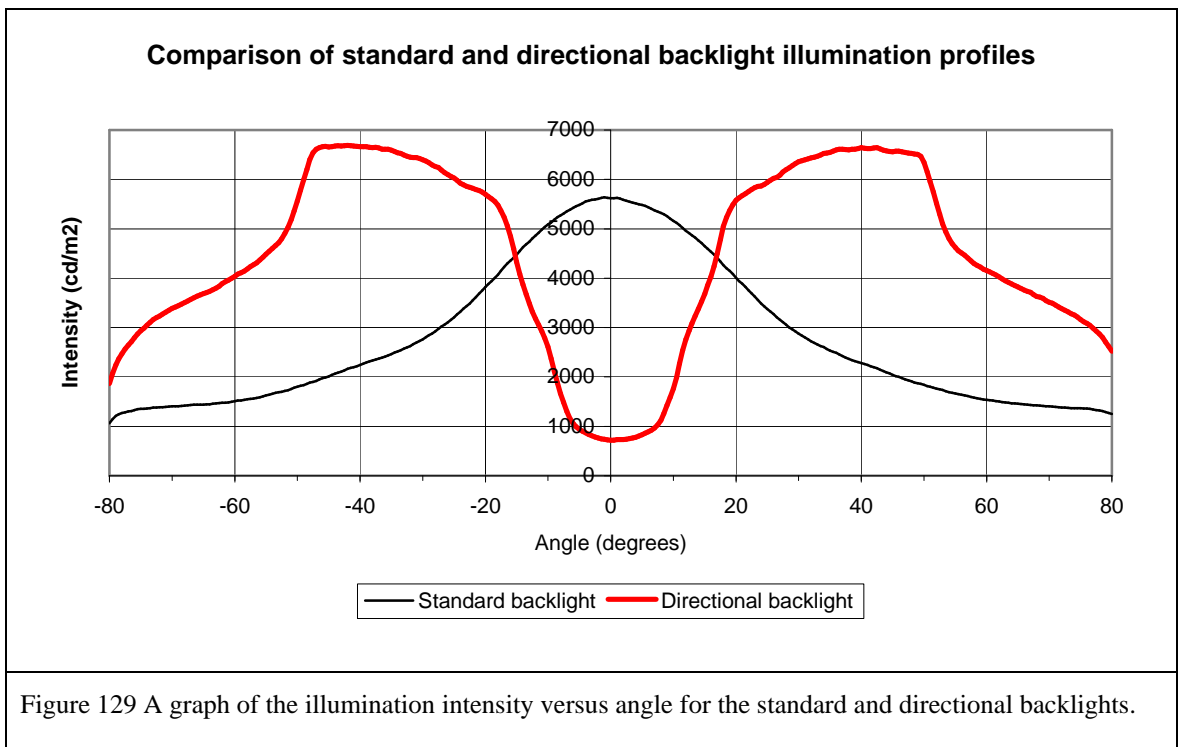
Figure 128: A graph showing which angles of light from the backlight cause crosstalk.

Figure 128 shows that;

- Crosstalk mostly occurs from on axis illumination of the panel.
- Some crosstalk occurs from light illuminating the secondary windows (from about -35 to -50 °).
- Little crosstalk comes from high angle light from the backlight (50 to 80 °).

Given that illumination on axis, and illumination from 35 to 50 °, contributes heavily to crosstalk, and given that this light does not contribute significantly to useful illumination of the panel, it seems sensible to remove these illumination angles from the backlight.

A backlight with the correct characteristics of high brightness at +/- 30 °, low brightness on axis, and low brightness at high angles has been described in chapter 1.



Using measurement data similar to that in Figure 111 it should be possible to predict the performance of such a backlight, in terms of crosstalk.

This can be done by;

1. Determining for each angle the contribution which the backlight illumination makes to the crosstalk image.
2. Determining for each angle the contribution which the backlight illumination makes to the correct image.
3. Weighting the information from 1 and 2 by the normalised intensity of the backlight at each angle (from Figure 129).
4. Sum the results from 3 for all angles. This gives the total contribution from the backlight to both the crosstalk image and the correct image.
5. Divide totals by 4 to obtain the crosstalk ratio.

The results of this calculation are shown in Table 23 for the standard dual view backlight, the directional backlight achieved in Figure 129, and a theoretical perfect directional backlight, which emits light only from +/- 12 to 35 ° with uniform intensity.

*A reduced crosstalk display by directional backlighting*

<b>Backlight</b>	<b>Predicted crosstalk (%)</b>	<b>Experimental measurement of crosstalk with photodiode (%)</b>
Standard backlight	0.46	0.46
Directional backlight	0.33	0.30
Perfect directional backlight (black central and black 2ndary windows).	0.19	No data.  Backlight Exists in theory only.

Table 23: The effect of different illumination profiles on crosstalk. Crosstalk levels from different backlights can be predicted from knowledge of the backlight illumination profile with angle, and the contribution each angle of illumination makes to crosstalk of the display. The predictions are verified with experimental data, for two different backlights. Crosstalk can be ~halved by creating a perfect directional backlight (compared with a standard automotive backlight).

The predictions made in the table above suggest that by using the directional backlight of Figure 129 with a dual view display, crosstalk should be reduced from 0.46% to 0.33%. This backlight is not perfect because still some stray light exists on axis and at high angles. The table above also includes a prediction of the crosstalk that could be achieved by use of a perfect backlight, which emits zero light on axis and to the secondary windows. The prediction suggests that crosstalk can be reduced to 0.19% if such a backlight could be constructed.

**4.2.2.3 Image separation angle**

As is known from Chapter 1, reducing the separation between the LCD pixels and the parallax barrier may increase the angle of separation between the left and right images. If a dual view display has a greater angle between the left and right image, this would mean that light causing crosstalk would have to deviate a larger angle away from the path predicted by geometric optics, in order to cause crosstalk. Experience suggests that light primarily follows the geometric path. Effects such as diffraction and scattering deviate light from the geometric path, but the further light is deviated from the geometric path, the less significant the intensity of the light at this angle becomes. Therefore you would expect that, for a dual view display of high angular image separation, the amount of light that is deviated from one image to the other would be low. The wider the image separation the lower the crosstalk should be.

This line of thought is tested in the experiment of Figure 130. The experiment was carried out on the original dual view panel (before the modifications of section 2.3.6).

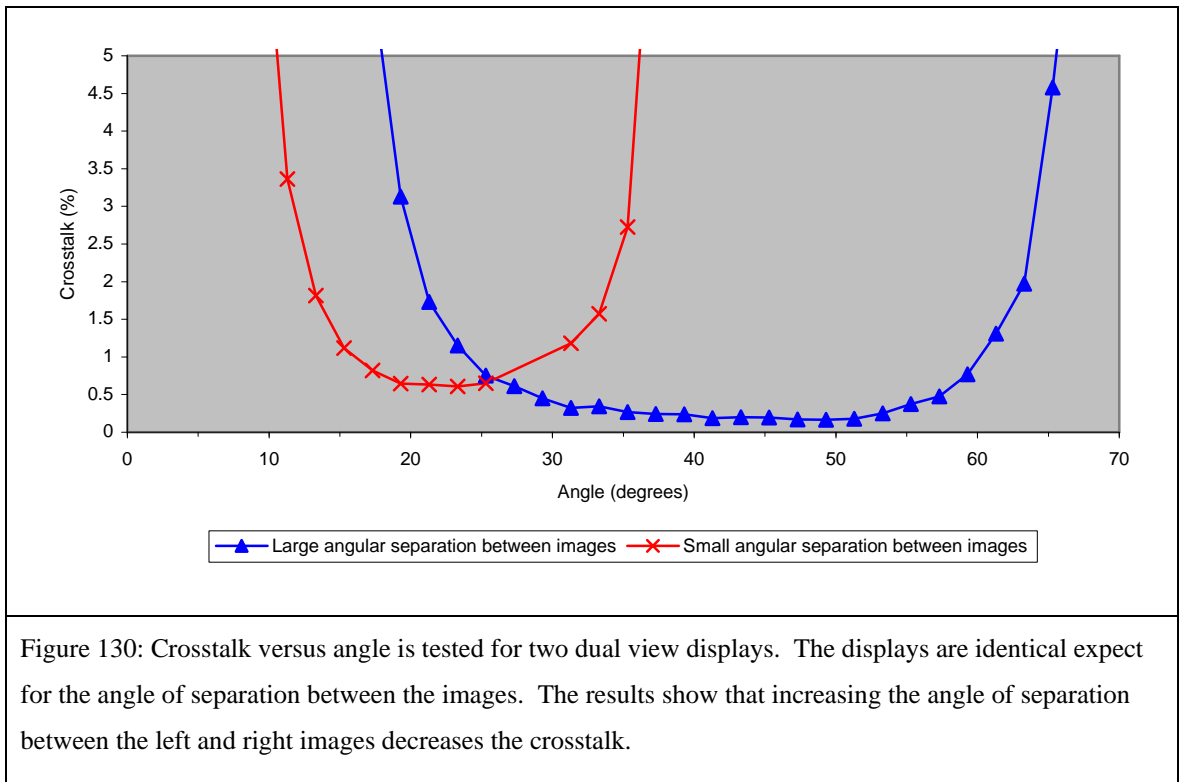


Figure 130: Crosstalk versus angle is tested for two dual view displays. The displays are identical except for the angle of separation between the images. The results show that increasing the angle of separation between the left and right images decreases the crosstalk.

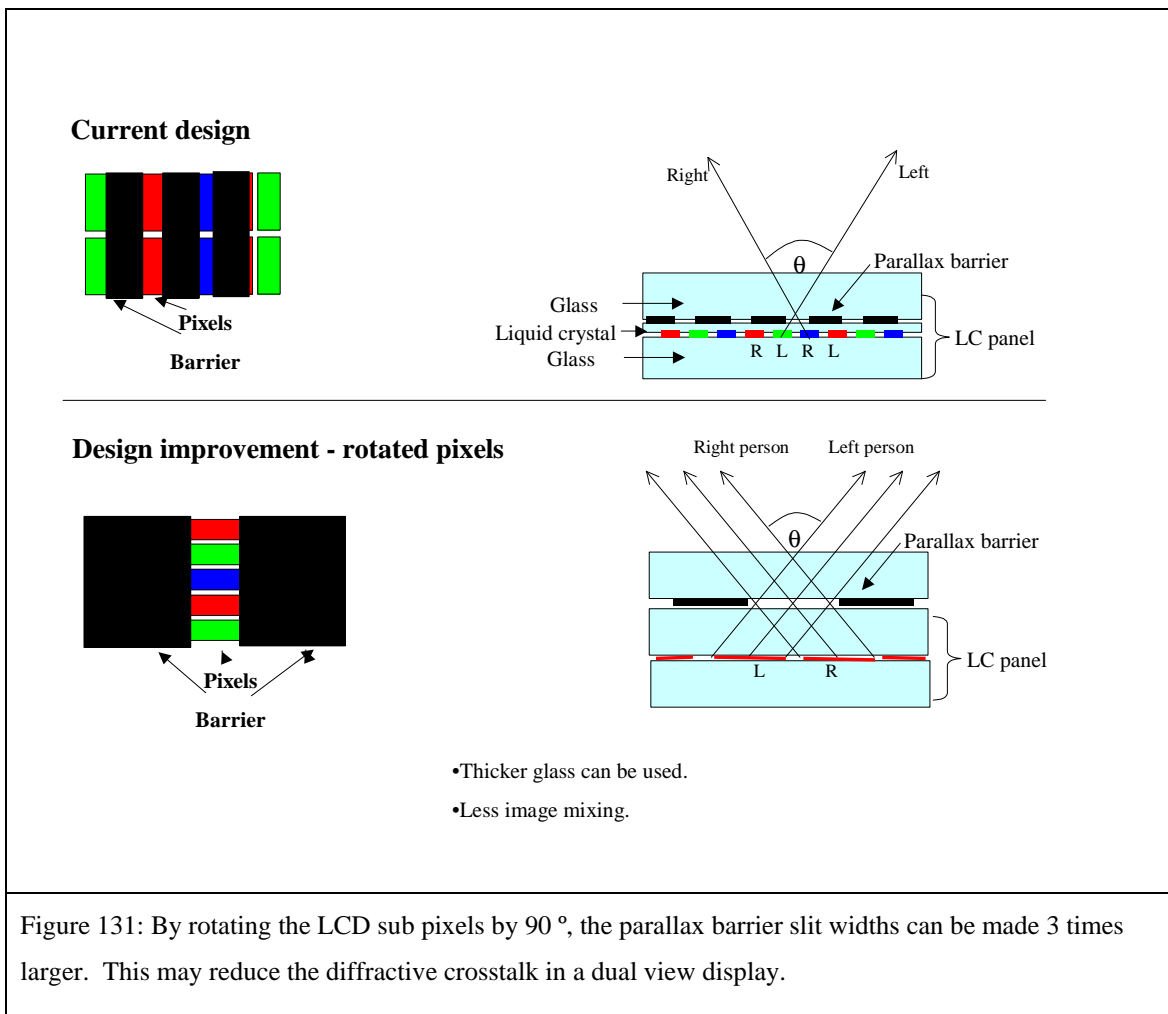
Results show that increasing the image separation of a dual view display decreases the crosstalk level. In addition the head freedom is increased for a wider angle of separation between images. This is consistent with geometric optical modelling of the dual view system, because light exiting the panel at high angles is refracted strongly due to the non-linearity of Snell's law.

In reality, increasing image separation is not a realistic option for reducing crosstalk in an automotive application, since the head freedom requirements are fixed by the positions of the driver and passenger. Increasing the image separation would increase the angular range of image mixing seen when viewing the display on axis, and so the head freedom requirements would not be met.

#### 4.2.2.4 Rotated pixels

The amount of diffraction from the parallax barrier would be expected to depend on the size of the parallax barrier aperture: the wider the slit the less diffraction should occur.

It is possible to create a dual view display which has a wider slit aperture by rotating the pixel apertures, as shown in Figure 131.



It is difficult to test the design of Figure 131 because by rotating the LCD panel, the angular intensity characteristics of the twisted nematic liquid crystal mode change considerably, and are likely to distort the result. To test the design properly would require a new TFT LCD panel to be made with the pixel apertures rotated but without changing the orientation of the LC and associated polarisers and so on. This option was too expensive to consider.

An experiment was carried out in which the LCD panel was replaced with a black and white mask, replicating the apertures of the LCD panel. A parallax optic was added to this mask to create a dual view test panel. ‘Test panels’ were made for the current and rotated designs of Figure 121 (the new pixel design). The crosstalk characteristics are shown in the figure below.

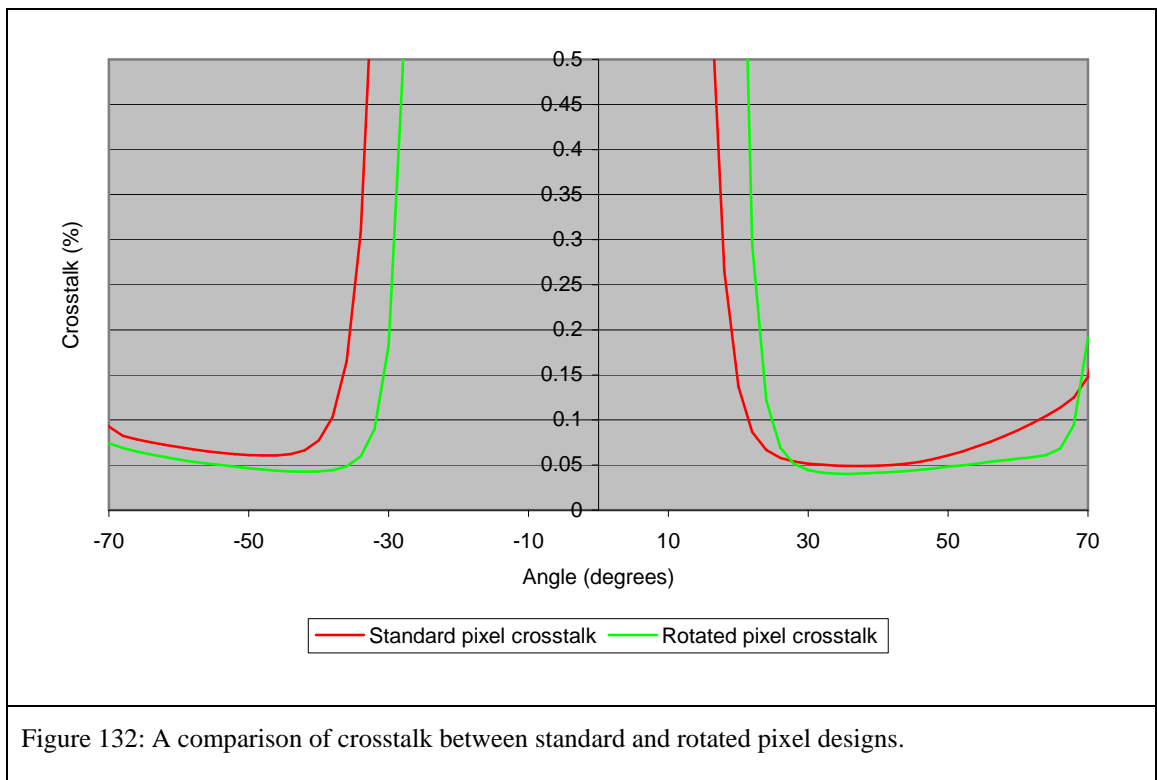


Figure 132: A comparison of crosstalk between standard and rotated pixel designs.

It is interesting that the pixel mask only produces 0.06% crosstalk, when previous experiments predict 0.1% from diffraction. I suggest two possibilities for this.

- The pixel masks do not contain black areas where the TFTs and capacitor lines would be on a real pixel. These features may increase the diffraction in a real panel.
- The difference seen could be due to construction error. For example, the image separation in this experiment is greater than in a standard dual view panel, which may account for the lower crosstalk.

The result shows that wider slit apertures do decrease crosstalk from 0.06% to 0.04%. Unfortunately this is not a hugely significant result and does not justify the cost of redesigning a panel to use rotated pixels.

#### 4.2.2 Reducing crosstalk from the polariser

The polariser and view film that cause crosstalk by scattering are not scattering by design. Polarisers of different scattering levels are available because they can help to prevent bright specular reflection from the display. The polarisers used on the dual view panel have the minimum scatter levels available. This implies that reducing scatter further may be difficult.

A simpler alternative method of reducing crosstalk by polariser scattering was demonstrated. This idea may be a workable remedy or, if not, it should demonstrate the impact that low scatter polarisers could have on crosstalk and encourage development of scatter free polarisers.

The idea to reduce crosstalk from the polariser was to space the polariser away from the display by 5 mm. This does not stop the polariser from scattering but image that is scattered to the other view becomes blurred and diffuse. When the polariser is placed 5 mm from the panel, the scattering from the passenger view increases the intensity at the drivers view, but no crosstalk image can be seen because the light from the passenger view is spread out evenly across the polariser.

By using this technique, the entire contribution of polariser scatter to the crosstalk image is removed. We believe this because as the polariser is moved from a position close to the panel to a position 5 mm from the panel the crosstalk from the polariser can be seen to blur increasingly to such an extent that no recognizable image is formed. Crosstalk by polariser scatter then only contributes to a small reduction in contrast ratio of the images.

An alternative remedy might be to use a polariser that is internal to the liquid crystal cell [53]. If the polariser were placed here, before the parallax barrier, then polariser scattering would have no effect on crosstalk. This is because the parallax barrier would block any polariser scatter. Such 'internal polarisers' are in development, but do not have sufficient performance to be used in a product as yet.

### **4.3 Summary of solutions**

This section summarises all the solutions to crosstalk proposed in section 4.

*Methods to reduce electrical crosstalk*

<b>Method</b>	<b>Comment</b>
Crosstalk correction	<p>Pros:</p> <ul style="list-style-type: none"> <li>• Successfully reduces the visibility of electrical crosstalk .</li> </ul> <p>Cons:</p> <ul style="list-style-type: none"> <li>• The extra electronics required adds cost.</li> </ul>
Re-design of TFT layout	<p><b>Best solution</b></p> <p>Pros:</p> <ul style="list-style-type: none"> <li>• Electrical crosstalk becomes almost invisible.</li> <li>• No extra electronics is needed for the panel.</li> </ul> <p>Cons:</p> <ul style="list-style-type: none"> <li>• Some capital investment is needed to re-design the panel.</li> </ul>

Table 24: A summary of methods to reduce electrical crosstalk.

*Methods to reduce optical crosstalk*

<b>Method</b>	<b>Comment</b>
Crosstalk correction	<p>Pros</p> <ul style="list-style-type: none"> <li>• Crosstalk can be eliminated for the main viewing positions.</li> </ul> <p>Cons</p> <ul style="list-style-type: none"> <li>• Crosstalk cannot be eliminated for all viewing angles.</li> <li>• Extra electronics is needed to perform the correction, adding cost to each display.</li> </ul>
Soft edge barrier	<p>Pros:</p> <ul style="list-style-type: none"> <li>• Diffractive crosstalk is reduced by about 50%.</li> </ul> <p>Cons:</p> <ul style="list-style-type: none"> <li>• The design is more complex to manufacture, which would add cost to the panel.</li> </ul>

Directional backlighting	<p>Pros</p> <ul style="list-style-type: none"> <li>• Crosstalk can be reduced by about one half.</li> <li>• The panel would look dark on axis, which is preferable over the current untidy mix of images.</li> </ul> <p>Cons</p> <ul style="list-style-type: none"> <li>• When the dual view panel is used as a single view panel (both images are set to display the same image), the panel would look dark on axis, which is not desirable. This makes the backlight design complex because the backlight must be switchable into a uniform mode for when the panel is in single view mode.</li> </ul>
Image separation angle	<p>Pros:</p> <ul style="list-style-type: none"> <li>• A slight crosstalk reduction (of about 20%) is achieved.</li> </ul> <p>Cons:</p> <ul style="list-style-type: none"> <li>• The image separation is substantially fixed by the driver and passenger positions, making the design impractical.</li> </ul>
Rotated pixels	<p>Pros</p> <ul style="list-style-type: none"> <li>• Crosstalk is reduced by an absolute value of 0.02%.</li> </ul> <p>Cons</p> <ul style="list-style-type: none"> <li>• The TFT layout would need redesigning. This is a significant task, which would increase the cost of the panel.</li> </ul>

Table 25: A summary of methods to reduce optical crosstalk.

The favoured ideas for reducing crosstalk are highlighted in green.

#### **4.4 Experimental demonstration of a low crosstalk dual view display**

We have seen from the previous work that the main sources of optical crosstalk are diffraction at the parallax barrier and scattering in the polariser and view films.

Therefore, if solutions that combat each of these causes are combined then a very low crosstalk dual view display should be produced. This should provide final evidence that

the suspected causes of crosstalk are correct. The resulting display did have a crosstalk level that was substantially invisible to the naked eye.

To reduce diffraction in the low crosstalk demonstration panel a soft edge barrier design was chosen. To reduce polariser scattering the method of spacing the polariser away from the LC display was chosen.

A dual view display was made with two regions. In region 1 the parallax barrier is hard edged, and the polariser is in its standard position close to the pixels. In region 2 the barrier is soft edged and the polariser is spaced away from the panel. In region 1 standard crosstalk of 0.18% is expected, in region 2 the diffraction (causing 60% of the crosstalk) should be reduced by 50% by the soft edge barrier, and the polariser scatter (causing 40% of the crosstalk) should be rendered invisible. Therefore we estimate that the panel should have only 0.05% crosstalk remaining. Unfortunately the effective crosstalk level of 0.05% cannot be measured since the spaced off polariser still scatters light to the detector used in the crosstalk measurement. The detector does not distinguish between light that contributes to the crosstalk image and light that is scattered uniformly from the polariser. However from section 3 a level of 0.05% is known to be substantially invisible, so that substantially invisible crosstalk from region 2 will mark a good result.

The test images viewed on this panel consisted of a pure black image to the left, and maximum intensity white text on a black background to the right. This configuration will produce the maximum possible visibility of optical crosstalk and is known not to suffer from electrical crosstalk.

The panel was examined. Crosstalk is quite clearly visible on region 1, and substantially invisible in region 2. This is further proof that crosstalk is caused by diffraction and polariser scatter.

## 5.0 Summary

The **world's first dual view display** based on sub 100  $\mu\text{m}$  pixel – barrier separation was produced. It was seen to have some crosstalk, such that the driver can see a ghost image of the passenger image, which is a possible distraction hazard, and makes the display appear of lower quality.

The causes of this crosstalk were analysed and quantified.

Crosstalk from the dual view optics was shown to consist of;

<i>Crosstalk source</i>	<i>Contribution to the total crosstalk in a the dual view system</i>
Diffraction	~60%
Polariser scattering	~40%
Barrier edge reflection	<1%
Barrier underside reflection	<5%
Barrier transmission	~0%
Barrier upper side scatter	~0%

Table 26: A summary the causes of crosstalk in a parallax barrier system and their magnitudes.

In addition, electrical crosstalk exists within the TFT electronics. This crosstalk depends on the image data that is applied to the panel.

Experimentation with the human visual system showed that crosstalk should be reduced by about 6 times, to make it invisible to the human eye.

Counter measures to crosstalk were developed to reduce the crosstalk.

Optical crosstalk could be reduced by;

Software compensation (for one viewing position only)

Apodised barrier slits (which reduce diffractive crosstalk by about 50%).

Modifying the illumination profile of the backlight (which reduced crosstalk by about 30%).

- Changing the LCD pixel configuration to allow the use of wider less diffractive slits (reduced diffraction by about 30%).
- Increasing the angular separation between left and right images.
- Spacing the polariser away from the display such that the polariser does not create a legible scattered image (reducing crosstalk by about 40%).

Electrical crosstalk could be reduced by;

- Software compensation (which works for all viewing positions).
- Modification to the panel electronics (reducing electrical crosstalk by about 8 times).

Some of these counter measures were used in Sharp's dual view LCD product which was launched in July 2005.

# **CHAPTER 4: A MICROLENS DUAL VIEW SYSTEM**

# Introduction

In chapter 2 a two lens dual view system was developed that allows the use of standard thickness glass, and has good brightness and head freedom.

As described in chapter 3 a dual view system based on thin glass was developed. It has poor brightness and head freedom, but crosstalk is 0.18% compared with  $> 1.5\%$  for the two lens system. Advances in manufacture techniques allowed thin glass displays to be produced with sufficient yield. So, the (eventual) simplicity of manufacture and low crosstalk meant the thin glass system now supersedes the thick glass system.

However the thin glass system has the major problem of low brightness. This chapter shows the development of an idea to increase the brightness using a combination of lenticular lenses and a parallax barrier.

The chapter breaks down into the following sections.

Section 1 provides an explanation of the design. Geometric optics is used to review possible simplifications and enhancements to the design but no substantial improvement is found.

The design is prototyped (section 2) so that factors such as crosstalk that are hard to predict can be assessed experimentally. The prototype demonstrates that this new lens design can produce dual view with 26% wider head freedom and lower crosstalk than a parallax barrier. The brightness data from this first prototype is invalid since the lenses are made from an absorbing material.

In section 3 a computer algorithm is developed to choose the best design parameters in the system to achieve the best head freedom and brightness. This program is used each time a new dual view panel is designed. The algorithm is accurate enough (predicting the angular brightness distribution of the panel with an  $r^2$  value of 0.987), yet is simple enough to produce results in less than 1 day. Crosstalk levels are not predicted.

Section 4 considers ways that clear micro-lenses could be produced. A second dual view prototype is made with clear micro-lenses and this demonstrates dual view with a brightness that is 1.7 times greater than a parallax barrier system.

The new combination of micro-lenses and a parallax barrier could be used to enhance the 3D and privacy displays mentioned in chapter 1. This is described in section 5.

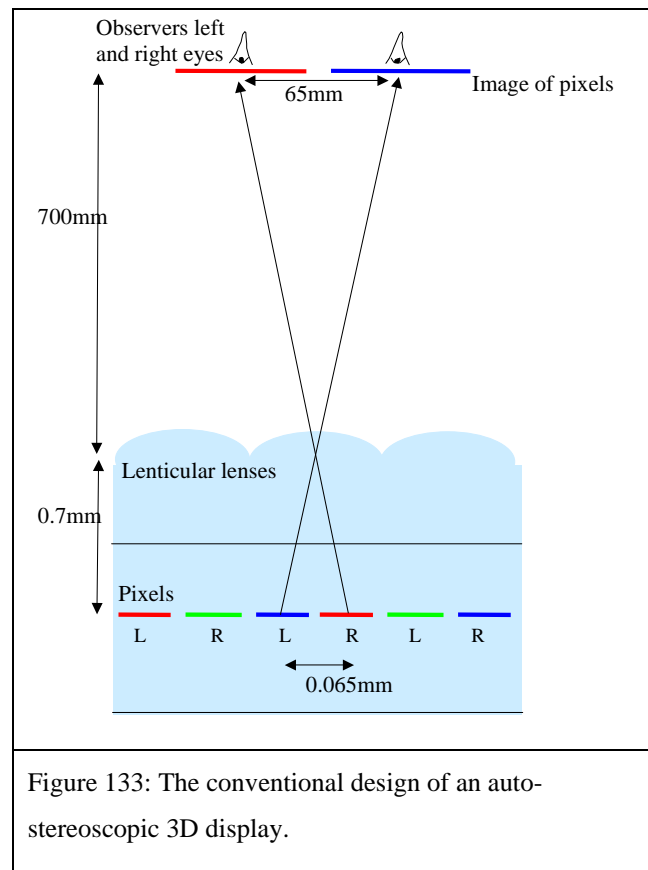
In section 6 the key points of this chapter are summarised.

# 1. Development of the idea

It has long been known in the field of stereoscopic 3D displays that the parallax barrier design is inefficient and absorbs a lot of light. The use of lenticular lenses is a well known solution to this problem. This section describes this known 3D technology and explains why it does not work for dual view displays. An equivalent lens design that is suitable for dual view displays is proposed and shown to work theoretically by ray tracing simulations. Finally some effort is made to improve on this design further but no significant improvement is found.

## 1.1 How a 3D lenticular system works

Figure 133 shows a conventional 3D system using lenticular lenses.

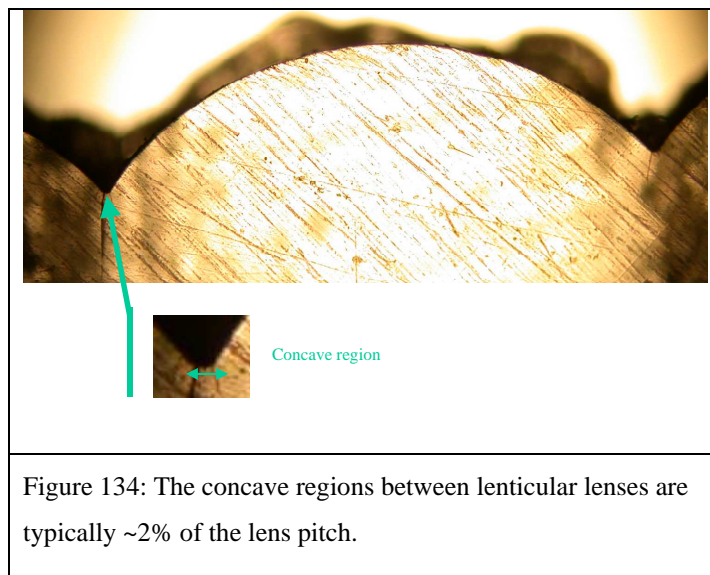


The lenses over the pixels image the pixels to a distance of approx 700mm where the observer is. As shown in the diagram, light from the left pixels is directed into the observers left eye, and vice versa.

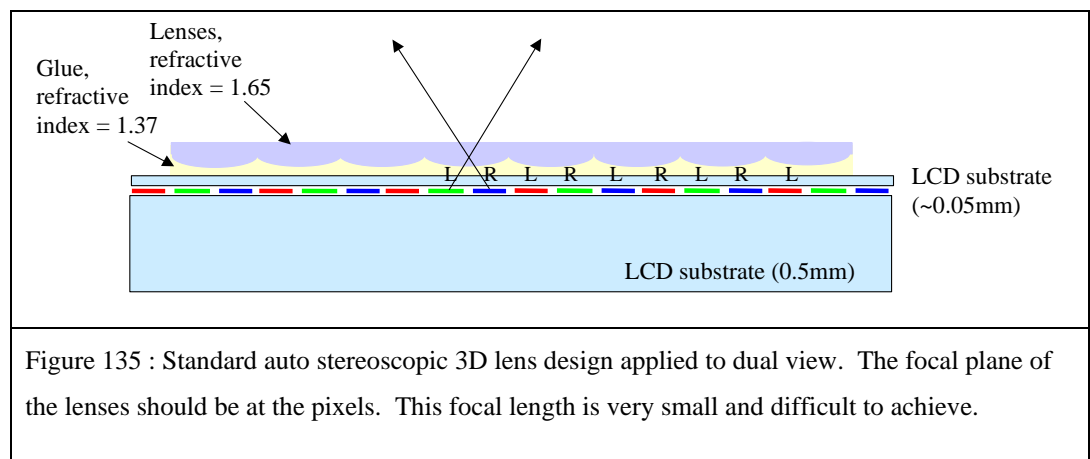
To achieve this the focal length must be  $\sim 0.7$  mm, (so that the focal length of the lens is approximately at the plane of the pixels).

## 1.2 Why the 3D lenticular system does not work for dual view

a). In a lens array, there are typically small round regions between each of the lenses. This is shown in Figure 134. These regions spread the light in all directions causing crosstalk. The width of the round regions is typically 2% of the lens pitch. We can make a rough estimate of the amount of crosstalk that this will cause. We can assume that 2% of the lens area scatters light in all directions, half of this will go to the left view, half of it will go to the right view. Therefore this will give approximately 1% crosstalk. This makes the production of a display with sub 0.4% crosstalk unrealistic for such a lenticular design.



b). In an example design (Figure 135), lens – pixel separation must be reduced to about  $80\ \mu\text{m}$  to give a large enough splitting angle between the left and right images. According to standard 3D lenticular design, the focal length of the lens should also be about  $80\ \mu\text{m}$ . This focal length is very short and it is very difficult to achieve.



Hemi-cylindrical lenses give the shortest focal length. For the 130  $\mu\text{m}$  pitch lenses of Figure 135, a hemi-cylindrical lens would have radius 65 $\mu\text{m}$ . Glue is needed between the lenses and very thin glass. The lowest refractive index glue on the market has refractive index 1.37 (custom made by Optical Polymer Research Inc.), and a typical lens material would have an index of up to 1.65 (e.g. Shipley “SPR” series photo-resist). The focal length of this lens is given by the equation [46]:

$$\text{focal length} = \text{lens radius} \times \frac{\text{glue refractive index}}{\text{lens refractive index} - \text{glue refractive index}}$$

$$\text{focal length} = 65 \times \frac{1.37}{1.65 - 1.37} \approx 320\mu\text{m}$$

That is to say, a hemi-cylindrical lens has a focal length that is by 4 times too long.

In addition, such a hemi-cylindrical lens is very thick, and it is not possible to get the lens centre close enough to the pixels to produce an image separation of 60° which is needed for an automotive dual view display.

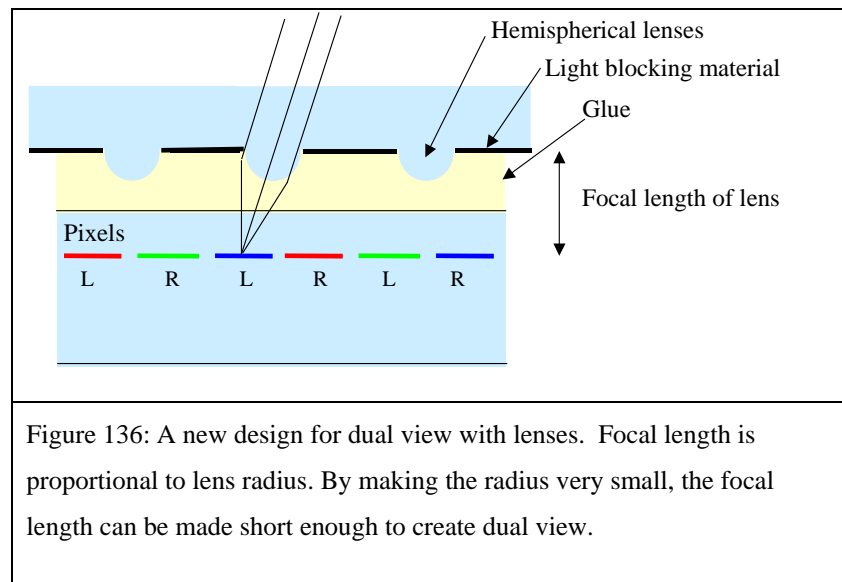
A system which does not use 1.37 index glue, but instead has an air gap of index 1.0 would help to reduce the focal length of the lenses but, as mentioned in chapter 1, this design would be mechanically unstable.

In summary the standard lenticular system used for 3D cannot be applied to dual view.

### **1.3 New lenticular design for dual view**

A standard lenticular system cannot work for dual view but, if a combination of lenses and a parallax barrier is used, a brightness improvement should be possible.

We can obtain a shorter focal length by making the lens smaller, Figure 136 . These smaller lenses can have a focal length short enough to image pixels to the observer.



The lens width is now less than the lens pitch, so that there are gaps between the lenses. These gaps must be filled with absorbing material so that light does not pass between the lenses to cause crosstalk.

Absorbing regions between the small lenses should remove the crosstalk problem associated with joins between lenses explained in section 1.2.

This design is not as efficient as the 3d system (since light falling between the lenses must be absorbed), however, the system should be more efficient than a parallax barrier. A parallax barrier relies solely on blocking rays travelling in the wrong direction. The lens and barrier system blocks some rays that travel in the wrong direction but others are bent from the wrong direction to the correct direction where they provide a useful brightness increase.

#### **1.4. What is the best lens- barrier design?**

Section 1.3 described the concept of the lens-barrier system and suggested that this system should be more efficient than a parallax barrier.

In this section the design is roughly optimised and simulated by optical ray tracing to quantify the improvement. A significant brightness enhancement of 1.7 times is predicted with an increase in head freedom as well.

Some effort is made to improve the design of the lens-barrier system further, for example by optimising the shape of the lens or adding reflective structures into the design. No significant improvement to the lens-barrier system could be found without significantly increasing the complexity of manufacture.

### 1.4.1 Cylindrical lenses and barrier

In order to quantify the brightness improvement that would be gained by the lens-barrier system sensible design parameters (focal length, and lens-pixel separation etc.) were chosen, and the performance of the system was compared with a parallax barrier by using optical ray tracing.

The design parameters are shown the table below with a brief explanation of why these values were chosen. The design parameters are presented diagrammatically in Figure 137.

<b>Design parameter</b>	<b>Value chosen</b>	<b>Comment/ reason for choice</b>
Pixel pitch	65 $\mu\text{m}$	These parameters are used in Sharp's dual view LCD panel.
Pixel aperture (horizontally)	44.5 $\mu\text{m}$	
Barrier-pixel separation	100 $\mu\text{m}$	Barrier- pixel separation controls the angle of separation between left and right images. This is explained in chapter 1 for the parallax barrier system. A cylindrical lens can be considered similar to a slit, in the same way that a pin-hole camera is similar to a camera with a simple lens. Therefore we will begin by placing the lens centre approximately in the same position as the slit.  A distance of $\sim 100 \mu\text{m}$ should give a good angular separation between the images.

Glue refractive index	1.37	The larger the lens radius the less barrier there will be to absorb light. So,
Lens refractive index	1.6	<p>Brightness <math>\propto</math> lens radius</p> <p>The focal length should be about equal to the pixel-barrier separation as described in Figure 136.</p> <p>Therefore a focal length of about 100 <math>\mu\text{m}</math> is needed.</p> <p>From the thin lens equations,</p> $\text{Focal length} \propto \frac{\text{lens radius}}{\text{lens to glue refractive index difference}}$ <p>So we can make a short 100 <math>\mu\text{m}</math> focal length by decreasing the lens radius (which reduces brightness) or increasing the refractive index difference between the lens and glue.</p> <p>Therefore to make the display as bright as possible we should use the highest refractive index difference we can. The 1.37 index glue is chosen as it is the lowest index glue known, and 1.6 is a typical index for a lens material.</p>
Lens radius	32.5 $\mu\text{m}$	Lens radius was chosen empirically so that a good dual view intensity profile was achieved in Figure 139.
Slit width	65 $\mu\text{m}$	The slit width is such that all the aperture of the lens is exposed for maximum brightness.

Table 27: A first iteration of the micro-lens dual view design.

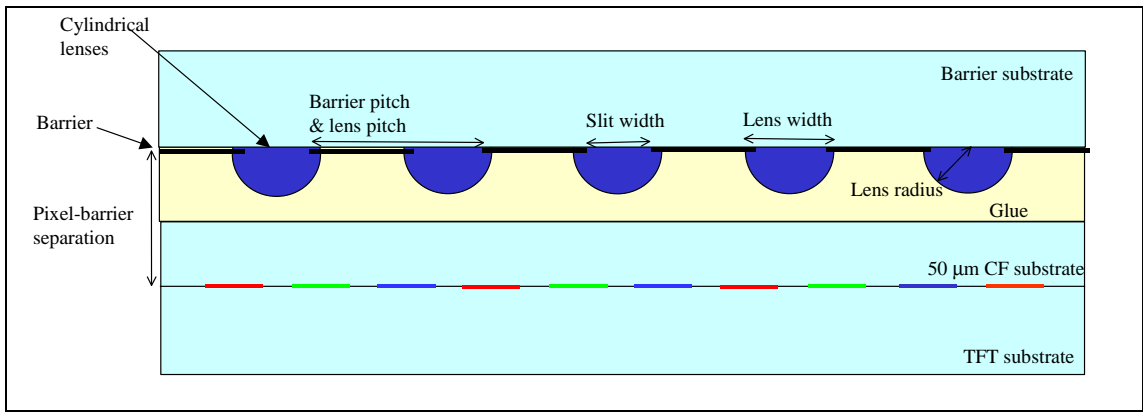


Figure 137: A cross sectional view of a novel lens-barrier dual view system. Various design parameters have been labelled on the diagram.

It was stated earlier in this text that the lenses on the barrier should have a focal length that is in the plane of the pixels. This is approximately correct but in fact a significant improvement can be achieved by de-focusing the system. This is explained in Figure 138.

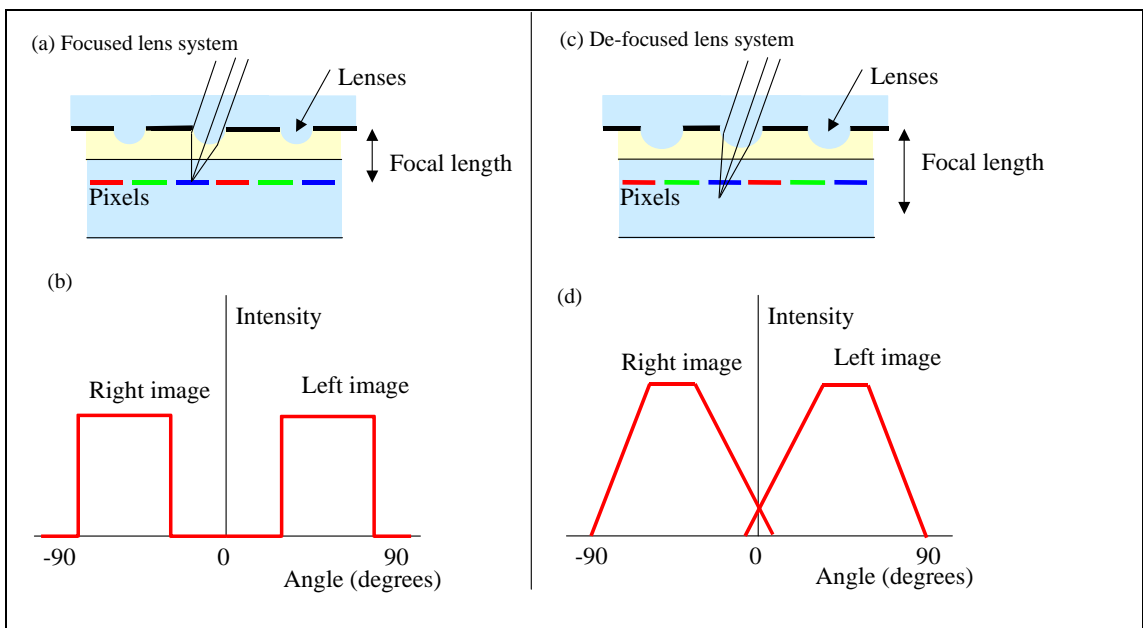


Figure 138: Previous sections have stated that the focal length of the lens should be at the pixels. In fact it is advantageous to defocus the lens from the pixels. (a) shows a system where the lenses focus on the pixels. (b) shows the intensity profile that an ideal lens would create. The pixels would be imaged to the left and right, and the black mask between the pixels would be imaged in the middle. A wide black region in the middle is not desirable. (c) shows a system where the lenses are larger. Firstly, these lenses have bigger apertures and so let more light pass. Secondly the pixels are defocused at the observer. This creates an intensity profile without a black central region.

In this first estimate of the design parameters for the lens-barrier system the lens radius was empirically chosen to be  $32.5 \mu\text{m}$ . This gives the lens a focal length of

approximately 160  $\mu\text{m}$  which is 1.6 times further away than the pixels are. This incorporates a de-focus into the design as described in Figure 138. The level of de-focus was chosen because it gives a sensible simulated angular intensity profile as shown in Figure 139.

Figure 139 is shown below. It shows the ray tracing simulation of the lens-barrier and parallax barrier systems.

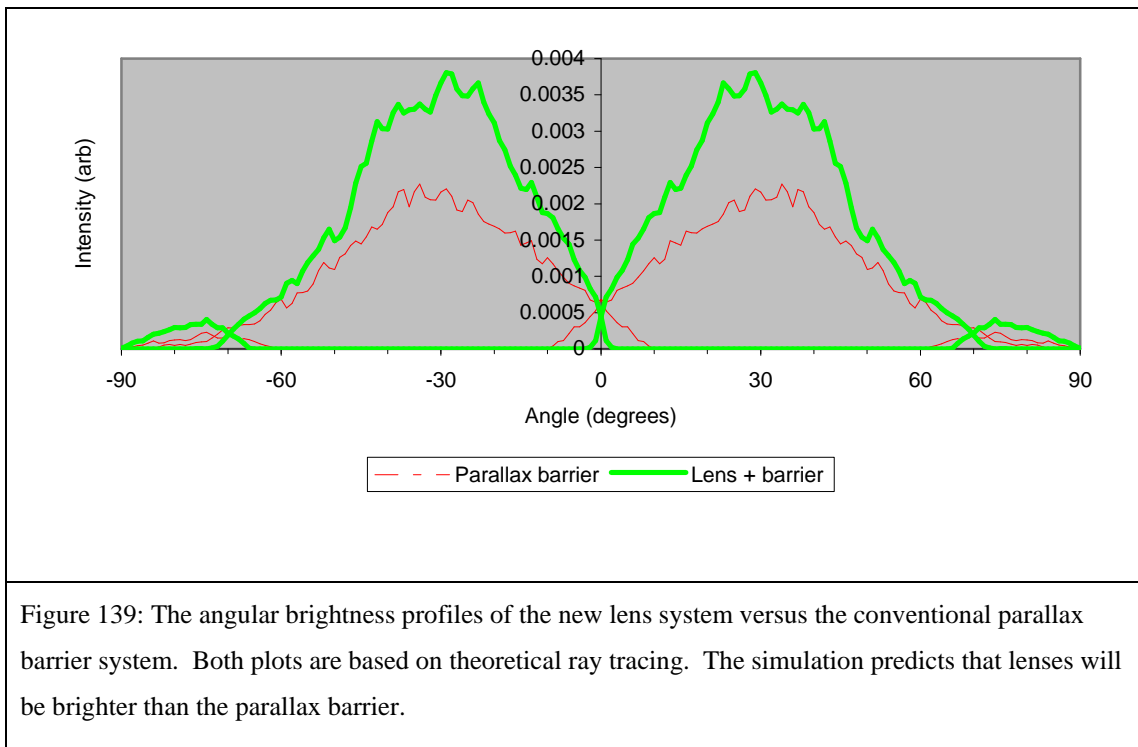


Figure 139: The angular brightness profiles of the new lens system versus the conventional parallax barrier system. Both plots are based on theoretical ray tracing. The simulation predicts that lenses will be brighter than the parallax barrier.

The lens-barrier system is 1.8 times brighter than the parallax barrier system at  $\pm 30^\circ$ . The head freedom of the lens-barrier system is from 3 to 65°, compared with 10 to 56 for the parallax barrier.

Therefore the lens-barrier system is predicted to be superior over the parallax-barrier system, however computer simulation can not accurately predict the lens-barrier crosstalk levels. The system will have to be tested experimentally to see if the lenses create too much crosstalk. The results of this testing are presented in section 2.

There is a significant amount of literature on 3D displays and some on dual view. However no literature was found to suggest that anyone else had considered the idea of combining micro-lenses with a parallax barrier. Perhaps this is because such a system is only needed when very high image separation is needed - for example in the automotive dual view application. Previous dual view posters and toys use a smaller image separation of about 30°.

The idea was patented in reference [17]. This patent looks set to give Sharp displays a significant advantage over its competitors.

### 1.4.2 Prisms + barrier

Until now designs have been attempting to image pixels to the observer. There is actually no need for the optics to image the pixels. To create dual view (or 3D) we only need to bend light anywhere within the correct direction. I.e. light from the left pixels needs only to be bent into the left direction anywhere between 0 to 90 °.

Lenses are tricky to make, prisms are much easier to make, they can be made from photo-resist lithographically under the right processing conditions.

This section investigates if prisms can produce a better dual view system than the lenses, and if they can not how much worse are they and does the ease of manufacture justify their use?

Figure 140 shows how the prisms can be used not to image pixels, but to bend light in the right directions to create dual view.

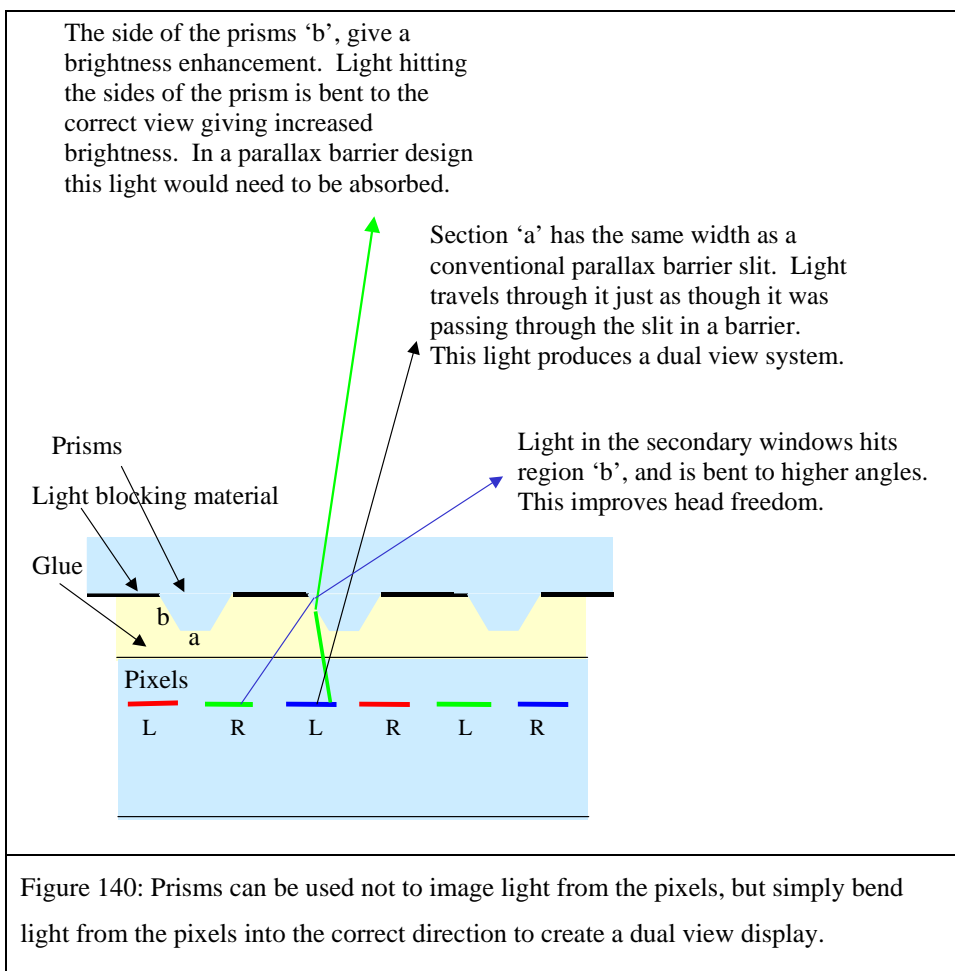
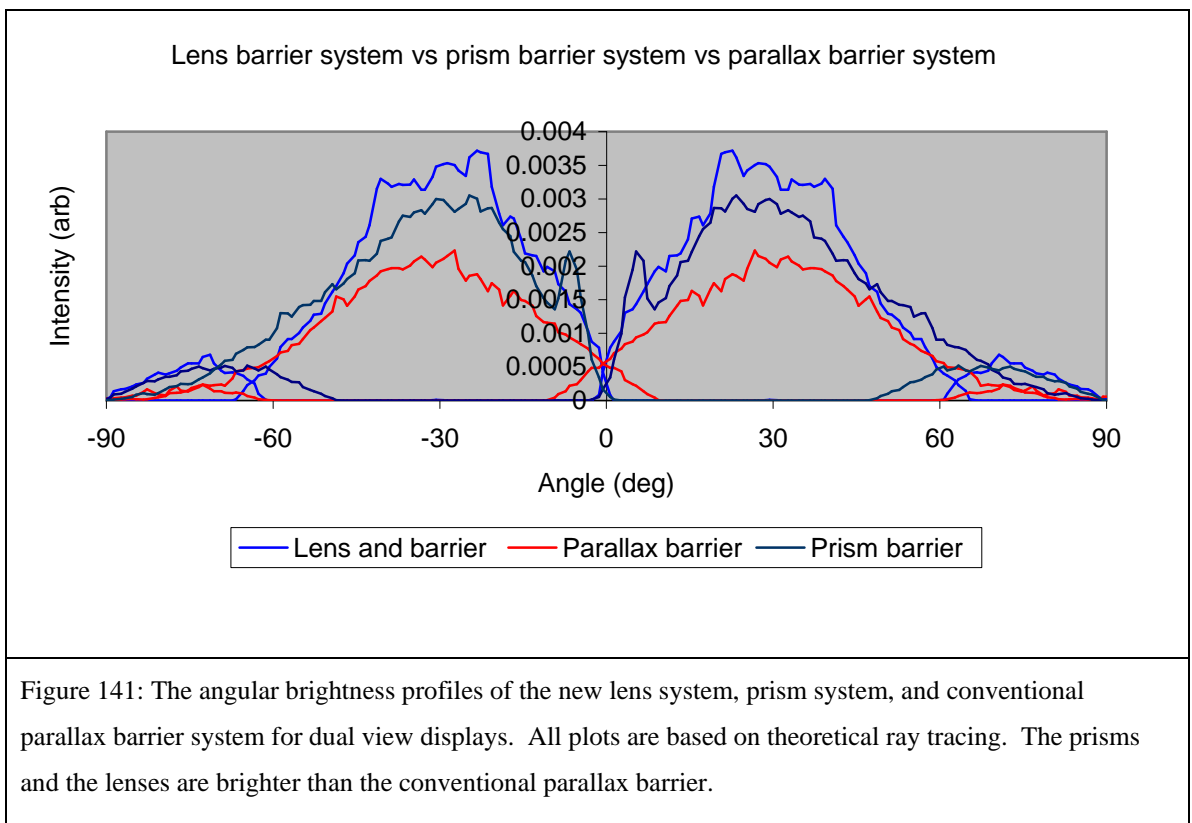


Figure 140: Prisms can be used not to image light from the pixels, but simply bend light from the pixels into the correct direction to create a dual view display.

Figure 141 below is a computer simulation of the intensity profiles created by the prisms compared with the lens- barrier and parallax barrier simulations.



The prism system is ~1.4 times brighter than the parallax barrier system at  $\pm 30^\circ$  and the head freedom is from  $3^\circ$  to  $48^\circ$ . The prism system is theoretically superior to the parallax barrier but the prisms are not as good as the lenses.

Lenses are better than prisms but are lenses the best shape? Figure 142 shows some reasons why a lens is not the perfect optic for a dual view display.

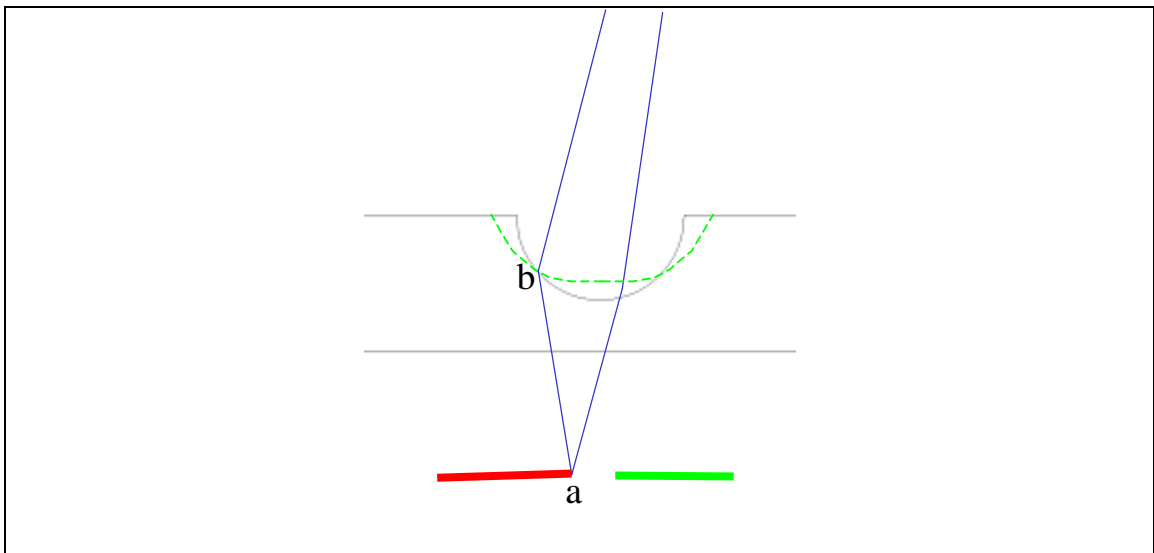


Figure 142: Lens shapes function better than prisms for dual view, but are lenses the best possible shape? The diagram shows rays of light from point a of the pixel passing through the lens.

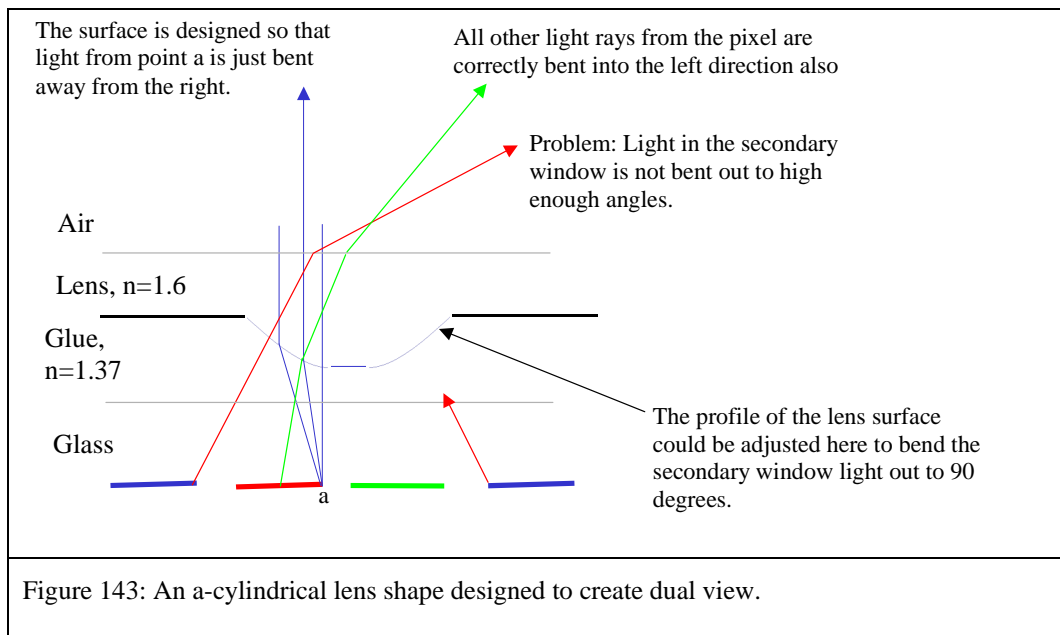
It can be seen that for point a the lens is not the best shape of refractive surface.

- At point b the gradient of the surface is unnecessarily steep. Light hitting point b is bent more than necessary (it only needs to be bent so that it does not head towards the right viewer).
- A lens with a steep gradient comes to an end (meets the barrier at 90 °) with a smaller aperture than a lens with a shallower gradient. Therefore it will have a lower light through put as more light is absorbed by the barrier. Therefore I suggest that the ideal surface would be as shallow as possible. An example is given by the dotted line. The dotted line is better because it has a wider aperture (will give brighter dual view).
- So long as the rays are bent away from the right, dual view is created.
- If light from point a is bent enough, then light from all the pixel will be bent enough, since light from point a needs bending the most.

Figure 10 describes a hypothesis that sounds plausible but it is difficult to be sure that it is correct. It is supposed that the hypothesis is correct in section 1.4.3, and the best design based on this theory is calculated analytically. The design is simulated by ray tracing and compared with a cylindrical lens system. We will see for sure if the new design out performs the cylindrical lens design.

### 1.4.3 A custom lens shape for dual view

Figure 143 shows the shape of the refractive surface that gives the shallowest and widest structure possible as specified in Figure 142. All light is bent in the correct direction.



It can be seen from inspection that the design will work well to create a sharp image transition between the left and right images on axis since light from the red pixel in Figure 143 can be directed on axis but never over into the left view. According to the hypothesis the light throughput should be high, however, the system is spoiled because the secondary windows are not bent out to high enough angles.

The secondary windows need to be taken into account during the design. The design of the refracting surface was changed so that it bends the secondary windows out to higher angles. Figure 144 shows the new design principles that were used to create a better refractive surface.

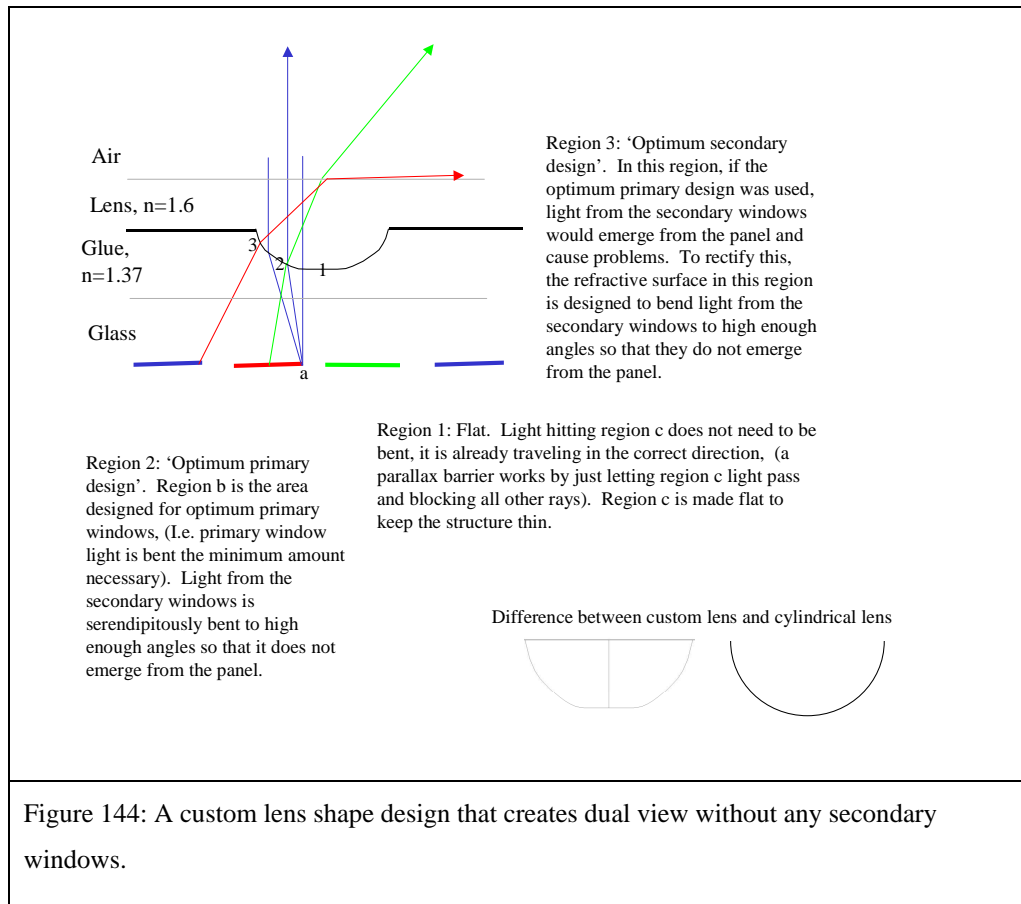


Figure 144: A custom lens shape design that creates dual view without any secondary windows.

The graph below shows computer simulated intensity profiles given by the custom lens shape, and a cylindrical lens shape.

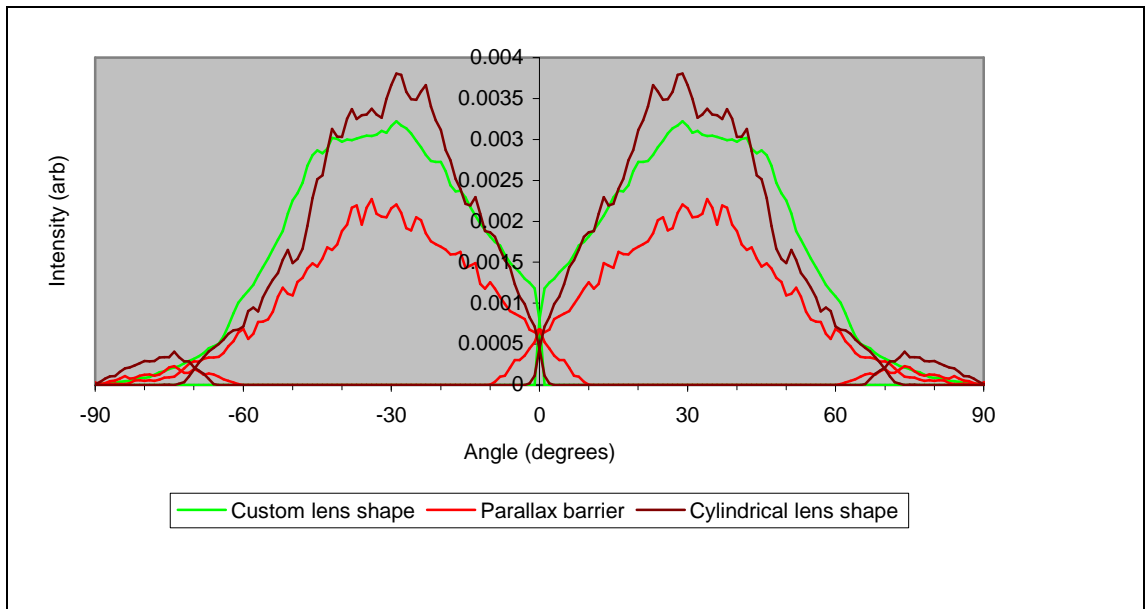


Figure 145: Theoretical predictions of the performance of a custom lens shape versus a cylindrical lens shape and parallax barrier. The custom lens shape has a sharp image transition between left and right views, and no secondary windows.

According to the ray tracing simulation the custom lens design successfully produces a dual view display and it produces viewing windows with interesting intensity profiles.

The image transition between the left and right view is very sharp. If a cylindrical lens shape was used to achieve this the on-axis brightness would drop to zero which may not be desirable if the display is to be viewed as a normal single view panel some of the time. With the custom lens shape the brightness remains reasonably high across the transition from left to right view.

The custom lens shape has virtually perfect viewing freedom. The viewing freedom ranges from 0 to 90 °.

The table below compares the performance of the custom lens shape with a cylindrical lens.

	<b>Custom lens shape</b>	<b>Cylindrical lens shape</b>	<b>Comment</b>
Aperture	63um	59um	The aperture of the custom lens is larger than that of the cylindrical lens, and it produces a greater range of head freedom.
Head freedom	1 to 90 °	2 to 67 °	
Brightness at 30 °	0.0031 (arbitrary units)	0.0035 (arbitrary units)	The cylindrical lens system puts a lot of light to +30 °, whilst the custom lens system spreads the light out from 0 to 90 ° resulting in less brightness at 30 °.
Useful light output	0.148 (arbitrary units)	0.142 (arbitrary units)	Useful light is defined as light within the head freedom limits of the lens system, e.g. 2 to 67 for the cylindrical lens.  Using this measurement criteria, the custom lens shape is slightly more efficient than the cylindrical lens.
On axis brightness	~0.0020 (arbitrary units)	0.0012 (arbitrary units)	Cylindrical lenses suffer a large brightness drop between the views. In single view mode (when left image = right image) this is undesirable because the display becomes very dim on axis.  The custom lens shape has no significant brightness drop on axis.

Table 28: The performances of cylindrical and custom designed lens shapes in a dual view system.

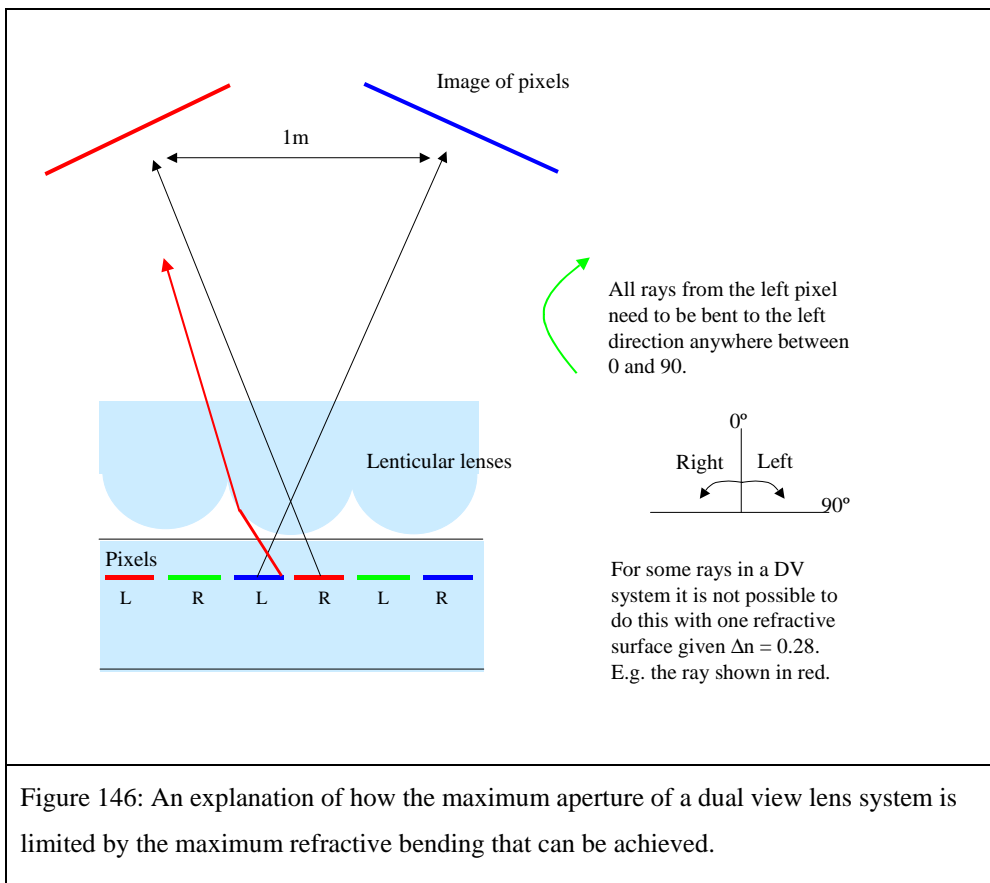
### *A summary of the custom lens design*

A custom lens shape has been designed that gives advantages over a cylindrical lens. What has been done is similar to aberration correction by aspheric lens design, however correcting for aberrations such as spherical, coma etc. is normally done to help all points on an object be imaged tightly. The lens has been adjusted to work well for 1 point on the pixel, knowing that all other points will be bent, not to a tight image point, but in the right direction. The image has been deliberately distorted. The secondary window is stretched out to higher angles than by an imaging lens.

This design produces a dual view display with a good angular brightness profile, good head freedom and a small increase in the efficiency over a cylindrical lens. However the difference between the shape of the custom lens and the cylindrical lens is small and the improvements are slight. The benefits of the custom lens shape do not justify any significant efforts that may be required to make the complex shape.

#### **1.4.4 Further possible improvements to the lens system**

The previous section considered whether or not the shape of the lens could be improved for dual view. In this section we consider alternative modifications to the lens system which could improve the brightness further. Figure 146 shows that a single refractive surface (such as a hemi-cylindrical lens) can not provide full brightness dual view.



In Figure 146 even if the ray shown in red hits the lens at grazing incidence it is not bent far enough to direct it to the correct view. It is not possible for one refractive surface to redirect this ray to the correct direction.

Three solutions to this problem were considered. Firstly, two refractive interfaces could be used to bend the ray further. Secondly a reflective surface could be used. Thirdly the ray could be blocked to prevent it causing crosstalk.

The third solution is used in the lens-barrier design but the absorption causes loss of light and so reduced efficiency. The first and second solutions could potentially give a brightness improvement.

Figure 147 shows sketches of designs which incorporate solutions 1 and 2. These ideas were investigated but neither looked like a promising and practical design.

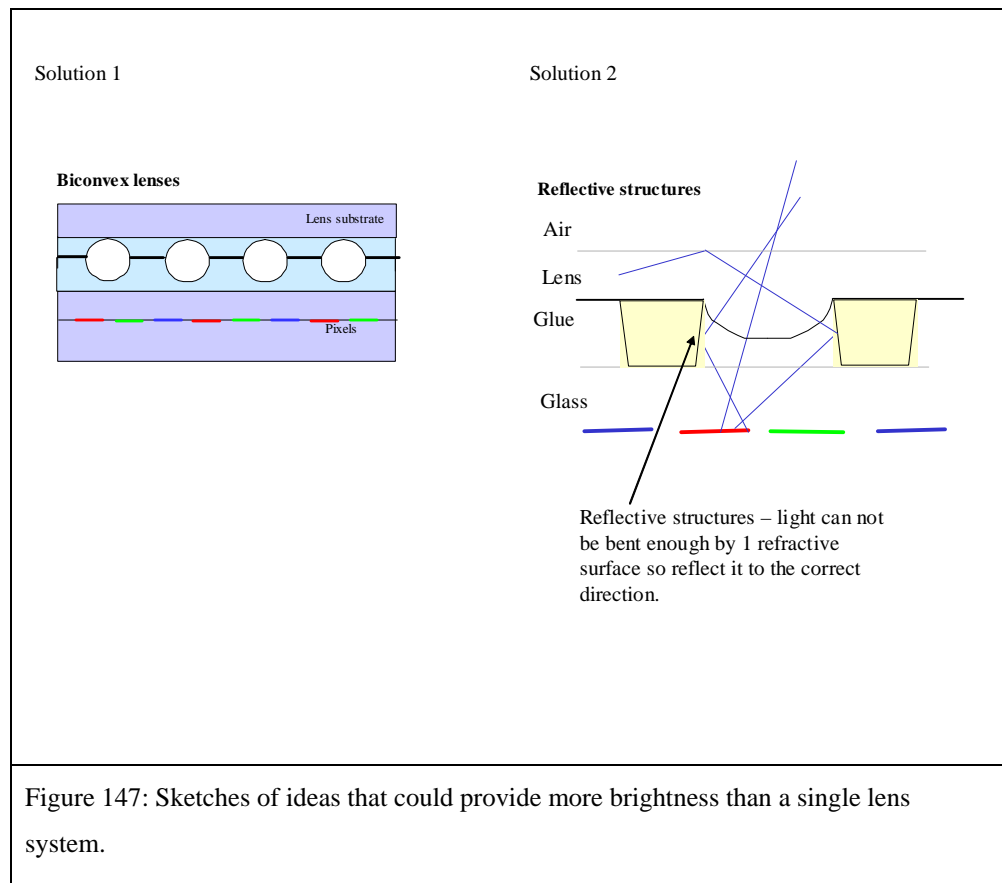


Figure 147: Sketches of ideas that could provide more brightness than a single lens system.

Solution 1 could theoretically produce a dual view system with higher brightness than the planar convex system originally proposed, however it would be harder to manufacture. If a simple manufacturing technique could be found for this design then it would be worthwhile to make it. However this is not considered any further in this thesis.

Solution 2 was investigated but it was found that the reflective structures could only increase the useful light output of the system by a small amount. This design would also be quite complicated to manufacture.

## **1.5 Summary of theoretical parallax optic designs**

In this section several designs were considered that might have improved the performance of the originally proposed lens-barrier system. The predicted brightness and head freedom for each design is summarised in the following table.

Design	Brightness at 30° (arbitrary units)	Head freedom
Single view panel	0.0052	-
Parallax barrier	0.0020	10 to 56°
Hemi-cylindrical lens	0.0035	2 to 67°
Prism	0.0028	3 to 48°
Custom lens	0.0031	1 to 90°

Table 29: A comparison of dual view systems based on different micro-optic lens shapes.

The parallax barrier reduces brightness of panel at 30° by more than half. All other systems improve on this but hemi-cylindrical lens-barrier system gives the most brightness at 30° (a 1.75 times improvement over the parallax barrier). The angular head freedom is also predicted to be improved by 1.4 times.

The custom lens gives good head freedom but it would be complicated to make such a shape. The prism system does not perform particularly well.

Of all of these systems the hemi-cylindrical lenses look to have the best compromise between performance and simplicity of manufacture. This is the design that was chosen to be prototyped and tested experimentally in the next section.

## 2. Experimental testing of the device

Section 1 showed that the proposed dual view lens-barrier system performs well theoretically. This theory is based on geometrical optics that ignores many subtle effects that could degrade the display. These effects might include crosstalk from diffraction, and the interplay between the lenses and LCD viewing films. The simulations assume that these effects are negligible.

In this section, the device is prototyped and tested. The assumptions are found to be substantially correct since the display performs well without significant crosstalk or degradation to the contrast ratio.

The micro-lenses were made by melting blocks of photo-resist. The material used in this process is not suitable for the final device because it is somewhat absorbing to visible light. However the resulting prototype could be used to test the new lens-barrier system.

The results show that crosstalk is not a problem in the system. The head freedom is increased over the parallax barrier system as predicted. The brightness of the new device was the same as the parallax barrier but this was expected since the lens material used in this prototype absorbs light heavily. The results imply that if the lens material was clear then the display would be much brighter than the parallax barrier system.

In summary the initial prototyping of the device showed that the new device has potential to significantly outperform a parallax barrier dual view system if the lenses were made from clear material. The testing did not show any major problems with the system.

## **2.1 Why test the device?**

Testing the lenses experimentally will allow us to test things that are not easy to predict by theory. For example;

1. Will the lenses diffract heavily and cause too much crosstalk?
2. Will the bending of the light by the lenses interfere with the viewing angle of the LCD?
3. Will variations between the modelled cylindrical lenses and actual imperfectly manufactured lenses create too much crosstalk, or is the design tolerant enough to withstand such errors?
4. Will polarisation sensitive Fresnel reflections in the system cause the intensity of the pixels to change with viewing angle?
5. Will unforeseen effects cause problems?

The problem associated with point 2 is described in more detail in Figure 148.

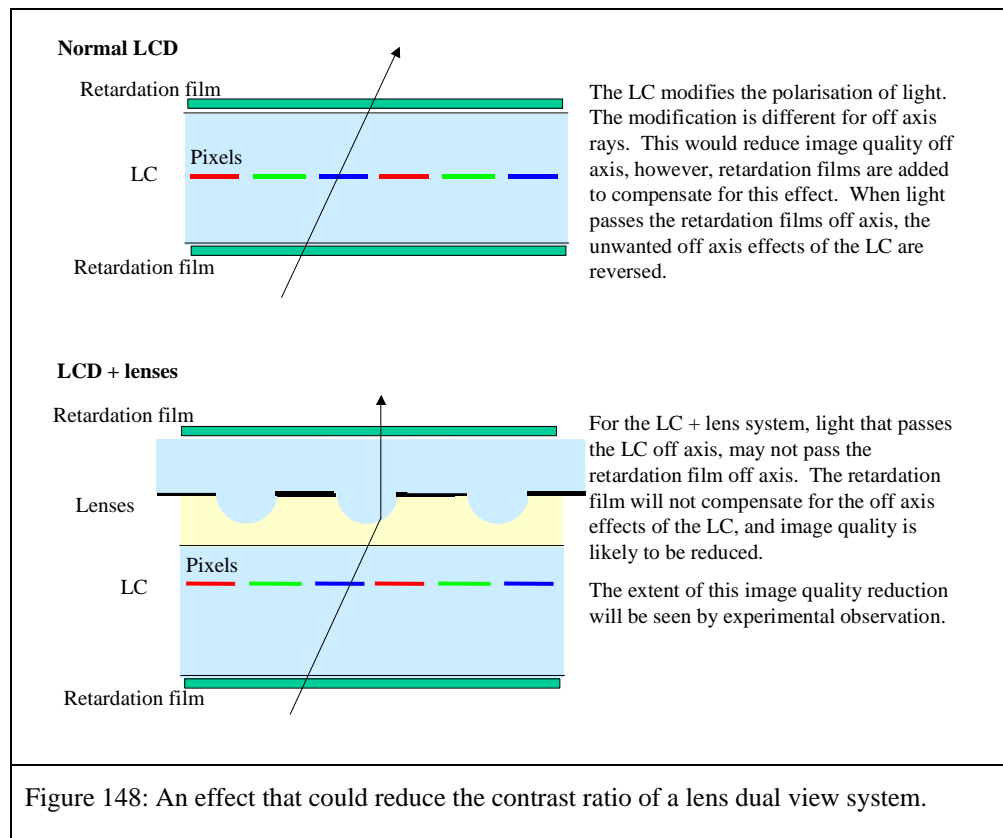
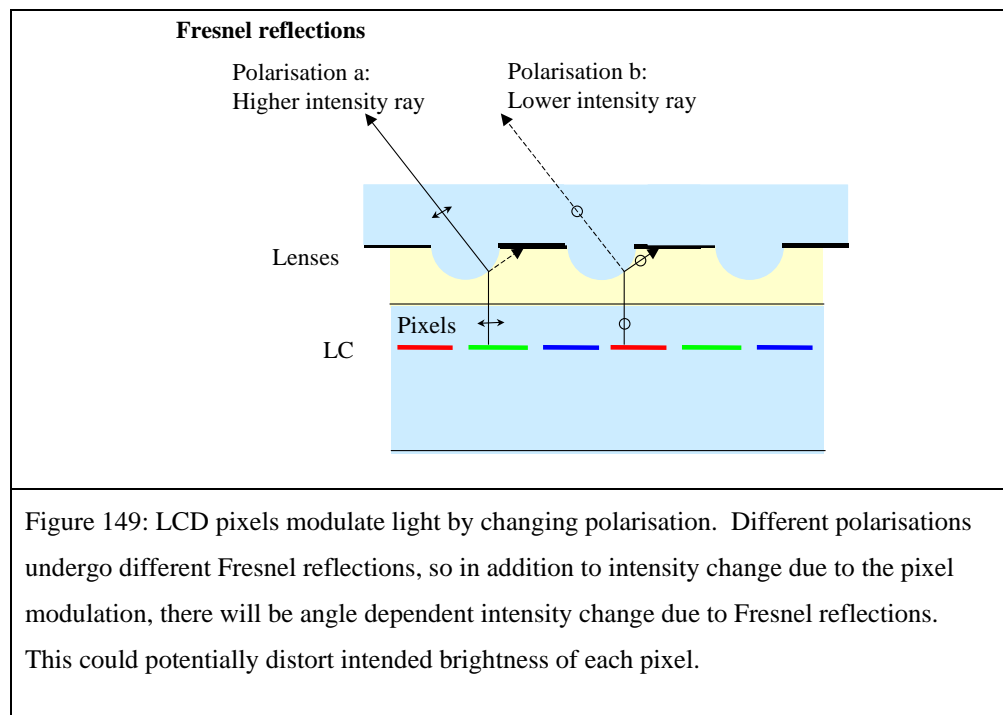


Figure 148: An effect that could reduce the contrast ratio of a lens dual view system.

The problem associated with point 4 is described in more detail Figure 149.



All of the points listed will be easy to assess by examination of a prototype device.

## **2.2 How to make the lenses**

The most common method of making micro lenses is embossing. However, there are disadvantages to prototyping using this method.

Firstly, embossing is expensive for prototyping due to the cost of the master stamp that is used to emboss the lens shape into plastic. The master is usually made by carving the desired shape into a metal by use of a fine diamond point. A typical cost for this is £10,000.

Secondly, embossed plastic lenses are likely to have thermal expansion problems. The glass of the LCD expands much less than the plastic. If the LCD and lenses are assembled and aligned at 25°C, at 50°C polycarbonate lenses will be 200 µm longer than the 156 mm LCD panel [54]. That is to say, at the edge of the panel the lenses could shift 100 µm (about 2 pixels) with respect to the pixels, which would cause unacceptable degradation of the dual view effect. This calculation assumes that the LCD glass and lenses are allowed to expand freely. In practice the lenses are adhered to the glass so that the glass may hold the lenses at the correct size by holding them under strain. Alternatively the lenses may break away from the glass due to this stress.

The embossing technique is expensive and is not guaranteed to work due to the possibility of thermal expansion causing problems.

For prototyping I decided to use micro-lens technology pioneered by Popovic et al in 1988 [55,56]. These lenses are made by melting blocks of resist. This method allows cheap prototyping, and more importantly, there is potential to develop it into a cheap mass manufacture process.

### **2.2.1 Prototyping by photo-resist micro-lenses**

Figure 150 shows how the lenses were made and gives an idea of how they perform.

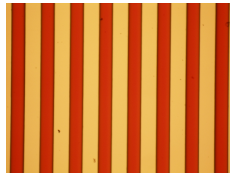
### Making lenses by melting photo-resist blocks



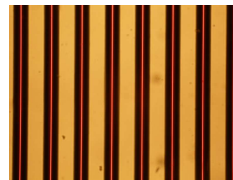
a). Photo-resist blocks made by standard wet lithography processing



b). Resist blocks after melting. The blocks have melted to form lenticular micro-lenses.



c). Top view of resist micro-lenses



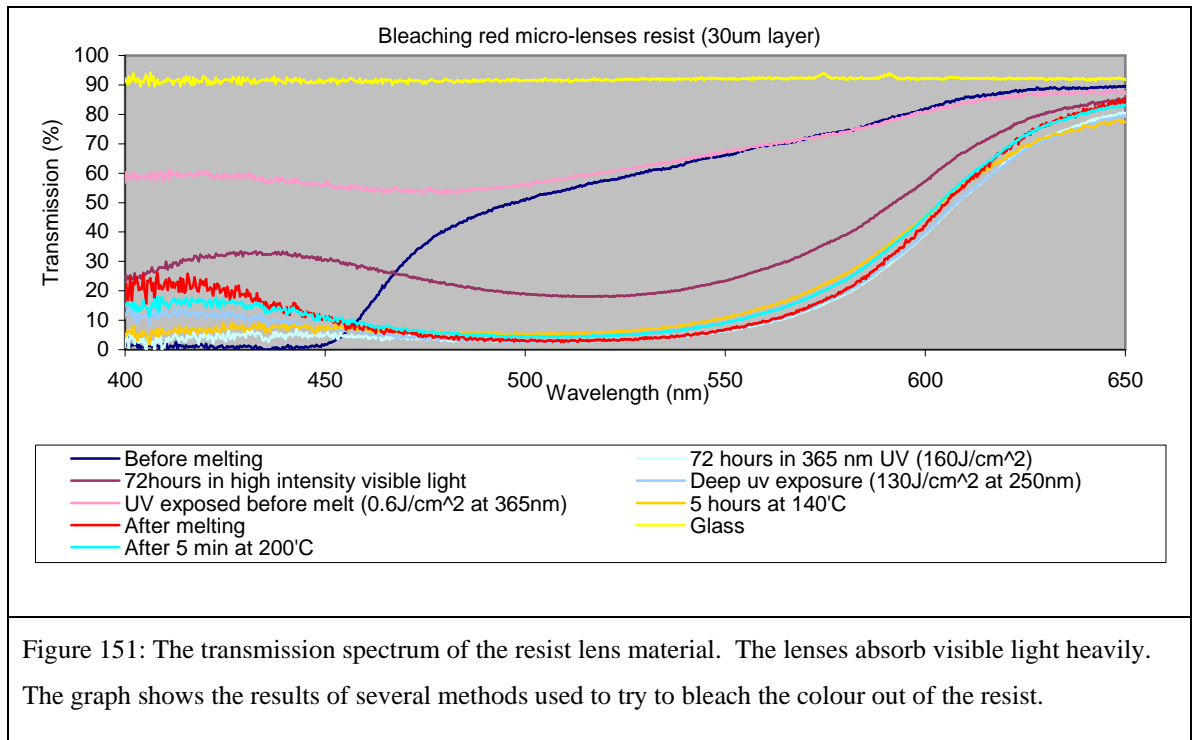
d). Top view of resist micro-lenses illuminated with collimated light. The lenses work well to focus the collimated light to a fine line.



Figure 150: Method used to prototype the first dual view lens system.

From the cross sectional photograph the lenses appear to be perfectly cylindrical, and they focus collimated light to a fine line very well. This suggests that the lenses are well formed by the surface tension effects that shape the lens. More detail about the manufacturing procedure are given in appendix 1.

Figure 151 shows the main problem with these melted micro-resist lenses. The resist that they are made from is strongly absorbing in green and blue (the resist is red in colour).



The photo-resist used is called ‘Megaposit SPR220’ from Rohm and Haas Electronic Materials. The red colour comes from the photo-initiator that absorbs UV light during the lithography process [57].

According to photo-resist suppliers, no positive photo resist exists with good transparency at 30  $\mu\text{m}$  thickness.

Transparent negative photo resist is available, however negative photo resist strengthen with heat – the more you heat it the harder it becomes, until it eventually burns. Blocks of negative resist will not melt on heating, so lenses cannot be made by this technique.

### 2.2.2 Can positive photo resist be bleached?

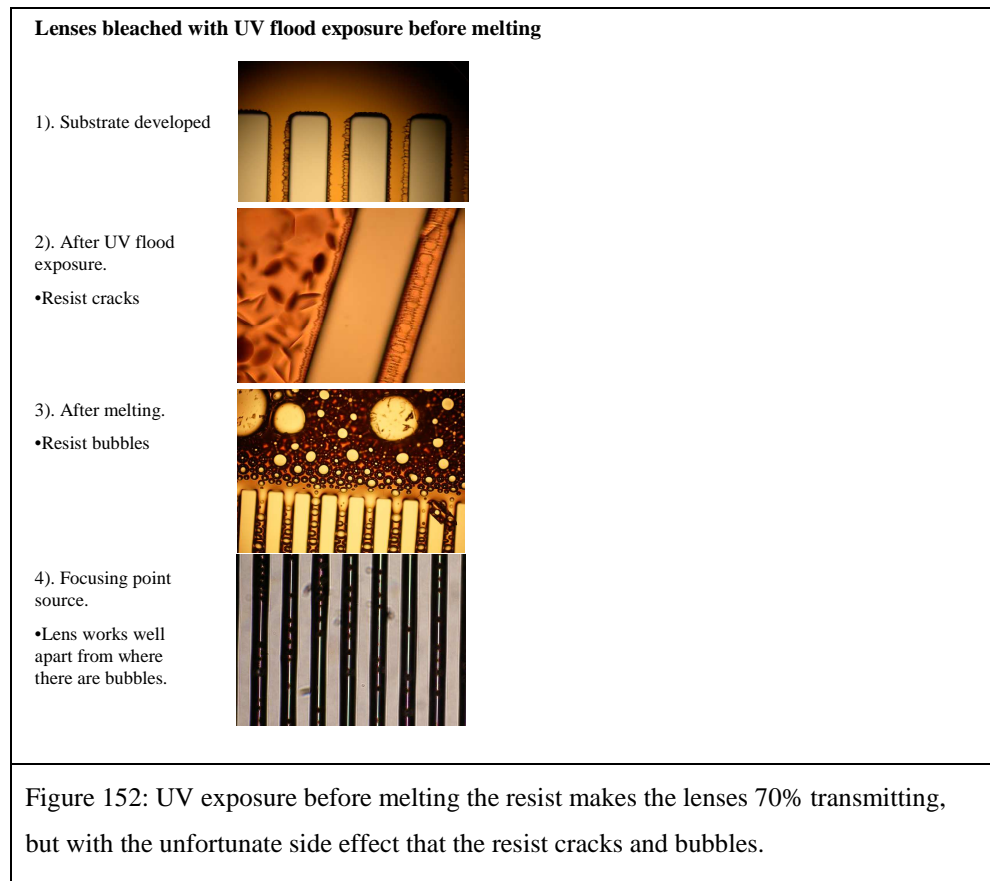
The absorbing material of the positive photo-resist is necessary for the lithographic process. Perhaps the absorbing material could be broken down into transparent components after the lithographic process is over.

The following methods were used to attempt this;

- UV exposure of the micro-lenses
- Deep UV exposure of the micro-lenses
- Intense visible light exposure of the micro-lenses
- Heat treatment of the micro-lenses

- UV exposure before melting the photo-resist

The results are shown in Figure 151. Heat treatment, and UV exposure after the lenses were formed had little effect. Exposing the photo resist to UV immediately before the melting step increased transmission of the resist to an average ~70%. Unfortunately this had a side effect that it caused the resist to crack and then bubble unacceptably upon melting. This is shown in Figure 152.



An alternative solution was to expose the formed lenses to intense visible light for 72 hours, which increased transmission to ~60%.

The lens system should give a 1.8x increase in brightness over the parallax barrier system, but the absorption of the lenses would give a ~0.6x reduction in brightness. In total the system would be about the same brightness, making the device no good as an efficient dual view system.

However, despite the low brightness, the red lenses can be used to test all other aspects of the design experimentally.

### 2.2.3 1<sup>st</sup> concept demo of the lens + barrier system

The red lenses were formed into a dual view display as detailed in appendix 1.

From an initial examination it could be seen that the dual view effect was created very well. A photo of the device is shown in Figure 153.

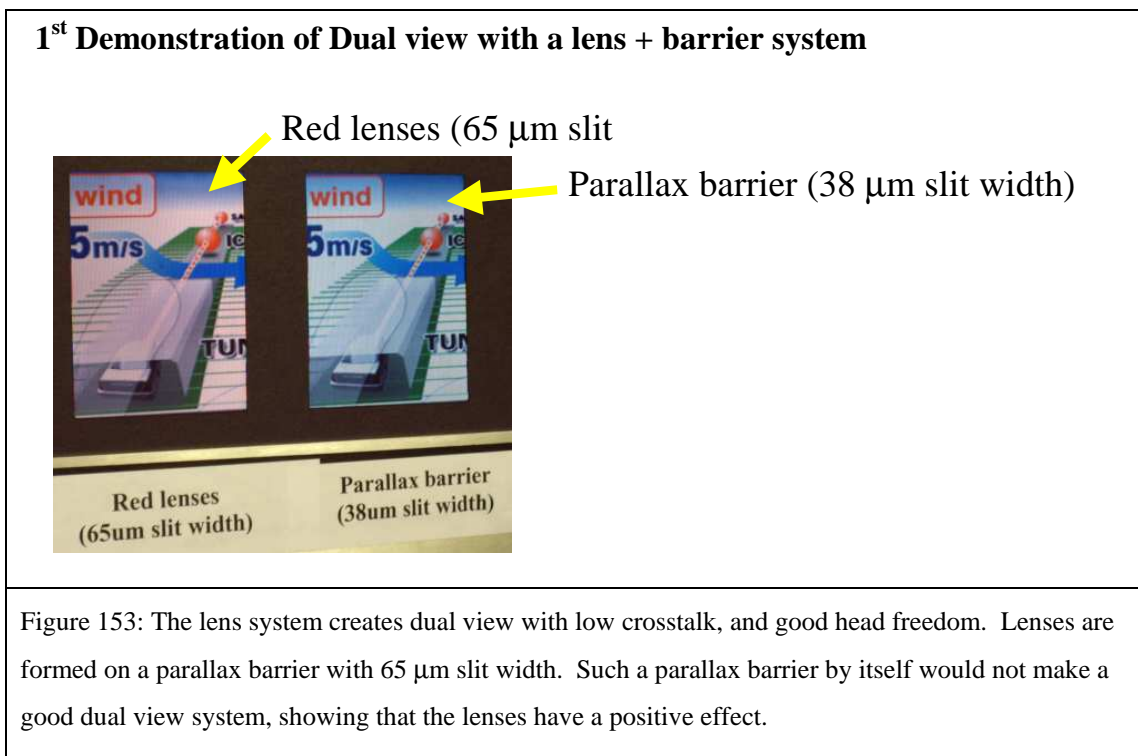
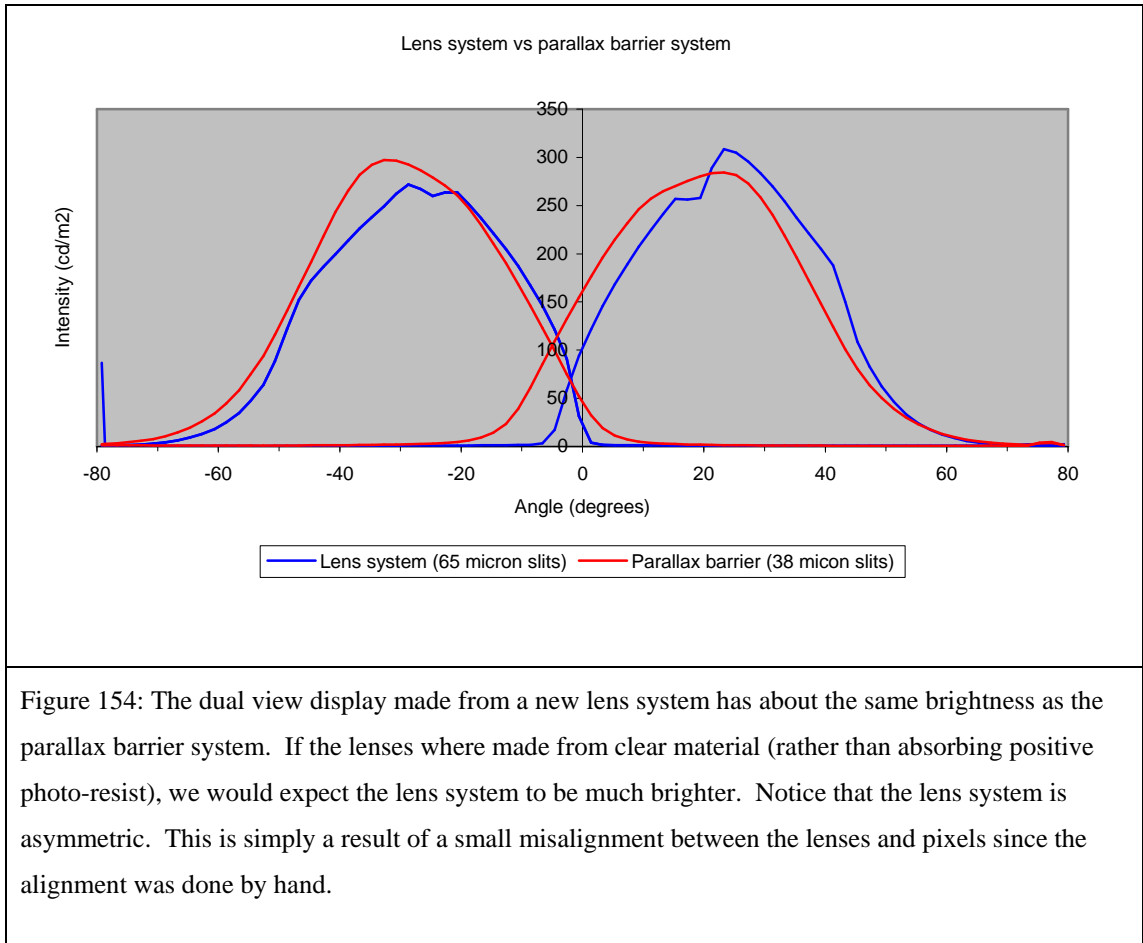


Figure 154 to Figure 156 show the quantified performance of the new lens system in comparison with a parallax barrier system.

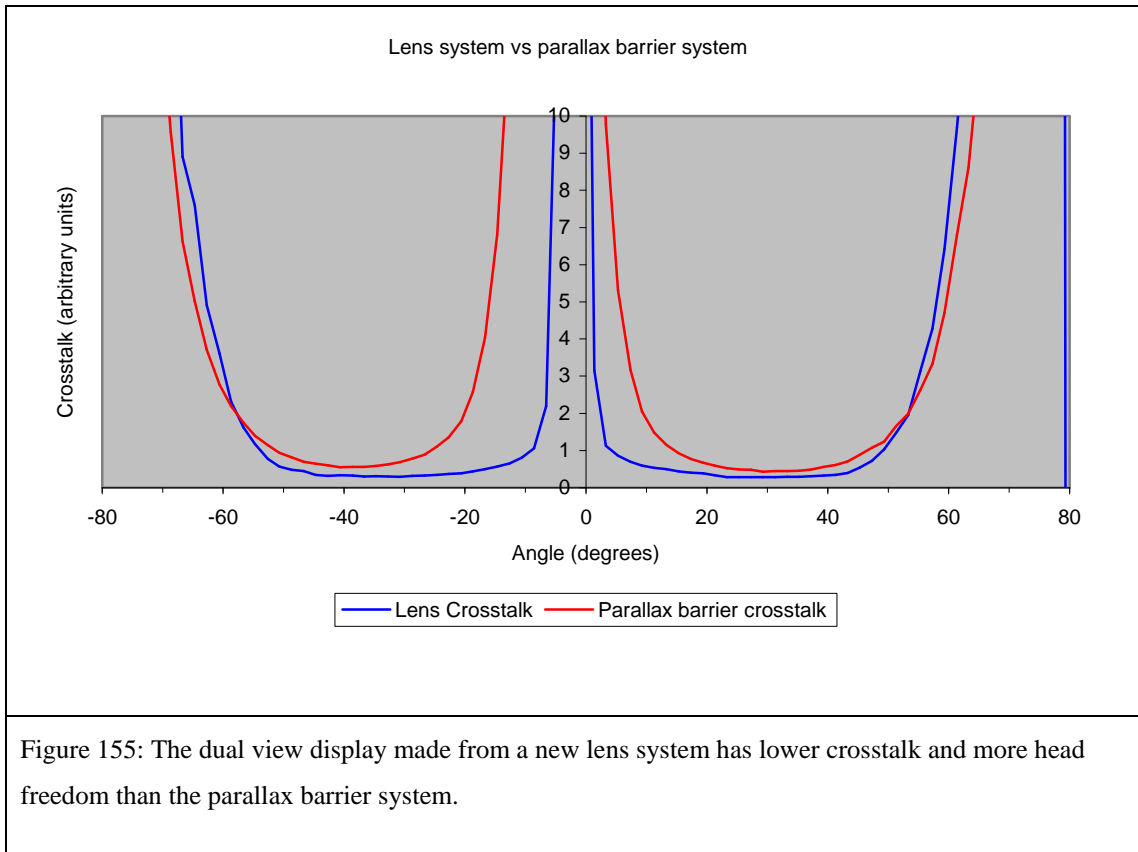
- Figure 154: The **brightness** is almost equal despite the absorption from the red lenses. A clear lens system would be expected to be genuinely brighter than the parallax barrier.
- Figure 155: As predicted the **image transition** between left and right images is sharper for the lens system than the parallax barrier system, giving the viewer more head freedom.
- Figure 157: The **crosstalk** is lower in the lens system. This is likely to be due to the larger apertures of the lens system suffering less diffraction.
- Figure 156: The **contrast ratio** of the lens system is lower than the parallax barrier system. This suggests that bending the light between the LC and the compensation layers is detrimental to their performance. However, the lens system contrast ratio is still reasonable.

There were no other adverse side effects of the lenses in the system. In summary, overall the lens system was a great success.

## Brightness measurements



## Crosstalk and head freedom measurements



It needs to be noted that these crosstalk measurements are comparative rather than absolute. This is because these measurements were measured with a photodiode that did not cut out wall reflections (see chapter 3). This means the crosstalk levels are overestimated for the parallax barrier and the lens system. The measurements do show that the crosstalk is lower for the lens system than the parallax barrier, and the head freedom is 26% greater.

Here I have defined head freedom as the region over which crosstalk is less than 2. This definition is designed to show the position where crosstalk rapidly begins to rise to a level that is quite decidedly unusable, rather than to show the region of head freedom where the display is of superbly low crosstalk.

With this definition of head freedom the parallax barrier has a head freedom from  $-56$  to  $-6$  and  $3$  to  $53^\circ$ , whilst the parallax barrier system has a head freedom from  $-56$  to  $-20$  and  $10$  to  $53^\circ$ . The usable angular range of the lens dual view system is increased by 26%.

A thorough investigation of the causes of crosstalk from the lens system has not been carried out, but from experience gained by studying the parallax barrier system we can make an estimate of what might happen. We would expect crosstalk from the polariser

scattering to remain about the same in the lens system and so this would cause about 0.07% crosstalk. The lens apertures are wider than the parallax barrier apertures so it is probable that since the crosstalk in the lens system is lower than in the barrier system, the diffraction from the system is much reduced. In fact the use of lenses is probably a simpler method of reducing crosstalk than using an apodised slit edge. We might also have expected some Fresnel reflections in the system from the boundaries between high and low index material, but since the crosstalk of the system is lower than the barrier system these effects can not be very significant. The same logic applies to manufacturing errors in the lens shape to say that they must be slight.

### *Contrast ratio measurements*

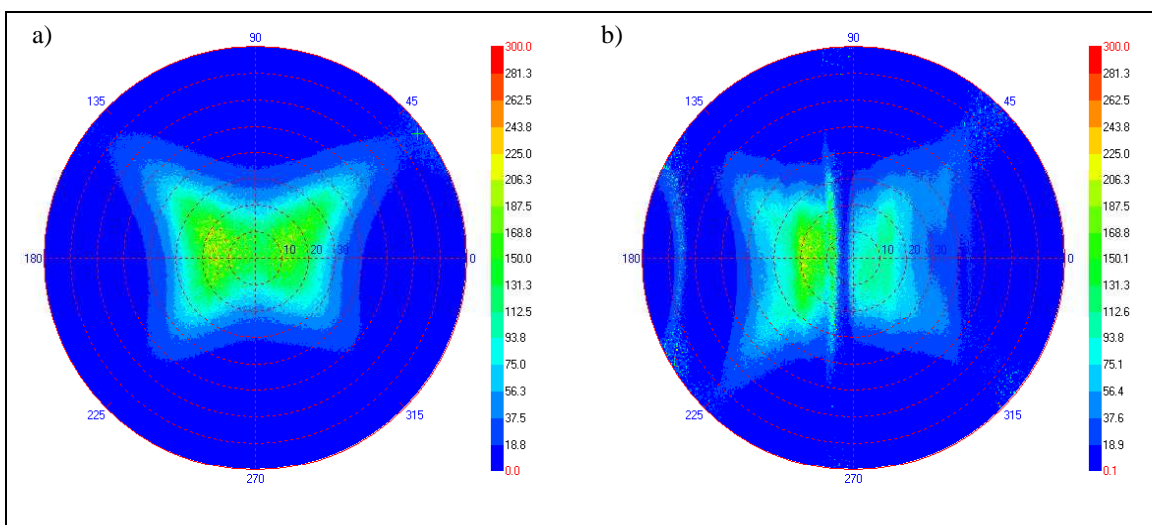
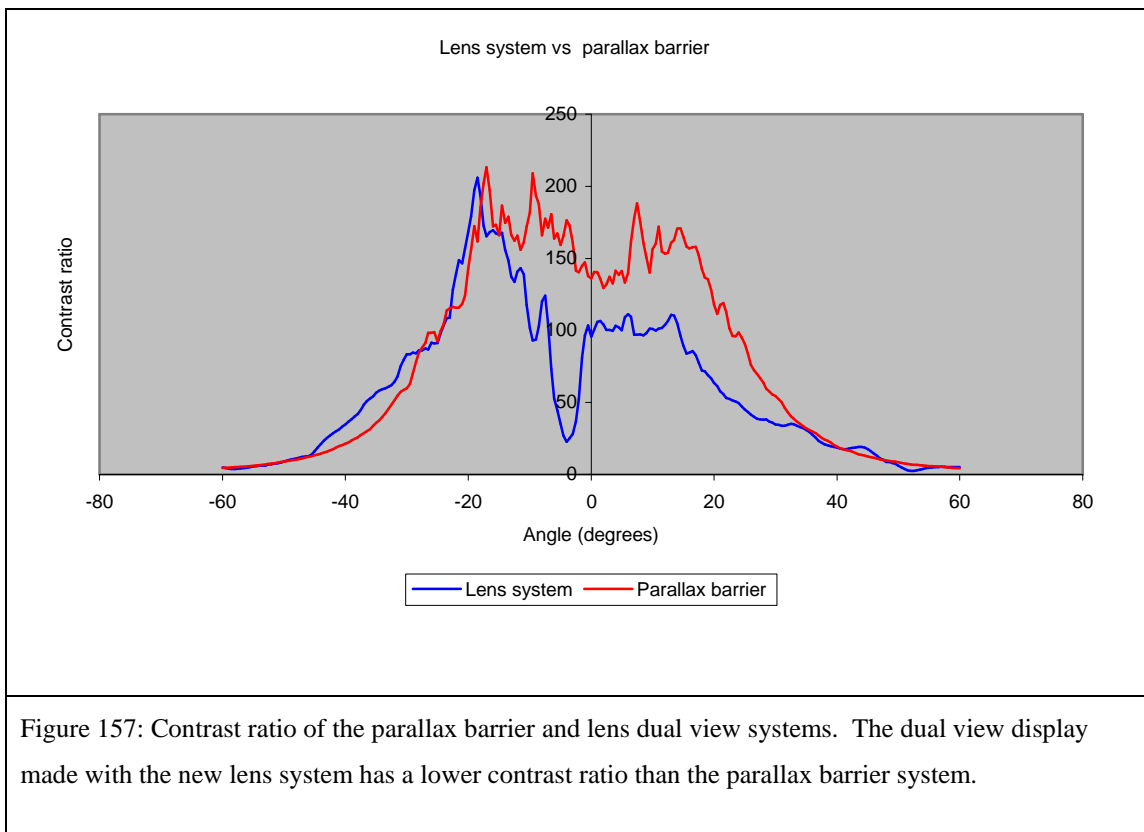


Figure 156: a) Contrast ratio of a dual view display with parallax barrier. b) Contrast ratio of dual view display with a lens system. The lens system bends light as it passes between the LC and the retardation film, thus causing a decrease in contrast ratio. Note that contrast ratio is lower on-axis, we would expect this since we are seeing light from the regions between pixels, where scattering, fringing fields, and disclinations may exist.



The contrast ratio reduction is more complex than shown in Figure 156. By inspection of the panel, reduction of contrast ratio was not obvious, but the image quality in the left or right views appeared much better in the lens system when looking from above or below the panel. Greyscale inversion does not become noticeable until higher vertical angles in the lens system. Greyscale inversion refers to an effect seen in some LCDs when viewed from high angles. At high angles areas that should be dark become brighter than other areas that should be of medium intensity. This degrades the picture quality.

Figure 158 shows contrast ratio plots of the lens and parallax barrier systems. Although contrast is reduced in the lens system whilst viewing approximately on axis, greyscale inversion is reduced at other viewing angles.

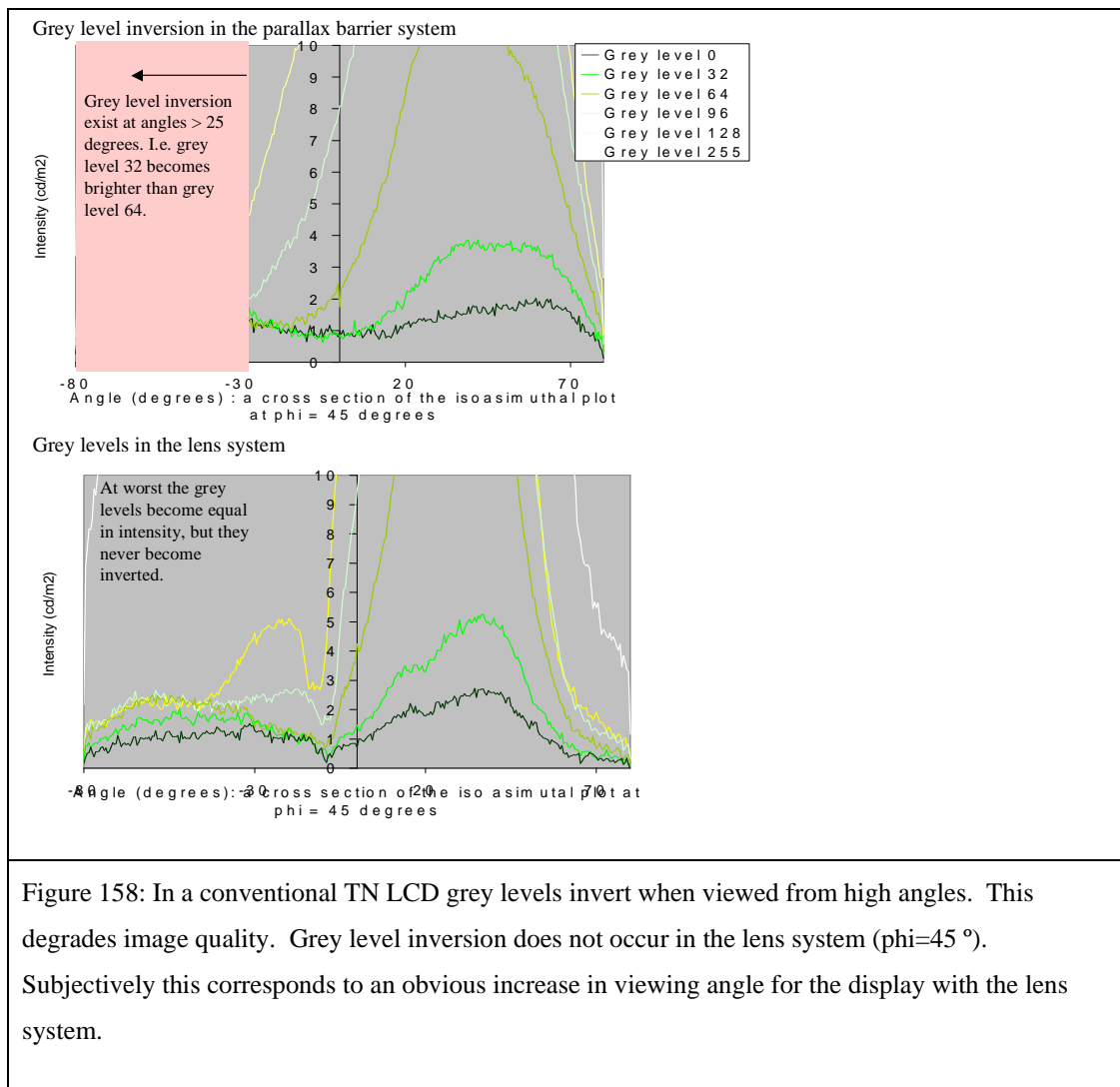


Figure 158: In a conventional TN LCD grey levels invert when viewed from high angles. This degrades image quality. Grey level inversion does not occur in the lens system ( $\phi=45^\circ$ ). Subjectively this corresponds to an obvious increase in viewing angle for the display with the lens system.

A possible explanation for this increase in vertical head freedom comes from considering the refraction that occurs at the lenses in all three dimensions.

It seems that even though the lenses are cylindrical the lenses have the effect of spreading light out vertically and horizontally. For light passing the LC at angles that are near on-axis the LC has good optical properties and no grey level inversion exists. When lenses are introduced into the system, the light passing the LC near on axis is spread out over a larger vertical range therefore increasing the vertical range over which no greyscale inversion exists.

The following text gives a description of how Snell's law can explain this.

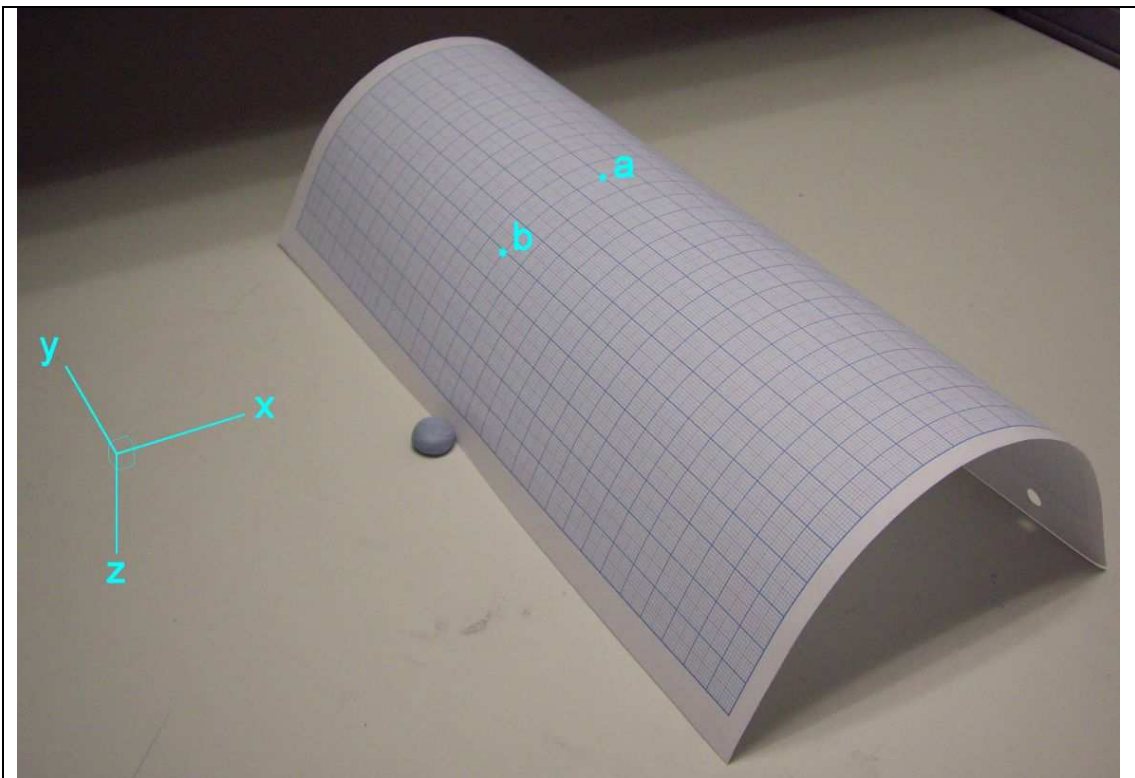


Figure 159: A paper representation of a cylindrical lens in the dual view system.

The figure shows a cylindrical lens viewed from the point of view of a pixel. Imagine light travelling from the camera to points 'a' and 'b' on the photograph.

By considering how Snell's law would affect the paths of each of these rays one would predict that path 'b' would be bent further in the x direction if the lens were not present. Therefore the lens allows the light to spread out more when compared with a parallax barrier system.

Figure 160 shows a simulation of this effect using the 'Zemax' ray tracing software.

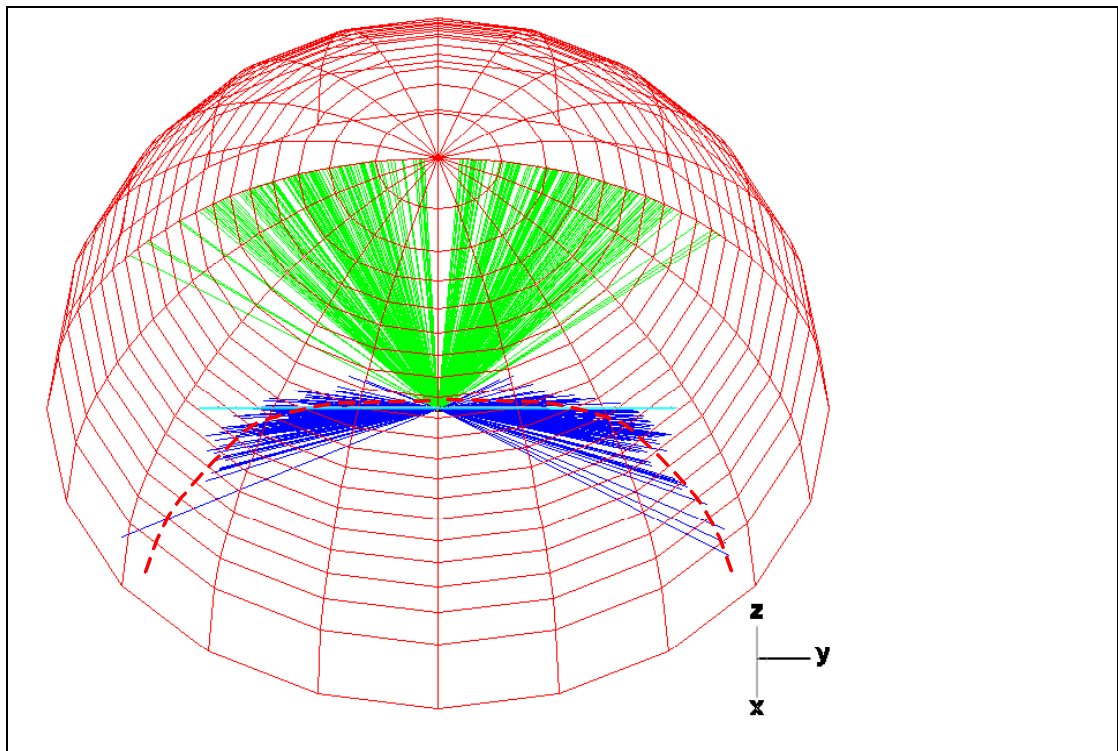


Figure 160: A simulation of a dual view system based on geometric optical ray tracing. The dual view system is at the centre of the dome. The green lines represent a  $\pm 30^\circ$  slice of light in the  $y$ - $z$  plane passing the lens system. The cyan lines represent the same slice passing a parallax barrier system angled  $40^\circ$  down (towards the positive  $x$  direction). The blue lines represent the same situation as the cyan lines but for a lens dual view system. The blue lines are more spread out vertically than for the parallax barrier system. The blue lines are more spread out vertically than for the parallax barrier system. The blue lines are more spread out vertically than for the parallax barrier system. The blue lines are more spread out vertically than for the parallax barrier system. The red dotted line is a guide for the eye showing where the blue lines hit on the dome.

The figure shows that spreading of light in the vertical ( $x$ ) direction is predicted by Snell's law. Light is spread from low vertical angles to high vertical angles. The low vertical angles have good optical properties without greyscale inversion, and this angular range is spread to a wider angular range giving a wider range without greyscale inversion.

It is also possible that another factor may contribute to the increased vertical head freedom. This is the interplay between the lenses and the view angle compensation films. As previously mentioned the lenses bend the light between the LC and view film, and the optical properties of the view film are angle dependent. The change in direction that the light passes the view film could also contribute to the change in image quality when the display is viewed from above or below. The effect of these films is quite complicated to model and is not included in this thesis.

## **2.3 Summary**

The table below summarises the key parameters of the new lens system compared with the original parallax barrier system.

<b>Parameter</b>	<b>Parallax barrier system</b>	<b>Red lens system</b>
Brightness at 30 °	272 cd/m <sup>2</sup>	277 cd/m <sup>2</sup>
Head freedom	~40 °	~50 °
Crosstalk	~0.2%	Lower
Contrast ratio at 30 °	56	58

Table 30: A comparison of a parallax barrier dual view system and the first micro-lens dual view system based on red lens material.

This prototype successfully proved the concept of the lens barrier system. The system was shown to work without major problems. This prototype showed that it was worth spending more effort to optimise the system and develop a simple method to create clear micro-lenses.

## **3. Optimisation tool for lens + barrier design**

Section 1 made a rough estimate of the best lens design for testing purposes.

With lenses being successful experimentally and looking set to become the basis of Sharp's dual view technology the design should be optimised with more rigour. This section is about the creation of an algorithm that can predict the performance of a lens-barrier dual view display and optimise the design parameters to provide the best possible performance for a product.

The ability of the model to predict dual view performance is compared with experimental data in section 3.2 and 4.3. The model is seen to predict the brightness profile from a dual view display with a correlation coefficient of  $r^2 = 0.987$ .

It is seen that an algorithm that tries all possible combinations of parameters would take an impractical amount of time. Deducing simplifications that could be made to the problem successfully reduced the run time of the algorithm to 1 day.

### **3.1 Requirements of the theoretical model**

Prototyping a dual view panel takes a lot of time and is expensive. Therefore adjusting the design parameters of the lens-barrier system by experimental trial and error is not ideal. It would be much better if the design could be optimised theoretically.

There are many parameters that need to be chosen: these include the lens radius, pixel aperture, pixel – barrier separation and so on. The theoretical model should be able to predict the performance of a dual view system with any given values of these parameters, and ultimately be able to automatically iterate the parameters until the best values are found.

In addition the theoretical model should help our understanding of what makes a good design. For example is it better to have a big lens aperture and a small pixel aperture or vice versa.

### **3.2 The assumptions used in the model**

Ideally the model would be able to predict all aspects of the displays performance including brightness, crosstalk and contrast ratio. The efforts that would be required to model each of these performance aspects were considered and it was decided that a model based purely on geometric optics should be sufficient to optimise the design parameters. The reasoning behind this is explained in this section, along with some of the assumptions that are used.

The table below suggests which optical properties might need to be modelled to predict different characteristics of the display.

<i>Display characteristic</i>	<i>Modelling required</i>
Brightness profile of the dual view windows	Geometric optics
Crosstalk in the system	Diffraction, polariser scattering and possible other unknown factors
Contrast ratio	Polarisation effects caused by the LC and retardation films.

Table 31: The complexity of modelling that might be required to predict different dual view parameters.

Given that parallax barrier systems can be designed satisfactorily with geometric optics, and that the ray tracing in section 1 made a sensible prediction of the first lens-barrier

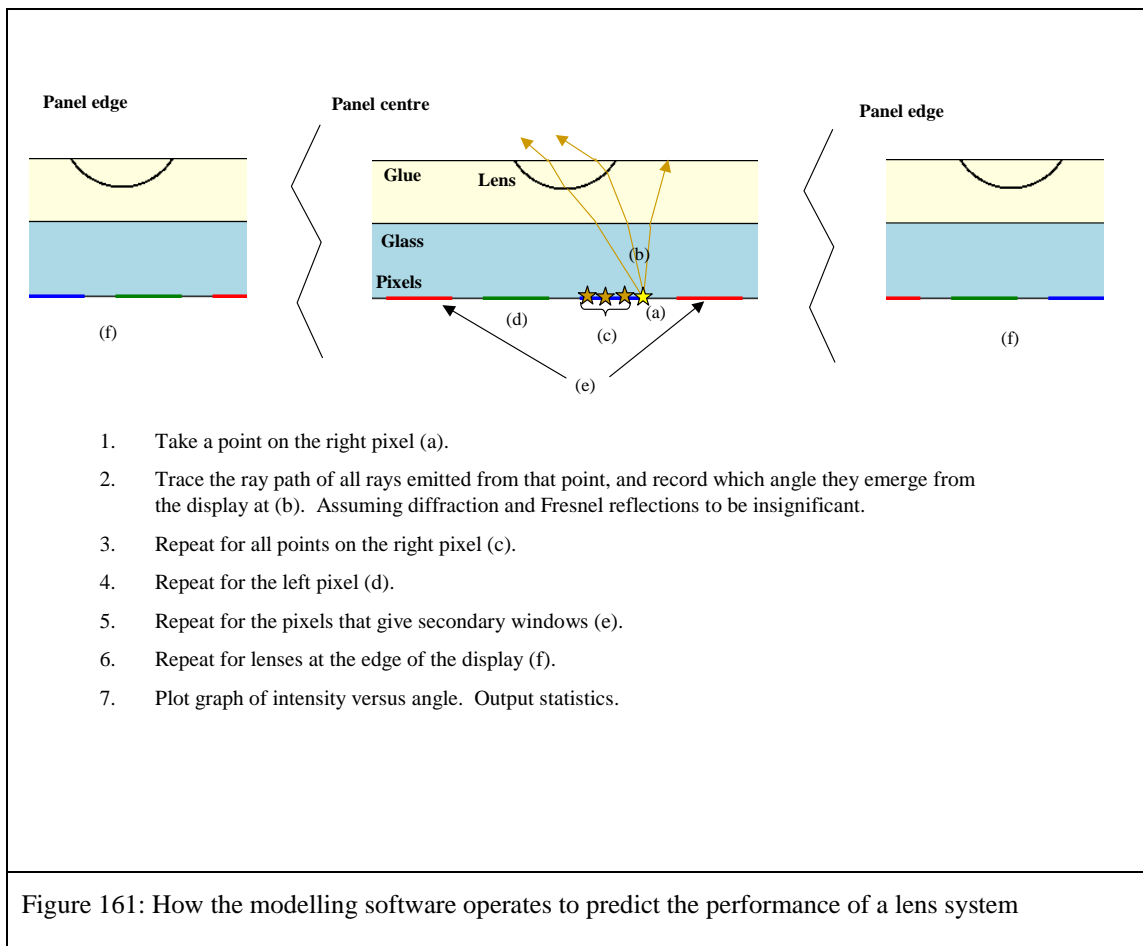
prototype, it was assumed that geometrical optic considerations only would be needed to simulate the brightness profile, and that diffraction could be assumed irrelevant. It was proposed that reflections in the system would not need to be considered though this could be changed if necessary if the results were not accurate enough.

Diffraction modelling is likely to be needed to predict crosstalk as well as scatter in polariser. However the origin of crosstalk from the lenses has not been studied so it may be that new factors need to be taken into account. Fresnel diffraction modelling did not work well in chapter 3 to predict the intensity at the barrier slits and so basic diffraction modelling would be unlikely to produce an accurate result for the lens system. These factors suggest that modelling crosstalk in the system will be very difficult. From work on parallax barrier systems it has been seen that factors such as slit width have a big effect on head freedom and a small effect on crosstalk. Therefore the slits widths are set by the head freedom requirements and are not modified to reduce crosstalk. For these reasons it was proposed that in the lens system a knowledge of crosstalk would not affect the how the design parameters are set, and so crosstalk could be considered separately at a later date.

It would be useful to be able to simulate contrast ratio. This would help to choose an LC mode that works well with the lenses. However modelling the performance of the liquid crystal and compensation films is complicated and would be likely to take a lot of computer time. Again it was proposed that a design which gives good head freedom should take precedence over a lens design that gives good contrast ratio. Therefore the LC mode characteristics can be modelled separately after good lens design is found. This would be a useful piece of work to do but it is not considered in this thesis.

The first design (of section 1) was simulated with optical ray tracing package Zemax. Zemax is complicated and time consuming to use. It is a universal piece of software that can be used for various optical systems but as such it is not as efficient with computer time as it could be. It is not easy to make Zemax automatically optimise the parameters of a system such as a dual view display.

For these reasons it was decided to write a custom piece of software that would optimise the system as efficiently as possible. The model only takes geometric optics into account for the purpose of predicting brightness and optimising the design parameters of the lens-barrier system. Figure 161 shows how it works.



Each ray from the pixel has its intensity weighted depending on the angle of the ray and position from which it came from on the pixel. This is explained in the following text.

The angular weighting of a ray depends on the intensity of the light that is emitted from the backlight and the transmission of the LC and polarisers etc. This data is obtained by measurement of a single view panel. This assumes that the transmission through the polariser is unaffected by the lenses. This is not true since lenses change the angle at which the ray passes the polariser and view films, the transmission through these elements is angularly dependant. This effect is assumed to be small.

The measured data from the single view panel takes into account the effect of Fresnel reflections that exist in the single view panel but Fresnel reflections from the lenses are not taken into account by the measurement or the modelling. Fresnel reflections will exist since there is a high index change between the glue and lenses. This would be expected to cause a loss of a few percent in the system (according to the Fresnel equation). This loss is assumed to be negligible.

Different positions on the pixel emit different intensities of light because the pixels have a black mask which block the light in some areas. This is taken into account by

weighting the intensity of the rays depending on the position from which they originate on the pixel.

Appendix 2 shows more about the program's functionality.

### 3.3 Experiment versus theory

Results from this model are compared with experimental data from the red lens prototype in the graph below.

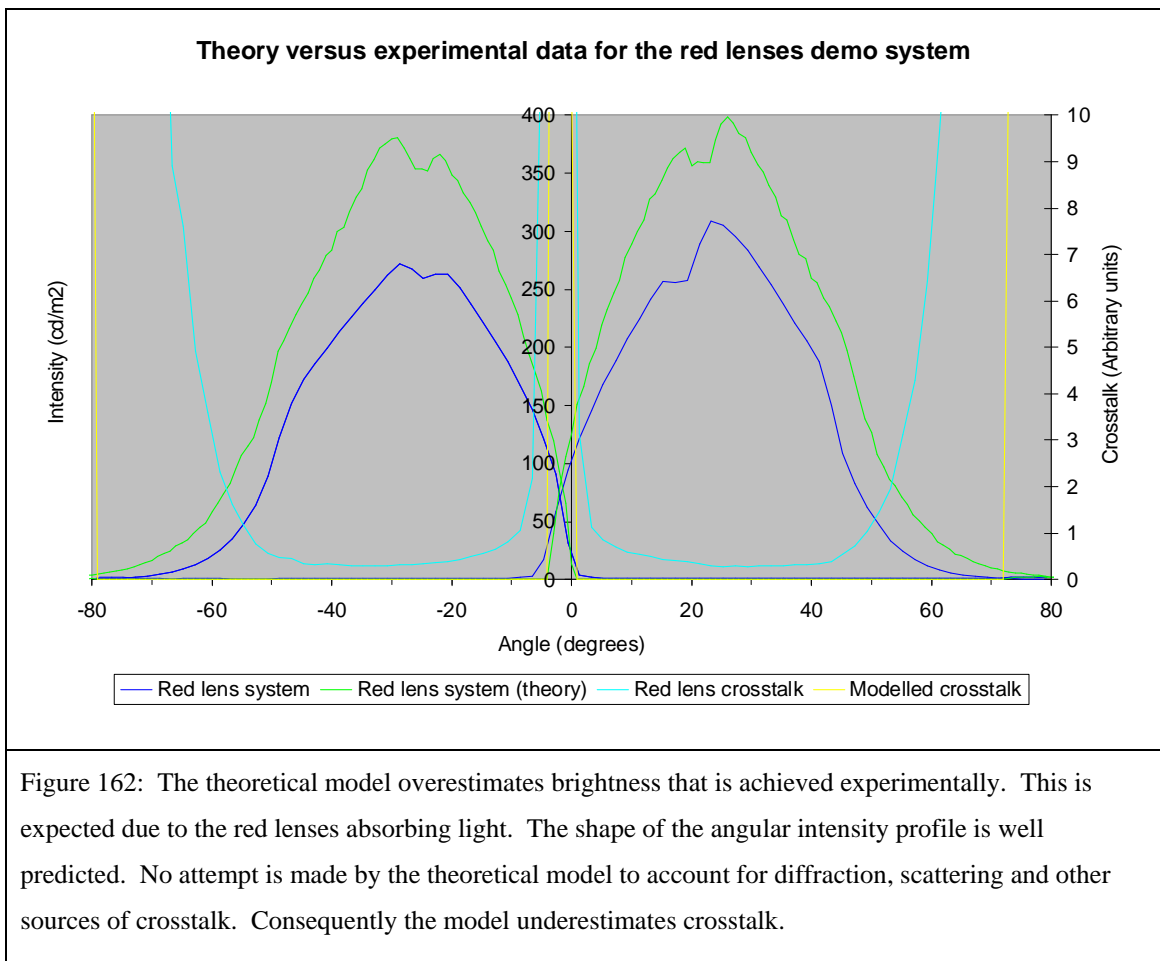


Figure 162: The theoretical model overestimates brightness that is achieved experimentally. This is expected due to the red lenses absorbing light. The shape of the angular intensity profile is well predicted. No attempt is made by the theoretical model to account for diffraction, scattering and other sources of crosstalk. Consequently the model underestimates crosstalk.

Essentially the theory fits the experimental data very well. The shape of the brightness profile is well predicted, but the intensity is underestimated by about 20% since the theory neglects the absorption of the red lenses. The table below discusses this in more detail.

	From experiment	From model	Comment
Brightness (at $\pm 30^\circ$ )	290 cd/m <sup>2</sup>	390 cd/m <sup>2</sup> (35% error)	High error, but this is expected since absorption by the red lenses is not taken into account.
Crosstalk	Low	0%	No attempt is made to model crosstalk, as achieving sufficient accuracy would be extremely difficult.
Head freedom	3 to 53°	1 to 72°	Over estimated by the simulation.
Window intensity versus angle	See graph		The shape of the theoretical intensity profile follows the experimental data very well.
Fresnel reflections	See graph		Model predicts window shape and brightness accurately so angular variation in Fresnel reflection losses must be insignificant.

Brightness is not modelled well but this is expected since the absorption of the lenses is not taken into account. The accuracy of the brightness data is considered later when a clear lens system is made.

Since the shape of the brightness intensity profile appears to be accurate this gives us confidence that the design can be designed based on theory that is the bases of section 3.4.

The head freedom of the design is overestimated by the geometric optics because crosstalk increases near the edges of the geometric viewing windows. This point will need to be considered when designing a dual view display.

The modelling explains why there is a dip in each of the peaks in brightness at  $\pm 30^\circ$ . According to the modelling this is caused by a region of black mask in the centre of the pixel which is imaged to  $\pm 30^\circ$  and so causes a reduction in intensity there.

The model also allowed each of the parameters to be considered individually to build up an understanding of what affects each parameter such as the lens radius has. Appendix 3 presents this information.

### **3.4 Finding the best design**

There are 6 design parameters that need to be chosen to give the best dual view design. Design choices include – exactly how much does the lens need to be defocused, and which is better – a big pixel aperture and small lens, or vice versa.

There are too many options to try by hand so we need a computer program to automatically iterate until the best design is found.

In this section an algorithm is designed that can perform this task in a sensible time. It is seen that an algorithm that tries all possible combinations of parameters would take an impractical amount of time. Deducing simplifications that could be made to the problem successfully reduced the run time of the algorithm.

#### **3.4.1 Success criteria for the dual view design**

In order to optimise the design the computer needs some way of assessing how good each design is. The best design was defined as follows. The user states the amount of head freedom that is required. For example, ‘the display must provide dual view from at least 10 to 56 °’. The best design is a design that meets or exceeds this criteria and has the highest brightness.

Brightness and head freedom are the two key requirements from the design.

#### **3.4.2 The optimisation algorithm**

The table below shows the variables that need to be optimised in a parallax barrier system, and the new lens- barrier system.

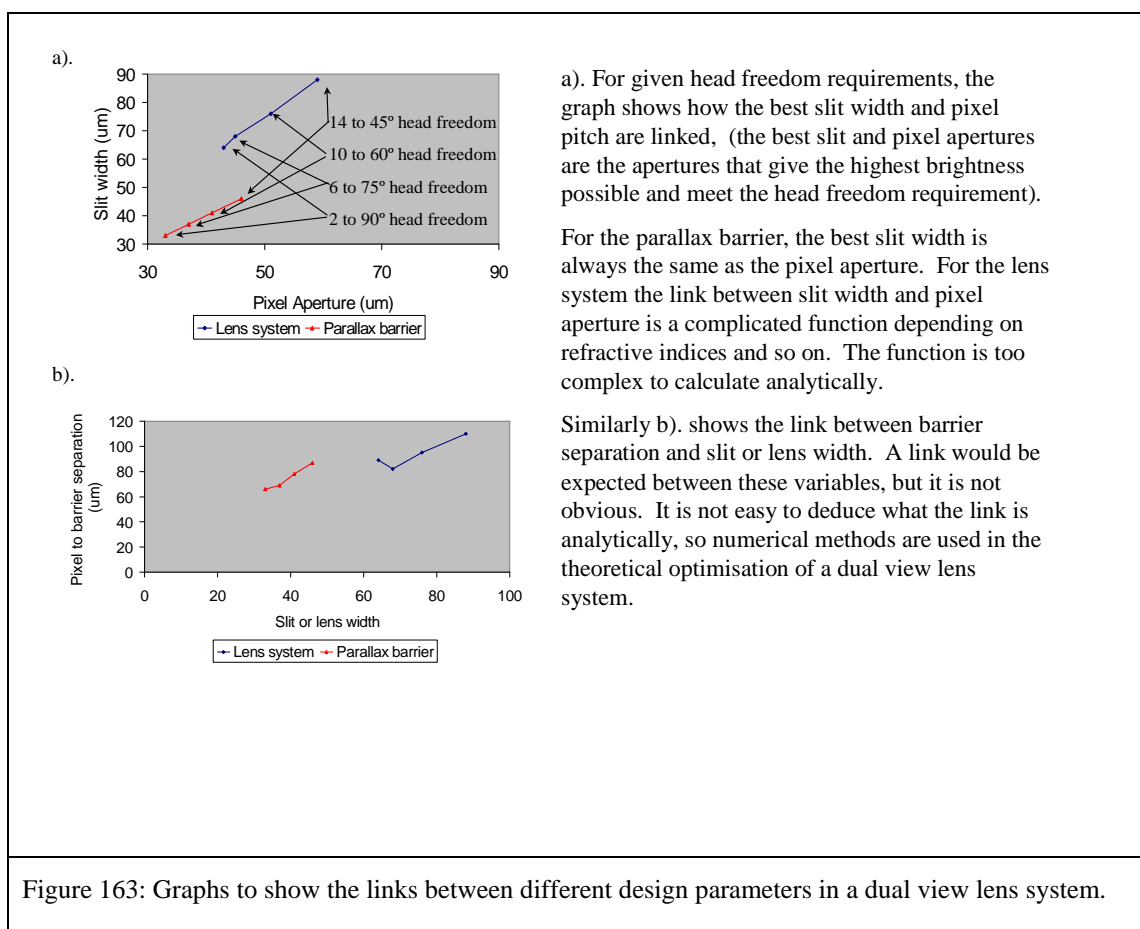
<b>Parameters in parallax barrier system</b>	<b>Parameters in lens barrier system</b>
Slit width	Slit width
Barrier separation	Barrier separation
Pixel aperture	Pixel aperture
	Lens radius
	Lens refractive index
	Glue refractive index

Table 32: The variables that must be optimised in the parallax barrier and micro-lens dual view systems.

Optimising a parallax barrier system is relatively simple. There are only three variables and two of the variables are linked (the slit width should be the same as the pixel aperture for the best brightness). This leaves two independent variables. These could have probably been solved analytically due to simplicity of the system, but they were solved numerically since this was adequately fast, and accurate.

For a lens-barrier system there are six variables so from experience in optimising the double lens system in Chapter 2 some simplification will be needed to solve the problem in a sensible time.

A neat method of simplifying the problem would be to find simple links between the variables, however the link between the best slit width and pixel aperture is not trivial (see Figure 163).



One might expect a link between the lens focal length and barrier separation, but as Figure 163b shows the link is not simple, the variables are linked to each other by a ray-tracing algorithm, which could be extremely difficult to calculate analytically.

Some simplifications are obvious from appendix 3. From this two simplifications were made. Firstly, the lenses should be hemi-cylindrical. Secondly, the difference in

refractive index between lens and glue should be as high as possible and the values that can be obtained should be input by the user.

This reduces the problem to 3 independent variables. The table below shows the 3 parameters and an estimate of the computer time that would be needed to simply try all possible combinations of these parameters. This is based on a measurement of the time taken for the software to simulate one set of parameters. It took 3 seconds.

<b>Parameter</b>	<b>Range of values</b>	<b>Accuracy required</b>	<b>Number of values to try</b>
Lens radius	13 to 130 $\mu\text{m}$	+1 $\mu\text{m}$	117
Glass thickness	40 to 195 $\mu\text{m}$	+3 $\mu\text{m}$	51
Pixel aperture	13 to 65 $\mu\text{m}$	+2 $\mu\text{m}$	26
Total number of design iterations needed:			155142
Time taken to try all iteration (3 seconds per iteration):			5 days

Table 33: An estimate of the amount of time required to test all possible combinations of variables in the micro-lens system.

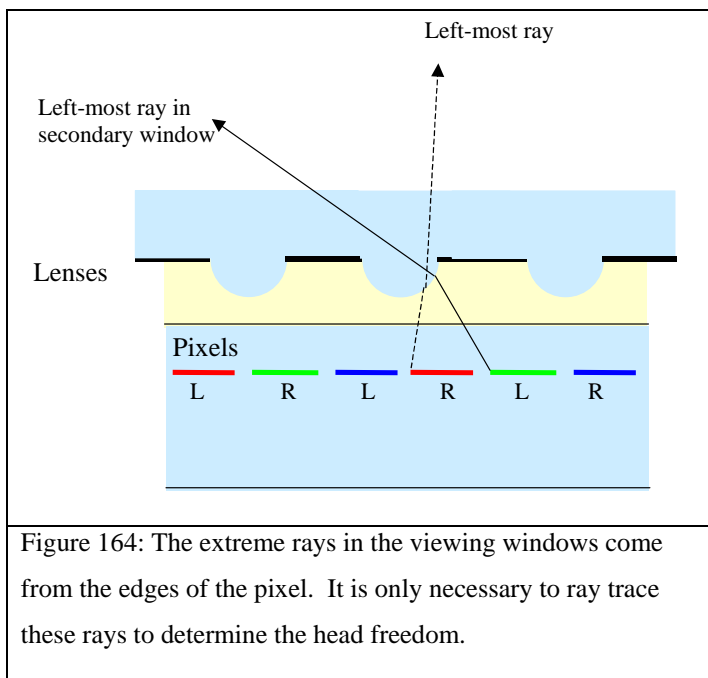
The ‘Ranges of value’ column refers to values of each parameter that could sensibly be used in a design. If all of these possibilities were tested then 5 days of computer time would be needed to obtain the result. This is an amount of time that is inconvenient. So further efficiency saving were sought.

Two further options for efficiency savings were considered. Firstly, use a clever optimisation routine that iterates towards the best design, rather than blindly trying all the possible designs, or secondly do a ‘fast ray trace’.

Option 1). Has the disadvantage that in the search for the global maximum of the success criteria, it may find by accident a local maximum and incorrectly conclude that it has found the best design. This was thought to be an unacceptable risk. In studying the design parameters local maxima were found to exist.

Option 2). The optimisation routine spends hours trying designs that are nowhere near good enough. Figure 164 shows how head freedom data can be obtained by ray tracing from just the 2 edges of a pixel. This is 50 times faster than a full ray trace. If the head freedom is met the algorithm continues to perform a full ray trace which determines

brightness. This reduces the time taken to optimise a design to approximately 1 day, which is acceptable.



Option 2 was chosen as the optimisation method.

### **3.5 Summary**

The software designed in this section predicts the brightness profile of a lens-barrier dual view display with good accuracy. More evidence of this is presented in section 4.3 when the modelling results are compared with a clear lens-barrier system.

The software is less effective at predicting the exact head freedom of a display because it does not model crosstalk that increases towards the edge of the geometric head freedom limits. For this reason this software is used in conjunction with experimental testing when a new dual view display is designed. The software provides the best starting point for the design and a few variations in slit width are tested experimentally around this initial design before the final choice is made.

## **4. Making a Manufacturable clear lens system**

Making lenses by melting blocks of resist is an ideal technique for Sharp, since all the lithographic production equipment needed already exists for the manufacture of LCDs. The lenses are made on glass with lithographic pitch accuracy and there is no difference between the thermal expansion of the lens and LCD substrates.

Unfortunately the red colouring of positive resists makes the idea unworkable.

This section is about experimentation to find an elegant process to make micro-lenses that is easy to perform using Sharp's manufacturing facilities. We start with a list of proposals that may work, each proposal is tested experimentally and the result is shown. Two methods were found to be successful and these were developed into dual view displays that showed all the high specifications we are looking for.

#### **4.1 Idea proposals**

Clear negative resist can be melted but only before it is cured. The process of curing the clear resist into blocks hardens it so that it cannot be melted into lenses.

It was determined that there must be some way to make clear lenses by a lithographic technique many possible manufacturing routes were thought of. Below are the top 10 ideas (some novel, some existing techniques), in no particular order.

Top 10 ideas to make clear micro-lenses.

1. Under-development of resist
2. Dry etch red lenses into glass
3. Use negative resist exposed through a mask with a diffusive light source.
4. Use negative resist and greyscale lithography [58].
5. Print negative resist blocks and melt them to form lenses.
6. Create resist pillars to shape negative resist into blocks, ready to melt.
7. A transfer technique.
8. Coating clear resist over blocks.
9. Embossing.
10. Patterned de-wetting.

#### **4.2 Experimental testing**

A short summary of each idea is given in this section. In each case an explanation of the method is given, the results that were obtained in each case are presented and a discussion is presented about its potential as a useful method.

Of the techniques tested ideas 8 and 9 stood out as the most promising.

Although embossing is not a lithographic method it is a method potentially suitable for manufacture. It was tested by using the method to create a working dual view display.

This showed that embossing is a workable method and gave confirmation that a clear lens system does have considerably more brightness than a parallax barrier system. This is described in section 4.3.

Idea 8 is a very elegant and simple (cheap) way of making high quality micro-lenses. In addition, very high index difference between the lens and surrounding material can be achieved, allowing a high brightness designs. This technique was also used to create a dual view display. This is described in section 4.4.

#### 4.2.1 Under development of resist

Resist is usually formed into blocks by a lithographic process and the shape that the blocks form depends on the processing conditions [58]. This idea involved under-developing the resist so that the corners become rounded and lens like.

##### *Results and comments*

The table below shows the cross sections that result from a range of different exposure and development conditions. The resist material is SU8 with a thickness of about 30  $\mu\text{m}$ .

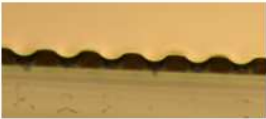
Development:	Exposure:		
	Low	Medium	High
Low			
Medium			
High			

Figure 165: Cross sections of resist blocks that are created with various exposure and development conditions.

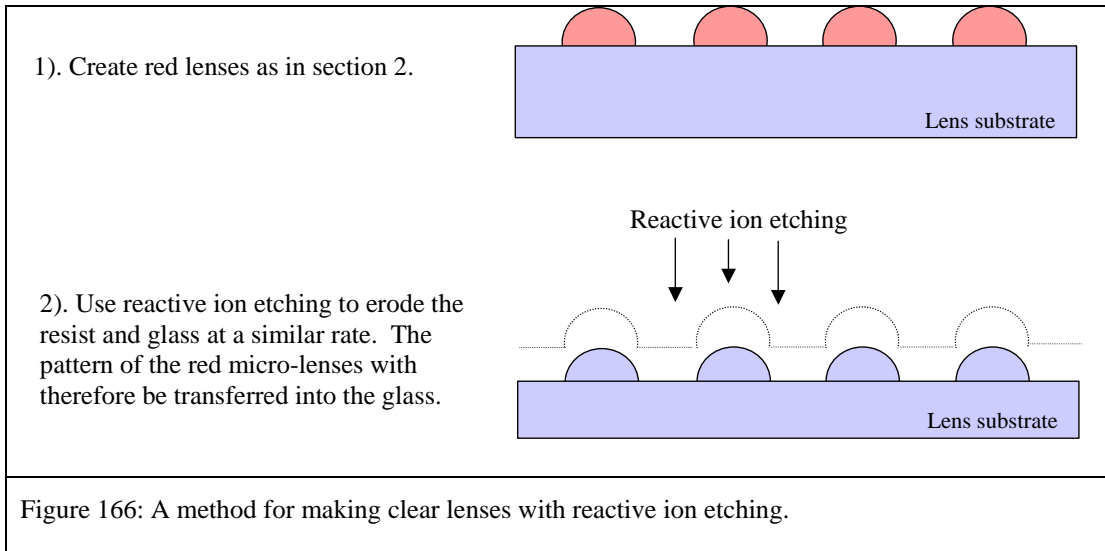
Some processing conditions give shapes approaching the required lens shapes.

However, the processing conditions required to obtain these shapes were very critical.

That is to say the lens shapes change rapidly depending on the amount of development

and exposure they receive. This means that small variations in exposure etc. across the substrate lead to non-uniformity. This would make the process very difficult to repeat exactly, furthermore the lens shapes produced are not particularly good.

#### 4.2.2. Dry etching red resist lenses into glass



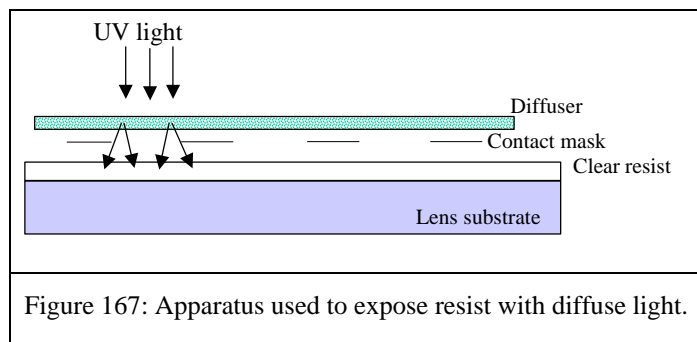
#### Results and comments

This is a standard technique that is known to work [59].

This idea was not tested because reactive ion etching is an expensive manufacturing process. It would be better if a technique could be found that made clear lenses and was cost effective to manufacture.

#### 4.2.3 Create rounded blocks in negative resist by use of a diffusive mask

Lithography is usually carried out by exposing the resist with a collimated ultra-violet light source. This is to keep the edges of the resist blocks straight to allow high resolution features to be made. If an un-collimated light source was used then perhaps the edges of the blocks would become round and a lens shape would be made. This idea was tested by adding a diffuser before the contact mask during the ultra violet exposure.



### Results and comments

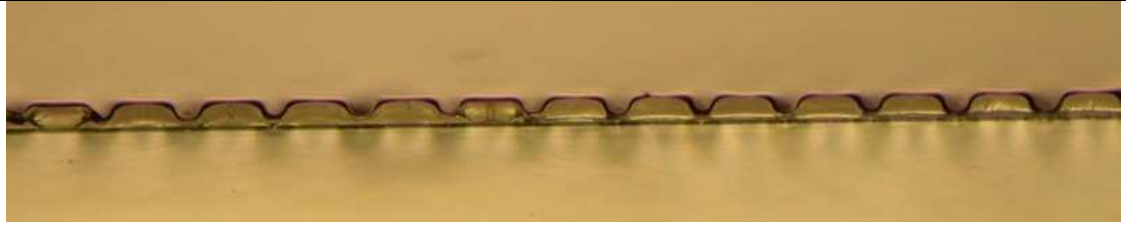


Figure 168: Resist blocks created by exposure with diffuse light.

The photograph above shows a cross section of resist blocks formed using this method. The resist was SU8 in a 30  $\mu\text{m}$  layer. The lens shapes could be developed much more robustly (with less tight tolerances) than in method 2. The lens shapes are reasonably well formed. The technique might produce reasonable results if developed further however I suspect that it will be difficult to create a precise cylindrical shape using this technique. The techniques that use surface tension effects to produce a cylinder are likely to create a better shape profile.

#### 4.2.4 Greyscale lithography on clear negative resist

In greyscale lithography the resist is exposed to ultra violet light through a contact mask. The mask has varying levels of transmission so that the resist can be given various levels of resistance to the solvent used to develop it. In this way it should be possible to create a lens shape.

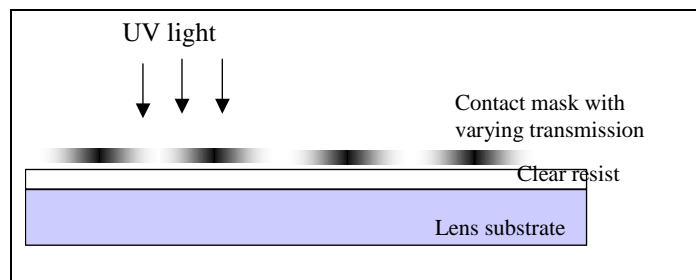


Figure 169: Apparatus used to create lithographic structures by using greyscale lithography.

### Results and comments

This is a standard technique that is known to work [58].

Like ideas 2 and 3 this idea is an analogue processing technique. This means the process conditions must be just right every time otherwise unacceptable variations could become present between different displays. This translates to many panels being

thrown away, low yield and so high cost. Although possible it is probably not the best manufacturing route.

#### 4.2.5 Print negative resist blocks and then melt them

Negative resist does melt and reflow before it is cured by UV light. By patterning the resist without UV lithography (for example by screen printing) the resist remains soft enough to melt. Once melted the resist naturally forms a cylindrical lens shape.

Therefore any method by which clear resist can be deposited into blocks without using lithography should enable lenses to be made.

#### *Results and comments*

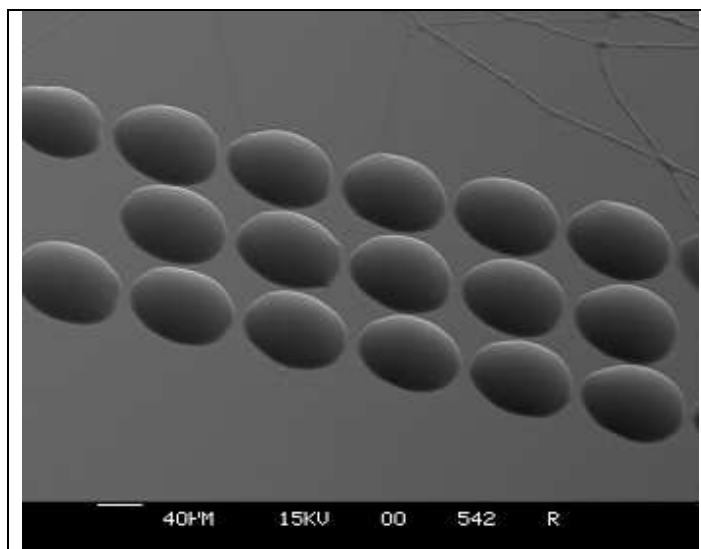


Figure 170: A picture of lenses made by depositing resist through a screen printing mask taken with an electron microscope by Micro-Stencil ltd.

The scanning electron microscope picture opposite shows lenses made by screen printing su-8 blocks and then melting them, (this technique was tested by Micro-Stencil ltd.).

The problems with this technique were that the lenses are too shallow. Micro-stencil could not deposit enough su-8 onto the substrate. The su-8 tended to stay in the screen printing mask. Also screen printing was not able to meet the required pitch accuracy. The pitch of the lenses would vary across the substrate which would cause the dual view windows to become smeared.

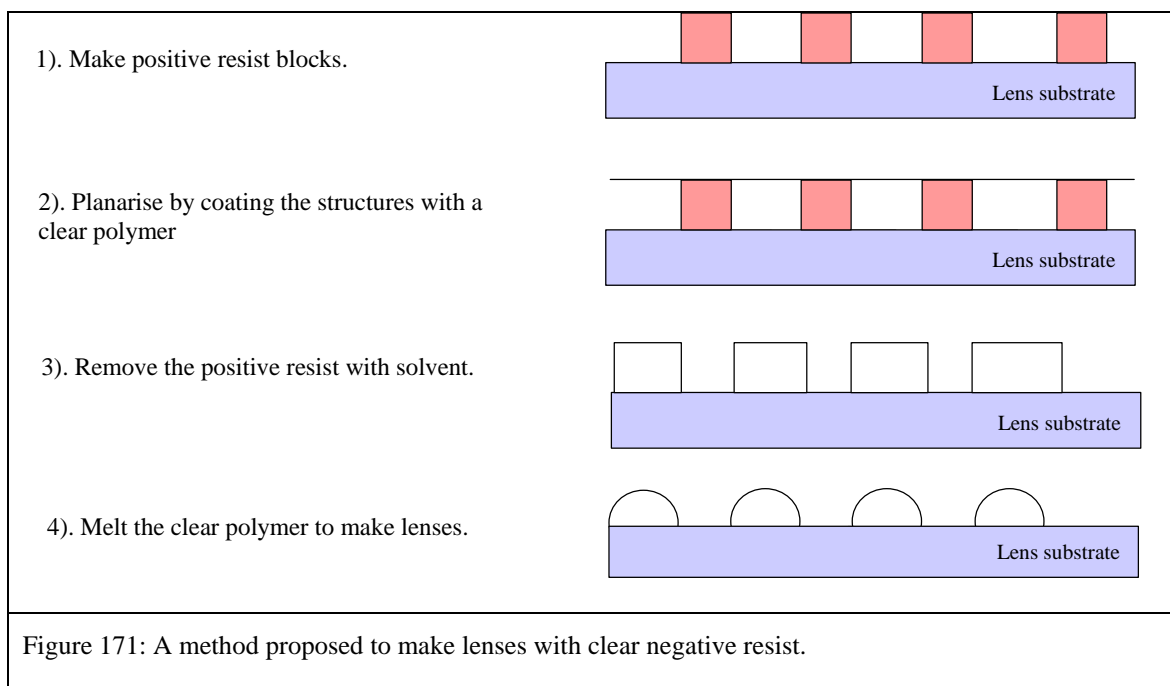
Apart from these problems lenses were formed which focused collimated light to a fine point. Unfortunately the problems associated with this technique could not be overcome.

Another technique was attempted to deposit the resist. That was to deposit the resist with a robotically controlled syringe [60]. This could deposit the resist with sufficient height but the pitch accuracy remained a problem.

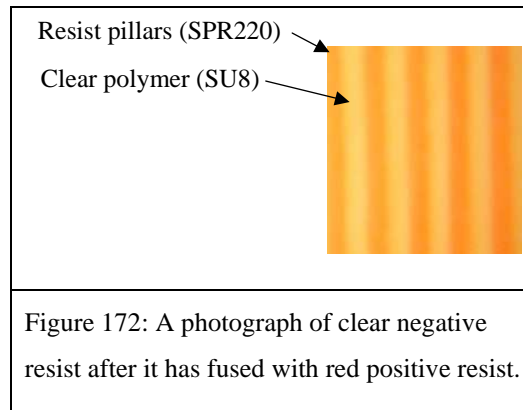
#### 4.2.6 Using resist pillars to shape clear resist

The main problem with method 5 was that the lenses could not be produced with sufficient pitch accuracy. Lithography is quite unique because of its ability to produce high positional accuracy. Therefore lithography was used to position blocks of clear resist, however in this process the negative resist was never exposed to ultra violet light so that it remained possible to melt them to form lenses at a later stage.

The process proposed was as follows.



## Results and comments



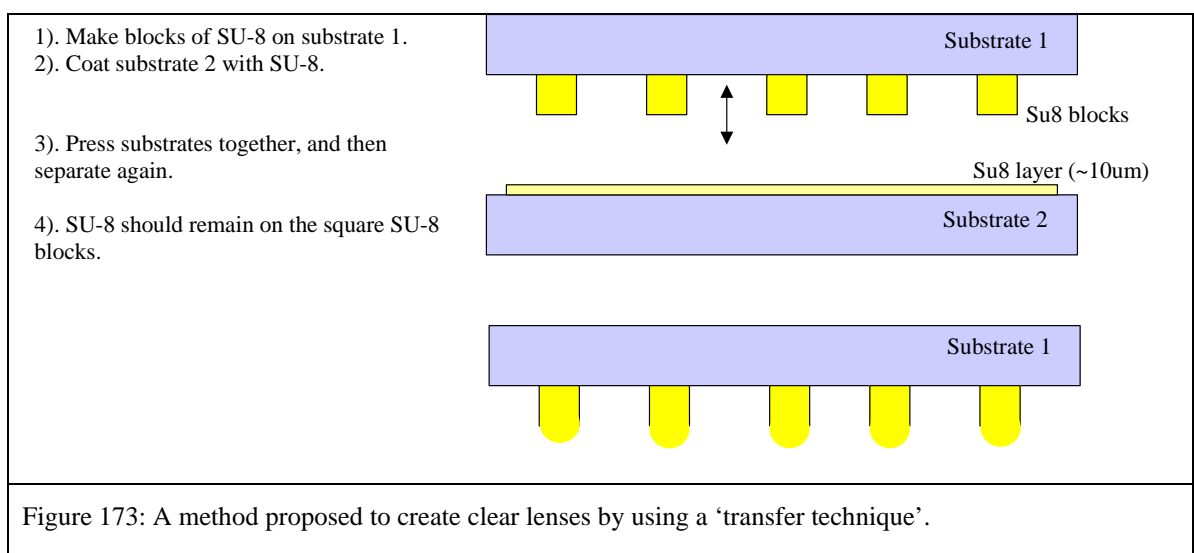
The photo opposite shows how (with the materials used in this experiment) the clear polymer and the resist pillars fused together making them impossible to separate.

The idea was not developed further due to the effort that may be required to find compatible materials. The technique could work if suitable material were found.

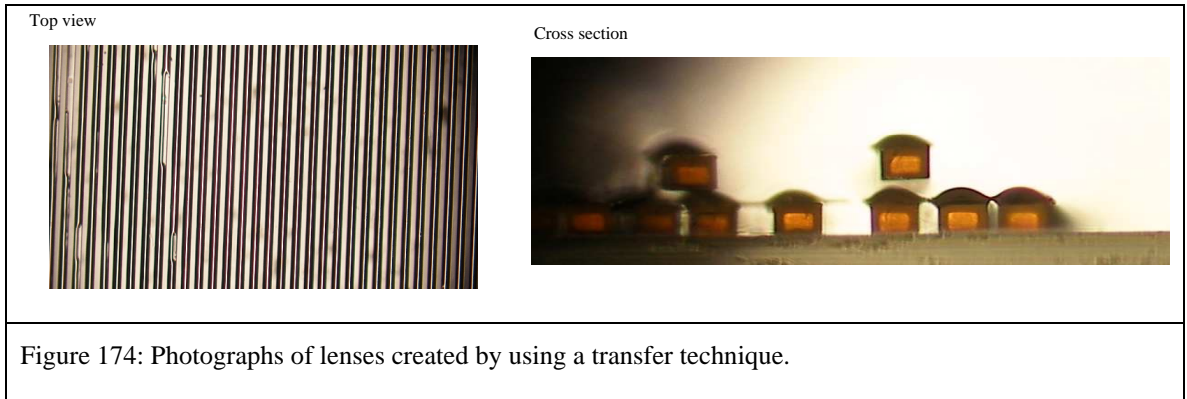
### 4.2.7 Lenses by transfer technique

It was known [61] that the tops of micro structures could be coated with a liquid by immersing their tips into a thin layer of the liquid which is formed by spin coating for example. It was suggested that if the liquid had the correct viscosity and thickness the liquid may form micro-lenses.

The method proposed was as follows.



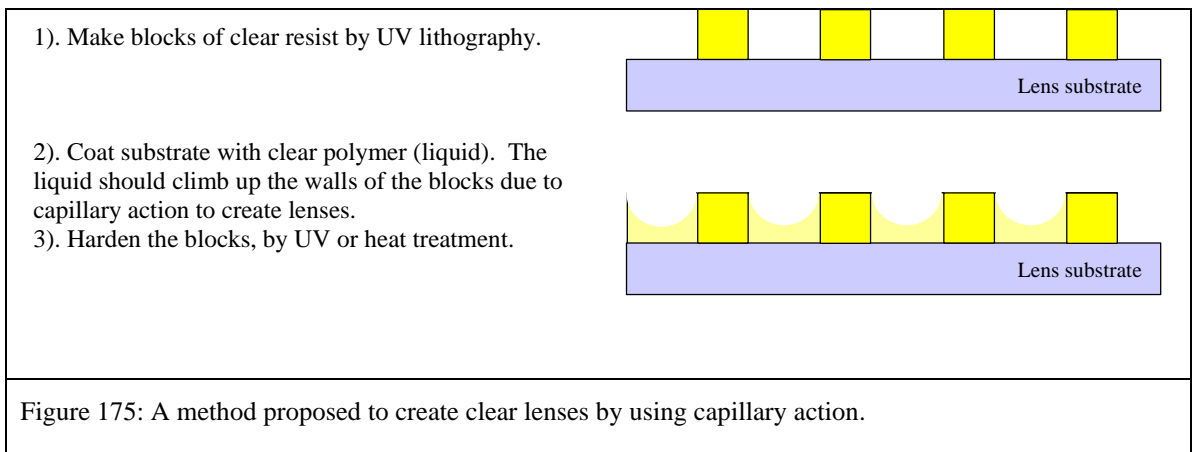
## Results and comments



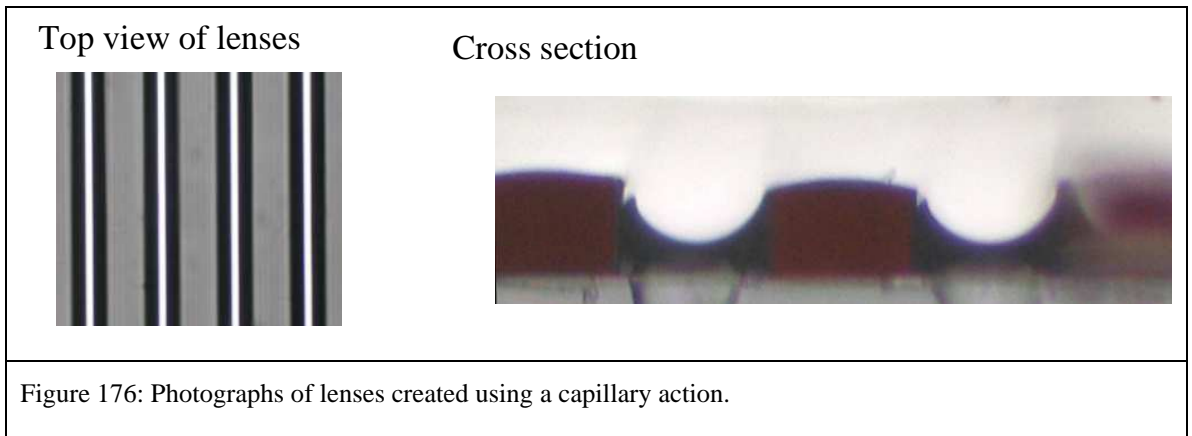
The technique substantially works. The lenses focus collimated light to a fine line (as shown in the top view). However the substrate uniformity is not good, and the lenses are shallower than needed. There is potential to develop this technique but the process looks inherently prone to defects.

### 4.2.8 Capillary lenses

Water in a tube will rise up at the edges of the tube due to capillary effects. It was thought possible that this effect might be used to create micro lenses. The following method was proposed.



### *Results and comments*



Lenses were successfully made by spinning a UV-curable polymer over resist blocks. The lenses work well to focus a collimated source as can be seen in the top view of the lenses. This is a very simple process giving lithographic pitch accuracy, high focal power lenses, with almost no transmission losses in the visible spectrum. These lenses could be produced using Sharp's standard lithographic manufacturing facilities.

This process was developed into a working dual view lens system in section 4.4.

#### **4.2.9 Embossing**

The procedure for embossing goes as follows. A mould is created (usually by diamond tooling) of the lens structure. This mould is pressed into a UV curable polymer. The polymer is exposed to UV light so that it solidifies and then the mould is removed.

In this case the mould was created by replicating the red lenses of section 2. The red lenses were created as in section 2 and then coated them with aluminium and Teflon to make them 'non stick' [62]. The mould was made by coating the 'non stick' red lenses with liquid silicon rubber which solidifies with time [63]. After the silicon rubber was removed it was used as the mould for the UV curable polymer.

### *Results and comments*

This technique is a variation on a standard technique that is known to work. The lenses were embossed into a thin 60  $\mu\text{m}$  layer of UV-curing glue on glass that was hoped to be thin enough so that the glass prevents the polymer from expanding thermally. This method is potentially a suitable process for manufacture provided thermal expansion does not cause problems.

The technique was successful and clear lenses were produced. This technique has a problem associated with the addition of black mask between the lenses. If the black mask was deposited on the glass substrate then the lenses would be separated from the black mask by the thickness of the UV polymer. This would create an unacceptable parallax between the lenses and black mask. Adding the black mask on top of the UV polymer solved this problem. This was achieved as shown in the figure below.

This process was developed into a working dual view lens system in section 4.3.

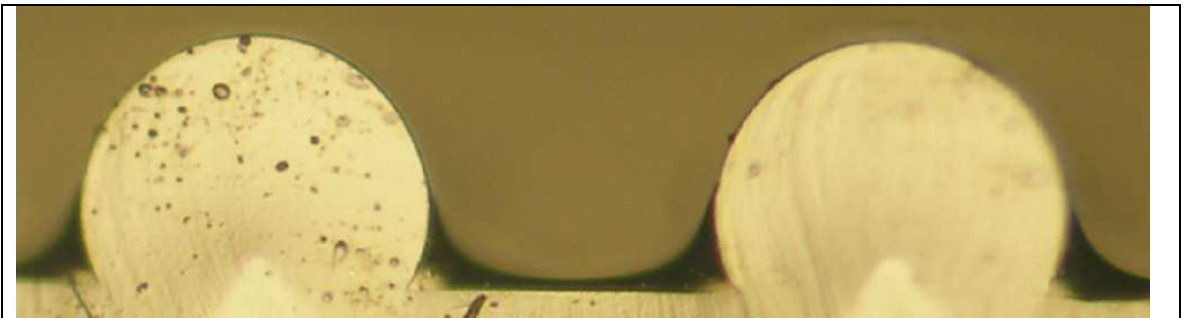


Figure 177: A cross sectional photograph of embossed lenses with black mask. The black mask used was a liquid solution that was coated onto the lenses. The dye naturally falls between the lenses. The lenses were made very tall (by using a thick layer of positive resist to create the mould) to help the dye fall between the lenses. The dye rises up the sides of the lens a little but, due to the extra lens height, the lens aperture is not significantly reduced.

#### **4.2.10 Patterned de-wetting.**

If the adhesion between a photo resist and a substrate is poor then the surface tension of the photo-resist will pull the photo resist together into a bead like a water droplet on glass. This is shown in the following photograph [64].

Therefore if the adhesion could be patterned so that there are lines of high and low adhesion, a resist coated over the lines might naturally form into micro-lenses.

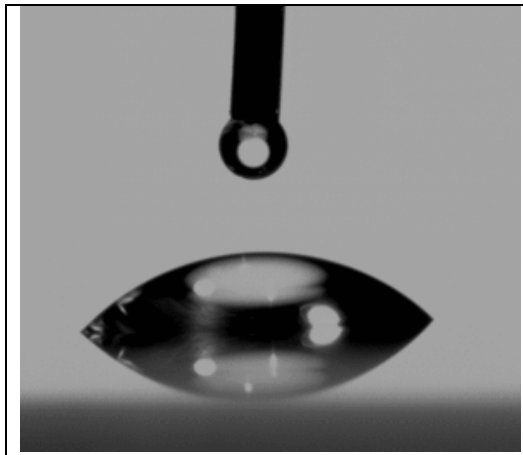


Figure 178: A photograph of a water droplet on a glass surface.

### *Results and comments*

Attempts were made to reduce the adhesion between resist and glass by using polyimides. This did not reduce the adhesion sufficiently to cause the resist to de-wet from the substrate. The only material that was found to cause de-wetting was a Teflon coating. Scratching this layer did enable crude micro-lenses to form, but the Teflon coating could not be patterned into lines. The method that was proposed to do this was to coat the Teflon with resist, pattern the resist lithographically, and then etch away the Teflon in the unprotected regions. Unfortunately no resist could be found that stuck to the Teflon. Therefore this idea was abandoned.

### **4.3 Embossing clear micro-lenses**

Clear lenses were made as in appendix 4, which also has an explanation of the manufacturing steps.

A summary of the system is shown in Figure 179.

## Embossed clear lens demo

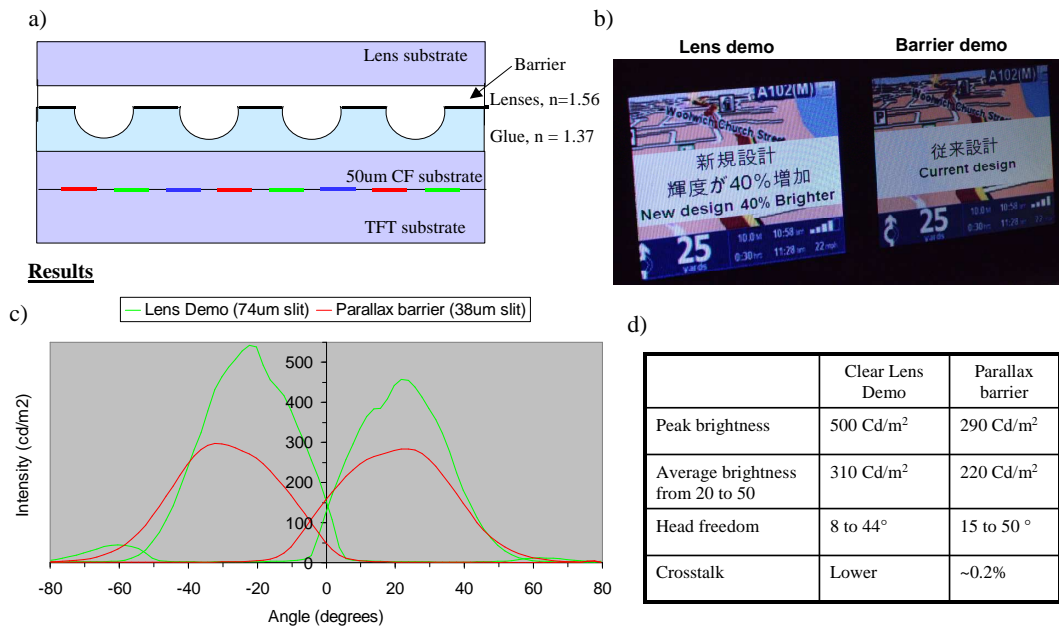


Figure 179: a) a cross section of the embossed lens demo structure. B). A photo of the embossed lens demo and conventional barrier system side by side. C) shows the brightness of the embossed lenses with angle, and d), shows the key performance statistics of the system.

The clear lens system demonstrates;

- **Peak brightness:** of 1.7 x that of a parallax barrier.
- **Thermal expansion** of embossed lenses: Thermal variation in the lens pitch matches that of the pixels on the LCD glass since there is no noticeable degradation in performance from 20 to 50 °C. It is thought that the polymer wants to expand due to its large thermal expansion coefficient, but the 700 μm glass substrate holds the 30 μm polymer layer under strain rather than allowing it to expand.
- **A test of theory:** Figure 180 shows the comparison between the experimental test of the embossed lenses and the theoretical prediction of the model. The model is tested in new circumstances, the lenses are now clear not red. In this case the brightness from the model matches the experimental brightness with an  $r^2$  correlation coefficient of 0.987.

### Theory versus experimental data for the embossed lenses system

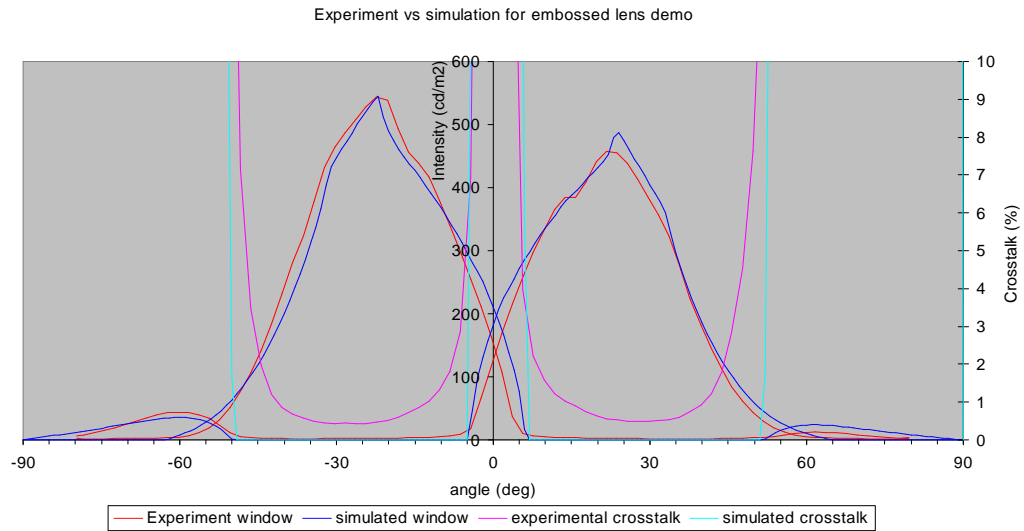


Figure 180: Modelling matches experimental brightness data very well. The model under estimates crosstalk since the model makes no attempt to take into account scattering, diffraction, and other subtle effects.

Note that the head freedom in the clear lens demo is less than that of the red lens demo tested in section 2. It is expected that this is because the clear lenses have a refractive index of 1.56 whereas the red material had a refractive index of 1.65. This reduction in refractive index difference between the lens and the glue reduces the focal power of the lens and so reduces the head freedom.

#### 4.4 Making clear micro-lenses by capillary action

Embossed lenses have a brightness advantage as explained in Figure 181.

### Capillary lenses for dual view

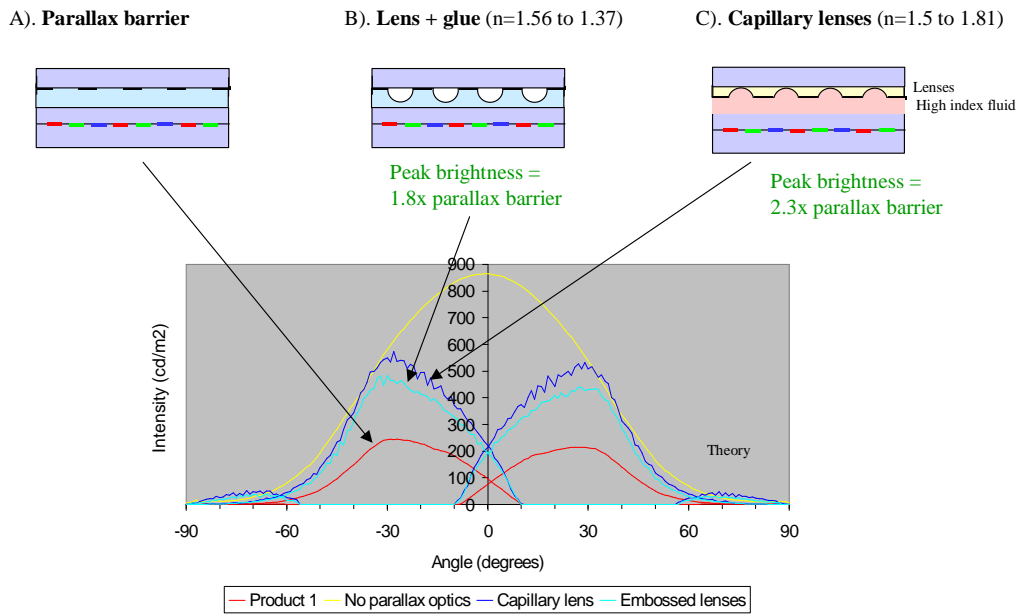


Figure 181: Capillary lenses can be brighter than embossed lenses because of a bigger change in refractive index that can be achieved. The refractive index of the capillary lenses depends on the index of the high index fluid. A fluid could be used with an index of 1.81. In this simulated graph the head freedom has been set from 10 to 56 ° and the system has been optimised (using the software from section 3) given the refractive indices of the different lenses a, b and c. The higher the focal power of the lens the more brightness is achieved.

Capillary lenses are ‘upside down’ compared with embossed lenses, so a different configuration of refractive indices is needed. Figure 182 shows 3 options of achieving this.

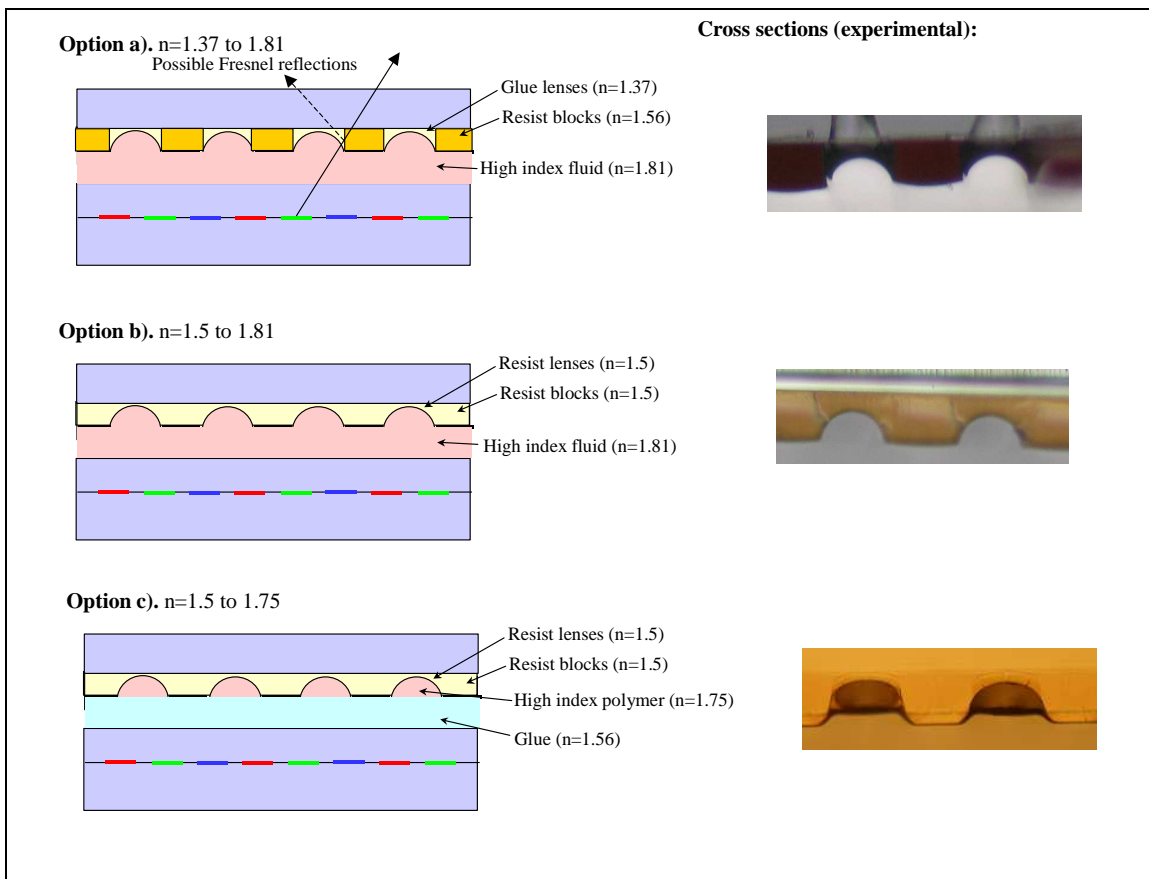


Figure 182: Three options for assembling lenses (formed by capillary action) into a dual view display.

Option a in Figure 182 has the highest focal power, so can achieve the highest brightness. Unfortunately, Fresnel reflections are created by this configuration making it unusable. The extent of the problem is shown in Figure 183 by simulation using Zemax ray tracing software which accounts for the effect of Fresnel reflections. Options b and c are both workable solutions.

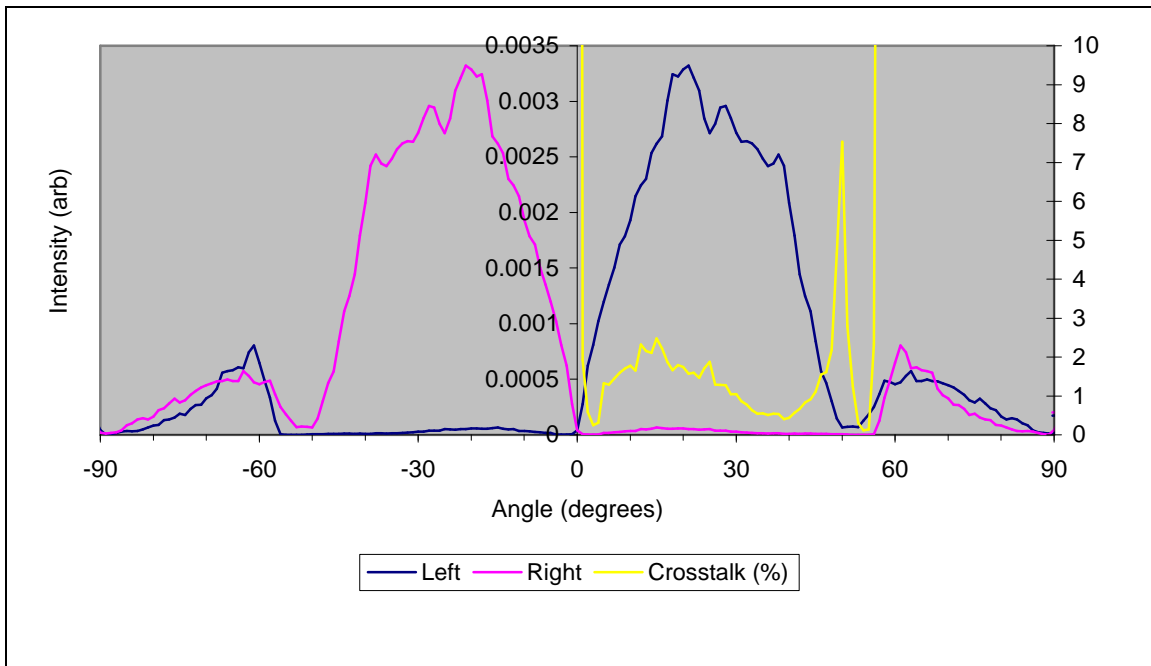


Figure 183: Modelling of crosstalk created by Fresnel reflection in 'low index capillary lenses'. Fresnel reflections occur between the low index glue and the higher index blocks (see Figure 182 option a). The Fresnel reflections would make the device too high in crosstalk, and therefore unusable. This modelling was performed using commercial ray tracing software called 'Zemax'.

Option 'b' was constructed into a dual view display as described in appendix [a], the results are shown in Figure 184.

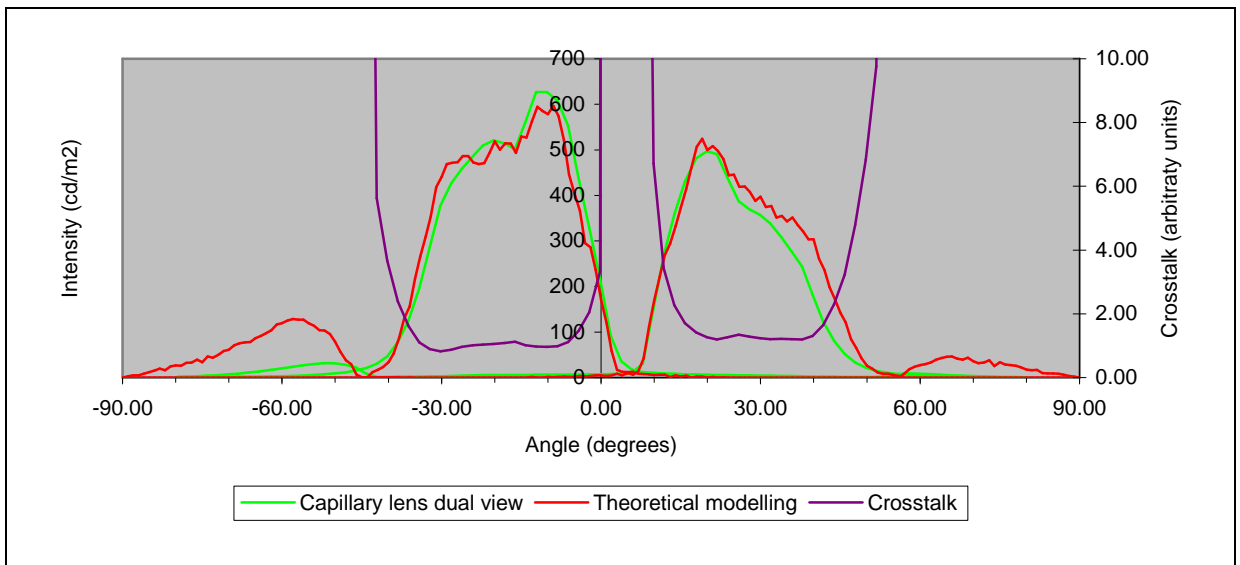


Figure 184: Experimental measurement of a dual view made with a capillary lens system. The device performs well, with reasonable crosstalk and high brightness.

The capillary lens system demonstrates;

- Peak **brightness**: about 2.2 x that of a parallax barrier.

- **Head freedom:** is too narrow in the constructed device. It is believed that this is because the lenses are too far away from the pixels (in error). This problem should be trivial to rectify.
- **Crosstalk** is about 2%. A little high. We believe that this is because the black barrier material does not adhere well to the polymer blocks (it is designed to be coated directly onto glass). The result is that the black material cracks in places and lets light through which causes crosstalk.
- A **test of theory:** The capillary lenses test the model of section 3 in a new situation. The capillary lenses are ‘upside down’ compared with the embossed lenses and this is not taken into account in the model. However, the model still matches the experimental data very well.

## **4.5 Summary**

The work on clear lenses demonstrated a lens system can produce dual view brightness that is 1.7 times that of a parallax barrier system. Two possible manufacturing routes were found to be suitable to create the clear micro-lenses.

# **5. Spin off designs for 3D and VAR**

## **5.1 Novel 3D systems**

The new lens design used for dual view (section 1.3) has fewer aberrations than the conventional 3D system (section 1.1). This allows us to design an autostereoscopic system with novel properties.

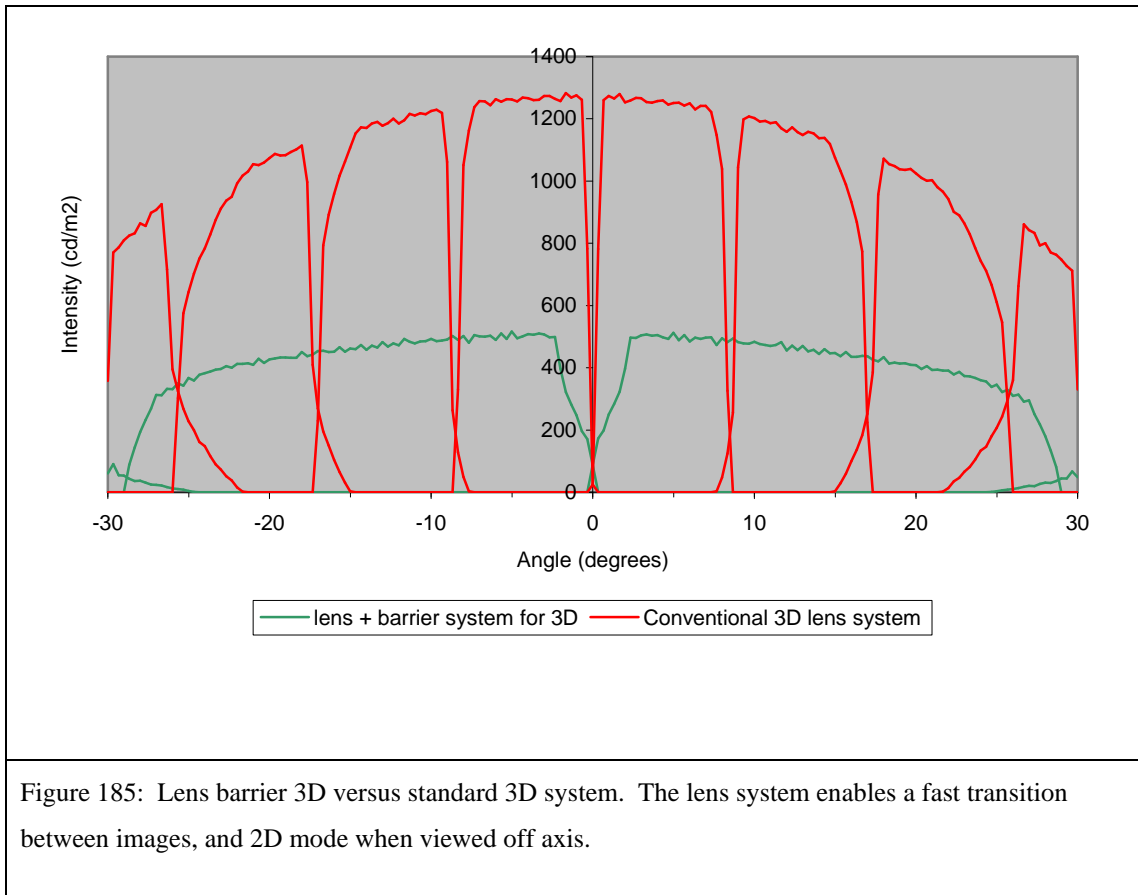
In a 3D system, aberrations blur the image of the pixels, consequently making the transition between left and right images less sharp. From the dual view theoretical model it can be seen that aberrations depend mostly on;

- The size of the lens aperture (small apertures give less aberration).
- The radius of the lens, (shallow lenses give less aberration).

Conventional 3D systems put the lens far from the pixels, this increasing the focal length, and so decreases the radius of the lens required, which decreases aberrations, and gives the fastest transition between left and right images. Fast transition means that the 3D image is viewable for a larger range of head movement.

The new lens system gives a different option for reducing aberrations of the system. Instead of putting the lens far from the pixels, we can put the lens close, and decrease aberrations by reducing the lens aperture.

Figure 185 shows that we can design a 3D system with an acceptably fast image transition, with the lenses close to the pixels. The theoretical model was used to optimise each design.



Putting the lenses close to the pixels gives us a significant advantage. When the user moves off axis, they see just 1 image in both eyes, i.e. a normal 2D image. In the old system the user would see the left and right imaged swapped around. This is an uncomfortable situation for the viewer since perceived depth is reversed. For example, perspective tells the brain that an object is running into the distance, stereoscopic vision tells the brain that it is running into the foreground. This can cause eyestrain and headaches.

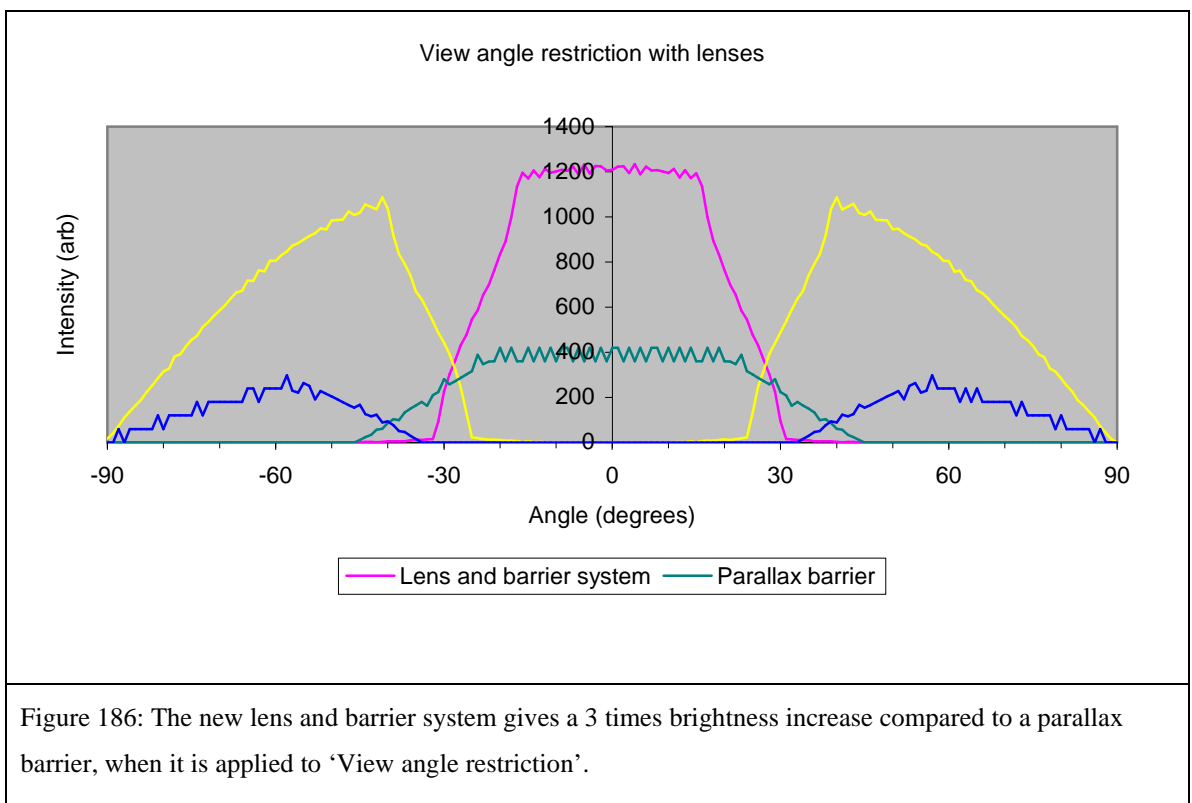
The new lens system is 'fail safe'. If the user is in the wrong position the image looks like a normal 2D image, if they are in the correct place the image jumps into 3D.

## 5.2 Improved view-angle restriction systems

A dual view display can be modified so that image 1 is on axis, and image 2 is visible from the left or right. These displays could be used in cash point machines, where the users data is confidential and is only displayed to the user, whilst surrounding people may be shown adverts.

Parallax barriers can be used achieve this effect, by offsetting them with respect to the pixels. The new lens system can be used to enhance the brightness of these ‘View angle restriction’ systems. In fact the lenses are more effective in this configuration, because the focal length can be longer, and so a bigger lens aperture can be used.

The new lens system gives a 3 times brightness improvement over an equivalent parallax barrier system (Figure 186).



## 6. Summary

A new optical system was designed to create dual view displays. This system was shown to have superior performance to the existing parallax barrier design by theoretical modelling. In comparison to the parallax barrier system the new system was predicted to be 1.8 times brighter with an increase in angular head freedom of 40%. These two parameters are the key parameters for a dual view display. Some thought

and analytical effort was put into improving the design further but no significant improvement was found.

Some methods for making clear micro-lenses with lithographic pitch accuracy were tested and two methods were developed into a complete dual view display. This allowed the device to be tested experimentally and the results substantially line up with the predictions.

A brief analysis showed that this new system might help to improve the performance of privacy and autostereoscopic 3D displays.

No previous literature was found that describes this type of system and so broad patent coverage has been filed for the device. This patent protection looks set to give Sharp displays a significant advantage over its competitors.

# SUMMARY

In 2002 Sharp was asked if they could make a new type of LCD display for a car. This display would be placed in the central console between the passenger and the driver, and it should show one image (such as GPS data) to the driver, whilst the passenger who views the display from a different angle could see different content (such as a movie).

Through a number of years of research this idea has been advanced from a concept to a commercial product. This process involved numerous people from disciplines such as engineering, sales, and marketing. My most significant contributions have been in pioneering the device and gaining a fundamental understanding of how the optics in such systems work. This has enabled me to create improved designs with higher efficiency and lower crosstalk.

I was asked to develop a dual view display because I had previously worked on stereoscopic 3D displays. These displays are very similar to dual view displays because they show different images to different angles. Instead of showing different images to different people they show a different perspective of an image to each eye, thus replicating the sense of depth that is seen in the natural world. In fact a 3D display can be redesigned to create a dual view display by decreasing the distance between the display pixels and the 3D optics. However to create a dual view display the optics would need to be placed about 80  $\mu\text{m}$  from the pixels which was at first thought to be unfeasible. This meant that the main objective was to find an alternative method that did not require small pixel-optic separation. Through experience of 3D systems a dual view device was created with a large pixel-optic separation by grouping pixels. The device showed a good dual view effect, but the image quality was fundamentally poor.

A new design was created that could potentially produce dual view with a large pixel-optic separation and high image quality. This design is the subject of chapter 2 in which the design is optimised theoretically and tested experimentally. The conclusion was that the display was too complicated and suffered too much crosstalk – that is to say the passenger image would be seen as a faint ghost image by the driver causing a potential distraction hazard.

It was decided that the use of a small pixel-optic separation was the most feasible method for creating a dual view display and this was achieved by the engineering efforts

of Sharp Japan. This design produced less crosstalk than that of chapter 2 but it was still visible. Crosstalk is a known problem in 3D displays where 5% crosstalk is common and acceptable. Human factors experiments were carried out and it was shown that in a dual view display less than 0.02% crosstalk is required for zero visibility. In order to achieve such low levels of crosstalk it was necessary to gain a more complete understanding of the sources of crosstalk the system than had ever been achieved before. This is the subject of chapter 3. Crosstalk was analysed through a combination of modelling and experimental tests to gain a quantitative break down of very low level crosstalk sources. The main sources of crosstalk were found to be diffraction, scatter in the polariser and view films of the LCD, and electrical interference within the display electronics. Counter measures were implemented into the system and a dual view display with approximately 0.05% crosstalk was produced. The distraction hazard from this level of crosstalk is thought to be minimal.

The design of chapter 3 was implemented in the world's first mass-produced dual view display which was launched in July 2005. The display worked well but its efficiency and the amount of head freedom within each view would both benefit from improvement. By considering bright but high crosstalk lens systems, and dim but low crosstalk parallax barrier systems a new design was created that was a hybrid of the two. This design works particularly well for dual view but can also be used to improve 3D displays and privacy displays. It is the subject of chapter 4 in which the design is optimised and tested. A customised ray tracing and optimisation package was written which can identify the parameters which give the most efficient dual view display. Prototyping of the device proved that it could produce dual view with 1.7 times greater brightness than the first Sharp product or a 40% increase in angular head freedom. With such good performance proven it was necessary to identify how the micro-lenses in the design could be manufactured. A number of different possibilities were considered and a method was found that could easily be integrated into an existing production line. This technology is ready to go into the next generation of Sharp's dual view displays. Through the research in this thesis a fundamental understanding of multi-view display optics has been achieved and this knowledge has been used to improve Sharp's products.

# APPENDICES

## Appendix 1

*Procedure for creating a lens-barrier dual view system with red lenses made by re-flowing resist*

*Creating the parallax barrier*

1. Clean glass.
2. Create a parallax barrier by using black photo-resist and a lithographic process.

*Creating the red micro-resist lenses*

1. Coat photoresist SPR220 by spinning. SPR220 thickness should approximately equal the lens radius for hemi-cylinder lenses. (e.g. a 60  $\mu\text{m}$  thick coating for 120  $\mu\text{m}$  diameter lenses).
  - a. 1000 rpm, 30 seconds, 400 rpmps – gives a  $\sim 20$   $\mu\text{m}$  coating.
  - b. Hotplate 50  $^{\circ}\text{C}$  1 minute.
  - c. Hotplate 115 $^{\circ}\text{C}$  for 4 minutes.
  - d. Hotplate 25 $^{\circ}\text{C}$  for 3 minutes.
  - e. Repeat for more 20  $\mu\text{m}$  coatings as necessary.
2. Expose resist to  $\sim 1.3$   $\text{J}/\text{cm}^2$  at 365 nm for 40  $\mu\text{m}$  of resist (exposure will need to be increased for thicker layers).
3. Develop in Shipley 351CD31 developer for about 10 minutes.
4. Rinse with water, and dry.
5. Hotplate 70 $^{\circ}\text{C}$  for 3 minutes to ensure resist is dry (water causes the resist to bubble on melting).
6. Melt the lenses on a hotplate at 140 $^{\circ}\text{C}$ . Stop when the lenses have been formed (after approximately 30 seconds to 1 minute). This can be seen by a change in substrate reflectivity.
7. Expose the lenses to intense white light from an arc lamp for 3 days to increase the lens transmission.

## Adhering the lens-barrier substrate to the LCD panel

1. Apply low refractive index glue to the LCD panel (custom made by Optical polymer research Inc.).
2. Lay the lens-barrier substrate onto the panel.
3. Place system in a vacuum for 20 minutes to degas the photoresist lenses.
4. Align the lenses with the pixels so that the moiré fringe is straight and on-axis.
5. Expose the glue to  $\sim 0.3 \text{ J/cm}^2$  to cure the glue.

## Appendix 2

### Instructions for using the simulation tool for the lens-barrier dual view system

#### Simulating a known design

The screenshot shows the 'Design' tab of the simulation tool. It is divided into several sections: 'Parallax Optic' with radio buttons for 'Parallax barrier' and 'Parallax barrier + lens'; 'Barrier Separation' with input fields for 'Glass thickness' (50 um) and 'Glue thickness' (42 um); 'Lens and barrier' with input fields for 'Lens radius' (40 um), 'Slit width' (68 um), 'Barrier offset' (0 um), and 'Viewing distance' (700 mm); and 'Refractive Indices' with input fields for 'Glass' (1.52), 'Glue' (1.37), and 'Lens' (1.56).

a). Enter design details.

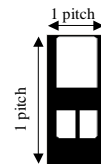
Note: this model can be used for parallax barriers and for lens designs.

The screenshot shows the 'Pixel shape' tab of the simulation tool. It has radio buttons for 'Load from picture' and 'Use general pixel shape'. The 'Pixel x pitch' is set to 65 um. There is a visual representation of a pixel with a central aperture. The 'Pixel x aperture' is 44.5 um and the 'Average y aperture' is 100 um. A file path 'Product1 Pixel.bmp' is shown at the bottom.

b). Enter pixel details.

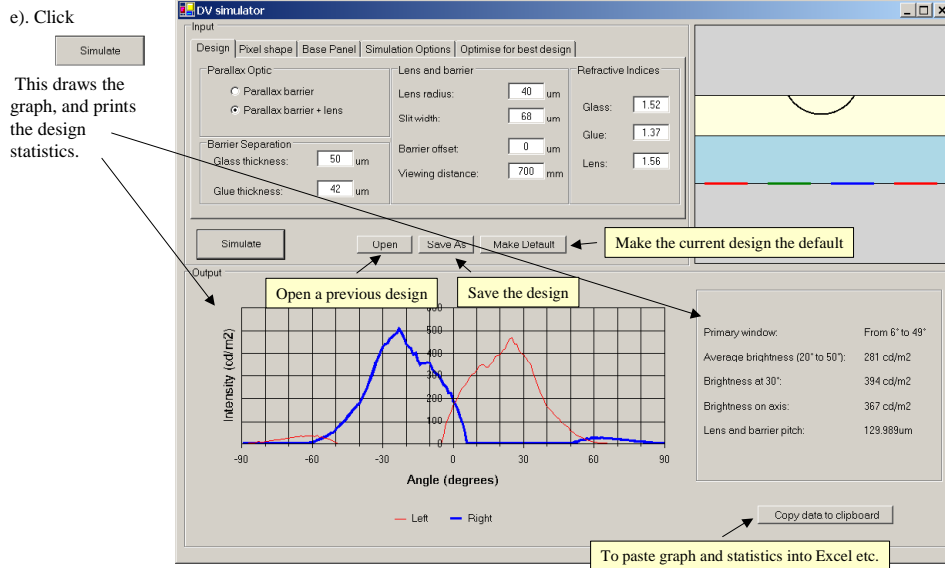
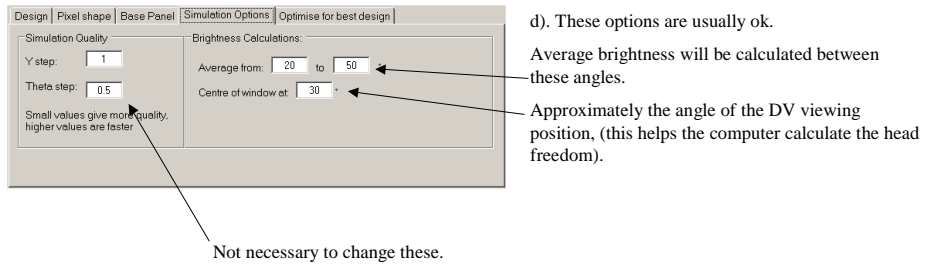
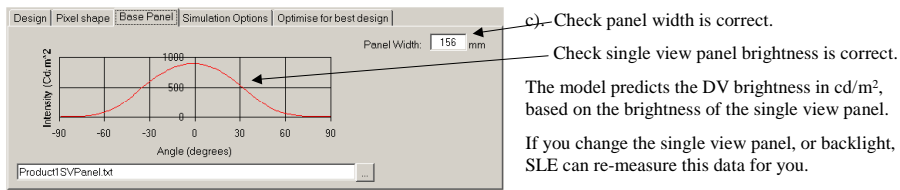
If you have a pixel bmp;

- Click to open it.
- Pixel bmp must be the correct size:



If you do not have a pixel bmp;

- Click Use general pixel shape
- Enter pixel details.



## Finding the best design

a). Enter design details as for example 1.

The screenshot shows the 'Optimise for best design' panel with the following settings:

- Parallel Optic:**  Parallel barrier + lens
- Barrier Separation:** Glass thickness: 50  $\mu\text{m}$ , Glue thickness: 42  $\mu\text{m}$
- Lens and barrier:** Lens radius: 40  $\mu\text{m}$ , Slit width: 68  $\mu\text{m}$ , Barrier offset: 0  $\mu\text{m}$ , Viewing distance: 700 mm
- Refractive Indices:** Glass: 1.52, Glue: 1.37, Lens: 1.56

The model can adjust the following parameters to give the best design;

- Glass thickness, glue thickness.
- Lens radius, slit width.
- Pixel x aperture

Enter any value for the unknown parameters.

The screenshot shows the 'Optimise for best design' panel with the following settings:

- Head Freedom:** From: 10 to 56, Estimated time left: [blank]
- Optimisation parameters:**
  - Lens radius or slit width
  - Barrier separation
  - Pixel aperture

b). Set head freedom requirements.

Click

The computer will find the design with the best average brightness that meets the head freedom.

Choose which parameters to optimise here.  
E.g.

Optimisation parameters

- Lens radius or slit width
- Barrier separation
- Pixel aperture

Gives best lens parameters for a fixed pixel aperture.

Optimisation parameters

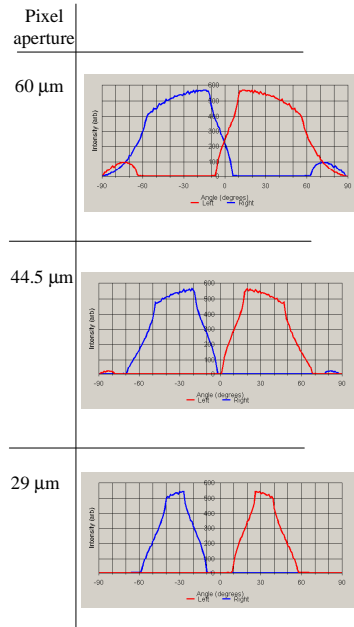
- Lens radius or slit width
- Barrier separation
- Pixel aperture

Gives best best lens, and pixel aperture.

## Appendix 3

### *The effect of different parameters on the angular light output distribution of a lens-barrier dual view system*

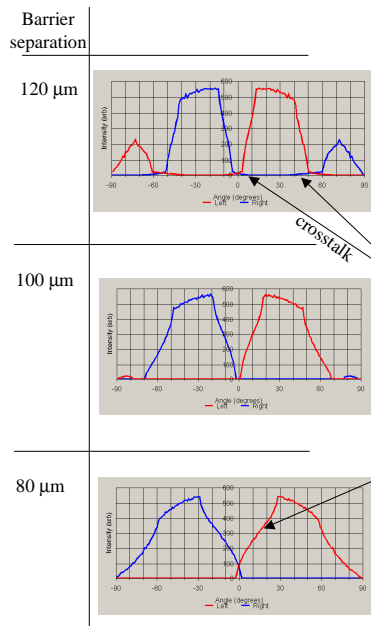
#### Parameter 1: Pixel aperture ratio



Changing pixel aperture ratio makes the windows wider or narrower.

**(Other parameters)**  
 Barrier separation=100 µm  
 Glue index=1.37  
 Lens index= 1.65  
 Lens radius =32.5 µm  
 Slit half width =32.5 µm

#### Parameter 2: Barrier separation



Changing barrier separation for lens + barrier has similar effect as for a parallax barrier.

It changes:

- Image separation angle.
- Angle of secondary windows.
- Image mixing region.

In addition:

- If barrier separation is too much, the lens becomes out of focus and crosstalk occurs, (use a bigger lens to solve this).
- If barrier separation is too small, no crosstalk occurs, but the intensity rises slower here.

crosstalk

**(Other parameters)**  
 Pixel aperture= 44.5 µm  
 Glue index=1.37  
 Lens index= 1.65  
 Lens radius =32.5 µm  
 Slit half width =32.5 µm

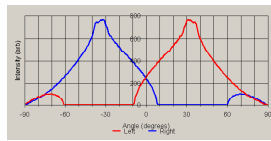
Parameters 3 and 4: Lens radius and slit width

(for half cylindrical lenses)

Lens radius and slit width

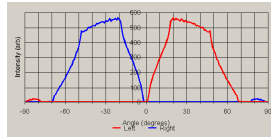


Lens radius 46  $\mu\text{m}$   
Slit half width 46  $\mu\text{m}$



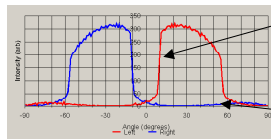
•Big lens radius = brighter, but less head freedom.

Lens radius 32.5  $\mu\text{m}$   
Slit half width 32.5  $\mu\text{m}$



•Smaller lens radius = dimmer, but more head freedom and makes intensity rise quicker here.

Lens radius 19  $\mu\text{m}$   
Slit half width 19  $\mu\text{m}$

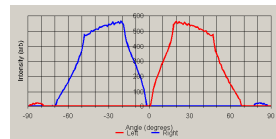


•Changing lens radius also changes the lenses focal length, so the barrier separation must be adjusted accordingly to remove crosstalk here

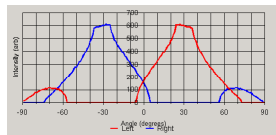
Parameters 5 and 6: lens and glue refractive index.

Lens and glue refractive index

Lens index 1.65  
Glue index 1.37



Lens index 1.59  
Glue index 1.45



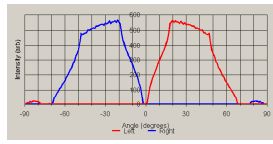
Lower  $\Delta n$  means less head freedom or less brightness.

$\Delta n$  should be as large as possible for DV.

## Parameter 7: Lens radius

Lens radius and slit width

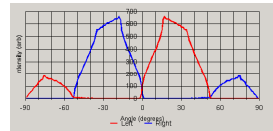
Lens radius 32.5  $\mu\text{m}$   
Slit half width 32.5  $\mu\text{m}$



(for half cylindrical lenses)



Lens radius 43  $\mu\text{m}$   
Slit half width 32.5  $\mu\text{m}$



(for shallow lenses)



Shallow lenses:

- make secondary windows visible at lower angles (bad).
- increase central image mixing (bad).
- increase brightness a little at 30 degrees, so it may be possible to get a slight advantage from them (to be investigated).

Probably, half cylindrical lenses are best, shallow lenses should not be used.

## Appendix 4

*Procedure for creating a lens-barrier dual view system with clear lenses made by embossing*

*Creating the red micro-resist lenses*

1. As described in appendix 1.

*Embossing from the red lenses*

1. Coat the red lenses with 100 nm of aluminium by vapour deposition.
2. Mix Teflon coating. Mix PTFE and Fluoroinert solvent in a ratio of 1:50. Leave for about 1 day to dissolve.
3. Spin coat Teflon over the red lenses at 3000rpm. Hotplate at 60°C for 10 minutes.
4. Mix silicon rubber (P4) with its hardener, in a ratio of 10:1.
5. Place in a vacuum until all bubbles are removed from the silicon mixture (about 5 minutes).
6. Pour silicon rubber onto a glass substrate, and lay the red lenses face down in the silicon rubber to create a negative copy of the lenses.
7. Wait for 16 hours for the silicon rubber to set.

8. Separate the red lenses from the silicon rubber.
9. Coat the silicon rubber mould in UV curable glue (Norland optical adhesive 71). Press a glass substrate into the glue, and cure for about 1 hour at 0.1 mW, 365 nm UV, (e.g. from a fluorescent UV tube). The glue will take the shape of the original red lenses.
10. Separate the silicon rubber from the UV glue.

*Forming a black barrier in between the lenses*

1. Spin coat PSK2000 over the glue to form a black barrier in between the lenses. The faster the spin speed the thinner the black mask layer will be, but the more the black will over lap with the lenses. A spin speed of about 1500rpm is good for lenses with 50% fill factor.

*Adhering the lens-barrier substrate to the LCD panel*

1. Apply low refractive index glue to the LCD panel (custom made by Optical polymer research Inc.).
2. Lay the lens-barrier substrate onto the panel.
3. Align the lenses with the pixels so that the moiré fringe is straight and on-axis.
4. Expose the glue to  $\sim 0.3 \text{ J/cm}^2$  to cure the glue.

**Appendix 5**

*Detailed acknowledgements*

*Chapter 1*

Section and subject	Whose idea was it	Who did the research
1.1 What is a dual view display	As referenced	The literature was interpreted by <b>JM</b> .
1.2 Why are dual view displays needed		
2. Dual view prior art		
2.1 Dual view paintings		

2.2 Dual view toys - still images		
2.3 Dual view displays		
2.3.1 Concept		
2.3.2 Multi-view		
2.3.3 Parallax barrier dual view		
2.4 Dual view prior art summary		
3.1 What are auto-stereoscopic 3D displays		
3.2 Parallax optic technology		
3.2.1 Basic design principles for 3D		
3.2.2 Extension of parallax barrier design principles to dual view	<b>JM</b>	<b>JM</b>
3.2.3 Techniques to increase image splitting		
Reduced pixel-barrier separation	<b>JM, DK, RW, GB, AN</b>	<b>JM</b> - dual view optics design MBLC – Dual view panel production
Rotated pixel designs	<b>JM, GJ, DK, DM</b>	-
Grouped pixel designs	<b>JM, DK</b>	-
First prototype design	<b>JM</b>	<b>JM</b> – construction of prototype
Increased refractive index	<b>JM</b>	-
3.2.4 Techniques for switching dual view	<b>JM</b>	-
3.2.5 Time multiplexing to increase resolution	As referenced	The literature was interpreted by <b>JM</b> .
3.2.6 Techniques to make a black central window – directional backlighting	<b>EW, JM, NB, DK</b>	<b>JM, NB</b>

3.2.7 Crosstalk reduction	As referenced	The literature was interpreted by <b>JM</b> .
3.3 Alternative methods of image splitting	<b>JM, DK</b>	<b>JM, DK, HS</b>
4. A spin off application for dual view	Mr K Sato	-

### *Chapter 2*

Section and subject	Whose idea was it	Who did the research
All sections	<b>JM</b>	<b>JM</b>

### *Chapter 3*

Section and subject	Whose idea was it	Who did the research
1.1 Description of the new design	Common knowledge	Designed by <b>JM</b> , built by MBLC.
Experiment vs. prediction based on geometric optics	<b>JM</b>	<b>JM</b>
1.2 The crosstalk problem	-	<b>JM</b>
2.1 Hypothesis on the causes of crosstalk	<b>JM</b>	-
2.2.1 Test images	<b>JM</b>	<b>JM</b>
2.2.2 Observations of single view panel.	<b>JM</b>	<b>JM</b>
2.2.3 A redesign of the panel electronics	MBLC	MBLC
2.3.1 Test images that show optical crosstalk.	<b>JM</b>	<b>JM</b>

2.3.2 Measurement of crosstalk	<b>JM</b>	Work on stray light reflections – <b>JM</b> .  Work on Azimuthal angle misalignment – LPJ, <b>JM</b> .  Robotics built by Heason Technologies ltd.  Use of Eldim system – <b>JM</b> .
2.3.3 Microscope pictures of optical crosstalk.	<b>JM</b>	<b>JM</b>
2.3.4 Further discussion supporting diffraction as a cause of crosstalk	DM	DM, <b>JM</b> .
2.3.5 Further investigation of light leakage through the parallax barrier	<b>JM, DK</b>	<b>JM</b>
2.3.6 A new panel design	MBLC	Manufacture - MBLC  TFT design - MBLC  Pixel apertures and barrier design – <b>JM</b>
2.3.7 Further evidence of diffractive crosstalk	<b>JM</b>	<b>JM</b>
2.3.8 Could crosstalk be caused by edge reflection?	<b>JM</b>	<b>JM</b> except for edge reflection modelling – EL, SEM pictures – JY
2.3.9 Could reflections from the underside of the barrier cause crosstalk?	<b>JM</b>	<b>JM</b> except for the measurement of Konica Minolta index - EL
2.3.10 Could crosstalk be caused by scatter at the polariser?	<b>JM, GB, DK</b>	Experiment designed and carried out by <b>JM</b> .
2.3.11 Experimentation on a giant dual view model	<b>JM</b>	<b>JM</b>

3.1 Review of factors influencing crosstalk visibility	DK	DK, <b>JM</b>
3.2 Experiments specific to dual view crosstalk visibility	<b>JM</b> , DK	<b>JM</b> , DK
3.3 Human factors techniques to reduce crosstalk visibility	<b>JM</b> , DK	<b>JM</b> , DK
4.1.1 Crosstalk correction for electrical crosstalk	<b>JM</b> , DK	<b>JM</b>
4.1.2 Redesign of TFT layout to reduce parasitic capacitance.	MBLC	MBLC
4.2.1 Crosstalk correction	GJ	GJ, <b>JM</b> , DK
Soft edge barriers	Concept – DM Prototyping technique - <b>JM</b>	<b>JM</b> except for, SEM pictures and RIE etching – JY, manufacture of the barriers – <b>JM</b> , PF
Directional backlighting	<b>JM</b>	<b>JM</b>
Image separation angle	<b>JM</b>	<b>JM</b> , DK
Rotated pixels	<b>JM</b> , DK	<b>JM</b>
4.2.2 Reducing crosstalk from the polariser	<b>JM</b>	<b>JM</b> , LPJ

#### *Chapter 4*

Section and subject	Whose idea was it	Who did the research
1.2 Why the 3D lenticular system does not work for DV	<b>JM</b>	<b>JM</b>
1.3 New lenticular design for DV	<b>JM</b>	<b>JM</b>
1.4. What is the best lens + barrier design?	<b>JM</b>	<b>JM</b>

1.4.1 Spherical lenses + barrier	<b>JM</b>	<b>JM</b>
1.4.2 Prisms + barrier	<b>JM</b>	<b>JM</b>
1.4.3 The ultimate refractive surface for dual view	<b>JM</b>	<b>JM</b>
1.4.4 Can we make the custom lens shape brighter?	<b>JM</b>	<b>JM</b>
1.4.5 Summary of theoretical parallax optic designs	<b>JM</b>	<b>JM</b>
2. Experimental testing of the device	<b>JM</b>	<b>JM</b>
2.1 Why test the device?	<b>JM</b>	<b>JM</b>
2.2 How to make the lenses	<b>JM</b>	<b>JM</b>
2.2.1 Prototyping by photo-resist micro-lenses	<b>JM</b> + [55]	<b>JM</b> – proof of concept <b>JM, MS</b> – manufacture of high quality prototype.
2.2.4 Further observations on contrast ratio	<b>JM</b>	<b>JM</b>
3. Optimisation tool for lens + barrier design		
3.1 Requirements of the theoretical model	<b>JM</b> + MBLC	
3.2 Assumptions used	<b>JM</b>	<b>JM</b>
3.3 Experiment versus theory	-	<b>JM</b>
3.4 Finding the best design	<b>JM</b>	<b>JM</b>
3.4.1 Success criteria for the dual view design	<b>JM</b>	<b>JM</b>
3.4.2 The optimisation algorithm	<b>JM</b>	<b>JM</b>

4.1 Idea proposals	<b>JM</b> except where referenced	
4.2 Experimental testing	<b>JM</b>	
4.3 Embossing clear micro-lenses	<b>JM + MK</b>	<b>JM, MS</b>
4.4 Making clear micro-lenses by capillary action	<b>JM</b>	<b>JM</b> – proof of concept EL – manufacture of prototype.
5.1 Novel 3D systems	<b>JM</b>	<b>JM</b>
5.2 Improved View angle restriction systems	<b>JM</b>	<b>JM</b>

Key:

DM = David Montgomery

DK = Diana Kean

**JM** = Jonathan Mather

LPJ = Lesley Parry Jones

PF= Peter Farah

MBLC = Mobile liquid crystal business group (Sharp Corporation Japan).

Heason = Heason Technologies Group Ltd.

JY = Jin Yu

GB = Grant Bourhill

AN = Akira.Nakagawa

NB = Neil Barret

MK = Marina Khazova

## References

References in [blue](#) are references to work of which I am an author.

---

- 1 “A Brief History of Stereo Images, Printing and Photography from 1692 – 2001”  
Milestones in the ever advancing world of 3D image technology, Frank X. Didik 2001,  
[http://www.didik.com/3d\\_hist.htm](http://www.didik.com/3d_hist.htm)
- 2 United states Patent number 1475430, ‘Advertising device or toy’, John Curwen, filed  
27 Feb 1922.
- 3 <http://www.medialive.ie/Newoutdoor/photo65.html>
- 4 Japanese patent number 6-236152, Nihon Denso, filed 23 Aug 1994.
- 5 Introduction to Liquid Crystals: Chemistry and Physics, P J Collings, Michael Hird,  
Taylor & Francis, 1997.
- 6 Journal of the Society for Information Display , -- Volume 13, Issue 7, pp. 605-608 ,  
Liquid-crystal displays using printed plastic TFT backplanes, T Wilkinson et al., July  
2005
- 7 Japanese patent number H9-046622, Matsushita, Published 14 Feb 1997.
- 8 European patent, EP0999088, Siemens, ‘ Display for motor vehicle’, Christoph Rupp,  
filed 29 Oct 1999.
- 9 United states patent number 6424323, Philips, ‘Electronic device having display’,  
David Bell et al., filed, 23 July 2002.
- 10 Japanese patent number H11-205822, Ricoh, filed 13 January 1998.
- 11 Japanese patent number 2000 – 137443, Sumitomo, filed 16 June 2000.
- 12 Pictures courtesy of <http://images.google.co.uk/>, or are photos taken by colleagues.
- 13 Optimum parameters and viewing areas of stereoscopic full colour LED display  
using parallax barrier, Hirotsugu Yamamoto et al., IEICE trans electron, vol E83-c no  
10 Oct 2000.
- 14 ‘Analysis of the performance of a flat panel display system convertible between 2D  
and autostereoscopic 3D modes’, David J. Montgomery et al, SPIE 2001.
- 15 Discussion with David Montgomery of Sharp Laboratories of Europe Ltd.
- 16 Japanese patent number 2004-231737, Sharp Laboratories of Europe Ltd, ‘Multiple  
view directional display’, Jonathan Mather et al., filed 13th August 2003.
- 17 United states patent number 11/223206, Sharp Laboratories of Europe Ltd,  
‘Techniques to put a Barrier close to an LCD’, Jonathan Mather et al., filed 30th August  
2003.

- 
- 18 United states patent number US05850269B1, Samsung, 'Liquid crystal display device wherein each scanning electrode includes three gate lines corresponding separate pixels for displaying three dimensional image', published 15<sup>th</sup> December 1998.
- 19 United States patent number 6791570, "Method and device for three dimensional representation of information with viewer movement compensation", Armin Schwerdtner et al., SeeReal Technologies GmbH, filed 15 December 1997.
- 20 Barten, Contrast sensitivity in the human eye and its effects on image quality, Press Monogram, Dec 1999.
- 21 British patent application number 0420945.8, Sharp Laboratories of Europe Ltd, 'Novel Barrier and Colour filter Designs for Multi-View Displays', Jonathan Mather et al, filed 21<sup>st</sup> August 2004.
- 22 J Harrold, A Jacobs, GJ Woodgate, D Ezra, Performance of a Convertible 2D and 3D Parallax Barrier Autostereoscopic Display, Proc SID 20th International Display Research Conference, September 2000, Florida, USA.
- 23 Philips and New Venture Partners announce creation of Liquavista, <http://www.research.philips.com/newscenter/archive/2006/060419-liquavista.html>, April 19, 2006.
- 24 Polymer network liquid crystal, Seiko, <http://www.seiko-denki.co.jp/site/view/contview.jsp?cateid=41&id=358&page=1>, presented at IDW 2005.
- 25 Rewritable Paper Using Leuco Dyes: Coloring/ Decoloring Effects of Long-chain Alkyl Group, S. Yamamoto et al., Advanced Technology, R&D center, Ricoh Co., Ltd., Numazu, Shizuoka, Japan, IDW 2005.
- 26 [http://www.kayelaby.npl.co.uk/general\\_physics/2\\_3/2\\_3\\_6.html](http://www.kayelaby.npl.co.uk/general_physics/2_3/2_3_6.html), [http://www.kayelaby.npl.co.uk/chemistry/3\\_11/3\\_11\\_1.html](http://www.kayelaby.npl.co.uk/chemistry/3_11/3_11_1.html)
- 27 <http://home.earthlink.net/~jimlux/energies.htm>
- 28 Power consumption determined by measurement of a commercially available CCFL automotive backlight, 2005.
- 29 [http://www.spocc.com/main\\_trans.htm](http://www.spocc.com/main_trans.htm)
- 30 British patent number 0611655.2, , Sharp Laboratories of Europe Ltd, 'Switching parallax optics using thermal rewritable technology', Etienne Lesage, Jonathan Mather, filed 13th June 2006.

- 
- 31 Kenneth Erbey, US patent number US6476850, filed October 1998, Apparatus for the generation of a stereoscopic display.
- 32 T.Sasagawa, A.Yuuki, S.Tahata, O.Murakami, and K.Oda , ‘P-51: Dual Directional Backlight for Stereoscopic LCD’, Mitsubishi Electric Corporation, Amagasaki, Hyogo, Japan, SID 2003 digest, p399.
- 33 ‘A display system with 2D/3D compatibility’, G Hamagishi et al, Sanyo Electric Co, SID 98 digest, p915, 1998.
- 34 Japanese patent number 11103475A, Three dimensional color video display - has filter having color sequence opposite to filter in liquid crystal panel display, placed in front of back light, Sanyo electric co ltd., filed 26 Sept 1997.
- 35 Okumura, Tagaya and Koike, “Highly efficient backlight for liquid crystal display having no optical films”, Applied Physics Letters, vol 83, no. 13, p2515, 29th September 2003.
- 36 World patent number WO2005/071474, Sharp Laboratories of Europe Ltd, ‘A multiple view display and a multi-direction display’, Jonathan Mather et al., filed 20th January 2004.
- 37 ‘Subjective evaluation of crosstalk disturbance in stereoscopic displays’, Atsuo Hanazato et al, NHK (Japan broadcasting corporation) science and technical research laboratories, SID, 2000.
- 38 Sci/Tech Look: 3D TV with no goggles,  
<http://news.bbc.co.uk/1/hi/sci/tech/271693.stm>, Wednesday, February 3, 1999.
- 39 Internal Sharp document, ‘3D Display Apparatus (Beamcombiner Application), author unknown, 1992.
- 40 Possibility of stereoscopic displays by using a viewing angle dependence of twisted nematic liquid crystal cells, Hiroyuki Okada et al, IEEE transactions on electron devices vol 45 no 7 July 1998.
- 41 Japanese patent number 2004-246019, Sharp Laboratories of Europe Ltd, ‘Display showing two images from one uniform panel’, H. Stevenson, J. Mather, D. Kean, filed 30th August 2003.
- 42 Japanese patent number 2004-251107, Sharp Laboratories of Europe Ltd, ‘Display that produces an image larger than the display size’, Jonathan Mather et al., filed 30th August 2003.
- 43 Discussion with Austin Schuman, Optical Polymer Research Inc., January 2007.

- 
- 44 Discussions with Sharp Corporation TFT designers, 2004.
- 45 E. Hecht, 'Optics', Addison-Wesley Publishing Company, 1987.
- 46 Pedrotti and Pedrotti, 'Introduction to Optics', Prentice Hall International, 1996.
- 47 H Hopkins, 1951, 'The concept of partial coherence in optics', Procedures of the Royal Society A, volume 208, page 263.
- 48 [http://en.wikipedia.org/wiki/Lens\\_flare](http://en.wikipedia.org/wiki/Lens_flare), January 2007.
- 49 H Hopkins, 1951, 'The concept of partial coherence in optics', Procedures of the Royal Society A, volume 208, page 263.
- 50 Peter G Barton, 'Contrast sensitivity in the human eye', Press Monograph PM72, Dec 1999.
- 51 Missing reference, downloaded from the internet 2004.
- 52 British patent application number 0501469.1, Sharp Laboratories of Europe Ltd, "Multiple-view display and display controller", Jonathan Mather et al, filed 26<sup>th</sup> January 2005.
- 53 Yasin Ekinici et al, "Bilayer Al wire-grids as broadband and high performance Polarizers", Paul Sherrer Institute, Switzerland, 2006 Optical Society of America.
- 54 Glass thermal expansion coefficient taken from a discussion with Sharp Corporation engineer Mr. Y. Koyama, August 2002. Plastic thermal expansion coefficient from discussion with Sharp Laboratories of Europe engineer Mr Stephen Fasham, March 2005.
- 55 D. Daly et al, 'The manufacture of microlenses by melting photoresist', Measurement Science Technology, volume 1 page 759-766, 1990.
- 56 Z Popovic et al, 'Technique for monolithic fabrication of microlens arrays', Applied optics 27, p1281, 1988.
- 57 Discussion with technical support engineer Russel Davies of Chestech ltd photoresist suppliers, July 2005.
- 58 M Madou, 'Fundamentals of microfabrication', Second edition, CRC Press, 2002.
- 59 T Mancebo, 'Interferometric monitoring of surface shaping processes in microlenses produced by melting photoresist', Journal of modern optics, vol 45, no 5, p1029, 1998.
- 60 Work carried out by Michel Sagadoyburu, at Sharp Laboratories of Europe Ltd., November 2005.
- 61 Discussion with Diana Kean, at Sharp Laboratories of Europe Ltd., February 2005.
- 62 Marina Khasova, Internal Document at Sharp Laboratories of Europe Ltd., 2001.

---

63 <http://www.sculptor-iangb.com/mould.htm>.

64 <http://content.answers.com/main/content/wp/en/thumb/3/34/300px->

Video\_contact\_angle.gif.